6.17 Two W8 × 31 rolled sections may be welded at A and B in either of the two ways shown in order to form a composite beam. Knowing that for each weld the allowable shearing force is 3000 lb per inch of weld, determine for each arrangement the maximum allowable vertical shear in the composite beam.

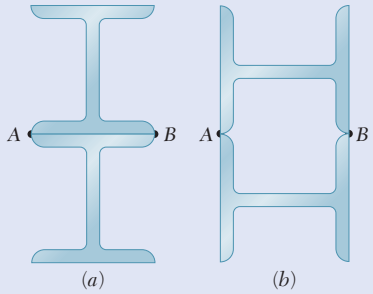


Fig. P6.17

6.18 For the beam and loading shown, determine the minimum required width b, knowing that for the grade of timber used, $\sigma_{all} = 12$ MPa and $\tau_{all} = 825$ kPa.

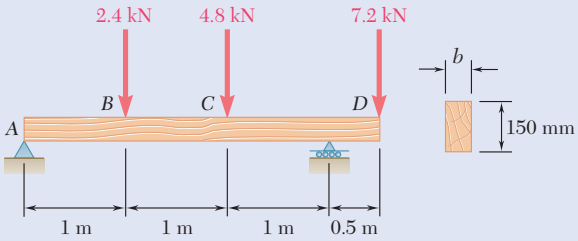


Fig. P6.18

6.19 A timber beam AB of length L and rectangular cross section carries a single concentrated load **P** at its midpoint C. (a) Show that the ratio τ_m/σ_m of the maximum values of the shearing and normal stresses in the beam is equal to $h/2L$, where h and L are, respectively, the depth and the length of the beam. (b) Determine the depth h and the width b of the beam, knowing that $L = 2$ m, $P = 40$ kN, $\tau_m = 960$ kPa, and $\sigma_m = 12$ MPa.

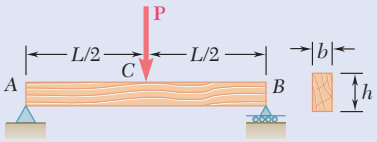


Fig. P6.19

6.20 A timber beam AB of length L and rectangular cross section carries a uniformly distributed load w and is supported as shown. (a) Show that the ratio τ_m/σ_m of the maximum values of the shearing and normal stresses in the beam is equal to $2h/L$, where h and L are, respectively, the depth and the length of the beam. (b) Determine the depth h and the width b of the beam, knowing that $L = 5$ m, $w = 8$ kN/m, $\tau_m = 1.08$ MPa, and $\sigma_m = 12$ MPa.

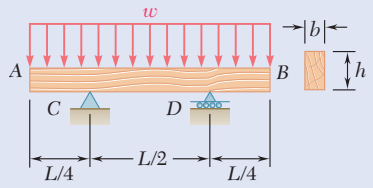


Fig. P6.20

Zhuhai CosMX Battery Co. - EX1018 (Part 2 of 2)
Zhuhai CosMX Battery Co. v. Ningde Amperex Tech. Ltd.

6.21 and 6.22 For the beam and loading shown, consider section n–n and determine the shearing stress at (a) point a, (b) point b.

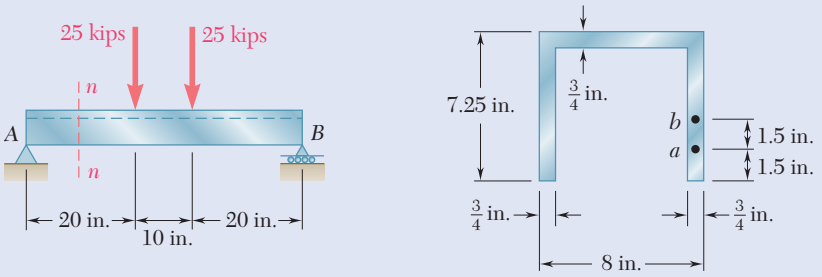


Fig. P6.21 and P6.23

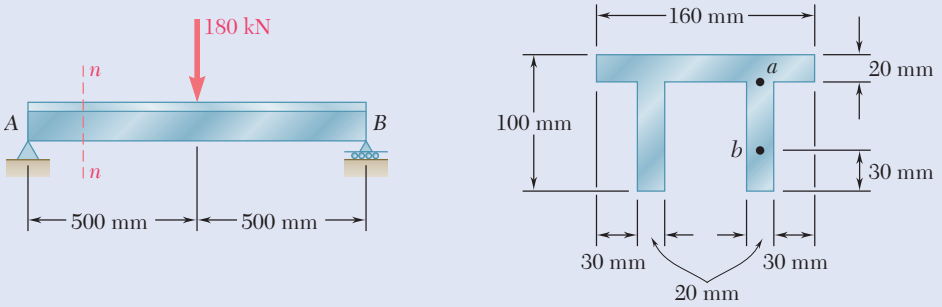


Fig. P6.22 and P6.24

6.23 and 6.24 For the beam and loading shown, determine the largest shearing stress in section n–n.

***6.25* through 6.28** A beam having the cross section shown is subjected to a vertical shear **V**. Determine (a) the horizontal line along which the shearing stress is maximum, (b) the constant k in the following expression for the maximum shearing stress

$$\tau_{\max} = k\frac{V}{A}$$

where A is the cross-sectional area of the beam.

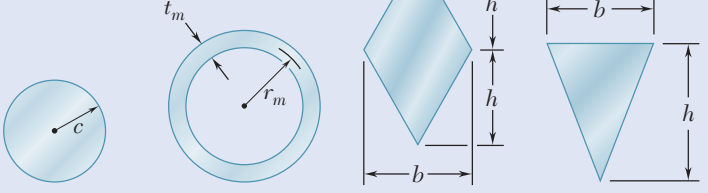


Fig. *P6.25* **Fig. P6.26** **Fig. *P6.27*** **Fig. P6.28**

6.3 LONGITUDINAL SHEAR ON A BEAM ELEMENT OF ARBITRARY SHAPE

Consider a box beam obtained by nailing together four planks, as shown in Fig. 6.21*a*. Sec. 6.1A showed how to determine the shear per unit length q on the horizontal surfaces along which the planks are joined. But could q be determined if the planks are joined along *vertical* surfaces, as shown in Fig. 6.21*b*? Section 6.2 showed the distribution of the vertical components τ_{xy} of the stresses on a transverse section of a W- or S-beam. These stresses had a fairly constant value in the web of the beam and were negligible in its flanges. But what about the *horizontal* components τ_{xz} of the stresses in the flanges? The procedure developed in Sec. 6.1A to determine the shear per unit length q applies to the cases just described.

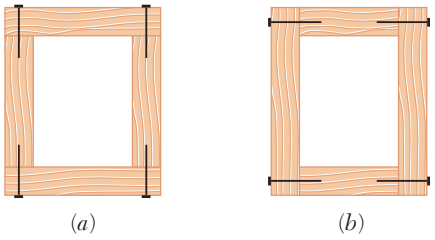


Fig. 6.21 Box beam formed by nailing planks together.

Consider the prismatic beam AB of Fig. 6.4, which has a vertical plane of symmetry and supports the loads shown. At a distance x from end A, detach an element $CDD'C'$ with a length of Δx. However, this element now extends from two sides of the beam to an arbitrary curved surface (Fig. 6.22). The forces exerted on the element include vertical shearing

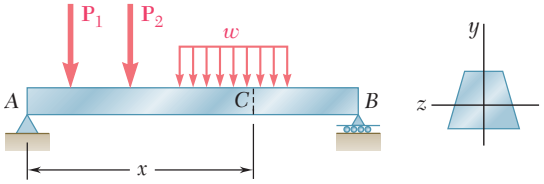


Fig. 6.4 (*repeated*) Beam example.

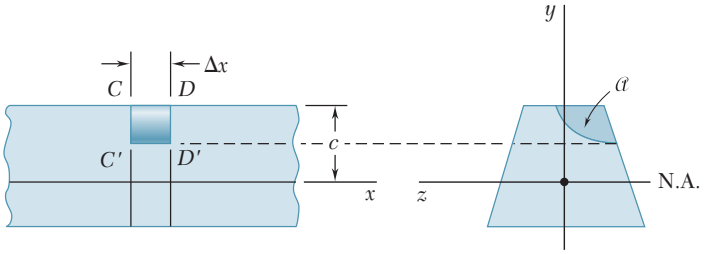


Fig. 6.22 Short segment of beam with element $CDD'C'$ of length Δx.

forces $\mathbf{V}'_C$ and $\mathbf{V}'_D$, elementary horizontal normal forces $\sigma_C dA$ and $\sigma_D dA$, possibly a load $w\,\Delta x$, and a longitudinal shearing force $\Delta\mathbf{H}$, which represent the resultant of the elementary longitudinal shearing forces exerted on the curved surface (Fig. 6.23). The equilibrium equation is

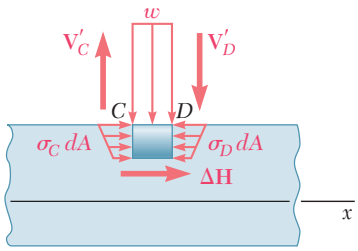


Fig. 6.23 Forces exerted on element $CDD'C'$.

$$\overset{+}{\rightarrow}\Sigma F_x = 0: \qquad \Delta H + \int_{\mathcal{A}} (\sigma_C - \sigma_D)\, dA = 0$$

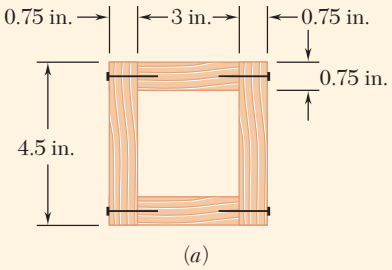
where the integral is to be computed over the shaded area $\mathcal{A}$ of the section in Fig. 6.22. This equation is the same as the one in Sec. 6.1A, but the shaded area $\mathcal{A}$ now extends to the curved surface.

The longitudinal shear exerted on the beam element is

$$\Delta H = \frac{VQ}{I}\Delta x \tag{6.4}$$

where I is the centroidal moment of inertia of the entire section, Q is the first moment of the shaded area $\mathcal{A}$ with respect to the neutral axis, and V is the vertical shear in the section. Dividing both members of Eq. (6.4) by Δx, the horizontal shear per unit length or shear flow is

$$q = \frac{\Delta H}{\Delta x} = \frac{VQ}{I} \tag{6.5}$$



(*a*)

Concept Application 6.4

A square box beam is made of two 0.75 × 3-in. planks and two 0.75 × 4.5-in. planks nailed together, as shown (Fig. 6.24*a*). Knowing that the spacing between nails is 1.75 in. and that the beam is subjected to a vertical shear with a magnitude of $V = 600$ lb, determine the shearing force in each nail.

Isolate the upper plank and consider the total force per unit length q exerted on its two edges. Use Eq. (6.5), where Q represents the first moment with respect to the neutral axis of the shaded area A' shown in Fig. 6.24*b* and I is the moment of inertia about the same axis of the entire cross-sectional area of the box beam (Fig. 6.24*c*).

$$Q = A'\bar{y} = (0.75 \text{ in.})(3 \text{ in.})(1.875 \text{ in.}) = 4.22 \text{ in}^3$$

Recalling that the moment of inertia of a square of side a about a centroidal axis is $I = \frac{1}{12}a^4$,

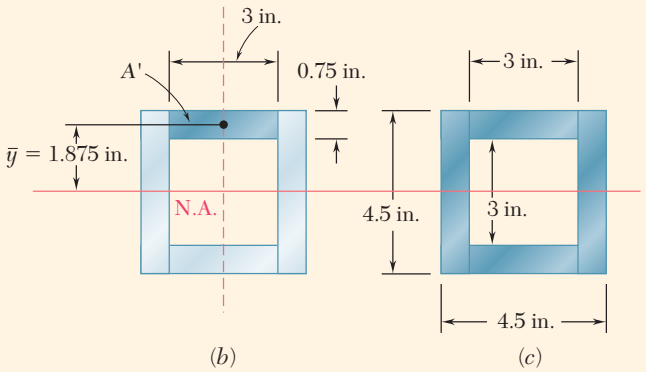
$$I = \tfrac{1}{12}(4.5 \text{ in.})^4 - \tfrac{1}{12}(3 \text{ in.})^4 = 27.42 \text{ in}^4$$

Substituting into Eq. (6.5),

$$q = \frac{VQ}{I} = \frac{(600 \text{ lb})(4.22 \text{ in}^3)}{27.42 \text{ in}^4} = 92.3 \text{ lb/in.}$$

Because both the beam and the upper plank are symmetric with respect to the vertical plane of loading, equal forces are exerted on both edges of the plank. The force per unit length on each of these edges is thus $\frac{1}{2}q = \frac{1}{2}(92.3) = 46.15$ lb/in. Since the spacing between nails is 1.75 in., the shearing force in each nail is

$$F = (1.75 \text{ in.})(46.15 \text{ lb/in.}) = 80.8 \text{ lb}$$



(*b*) (*c*)

Fig. 6.24 (*a*) Box beam made from planks nailed together. (*b*) Geometry for finding first moment of area of top plank. (*c*) Geometry for finding the moment of inertia of entire cross section.

6.4 SHEARING STRESSES IN THIN-WALLED MEMBERS

We saw in the preceding section that Eq. (6.4) may be used to determine the longitudinal shear $\Delta\mathbf{H}$ exerted on the walls of a beam element of arbitrary shape and Eq. (6.5) to determine the corresponding shear flow q. Equations (6.4) and (6.5) are used in this section to calculate both the shear flow and the average shearing stress in thin-walled members such as the flanges of wide-flange beams (Photo 6.2), box beams, or the walls of structural tubes (Photo 6.3).



Photo 6.2 Wide-flange beams.



Photo 6.3 Structural tubes.

Consider a segment of length Δx of a wide-flange beam (Fig. 6.25*a*) where **V** is the vertical shear in the transverse section shown. Detach an element $ABB'A'$ of the upper flange (Fig. 6.25*b*). The longitudinal shear $\Delta\mathbf{H}$ exerted on that element can be obtained from Eq. (6.4):

$$\Delta H = \frac{VQ}{I}\,\Delta x \tag{6.4}$$

Dividing ΔH by the area $\Delta A = t\,\Delta x$ of the cut, the average shearing stress exerted on the element is the same expression obtained in Sec. 6.1B for a horizontal cut:

$$\tau_{\text{ave}} = \frac{VQ}{It} \tag{6.6}$$

Note that τ_{ave} now represents the average value of the shearing stress τ_{zx} over a vertical cut, but since the thickness t of the flange is small, there is very little variation of τ_{zx} across the cut. Recalling that $\tau_{xz} = \tau_{zx}$

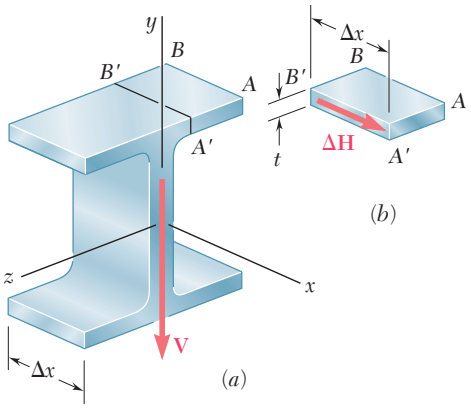


Fig. 6.25 (*a*) Wide-flange beam section with vertical shear *V*. (*b*) Segment of flange with longitudinal shear ΔH.

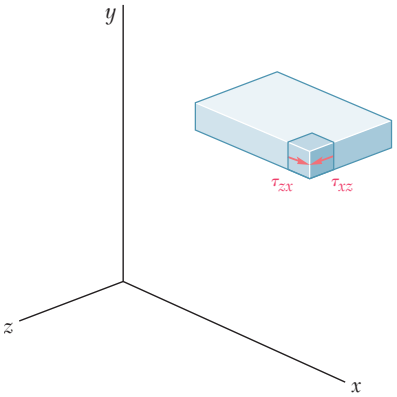


Fig. 6.26 Stress element within flange segment.

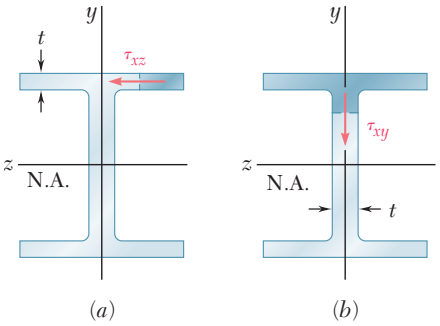


Fig. 6.27 Wide-flange beam sections showing shearing stress (*a*) in flange and (*b*) in web. The shaded area is that used for calculating the first moment of area.

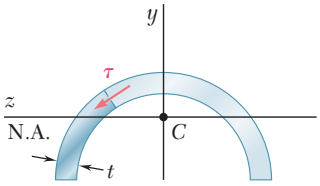


Fig. 6.29 Half pipe section showing shearing stress, and shaded area for calculating first moment of area.

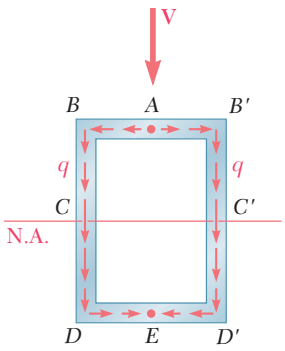


Fig. 6.30 Shear flow, *q*, in a box beam section.

(Fig. 6.26), the horizontal component τ_{xz} of the shearing stress at any point of a transverse section of the flange can be obtained from Eq. (6.6), where Q is the first moment of the shaded area about the neutral axis (Fig. 6.27*a*). A similar result was obtained for the vertical component τ_{xy} of the shearing stress in the web (Fig. 6.27*b*). Equation (6.6) can be used to determine shearing stresses in box beams (Fig. 6.28), half pipes (Fig. 6.29), and other thin-walled members, as long as the loads are applied in a plane of symmetry. In each case, the cut must be perpendicular to the surface of the member, and Eq. (6.6) will yield the component of the shearing stress in the direction tangent to that surface. (The other component is assumed to be equal to zero, because of the proximity of the two free surfaces.)

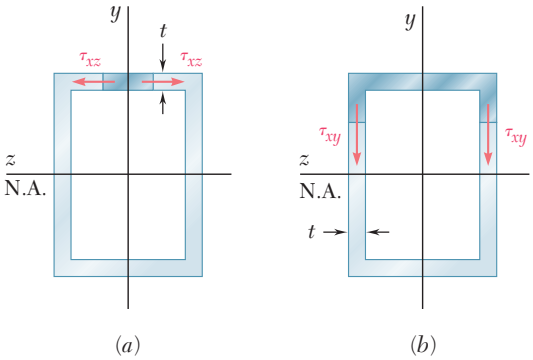


Fig. 6.28 Box beam showing shearing stress (*a*) in flange, (*b*) in web. Shaded area is that used for calculating the first moment of area.

Comparing Eqs. (6.5) and (6.6), the product of the shearing stress τ at a given point of the section and the thickness t at that point is equal to q. Since V and I are constant, q depends only upon the first moment Q and easily can be sketched on the section. For a box beam (Fig. 6.30), q grows smoothly from zero at A to a maximum value at C and C' on the neutral axis and decreases back to zero as E is reached. There is no sudden variation in the magnitude of q as it passes a corner at B, D, B', or D', and the sense of q in the horizontal portions of the section is easily obtained from its sense in the vertical portions (the sense of the shear **V**). In a wide-flange section (Fig. 6.31), the values of q in portions AB and $A'B$ of the upper flange are distributed symmetrically. At B in the web, q corresponds to the two halves of the flange, which must be combined to obtain the value of q at the top of the web. After reaching a maximum value at C on the neutral axis, q decreases and splits into two equal parts at D, which corresponds at D to the two halves of the lower flange. The shear per unit length q is commonly called the *shear flow* and reflects the similarity between the properties of q just described and some of the characteristics of a fluid flow through an open channel or pipe.[†]

So far, all of the loads were applied in a plane of symmetry of the member. In the case of members possessing two planes of symmetry (Fig. 6.27 or 6.30), any load applied through the centroid of a given cross

[†]Recall that the concept of shear flow was used to analyze the distribution of shearing stresses in thin-walled hollow shafts (Sec. 3.10). However, while the shear flow in a hollow shaft is constant, the shear flow in a member under a transverse loading is not.

section can be resolved into components along the two axes of symmetry. Each component will cause the member to bend in a plane of symmetry, and the corresponding shearing stresses can be obtained from Eq. (6.6). The principle of superposition can then be used to determine the resulting stresses.

However, if the member possesses no plane of symmetry or a single plane of symmetry and is subjected to a load that is not contained in that plane, that member is observed to *bend and twist* at the same time—except when the load is applied at a specific point called the *shear center*. The shear center normally does *not* coincide with the centroid of the cross section. The shear center of various thin-walled shapes is discussed in Sec. 6.6.

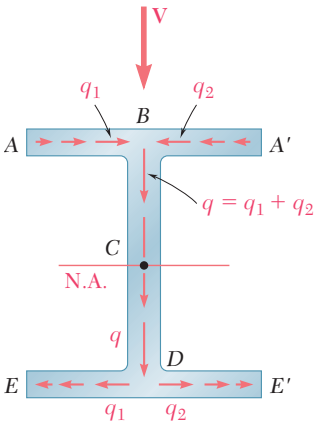


Fig. 6.31 Shear flow, q, in a wide-flange beam section.

*6.5 PLASTIC DEFORMATIONS

Consider a cantilever beam AB with a length of L and a rectangular cross section subjected to a concentrated load **P** at its free end A (Fig. 6.32). The largest bending moment occurs at the fixed end B and is equal to $M = PL$. As long as this value does not exceed the maximum elastic moment M_Y (i.e., $PL \le M_Y$), the normal stress σ_x will not exceed the yield strength σ_Y anywhere in the beam. However, as P is increased beyond M_Y/L, yield is initiated at points B and B' and spreads toward the free end of the beam. Assuming the material is elastoplastic and considering a cross section CC' located a distance x from the free end A of the beam (Fig. 6.33), the half-thickness y_Y of the elastic core in that section is obtained by making $M = Px$ in Eq. (4.38). Thus,

$$Px = \frac{3}{2}M_Y\left(1 - \frac{1}{3}\frac{y_Y^2}{c^2}\right) \tag{6.14}$$

where c is the half-depth of the beam. Plotting y_Y against x gives the boundary between the elastic and plastic zones.

As long as $PL < \frac{3}{2}M_Y$, the parabola from Eq. (6.14) intersects the line BB', as shown in Fig. 6.33. However, when PL reaches the value $\frac{3}{2}M_Y$ ($PL = M_p$) where M_p is the plastic moment, Eq. (6.14) yields $y_Y = 0$ for $x = L$, which shows that the vertex of the parabola is now located in section BB' and that this section has become fully plastic (Fig. 6.34). Recalling Eq. (4.40), the radius of curvature ρ of the neutral surface at that point is equal to zero, indicating the presence of a sharp bend in the beam at its fixed end. Thus, a *plastic hinge* has developed at that point. The load $P = M_p/L$ is the largest load that can be supported by the beam.

This discussion is based only on the analysis of the normal stresses in the beam. Now examine the distribution of the shearing stresses in a section

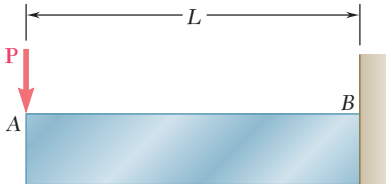


Fig. 6.32 Cantilever beam having maximum moment PL at section B-B'. As long as $PL \le M_Y$, the beam remains elastic.

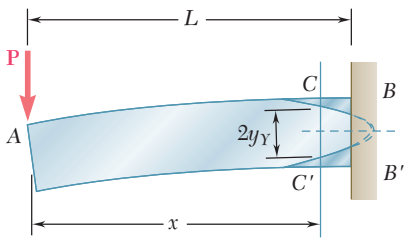


Fig. 6.33 Cantilever beam exhibiting partial yielding, showing the elastic core at section C–C'.

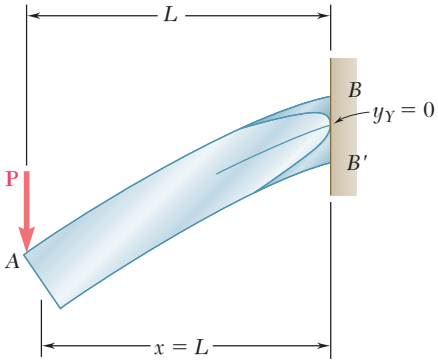


Fig. 6.34 Fully plastic cantilever beam having $PL = M_P = 1.5\ M_Y$.

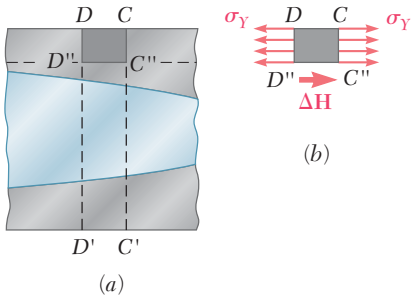


Fig. 6.35 (*a*) Beam segment in partially plastic area. (*b*) Element *DCC″D″* is fully plastic.

that has become partly plastic. Consider the portion of beam *CC″D″D* located between the transverse sections *CC′* and *DD′* and above the horizontal plane *D″C″* (Fig. 6.35*a*). If this portion is located entirely in the plastic zone, the normal stresses exerted on the faces *CC″* and *DD″* will be uniformly distributed and equal to the yield strength σ_Y (Fig. 6.35*b*). The equilibrium of the free body *CC″D″D* requires that the horizontal shearing force **ΔH** exerted on its lower face is equal to zero. The average value of the horizontal shearing stress τ_{yx} across the beam at *C″* is also zero, as well as the average value of the vertical shearing stress τ_{xy}. Thus, the vertical shear $V = P$ in section *CC′* must be distributed entirely over the portion *EE′* of the section located within the elastic zone (Fig. 6.36). The distribution of the shearing stresses over *EE′* is the same as that in an elastic rectangular beam with the same width *b* as beam *AB* and depth equal to the thickness $2y_Y$ of the elastic zone.† The area $2by_Y$ of the elastic portion of the cross section *A′* gives

$$\tau_{xy} = \frac{3}{2}\frac{P}{A'}\left(1 - \frac{y^2}{y_Y^2}\right) \tag{6.15}$$

The maximum value of the shearing stress occurs for $y = 0$ and is

$$\tau_{\max} = \frac{3}{2}\frac{P}{A'} \tag{6.16}$$

As the area *A′* of the elastic portion of the section decreases, $\tau_{\max}$ increases and eventually reaches the yield strength in shear τ_Y. Thus, shear contributes to the ultimate failure of the beam. A more exact analysis of this mode of failure should take into account the combined effect of the normal and shearing stresses.

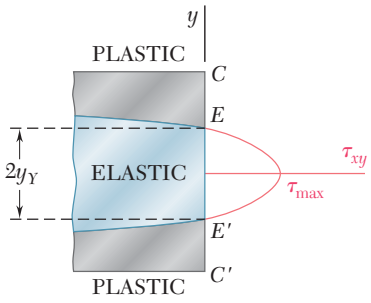


Fig. 6.36 Parabolic shear distribution in elastic core.

†See Prob. 6.60.

Sample Problem 6.3

Knowing that the vertical shear is 50 kips in a W10 × 68 rolled-steel beam, determine the horizontal shearing stress in the top flange at a point a located 4.31 in. from the edge of the beam. The dimensions and other geometric data of the rolled-steel section are given in Appendix C.

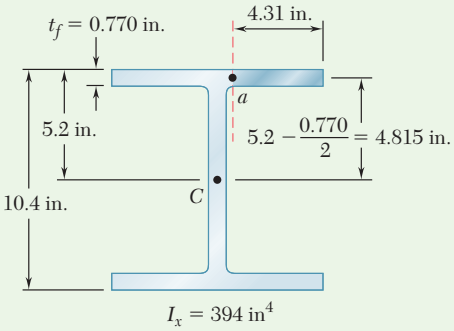


Fig. 1 Cross section dimensions for W10 × 68 steel beam.

STRATEGY: Determine the horizontal shearing stress at the required section.

MODELING and ANALYSIS:

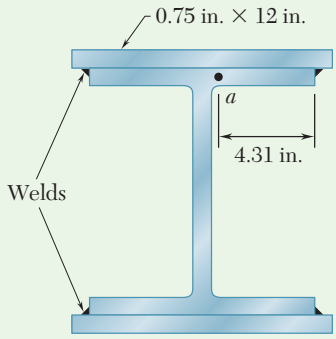
As shown in Fig. 1, we isolate the shaded portion of the flange by cutting along the dashed line that passes through point a.

$$Q = (4.31 \text{ in.})(0.770 \text{ in.})(4.815 \text{ in.}) = 15.98 \text{ in}^3$$

$$\tau = \frac{VQ}{It} = \frac{(50 \text{ kips})(15.98 \text{ in}^3)}{(394 \text{ in}^4)(0.770 \text{ in.})} \qquad \tau = 2.63 \text{ ksi}$$

Sample Problem 6.4

Solve Sample Prob. 6.3, assuming that 0.75 × 12-in. plates have been attached to the flanges of the W10 × 68 beam by continuous fillet welds as shown.



STRATEGY: Calculate the properties for the composite beam and then determine the shearing stress at the required section.

(continued)

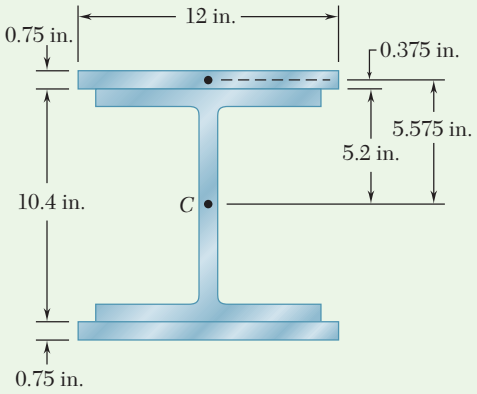


Fig. 1 Cross section dimensions for calculating moment of inertia.

MODELING and ANALYSIS:

For the composite beam shown in Fig. 1, the centroidal moment of inertia is

$$I = 394\text{ in}^4 + 2\left[\tfrac{1}{12}(12\text{ in.})(0.75\text{ in.})^3 + (12\text{ in.})(0.75\text{ in.})(5.575\text{ in.})^2\right]$$
$$I = 954\text{ in}^4$$

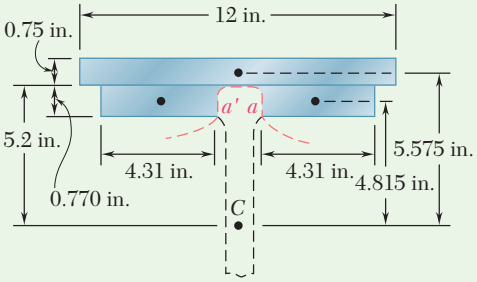


Fig. 2 Dimensions used to find first moment of area and shearing stress at flange-web junction.

Since the top plate and the flange are connected only at the welds, the shearing stress is found at a by passing a section through the flange at a, *between* the plate and the flange, and again through the flange at the symmetric point a' (Fig. 2).

For the shaded area,

$$t = 2t_f = 2(0.770\text{ in.}) = 1.540\text{ in.}$$

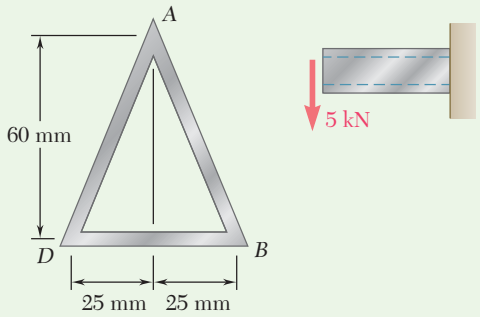
$$Q = 2[(4.31\text{ in.})(0.770\text{ in.})(4.815\text{ in.})] + (12\text{ in.})(0.75\text{ in.})(5.575\text{ in.})$$

$$Q = 82.1\text{ in}^3$$

$$\tau = \frac{VQ}{It} = \frac{(50\text{ kips})(82.1\text{ in}^3)}{(954\text{ in}^4)(1.540\text{ in.})} \qquad \tau = 2.79\text{ ksi}$$

Sample Problem 6.5

The thin-walled extruded beam shown is made of aluminum and has a uniform 3-mm wall thickness. Knowing that the shear in the beam is 5 kN, determine (*a*) the shearing stress at point *A*, (*b*) the maximum shearing stress in the beam. *Note:* The dimensions given are to lines midway between the outer and inner surfaces of the beam.



STRATEGY: Determine the location of the centroid and then calculate the moment of inertia. Calculate the two required stresses.

MODELING and ANALYSIS:

Centroid. Using Fig. 1, we note that $AB = AD = 65$ mm.

$$\bar{Y} = \frac{\Sigma\, \bar{y}\mathrm{A}}{\Sigma\, \mathrm{A}} = \frac{2[(65\text{ mm})(3\text{ mm})(30\text{ mm})]}{2[(65\text{ mm})(3\text{ mm})] + (50\text{ mm})(3\text{ mm})}$$

$$\bar{Y} = 21.67\text{ mm}$$

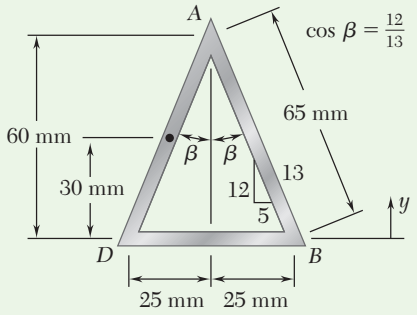


Fig. 1 Section dimensions for finding centroid.

(continued)

Centroidal Moment of Inertia. Each side of the thin-walled beam can be considered as a parallelogram (Fig. 2), and we recall that for the case shown $I_{nn} = bh^3/12$, where b is measured parallel to the axis nn. Using Fig. 3 we write

$$b = (3\text{ mm})/\cos\beta = (3\text{ mm})/(12/13) = 3.25\text{ mm}$$

$$I = \Sigma(\bar{I} + Ad^2) = 2[\tfrac{1}{12}(3.25\text{ mm})(60\text{ mm})^3 + (3.25\text{ mm})(60\text{ mm})(8.33\text{ mm})^2] + [\tfrac{1}{12}(50\text{ mm})(3\text{ mm})^3 + (50\text{ mm})(3\text{ mm})(21.67\text{ mm})^2]$$

$$I = 214.6 \times 10^3\text{ mm}^4 \qquad I = 0.2146 \times 10^{-6}\text{ m}^4$$

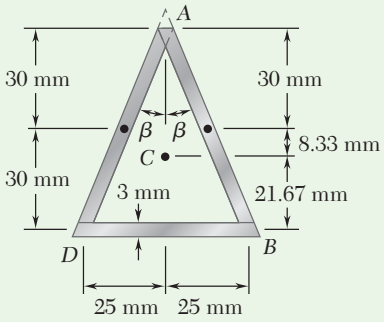


Fig. 2 Dimensions locating centroid.

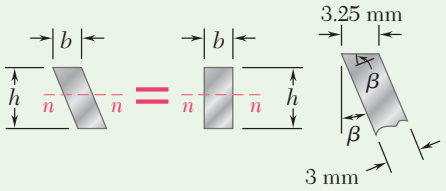


Fig. 3 Determination of horizontal width for side elements.

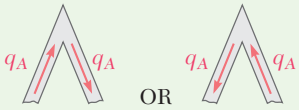


Fig. 4 Possible directions for shear flow at *A*.

a. Shearing Stress at *A*. If a shearing stress τ_A occurs at A, the shear flow will be $q_A = \tau_A t$ and must be directed in one of the two ways shown in Fig 4. But the cross section and the loading are symmetric about a vertical line through A, and thus the shear flow must also be symmetric. Since neither of the possible shear flows is symmetric, we conclude that

$$\tau_A = 0.$$

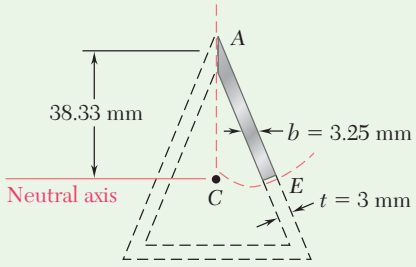


Fig. 5 Section for finding the maximum shearing stress.

b. Maximum Shearing Stress. Since the wall thickness is constant, the maximum shearing stress occurs at the neutral axis, where Q is maximum. Since we know that the shearing stress at A is zero, we cut the section along the dashed line shown and isolate the shaded portion of the beam (Fig. 5). In order to obtain the largest shearing stress, the cut at the neutral axis is made perpendicular to the sides and is of length $t = 3$ mm.

$$Q = [(3.25\text{ mm})(38.33\text{ mm})]\left(\frac{38.33\text{ mm}}{2}\right) = 2387\text{ mm}^3$$

$$Q = 2.387 \times 10^{-6}\text{ m}^3$$

$$\tau_E = \frac{VQ}{It} = \frac{(5\text{ kN})(2.387 \times 10^{-6}\text{ m}^3)}{(0.2146 \times 10^{-6}\text{ m}^4)(0.003\text{ m})} \qquad \tau_{\max} = \tau_E = 18.54\text{ MPa}$$

Problems

6.29 The built-up timber beam shown is subjected to a vertical shear of 1200 lb. Knowing that the allowable shearing force in the nails is 75 lb, determine the largest permissible spacing s of the nails.

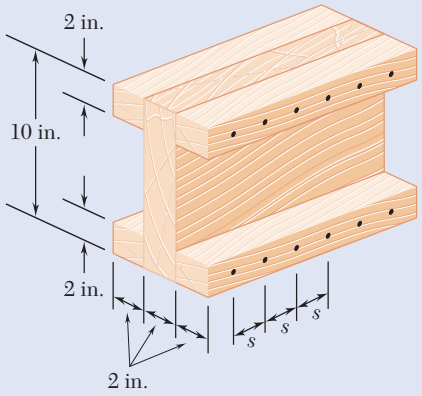


Fig. P6.29

6.30 The built-up beam shown is made by gluing together two 20 × 250-mm plywood strips and two 50 × 100-mm planks. Knowing that the allowable average shearing stress in the glued joints is 350 kPa, determine the largest permissible vertical shear in the beam.

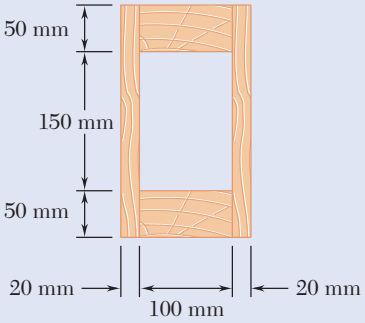


Fig. P6.30

6.31 The built-up beam was made by gluing together several wooden planks. Knowing that the beam is subjected to a 1200-lb vertical shear, determine the average shearing stress in the glued joint (*a*) at *A*, (*b*) at *B*.

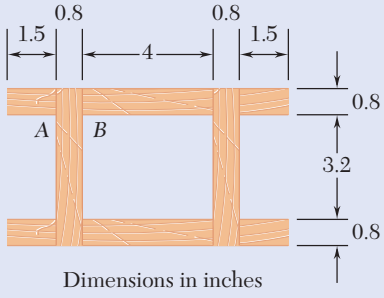


Fig. P6.31

6.32 Several wooden planks are glued together to form the box beam shown. Knowing that the beam is subjected to a vertical shear of 3 kN, determine the average shearing stress in the glued joint (*a*) at *A*, (*b*) at *B*.

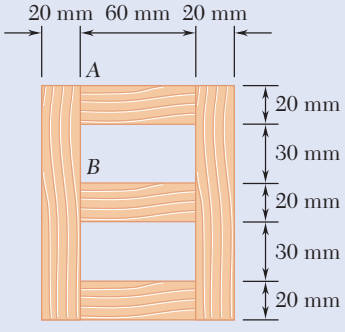
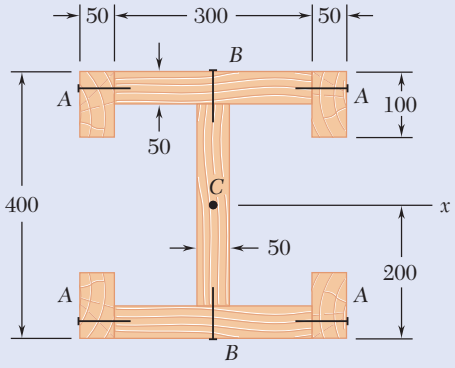


Fig. P6.32



Dimensions in mm

Fig. P6.33

6.33 The built-up wooden beam shown is subjected to a vertical shear of 8 kN. Knowing that the nails are spaced longitudinally every 60 mm at A and every 25 mm at B, determine the shearing force in the nails (a) at A, (b) at B. (*Given*: $I_x = 1.504 \times 10^9$ mm^4.)

6.34 Knowing that a W360 × 122 rolled-steel beam is subjected to a 250-kN vertical shear, determine the shearing stress (a) at point A, (b) at the centroid C of the section.

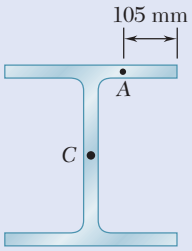
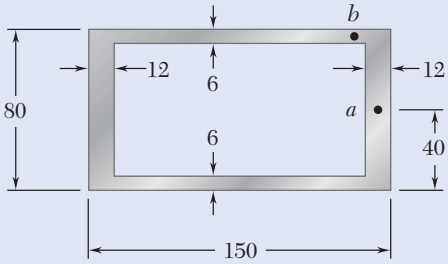


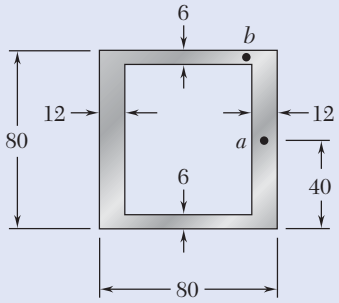
Fig. P6.34

6.35 and 6.36 An extruded aluminum beam has the cross section shown. Knowing that the vertical shear in the beam is 150 kN, determine the shearing stress at (a) point a, (b) point b.



Dimensions in mm

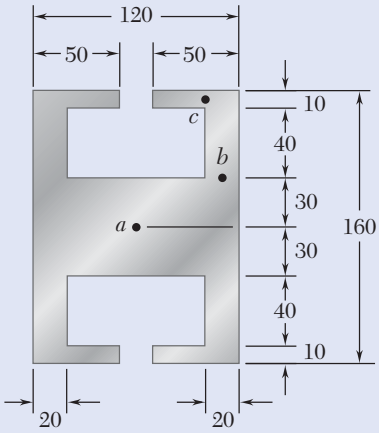
Fig. P6.35



Dimensions in mm

Fig. P6.36

6.37 Knowing that a given vertical shear **V** causes a maximum shearing stress of 75 MPa in an extruded beam having the cross section shown, determine the shearing stress at the three points indicated.



Dimensions in mm

Fig. P6.37

6.38 The vertical shear is 1200 lb in a beam having the cross section shown. Knowing that $d = 4$ in., determine the shearing stress at (*a*) point *a*, (*b*) point *b*.

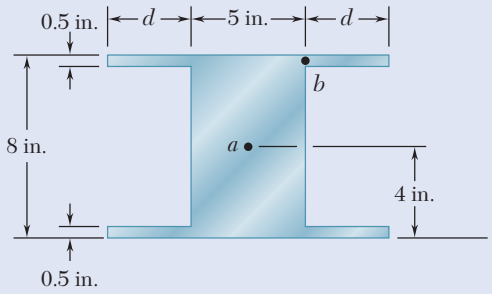


Fig. P6.38 and *P6.39*

6.39 The vertical shear is 1200 lb in a beam having the cross section shown. Determine (*a*) the distance *d* for which $\tau_a = \tau_b$, (*b*) the corresponding shearing stress at points *a* and *b*.

6.40 and *6.41* The extruded aluminum beam has a uniform wall thickness of $\frac{1}{8}$ in. Knowing that the vertical shear in the beam is 2 kips, determine the corresponding shearing stress at each of the five points indicated.

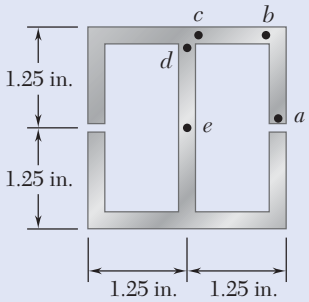


Fig. P6.40

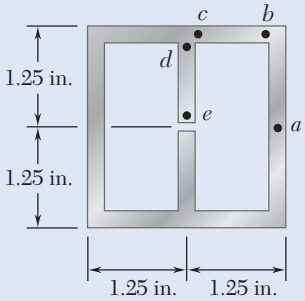


Fig. *P6.41*

6.42 Knowing that a given vertical shear **V** causes a maximum shearing stress of 50 MPa in a thin-walled member having the cross section shown, determine the corresponding shearing stress at (*a*) point *a*, (*b*) point *b*, (*c*) point *c*.

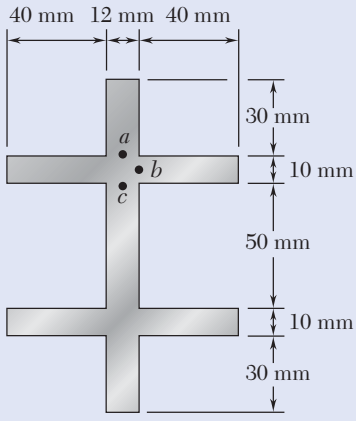


Fig. P6.42

6.43 Three planks are connected as shown by bolts of $\frac{3}{8}$-in. diameter spaced every 6 in. along the longitudinal axis of the beam. For a vertical shear of 2.5 kips, determine the average shearing stress in the bolts.

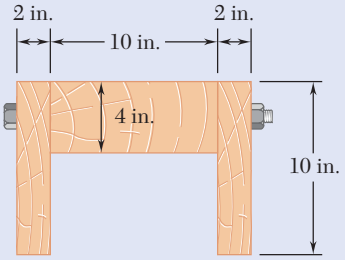


Fig. P6.43

6.44 A beam consists of three planks connected as shown by steel bolts with a longitudinal spacing of 225 mm. Knowing that the shear in the beam is vertical and equal to 6 kN and that the allowable average shearing stress in each bolt is 60 MPa, determine the smallest permissible bolt diameter that can be used.

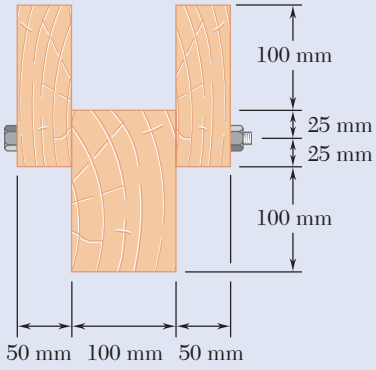


Fig. P6.44

6.45 A beam consists of five planks of 1.5 × 6-in. cross section connected by steel bolts with a longitudinal spacing of 9 in. Knowing that the shear in the beam is vertical and equal to 2000 lb and that the allowable average shearing stress in each bolt is 7500 psi, determine the smallest permissible bolt diameter that can be used.

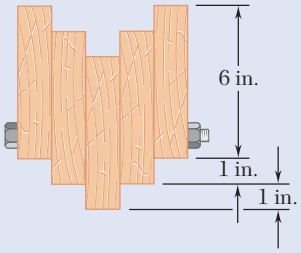


Fig. P6.45

6.46 Four L102 × 102 × 9.5 steel angle shapes and a 12 × 400-mm plate are bolted together to form a beam with the cross section shown. The bolts are of 22-mm diameter and are spaced longitudinally every 120 mm. Knowing that the beam is subjected to a vertical shear of 240 kN, determine the average shearing stress in each bolt.

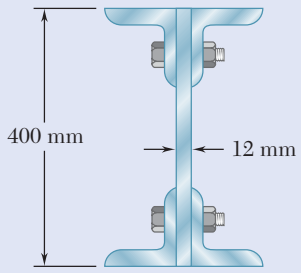


Fig. P6.46

6.47 A plate of $\frac{1}{4}$-in. thickness is corrugated as shown and then used as a beam. For a vertical shear of 1.2 kips, determine (*a*) the maximum shearing stress in the section, (*b*) the shearing stress at point *B*. Also sketch the shear flow in the cross section.

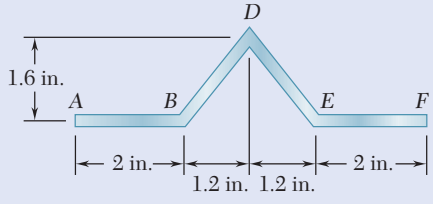


Fig. *P6.47*

6.48 A plate of 2-mm thickness is bent as shown and then used as a beam. For a vertical shear of 5 kN, determine the shearing stress at the five points indicated and sketch the shear flow in the cross section.

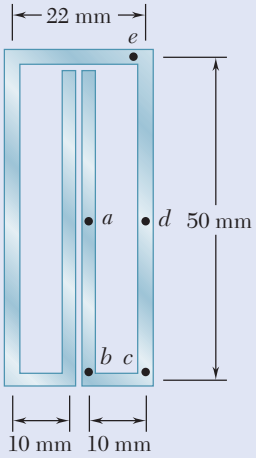


Fig. P6.48

6.49 An extruded beam has the cross section shown and a uniform wall thickness of 3 mm. For a vertical shear of 10 kN, determine (*a*) the shearing stress at point *A*, (*b*) the maximum shearing stress in the beam. Also sketch the shear flow in the cross section.

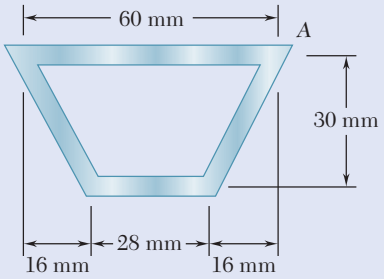


Fig. P6.49

6.50 A plate of thickness *t* is bent as shown and then used as a beam. For a vertical shear of 600 lb, determine (*a*) the thickness *t* for which the maximum shearing stress is 300 psi, (*b*) the corresponding shearing stress at point *E*. Also sketch the shear flow in the cross section.

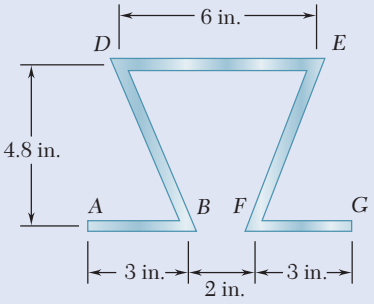


Fig. *P6.50*

6.51 The design of a beam calls for connecting two vertical rectangular $\frac{3}{8} \times 4$-in. plates by welding them to two horizontal $\frac{1}{2} \times 2$-in. plates as shown. For a vertical shear **V**, determine the dimension *a* for which the shear flow through the welded surfaces is maximum.

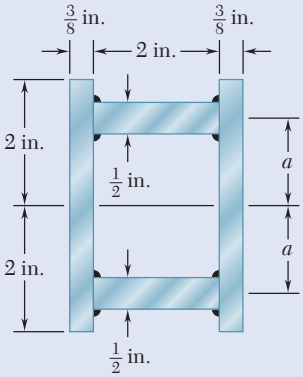


Fig. P6.51

6.52 The cross section of an extruded beam is a hollow square of side $a = 3$ in. and thickness $t = 0.25$ in. For a vertical shear of 15 kips, determine the maximum shearing stress in the beam and sketch the shear flow in the cross section.

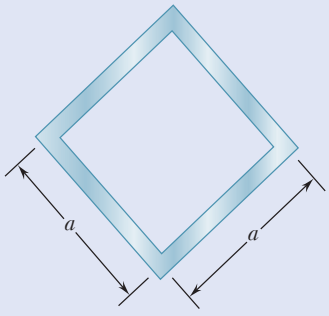


Fig. P6.52

6.53 An extruded beam has a uniform wall thickness t. Denoting by $\mathbf{V}$ the vertical shear and by A the cross-sectional area of the beam, express the maximum shearing stress as $\tau_{max} = k(V/A)$ and determine the constant k for each of the two orientations shown.

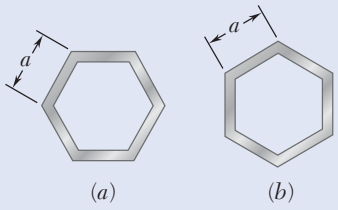


Fig. P6.53

6.54 (a) Determine the shearing stress at point P of a thin-walled pipe of the cross section shown caused by a vertical shear $\mathbf{V}$. (b) Show that the maximum shearing stress occurs for $\theta = 90°$ and is equal to $2V/A$, where A is the cross-sectional area of the pipe.

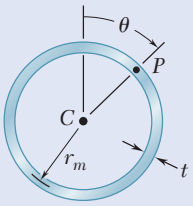


Fig. P6.54

6.55 For a beam made of two or more materials with different moduli of elasticity, show that Eq. (6.6)

$$\tau_{ave} = \frac{VQ}{It}$$

remains valid provided that both Q and I are computed by using the transformed section of the beam (see Sec. 4.4) and provided further that t is the actual width of the beam where τ_{ave} is computed.

6.56 and 6.57 A composite beam is made by attaching the timber and steel portions shown with bolts of 12-mm diameter spaced longitudinally every 200 mm. The modulus of elasticity is 10 GPa for the wood and 200 GPa for the steel. For a vertical shear of 4 kN, determine (a) the average shearing stress in the bolts, (b) the shearing stress at the center of the cross section. (*Hint*: Use the method indicated in Prob. 6.55.)

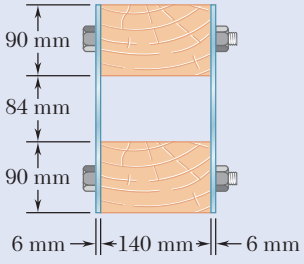


Fig. P6.56

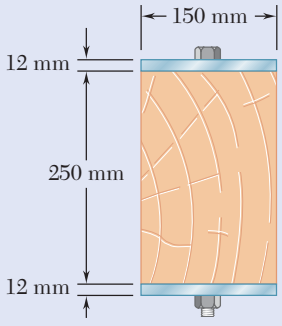


Fig. P6.57

6.58 and 6.59 A steel bar and an aluminum bar are bonded together as shown to form a composite beam. Knowing that the vertical shear in the beam is 4 kips and that the modulus of elasticity is 29×10^6 psi for the steel and 10.6×10^6 psi for the aluminum, determine (*a*) the average shearing stress at the bonded surface, (*b*) the maximum shearing stress in the beam. (*Hint*: Use the method indicated in Prob. 6.55.)

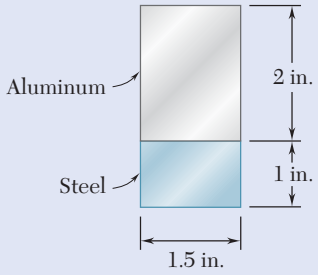


Fig. P6.58

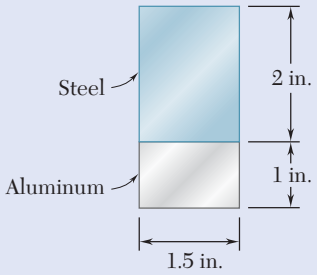


Fig. P6.59

6.60 Consider the cantilever beam *AB* discussed in Sec. 6.5 and the portion *ACKJ* of the beam that is located to the left of the transverse section *CC′* and above the horizontal plane *JK*, where *K* is a point at a distance $y < y_Y$ above the neutral axis (Fig. P6.60). (*a*) Recalling that $\sigma_x = \sigma_Y$ between *C* and *E* and $\sigma_x = (\sigma_Y/y_Y)y$ between *E* and *K*, show that the magnitude of the horizontal shearing force **H** exerted on the lower face of the portion of beam *ACKJ* is

$$H = \frac{1}{2} b\sigma_Y \left(2c - y_Y - \frac{y^2}{y_Y} \right)$$

(*b*) Observing that the shearing stress at *K* is

$$\tau_{xy} = \lim_{\Delta A \to 0} \frac{\Delta H}{\Delta A} = \lim_{\Delta x \to 0} \frac{1}{b} \frac{\Delta H}{\Delta x} = \frac{1}{b} \frac{\partial H}{\partial x}$$

and recalling that y_Y is a function of *x* defined by Eq. (6.14), derive Eq. (6.15).

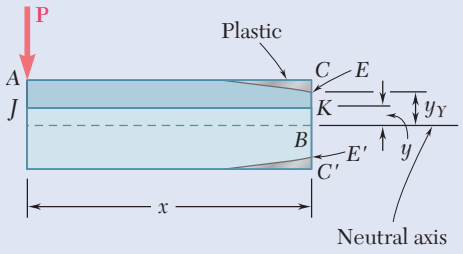


Fig. P6.60

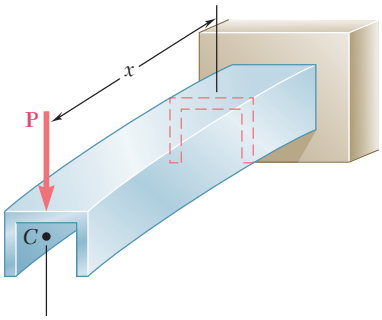


Fig. 6.37 Cantilevered channel beam with vertical plane of symmetry.

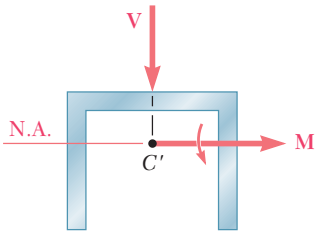
*6.6 UNSYMMETRIC LOADING OF THIN-WALLED MEMBERS AND SHEAR CENTER

Our analysis of the effects of transverse loadings has been limited to members possessing a vertical plane of symmetry and to loads applied in that plane. The members were observed to bend in the plane of loading (Fig. 6.37), and in any given cross section, the bending couple **M** and the shear **V** (Fig. 6.38) were found to result in normal and shearing stresses:

$$\sigma_x = -\frac{My}{I} \tag{4.16}$$

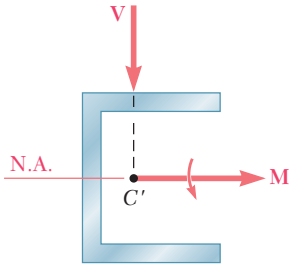
and

$$\tau_{\text{ave}} = \frac{VQ}{It} \tag{6.6}$$



$(V = P, M = Px)$

Fig. 6.38 Load applied in vertical plane of symmetry.



$(V = P, M = Px)$

Fig. 6.39 Load perpendicular to plane of symmetry.

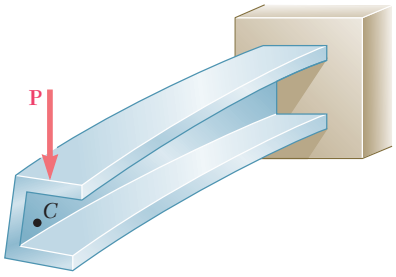


Fig. 6.40 Deformation of channel when not loaded in plane of symmetry.

In this section, the effects of transverse loads on *thin-walled members that do not possess a vertical plane of symmetry* are examined. Assume that the channel member of Fig. 6.37 has been rotated through 90° and that the line of action of **P** still passes through the centroid of the end section. The couple vector **M** representing the bending moment in a given cross section is still directed along a principal axis of the section (Fig. 6.39), and the neutral axis will coincide with that axis (see Sec. 4.8). Equation (4.16) can be used to compute the normal stresses in the section. However, Eq. (6.6) cannot be used to determine the shearing stresses, since this equation was derived for a member possessing a vertical plane of symmetry (see Sec. 6.4). Actually, the member will be observed to *bend and twist* under the applied load (Fig. 6.40), and the resulting distribution of shearing stresses will be quite different from that given by Eq. (6.6).

Is it possible to apply the vertical load **P** so that the channel member of Fig. 6.40 will *bend without twisting?* If so, where should the load **P** be applied? If the member bends without twisting, the shearing stress at any point of a given cross section can be obtained from Eq. (6.6), where Q is the first moment of the shaded area with respect to the neutral axis (Fig. 6.41*a*) and the distribution of stresses is as shown in Fig. 6.41*b* with $\tau = 0$ at both A and E. The shearing force exerted on a small element of cross-sectional area $dA = t\,ds$ is $dF = \tau\,dA = \tau t\,ds$ or $dF = q\,ds$ (Fig. 6.42*a*), where q is the shear flow $q = \tau t = VQ/I$. The resultant of the shearing

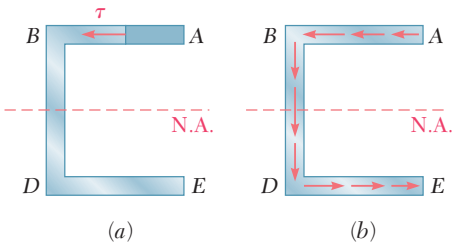


Fig. 6.41 Shearing stress and shear flow as a result of unsymmetric loading. (*a*) Shearing stress. (*b*) Shear flow *q*.

forces exerted on the elements of the upper flange *AB* of the channel is a horizontal force **F** (Fig. 6.42*b*) of magnitude

$$F = \int_A^B q\,ds \tag{6.17}$$

Because of the symmetry of the channel section about its neutral axis, the resultant of the shearing forces exerted on the lower flange *DE* is a force **F**′ of the same magnitude as **F** but of opposite sense. The resultant of the shearing forces exerted on the web *BD* must be equal to the vertical shear **V** in the section:

$$V = \int_B^D q\,ds \tag{6.18}$$

The forces **F** and **F**′ form a couple of moment *Fh*, where *h* is the distance between the center lines of the flanges *AB* and *DE* (Fig. 6.43*a*). This couple can be eliminated if the vertical shear **V** is moved to the left through a distance *e* so the moment of **V** about *B* is equal to *Fh* (Fig. 6.43*b*). Thus, $Ve = Fh$ or

$$e = \frac{Fh}{V} \tag{6.19}$$

When the force **P** is applied at a distance *e* to the left of the center line of the web *BD*, the member bends in a vertical plane without twisting (Fig. 6.44).

The point *O* where the line of action of **P** intersects the axis of symmetry of the end section is the *shear center* of that section. In the case of an oblique load **P** (Fig. 6.45*a*), the member will also be free of twist if the load **P** is applied at the shear center of the section. The load **P** then can be resolved into two components $\mathbf{P}_z$ and $\mathbf{P}_y$ (Fig. 6.45*b*) corresponding to the load conditions of Figs. 6.37 and 6.44, neither of which causes the member to twist.

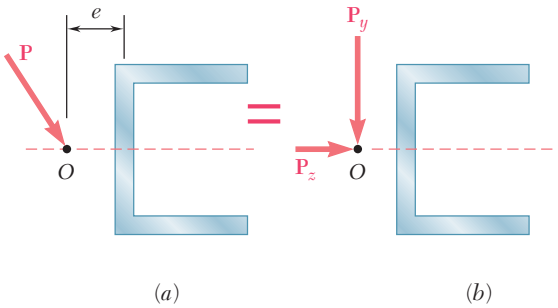


Fig. 6.45 (*a*) Oblique load applied at shear center will not cause twist, since (*b*) it can be resolved into components that do not cause twist.

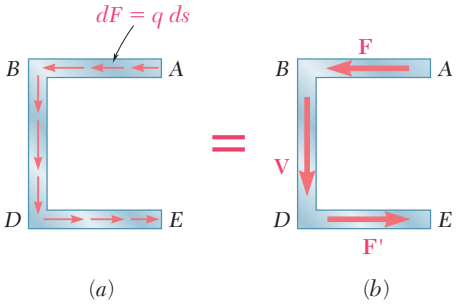
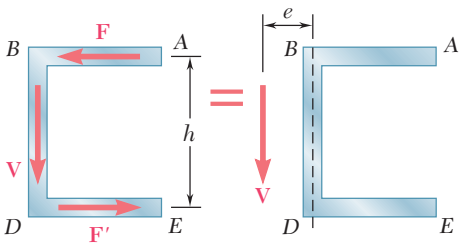


Fig. 6.42 Shear flow in each element results in a vertical shear and couple. **(***a***)** Shear flow *q*. **(***b***)** Resultant forces on elements.



(*a*) Resultant forces on elements (*b*) Placement of **V** to eliminate twisting

Fig. 6.43 Resultant force-couple for bending without twisting, and relocation of **V** to create same effect.

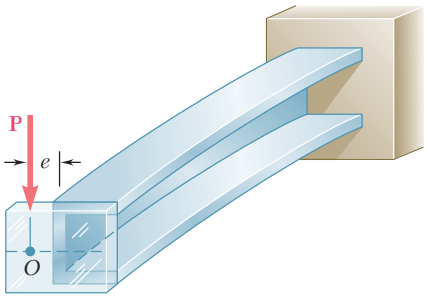


Fig. 6.44 Placement of load to eliminate twisting through the use of an attached bracket.

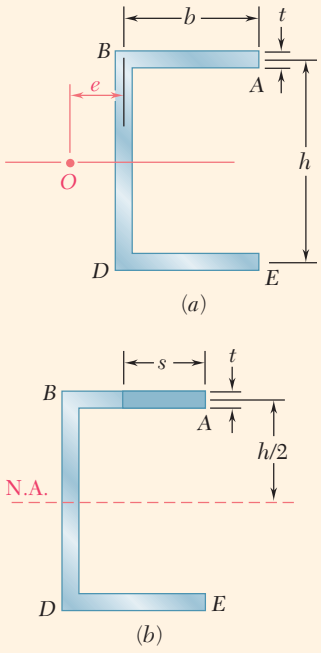


Fig. 6.46 (*a*) Channel section. (*b*) Flange segment used for calculation of shear flow.

Concept Application 6.5

Determine the shear center O of a channel section of uniform thickness (Fig. 6.46*a*), knowing that $b = 4$ in., $h = 6$ in., and $t = 0.15$ in.

Assuming that the member does not twist, determine the shear flow q in flange AB at a distance s from A (Fig. 6.46*b*). Recalling Eq. (6.5) and observing that the first moment Q of the shaded area with respect to the neutral axis is $Q = (st)(h/2)$,

$$q = \frac{VQ}{I} = \frac{Vsth}{2I} \tag{6.20}$$

where V is the vertical shear and I is the moment of inertia of the section with respect to the neutral axis.

Recalling Eq. (6.17), the magnitude of the shearing force **F** exerted on flange AB is found by integrating the shear flow q from A to B

$$F = \int_0^b q\,ds = \int_0^b \frac{Vsth}{2I}\,ds = \frac{Vth}{2I}\int_0^b s\,ds$$

$$F = \frac{Vthb^2}{4I} \tag{6.21}$$

The distance e from the center line of the web BD to the shear center O can be obtained from Eq. (6.19):

$$e = \frac{Fh}{V} = \frac{Vthb^2}{4I}\frac{h}{V} = \frac{th^2b^2}{4I} \tag{6.22}$$

The moment of inertia I of the channel section can be expressed as

$$I = I_{\text{web}} + 2I_{\text{flange}}$$
$$= \frac{1}{12}th^3 + 2\left[\frac{1}{12}bt^3 + bt\left(\frac{h}{2}\right)^2\right]$$

Neglecting the term containing t^3, which is very small, gives

$$I = \tfrac{1}{12}th^3 + \tfrac{1}{2}tbh^2 = \tfrac{1}{12}th^2(6b + h) \tag{6.23}$$

Substituting this expression into Eq. (6.22) gives

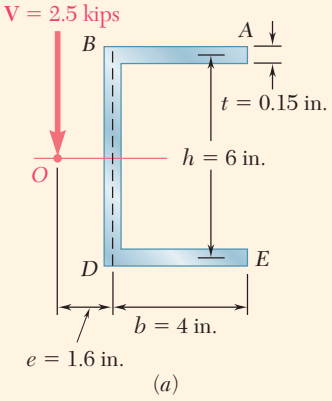
$$e = \frac{3b^2}{6b + h} = \frac{b}{2 + \dfrac{h}{3b}} \tag{6.24}$$

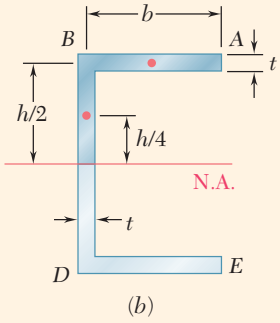
Note that the distance e does not depend upon t and can vary from 0 to $b/2$, depending upon the value of the ratio $h/3b$. For the given channel section,

$$\frac{h}{3b} = \frac{6\text{ in.}}{3(4\text{ in.})} = 0.5$$

and

$$e = \frac{4\text{ in.}}{2 + 0.5} = 1.6\text{ in.}$$





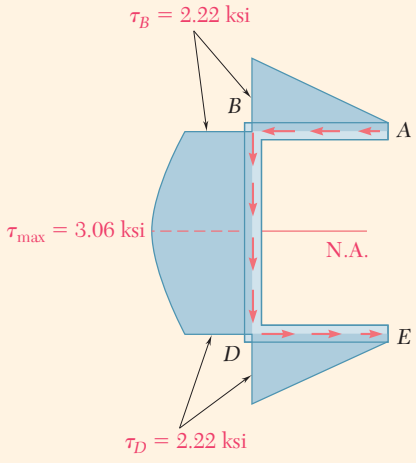


Fig. 6.47 (*a*) Channel section loaded at shear center. (*b*) Section used to find the maximum shearing stress. (*c*) Shearing stress distribution.

Concept Application 6.6

For the channel section of Concept Application 6.5, determine the distribution of the shearing stresses caused by a 2.5-kip vertical shear **V** applied at the shear center *O* (Fig. 6.47*a*).

Shearing Stresses in Flanges. Since **V** is applied at the shear center, there is no torsion, and the stresses in flange *AB* are obtained from Eq. (6.20), so

$$\tau = \frac{q}{t} = \frac{VQ}{It} = \frac{Vh}{2I}s \tag{6.25}$$

which shows that the stress distribution in flange *AB* is linear. Letting $s = b$ and substituting for *I* from Eq. (6.23), we obtain the value of the shearing stress at *B:*

$$\tau_B = \frac{Vhb}{2(\frac{1}{12}th^2)(6b + h)} = \frac{6Vb}{th(6b + h)} \tag{6.26}$$

Letting $V = 2.5$ kips and using the given dimensions,

$$\tau_B = \frac{6(2.5 \text{ kips})(4 \text{ in.})}{(0.15 \text{ in.})(6 \text{ in.})(6 \times 4 \text{ in.} + 6 \text{ in.})}$$
$$= 2.22 \text{ ksi}$$

Shearing Stresses in Web. The distribution of the shearing stresses in the web *BD* is parabolic, as in the case of a W-beam, and the maximum stress occurs at the neutral axis. Computing the first moment of the upper half of the cross section with respect to the neutral axis (Fig. 6.47*b*),

$$Q = bt(\tfrac{1}{2}h) + \tfrac{1}{2}ht(\tfrac{1}{4}h) = \tfrac{1}{8}ht(4b + h) \tag{6.27}$$

Substituting for *I* and *Q* from Eqs. (6.23) and (6.27), respectively, into the expression for the shearing stress,

$$\tau_{\max} = \frac{VQ}{It} = \frac{V(\frac{1}{8}ht)(4b + h)}{\frac{1}{12}th^2(6b + h)t} = \frac{3V(4b + h)}{2th(6b + h)}$$

or with the given data,

$$\tau_{\max} = \frac{3(2.5 \text{ kips})(4 \times 4 \text{ in.} + 6 \text{ in.})}{2(0.15 \text{ in.})(6 \text{ in.})(6 \times 4 \text{ in.} + 6 \text{ in.})}$$
$$= 3.06 \text{ ksi}$$

Distribution of Stresses Over the Section. The distribution of the shearing stresses over the entire channel section has been plotted in Fig. 6.47*c*.

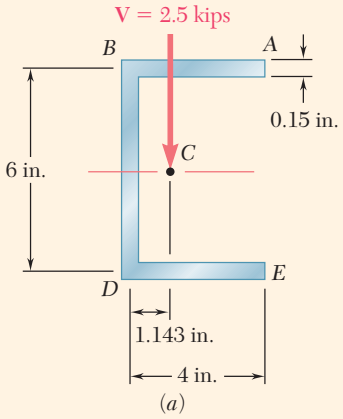


Fig. 6.48 (*a*) Channel section loaded at centroid (not shear center).

Concept Application 6.7

For the channel section of Concept Application 6.5, and neglecting stress concentrations, determine the maximum shearing stress caused by a 2.5-kip vertical shear **V** applied at the centroid *C* of the section, which is located 1.143 in. to the right of the center line of the web *BD* (Fig. 6.48*a*).

Equivalent Force-Couple System at Shear Center. The shear center *O* of the cross section was determined in Concept Application 6.5 and found to be at a distance $e = 1.6$ in. to the left of the center line of the web *BD*. We replace the shear **V** (Fig. 6.48*b*) by an equivalent force-couple system at the shear center *O* (Fig. 6.48*c*). This system consists of a 2.5-kip force **V** and of a torque **T** of magnitude

$$T = V(OC) = (2.5 \text{ kips})(1.6 \text{ in.} + 1.143 \text{ in.})$$
$$= 6.86 \text{ kip·in.}$$

Stresses Due to Bending. The 2.5-kip force **V** causes the member to bend, and the corresponding distribution of shearing stresses in the section (Fig. 6.48*d*) was determined in Concept Application 6.6. Recall that the maximum value of the stress due to this force was found to be

$$(\tau_{\max})_{\text{bending}} = 3.06 \text{ ksi}$$

Stresses Due to Twisting. The torque **T** causes the member to twist, and the corresponding distribution of stresses is shown in Fig. 6.48*e*. Recall from Chap. 3 that the membrane analogy shows that in a thin-walled member of uniform thickness, the stress caused by a torque **T** is maximum along the edge of the section. Using Eqs. (3.42) and (3.40) with

$$a = 4 \text{ in.} + 6 \text{ in.} + 4 \text{ in.} = 14 \text{ in.}$$
$$b = t = 0.15 \text{ in.} \qquad b/a = 0.0107$$

So,

$$c_1 = \tfrac{1}{3}(1 - 0.630b/a) = \tfrac{1}{3}(1 - 0.630 \times 0.0107) = 0.331$$

$$(\tau_{\max})_{\text{twisting}} = \frac{T}{c_1 ab^2} = \frac{6.86 \text{ kip·in.}}{(0.331)(14 \text{ in.})(0.15 \text{ in.})^2} = 65.8 \text{ ksi}$$

Combined Stresses. The maximum shearing stress due to the combined bending and twisting occurs at the neutral axis on the inside surface of the web and is

$$\tau_{\max} = 3.06 \text{ ksi} + 65.8 \text{ ksi} = 68.9 \text{ ksi}$$

As a practical observation, this exceeds the shearing stress at yield for commonly available steels. This analysis demonstrates the potentially large effect that torsion can have on the shearing stresses in channels and similar structural shapes.

(continued)

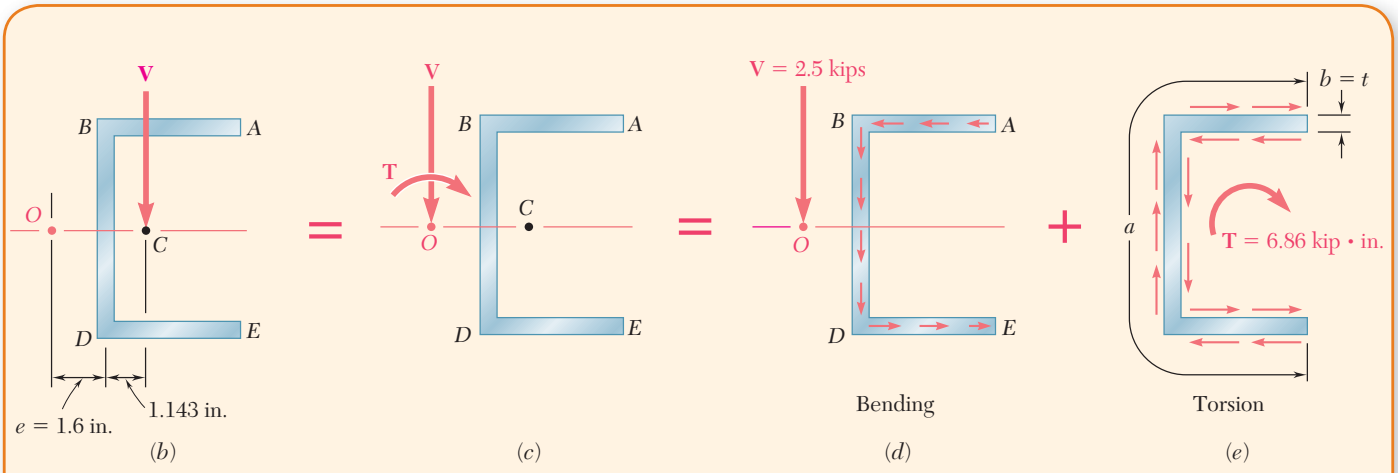


Fig. 6.48 (*cont.*) (*b*) Load at the centroid (*c*) is equivalent to a force-torque at the shear center, which is the superposition of shearing stress due to (*d*) bending and (*e*) torsion.

We now consider thin-walled members possessing no plane of symmetry. Consider an angle shape subjected to a vertical load **P.** If the member is oriented in such a way that the load **P** is perpendicular to one of the principal centroidal axes *Cz* of the cross section, the couple vector **M** representing the bending moment in a given section will be directed along *Cz* (Fig. 6.49), and the neutral axis will coincide with that axis (see Sec. 4.8). Equation (4.16) is applicable and can be used to compute the normal stresses in the section. We will now determine where the load **P** should be applied so that Eq. (6.6) can be used to determine the shearing stresses in the section, i.e., so that the member is to *bend without twisting*.

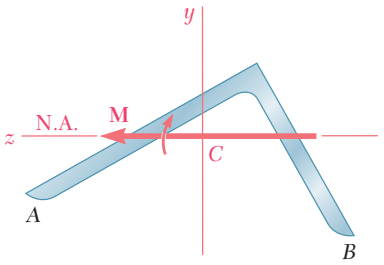
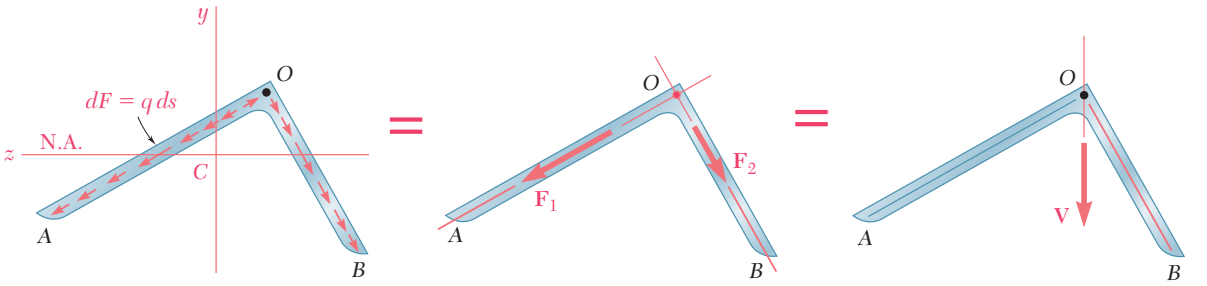


Fig. 6.49 Beam without plane of symmetry subject to bending moment.

Assume that the shearing stresses in the section are defined by Eq. (6.6). As in the channel member, the elementary shearing forces exerted on the section can be expressed as $dF = q\,ds$, with $q = VQ/I$, where Q represents a first moment with respect to the neutral axis (Fig. 6.50*a*). The resultant of the shearing forces exerted on portion OA of the cross section is force $\mathbf{F}_1$ directed along OA, and the resultant of the shearing forces exerted on portion OB is a force $\mathbf{F}_2$ along OB (Fig. 6.50*b*). Since both $\mathbf{F}_1$ and $\mathbf{F}_2$ pass through point O at the corner of



(*a*) Elementary shearing forces (*b*) Resultant forces on elements (*c*) Placement of **V** to eliminate twisting

Fig. 6.50 Determination of shear center, *O*, in an angle shape.

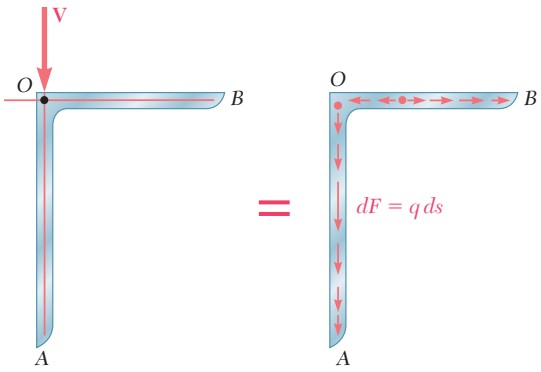


Fig. 6.51 Vertically loaded angle section and resulting shear flow.

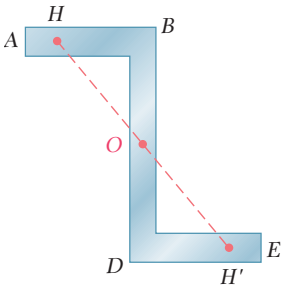


Fig. 6.52 *Z* section has centroid and shear center coinciding.

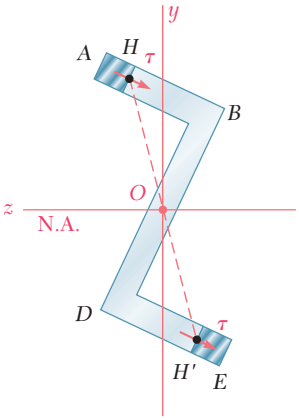


Fig. 6.53 Neutral axis location for load applied in a plane perpendicular to principal axis *z*.

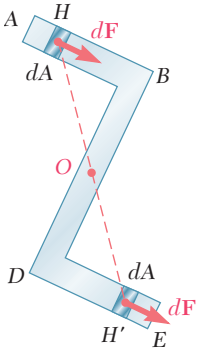


Fig. 6.54 For member bending without twisting, equal and opposite moments about *O* occur for any pair of symmetric elements.

the angle, their own resultant, which is the shear **V** in the section, must also pass through *O* (Fig. 6.50*c*). The member will not be twisted if the line of action of the load **P** passes through the corner *O* of the section in which it is applied.

The same reasoning can be applied when load **P** is perpendicular to the other principal centroidal axis *Cy* of the angle section. Since any load **P** applied at the corner *O* of a cross section also can be resolved into components perpendicular to the principal axes, the member will not be twisted if each load is applied at the corner *O* of a cross section. Thus, *O* is the shear center of the section.

Angle shapes with one vertical and one horizontal leg are encountered in many structures. Such members will not be twisted if vertical loads are applied along the center line of their vertical leg. Note from Fig. 6.51 that the resultant of the elementary shearing forces exerted on the vertical portion *OA* of a given section will be equal to the shear **V,** while the resultant of the shearing forces on the horizontal portion *OB* will be zero:

$$\int_O^A q\,ds = V \qquad \int_O^B q\,ds = 0$$

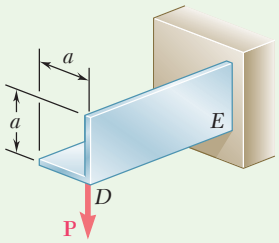
This does *not* mean that there will be no shearing stress in the horizontal leg of the member. By resolving the shear **V** into components perpendicular to the principal centroidal axes of the section and computing the shearing stress at every point, τ is zero at only one point between *O* and *B* (see Sample Prob. 6.6).

Another type of thin-walled member frequently encountered in practice is the Z shape. While the cross section of a Z shape does not possess any axis of symmetry, it does possess a *center of symmetry O* (Fig. 6.52). This means that any point *H* of the cross section corresponds another point *H′*, so that the segment of straight line *HH′* is bisected by *O*. Clearly, the center of symmetry *O* coincides with the centroid of the cross section. As we will now demonstrate, point *O* is also the shear center of the cross section.

As for an angle shape, we assume that the loads are applied in a plane perpendicular to one of the principal axes of the section, so that this axis is also the neutral axis of the section (Fig. 6.53). We further assume that the shearing stresses in the section are defined by Eq. (6.6), where the member is bent without being twisted. Denoting by *Q* the first moment about the neutral axis of portion *AH* of the cross section and by *Q′* the first moment of portion *EH′*, we note that $Q' = -Q$. Thus, the shearing stresses at *H* and *H′* have the same magnitude and the same direction, and the shearing forces exerted on small elements of area *dA* located respectively at *H* and *H′* are equal forces that have equal and opposite moments about *O* (Fig. 6.54). Since this is true for any pair of symmetric elements, the resultant of the shearing forces exerted on the section has a zero moment about *O*. This means that the shear **V** in the section is directed along a line that passes through *O*. Since this analysis can be repeated when the loads are applied in a plane perpendicular to the other principal axis, point *O* is the shear center of the section.

Sample Problem 6.6

Determine the distribution of shearing stresses in the thin-walled angle shape DE of uniform thickness t for the loading shown.



STRATEGY: Locate the centroid of the cross section and determine the two principal moments of inertia. Resolve the load **P** into components parallel to the principal axes, equal to the shear forces. The two sets of shearing stresses are then calculated at locations along the two angle legs. These are then superposed to obtain the shearing stress distribution.

MODELING and ANALYSIS:

Shear Center. We recall from Sec. 6.6 that the shear center of the cross section of a thin-walled angle shape is located at its corner. Since the load **P** is applied at D, it causes bending but no twisting of the shape.

Principal Axes. We locate the centroid C of a given cross section AOB (Fig. 1). Since the y' axis is an axis of symmetry, the y' and z' axes are the principal centroidal axes of the section. We recall that for the parallelogram shown (Fig. 2), $I_{nn} = \frac{1}{12}bh^3$ and $I_{mm} = \frac{1}{3}bh^3$. Considering each leg of the section as a parallelogram, we now determine the centroidal moments of inertia $I_{y'}$ and $I_{z'}$:

$$I_{y'} = 2\left[\frac{1}{3}\left(\frac{t}{\cos 45^\circ}\right)(a\cos 45^\circ)^3\right] = \frac{1}{3}ta^3$$

$$I_{z'} = 2\left[\frac{1}{12}\left(\frac{t}{\cos 45^\circ}\right)(a\cos 45^\circ)^3\right] = \frac{1}{12}ta^3$$

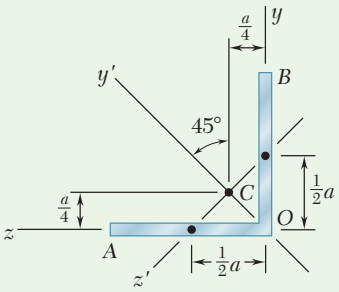


Fig. 1 Angle section with principal axes y' and z'.

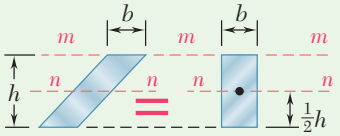


Fig. 2 Parallelogram and equivalent rectangle for determining moments of inertia.

(continued)

Superposition. The shear **V** in the section is equal to the load **P**. As shown in Fig. 3, we resolve it into components parallel to the principal axes.

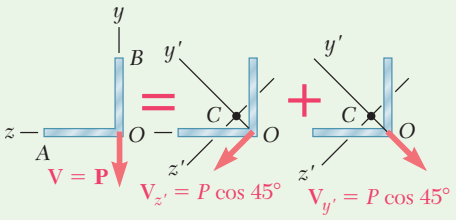


Fig. 3 Resolution of the load into components parallel to principal axes.

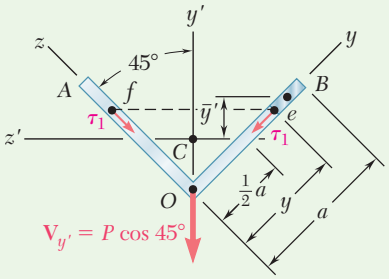


Fig. 4 Load component in plane of symmetry.

Shearing Stresses Due to $V_{y'}$. Using Fig. 4, we determine the shearing stress at point e of coordinate y:

$$\bar{y}' = \tfrac{1}{2}(a + y)\cos 45° - \tfrac{1}{2}a\cos 45° = \tfrac{1}{2}y\cos 45°$$

$$Q = t(a - y)\bar{y}' = \tfrac{1}{2}t(a - y)y\cos 45°$$

$$\tau_1 = \frac{V_{y'}Q}{I_{z'}t} = \frac{(P\cos 45°)[\frac{1}{2}t(a - y)y\cos 45°]}{(\frac{1}{12}ta^3)t} = \frac{3P(a - y)y}{ta^3}$$

The shearing stress at point f is represented by a similar function of z.

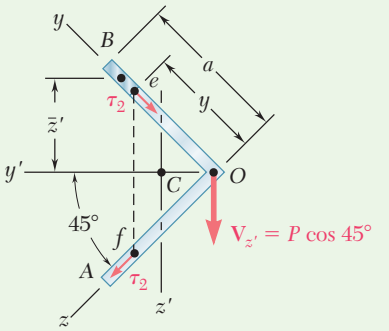


Fig. 5 Load component perpendicular to plane of symmetry.

Shearing Stresses Due to $V_{z'}$. Using Fig. 5, reconsider point e:

$$\bar{z}' = \tfrac{1}{2}(a + y)\cos 45°$$

$$Q = (a - y)t\bar{z}' = \tfrac{1}{2}(a^2 - y^2)t\cos 45°$$

$$\tau_2 = \frac{V_{z'}Q}{I_{y'}t} = \frac{(P\cos 45°)[\frac{1}{2}(a^2 - y^2)t\cos 45°]}{(\frac{1}{3}ta^3)t} = \frac{3P(a^2 - y^2)}{4ta^3}$$

The shearing stress at point f is represented by a similar function of z.

Combined Stresses. ***Along the Vertical Leg.*** The shearing stress at point e is

$$\tau_e = \tau_2 + \tau_1 = \frac{3P(a^2 - y^2)}{4ta^3} + \frac{3P(a - y)y}{ta^3} = \frac{3P(a - y)}{4ta^3}[(a + y) + 4y]$$

$$\tau_e = \frac{3P(a - y)(a + 5y)}{4ta^3}$$

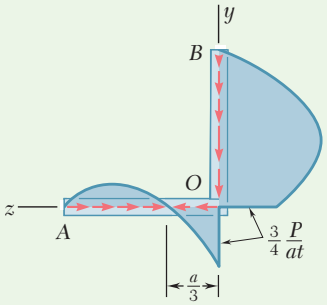


Fig. 6 Shearing stress distribution.

Along the Horizontal Leg. The shearing stress at point f is

$$\tau_f = \tau_2 - \tau_1 = \frac{3P(a^2 - z^2)}{4ta^3} - \frac{3P(a - z)z}{ta^3} = \frac{3P(a - z)}{4ta^3}[(a + z) - 4z]$$

$$\tau_f = \frac{3P(a - z)(a - 3z)}{4ta^3}$$

REFLECT and THINK: The combined stresses are plotted in Fig. 6.

Problems

6.61 through 6.64 Determine the location of the shear center O of a thin-walled beam of uniform thickness having the cross section shown.

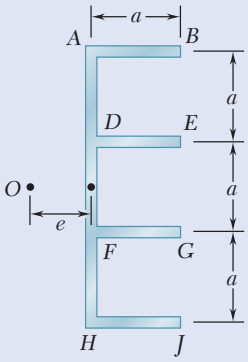


Fig. P6.61

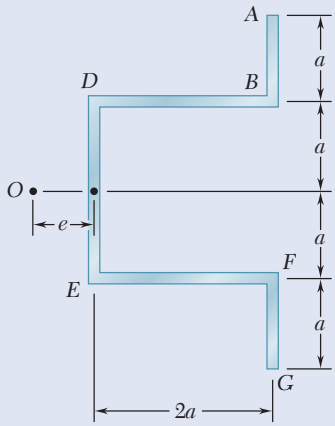


Fig. P6.62

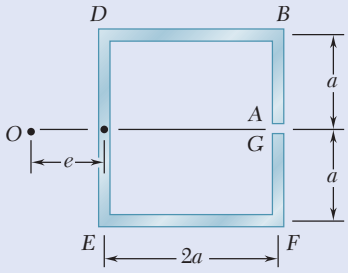


Fig. P6.63

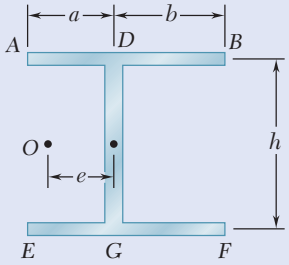


Fig. P6.64

6.65 through 6.68 An extruded beam has the cross section shown. Determine (*a*) the location of the shear center O, (*b*) the distribution of the shearing stresses caused by the vertical shearing force **V** shown applied at O.

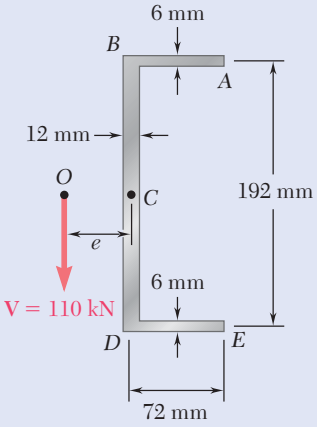


Fig. P6.65

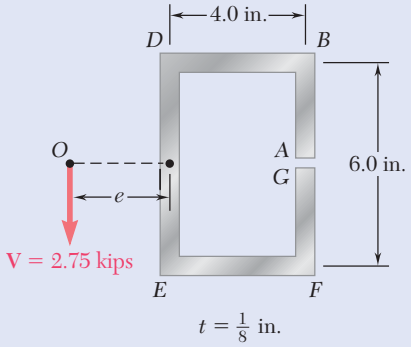


Fig. *P6.66*

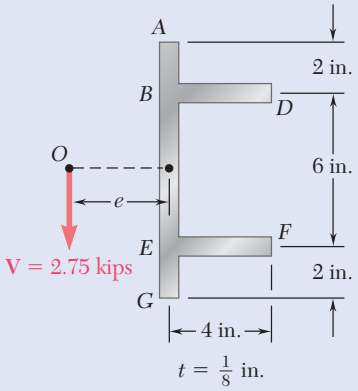


Fig. *P6.67*

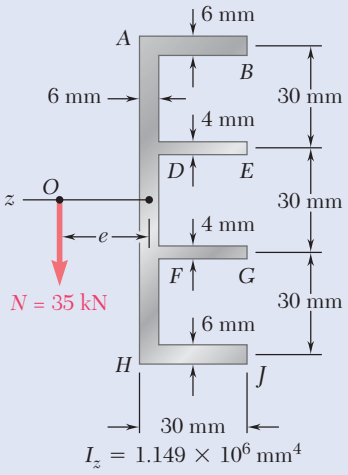


Fig. P6.68

6.69 through 6.74 Determine the location of the shear center O of a thin-walled beam of uniform thickness having the cross section shown.

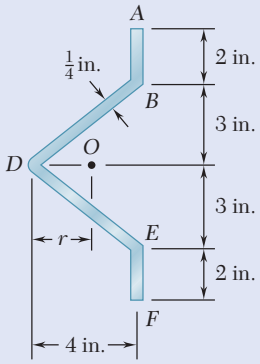


Fig. P6.69

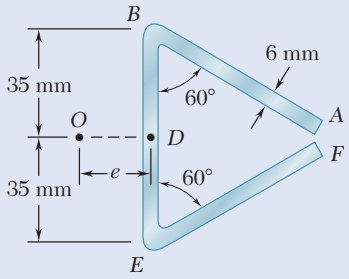


Fig. P6.70

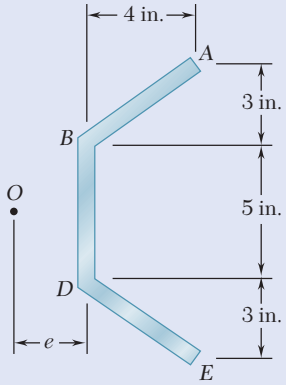


Fig. P6.71

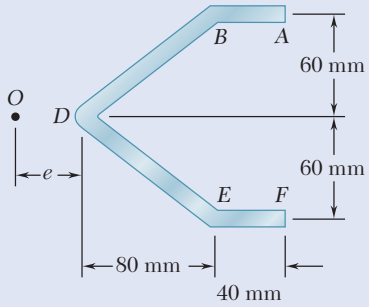


Fig. P6.72

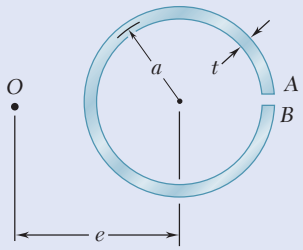


Fig. *P6.73*

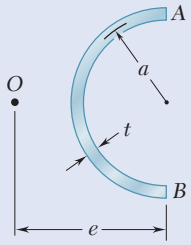


Fig. *P6.74*

6.75 and 6.76 A thin-walled beam has the cross section shown. Determine the location of the shear center O of the cross section.

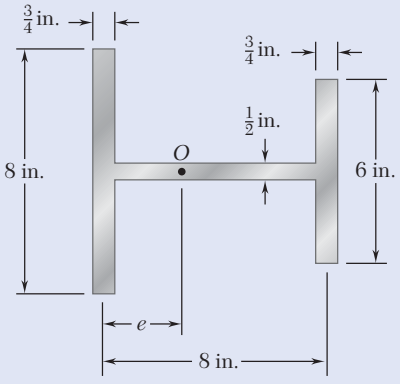


Fig. P6.75

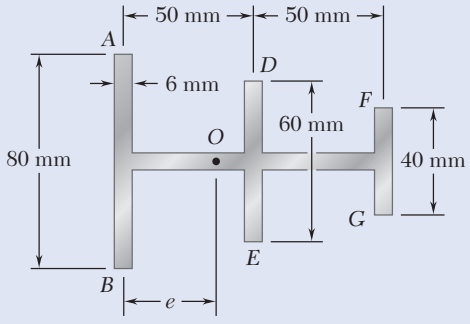


Fig. P6.76

6.77 and 6.78 A thin-walled beam of uniform thickness has the cross section shown. Determine the dimension b for which the shear center O of the cross section is located at the point indicated.

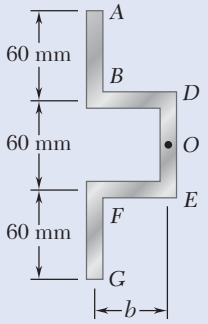


Fig. P6.77

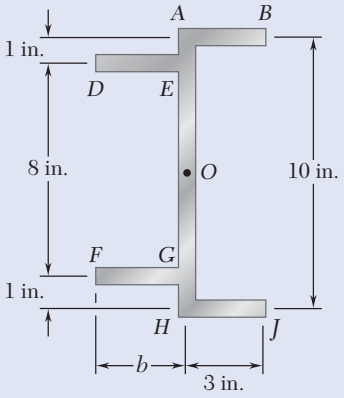


Fig. P6.78

6.79 For the angle shape and loading of Sample Prob. 6.6, check that $\int q\,dz = 0$ along the horizontal leg of the angle and $\int q\,dy = P$ along its vertical leg.

6.80 For the angle shape and loading of Sample Prob. 6.6, (a) determine the points where the shearing stress is maximum and the corresponding values of the stress, (b) verify that the points obtained are located on the neutral axis corresponding to the given loading.

***6.81** Determine the distribution of the shearing stresses along line $D'B'$ in the horizontal leg of the angle shape for the loading shown. The x' and y' axes are the principal centroidal axes of the cross section.

***6.82** For the angle shape and loading of Prob. 6.81, determine the distribution of the shearing stresses along line $D'A'$ in the vertical leg.

***6.83** A steel plate, 160 mm wide and 8 mm thick, is bent to form the channel shown. Knowing that the vertical load **P** acts at a point in the midplane of the web of the channel, determine (a) the torque **T** that would cause the channel to twist in the same way that it does under the load **P**, (b) the maximum shearing stress in the channel caused by the load **P**.

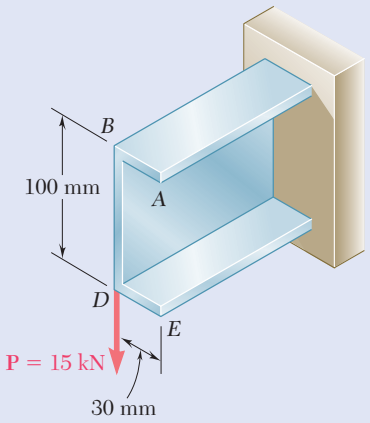
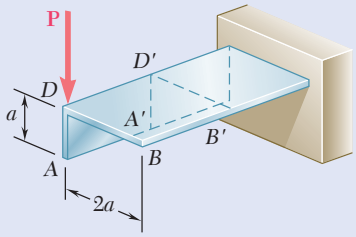


Fig. P6.83

***6.84** Solve Prob. 6.83, assuming that a 6-mm-thick plate is bent to form the channel shown.



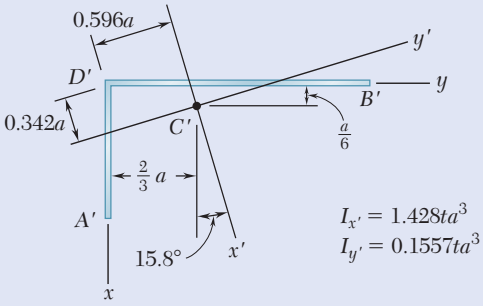


Fig. P6.81

***6.85** The cantilever beam AB, consisting of half of a thin-walled pipe of 1.25-in. mean radius and $\frac{3}{8}$-in. wall thickness, is subjected to a 500-lb vertical load. Knowing that the line of action of the load passes through the centroid C of the cross section of the beam, determine (*a*) the equivalent force-couple system at the shear center of the cross section, (*b*) the maximum shearing stress in the beam. (*Hint*: The shear center O of this cross section was shown in Prob. 6.74 to be located twice as far from its vertical diameter as its centroid C.)

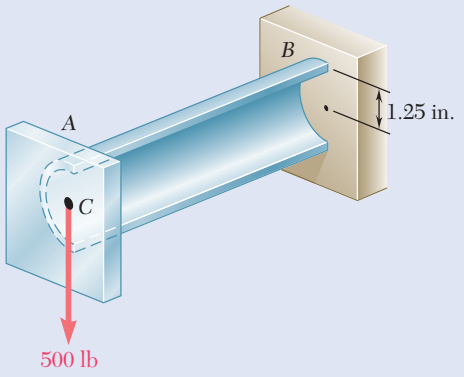


Fig. *P6.85*

***6.86** Solve Prob. 6.85, assuming that the thickness of the beam is reduced to $\frac{1}{4}$ in.

***6.87** The cantilever beam shown consists of a Z shape of $\frac{1}{4}$-in. thickness. For the given loading, determine the distribution of the shearing stresses along line $A'B'$ in the upper horizontal leg of the Z shape. The x' and y' axes are the principal centroidal axes of the cross section, and the corresponding moments of inertia are $I_{x'} = 166.3 \text{ in}^4$ and $I_{y'} = 13.61 \text{ in}^4$.

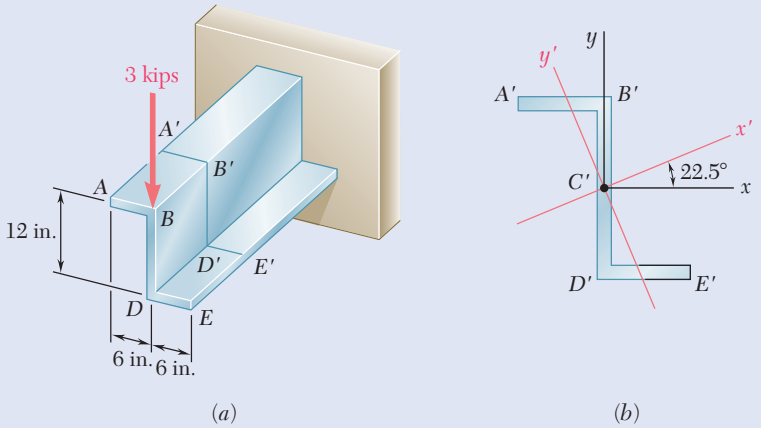


Fig. P6.87

***6.88** For the cantilever beam and loading of Prob. 6.87, determine the distribution of the shearing stresses along line $B'D'$ in the vertical web of the Z shape.

Review and Summary

Stresses on a Beam Element

A small element located in the vertical plane of symmetry of a beam under a transverse loading was considered (Fig. 6.55), and it was found that normal stresses σ_x and shearing stresses τ_{xy} are exerted on the transverse faces of that element, while shearing stresses τ_{yx}, equal in magnitude to τ_{xy}, are exerted on its horizontal faces.

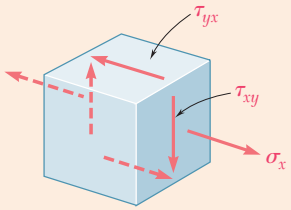


Fig. 6.55 Stress element from section of transversely loaded beam.

Horizontal Shear

For a prismatic beam AB with a vertical plane of symmetry supporting various concentrated and distributed loads (Fig. 6.56), at a distance x from end A we can detach an element $CDD'C'$ of length Δx that extends

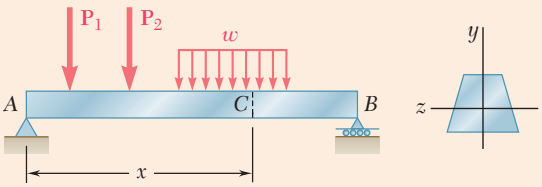


Fig. 6.56 Transversely loaded beam with vertical plane of symmetry.

across the width of the beam from the upper surface of the beam to a horizontal plane located at a distance y_1 from the neutral axis (Fig. 6.57). The magnitude of the shearing force $\Delta\mathbf{H}$ exerted on the lower face of the beam element is

$$\Delta H = \frac{VQ}{I}\Delta x \tag{6.4}$$

where V = vertical shear in the given transverse section
Q = first moment with respect to the neutral axis of the shaded portion $\mathcal{A}$ of the section
I = centroidal moment of inertia of the entire cross-sectional area

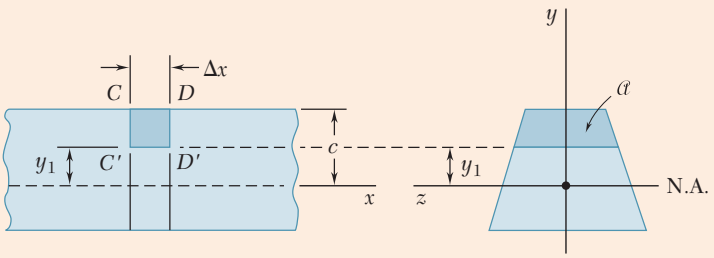


Fig. 6.57 Short segment of beam with stress element $CDD'C'$.

Shear Flow

The *horizontal shear per unit length* or *shear flow*, denoted by the letter q, is obtained by dividing both members of Eq. (6.4) by Δx:

$$q = \frac{\Delta H}{\Delta x} = \frac{VQ}{I} \tag{6.5}$$

Shearing Stresses in a Beam

Dividing both members of Eq. (6.4) by the area ΔA of the horizontal face of the element and observing that $\Delta A = t\,\Delta x$, where t is the width of the element at the cut, the *average shearing stress* on the horizontal face of the element is

$$\tau_{\text{ave}} = \frac{VQ}{It} \tag{6.6}$$

Since the shearing stresses τ_{xy} and τ_{yx} are exerted on a transverse and a horizontal plane through D' and are equal, Eq. (6.6) also represents the average value of τ_{xy} along the line $D'_1D'_2$ (Fig. 6.58).

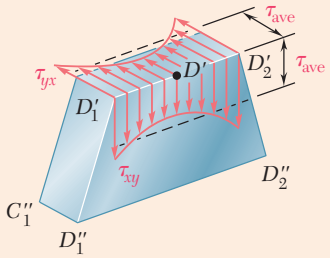


Fig. 6.58 Shearing stress distribution across horizontal and transverse planes.

Shearing Stresses in a Beam of Rectangular Cross Section

The distribution of shearing stresses in a beam of rectangular cross section was found to be parabolic, and the maximum stress, which occurs at the center of the section, is

$$\tau_{\text{max}} = \frac{3}{2}\frac{\text{V}}{\text{A}} \tag{6.10}$$

where A is the area of the rectangular section. For wide-flange beams, a good approximation of the maximum shearing stress is obtained by dividing the shear V by the cross-sectional area of the web.

Longitudinal Shear on Curved Surface

Equations (6.4) and (6.5) can be used to determine the longitudinal shearing force $\Delta\mathbf{H}$ and the shear flow q exerted on a beam element if the element is bounded by an arbitrary curved surface instead of a horizontal plane (Fig. 6.59).

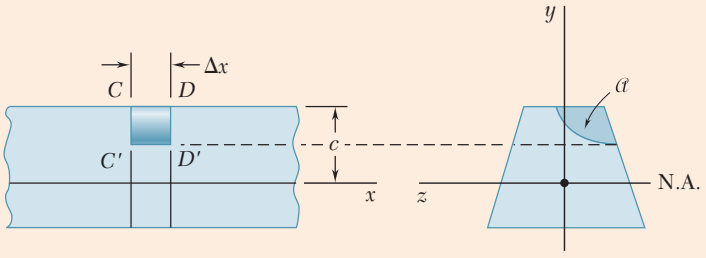


Fig. 6.59 Segment of beam showing element CDD′C′ of length Δx.

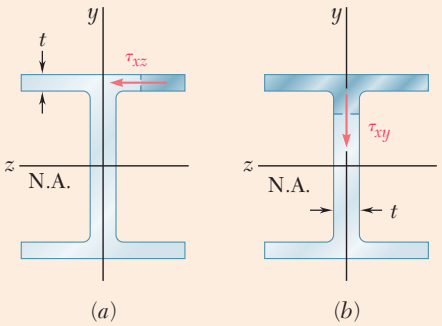


Fig. 6.60 Wide-flange beam sections showing shearing stress (*a*) in flange, (*b*) in web. The shaded area is that used for calculating the first moment of area.

Shearing Stresses in Thin-Walled Members

We found that we could extend the use of Eq. (6.6) to determine the average shearing stress in both the webs and flanges of thin-walled members, such as wide-flange beams and box beams (Fig. 6.60).

Plastic Deformations

Once plastic deformation has been initiated, additional loading causes plastic zones to penetrate into the elastic core of a beam. Because shearing stresses can occur only in the elastic core of a beam, both an increase in loading and the resulting decrease in the size of the elastic core contribute to an increase in shearing stresses.

Unsymmetric Loading and Shear Center

Prismatic members that are *not* loaded in their plane of symmetry will have both bending and twisting. Twisting is prevented if the load is applied at the point *O* of the cross section. This point is known as the *shear center*, where the loads may be applied so the member only bends (Fig. 6.61). If the loads are applied at that point,

$$\sigma_x = -\frac{My}{I} \qquad \tau_{\text{ave}} = \frac{VQ}{It} \qquad \textbf{(4.16, 6.6)}$$

The principle of superposition can be used to find the stresses in unsymmetric thin-walled members such as channels, angles, and extruded beams.

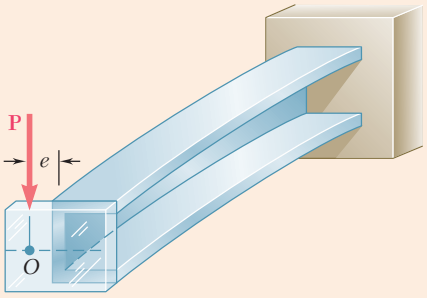


Fig. 6.61 Placement of load to eliminate twisting through the use of an attached bracket.

Review Problems

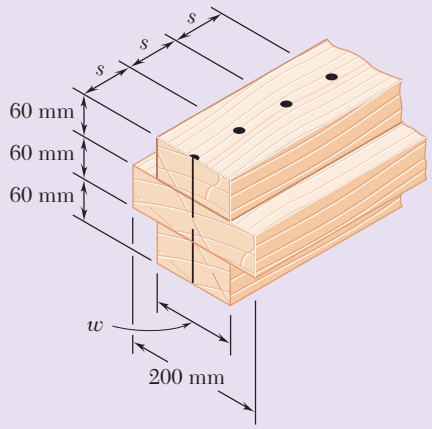


Fig. P6.89

6.89 Three boards are nailed together to form the beam shown, which is subjected to a vertical shear. Knowing that the spacing between the nails is $s = 75$ mm and that the allowable shearing force in each nail is 400 N, determine the allowable shear when $w = 120$ mm.

6.90 For the beam and loading shown, consider section n–n and determine (a) the largest shearing stress in that section, (b) the shearing stress at point a.

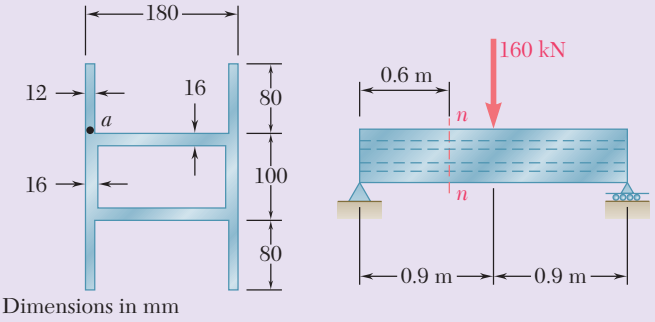


Fig. P6.90

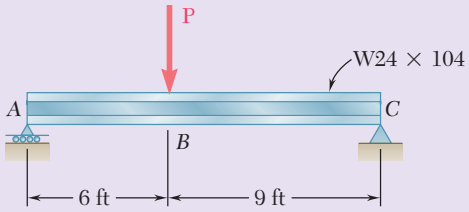
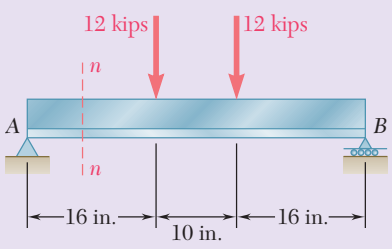


Fig. P6.91

6.91 For the wide-flange beam with the loading shown, determine the largest **P** that can be applied, knowing that the maximum normal stress is 24 ksi and the largest shearing stress, using the approximation $\tau_m = V/A_{\text{web}}$, is 14.5 ksi.

6.92 For the beam and loading shown, consider section n–n and determine the shearing stress at (a) point a, (b) point b.



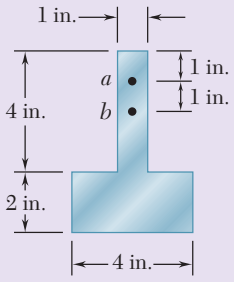


Fig. P6.92

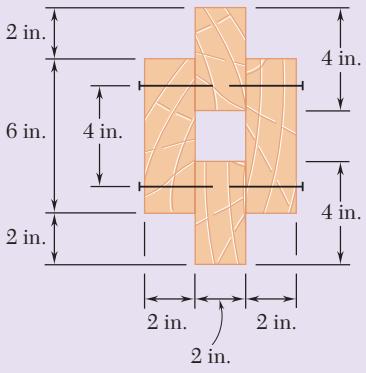


Fig. P6.93

6.93 The built-up timber beam is subjected to a 1500-lb vertical shear. Knowing that the longitudinal spacing of the nails is $s = 2.5$ in. and that each nail is 3.5 in. long, determine the shearing force in each nail.

6.94 Knowing that a given vertical shear **V** causes a maximum shearing stress of 75 MPa in the hat-shaped extrusion shown, determine the corresponding shearing stress at (*a*) point *a*, (*b*) point *b*.

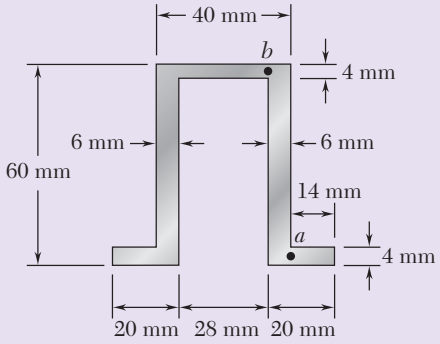


Fig. P6.94

6.95 Three planks are connected as shown by bolts of 14-mm diameter spaced every 150 mm along the longitudinal axis of the beam. For a vertical shear of 10 kN, determine the average shearing stress in the bolts.

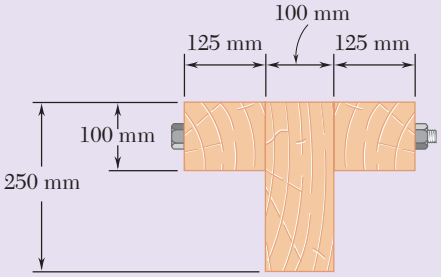


Fig. P6.95

6.96 Three 1 × 18-in. steel plates are bolted to four L6 × 6 × 1 angles to form a beam with the cross section shown. The bolts have a $\frac{7}{8}$-in. diameter and are spaced longitudinally every 5 in. Knowing that the allowable average shearing stress in the bolts is 12 ksi, determine the largest permissible vertical shear in the beam. (*Given:* $I_x = 6123$ in^4.)

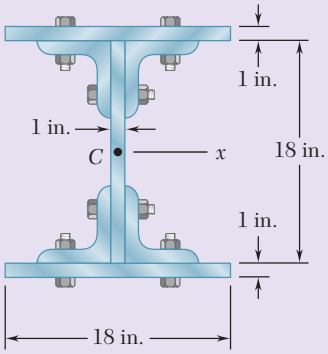


Fig. P6.96

6.97 The composite beam shown is made by welding C200 × 17.1 rolled-steel channels to the flanges of a W250 × 80 wide-flange rolled-steel shape. Knowing that the beam is subjected to a vertical shear of 200 kN, determine (*a*) the horizontal shearing force per meter at each weld, (*b*) the shearing stress at point *a* of the flange of the wide-flange shape.

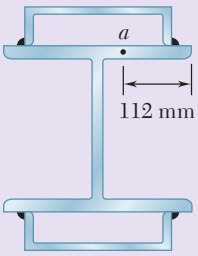


Fig. P6.97

6.98 The design of a beam requires welding four horizontal plates to a vertical 0.5 × 5-in. plate as shown. For a vertical shear **V**, determine the dimension h for which the shear flow through the welded surfaces is maximum.

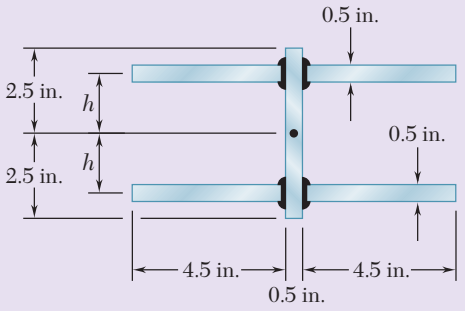


Fig. *P6.98*

6.99 A thin-walled beam of uniform thickness has the cross section shown. Determine the dimension b for which the shear center O of the cross section is located at the point indicated.

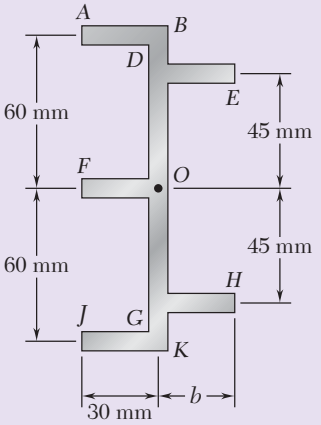


Fig. P6.99

6.100 Determine the location of the shear center O of a thin-walled beam of uniform thickness having the cross section shown.

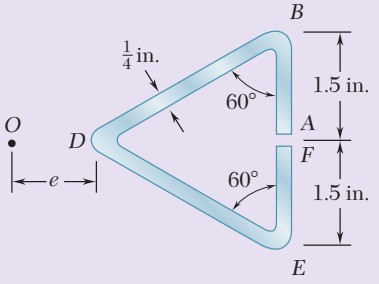


Fig. P6.100

Computer Problems

The following problems are designed to be solved with a computer.

6.C1 A timber beam is to be designed to support a distributed load and up to two concentrated loads as shown. One of the dimensions of its uniform rectangular cross section has been specified, and the other is to be determined so that the maximum normal stress and the maximum shearing stress in the beam will not exceed given allowable values σ_{all} and τ_{all}. Measuring x from end A and using either SI or U.S. customary units, write a computer program to calculate for successive cross sections, from $x = 0$ to $x = L$ and using given increments Δx, the shear, the bending moment, and the smallest value of the unknown dimension that satisfies in that section (1) the allowable normal stress requirement and (2) the allowable shearing stress requirement. Use this program to solve Prob. 5.65, assuming $\sigma_{all} = 12$ MPa and $\tau_{all} = 825$ kPa and using $\Delta x = 0.1$ m.

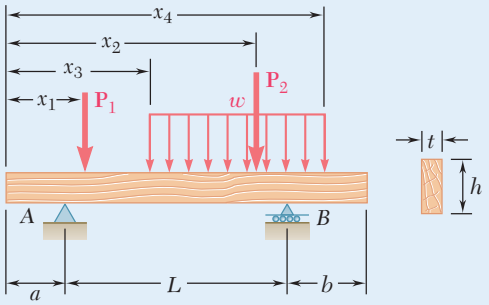


Fig. P6.C1

6.C2 A cantilever timber beam AB of length L and of uniform rectangular section shown supports a concentrated load **P** at its free end and a uniformly distributed load w along its entire length. Write a computer program to determine the length L and the width b of the beam for which both the maximum normal stress and the maximum shearing stress in the beam reach their largest allowable values. Assuming $\sigma_{all} = 1.8$ ksi and $\tau_{all} = 120$ psi, use this program to determine the dimensions L and b when (*a*) $P = 1000$ lb and $w = 0$, (*b*) $P = 0$ and $w = 12.5$ lb/in., and (*c*) $P = 500$ lb and $w = 12.5$ lb/in.

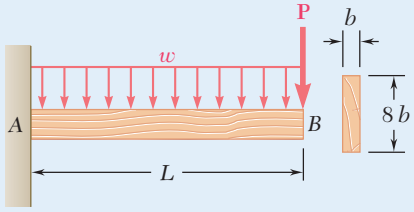


Fig. P6.C2

6.C3 A beam having the cross section shown is subjected to a vertical shear **V.** Write a computer program that, for loads and dimensions expressed in either SI or U.S. customary units, can be used to calculate the shearing stress along the line between any two adjacent rectangular areas forming the cross section. Use this program to solve (*a*) Prob. 6.10, (*b*) Prob. 6.12, (*c*) Prob. 6.22.

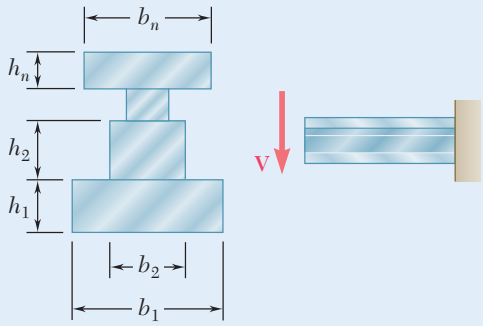


Fig. P6.C3

6.C4 A plate of uniform thickness t is bent as shown into a shape with a vertical plane of symmetry and is then used as a beam. Write a computer program that, for loads and dimensions expressed in either SI or U.S. customary units, can be used to determine the distribution of shearing stresses caused by a vertical shear **V**. Use this program (*a*) to solve Prob. 6.47, (*b*) to find the shearing stress at a point E for the shape and load of Prob. 6.50, assuming a thickness $t = \frac{1}{4}$ in.

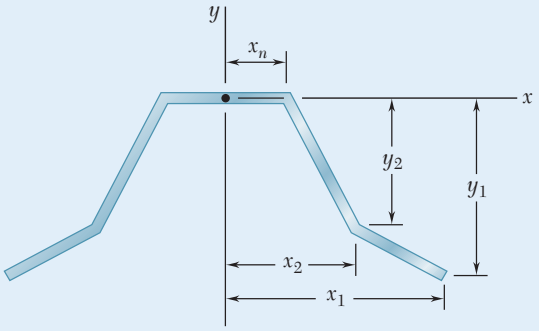


Fig. P6.C4

6.C5 The cross section of an extruded beam is symmetric with respect to the x axis and consists of several straight segments as shown. Write a computer program that, for loads and dimensions expressed in either SI or U.S. customary units, can be used to determine (a) the location of the shear center O, (b) the distribution of shearing stresses caused by a vertical force applied at O. Use this program to solve Prob. 6.70.

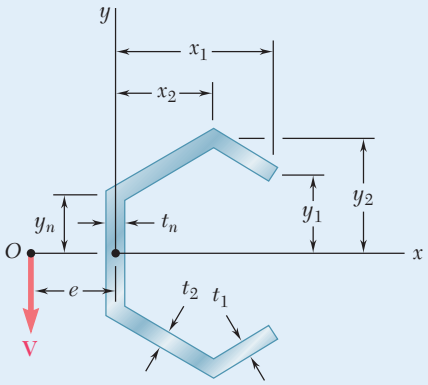


Fig. P6.C5

6.C6 A thin-walled beam has the cross section shown. Write a computer program that, for loads and dimensions expressed in either SI or U.S. customary units, can be used to determine the location of the shear center O of the cross section. Use the program to solve Prob. 6.75.

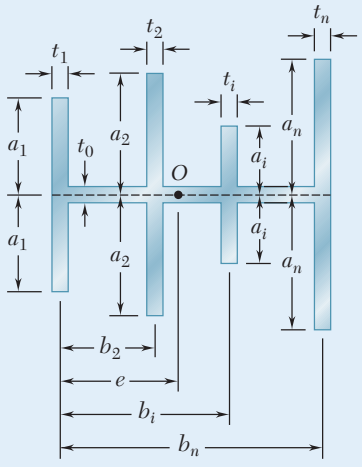
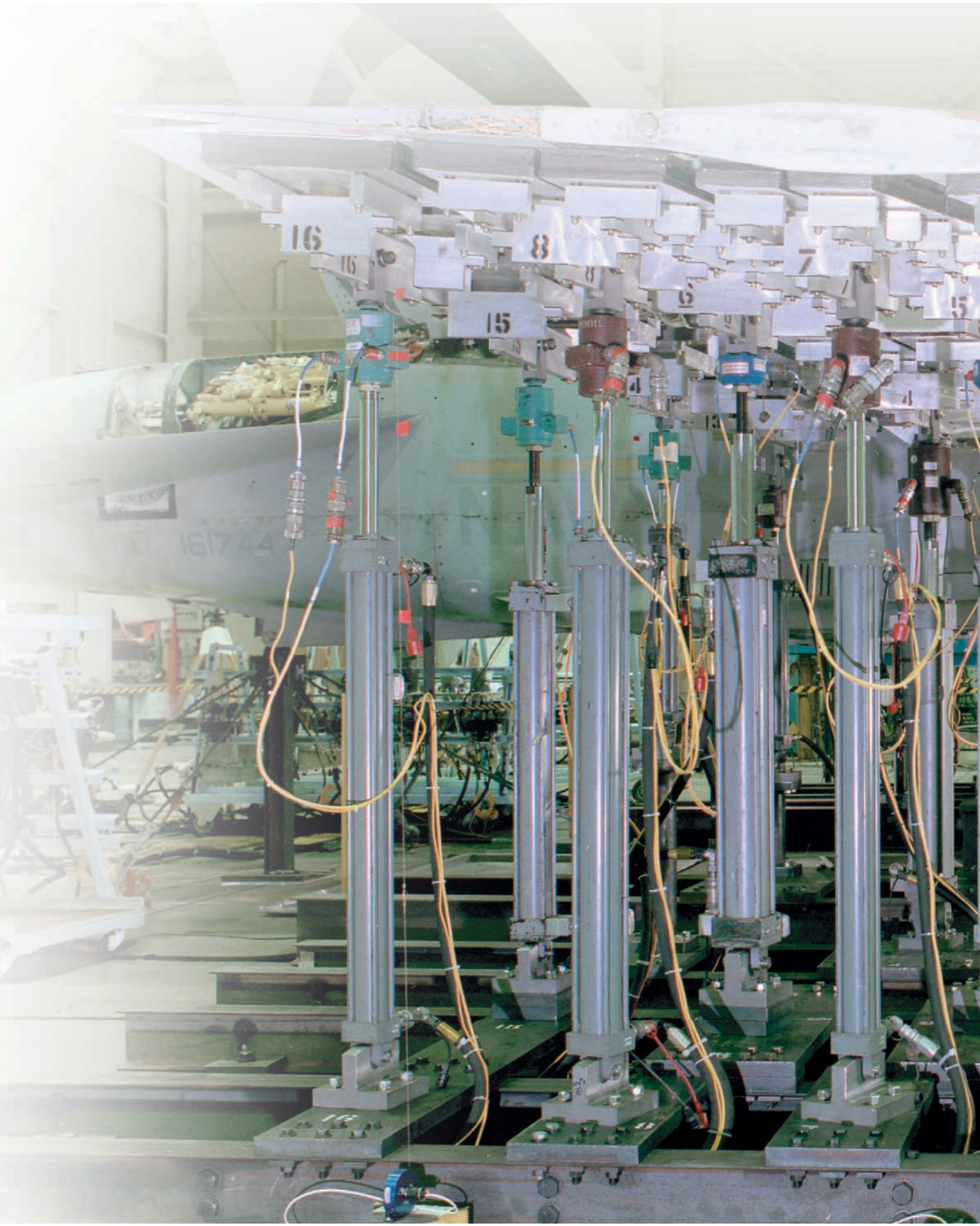
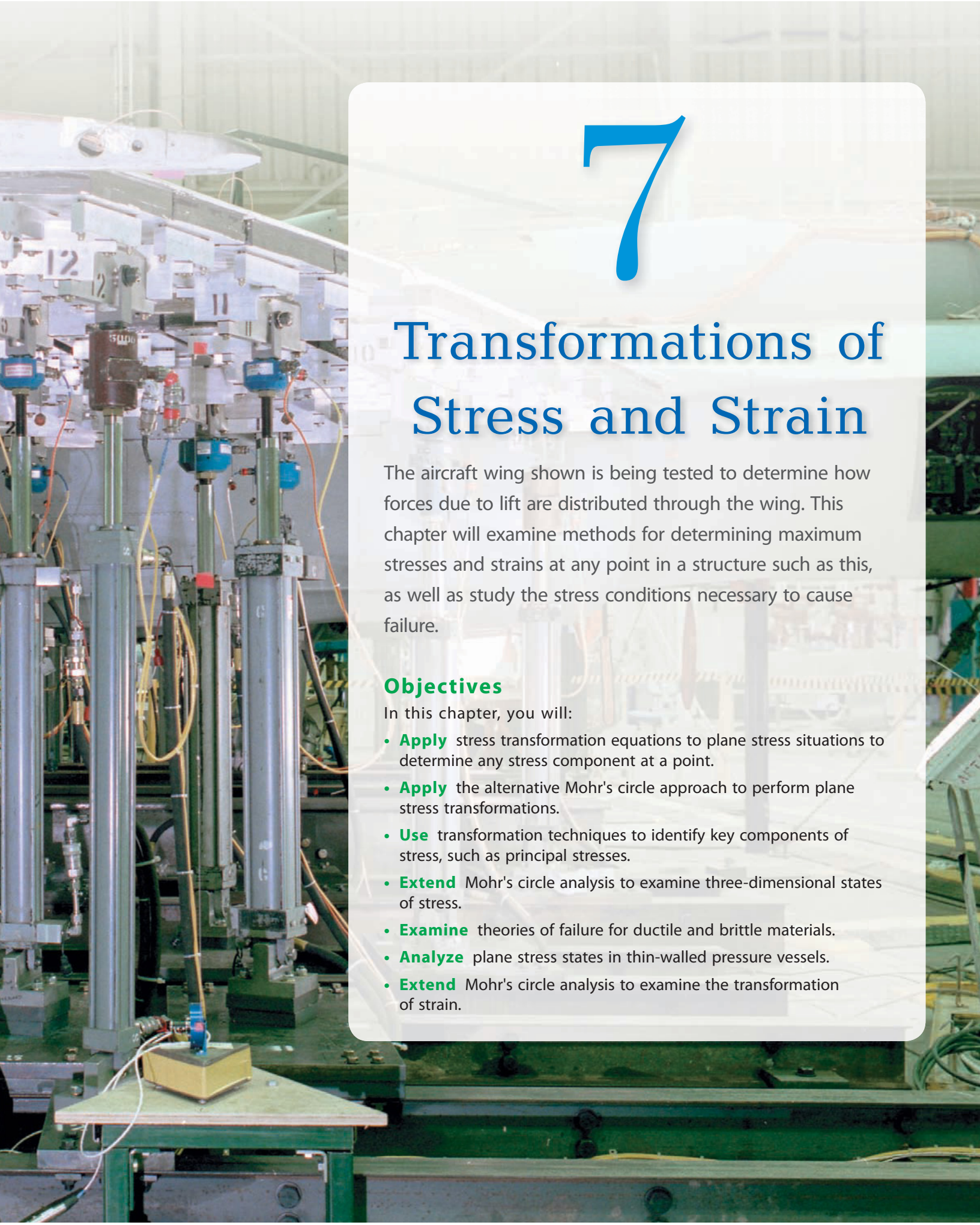


Fig. P6.C6


16
15



7

Transformations of Stress and Strain

The aircraft wing shown is being tested to determine how forces due to lift are distributed through the wing. This chapter will examine methods for determining maximum stresses and strains at any point in a structure such as this, as well as study the stress conditions necessary to cause failure.

Objectives

In this chapter, you will:

- **Apply** stress transformation equations to plane stress situations to determine any stress component at a point.
- **Apply** the alternative Mohr's circle approach to perform plane stress transformations.
- **Use** transformation techniques to identify key components of stress, such as principal stresses.
- **Extend** Mohr's circle analysis to examine three-dimensional states of stress.
- **Examine** theories of failure for ductile and brittle materials.
- **Analyze** plane stress states in thin-walled pressure vessels.
- **Extend** Mohr's circle analysis to examine the transformation of strain.

Introduction

7.1 TRANSFORMATION OF PLANE STRESS
7.1A Transformation Equations
7.1B Principal Stresses and Maximum Shearing Stress
7.2 MOHR'S CIRCLE FOR PLANE STRESS
7.3 GENERAL STATE OF STRESS
7.4 THREE-DIMENSIONAL ANALYSIS OF STRESS
7.5 THEORIES OF FAILURE
*7.5A Yield Criteria for Ductile Materials
*7.5B Fracture Criteria for Brittle Materials
7.6 STRESSES IN THIN-WALLED PRESSURE VESSELS
7.7 TRANSFORMATION OF PLANE STRAIN
*7.7A Transformation Equations
*7.7B Mohr's Circle for Plane Strain
*7.8 THREE-DIMENSIONAL ANALYSIS OF STRAIN
*7.9 MEASUREMENTS OF STRAIN; STRAIN ROSETTE

Introduction

The most general state of stress at a given point Q is represented by six components (Sec. 1.4). Three of these components, σ_x, σ_y, and σ_z, are the normal stresses exerted on the faces of a small cubic element centered at Q with the same orientation as the coordinate axes (Fig. 7.1*a*). The other three, τ_{xy}, τ_{yz}, and τ_{zx},† are the components of the shearing stresses on the same element. The same state of stress will be represented by a different set of components if the coordinate axes are rotated (Fig. 7.1*b*). The first part of this chapter determines how the components of stress are transformed under a rotation of the coordinate axes. The second part of the chapter is devoted to a similar analysis of the transformation of strain components.

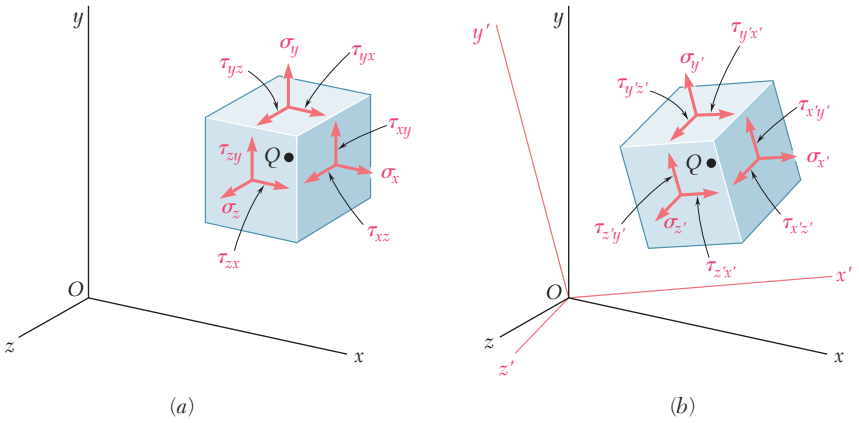


Fig. 7.1 General state of stress at a point: (*a*) referred to {*xyz*}, (*b*) referred to {*x′y′z′*}.

Our discussion of the transformation of stress will deal mainly with *plane stress*, i.e., with a situation in which two of the faces of the cubic element are free of any stress. If the z axis is chosen perpendicular to these faces, $\sigma_z = \tau_{zx} = \tau_{zy} = 0$, and the only remaining stress components are σ_x, σ_y, and τ_{xy} (Fig. 7.2). This situation occurs in a thin plate subjected to forces acting in the midplane of the plate (Fig. 7.3). It also occurs on the

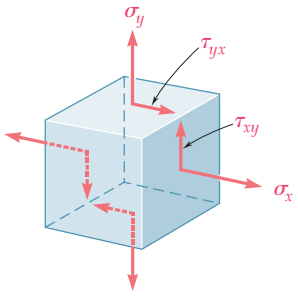


Fig. 7.2 Non-zero stress components for state of plane stress.

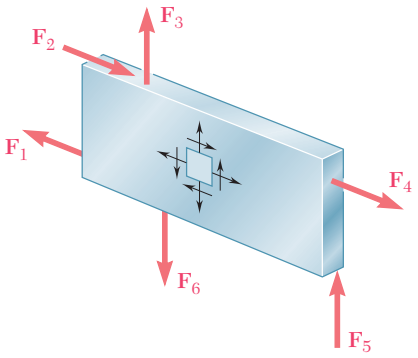


Fig. 7.3 Example of plane stress: thin plate subjected to only in-plane loads.

†Recall that $\tau_{yx} = \tau_{xy}$, $\tau_{zy} = \tau_{yz}$, and $\tau_{xz} = \tau_{zx}$ (Sec. 1.4).

free surface of a structural element or machine component where any point of the surface of that element or component is not subjected to an external force (Fig. 7.4).

In Sec. 7.1A, a state of plane stress at a given point Q is characterized by the stress components σ_x, σ_y, and τ_{xy} associated with the element shown in Fig. 7.5*a*. Components $\sigma_{x'}$, $\sigma_{y'}$, and $\tau_{x'y'}$ associated with that element after it has been rotated through an angle θ about the z axis (Fig. 7.5*b*) will then be determined. In Sec. 7.1B, the value θ_p of θ will be found, where the stresses $\sigma_{x'}$ and $\sigma_{y'}$ are the maximum and minimum stresses. These values of the normal stress are the *principal stresses* at point Q, and the faces of the corresponding element define the *principal planes of stress* at that point. The angle of rotation θ_s for which the shearing stress is maximum also is discussed.

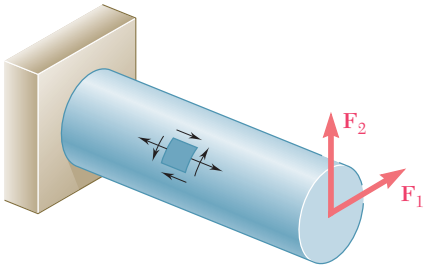


Fig. 7.4 Example of plane stress: free surface of a structural component.

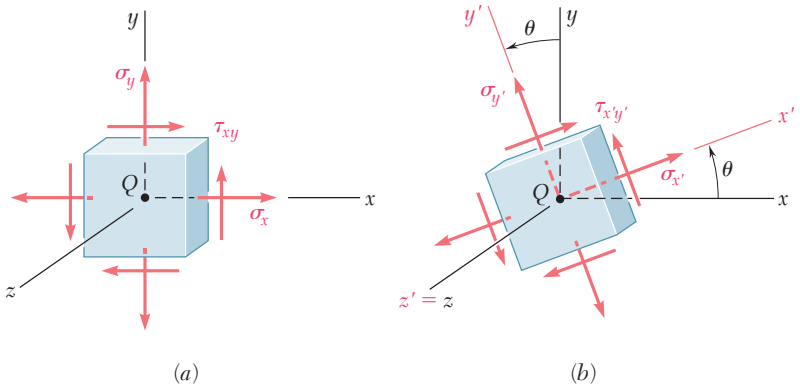


Fig. 7.5 State of plane stress: (*a*) referred to {*xyz*}, (*b*) referred to {*x*′*y*′*z*′}.

In Sec. 7.2, an alternative method to solve problems involving the transformation of plane stress, based on the use of *Mohr's circle*, is presented.

In Sec. 7.3, the *three-dimensional state of stress* at a given point is discussed, and the normal stress on a plane of arbitrary orientation at that point is determined. In Sec. 7.4, the rotations of a cubic element about each of the principal axes of stress and the corresponding transformations of stress are described by three different Mohr's circles. For a state of *plane stress* at a given point, the maximum value of the shearing stress obtained using rotations in the plane of stress does not necessarily represent the maximum shearing stress at that point. This make it necessary to distinguish *in-plane* and *out-of-plane* maximum shearing stresses.

Yield criteria for ductile materials under plane stress are discussed in Sec. 7.5A. To predict whether a material yields at some critical point under given load conditions, the principal stresses σ_a and σ_b will be determined at that point, and then used with the yield strength σ_Y of the material to evaluate a certain criterion. Two criteria in common use are the *maximum-shearing-strength criterion* and the *maximum-distortion-energy criterion*. In Sec. 7.5B, *fracture criteria* for brittle materials under plane stress are developed using the principal stresses σ_a and σ_b at some critical point and the ultimate strength σ_U of the material. Two criteria discussed here are the *maximum-normal-stress* criterion and *Mohr's criterion*.

Thin-walled pressure vessels are an important application of the analysis of plane stress. Stresses in both cylindrical and spherical pressure vessels (Photos 7.1 and 7.2) are discussed in Sec. 7.6.



Photo 7.1 Cylindrical pressure vessels.



Photo 7.2 Spherical pressure vessel.

Section 7.7 is devoted to the *transformation of plane strain* and *Mohr's circle for plane strain*. In Sec. 7.8, the three-dimensional analysis of strain shows how Mohr's circles can be used to determine the maximum shearing strain at a given point. These two particular cases are of special interest and should not be confused: the case of *plane strain* and the case of *plane stress*.

The application of *strain gages* to measure the normal strain on the surface of a structural element or machine component is considered in Sec. 7.9. The components ϵ_x, ϵ_y, and γ_{xy} characterizing the state of strain at a given point are computed from the measurements made with three strain gages forming a *strain rosette*.

7.1 TRANSFORMATION OF PLANE STRESS

7.1A Transformation Equations

Assume that a state of plane stress exists at point Q (with $\sigma_z = \tau_{zx} = \tau_{zy} = 0$) and is defined by the stress components σ_x, σ_y, and τ_{xy} associated with the element shown in Fig. 7.5*a*. The stress components $\sigma_{x'}$, $\sigma_{y'}$, and $\tau_{x'y'}$ associated with the element are determined after it has been rotated through an angle θ about the z axis (Fig. 7.5*b*). These components are given in terms of σ_x, σ_y, τ_{xy}, and θ.

In order to determine the normal stress $\sigma_{x'}$ and shearing stress $\tau_{x'y'}$ exerted on the face perpendicular to the x' axis, consider a prismatic element with faces perpendicular to the x, y, and x' axes (Fig. 7.6*a*). If the area of the oblique face is ΔA, the areas of the vertical and horizontal faces are equal to $\Delta A \cos\theta$ and $\Delta A \sin\theta$, respectively. The *forces* exerted on the three faces are as shown in Fig. 7.6*b*. (No forces are exerted on the

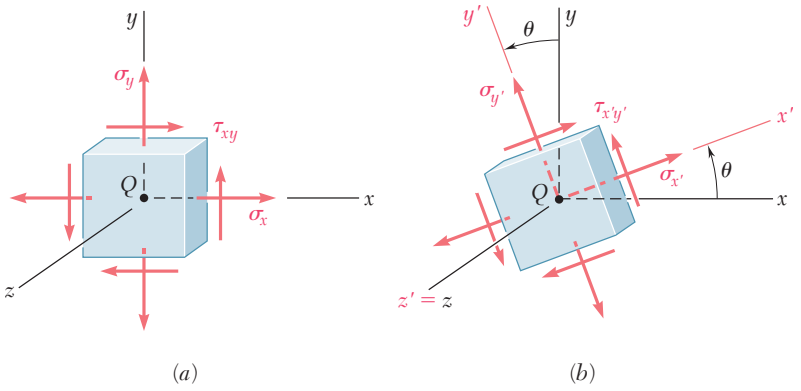


Fig. 7.5 (repeated) State of plane stress: (*a*) referred to {*xyz*}, (*b*) referred to {*x*′*y*′*z*′}.

triangular faces of the element, since the corresponding normal and shearing stresses are assumed equal to zero.) Using components along the x' and y' axes, the equilibrium equations are

$$\Sigma F_{x'} = 0: \quad \sigma_{x'}\,\Delta A - \sigma_x(\Delta A\cos\theta)\cos\theta - \tau_{xy}(\Delta A\cos\theta)\sin\theta - \sigma_y(\Delta A\sin\theta)\sin\theta - \tau_{xy}(\Delta A\sin\theta)\cos\theta = 0$$

$$\Sigma F_{y'} = 0: \quad \tau_{x'y'}\,\Delta A + \sigma_x(\Delta A\cos\theta)\sin\theta - \tau_{xy}(\Delta A\cos\theta)\cos\theta - \sigma_y(\Delta A\sin\theta)\cos\theta + \tau_{xy}(\Delta A\sin\theta)\sin\theta = 0$$

Solving the first equation for $\sigma_{x'}$ and the second for $\tau_{x'y'}$,

$$\sigma_{x'} = \sigma_x\cos^2\theta + \sigma_y\sin^2\theta + 2\tau_{xy}\sin\theta\cos\theta \tag{7.1}$$

$$\tau_{x'y'} = -(\sigma_x - \sigma_y)\sin\theta\cos\theta + \tau_{xy}(\cos^2\theta - \sin^2\theta) \tag{7.2}$$

Recalling the trigonometric relations

$$\sin 2\theta = 2\sin\theta\cos\theta \qquad \cos 2\theta = \cos^2\theta - \sin^2\theta \tag{7.3}$$

and

$$\cos^2\theta = \frac{1 + \cos 2\theta}{2} \qquad \sin^2\theta = \frac{1 - \cos 2\theta}{2} \tag{7.4}$$

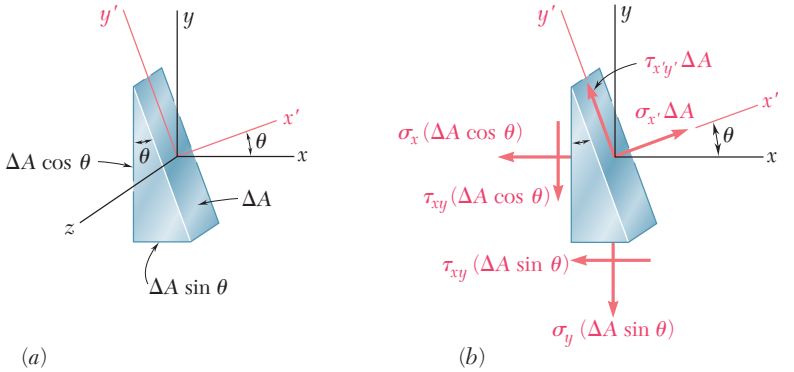


Fig. 7.6 Stress transformation equations are determined by considering an arbitrary prismatic wedge element. (*a*) Geometry of the element. (*b*) Free-body diagram.

Eq. (7.1) is rewritten as

$$\sigma_{x'} = \sigma_x \frac{1 + \cos 2\theta}{2} + \sigma_y \frac{1 - \cos 2\theta}{2} + \tau_{xy} \sin 2\theta$$

or

$$\sigma_{x'} = \frac{\sigma_x + \sigma_y}{2} + \frac{\sigma_x - \sigma_y}{2} \cos 2\theta + \tau_{xy} \sin 2\theta \tag{7.5}$$

Using the relationships of Eq. (7.3), Eq. (7.2) is now

$$\tau_{x'y'} = -\frac{\sigma_x - \sigma_y}{2} \sin 2\theta + \tau_{xy} \cos 2\theta \tag{7.6}$$

The normal stress $\sigma_{y'}$ is obtained by replacing θ in Eq. (7.5) by the angle $\theta + 90°$ that the y' axis forms with the x axis. Since $\cos(2\theta + 180°) = -\cos 2\theta$ and $\sin(2\theta + 180°) = -\sin 2\theta$,

$$\sigma_{y'} = \frac{\sigma_x + \sigma_y}{2} - \frac{\sigma_x - \sigma_y}{2} \cos 2\theta - \tau_{xy} \sin 2\theta \tag{7.7}$$

Adding Eqs. (7.5) and (7.7) member to member,

$$\sigma_{x'} + \sigma_{y'} = \sigma_x + \sigma_y \tag{7.8}$$

Since $\sigma_z = \sigma_{z'} = 0$, we thus verify for plane stress that the sum of the normal stresses exerted on a cubic element of material is independent of the orientation of that element.†

7.1B Principal Stresses and Maximum Shearing Stress

Equations (7.5) and (7.6) are the parametric equations of a circle. This means that, if a set of rectangular axes is used to plot a point M of abscissa $\sigma_{x'}$ and ordinate $\tau_{x'y'}$ for any given parameter θ, all of the points obtained will lie on a circle. To establish this property, we eliminate θ from Eqs. (7.5) and (7.6) by first transposing $(\sigma_x + \sigma_y)/2$ in Eq. (7.5) and squaring both members of the equation, then squaring both members of Eq. (7.6), and finally adding member to member the two equations obtained:

$$\left(\sigma_{x'} - \frac{\sigma_x + \sigma_y}{2}\right)^2 + \tau_{x'y'}^2 = \left(\frac{\sigma_x - \sigma_y}{2}\right)^2 + \tau_{xy}^2 \tag{7.9}$$

Setting

$$\sigma_{\text{ave}} = \frac{\sigma_x + \sigma_y}{2} \qquad \text{and} \qquad R = \sqrt{\left(\frac{\sigma_x - \sigma_y}{2}\right)^2 + \tau_{xy}^2} \tag{7.10}$$

the identity of Eq. (7.9) is given as

$$(\sigma_{x'} - \sigma_{\text{ave}})^2 + \tau_{x'y'}^2 = R^2 \tag{7.11}$$

†This verifies the property of dilatation as discussed in the first footnote of Sec. 2.6.

which is the equation of a circle of radius R centered at the point C of abscissa σ_{ave} and ordinate 0 (Fig. 7.7). Due to the symmetry of the circle about the horizontal axis, the same result is obtained if a point N of abscissa $\sigma_{x'}$ and ordinate $-\tau_{x'y'}$ is plotted instead of M. (Fig. 7.8). This property will be used in Sec. 7.2.

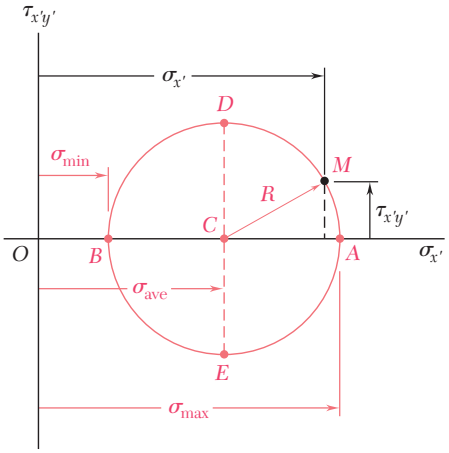


Fig. 7.7 Circular relationship of transformed stresses.

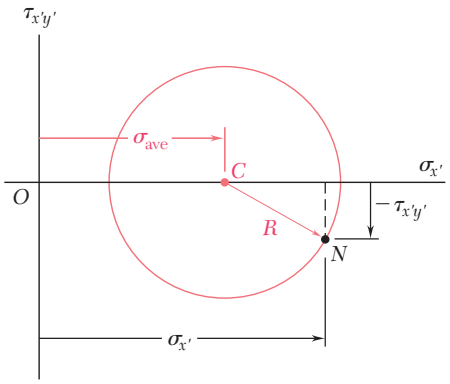


Fig. 7.8 Equivalent formation of stress transformation circle.

The points A and B where the circle of Fig. 7.7 intersects the horizontal axis are of special interest: point A corresponds to the maximum value of the normal stress $\sigma_{x'}$, while point B corresponds to its minimum value. Both points also correspond to a zero value of the shearing stress $\tau_{x'y'}$. Thus, the values θ_p of the parameter θ which correspond to points A and B can be obtained by setting $\tau_{x'y'} = 0$ in Eq. (7.6).†

$$\tan 2\theta_p = \frac{2\tau_{xy}}{\sigma_x - \sigma_y} \tag{7.12}$$

This equation defines two values $2\theta_p$ that are 180° apart and thus two values θ_p that are 90° apart. Either value can be used to determine the orientation of the corresponding element (Fig. 7.9). The planes containing the faces of the element obtained in this way are the *principal planes of stress* at point Q, and the corresponding values σ_{max} and σ_{min} exerted on these planes are the *principal stresses* at Q. Since both values θ_p defined by Eq. (7.12) are obtained by setting $\tau_{x'y'} = 0$ in Eq. (7.6), it is clear that no shearing stress is exerted on the principal planes.

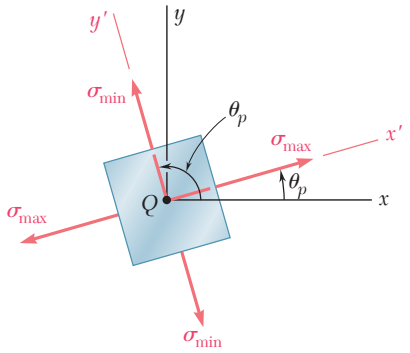


Fig. 7.9 Principal stresses.

From Fig. 7.7,

$$\sigma_{max} = \sigma_{ave} + R \quad \text{and} \quad \sigma_{min} = \sigma_{ave} - R \tag{7.13}$$

Substituting for σ_{ave} and R from Eq. (7.10),

$$\sigma_{max,\,min} = \frac{\sigma_x + \sigma_y}{2} \pm \sqrt{\left(\frac{\sigma_x - \sigma_y}{2}\right)^2 + \tau_{xy}^2} \tag{7.14}$$

†This relationship also can be obtained by differentiating $\sigma_{x'}$ in Eq. (7.5) and setting the derivative equal to zero: $d\sigma_{x'}/d\theta = 0$.

Unless it is possible to tell by inspection which of these principal planes is subjected to σ_{max} and which is subjected to σ_{min}, it is necessary to substitute one of the values θ_p into Eq. (7.5) in order to determine which corresponds to the maximum value of the normal stress.

Referring again to Fig. 7.7, points D and E located on the vertical diameter of the circle correspond to the largest value of the shearing stress $\tau_{x'y'}$. Since the abscissa of points D and E is $\sigma_{ave} = (\sigma_x + \sigma_y)/2$, the values θ_s of the parameter θ corresponding to these points are obtained by setting $\sigma_{x'} = (\sigma_x + \sigma_y)/2$ in Eq. (7.5). The sum of the last two terms in that equation must be zero. Thus, for $\theta = \theta_s$,[†]

$$\frac{\sigma_x - \sigma_y}{2} \cos 2\theta_s + \tau_{xy} \sin 2\theta_s = 0$$

or

$$\tan 2\theta_s = -\frac{\sigma_x - \sigma_y}{2\tau_{xy}} \tag{7.15}$$

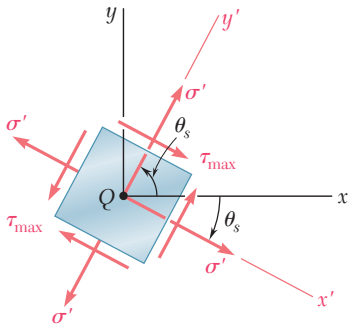


Fig. 7.10 Maximum shearing stress.

This equation defines two values $2\theta_s$ that are 180° apart, and thus two values θ_s that are 90° apart. Either of these values can be used to determine the orientation of the element corresponding to the maximum shearing stress (Fig. 7.10). Fig. 7.7 shows that the maximum value of the shearing stress is equal to the radius R of the circle. Recalling the second of Eqs. (7.10),

$$\tau_{max} = \sqrt{\left(\frac{\sigma_x - \sigma_y}{2}\right)^2 + \tau_{xy}^2} \tag{7.16}$$

As observed earlier, the normal stress corresponding to the condition of maximum shearing stress is

$$\sigma' = \sigma_{ave} = \frac{\sigma_x + \sigma_y}{2} \tag{7.17}$$

Comparing Eqs. (7.12) and (7.15), $\tan 2\theta_s$ is the negative reciprocal of $\tan 2\theta_p$. Thus, angles $2\theta_s$ and $2\theta_p$ are 90° apart, and therefore angles θ_s and θ_p are 45° apart. Thus, *the planes of maximum shearing stress are at 45° to the principal planes*. This confirms the results found in Sec. 1.4 for a centric axial load (Fig. 1.38) and in Sec. 3.1C for a torsional load (Fig. 3.17).

Be aware that the analysis of the transformation of plane stress has been limited to rotations *in the plane of stress*. If the cubic element of Fig. 7.5 is rotated about an axis other than the z axis, its faces may be subjected to shearing stresses larger than defined by Eq. (7.16). In Sec. 7.3, this occurs when the principal stresses in Eq. (7.14) have the same sign (i.e., either both tensile or both compressive). In these cases, the value given by Eq. (7.16) is referred to as the maximum *in-plane* shearing stress.

[†]This relationship also can be obtained by differentiating $\tau_{x'y'}$ in Eq. (7.6) and setting the derivative equal to zero: $d\tau_{x'y'}/d\theta = 0$.

Concept Application 7.1

For the state of plane stress shown in Fig. 7.11*a*, determine (*a*) the principal planes, (*b*) the principal stresses, (*c*) the maximum shearing stress and the corresponding normal stress.

a. Principal Planes. Following the usual sign convention, the stress components are

$$\sigma_x = +50 \text{ MPa} \qquad \sigma_y = -10 \text{ MPa} \qquad \tau_{xy} = +40 \text{ MPa}$$

Substituting into Eq. (7.12),

$$\tan 2\theta_p = \frac{2\tau_{xy}}{\sigma_x - \sigma_y} = \frac{2(+40)}{50 - (-10)} = \frac{80}{60}$$

$$2\theta_p = 53.1^\circ \quad \text{and} \quad 180^\circ + 53.1^\circ = 233.1^\circ$$

$$\theta_p = 26.6^\circ \quad \text{and} \quad 116.6^\circ$$

b. Principal Stresses. Equation (7.14) yields

$$\sigma_{\max,\min} = \frac{\sigma_x + \sigma_y}{2} \pm \sqrt{\left(\frac{\sigma_x - \sigma_y}{2}\right)^2 + \tau_{xy}^2}$$

$$= 20 \pm \sqrt{(30)^2 + (40)^2}$$

$$\sigma_{\max} = 20 + 50 = 70 \text{ MPa}$$

$$\sigma_{\min} = 20 - 50 = -30 \text{ MPa}$$

The principal planes and principal stresses are shown in Fig. 7.11*b*. Making $2\theta = 53.1^\circ$ in Eq. (7.5), it is confirmed that the normal stress exerted on face *BC* of the element is the maximum stress:

$$\sigma_{x'} = \frac{50 - 10}{2} + \frac{50 + 10}{2}\cos 53.1^\circ + 40 \sin 53.1^\circ$$

$$= 20 + 30 \cos 53.1^\circ + 40 \sin 53.1^\circ = 70 \text{ MPa} = \sigma_{\max}$$

c. Maximum Shearing Stress. Equation (7.16) yields

$$\tau_{\max} = \sqrt{\left(\frac{\sigma_x - \sigma_y}{2}\right)^2 + \tau_{xy}^2} = \sqrt{(30)^2 + (40)^2} = 50 \text{ MPa}$$

Since $\sigma_{\max}$ and $\sigma_{\min}$ have opposite signs, $\tau_{\max}$ actually represents the maximum value of the shearing stress at the point. The orientation of the planes of maximum shearing stress and the sense of the shearing stresses are determined by passing a section along the diagonal plane *AC* of the element of Fig. 7.11*b*. Since the faces *AB* and *BC* of the element are in the principal planes, the diagonal plane *AC* must be one of the planes of maximum shearing stress (Fig. 7.11*c*). Furthermore, the equilibrium conditions for the prismatic element *ABC* require that the shearing stress exerted on *AC* be directed as shown. The cubic element corresponding to the maximum shearing stress is shown in Fig. 7.11*d*. The normal stress on each of the four faces of the element is given by Eq. (7.17):

$$\sigma' = \sigma_{\text{ave}} = \frac{\sigma_x + \sigma_y}{2} = \frac{50 - 10}{2} = 20 \text{ MPa}$$

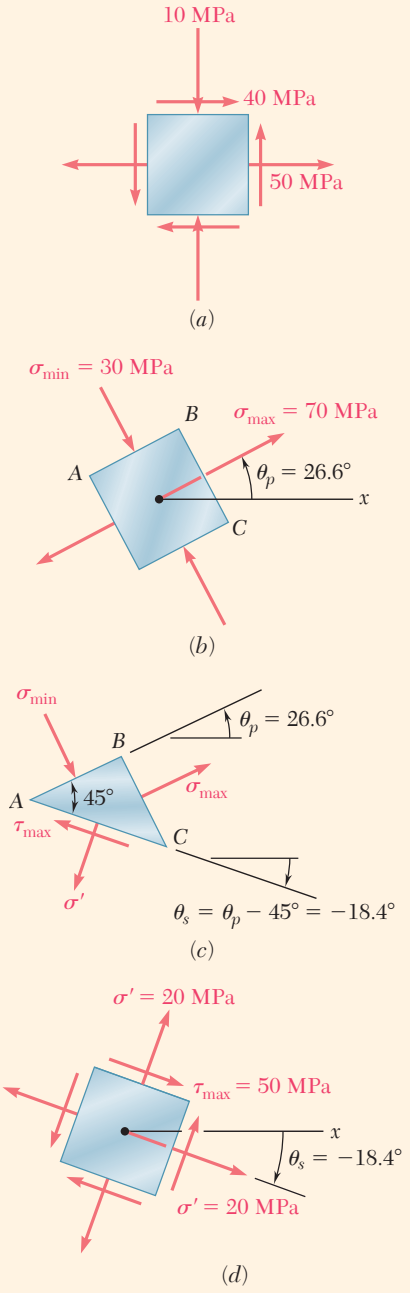
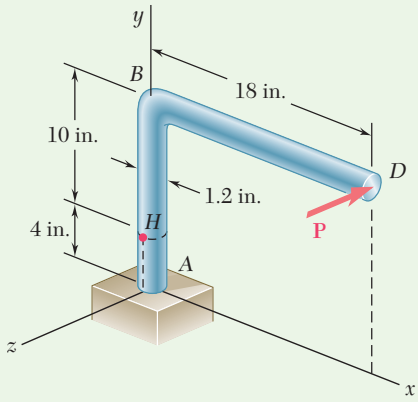


Fig. 7.11 (*a*) Plane stress element. (*b*) Plane stress element oriented in principal directions. (*c*) Plane stress element showing principal and maximum shear planes. (*d*) Plane stress element showing maximum shear orientation.

Sample Problem 7.1

A single horizontal force **P** with a magnitude of 150 lb is applied to end *D* of lever *ABD*. Knowing that portion *AB* of the lever has a diameter of 1.2 in., determine (*a*) the normal and shearing stresses located at point *H* and having sides parallel to the *x* and *y* axes, (*b*) the principal planes and principal stresses at point *H*.



STRATEGY: You can begin by determining the forces and couples acting on the section containing the point of interest, and then use them to calculate the normal and shearing stresses acting at that point. These stresses can then be transformed to obtain the principal stresses and their orientation.

MODELING and ANALYSIS:

Force-Couple System. We replace the force **P** by an equivalent force-couple system at the center *C* of the transverse section containing point *H* (Fig.1):

$$P = 150 \text{ lb} \qquad T = (150 \text{ lb})(18 \text{ in.}) = 2.7 \text{ kip·in.}$$

$$M_x = (150 \text{ lb})(10 \text{ in.}) = 1.5 \text{ kip·in.}$$

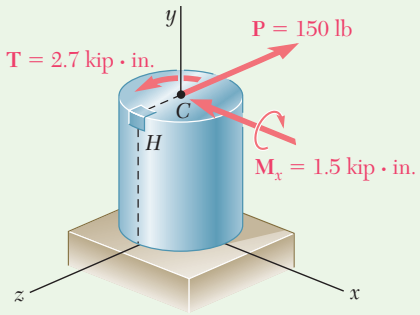


Fig. 1 Equivalent force-couple system acting on transverse section containing point *H*.

(continued)

a. Stresses σ_x, σ_y, τ_{xy} at Point H. Using the sign convention shown in Fig. 7.2, the sense and the sign of each stress component are found by carefully examining the force-couple system at point C (Fig. 1):

$$\sigma_x = 0 \qquad \sigma_y = +\frac{Mc}{I} = +\frac{(1.5 \text{ kip·in.})(0.6 \text{ in.})}{\frac{1}{4}\pi\,(0.6 \text{ in.})^4} \qquad \sigma_y = +8.84 \text{ ksi}$$

$$\tau_{xy} = +\frac{Tc}{J} = +\frac{(2.7 \text{ kip·in.})(0.6 \text{ in.})}{\frac{1}{2}\pi\,(0.6 \text{ in.})^4} \qquad \tau_{xy} = +7.96 \text{ ksi}$$

We note that the shearing force **P** does not cause any shearing stress at point H. The general plane stress element (Fig. 2) is completed to reflect these stress results (Fig. 3).

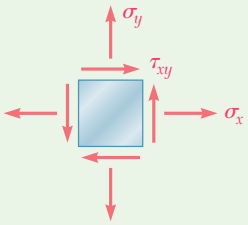


Fig. 2 General plane stress element (showing positive directions).

b. Principal Planes and Principal Stresses. Substituting the values of the stress components into Eq. (7.12), the orientation of the principal planes is

$$\tan 2\theta_p = \frac{2\tau_{xy}}{\sigma_x - \sigma_y} = \frac{2(7.96)}{0 - 8.84} = -1.80$$

$$2\theta_p = -61.0^\circ \qquad \text{and} \qquad 180^\circ - 61.0^\circ = +119^\circ$$

$$\theta_p = -30.5^\circ \qquad \text{and} \qquad +59.5^\circ$$

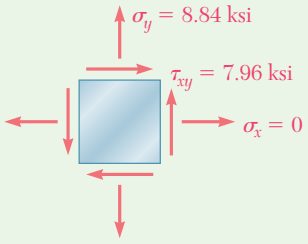


Fig. 3 Stress element at point H.

Substituting into Eq. (7.14), the magnitudes of the principal stresses are

$$\sigma_{\max,\,\min} = \frac{\sigma_x + \sigma_y}{2} \pm \sqrt{\left(\frac{\sigma_x - \sigma_y}{2}\right)^2 + \tau_{xy}^2}$$

$$= \frac{0 + 8.84}{2} \pm \sqrt{\left(\frac{0 - 8.84}{2}\right)^2 + (7.96)^2} = +4.42 \pm 9.10$$

$$\sigma_{\max} = +13.52 \text{ ksi}$$

$$\sigma_{\min} = -4.68 \text{ ksi}$$

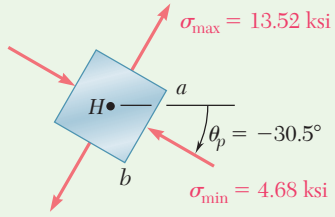


Fig. 4 Stress element at point H oriented in principal directions.

Considering face ab of the element shown, $\theta_p = -30.5^\circ$ in Eq. (7.5) and $\sigma_{x'} = -4.68$ ksi. The principal stresses are as shown in Fig. 4.

Problems

7.1 through 7.4 For the given state of stress, determine the normal and shearing stresses exerted on the oblique face of the shaded triangular element shown. Use a method of analysis based on the equilibrium of that element, as was done in the derivations of Sec. 7.1A.

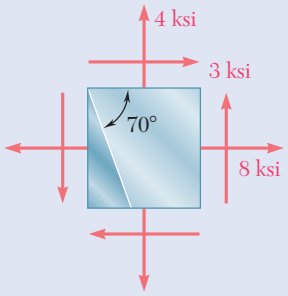


Fig. P7.1

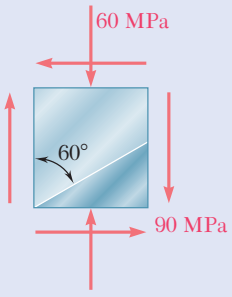


Fig. P7.2

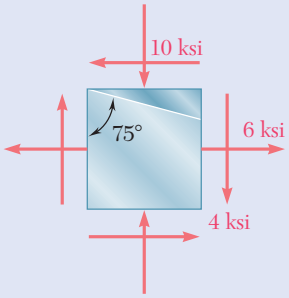


Fig. P7.3

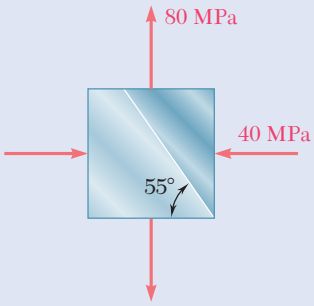


Fig. P7.4

7.5 through *7.8* For the given state of stress, determine (*a*) the principal planes, (*b*) the principal stresses.

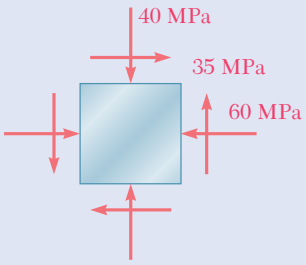


Fig. P7.5 and P7.9

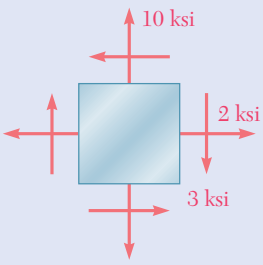


Fig. *P7.6* and P7.10

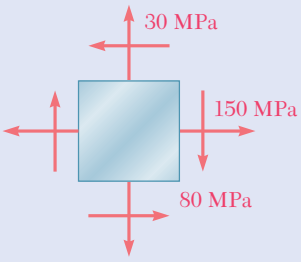


Fig. P7.7 and P7.11

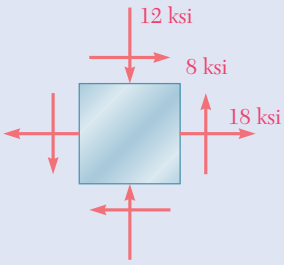


Fig. *P7.8* and P7.12

7.9 through 7.12 For the given state of stress, determine (*a*) the orientation of the planes of maximum in-plane shearing stress, (*b*) the maximum in-plane shearing stress, (*c*) the corresponding normal stress.

7.13 through *7.16* For the given state of stress, determine the normal and shearing stresses after the element shown has been rotated through (*a*) 25° clockwise, (*b*) 10° counterclockwise.

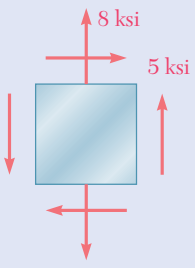


Fig. P7.13

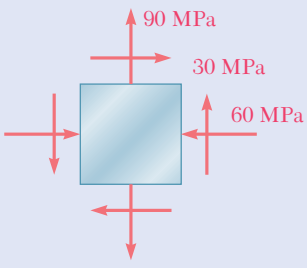


Fig. *P7.14*

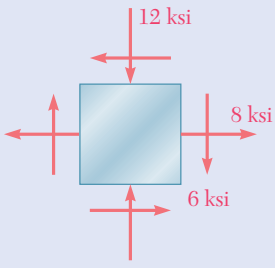


Fig. P7.15

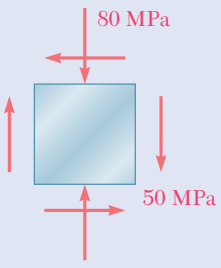


Fig. *P7.16*

7.17 and 7.18 The grain of a wooden member forms an angle of 15° with the vertical. For the state of stress shown, determine (*a*) the in-plane shearing stress parallel to the grain, (*b*) the normal stress perpendicular to the grain.

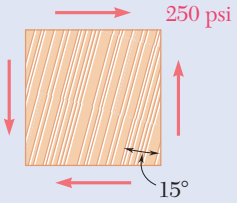


Fig. P7.17

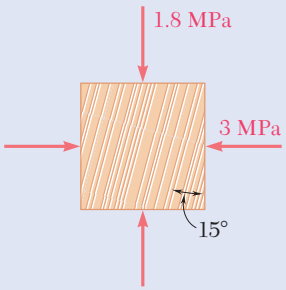


Fig. P7.18

7.19 Two wooden members of 80 × 120-mm uniform rectangular cross section are joined by the simple glued scarf splice shown. Knowing that $\beta = 22°$ and that the maximum allowable stresses in the joint are, respectively, 400 kPa in tension (perpendicular to the splice) and 600 kPa in shear (parallel to the splice), determine the largest centric load **P** that can be applied.

7.20 Two wooden members of 80 × 120-mm uniform rectangular cross section are joined by the simple glued scarf splice shown. Knowing that $\beta = 25°$ and that centric loads of magnitude $P = 10$ kN are applied to the members as shown, determine (*a*) the in-plane shearing stress parallel to the splice, (*b*) the normal stress perpendicular to the splice.

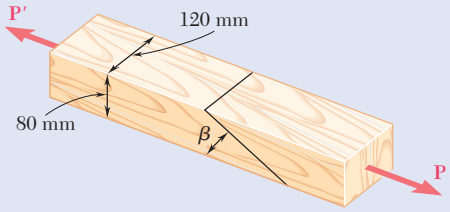


Fig. P7.19 and *P7.20*

7.21 The centric force **P** is applied to a short post as shown. Knowing that the stresses on plane *a*-*a* are $\sigma = -15$ ksi and $\tau = 5$ ksi, determine (*a*) the angle β that plane *a*-*a* forms with the horizontal, (*b*) the maximum compressive stress in the post.

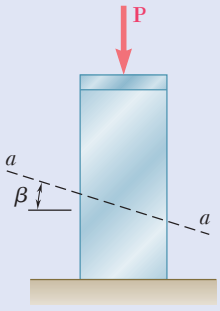


Fig. P7.21

7.22 Two members of uniform cross section 50 × 80 mm are glued together along plane *a*-*a* that forms an angle of 25° with the horizontal. Knowing that the allowable stresses for the glued joint are $\sigma = 800$ kPa and $\tau = 600$ kPa, determine the largest centric load **P** that can be applied.

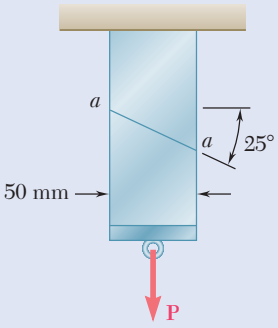


Fig. *P7.22*

7.23 The axle of an automobile is acted upon by the forces and couple shown. Knowing that the diameter of the solid axle is 32 mm, determine (*a*) the principal planes and principal stresses at point *H* located on top of the axle, (*b*) the maximum shearing stress at the same point.

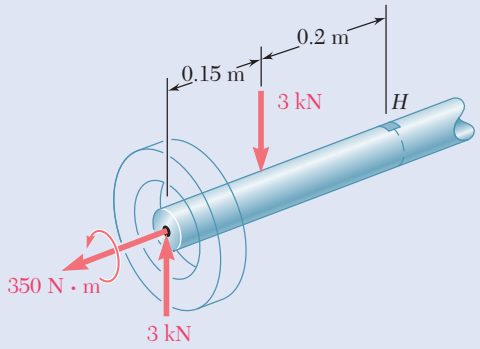


Fig. P7.23

7.24 A 400-lb vertical force is applied at *D* to a gear attached to the solid 1-in. diameter shaft *AB*. Determine the principal stresses and the maximum shearing stress at point *H* located as shown on top of the shaft.

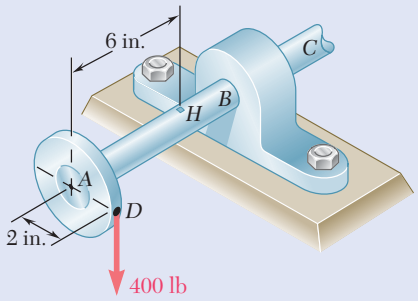


Fig. P7.24

7.25 A mechanic uses a crowfoot wrench to loosen a bolt at *E*. Knowing that the mechanic applies a vertical 24-lb force at *A*, determine the principal stresses and the maximum shearing stress at point *H* located as shown on top of the $\frac{3}{4}$-in. diameter shaft.

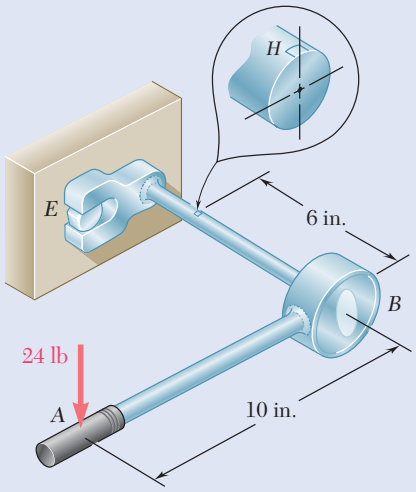


Fig. P7.25

7.26 The steel pipe *AB* has a 102-mm outer diameter and a 6-mm wall thickness. Knowing that arm *CD* is rigidly attached to the pipe, determine the principal stresses and the maximum shearing stress at point *K*.

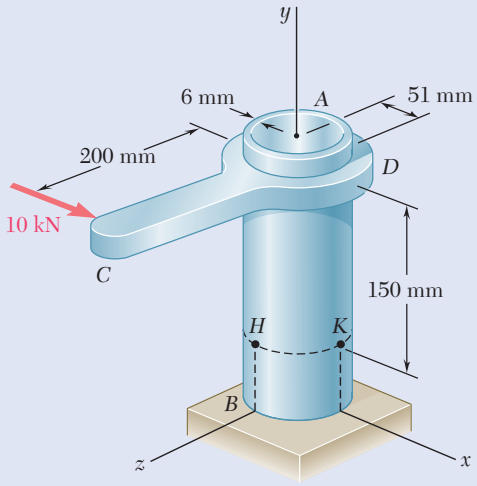


Fig. P7.26

7.27 For the state of plane stress shown, determine the largest value of σ_y for which the maximum in-plane shearing stress is equal to or less than 75 MPa.

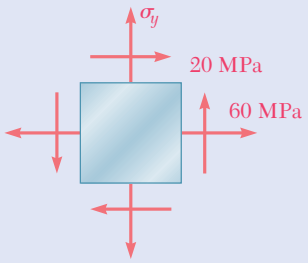


Fig. P7.27

7.28 For the state of plane stress shown, determine (*a*) the largest value of τ_{xy} for which the maximum in-plane shearing stress is equal to or less than 12 ksi, (*b*) the corresponding principal stresses.

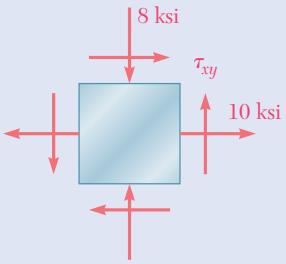


Fig. *P7.28*

7.29 For the state of plane stress shown, determine (*a*) the value of τ_{xy} for which the in-plane shearing stress parallel to the weld is zero, (*b*) the corresponding principal stresses.

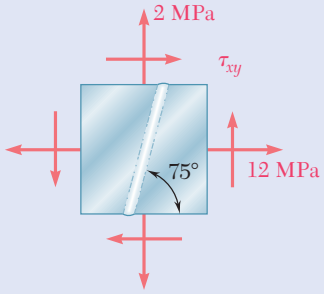


Fig. P7.29

7.30 Determine the range of values of σ_x for which the maximum in-plane shearing stress is equal to or less than 10 ksi.

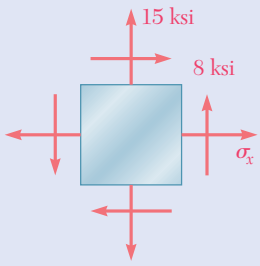


Fig. *P7.30*

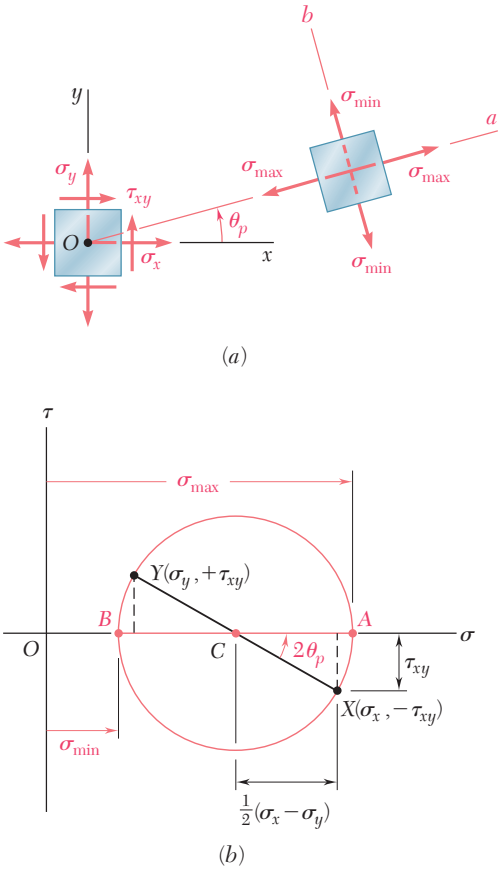


Fig. 7.12 (*a*) Plane stress element and the orientation of principal planes. (*b*) Corresponding Mohr's circle.

7.2 MOHR'S CIRCLE FOR PLANE STRESS

The circle used in the preceding section to derive the equations relating to the transformation of plane stress was introduced by the German engineer Otto Mohr (1835–1918) and is known as *Mohr's circle* for plane stress. This circle can be used to obtain an alternative method for the solution of the problems considered in Sec. 7.1. This method is based on simple geometric considerations and does not require the use of specialized equations. While originally designed for graphical solutions, a calculator may also be used.

Consider a square element of a material subjected to plane stress (Fig. 7.12*a*), and let σ_x, σ_y, and τ_{xy} be the components of the stress exerted on the element. A point X of coordinates σ_x and $-\tau_{xy}$ and a point Y of coordinates σ_y and $+\tau_{xy}$ are plotted (Fig. 7.12*b*). If τ_{xy} is positive, as assumed in Fig. 7.12*a*, point X is located below the σ axis and point Y above, as shown in Fig. 7.12*b*. If τ_{xy} is negative, X is located above the σ axis and Y below. Joining X and Y by a straight line, the point C is at the intersection of line XY with the σ axis, and the circle is drawn with its center at C and having a diameter XY. The abscissa of C and the radius of the circle are respectively equal to σ_{ave} and R in Eqs. (7.10). The circle obtained is Mohr's circle for plane stress. Thus, the abscissas of points A and B where the circle intersects the σ axis represent the principal stresses σ_{max} and σ_{min} at the point considered.

Since $\tan(XCA) = 2\tau_{xy}/(\sigma_x - \sigma_y)$, the angle XCA is equal in magnitude to one of the angles $2\theta_p$ that satisfy Eq. (7.12). Thus, the angle θ_p in Fig. 7.12*a* defines the orientation of the principal plane corresponding to point A in Fig. 7.12*b* and can be obtained by dividing the angle XCA measured on Mohr's circle in half. If $\sigma_x > \sigma_y$ and $\tau_{xy} > 0$, as in the case considered here, the rotation that brings CX into CA is counterclockwise. But, in that case, the angle θ_p obtained from Eq. (7.12) and defining the direction of the normal Oa to the principal plane is positive; thus, the rotation bringing Ox into Oa is also counterclockwise. Therefore, the senses of rotation in both parts of Fig. 7.12 are the same. So, if a counterclockwise rotation through $2\theta_p$ is required to bring CX into CA on Mohr's circle, a counterclockwise rotation through θ_p will bring Ox into Oa in Fig. 7.12*a*.†

Since Mohr's circle is uniquely defined, the same circle can be obtained from the stress components $\sigma_{x'}$, $\sigma_{y'}$, and $\tau_{x'y'}$, which correspond to the x' and y' axes shown in Fig. 7.13*a*. Point X' of coordinates $\sigma_{x'}$ and $-\tau_{x'y'}$ and point Y' of coordinates $\sigma_{y'}$ and $+\tau_{x'y'}$ are located on Mohr's circle, and the angle $X'CA$ in Fig. 7.13*b* must be equal to twice the angle $x'Oa$ in Fig. 7.13*a*. Since the angle XCA is twice the angle xOa, the angle XCX' in Fig. 7.13*b* is twice the angle xOx' in Fig. 7.13*a*. Thus the diameter $X'Y'$ defining the normal and shearing stresses $\sigma_{x'}$, $\sigma_{y'}$, and $\tau_{x'y'}$ is obtained by rotating the diameter XY through an angle equal to twice the angle θ formed by the x' and x axes in Fig. 7.13*a*. The rotation that brings the diameter XY into the diameter $X'Y'$ in Fig. 7.13*b* has the same sense as the rotation that brings the xy axes into the $x'y'$ axes in Fig. 7.13*a*.

This property can be used to verify that planes of maximum shearing stress are at 45° to the principal planes. Indeed, points D and E on

†This is due to the fact that we are using the circle of Fig 7.8 rather than the circle of Fig. 7.7 as Mohr's circle.

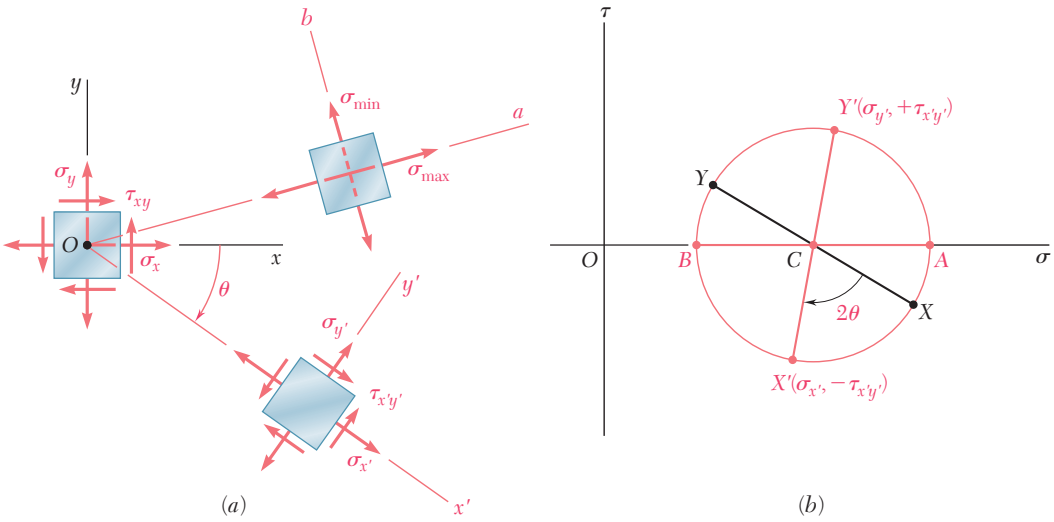


Fig. 7.13 (*a*) Stress element referenced to *xy* axes, transformed to obtain components referenced to *x'y'* axes. (*b*) Corresponding Mohr's circle.

Mohr's circle correspond to the planes of maximum shearing stress, while *A* and *B* correspond to the principal planes (Fig. 7.14*b*). Since the diameters *AB* and *DE* of Mohr's circle are at 90° to each other, the faces of the corresponding elements are at 45° to each other (Fig. 7.14*a*).

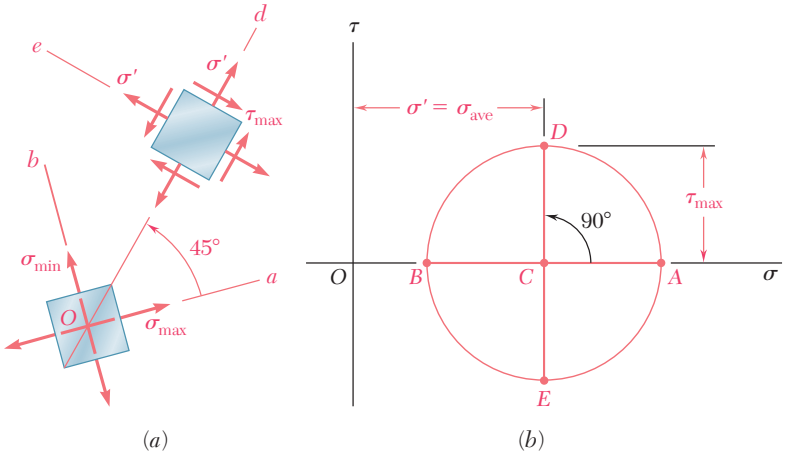


Fig. 7.14 (*a*) Stress elements showing orientation of planes of maximum shearing stress relative to principal planes. (*b*) Corresponding Mohr's circle.

The construction of Mohr's circle for plane stress is simplified if each face of the element used to define the stress components is considered separately. From Figs. 7.12 and 7.13, when the shearing stress exerted *on a given face* tends to rotate the element *clockwise*, the point on Mohr's circle corresponding to that face is located *above* the σ axis. When the shearing stress on a given face tends to rotate the element *counterclockwise*, the point corresponding to that face is located *below* the σ axis (Fig. 7.15).† As far as the normal stresses are concerned, the usual convention holds, so that a tensile stress is positive and is plotted to the right, while a compressive stress is considered negative and is plotted to the left.

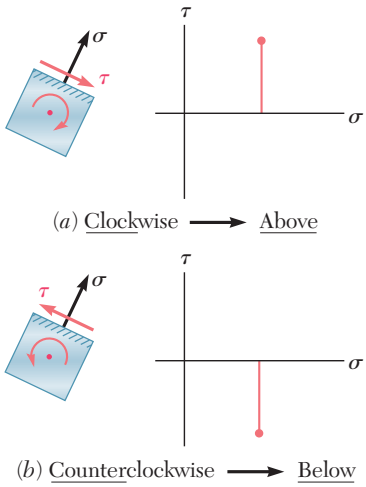


Fig. 7.15 Convention for plotting shearing stress on Mohr's circle.

†To remember this convention, think "In the kitchen, the *clock* is above, and the *counter* is below."

Concept Application 7.2

For the state of plane stress considered in Concept Application 7.1, (*a*) construct Mohr's circle, (*b*) determine the principal stresses, (*c*) determine the maximum shearing stress and the corresponding normal stress.

a. Construction of Mohr's Circle. Note from Fig. 7.16*a* that the normal stress exerted on the face oriented toward the *x* axis is tensile (positive) and the shearing stress tends to rotate the element counterclockwise. Therefore, point *X* of Mohr's circle is plotted to the right of the vertical axis and below the horizontal axis (Fig. 7.16*b*). A similar inspection of the normal and shearing stresses exerted on the upper face of the element shows that point *Y* should be plotted to the left of the vertical axis and above the horizontal axis. Drawing the line *XY*, the center *C* of Mohr's circle is found. Its abscissa is

$$\sigma_{\text{ave}} = \frac{\sigma_x + \sigma_y}{2} = \frac{50 + (-10)}{2} = 20 \text{ MPa}$$

Since the sides of the shaded triangle are

$$CF = 50 - 20 = 30 \text{ MPa} \quad \text{and} \quad FX = 40 \text{ MPa}$$

the radius of the circle is

$$R = CX = \sqrt{(30)^2 + (40)^2} = 50 \text{ MPa}$$

b. Principal Planes and Principal Stresses. The principal stresses are

$$\sigma_{\max} = OA = OC + CA = 20 + 50 = 70 \text{ MPa}$$

$$\sigma_{\min} = OB = OC - BC = 20 - 50 = -30 \text{ MPa}$$

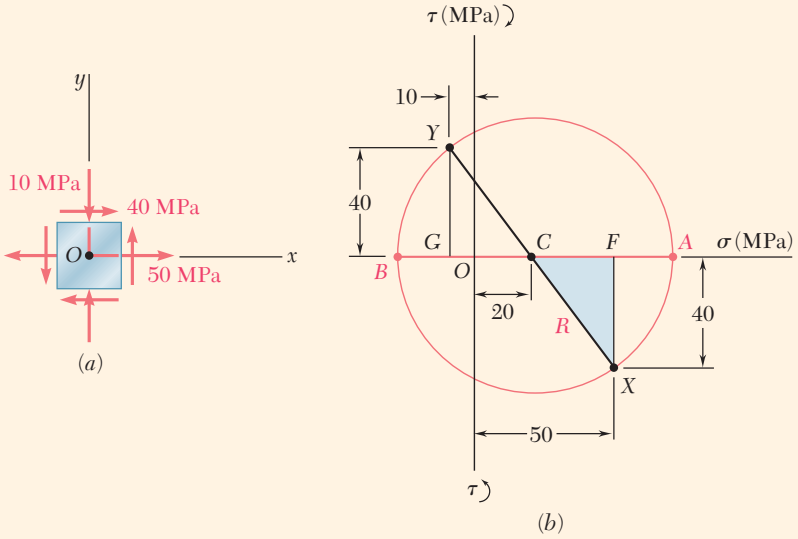


Fig. 7.16 (*a*) Plane stress element. (*b*) Corresponding Mohr's circle.

(continued)

Recalling that the angle ACX represents $2\theta_p$ (Fig. 7.16*b*),

$$\tan 2\theta_p = \frac{FX}{CF} = \frac{40}{30}$$

$$2\theta_p = 53.1^\circ \qquad \theta_p = 26.6^\circ$$

Since the rotation that brings CX into CA in Fig. 7.16*d* is counterclockwise, the rotation that brings Ox into the axis Oa corresponding to $\sigma_{\max}$ in Fig. 7.16*c* is also counterclockwise.

c. Maximum Shearing Stress. Since a further rotation of 90° counterclockwise brings CA into CD in Fig. 7.16*d*, a further rotation of 45° counterclockwise will bring the axis Oa into the axis Od corresponding to the maximum shearing stress in Fig. 7.16*d*. Note from Fig. 7.16*d* that $\tau_{\max} = R = 50$ MPa and the corresponding normal stress is $\sigma' = \sigma_{\text{ave}} = 20$ MPa. Since point D is located above the σ axis in Fig. 7.16*c*, the shearing stresses exerted on the faces perpendicular to Od in Fig. 7.16*d* must be directed so that they will tend to rotate the element clockwise.

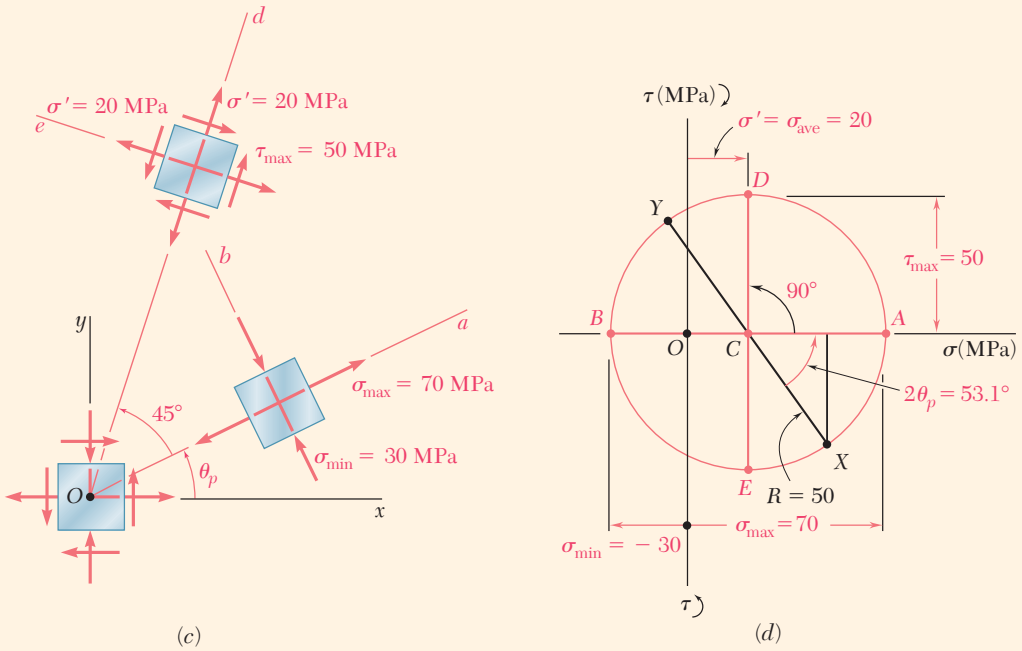


Fig. 7.16 (*cont.*) (*c*) Stress element orientations for principal and maximum shearing stresses. (*d*) Mohr's circle used to determine principal and maximum shearing stresses.

Mohr's circle provides a convenient way of checking the results obtained earlier for stresses under a centric axial load (Sec. 1.4) and under a torsional load (Sec. 3.1C). In the first case (Fig. 7.17*a*), $\sigma_x = P/A$, $\sigma_y = 0$, and $\tau_{xy} = 0$. The corresponding points X and Y define a circle of radius $R = P/2A$ that passes through the origin of coordinates (Fig. 7.17*b*). Points D and E yield the orientation of the planes of maximum shearing stress (Fig. 7.17*c*), as well as $\tau_{\max}$ and the corresponding normal stresses σ':

$$\tau_{\max} = \sigma' = R = \frac{P}{2A} \tag{7.18}$$

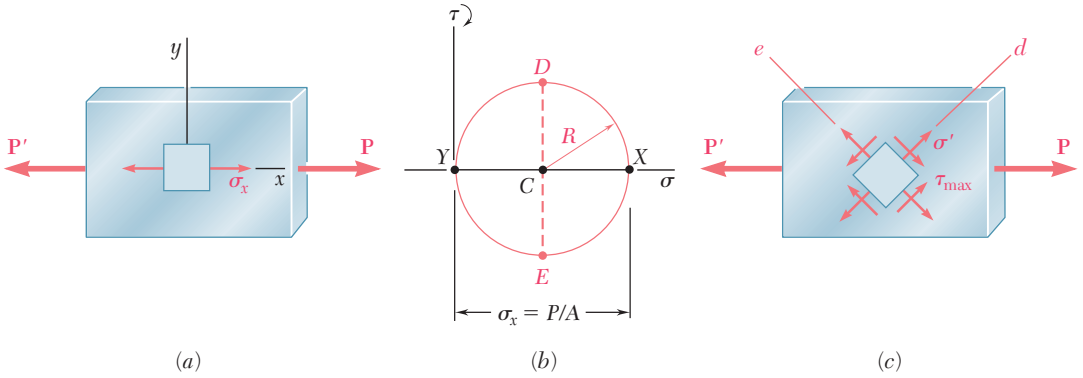


Fig. 7.17 (*a*) Member under centric axial load. (*b*) Mohr's circle. (*c*) Element showing planes of maximum shearing stress.

In the case of torsion (Fig. 7.18*a*), $\sigma_x = \sigma_y = 0$ and $\tau_{xy} = \tau_{\max} = Tc/J$. Therefore, points X and Y are located on the τ axis, and Mohr's circle has a radius of $R = Tc/J$ centered at the origin (Fig. 7.18*b*). Points A and B define the principal planes (Fig. 7.18*c*) and the principal stresses:

$$\sigma_{\max,\,\min} = \pm R = \pm \frac{Tc}{J} \tag{7.19}$$

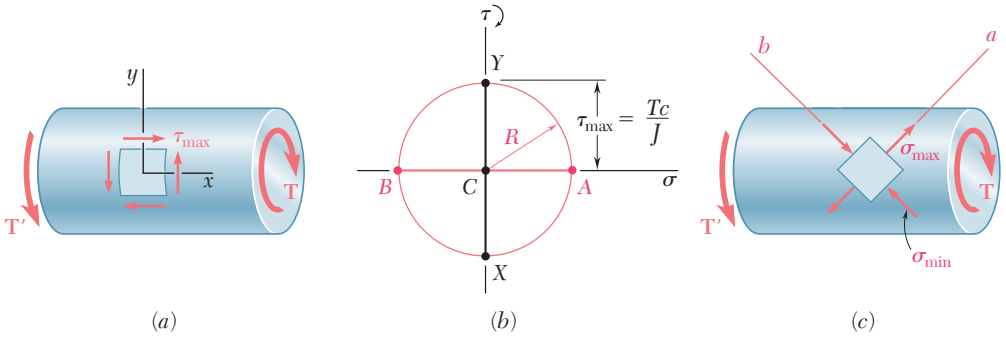
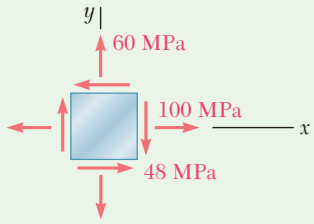


Fig. 7.18 (*a*) Member under torsional load. (*b*) Mohr's circle. (*c*) Element showing orientation of principal stresses.



Sample Problem 7.2

For the state of plane stress shown determine (*a*) the principal planes and the principal stresses, (*b*) the stress components exerted on the element obtained by rotating the given element counterclockwise through 30°.

STRATEGY: Since the given state of stress represents two points on Mohr's circle, you can use these points to generate the circle. The state of stress on any other plane, including the principal planes, can then be readily determined through the geometry of the circle.

MODELING and ANALYSIS:

Construction of Mohr's Circle (Fig 1). On a face perpendicular to the x axis, the normal stress is tensile, and the shearing stress tends to rotate the element clockwise. Thus, X is plotted at a point 100 units to the right of the vertical axis and 48 units above the horizontal axis. By examining the stress components on the upper face, point $Y(60, -48)$ is plotted. Join points X and Y by a straight line to define the center C of Mohr's circle. The abscissa of C, which represents σ_{ave}, and the radius R of the circle, can be measured directly or calculated as

$$\sigma_{\text{ave}} = OC = \tfrac{1}{2}(\sigma_x + \sigma_y) = \tfrac{1}{2}(100 + 60) = 80 \text{ MPa}$$

$$R = \sqrt{(CF)^2 + (FX)^2} = \sqrt{(20)^2 + (48)^2} = 52 \text{ MPa}$$

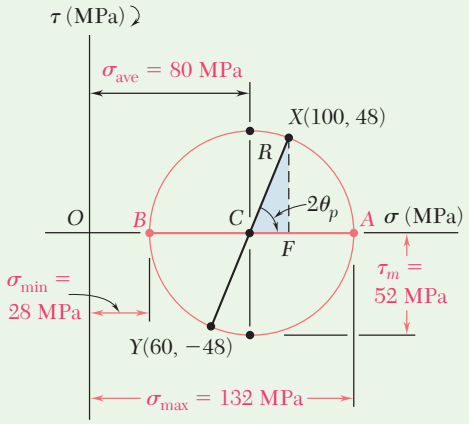


Fig. 1 Mohr's circle for given stress state.

a. Principal Planes and Principal Stresses. We rotate the diameter XY clockwise through $2\theta_p$ until it coincides with the diameter AB. Thus,

$$\tan 2\theta_p = \frac{XF}{CF} = \frac{48}{20} = 2.4 \quad 2\theta_p = 67.4° \circlearrowright \qquad \theta_p = 33.7° \circlearrowright$$

(continued)

The principal stresses are represented by the abscissas of points A and B:

$$\sigma_{\max} = OA = OC + CA = 80 + 52 \qquad \sigma_{\max} = +132 \text{ MPa}$$

$$\sigma_{\min} = OB = OC - BC = 80 - 52 \qquad \sigma_{\min} = +28 \text{ MPa}$$

Since the rotation that brings XY into AB is clockwise, the rotation that brings Ox into the axis Oa corresponding to $\sigma_{\max}$ is also clockwise; we obtain the orientation shown in Fig. 2 for the principal planes.

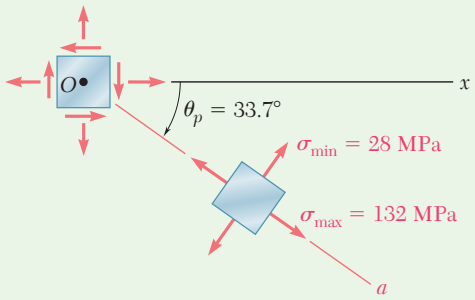


Fig. 2 Orientation of principal stress element.

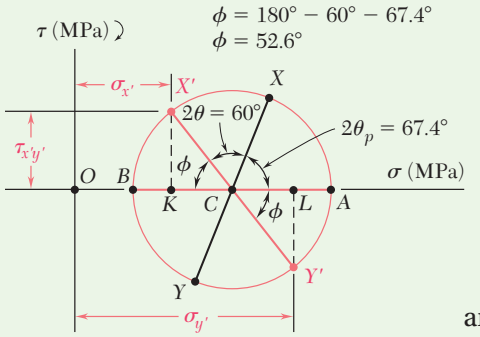


Fig. 3 Mohr's circle analysis for element rotation of 30° counterclockwise.

b. Stress Components on Element Rotated 30°↰. Points X' and Y' on Mohr's circle that correspond to the stress components on the rotated element are obtained by rotating XY counterclockwise through $2\theta = 60°$ (Fig. 3). We find

$$\phi = 180° - 60° - 67.4° \qquad \phi = 52.6°$$

$$\sigma_{x'} = OK = OC - KC = 80 - 52\cos 52.6° \qquad \sigma_{x'} = +48.4 \text{ MPa}$$

$$\sigma_{y'} = OL = OC + CL = 80 + 52\cos 52.6° \qquad \sigma_{y'} = +111.6 \text{ MPa}$$

$$\tau_{x'y'} = KX' = 52\sin 52.6° \qquad \tau_{x'y'} = 41.3 \text{ MPa}$$

Since X' is located above the horizontal axis, the shearing stress on the face perpendicular to Ox' tends to rotate the element clockwise. The stresses, along with their orientation, are shown in Fig. 4.

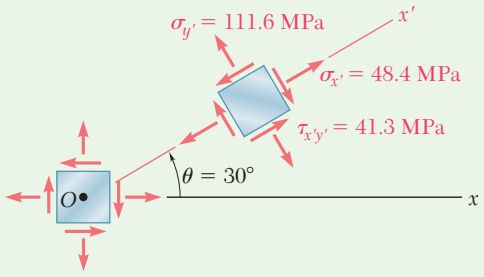


Fig. 4 Stress components obtained by rotating original element 30° counterclockwise.

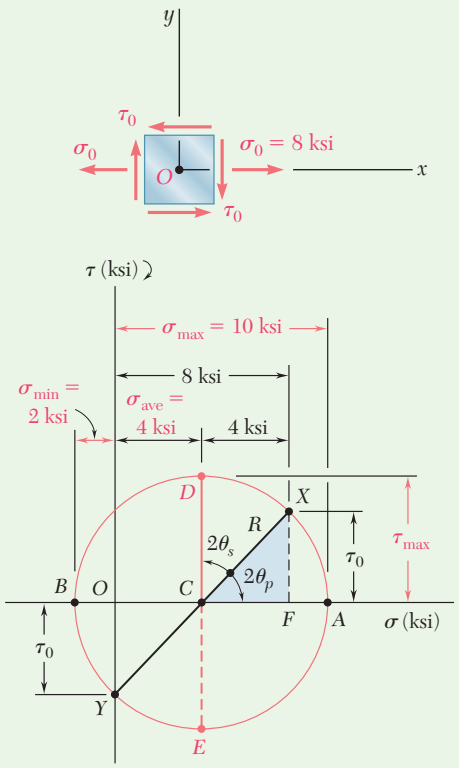


Fig. 1 Mohr's circle for given state of stress.

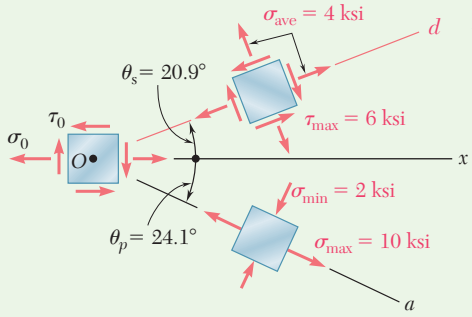


Fig. 2 Orientation of principal and maximum shearing stress planes for assumed sense of τ_0.

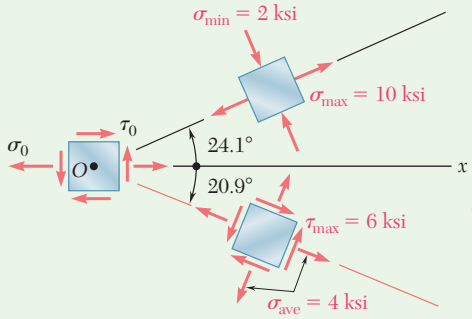


Fig. 3 Orientation of principal and maximum shearing stress planes for opposite sense of τ_0.

Sample Problem 7.3

A state of plane stress consists of a tensile stress $\sigma_0 = 8$ ksi exerted on vertical surfaces and of unknown shearing stresses. Determine (*a*) the magnitude of the shearing stress τ_0 for which the largest normal stress is 10 ksi, (*b*) the corresponding maximum shearing stress.

STRATEGY: You can use the normal stresses on the given element to determine the average normal stress, thereby establishing the center of Mohr's circle. Knowing that the given maximum normal stress is also a principal stress, you can use this to complete the construction of the circle.

MODELING and ANALYSIS:

Construction of Mohr's Circle (Fig.1). Assume that the shearing stresses act in the senses shown. Thus, the shearing stress τ_0 on a face perpendicular to the x axis tends to rotate the element clockwise, and point X of coordinates 8 ksi and τ_0 is plotted above the horizontal axis. Considering a horizontal face of the element, $\sigma_y = 0$ and τ_0 tends to rotate the element counterclockwise. Thus, Y is plotted at a distance τ_0 below O.

The abscissa of the center C of Mohr's circle is

$$\sigma_{ave} = \tfrac{1}{2}(\sigma_x + \sigma_y) = \tfrac{1}{2}(8 + 0) = 4 \text{ ksi}$$

The radius R of the circle is found by observing that $\sigma_{max} = 10$ ksi and is represented by the abscissa of point A:

$$\sigma_{max} = \sigma_{ave} + R$$
$$10 \text{ ksi} = 4 \text{ ksi} + R \qquad R = 6 \text{ ksi}$$

a. Shearing Stress τ_0. Considering the right triangle CFX,

$$\cos 2\theta_p = \frac{CF}{CX} = \frac{CF}{R} = \frac{4 \text{ ksi}}{6 \text{ ksi}} \qquad 2\theta_p = 48.2^\circ \text{ ⤵} \qquad \theta_p = 24.1^\circ \text{ ⤵}$$
$$\tau_0 = FX = R \sin 2\theta_p = (6 \text{ ksi}) \sin 48.2^\circ \qquad \tau_0 = 4.47 \text{ ksi}$$

b. Maximum Shearing Stress. The coordinates of point D of Mohr's circle represent the maximum shearing stress and the corresponding normal stress.

$$\tau_{max} = R = 6 \text{ ksi} \qquad \tau_{max} = 6 \text{ ksi}$$
$$2\theta_s = 90^\circ - 2\theta_p = 90^\circ - 48.2^\circ = 41.8^\circ \text{ ↰} \qquad \theta_x = 20.9^\circ \text{ ↰}$$

The maximum shearing stress is exerted on an element that is oriented as shown in Fig. 2. (The element upon which the principal stresses are exerted is also shown.)

REFLECT and THINK. If our original assumption regarding the sense of τ_0 was reversed, we would obtain the same circle and the same answers, but the orientation of the elements would be as shown in Fig. 3.

Problems

7.31 Solve Probs. 7.5 and 7.9, using Mohr's circle.

7.32 Solve Probs. 7.7 and 7.11, using Mohr's circle.

7.33 Solve Prob. 7.10, using Mohr's circle.

7.34 Solve Prob. 7.12, using Mohr's circle.

7.35 Solve Prob. 7.13, using Mohr's circle.

7.36 Solve Prob. 7.14, using Mohr's circle.

7.37 Solve Prob. 7.15, using Mohr's circle.

7.38 Solve Prob. 7.16, using Mohr's circle.

7.39 Solve Prob. 7.17, using Mohr's circle.

7.40 Solve Prob. 7.18, using Mohr's circle.

7.41 Solve Prob. 7.19, using Mohr's circle.

7.42 Solve Prob. 7.20, using Mohr's circle.

7.43 Solve Prob. 7.21, using Mohr's circle.

7.44 Solve Prob. 7.22, using Mohr's circle.

7.45 Solve Prob. 7.23, using Mohr's circle.

7.46 Solve Prob. 7.24, using Mohr's circle.

7.47 Solve Prob. 7.25, using Mohr's circle.

7.48 Solve Prob. 7.26, using Mohr's circle.

7.49 Solve Prob. 7.27, using Mohr's circle.

7.50 Solve Prob. 7.28, using Mohr's circle.

7.51 Solve Prob. 7.29, using Mohr's circle.

7.52 Solve Prob. 7.30, using Mohr's circle.

7.53 Solve Prob. 7.29, using Mohr's circle and assuming that the weld forms an angle of 60° with the horizontal.

7.54 and 7.55 Determine the principal planes and the principal stresses for the state of plane stress resulting from the superposition of the two states of stress shown.

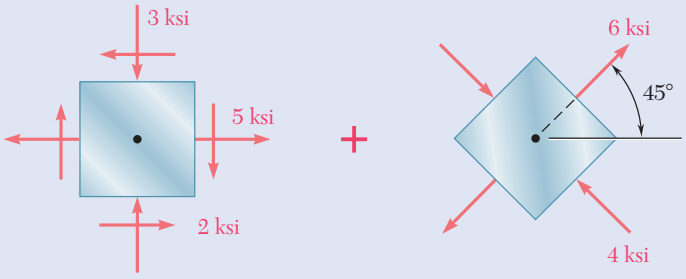


Fig. *P7.54*

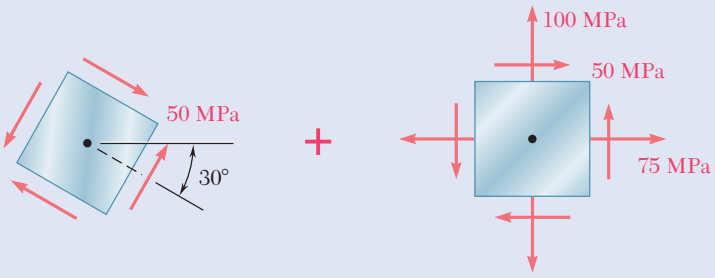


Fig. P7.55

7.56 and 7.57 Determine the principal planes and the principal stresses for the state of plane stress resulting from the superposition of the two states of stress shown.

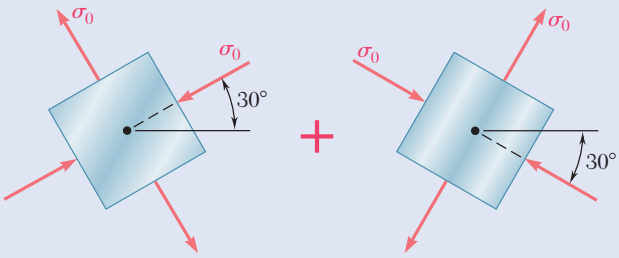


Fig. P7.56

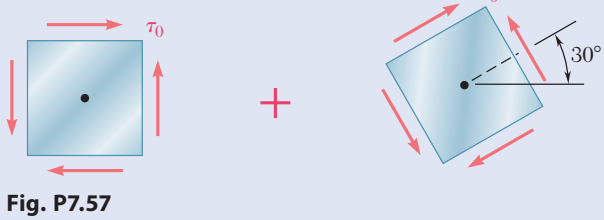


Fig. P7.57

7.58 For the element shown, determine the range of values of τ_{xy} for which the maximum tensile stress is equal to or less than 60 MPa.

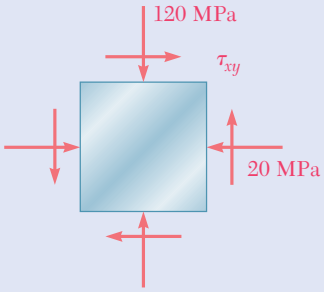


Fig. P7.58 and P7.59

7.59 For the element shown, determine the range of values of τ_{xy} for which the maximum in-plane shearing stress is equal to or less than 150 MPa.

7.60 For the state of stress shown, determine the range of values of θ for which the magnitude of the shearing stress $\tau_{x'y'}$ is equal to or less than 8 ksi.

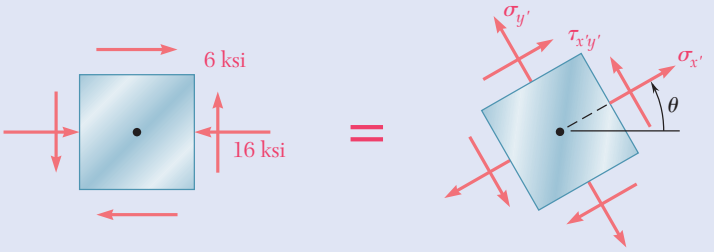


Fig. *P7.60*

7.61 For the state of stress shown, determine the range of values of θ for which the normal stress $\sigma_{x'}$ is equal to or less than 50 MPa.

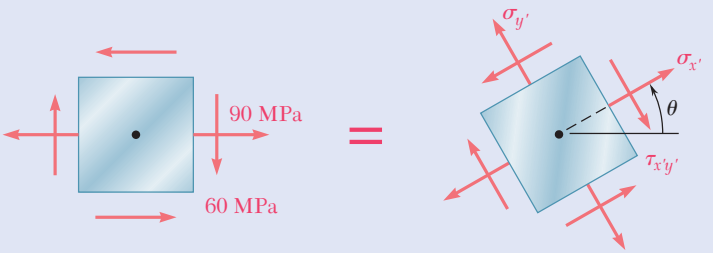


Fig. P7.61 and P7.62

7.62 For the state of stress shown, determine the range of values of θ for which the normal stress $\sigma_{x'}$ is equal to or less than 100 MPa.

7.63 For the state of stress shown, it is known that the normal and shearing stresses are directed as shown and that $\sigma_x = 14$ ksi, $\sigma_y = 9$ ksi, and $\sigma_{\min} = 5$ ksi. Determine (*a*) the orientation of the principal planes, (*b*) the principal stress $\sigma_{\max}$, (*c*) the maximum in-plane shearing stress.

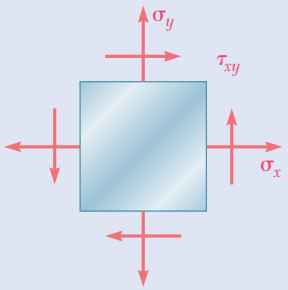


Fig. P7.63

7.64 The Mohr's circle shown corresponds to the state of stress given in Fig. 7.5*a* and *b*. Noting that $\sigma_{x'} = OC + (CX') \cos (2\theta_p - 2\theta)$ and that $\tau_{x'y'} = (CX') \sin (2\theta_p - 2\theta)$, derive the expressions for $\sigma_{x'}$ and $\tau_{x'y'}$ given in Eqs. (7.5) and (7.6), respectively. [*Hint:* Use $\sin (A + B) = \sin A \cos B + \cos A \sin B$ and $\cos (A + B) = \cos A \cos B - \sin A \sin B$.]

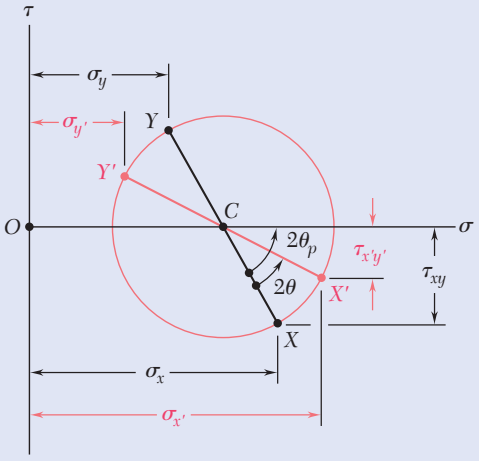


Fig. P7.64

7.65 (*a*) Prove that the expression $\sigma_{x'}\sigma_{y'} - \tau^2_{x'y'}$, where $\sigma_{x'}$, $\sigma_{y'}$, and $\tau_{x'y'}$ are components of the stress along the rectangular axes x' and y', is independent of the orientation of these axes. Also, show that the given expression represents the square of the tangent drawn from the origin of the coordinates to Mohr's circle. (*b*) Using the invariance property established in part *a*, express the shearing stress τ_{xy} in terms of σ_x, σ_y, and the principal stresses $\sigma_{\max}$ and $\sigma_{\min}$.

7.3 GENERAL STATE OF STRESS

In the preceding sections, we have assumed a state of plane stress with $\sigma_z = \tau_{zx} = \tau_{zy} = 0$, and have considered only transformations of stress associated with a rotation about the z axis. We will now consider the general state of stress represented in Fig. 7.1*a* and the transformation of stress associated with the rotation of axes shown in Fig. 7.1*b*. However, our analysis will be limited to the determination of the *normal stress* σ_n on a plane of arbitrary orientation.

Three of the faces in the tetrahedron shown in Fig. 7.19 are parallel to the coordinate planes, while the fourth face, *ABC*, is perpendicular to the line *QN*. Denoting the area of face *ABC* as ΔA and the direction cosines of line *QN* as λ_x, λ_y, λ_z, the areas of the faces perpendicular to the x, y, and z axes are $(\Delta A)\lambda_x$, $(\Delta A)\lambda_y$, and $(\Delta A)\lambda_z$. If the state of stress at point Q is defined by the stress components σ_x, σ_y, σ_z, τ_{xy}, τ_{yz}, and τ_{zx}, the *forces* exerted on the faces parallel to the coordinate planes are obtained by multiplying the appropriate stress components by the area of each face (Fig. 7.20). On the other hand, the forces exerted on face *ABC* consist of a normal force of magnitude $\sigma_n \Delta A$ directed along *QN* and a shearing force with a magnitude $\tau \Delta A$ perpendicular to *QN* but of unknown direction. Since *QBC*, *QCA*, and *QAB* face the negative x, y, and z axes respectively, the forces exerted must be shown with negative senses.

The sum of the components along *QN* of all the forces acting on the tetrahedron is zero. The component along *QN* of a force parallel to the x axis is obtained by multiplying the magnitude of that force by the direction cosine λ_x. The components of forces parallel to the y and z axes are obtained in a similar way. Thus,

$$\begin{aligned}\Sigma F_n = 0: \quad & \sigma_n \Delta A - (\sigma_x \Delta A\, \lambda_x)\lambda_x - (\tau_{xy} \Delta A\, \lambda_x)\lambda_y - (\tau_{xz} \Delta A\, \lambda_x)\lambda_z \\ & -(\tau_{yx} \Delta A\, \lambda_y)\lambda_x - (\sigma_y \Delta A\, \lambda_y)\lambda_y - (\tau_{yz} \Delta A\, \lambda_y)\lambda_z \\ & -(\tau_{zx} \Delta A\, \lambda_z)\lambda_x - (\tau_{zy} \Delta A\, \lambda_z)\lambda_y - (\sigma_z \Delta A\, \lambda_z)\lambda_z = 0\end{aligned}$$

Dividing through by ΔA and solving for σ_n gives

$$\sigma_n = \sigma_x\lambda_x^2 + \sigma_y\lambda_y^2 + \sigma_z\lambda_z^2 + 2\tau_{xy}\lambda_x\lambda_y + 2\tau_{yz}\lambda_y\lambda_z + 2\tau_{zx}\lambda_z\lambda_x \quad \textbf{(7.20)}$$

Note that the equation for the normal stress σ_n is a *quadratic form* in λ_x, λ_y, and λ_z. The coordinate axes are found when the right-hand member of Eq. (7.20) reduces to the three terms containing the squares of the direction cosines.[†] Calling these axes a, b, and c, the corresponding normal stresses σ_a, σ_b, and σ_c, and the direction cosines of *QN* with respect to these axes λ_a, λ_b, and λ_c, gives

$$\sigma_n = \sigma_a\lambda_a^2 + \sigma_b\lambda_b^2 + \sigma_c\lambda_c^2 \quad \textbf{(7.21)}$$

[†]In Sec. 9.16 of F. P. Beer and E. R. Johnston, *Vector Mechanics for Engineers*, 10th ed., McGraw-Hill Book Company, 2013, a similar quadratic form is found to represent the moment of inertia of a rigid body with respect to an arbitrary axis. It is shown in Sec. 9.17 that this form is associated with a *quadric surface* and reducing the quadratic form to terms containing only the squares of the direction cosines is equivalent to determining the principal axes of that surface.

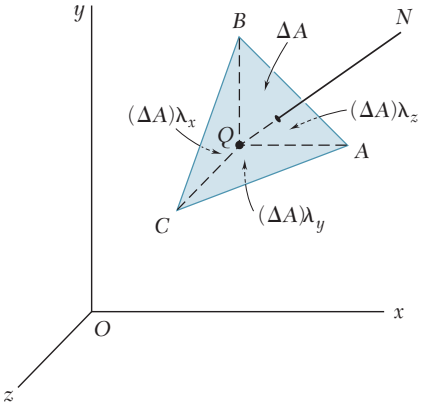


Fig. 7.19 Stress tetrahedron at point *Q* with three faces parallel to the coordinate planes.

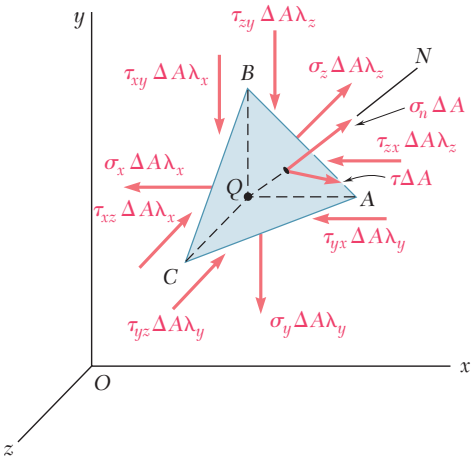


Fig. 7.20 Free-body diagram of stress tetrahedron at point *Q*.

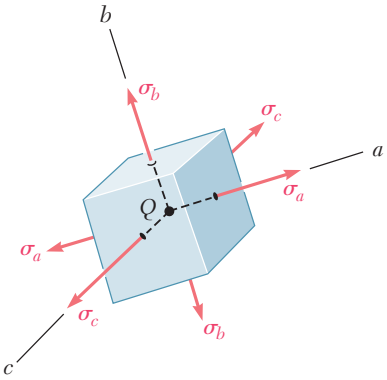


Fig. 7.21 General stress element oriented to principal axes.

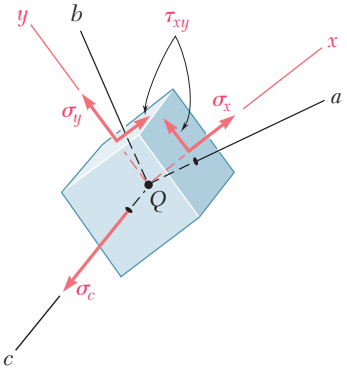


Fig. 7.22 Stress element rotated about *c* axis.

The coordinate axes *a*, *b*, *c* are the *principal axes of stress*. Since their orientation depends upon the state of stress at *Q* and thus upon the position of *Q*, these axes are represented in Fig. 7.21 as attached to *Q*. The corresponding coordinate planes are known as the *principal planes of stress*, and the corresponding normal stresses σ_a, σ_b, and σ_c are the *principal stresses* at *Q*.[†]

7.4 THREE-DIMENSIONAL ANALYSIS OF STRESS

If the element in Fig. 7.21 is rotated about one of the principal axes at *Q*, say the *c* axis (Fig. 7.22), the corresponding transformation of stress can be analyzed using Mohr's circle as a transformation of plane stress. The shearing stresses exerted on the faces perpendicular to the *c* axis remain equal to zero. The normal stress σ_c is perpendicular to the plane *ab* where the transformation takes place and does not affect this transformation. Therefore, the circle of diameter *AB* is used to determine the normal and shearing stresses exerted on the faces of the element as it is rotated about the *c* axis (Fig. 7.23). Similarly, circles of diameter *BC* and *CA* can be used to determine the stresses on the element as it is rotated about the *a* and *b* axes, respectively. While this analysis is limited to rotations about the principal axes, it could be shown that any other transformation of axes would lead to stresses represented in Fig. 7.23 by a point located within

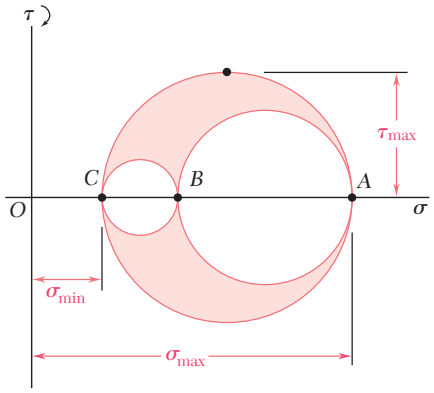


Fig. 7.23 Mohr's circles for general state of stress.

the shaded area. Thus, the radius of the largest circle yields the maximum value of the shearing stress at point *Q*. Noting that the diameter of that circle is equal to the difference between σ_{max} and σ_{min},

$$\tau_{max} = \tfrac{1}{2}|\sigma_{max} - \sigma_{min}| \tag{7.22}$$

where σ_{max} and σ_{min} represent the *algebraic* values of the maximum and minimum stresses at point *Q*.

[†]For a discussion of the determination of the principal planes of stress and of the principal stresses, see S. P. Timoshenko and J. N. Goodier, *Theory of Elasticity*, 3d ed., McGraw-Hill Book Company, 1970, Sec. 77.

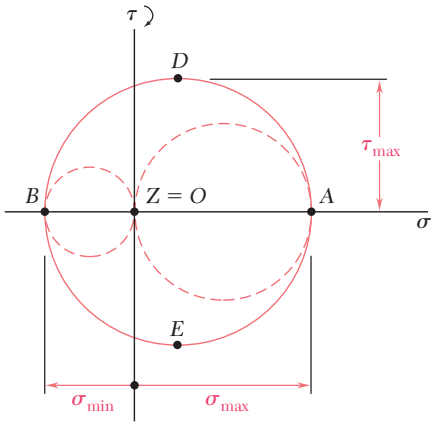


Fig. 7.24 Three-dimensional Mohr's circles for state of plane stress where $\sigma_a > 0 > \sigma_b$.

Recall that in *plane stress*, if the x and y axes are selected, we have $\sigma_z = \tau_{zx} = \tau_{zy} = 0$. This means that the z axis (i.e., the axis perpendicular to the plane of stress) is one of the three principal axes of stress. In a Mohr-circle diagram, this axis corresponds to the origin O, where $\sigma = \tau = 0$. The other two principal axes correspond to points A and B where Mohr's circle for the xy plane intersects the σ axis. If A and B are located on opposite sides of the origin O (Fig. 7.24), the corresponding principal stresses represent the maximum and minimum normal stresses at point Q, and the maximum shearing stress is equal to the maximum "in-plane" shearing stress. Recall that in Sec. 7.1B the planes of maximum shearing stress correspond to points D and E of Mohr's circle and are at 45° to the principal planes corresponding to points A and B. These are shown in the shaded diagonal planes of Figs. 7.25*a* and *b*.

However, if A and B are on the same side of O, where σ_a and σ_b have the same sign, the circle defining $\sigma_{\max}$, $\sigma_{\min}$, and $\tau_{\max}$ is *not* the circle corresponding to a transformation of stress within the xy plane. If $\sigma_a > \sigma_b > 0$, as assumed in Fig. 7.26, $\sigma_{\max} = \sigma_a$, $\sigma_{\min} = 0$, and $\tau_{\max}$ is equal to the radius of the circle defined by points O and A. Thus, $\tau_{\max} = \frac{1}{2}\sigma_{\max}$. The normals Qd' and Qe' to the planes of maximum shearing stress are obtained by rotating the axis Qa through 45° within the za plane. These planes of maximum shearing stress are shown in the shaded diagonal planes of Figs. 7.27*a* and *b*.

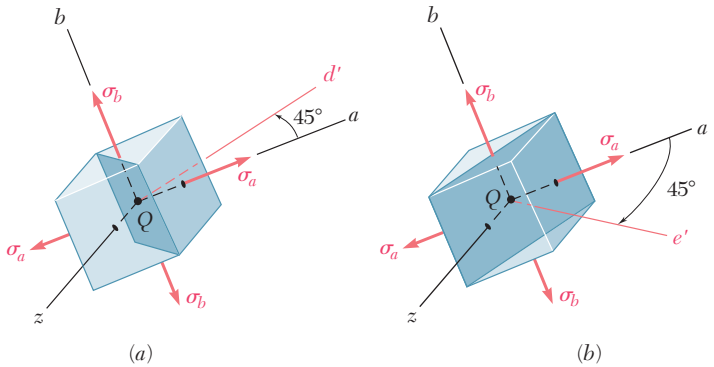


Fig. 7.27 Out-of-plane of maximum shearing stress for plane stress element. (*a*) 45° counterclockwise from principal axis *a*. (*b*) 45° clockwise from principal axis *a*.

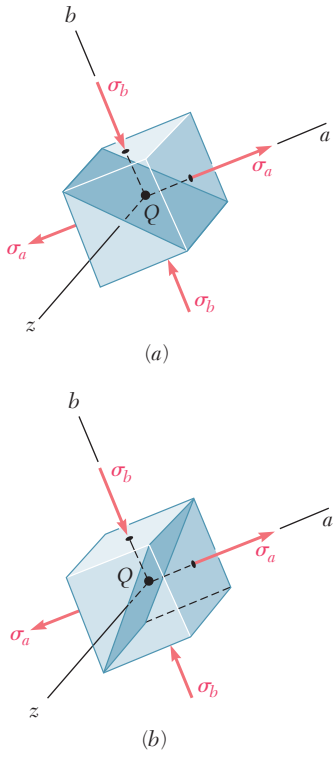


Fig. 7.25 In-plane maximum shearing stress for an element having a principal axis aligned with the z-axis. (*a*) 45° clockwise from principal axis *a*. (*b*) 45° counterclockwise from principal axis *a*.

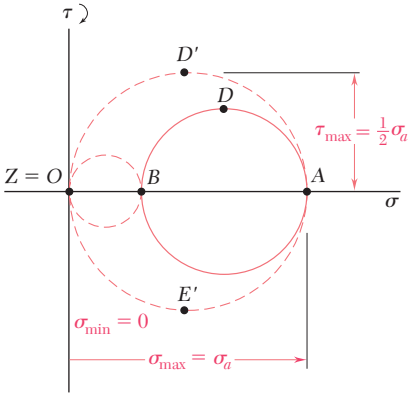


Fig. 7.26 Three-dimensional Mohr's circles for state of plane stress where $\sigma_a > \sigma_b > 0$.

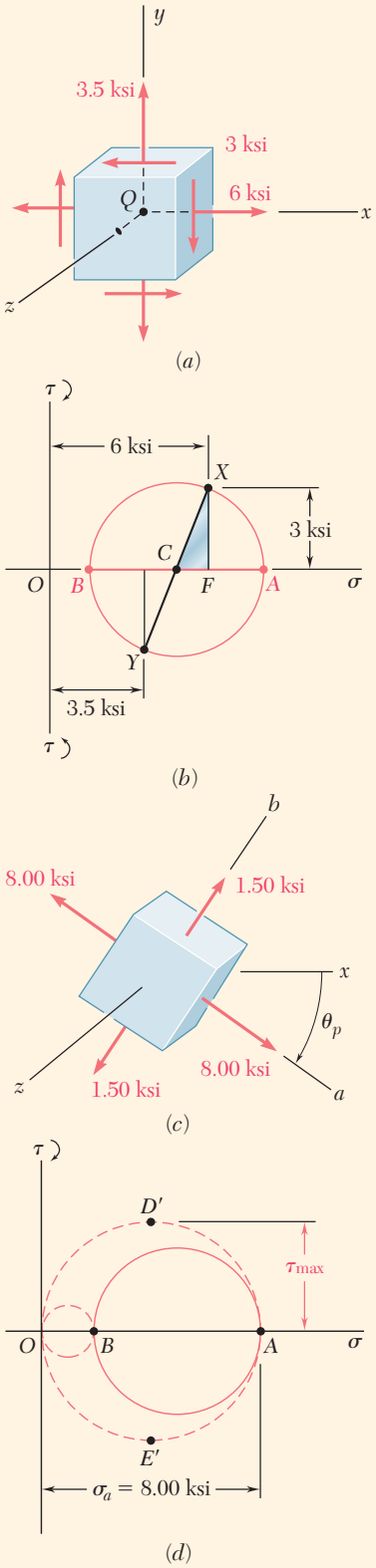


Fig. 7.28 (*a*) Plane stress element. (*b*) Mohr's circle for stress transformation in *xy* plane. (*c*) Orientation of principal stresses. (*d*) Three-dimensional Mohr's circles.

Concept Application 7.3

For the state of plane stress shown in Fig. 7.28*a*, determine (*a*) the three principal planes and principal stresses and (*b*) the maximum shearing stress.

a. Principal Planes and Principal Stresses. Construct Mohr's circle for the transformation of stress in the *xy* plane (Fig. 7.28*b*). Point *X* is plotted 6 units to the right of the τ axis and 3 units above the σ axis (since the corresponding shearing stress tends to rotate the element clockwise). Point *Y* is plotted 3.5 units to the right of the τ axis and 3 units below the σ axis. Drawing the line *XY*, the center *C* of Mohr's circle is found for the *xy* plane. Its abscissa is

$$\sigma_{\text{ave}} = \frac{\sigma_x + \sigma_y}{2} = \frac{6 + 3.5}{2} = 4.75 \text{ ksi}$$

Since the sides of the right triangle *CFX* are $CF = 6 - 4.75 = 1.25$ ksi and $FX = 3$ ksi, the radius of the circle is

$$R = CX = \sqrt{(1.25)^2 + (3)^2} = 3.25 \text{ ksi}$$

The principal stresses in the plane of stress are

$$\sigma_a = OA = OC + CA = 4.75 + 3.25 = 8.00 \text{ ksi}$$
$$\sigma_b = OB = OC - BC = 4.75 - 3.25 = 1.50 \text{ ksi}$$

Since the faces of the element perpendicular to the *z* axis are free of stress, they define one of the principal planes, and the corresponding principal stress is $\sigma_z = 0$. The other two principal planes are defined by points *A* and *B* on Mohr's circle. The angle θ_p through which the element should be rotated about the *z* axis to bring its faces to coincide with these planes (Fig. 7.28*c*) is half the angle *ACX*.

$$\tan 2\theta_p = \frac{FX}{CF} = \frac{3}{1.25}$$
$$2\theta_p = 67.4^\circ \circlearrowright \qquad \theta_p = 33.7^\circ \circlearrowright$$

b. Maximum Shearing Stress. Now draw the circles of diameter *OB* and *OA* that correspond to rotations of the element about the *a* and *b* axes (Fig. 7.28*d*). Note that the maximum shearing stress is equal to the radius of the circle of diameter *OA*. Thus,

$$\tau_{\max} = \tfrac{1}{2}\sigma_a = \tfrac{1}{2}(8.00 \text{ ksi}) = 4.00 \text{ ksi}$$

Since points D' and E', which define the planes of maximum shearing stress, are located at the ends of the vertical diameter of the circle corresponding to a rotation about the *b* axis, the faces of the element of Fig. 7.28*c* can be brought to coincide with the planes of maximum shearing stress through a rotation of 45° about the *b* axis.

*7.5 THEORIES OF FAILURE

7.5A Yield Criteria for Ductile Materials

Structural elements and machine components made of a ductile material are usually designed so that the material will not yield under the expected loading conditions. When the element or component is under uniaxial stress (Fig. 7.29), the value of the normal stress σ_x that causes the material to yield is obtained from a tensile test of the same material, since the test specimen and the structural element or machine component are in the same state of stress. Thus, regardless of the actual mechanism that causes the material to yield, the element or component will be safe as long as $\sigma_x < \sigma_Y$, where σ_Y is the yield strength of the test specimen.

On the other hand, when a structural element or machine component is in a state of plane stress (Fig. 7.30*a*), it is convenient to use one of the methods developed earlier to determine the principal stresses σ_a and σ_b at any given point (Fig. 7.30*b*). The material can then be considered to be in a state of biaxial stress at that point. Since this state is different from the state of uniaxial stress, it is not possible to predict from such a test whether or not the structural element or machine component under investigation will fail. Some criterion regarding the actual mechanism of failure of the material must be established that will make it possible to compare the effects of both states of stress. The purpose of this section is to present the two yield criteria most frequently used for ductile materials.

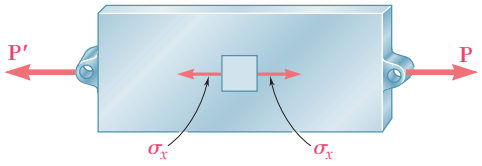
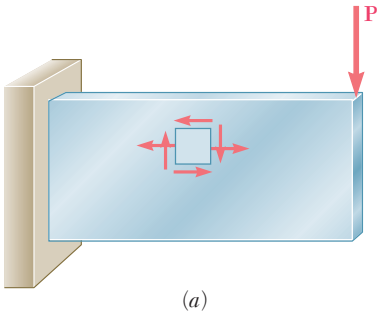
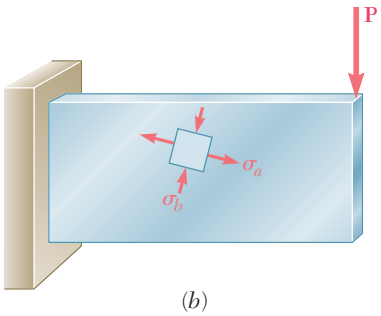


Fig. 7.29 Structural element under uniaxial stress.



(*a*)



(*b*)

Fig. 7.30 Structural element in a state of plane stress. (*a*) Stress element referred to coordinate axes. (*b*) Stress element referred to principal axes.

Maximum-Shearing-Stress Criterion. This criterion is based on the observation that yield in ductile materials is caused by slippage of the material along oblique surfaces and is due primarily to shearing stresses (see. Sec. 2.1B). According to this criterion, a structural component is safe as long as the maximum value $\tau_{\max}$ of the shearing stress in that component remains smaller than the corresponding shearing stress in a tensile-test specimen of the same material as the specimen starts to yield.

Recalling from Sec. 1.3 that the maximum value of the shearing stress under a centric axial load is equal to half the value of the corresponding normal stress, we conclude that the maximum shearing stress in a tensile-test specimen is $\frac{1}{2}\sigma_Y$ as the specimen starts to yield. On the other hand, Sec. 7.4 showed, for plane stress, that $\tau_{\max}$ of the shearing stress is equal to $\frac{1}{2}|\sigma_{\max}|$ if the principal stresses are either both positive or both negative and to $\frac{1}{2}|\sigma_{\max} - \sigma_{\min}|$ if the maximum stress is positive and the minimum stress is negative. Thus, if the principal stresses σ_a and σ_b have the same sign, the maximum-shearing-stress criterion gives

$$|\sigma_a| < \sigma_Y \qquad |\sigma_b| < \sigma_Y \tag{7.23}$$

If the principal stresses σ_a and σ_b have opposite signs, the maximum-shearing-stress criterion yields

$$|\sigma_a - \sigma_b| < \sigma_Y \tag{7.24}$$

These relationships have been represented graphically in Fig. 7.31. Any given state of stress is represented by a point of coordinates σ_a and σ_b, where σ_a and σ_b are the two principal stresses. If this point falls within the area shown, the structural component is safe. If it falls outside this area,

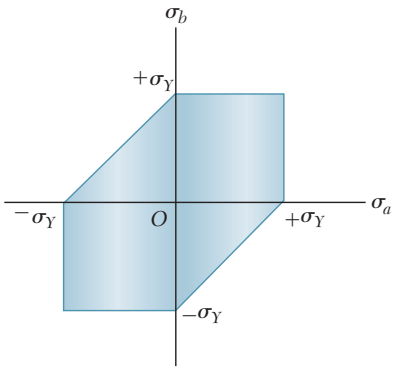


Fig. 7.31 Tresca's hexagon for maximum-shearing-stress criterion.

the component fails as a result of yield in the material. The hexagon associated with the initiation of yield is known as *Tresca's hexagon* after the French engineer Henri Edouard Tresca (1814–1885).

Maximum-Distortion-Energy Criterion. This criterion is based on the determination of the distortion energy in a given material. This is the energy associated with changes in shape in that material (as opposed to the energy associated with changes in volume in the same material). This criterion is also known as the *von Mises criterion* after the German-American applied mathematician Richard von Mises (1883–1953). Here, a given structural component is safe as long as the maximum value of the distortion energy per unit volume in that material remains smaller than the distortion energy per unit volume required to cause yield in a tensile-test specimen of the same material. The distortion energy per unit volume in an isotropic material under plane stress is

$$u_d = \frac{1}{6G}(\sigma_a^2 - \sigma_a\sigma_b + \sigma_b^2) \tag{7.25}$$

where σ_a and σ_b are the principal stresses and G is the modulus of rigidity. In a tensile-test specimen that is starting to yield, $\sigma_a = \sigma_Y$, $\sigma_b = 0$, and $(u_d)_Y = \sigma_Y^2/6G$. Thus, the maximum-distortion-energy criterion indicates that the structural component is safe as long as $u_d < (u_d)_Y$, or

$$\sigma_a^2 - \sigma_a\sigma_b + \sigma_b^2 < \sigma_Y^2 \tag{7.26}$$

where the point of coordinates σ_a and σ_b falls within the area shown in Fig. 7.32. This area is bounded by the ellipse

$$\sigma_a^2 - \sigma_a\sigma_b + \sigma_b^2 = \sigma_Y^2 \tag{7.27}$$

which intersects the coordinate axes at $\sigma_a = \pm\sigma_Y$ and $\sigma_b = \pm\sigma_Y$. The major axis of the ellipse bisects the first and third quadrants and extends from A ($\sigma_a = \sigma_b = \sigma_Y$) to B ($\sigma_a = \sigma_b = -\sigma_Y$), while its minor axis extends from C ($\sigma_a = -\sigma_b = -0.577\sigma_Y$) to D ($\sigma_a = -\sigma_b = 0.577\sigma_Y$).

The maximum-shearing-stress criterion and the maximum-distortion-energy criterion are compared in Fig. 7.33. The ellipse passes through the vertices of the hexagon. Thus, for the states of stress represented by these six points, the two criteria give the same results. For any other state of stress, the maximum-shearing-stress criterion is more conservative than the maximum-distortion-energy criterion, since the hexagon is located within the ellipse.

A state of stress of particular interest is associated with yield in a torsion test. Recall from Fig. 7.18 that, for torsion, $\sigma_{\min} = -\sigma_{\max}$. Thus, the corresponding points in Fig. 7.33 are located on the bisector of the second and fourth quadrants. It follows that yield occurs in a torsion test when $\sigma_a = -\sigma_b = \pm 0.5\sigma_Y$ according to the maximum-shearing-stress criterion and $\sigma_a = -\sigma_b = \pm 0.577\sigma_Y$ according to the maximum-distortion-energy criterion. But again recalling Fig. 7.18, σ_a and σ_b must be equal in magnitude to $\tau_{\max}$, which is obtained from a torsion test for the yield strength τ_Y of the material. Since the yield strength σ_Y in tension and τ_Y in shear are given for various ductile materials in Appendix B, the ratio τ_Y/σ_Y can be determined for these materials where the range is from 0.55 to 0.60. Thus, the maximum-distortion-energy criterion appears somewhat more accurate than the maximum-shearing-stress criterion for predicting yield in torsion.

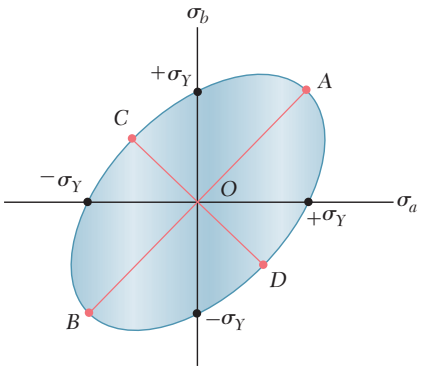


Fig. 7.32 Von Mises surface based on maximum-distortion-energy criterion.

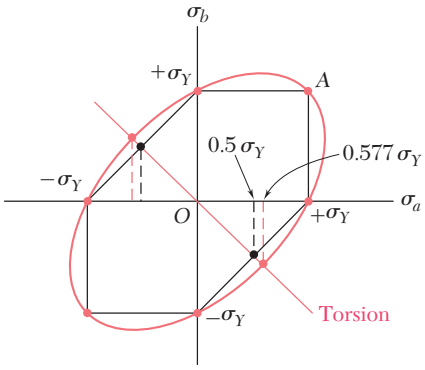


Fig. 7.33 Comparison of Tresca and von Mises criteria.

7.5B Fracture Criteria for Brittle Materials Under Plane Stress

When brittle materials are subjected to a tensile test, they fail suddenly through rupture—or fracture—without any prior yielding. When a structural element or machine component made of a brittle material is under uniaxial tensile stress, the normal stress that causes it to fail is equal to the ultimate strength σ_U as determined from a tensile test, since both the specimen and the element or component are in the same state of stress. However, when a structural element or machine component is in a state of plane stress, it is found convenient to determine the principal stresses σ_a and σ_b at any given point and to use one of the criteria presented in this section to predict whether or not the structural element or machine component will fail.

Maximum-Normal-Stress Criterion. According to this criterion, a given structural component fails when the maximum normal stress reaches the ultimate strength σ_U obtained from the tensile test of a specimen of the same material. Thus, the structural component will be safe as long as the absolute values of the principal stresses σ_a and σ_b are both less than σ_U:

$$|\sigma_a| < \sigma_U \qquad |\sigma_b| < \sigma_U \tag{7.28}$$

The maximum-normal-stress criterion is shown graphically in Fig. 7.34. If the point obtained by plotting the values σ_a and σ_b of the principal stresses falls within the square area shown, the structural component is safe. If it falls outside that area, the component will fail.

The maximum-normal-stress criterion is known as *Coulomb's criterion* after the French physicist Charles Augustin de Coulomb (1736–1806). This criterion suffers from an important shortcoming: it is based on the assumption that the ultimate strength of the material is the same in tension and in compression. As noted in Sec. 2.1B, this is seldom the case because the presence of flaws in the material, such as microscopic cracks or cavities, tends to weaken the material in tension, while not appreciably affecting its resistance to compressive failure. This criterion also makes no allowance for effects other than those of the normal stresses on the failure mechanism of the material.†

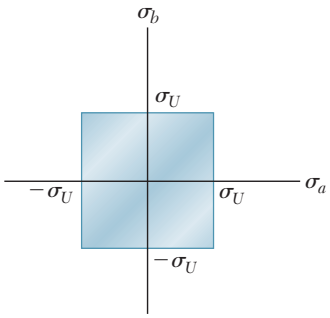


Fig. 7.34 Coulomb's surface for maximum-normal-stress criterion.

†Another failure criterion known as the *maximum-normal-strain criterion,* or Saint-Venant's criterion, was widely used during the nineteenth century. According to this criterion, a given structural component is safe as long as the maximum value of the normal strain in that component remains smaller than the value ϵ_U of the strain at which a tensile-test specimen of the same material will fail. But, as will be shown in Sec. 7.8, the strain is maximum along one of the principal axes of stress, if the deformation is elastic and the material homogeneous and isotropic. Thus, denoting by ϵ_a and ϵ_b the values of the normal strain along the principal axes in the plane of stress, we write

$$|\epsilon_a| < \epsilon_U \qquad |\epsilon_b| < \epsilon_U \tag{7.29}$$

Making use of the generalized Hooke's law (Sec. 2.5), we could express these relations in terms of the principal stresses σ_a and σ_b and the ultimate strength σ_U of the material. We would find that, according to the maximum-normal-strain criterion, the structural component is safe as long as the point obtained by plotting σ_a and σ_b falls within the area shown in Fig. 7.35, where ν is Poisson's ratio for the given material.

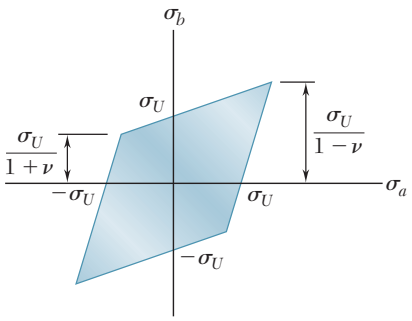


Fig. 7.35 Saint-Venant's surface for maximum-normal-strain criterion.

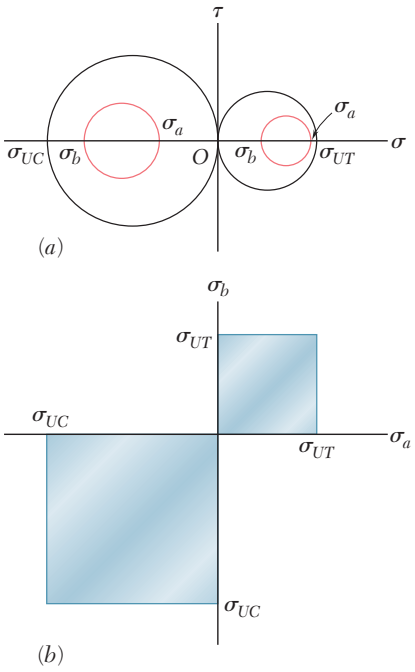


Fig. 7.36 Mohr's criterion for brittle materials having different ultimate strengths in tension and compression. (*a*) Mohr's circles for uniaxial compression (left) and tension (right) tests at rupture. (*b*) Safe stress states when σ_a and σ_b have the same sign.

Mohr's Criterion. Suggested by the German engineer Otto Mohr, this criterion is used to predict the effect of a given state of plane stress on a brittle material when the results of various types of tests are available.

Assume that tensile compressive tests have been conducted on a given material and that σ_{UT} and σ_{UC} of the ultimate strength in tension and compression have been determined. The state of stress corresponding to the rupture of the tensile-test specimen is represented on a Mohr-circle diagram where the circle intersects the horizontal axis at O and σ_{UT} (Fig. 7.36*a*). Similarly, the state of stress corresponding to the failure of the compressive-test specimen is represented by the circle intersecting the horizontal axis at O and σ_{UC}. Clearly, a state of stress represented by a circle entirely contained in either of these circles will be safe. Thus, if both principal stresses are positive, the state of stress is safe as long as $\sigma_a < \sigma_{UT}$ and $\sigma_b < \sigma_{UT}$. If both principal stresses are negative, the state of stress is safe as long as $|\sigma_a| < |\sigma_{UC}|$ and $|\sigma_b| < |\sigma_{UC}|$. Plotting the point of coordinates σ_a and σ_b (Fig. 7.36*b*), the state of stress is safe as long as that point falls within one of the square areas shown in that figure.

In order to analyze σ_a and σ_b when they have opposite signs, assume that a torsion test has been conducted on the material and that its ultimate strength in shear, τ_U, has been determined. Drawing the circle centered at O representing the state of stress corresponding to the failure of the torsion-test specimen (Fig. 7.37*a*), observe that any state of stress represented by a circle entirely contained in that circle is also safe. According to Mohr's criterion, a state of stress is safe if it is represented by a circle located entirely within the area bounded by the envelope of the circles corresponding to the available data. The remaining portions of the principal-stress diagram are obtained by drawing various circles tangent to this envelope, determining the corresponding values of σ_a and σ_b, and plotting the points of coordinates σ_a and σ_b (Fig. 7.37*b*).

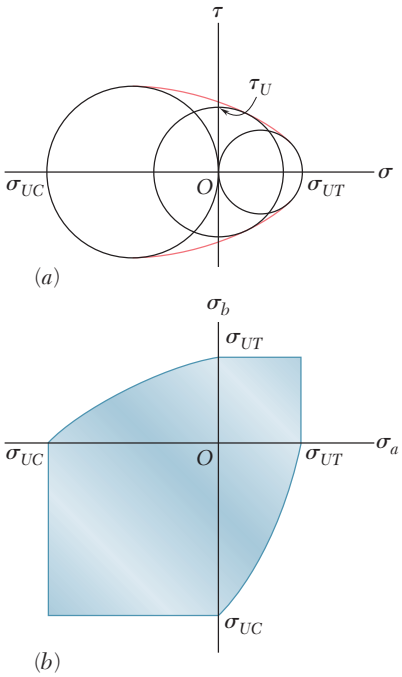


Fig. 7.37 Mohr's criterion for brittle materials. (*a*) Mohr's circles for uniaxial compression (left), torsion (middle), and uniaxial tension (right) tests at rupture. (*b*) Envelope of safe stress states.

More accurate diagrams can be drawn when test results corresponding to various states of stress are available. If the only available data consists of the ultimate strengths σ_{UT} and σ_{UC}, the envelope in Fig. 7.37*a* is replaced by the tangents AB and $A'B'$ to the circles corresponding to failure in tension and compression (Fig. 7.38*a*). From the similar triangles in Fig. 7.38, the abscissa of the center C of a circle tangent to AB and $A'B'$ is linearly related to its radius R. Since $\sigma_a = OC + R$ and $\sigma_b = OC - R$, σ_a and σ_b are also related linearly. Thus, the shaded area corresponding to this simplified Mohr's criterion is bounded by straight lines in the second and fourth quadrants (Fig. 7.38*b*).

In order to determine whether a structural component is safe under a given load, the state of stress should be calculated at all critical points of the component (i.e., where stress concentrations are likely to occur). This can be done by using the stress-concentration factors given in Figs. 2.52, 3.28, 4.24, and 4.25. However, there are many instances when the theory of elasticity must be used to determine the state of stress at a critical point.

Special care should be taken when *macroscopic cracks* are detected in a structural component. While it can be assumed that the test specimen used to determine the ultimate tensile strength of the material contained the same type of flaws (i.e., *microscopic* cracks or cavities) as the structural component, the specimen was certainly free of any noticeable macroscopic cracks. When a crack is detected in a structural component, it is necessary to determine whether that crack will propagate under the expected load and cause the component to fail or will remain stable. This requires an analysis involving the energy associated with the growth of the crack. Such an analysis is beyond the scope of this text and should be carried out using by the methods of fracture mechanics.

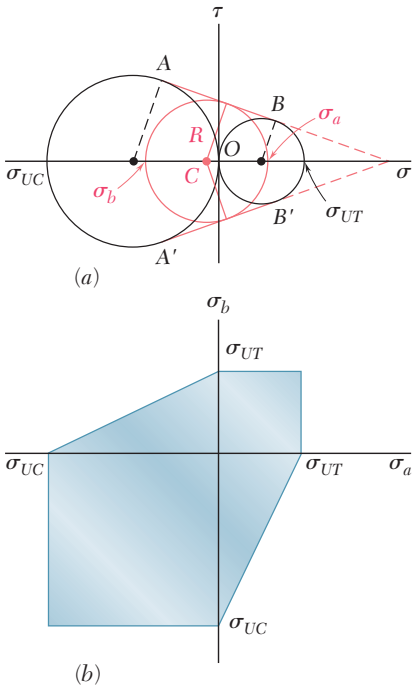
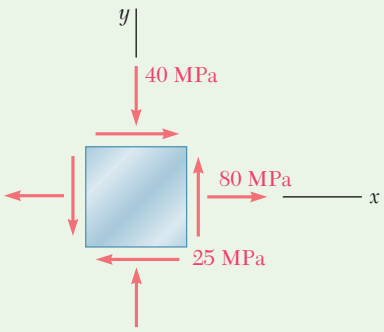


Fig. 7.38 Simplified Mohr's criterion for brittle materials. (*a*) Mohr's circles for uniaxial compression (left), torsion (middle), and uniaxial tension (right) tests at rupture. (*b*) Envelope of safe stress states.



Sample Problem 7.4

The state of plane stress shown occurs at a critical point of a steel machine component. As a result of several tensile tests, the tensile yield strength is $\sigma_Y = 250$ MPa for the grade of steel used. Determine the factor of safety with respect to yield using (*a*) the maximum-shearing-stress criterion, (*b*) the maximum-distortion-energy criterion.

STRATEGY: Draw Mohr's circle from the given state of plane stress. Analyzing this circle to obtain the principal stresses and the maximum shearing stress, you can then apply the maximum-shearing-stress and maximum-distortion-energy criteria.

MODELING and ANALYSIS:

Mohr's Circle. We construct Mohr's circle (Fig. 1) for the given state of stress and find

$$\sigma_{\text{ave}} = OC = \tfrac{1}{2}(\sigma_x + \sigma_y) = \tfrac{1}{2}(80 - 40) = 20 \text{ MPa}$$

$$\tau_m = R = \sqrt{(CF)^2 + (FX)^2} = \sqrt{(60)^2 + (25)^2} = 65 \text{ MPa}$$

Principal Stresses

$$\sigma_a = OC + CA = 20 + 65 = +85 \text{ MPa}$$

$$\sigma_b = OC - BC = 20 - 65 = -45 \text{ MPa}$$

a. Maximum-Shearing-Stress Criterion. Since the tensile strength is $\sigma_Y = 250$ MPa, the corresponding shearing stress at yield is

$$\tau_Y = \tfrac{1}{2}\sigma_Y = \tfrac{1}{2}(250 \text{ MPa}) = 125 \text{ MPa}$$

For $\tau_m = 65$ MPa,

$$F.S. = \frac{\tau_Y}{\tau_m} = \frac{125 \text{ MPa}}{65 \text{ MPa}} \qquad F.S. = 1.92$$

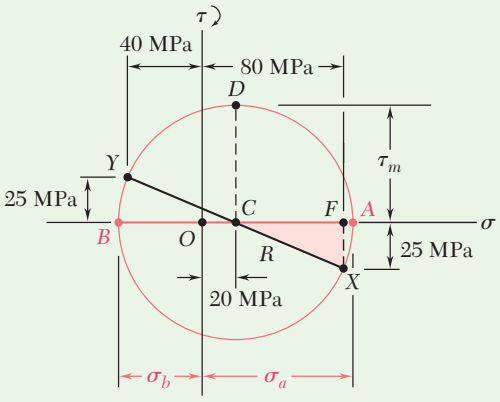


Fig. 1 Mohr's circle for given stress element.

(continued)

b. Maximum-Distortion-Energy Criterion. Introducing a factor of safety into Eq. (7.26) gives

$$\sigma_a^2 - \sigma_a\sigma_b + \sigma_b^2 = \left(\frac{\sigma_Y}{F.S.}\right)^2$$

For $\sigma_a = +85$ MPa, $\sigma_b = -45$ MPa, and $\sigma_Y = 250$ MPa, we have

$$(85)^2 - (85)(-45) + (45)^2 = \left(\frac{250}{F.S.}\right)^2$$

$$114.3 = \frac{250}{F.S.} \qquad F.S. = 2.19$$

REFLECT and THINK. For a ductile material with $\sigma_Y = 250$ MPa, we have drawn the hexagon associated with the maximum-shearing-stress criterion and the ellipse associated with the maximum-distortion-energy criterion (Fig. 2). The given state of plane stress is represented by point H with coordinates $\sigma_a = 85$ MPa and $\sigma_b = -45$ MPa. The straight line drawn through points O and H intersects the hexagon at point T and the ellipse at point M. For each criterion, $F.S.$ is verified by measuring the line segments indicated and computing their ratios:

$$(a)\ F.S. = \frac{OT}{OH} = 1.92 \qquad (b)\ F.S. = \frac{OM}{OH} = 2.19$$

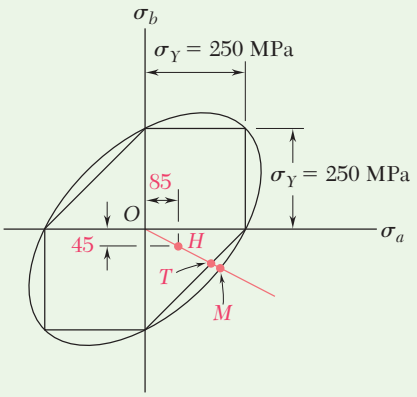


Fig. 2 Tresca and von Mises envelopes and given stress state (point H).

Problems

7.66 For the state of plane stress shown, determine the maximum shearing stress when (*a*) $\sigma_x = 14$ ksi and $\sigma_y = 4$ ksi, (*b*) $\sigma_x = 21$ ksi and $\sigma_y = 14$ ksi. (*Hint:* Consider both in-plane and out-of-plane shearing stresses.)

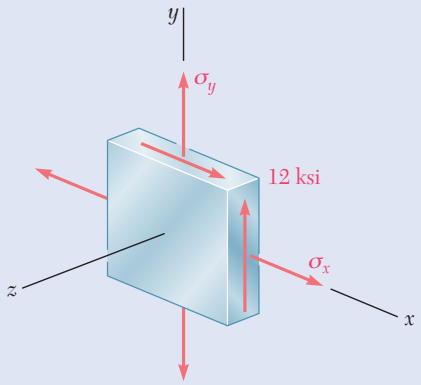


Fig. P7.66 and *P7.67*

7.67 For the state of plane stress shown, determine the maximum shearing stress when (*a*) $\sigma_x = 20$ ksi and $\sigma_y = 10$ ksi, (*b*) $\sigma_x = 12$ ksi and $\sigma_y = 5$ ksi. (*Hint:* Consider both in-plane and out-of-plane shearing stresses.)

7.68 For the state of stress shown, determine the maximum shearing stress when (*a*) $\sigma_y = 40$ MPa, (*b*) $\sigma_y = 120$ MPa. (*Hint:* Consider both in-plane and out-of-plane shearing stresses.)

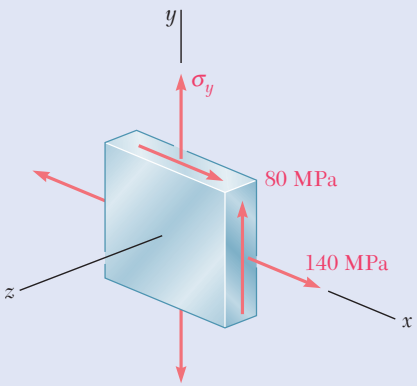


Fig. P7.68 and P7.69

7.69 For the state of stress shown, determine the maximum shearing stress when (*a*) $\sigma_y = 20$ MPa, (*b*) $\sigma_y = 140$ MPa. (*Hint:* Consider both in-plane and out-of-plane shearing stresses.)

7.70 and 7.71 For the state of stress shown, determine the maximum shearing stress when (*a*) $\sigma_z = 0$, (*b*) $\sigma_z = +60$ MPa, (*c*) $\sigma_z = -60$ MPa.

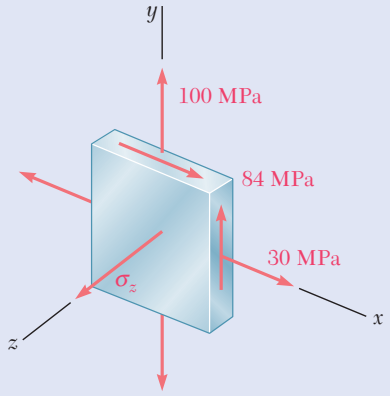


Fig. P7.70

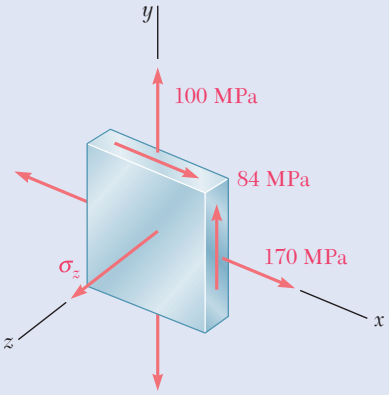


Fig. P7.71

***7.72* and 7.73** For the state of stress shown, determine the maximum shearing stress when (*a*) $\tau_{yz} = 17.5$ ksi, (*b*) $\tau_{yz} = 8$ ksi, (*c*) $\tau_{yz} = 0$.

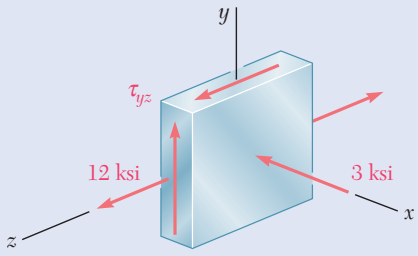


Fig. *P7.72*

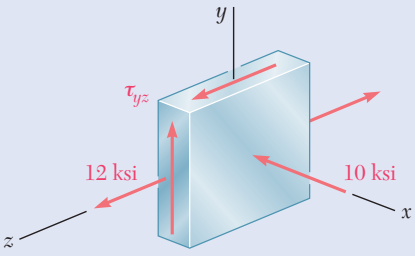


Fig. P7.73

7.74 For the state of stress shown, determine the value of τ_{xy} for which the maximum shearing stress is (*a*) 9 ksi, (*b*) 12 ksi.

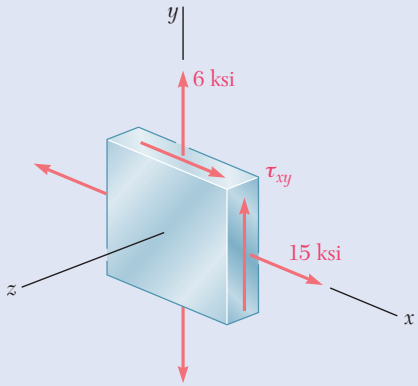


Fig. P7.74

7.75 For the state of stress shown, determine the value of τ_{xy} for which the maximum shearing stress is 80 MPa.

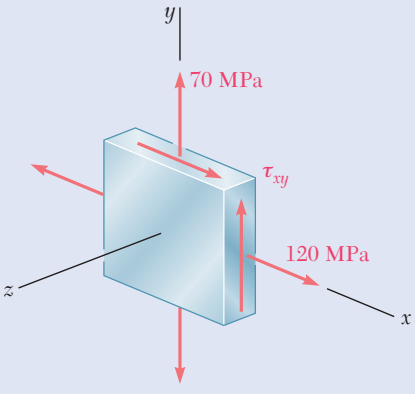


Fig. P7.75

7.76 For the state of stress shown, determine two values of σ_y for which the maximum shearing stress is 73 MPa.

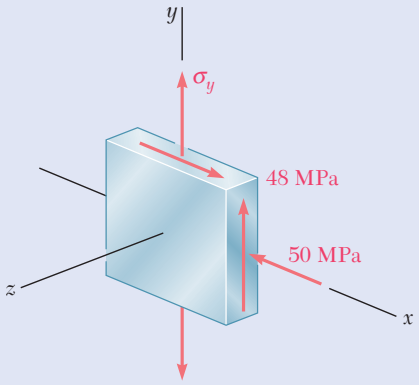


Fig. *P7.76*

7.77 For the state of stress shown, determine two values of σ_y for which the maximum shearing stress is 10 ksi.

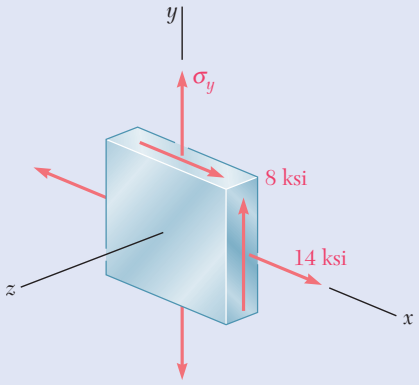


Fig. P7.77

7.78 For the state of stress shown, determine the range of values of τ_{xz} for which the maximum shearing stress is equal to or less than 60 MPa.

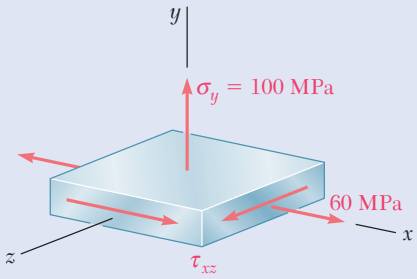


Fig. *P7.78*

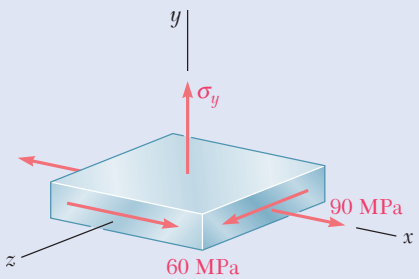


Fig. P7.79

7.79 For the state of stress shown, determine two values of σ_y for which the maximum shearing stress is 80 MPa.

***7.80** For the state of stress of Prob. 7.69, determine (*a*) the value of σ_y for which the maximum shearing stress is as small as possible, (*b*) the corresponding value of the shearing stress.

7.81 The state of plane stress shown occurs in a machine component made of a steel with $\sigma_Y = 325$ MPa. Using the maximum-distortion-energy criterion, determine whether yield will occur when (*a*) $\sigma_0 = 200$ MPa, (*b*) $\sigma_0 = 240$ MPa, (*c*) $\sigma_0 = 280$ MPa. If yield does not occur, determine the corresponding factor of safety.

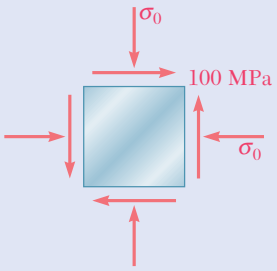


Fig. P7.81

7.82 Solve Prob. 7.81, using the maximum-shearing-stress criterion.

7.83 The state of plane stress shown occurs in a machine component made of a steel with $\sigma_Y = 45$ ksi. Using the maximum-distortion-energy criterion, determine whether yield will occur when (*a*) $\tau_{xy} = 9$ ksi, (*b*) $\tau_{xy} = 18$ ksi, (*c*) $\tau_{xy} = 20$ ksi. If yield does not occur, determine the corresponding factor of safety.

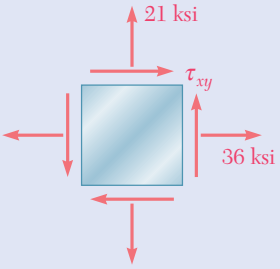


Fig. P7.83

7.84 Solve Prob. 7.83, using the maximum-shearing-stress criterion.

***7.85** The 38-mm-diameter shaft *AB* is made of a grade of steel for which the yield strength is $\sigma_Y = 250$ MPa. Using the maximum-shearing-stress criterion, determine the magnitude of the torque **T** for which yield occurs when $P = 240$ kN.

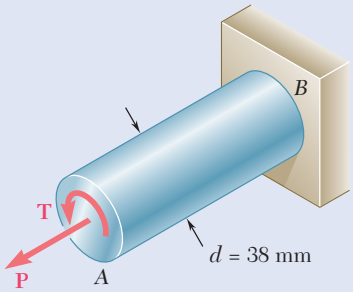


Fig. *P7.85*

***7.86** Solve Prob. 7.85, using the maximum-distortion-energy criterion.

7.87 The 1.5-in.-diameter shaft *AB* is made of a grade of steel with a 42-ksi tensile yield stress. Using the maximum-shearing-stress criterion, determine the magnitude of the torque **T** for which yield occurs when $P = 60$ kips.

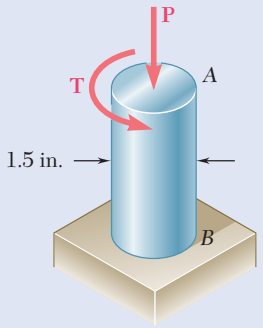


Fig. P7.87

7.88 Solve Prob. 7.87, using the maximum-distortion-energy criterion.

7.89 and 7.90 The state of plane stress shown is expected to occur in an aluminum casting. Knowing that for the aluminum alloy used $\sigma_{UT} = 80$ MPa and $\sigma_{UC} = 200$ MPa and using Mohr's criterion, determine whether rupture of the casting will occur.

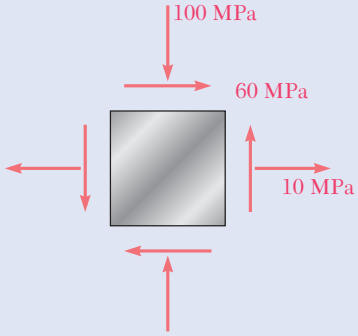


Fig. P7.89

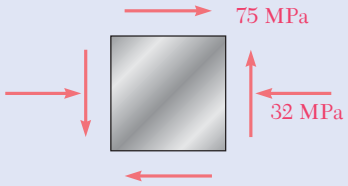


Fig. P7.90

7.91 and 7.92 The state of plane stress shown is expected to occur in an aluminum casting. Knowing that for the aluminum alloy used $\sigma_{UT} = 10$ ksi and $\sigma_{UC} = 30$ ksi and using Mohr's criterion, determine whether rupture of the casting will occur.

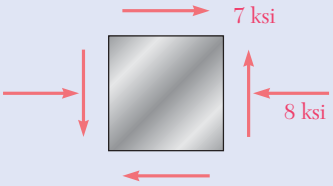


Fig. P7.91

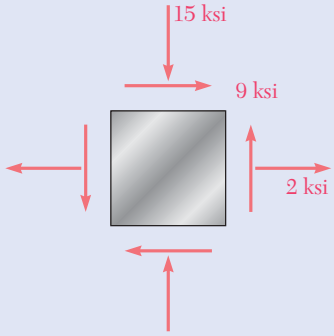


Fig. P7.92

7.93 The state of plane stress shown will occur at a critical point in an aluminum casting that is made of an alloy for which $\sigma_{UT} = 10$ ksi and $\sigma_{UC} = 25$ ksi. Using Mohr's criterion, determine the shearing stress τ_0 for which failure should be expected.

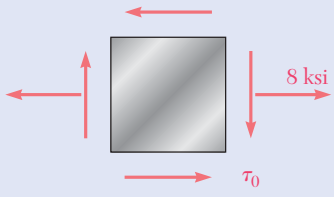


Fig. *P7.93*

7.94 The state of plane stress shown will occur at a critical point in a pipe made of an aluminum alloy for which $\sigma_{UT} = 75$ MPa and $\sigma_{UC} = 150$ MPa. Using Mohr's criterion, determine the shearing stress τ_0 for which failure should be expected.

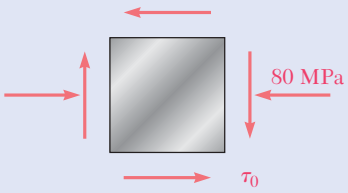


Fig. P7.94

7.95 The cast-aluminum rod shown is made of an alloy for which $\sigma_{UT} = 70$ MPa and $\sigma_{UC} = 175$ MPa. Knowing that the magnitude T of the applied torques is slowly increased and using Mohr's criterion, determine the shearing stress τ_0 that should be expected at rupture.

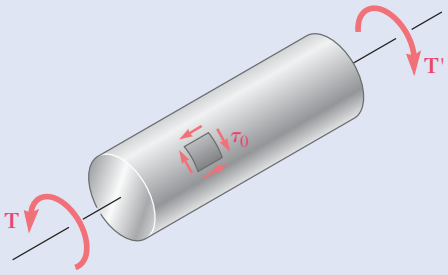


Fig. P7.95

7.96 The cast-aluminum rod shown is made of an alloy for which $\sigma_{UT} = 60$ MPa and $\sigma_{UC} = 120$ MPa. Using Mohr's criterion, determine the magnitude of the torque **T** for which failure should be expected.

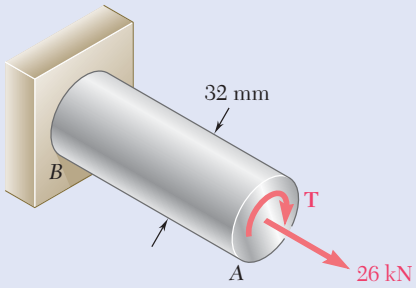


Fig. P7.96

7.97 A machine component is made of a grade of cast iron for which $\sigma_{UT} = 8$ ksi and $\sigma_{UC} = 20$ ksi. For each of the states of stress shown and using Mohr's criterion, determine the normal stress σ_0 at which rupture of the component should be expected.

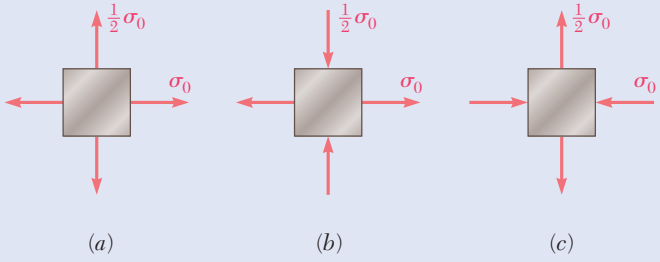


Fig. *P7.97*

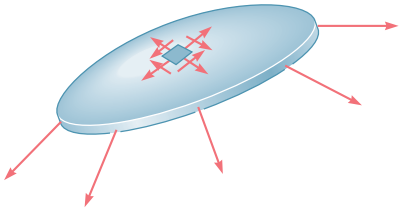


Fig. 7.39 Assumed stress distribution in thin-walled pressure vessels.

7.6 STRESSES IN THIN-WALLED PRESSURE VESSELS

Thin-walled pressure vessels provide an important application of the analysis of plane stress. Since their walls offer little resistance to bending, it can be assumed that the internal forces exerted on a given portion of wall are tangent to the surface of the vessel (Fig. 7.39). The resulting stresses on an element of wall will be contained in a plane tangent to the surface of the vessel.

This analysis of stresses in thin-walled pressure vessels is limited to two types of vessels: cylindrical and spherical (Photos 7.3 and 7.4).



Photo 7.3 Cylindrical pressure vessels for liquid propane.



Photo 7.4 Spherical pressure vessels at a chemical plant.

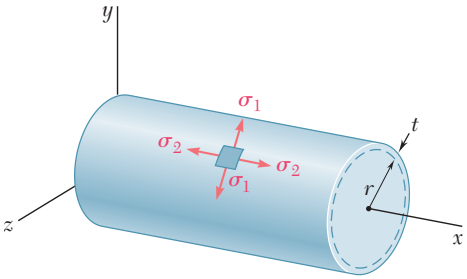


Fig. 7.40 Pressurized cylindrical vessel.

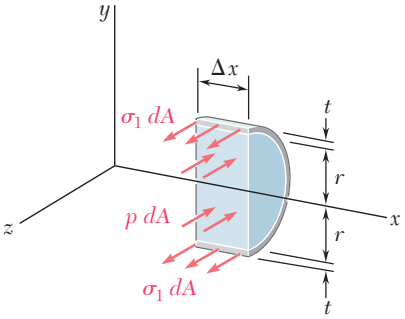


Fig. 7.41 Free-body diagram to determine hoop stress in a cylindrical pressure vessel.

Cylindrical Pressure Vessels. Consider a cylindrical vessel with an inner radius r and a wall thickness t containing a fluid under pressure (Fig. 7.40). The stresses exerted on a small element of wall with sides respectively parallel and perpendicular to the axis of the cylinder will be determined. Because of the axisymmetry of the vessel and its contents, no shearing stress is exerted on the element. The normal stresses σ_1 and σ_2 shown in Fig. 7.40 are therefore principal stresses. The stress σ_1 is called the *hoop stress*, because it is the type of stress found in hoops used to hold together the various slats of a wooden barrel. Stress σ_2 is called the *longitudinal stress*.

To determine the hoop stress σ_1, detach a portion of the vessel and its contents bounded by the xy plane and by two planes parallel to the yz plane at a distance Δx from each other (Fig. 7.41). The forces parallel to the z axis acting on the free body consist of the elementary internal forces $\sigma_1\, dA$ on the wall sections and the elementary pressure forces $p\, dA$ exerted on the portion of fluid included in the free body. Note that the *gage pressure* of the fluid p is the excess of the inside pressure over the outside atmospheric pressure. The resultant of the internal forces $\sigma_1\, dA$ is equal to the product of σ_1 and the cross-sectional area $2t\,\Delta x$ of the wall, while the resultant of the pressure forces $p\, dA$ is equal to the product of p and the area $2r\,\Delta x$. The equilibrium equation $\Sigma F_z = 0$ gives

$$\Sigma F_z = 0: \qquad \sigma_1(2t\,\Delta x) - p(2r\,\Delta x) = 0$$

and solving for the hoop stress σ_1,

$$\sigma_1 = \frac{pr}{t} \tag{7.30}$$

To determine the longitudinal stress σ_2, pass a section perpendicular to the x axis and consider the free body consisting of the portion of the vessel and its contents located to the left of the section (Fig. 7.42). The forces acting on this free body are the elementary internal forces $\sigma_2\,dA$ on the wall section and the elementary pressure forces $p\,dA$ exerted on the portion of fluid included in the free body. Noting that the area of the fluid section is πr^2 and that the area of the wall section can be obtained by multiplying the circumference $2\pi r$ of the cylinder by its wall thickness t, the equilibrium equation is:†

$$\Sigma F_x = 0: \qquad \sigma_2(2\pi rt) - p(\pi r^2) = 0$$

and solving for the longitudinal stress σ_2,

$$\sigma_2 = \frac{pr}{2t} \tag{7.31}$$

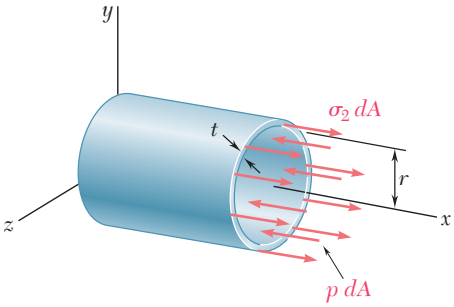


Fig. 7.42 Free-body diagram to determine longitudinal stress.

Note from Eqs. (7.30) and (7.31) that the hoop stress σ_1 is twice as large as the longitudinal stress σ_2:

$$\sigma_1 = 2\sigma_2 \tag{7.32}$$

Drawing Mohr's circle through the points A and B that correspond to the principal stresses σ_1 and σ_2 (Fig. 7.43), and recalling that the maximum in-plane shearing stress is equal to the radius of this circle, we obtain

$$\tau_{\max\,(\text{in plane})} = \tfrac{1}{2}\sigma_2 = \frac{pr}{4t} \tag{7.33}$$

This stress corresponds to points D and E and is exerted on an element obtained by rotating the original element of Fig. 7.40 through 45° *within*

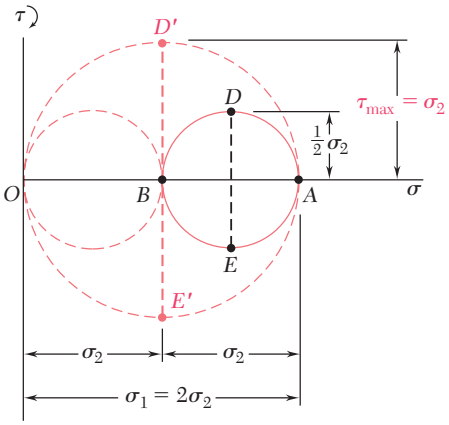


Fig. 7.43 Mohr's circle for element of cylindrical pressure vessel.

†Using the mean radius of the wall section, $r_m = r + \frac{1}{2}t$, to compute the resultant of the forces, a more accurate value of the longitudinal stress is

$$\sigma_2 = \frac{pr}{2t}\frac{1}{1 + \dfrac{t}{2r}}$$

However, for a thin-walled pressure vessel, the term $t/2r$ is sufficiently small to allow the use of Eq. (7.31) for engineering design and analysis. If a pressure vessel is not thin-walled (i.e., if $t/2r$ is not small), the stresses σ_1 and σ_2 vary across the wall and must be determined by the methods of the theory of elasticity.

the plane tangent to the surface of the vessel. However, the maximum shearing stress in the wall of the vessel is larger. It is equal to the radius of the circle of diameter *OA* and corresponds to a rotation of 45° about a longitudinal axis and *out of the plane* of stress.[†]

$$\tau_{\max} = \sigma_2 = \frac{pr}{2t} \tag{7.34}$$

Spherical Pressure Vessels. Now consider a spherical vessel of inner radius r and wall thickness t, containing a fluid under a gage pressure p. For reasons of symmetry, the stresses exerted on the four faces of a small element of wall must be equal (Fig. 7.44).

$$\sigma_1 = \sigma_2 \tag{7.35}$$

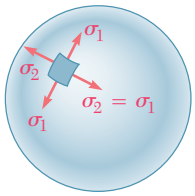


Fig. 7.44 Pressurized spherical vessel.

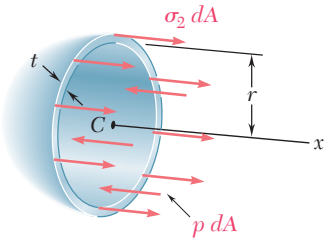


Fig. 7.45 Free-body diagram to determine spherical pressure vessel stress.

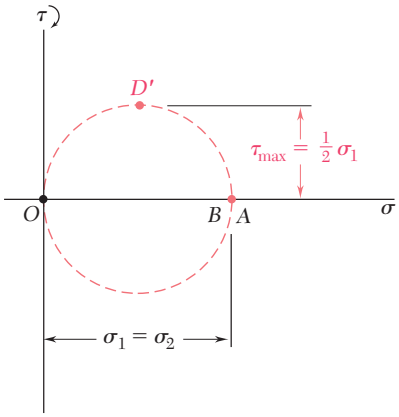


Fig. 7.46 Mohr's circle for element of spherical pressure vessel.

To determine the stress, pass a section through the center C of the vessel and consider the free body consisting of the portion of the vessel and its contents located to the left of the section (Fig. 7.45). The equation of equilibrium for this free body is the same as for the free body of Fig. 7.42. So for a spherical vessel,

$$\sigma_1 = \sigma_2 = \frac{pr}{2t} \tag{7.36}$$

Since the principal stresses σ_1 and σ_2 are equal, Mohr's circle for transformations of stress within the plane tangent to the surface of the vessel reduces to a point (Fig. 7.46). The in-plane normal stress is constant, and the in-plane maximum shearing stress is zero. However, the maximum shearing stress in the wall of the vessel is not zero; it is equal to the radius of the circle with the diameter *OA* and corresponds to a rotation of 45° out of the plane of stress. Thus,

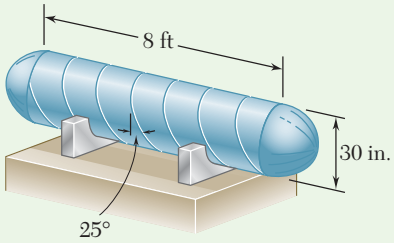
$$\tau_{\max} = \tfrac{1}{2}\sigma_1 = \frac{pr}{4t} \tag{7.37}$$

[†]While the third principal stress is zero on the outer surface of the vessel, it is equal to $-p$ on the inner surface and is represented by a point $C(-p, 0)$ on a Mohr-circle diagram. Thus, close to the inside surface of the vessel, the maximum shearing stress is equal to the radius of a circle of diameter *CA*, or

$$\tau_{\max} = \frac{1}{2}(\sigma_1 + p) = \frac{pr}{2t}\left(1 + \frac{t}{r}\right)$$

However, for a thin-walled vessel, t/r is small, and the variation of τ_{max} across the wall section can be neglected. This also applies to spherical pressure vessels.

Sample Problem 7.5



A compressed-air tank is supported by two cradles as shown. One of the cradles is designed so that it does not exert any longitudinal force on the tank. The cylindrical body of the tank has a 30-in. outer diameter and is made of a $\frac{3}{8}$-in. steel plate by butt welding along a helix that forms an angle of 25° with a transverse plane. The end caps are spherical and have a uniform wall thickness of $\frac{5}{16}$ in. For an internal gage pressure of 180 psi, determine (*a*) the normal stress and the maximum shearing stress in the spherical caps, (*b*) the stresses in directions perpendicular and parallel to the helical weld.

STRATEGY: Using the equations for thin-walled pressure vessels, you can determine the state of plane stress at any point within the spherical end cap and within the cylindrical body. You can then plot the corresponding Mohr's circles and use them to determine the stress components of interest.

MODELING and ANALYSIS:

a. Spherical Cap. The state of stress within any point in the spherical cap is shown in Fig. 1. Using Eq. (7.36), we write

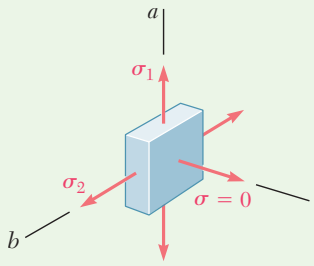


Fig. 1 State of stress at any point in spherical cap.

$$p = 180 \text{ psi}, \quad t = \tfrac{5}{16} \text{ in.} = 0.3125 \text{ in.}, \quad r = 15 - 0.3125 = 14.688 \text{ in.}$$

$$\sigma_1 = \sigma_2 = \frac{pr}{2t} = \frac{(180 \text{ psi})(14.688 \text{ in.})}{2(0.3125 \text{ in.})} \qquad \sigma = 4230 \text{ psi}$$

We note that for stresses in a plane tangent to the cap, Mohr's circle reduces to a point (*A*, *B*) on the horizontal axis, and that all in-plane shearing stresses are zero (Fig. 2). On the surface of the cap, the third principal stress is zero and corresponds to point *O*. On a Mohr's circle with a diameter of *AO*, point *D*′ represents the maximum shearing stress that occurs on planes at 45° to the plane tangent to the cap.

$$\tau_{\max} = \tfrac{1}{2}(4230 \text{ psi}) \qquad \tau_{\max} = 2115 \text{ psi}$$

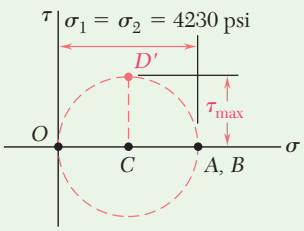


Fig. 2 Mohr's circle for stress element in spherical cap.

(continued)

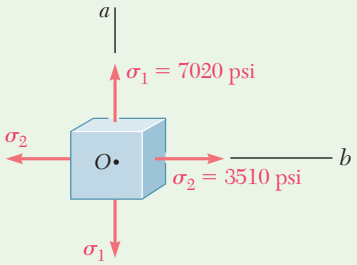


Fig. 3 State of stress at any point in cylindrical body.

b. Cylindrical Body of the Tank. The state of stress within any point in the cylindrical body is as shown in Fig. 3. We determine the hoop stress σ_1 and the longitudinal stress σ_2 using Eqs. (7.30) and (7.32). We write

$$p = 180 \text{ psi}, \; t = \tfrac{3}{8} \text{ in.} = 0.375 \text{ in.}, \; r = 15 - 0.375 = 14.625 \text{ in.}$$

$$\sigma_1 = \frac{pr}{t} = \frac{(180 \text{ psi})(14.625 \text{ in.})}{0.375 \text{ in.}} = 7020 \text{ psi} \qquad \sigma_2 = \tfrac{1}{2}\sigma_1 = 3510 \text{ psi}$$

$$\sigma_{\text{ave}} = \tfrac{1}{2}(\sigma_1 + \sigma_2) = 5265 \text{ psi} \qquad R = \tfrac{1}{2}(\sigma_1 - \sigma_2) = 1755 \text{ psi}$$

Stresses at the Weld. Noting that both the hoop stress and the longitudinal stress are principal stresses, we draw Mohr's circle as shown in Fig 4.

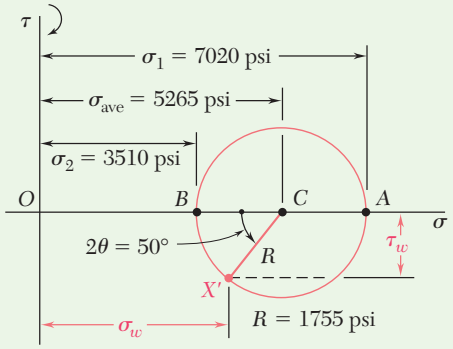


Fig. 4 Mohr's circle for stress element in cylindrical body.

An element having a face parallel to the weld is obtained by rotating the face perpendicular to the axis *Ob* (Fig. 3) counterclockwise through 25°. Therefore, on Mohr's circle (Fig. 4), point X' corresponds to the stress components on the weld by rotating radius *CB* counterclockwise through $2\theta = 50°$.

$$\sigma_w = \sigma_{\text{ave}} - R\cos 50° = 5265 - 1755\cos 50° \qquad \sigma_w = +4140 \text{ psi}$$

$$\tau_w = R\sin 50° = 1755\sin 50° \qquad \tau_w = 1344 \text{ psi}$$

Since X' is below the horizontal axis, τ_w tends to rotate the element counterclockwise. The stress components on the weld are shown in Fig. 5.

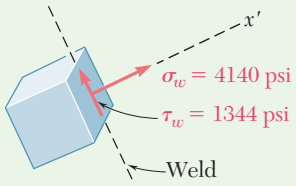


Fig. 5 Stress components on the weld.

Problems

7.98 A spherical pressure vessel has an outer diameter of 3 m and a wall thickness of 12 mm. Knowing that for the steel used $\sigma_{all} = 80$ MPa, $E = 200$ GPa, and $\nu = 0.29$, determine (*a*) the allowable gage pressure, (*b*) the corresponding increase in the diameter of the vessel.

7.99 A spherical gas container having an inner diameter of 5 m and a wall thickness of 24 mm is made of steel for which $E = 200$ GPa and $\nu = 0.29$. Knowing that the gage pressure in the container is increased from zero to 1.8 MPa, determine (*a*) the maximum normal stress in the container, (*b*) the corresponding increase in the diameter of the container.

7.100 The maximum gage pressure is known to be 1150 psi in a spherical steel pressure vessel having a 10-in. outer diameter and a 0.25-in. wall thickness. Knowing that the ultimate stress in the steel used is $\sigma_U = 60$ ksi, determine the factor of safety with respect to tensile failure.

7.101 A spherical pressure vessel of 750-mm outer diameter is to be fabricated from a steel having an ultimate stress $\sigma_U = 400$ MPa. Knowing that a factor of safety of 4.0 is desired and that the gage pressure can reach 4.2 MPa, determine the smallest wall thickness that should be used.

7.102 A spherical gas container made of steel has a 20-ft outer diameter and a wall thickness of $\frac{7}{16}$ in. Knowing that the internal pressure is 75 psi, determine the maximum normal stress and the maximum shearing stress in the container.

7.103 A basketball has a 300-mm outer diameter and a 3-mm wall thickness. Determine the normal stress in the wall when the basketball is inflated to a 120-kPa gage pressure.

7.104 The unpressurized cylindrical storage tank shown has a 5-mm wall thickness and is made of steel having a 400-MPa ultimate strength in tension. Determine the maximum height h to which it can be filled with water if a factor of safety of 4.0 is desired. (Density of water = 1000 kg/m^3.)

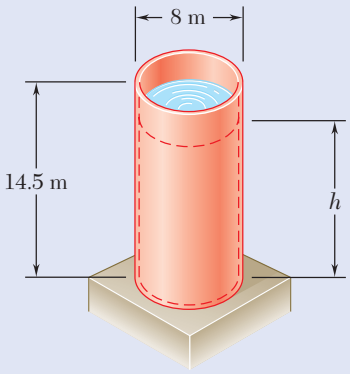


Fig. P7.104

7.105 For the storage tank of Prob. 7.104, determine the maximum normal stress and the maximum shearing stress in the cylindrical wall when the tank is filled to capacity ($h = 14.5$ m).

7.106 The bulk storage tank shown in Photo 7.3 has an outer diameter of 3.3 m and a wall thickness of 18 mm. At a time when the internal pressure of the tank is 1.5 MPa, determine the maximum normal stress and the maximum shearing stress in the tank.

7.107 A standard-weight steel pipe of 12-in. nominal diameter carries water under a pressure of 400 psi. (*a*) Knowing that the outside diameter is 12.75 in. and the wall thickness is 0.375 in., determine the maximum tensile stress in the pipe. (*b*) Solve part *a*, assuming an extra-strong pipe is used, of 12.75-in. outside diameter and 0.5-in. wall thickness.

7.108 A cylindrical storage tank contains liquefied propane under a pressure of 1.5 MPa at a temperature of 38°C. Knowing that the tank has an outer diameter of 320 mm and a wall thickness of 3 mm, determine the maximum normal stress and the maximum shearing stress in the tank.

7.109 Determine the largest internal pressure that can be applied to a cylindrical tank of 5.5-ft outer diameter and $\frac{5}{8}$-in. wall thickness if the ultimate normal stress of the steel used is 65 ksi and a factor of safety of 5.0 is desired.

7.110 A steel penstock has a 36-in. outer diameter, a 0.5-in. wall thickness, and connects a reservoir at *A* with a generating station at *B*. Knowing that the specific weight of water is 62.4 lb/ft^3, determine the maximum normal stress and the maximum shearing stress in the penstock under static conditions.

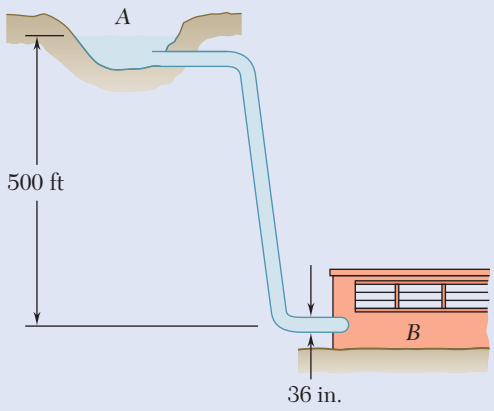


Fig. P7.110 and P7.111

7.111 A steel penstock has a 36-in. outer diameter and connects a reservoir at *A* with a generating station at *B*. Knowing that the specific weight of water is 62.4 lb/ft^3 and that the allowable normal stress in the steel is 12.5 ksi, determine the smallest thickness that can be used for the penstock.

7.112 The cylindrical portion of the compressed-air tank shown is fabricated of 8-mm-thick plate welded along a helix forming an angle $\beta = 30°$ with the horizontal. Knowing that the allowable stress normal to the weld is 75 MPa, determine the largest gage pressure that can be used in the tank.

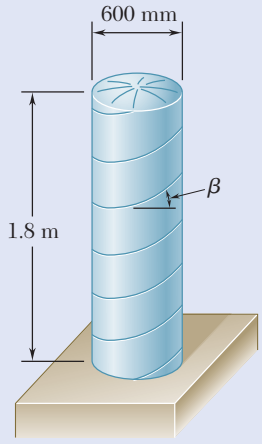


Fig. P7.112

7.113 For the compressed-air tank of Prob. 7.112, determine the gage pressure that will cause a shearing stress parallel to the weld of 30 MPa.

7.114 The steel pressure tank shown has a 750-mm inner diameter and a 9-mm wall thickness. Knowing that the butt-welded seams form an angle $\beta = 50°$ with the longitudinal axis of the tank and that the gage pressure in the tank is 1.5 MPa, determine, (*a*) the normal stress perpendicular to the weld, (*b*) the shearing stress parallel to the weld.

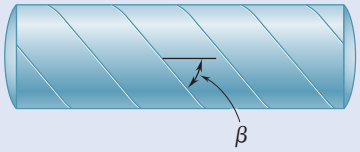


Fig. P7.114 and P7.115

7.115 The pressurized tank shown was fabricated by welding strips of plate along a helix forming an angle β with a transverse plane. Determine the largest value of β that can be used if the normal stress perpendicular to the weld is not to be larger than 85 percent of the maximum stress in the tank.

7.116 Square plates, each of 0.5-in. thickness, can be bent and welded together in either of the two ways shown to form the cylindrical portion of a compressed-air tank. Knowing that the allowable normal stress perpendicular to the weld is 12 ksi, determine the largest allowable gage pressure in each case.

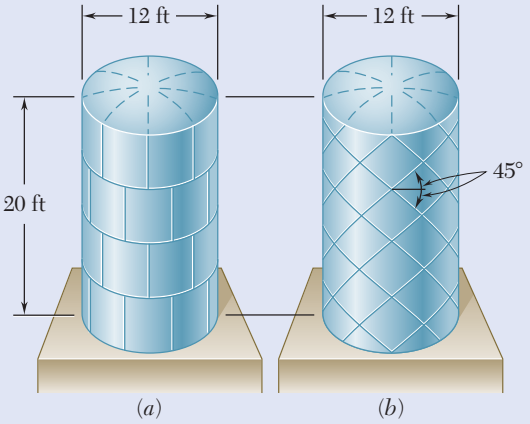


Fig. *P7.116*

7.117 The pressure tank shown has a 0.375-in. wall thickness and butt-welded seams forming an angle $\beta = 20°$ with a transverse plane. For a gage pressure of 85 psi, determine, (*a*) the normal stress perpendicular to the weld, (*b*) the shearing stress parallel to the weld.

7.118 For the tank of Prob. 7.117, determine the largest allowable gage pressure, knowing that the allowable normal stress perpendicular to the weld is 18 ksi and the allowable shearing stress parallel to the weld is 10 ksi.

7.119 For the tank of Prob. 7.117, determine the range of values of β that can be used if the shearing stress parallel to the weld is not to exceed 1350 psi when the gage pressure is 85 psi.

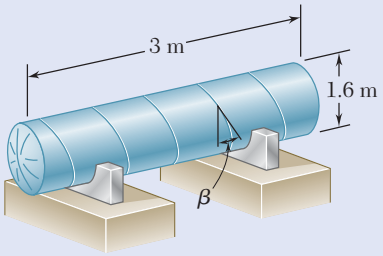


Fig. P7.117

7.120 A pressure vessel of 10-in. inner diameter and 0.25-in. wall thickness is fabricated from a 4-ft section of spirally-welded pipe *AB* and is equipped with two rigid end plates. The gage pressure inside the vessel is 300 psi and 10-kip centric axial forces **P** and **P′** are applied to the end plates. Determine (*a*) the normal stress perpendicular to the weld, (*b*) the shearing stress parallel to the weld.

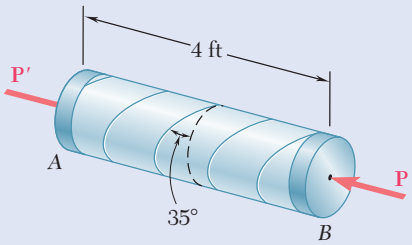


Fig. P7.120

7.121 Solve Prob. 7.120, assuming that the magnitude P of the two forces is increased to 30 kips.

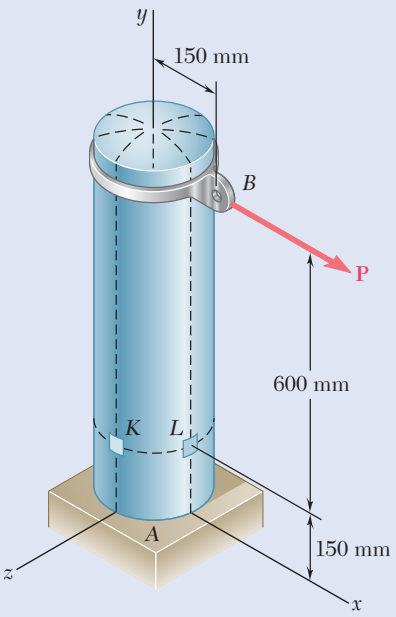


Fig. P7.124

7.122 A torque of magnitude $T = 12$ kN·m is applied to the end of a tank containing compressed air under a pressure of 8 MPa. Knowing that the tank has a 180-mm inner diameter and a 12-mm wall thickness, determine the maximum normal stress and the maximum shearing stress in the tank.

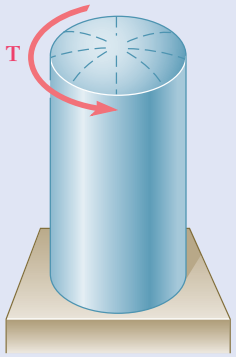


Fig. P7.122 and *P7.123*

7.123 The tank shown has a 180-mm inner diameter and a 12-mm wall thickness. Knowing that the tank contains compressed air under a pressure of 8 MPa, determine the magnitude T of the applied torque for which the maximum normal stress is 75 MPa.

7.124 The compressed-air tank AB has a 250-mm outside diameter and an 8-mm wall thickness. It is fitted with a collar by which a 40-kN force **P** is applied at B in the horizontal direction. Knowing that the gage pressure inside the tank is 5 MPa, determine the maximum normal stress and the maximum shearing stress at point K.

7.125 In Prob. 7.124, determine the maximum normal stress and the maximum shearing stress at point L.

7.126 A brass ring of 5-in. outer diameter and 0.25-in. thickness fits exactly inside a steel ring of 5-in. inner diameter and 0.125-in. thickness when the temperature of both rings is 50°F. Knowing that the temperature of both rings is then raised to 125°F, determine (*a*) the tensile stress in the steel ring, (*b*) the corresponding pressure exerted by the brass ring on the steel ring.

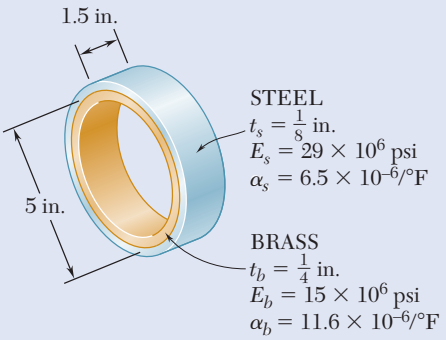


Fig. P7.126

7.127 Solve Prob. 7.126, assuming that the brass ring is 0.125 in. thick and the steel ring is 0.25 in. thick.

*7.7 TRANSFORMATION OF PLANE STRAIN

7.7A Transformation Equations

Transformations of *strain* under a rotation of the coordinate axes will now be considered. Our analysis will first be limited to states of *plane strain.* These are situations where the deformations of the material take place within parallel planes and are the same in each of these planes. If the z axis is chosen perpendicular to the planes in which the deformations take place, $\epsilon_z = \gamma_{zx} = \gamma_{zy} = 0$, and the only remaining strain components are ϵ_x, ϵ_y, and γ_{xy}. This occurs in a plate subjected to uniformly distributed loads along its edges and restrained from expanding or contracting laterally by smooth, rigid, and fixed supports (Fig. 7.47). It is also found in a bar of infinite length subjected to uniformly distributed loads on its sides, because by reason of symmetry, the elements located in a transverse plane cannot move out of that plane. This idealized model shows that a long bar subjected to uniformly distributed transverse loads (Fig. 7.48) is in a state of plane strain in any given transverse section that is not located too close to either end of the bar.[†]

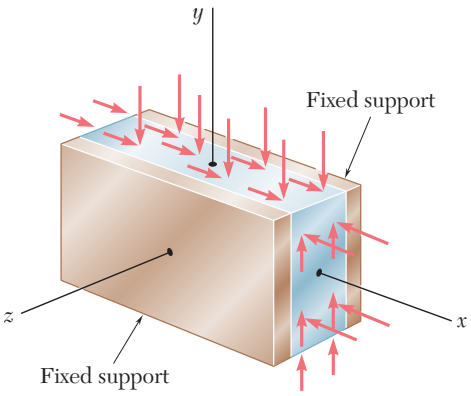


Fig. 7.47 Plane strain example: laterally restrained by fixed supports.

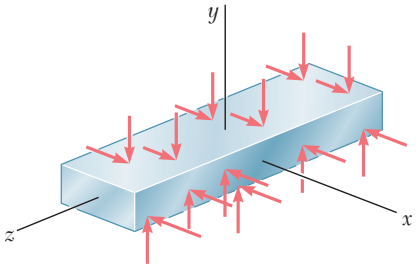


Fig. 7.48 Plane strain example: bar of infinite length in z direction.

Assume that a state of plane strain exists at point Q (with $\epsilon_z = \gamma_{zx} = \gamma_{zy} = 0$) and that it is defined by the strain components ϵ_x, ϵ_y, and γ_{xy} associated with the x and y axes. Recalling Secs. 2.5 and 2.7, a square element of center Q with sides of a length Δs and parallel to the x and y axes is deformed into a parallelogram where the sides are now equal to $\Delta s\,(1 + \epsilon_x)$ and $\Delta s\,(1 + \epsilon_y)$, forming angles of $\frac{\pi}{2} - \gamma_{xy}$ and $\frac{\pi}{2} + \gamma_{xy}$ with each other (Fig. 7.49). As a result of the deformations of the other elements located in the xy plane, the element can also undergo a rigid-body motion, but such a motion is irrelevant to the strains at point Q and will be ignored in this analysis. Our purpose is to determine in terms of ϵ_x, ϵ_y, γ_{xy}, and θ the strain components $\epsilon_{x'}$, $\epsilon_{y'}$, and $\gamma_{x'y'}$ associated with the frame of reference $x'y'$ obtained by rotating the x and y axes through angle θ. As shown in Fig. 7.50, these new strain components define the parallelogram into which a square with sides parallel to the x' and y' axes is deformed.

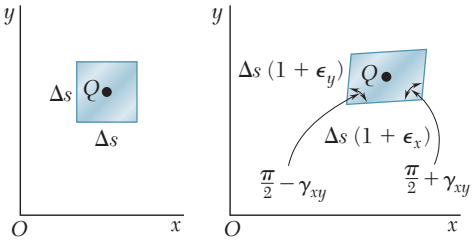


Fig. 7.49 Plane strain element: undeformed and deformed.

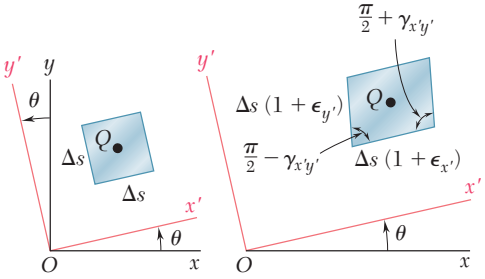


Fig. 7.50 Transformation of plane strain element in undeformed and deformed orientations.

[†]A state of *plane strain* and a state of *plane stress* do not occur simultaneously, except for ideal materials with a Poisson ratio equal to zero. The constraints placed on the elements of the plate of Fig. 7.47 and of the bar of Fig. 7.48 result in a stress σ_z different from zero. On the other hand, in the case of the plate of Fig. 7.3, the absence of any lateral restraint results in $\sigma_z = 0$ and $\epsilon_z \neq 0$.

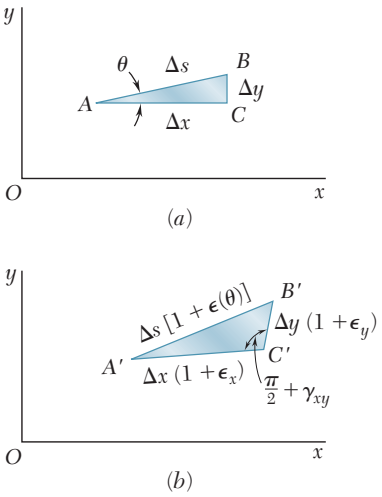


Fig. 7.51 Evaluating strain along line *AB*. (*a*) Undeformed; (*b*) deformed.

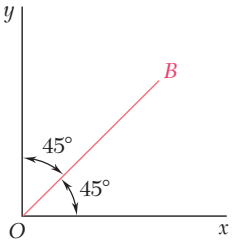


Fig. 7.52 Bisector *OB*.

The normal strain $\epsilon(\theta)$ along a line AB forms an arbitrary angle θ with the x axis. This strain is determined by using the right triangle ABC, which has AB for hypothenuse (Fig. 7.51*a*), and the oblique triangle $A'B'C'$ into which triangle ABC is deformed (Fig. 7.51*b*). With the length of AB denoted as Δs, the length of $A'B'$ is $\Delta s\,[1 + \epsilon(\theta)]$. Similarly, using Δx and Δy as the lengths of sides AC and CB, the lengths of $A'C'$ and $C'B'$ are $\Delta x\,(1 + \epsilon_x)$ and $\Delta y\,(1 + \epsilon_y)$, respectively. Recall from Fig. 7.49 that the right angle at C in Fig. 7.51*a* deforms into an angle equal to $\frac{\pi}{2} + \gamma_{xy}$ in Fig. 7.51*b*, and apply the law of cosines to triangle $A'B'C'$ to obtain

$$(A'B')^2 = (A'C')^2 + (C'B')^2 - 2(A'C')(C'B')\cos\left(\frac{\pi}{2} + \gamma_{xy}\right)$$

$$(\Delta s)^2[1 + \epsilon(\theta)]^2 = (\Delta x)^2(1 + \epsilon_x)^2 + (\Delta y)^2(1 + \epsilon_y)^2$$

$$-2(\Delta x)(1 + \epsilon_x)(\Delta y)(1 + \epsilon_y)\cos\left(\frac{\pi}{2} + \gamma_{xy}\right) \qquad \textbf{(7.38)}$$

But from Fig. 7.51*a*,

$$\Delta x = (\Delta s)\cos\theta \qquad \Delta y = (\Delta s)\sin\theta \qquad \textbf{(7.39)}$$

and since γ_{xy} is very small,

$$\cos\left(\frac{\pi}{2} + \gamma_{xy}\right) = -\sin\gamma_{xy} \approx -\gamma_{xy} \qquad \textbf{(7.40)}$$

Substituting from Eqs. (7.39) and (7.40) into Eq. (7.38), recalling that $\cos^2\theta + \sin^2\theta = 1$, and neglecting second-order terms in $\epsilon(\theta)$, ϵ_x, ϵ_y, and γ_{xy} gives

$$\epsilon(\theta) = \epsilon_x\cos^2\theta + \epsilon_y\sin^2\theta + \gamma_{xy}\sin\theta\cos\theta \qquad \textbf{(7.41)}$$

Equation (7.41) enables us to determine the normal strain $\epsilon(\theta)$ in any direction AB in terms of the strain components ϵ_x, ϵ_y, γ_{xy}, and the angle θ that AB forms with the x axis. We check that for $\theta = 0$, Eq. (7.41) yields $\epsilon(0) = \epsilon_x$ and for $\theta = 90°$, it yields $\epsilon(90°) = \epsilon_y$. On the other hand, making $\theta = 45°$ in Eq. (7.41), we obtain the normal strain in the direction of the bisector OB of the angle formed by the x and y axes (Fig. 7.52). Denoting this strain by ϵ_{OB}, we write

$$\epsilon_{OB} = \epsilon(45°) = \tfrac{1}{2}(\epsilon_x + \epsilon_y + \gamma_{xy}) \qquad \textbf{(7.42)}$$

Solving Eq. (7.42) for γ_{xy},

$$\gamma_{xy} = 2\epsilon_{OB} - (\epsilon_x + \epsilon_y) \qquad \textbf{(7.43)}$$

This relationship makes it possible to express the *shearing strain* associated with a given pair of rectangular axes in terms of the *normal strains* measured along these axes and their bisector. It plays a fundamental role in the present derivation and will also be used in Sec. 7.9 for the experimental determination of shearing strains.

The main purpose of this section is to express the strain components associated with the frame of reference $x'y'$ of Fig. 7.50 in terms of the angle θ and the strain components ϵ_x, ϵ_y, and γ_{xy} associated with the x and y axes. Thus, we note that the normal strain $\epsilon_{x'}$ along the x' axis is given by

Eq. (7.41). Using the trigonometric relationships in Eqs. (7.3) and (7.4), the alternative form of Eq. (7.41) is

$$\epsilon_{x'} = \frac{\epsilon_x + \epsilon_y}{2} + \frac{\epsilon_x - \epsilon_y}{2}\cos 2\theta + \frac{\gamma_{xy}}{2}\sin 2\theta \tag{7.44}$$

The normal strain along the y' axis is obtained by replacing θ with $\theta + 90°$. Since $\cos(2\theta + 180°) = -\cos 2\theta$ and $\sin(2\theta + 180°) = -\sin 2\theta$,

$$\epsilon_{y'} = \frac{\epsilon_x + \epsilon_y}{2} - \frac{\epsilon_x - \epsilon_y}{2}\cos 2\theta - \frac{\gamma_{xy}}{2}\sin 2\theta \tag{7.45}$$

Adding Eqs. (7.44) and (7.45) member to member gives

$$\epsilon_{x'} + \epsilon_{y'} = \epsilon_x + \epsilon_y \tag{7.46}$$

Since $\epsilon_z = \epsilon_{z'} = 0$, the sum of the normal strains associated with a cubic element of material is independent of the orientation of that element in plane strain.†

Replacing θ by $\theta + 45°$ in Eq. (7.44), an expression is obtained for the normal strain along the bisector OB' of the angle formed by the x' and y' axes. Since $\cos(2\theta + 90°) = -\sin 2\theta$ and $\sin(2\theta + 90°) = \cos 2\theta$,

$$\epsilon_{OB'} = \frac{\epsilon_x + \epsilon_y}{2} - \frac{\epsilon_x - \epsilon_y}{2}\sin 2\theta + \frac{\gamma_{xy}}{2}\cos 2\theta \tag{7.47}$$

Writing Eq. (7.43) with respect to the x' and y' axes, the shearing strain $\gamma_{x'y'}$ is expressed in terms of the normal strains measured along the x' and y' axes and the bisector OB':

$$\gamma_{x'y'} = 2\epsilon_{OB'} - (\epsilon_{x'} + \epsilon_{y'}) \tag{7.48}$$

Substituting from Eqs. (7.46) and (7.47) into Eq. (7.48) gives

$$\gamma_{x'y'} = -(\epsilon_x - \epsilon_y)\sin 2\theta + \gamma_{xy}\cos 2\theta \tag{7.49a}$$

Equations (7.44), (7.45), and (7.49a) are the desired equations defining the transformation of plane strain under a rotation of axes in the plane of strain. Dividing all terms in Eq. (7.49a) by 2, the alternative form is

$$\frac{\gamma_{x'y'}}{2} = -\frac{\epsilon_x - \epsilon_y}{2}\sin 2\theta + \frac{\gamma_{xy}}{2}\cos 2\theta \tag{7.49b}$$

Observe that Eqs. (7.44), (7.45), and (7.49b) for the transformation of plane strain closely resemble those for the transformation of plane stress (Sec 7.1). While the former can be obtained from the latter by replacing the normal stresses by the corresponding normal strains, it should be noted that the shearing stresses τ_{xy} and $\tau_{x'y'}$ should be replaced by *half* of the corresponding shearing strains (i.e., by $\frac{1}{2}\gamma_{xy}$ and $\frac{1}{2}\gamma_{x'y'}$).

†Cf. first footnote on page 98.

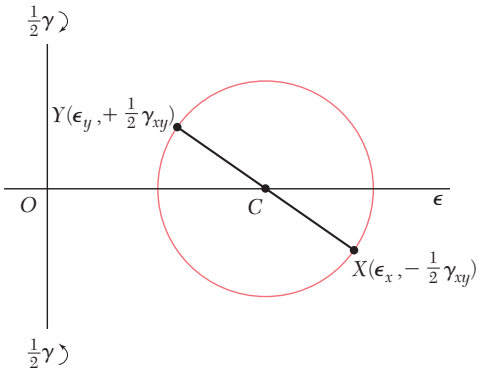


Fig. 7.53 Mohr's circle for plane strain.

7.7B Mohr's Circle for Plane Strain

Since the equations for the transformation of plane strain are of the same form as those for plane stress, Mohr's circle can be used for analysis of plane strain. Given the strain components ϵ_x, ϵ_y, and γ_{xy} defining the deformation in Fig. 7.49, point $X(\epsilon_x, -\frac{1}{2}\gamma_{xy})$ of abscissa equal to the normal strain ϵ_x and of ordinate equal to minus half the shearing strain γ_{xy}, and point $Y(\epsilon_y, +\frac{1}{2}\gamma_{xy})$ are plotted (Fig. 7.53). Drawing the diameter XY, the center C of Mohr's circle for plane strain is defined. The abscissa of C and the radius R of the circle are

$$\epsilon_{\text{ave}} = \frac{\epsilon_x + \epsilon_y}{2} \qquad \text{and} \qquad R = \sqrt{\left(\frac{\epsilon_x - \epsilon_y}{2}\right)^2 + \left(\frac{\gamma_{xy}}{2}\right)^2} \tag{7.50}$$

If γ_{xy} is positive, as assumed in Fig. 7.49, points X and Y are plotted below and above the horizontal axis in Fig. 7.53. But in the absence of any overall rigid-body rotation, the side of the element in Fig. 7.49 that is associated with ϵ_x rotates counterclockwise, while the side associated with ϵ_y rotates clockwise. Thus, if the shear deformation causes a given side to rotate *clockwise*, the corresponding point on Mohr's circle for plane strain is plotted *above* the horizontal axis, and if the deformation causes the side to rotate *counterclockwise*, the corresponding point is plotted *below* the horizontal axis. This convention matches the convention used to draw Mohr's circle for plane stress.

Points A and B where Mohr's circle intersects the horizontal axis correspond to the *principal strains* $\epsilon_{\max}$ and $\epsilon_{\min}$ (Fig. 7.54*a*). Thus,

$$\epsilon_{\max} = \epsilon_{\text{ave}} + R \qquad \text{and} \qquad \epsilon_{\min} = \epsilon_{\text{ave}} - R \tag{7.51}$$

where ϵ_{ave} and R are defined by Eqs. (7.50). The corresponding value θ_p of angle θ is obtained by observing that the shearing strain is zero for A and B. Setting $\gamma_{x'y'} = 0$ in Eq. (7.49*a*),

$$\tan 2\theta_p = \frac{\gamma_{xy}}{\epsilon_x - \epsilon_y} \tag{7.52}$$

The corresponding axes a and b in Fig. 7.54*b* are the *principal axes of strain*. Angle θ_p, which defines the direction of the principal axis Oa in Fig. 7.54*b* corresponding to point A in Fig. 7.54*a*, is equal to half of the

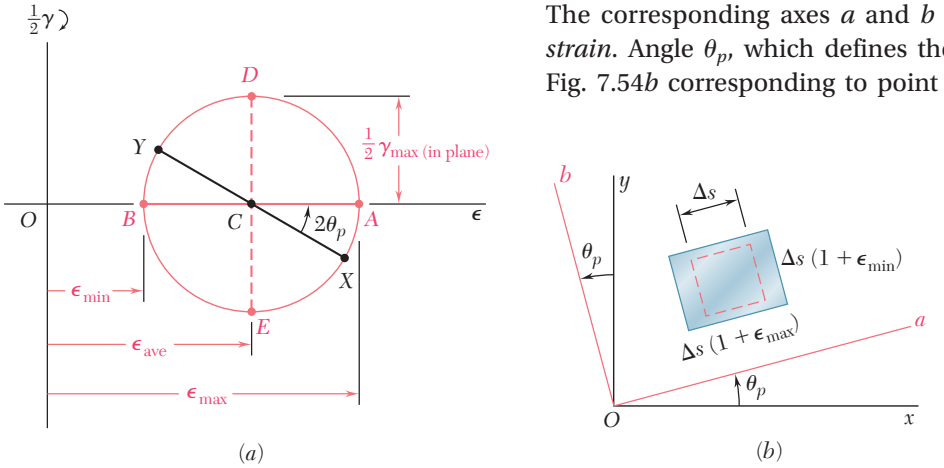


Fig. 7.54 (*a*) Mohr's circle for plane strain, showing principal strains and maximum in-plane shearing strain. (*b*) Strain element oriented to principal directions.

angle XCA measured on Mohr's circle, and the rotation that brings Ox into Oa has the same sense as the rotation that brings the diameter XY of Mohr's circle into the diameter AB.

Recall from Sec. 2.7 that in the elastic deformation of a homogeneous, isotropic material, Hooke's law for shearing stress and strain applies and yields $\tau_{xy} = G\gamma_{xy}$ for any pair of rectangular x and y axes. Thus, $\gamma_{xy} = 0$ when $\tau_{xy} = 0$, which indicates that the principal axes of strain coincide with the principal axes of stress.

The maximum in-plane shearing strain is defined by points D and E in Fig. 7.54*a*. This is equal to the diameter of Mohr's circle. From the second of Eqs. (7.50),

$$\gamma_{\max\,(\text{in plane})} = 2R = \sqrt{(\epsilon_x - \epsilon_y)^2 + \gamma_{xy}^2} \tag{7.53}$$

Finally, points X' and Y', which define the components of strain corresponding to a rotation of the coordinate axes through an angle θ (Fig. 7.50), are obtained by rotating the diameter XY of Mohr's circle in the same sense through an angle 2θ (Fig. 7.55).

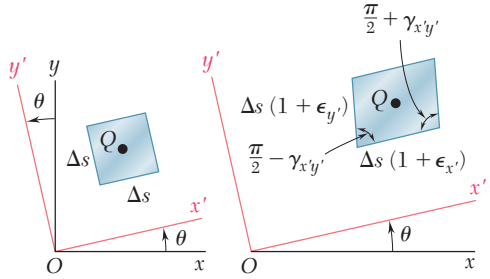


Fig. 7.50 *(repeated)* Transformation of plane strain element in undeformed and deformed orientations.

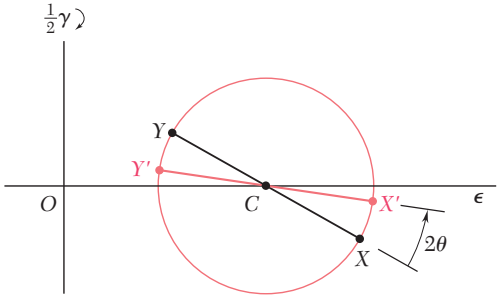


Fig. 7.55 Strains on arbitrary planes X' and Y' referenced to original planes X and Y on Mohr's circle.

Concept Application 7.4

For a material in a state of plane strain, it is found that the horizontal side of a 10 × 10-mm square elongates by 4 μm, its vertical side remains unchanged, and the angle at the lower-left corner increases by 0.4×10^{-3} rad (Fig. 7.56*a*). Determine (*a*) the principal axes and principal strains and (*b*) the maximum shearing strain and the corresponding normal strain.

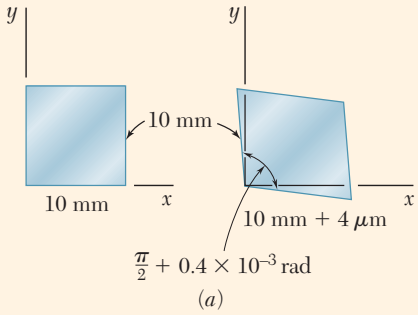


Fig. 7.56 Analysis of plane strain state. (*a*) Strain element: undeformed and deformed.

a. Principal Axes and Principal Strains. Determine the coordinates of points X and Y on Mohr's circle for strain.

$$\epsilon_x = \frac{+4 \times 10^{-6}\,\text{m}}{10 \times 10^{3}\,\text{m}} = +400\,\mu \qquad \epsilon_y = 0 \qquad \left|\frac{\gamma_{xy}}{2}\right| = 200\,\mu$$

Since the side of the square associated with ϵ_x rotates *clockwise*, point X of coordinates ϵ_x and $|\gamma_{xy}/2|$ is plotted *above* the horizontal axis. Since $\epsilon_y = 0$ and the corresponding side rotates *counterclockwise*, point Y is

(continued)

plotted directly *below* the origin (Fig. 7.56*b*). Drawing the diameter *XY*, determine the center *C* of Mohr's circle and its radius *R*.

$$OC = \frac{\epsilon_x + \epsilon_y}{2} = 200\,\mu \qquad OY = 200\,\mu$$

$$R = \sqrt{(OC)^2 + (OY)^2} = \sqrt{(200\,\mu)^2 + (200\,\mu)^2} = 283\,\mu$$

The principal strains are defined by the abscissas of points *A* and *B*.

$$\epsilon_a = OA = OC + R = 200\,\mu + 283\,\mu = 483\,\mu$$
$$\epsilon_b = OB = OC - R = 200\,\mu - 283\,\mu = -83\,\mu$$

The principal axes *Oa* and *Ob* are shown in Fig. 7.56c. Since $OC = OY$, the angle at *C* in triangle *OCY* is 45°. Thus, the angle $2\theta_p$ that brings *XY* into *AB* is 45°↓ and angle θ_p bringing *Ox* into *Oa* is 22.5°↓.

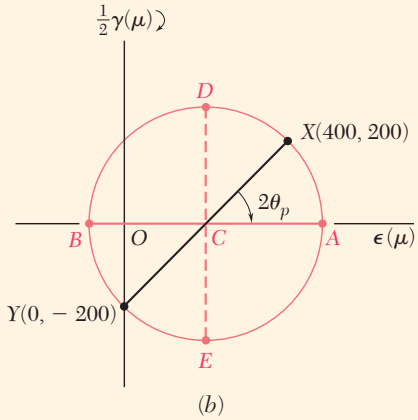
b. Maximum Shearing Strain. Points *D* and *E* define the maximum in-plane shearing strain which, since the principal strains have opposite signs, is also the actual maximum shearing strain (see Sec. 7.8).

$$\frac{\gamma_{\max}}{2} = R = 283\,\mu \qquad \gamma_{\max} = 566\,\mu$$

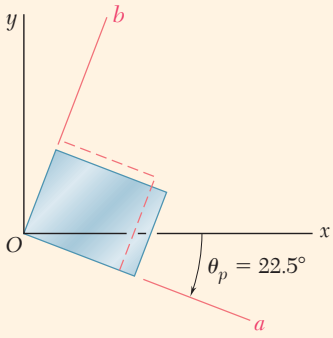
The corresponding normal strains are both equal to

$$\epsilon' = OC = 200\,\mu$$

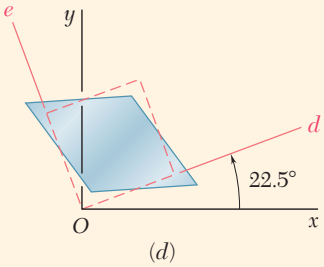
The axes of maximum shearing strain are shown in Fig. 7.56*d*.



(*b*)



(*c*)



(*d*)

Fig. 7.56 (*cont.*) (*b*) Mohr's circle for given plane strain element. (*c*) Undeformed and deformed principal strain elements. (*d*) Undeformed and deformed maximum shearing strain elements.

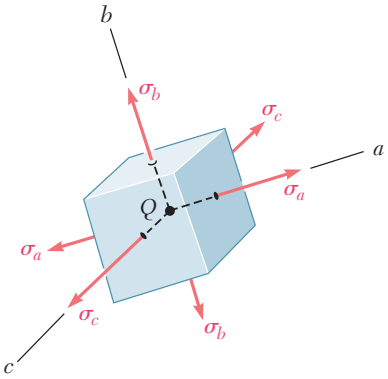


Fig. 7.21 (*repeated*) General stress element oriented to principal axes.

*7.8 THREE-DIMENSIONAL ANALYSIS OF STRAIN

We saw in Sec. 7.3 that, in the most general case of stress, we can determine three coordinate axes *a*, *b*, and *c*, called the principal axes of stress. A small cubic element with faces perpendicular to these axes is free of shearing stresses (Fig. 7.21), as $\tau_{ab} = \tau_{bc} = \tau_{ca} = 0$. Hooke's law for shearing stress and strain applies when the deformation is elastic and the material homogeneous and isotropic. Thus, $\gamma_{ab} = \gamma_{bc} = \gamma_{ca} = 0$, so the axes *a*, *b*, and *c* are also *principal axes of strain*. A small cube with sides equal to unity, centered at *Q*, and with faces perpendicular to the principal axes is

deformed into a rectangular parallelepiped with sides $1 + \epsilon_a$, $1 + \epsilon_b$, and $1 + \epsilon_c$ (Fig. 7.57).

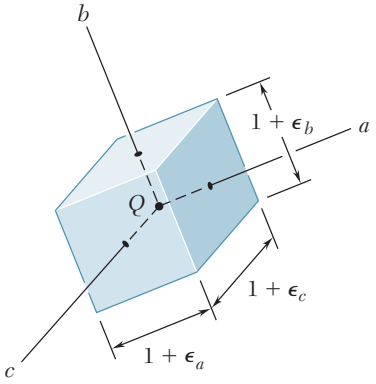


Fig. 7.57 Strain element oriented to directions of principal axes.

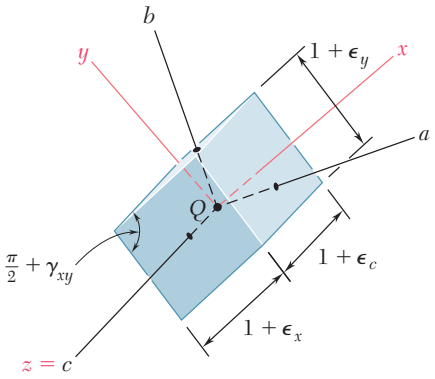


Fig. 7.58 Strain element having one axis coincident with a principal strain axis.

If the element of Fig. 7.57 is rotated about one of the principal axes at Q, say the c axis (Fig. 7.58), the method of analysis for the transformation of plane strain also can be used to determine the strain components ϵ_x, ϵ_y, and γ_{xy} associated with the faces perpendicular to the c axis, since this method did not involve any of the other strain components.† Therefore, Mohr's circle is drawn through the points A and B corresponding to the principal axes a and b (Fig. 7.59). Similarly, circles of diameters BC and CA are used to analyze the transformation of strain as the element is rotated about the a and b axes, respectively.

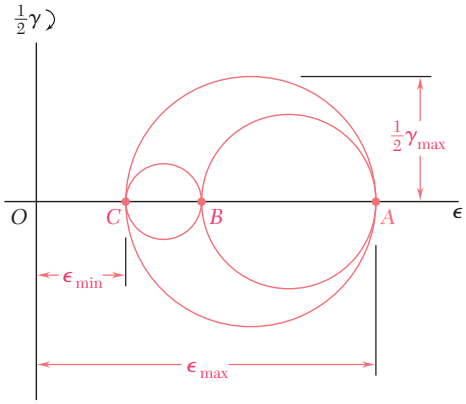


Fig. 7.59 Mohr's circle for three-dimensional analysis of strain.

The three-dimensional analysis of strain using Mohr's circle is limited here to rotations about principal axes (as for the analysis of stress) and is used to determine the maximum shearing strain γ_{max} at point Q. Since γ_{max} is equal to the diameter of the largest of the three circles shown in Fig. 7.59,

$$\gamma_{max} = |\epsilon_{max} - \epsilon_{min}| \tag{7.54}$$

†The other four faces of the element remain rectangular, and the edges parallel to the c axis remain unchanged.

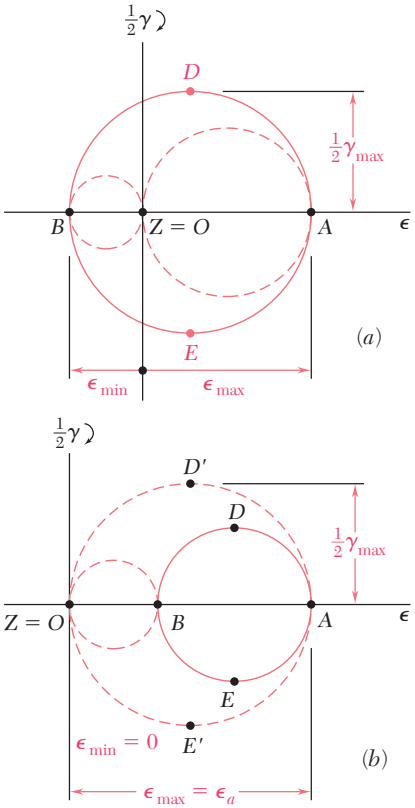


Fig. 7.60 Possible configurations of Mohr's circle for plane strain. (*a*) Principal strains having mixed signs. (*b*) Principal strains having positive signs.

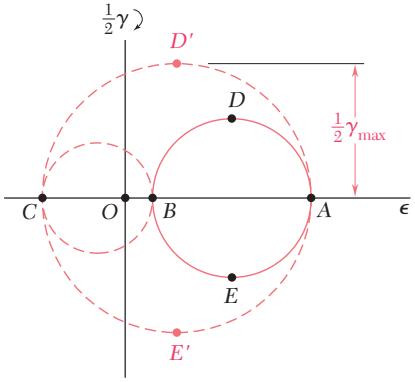


Fig. 7.61 Mohr's circle strain analysis for plane stress.

where ϵ_{max} and ϵ_{min} represent the *algebraic* values of the maximum and minimum strains at point Q.

Returning to the particular case of *plane strain*, and selecting the x and y axes in the plane of strain, we have $\epsilon_z = \gamma_{zx} = \gamma_{zy} = 0$. Thus, the z axis is one of the three principal axes at Q, and the corresponding point in the Mohr's circle diagram is the origin O, where $\epsilon = \gamma = 0$. If points A and B defining the principal axes within the plane of strain fall on opposite sides of O (Fig. 7.60*a*), the corresponding principal strains represent the maximum and minimum normal strains at point Q, and the maximum shearing strain is equal to the maximum in-plane shearing strain corresponding to points D and E. However, if A and B are on the same side of O (Fig. 7.60*b*), so that ϵ_a and ϵ_b have the same sign, the maximum shearing strain is defined by points D' and E' on the circle of diameter OA, and $\gamma_{max} = \epsilon_{max}$.

Now consider the particular case of *plane stress* encountered in a thin plate or on the free surface of a structural element or machine component. Selecting the x and y axes in the plane of stress, $\sigma_z = \tau_{zx} = \tau_{zy} = 0$, and the z axis is a principal axis of stress. If the deformation is elastic and the material is homogeneous and isotropic, Hooke's law shows that $\gamma_{zx} = \gamma_{zy} = 0$. Thus, the z axis is also a principal axis of strain, and Mohr's circle can be used to analyze the transformation of strain in the xy plane. However, as we shall see presently, Hooke's law does *not* show that $\epsilon_z = 0$; indeed, a state of plane stress does not, in general, result in a state of plane strain.

Using a and b as the principal axes within the plane of stress and c as the principal axis perpendicular to that plane, we let $\sigma_x = \sigma_a$, $\sigma_y = \sigma_b$, and $\sigma_z = 0$ in Eqs. (2.20) for the generalized Hooke's law (Sec. 2.5), and obtain

$$\epsilon_a = \frac{\sigma_a}{E} - \frac{\nu\sigma_b}{E} \tag{7.55}$$

$$\epsilon_b = -\frac{\nu\sigma_a}{E} + \frac{\sigma_b}{E} \tag{7.56}$$

$$\epsilon_c = -\frac{\nu}{E}(\sigma_a + \sigma_b) \tag{7.57}$$

Adding Eqs. (7.55) and (7.56) member to member gives

$$\epsilon_a + \epsilon_b = \frac{1-\nu}{E}(\sigma_a + \sigma_b) \tag{7.58}$$

Solving Eq. (7.58) for $\sigma_a + \sigma_b$ and substituting into Eq. (7.57), we write

$$\epsilon_c = -\frac{\nu}{1-\nu}(\epsilon_a + \epsilon_b) \tag{7.59}$$

The relationship obtained defines the third principal strain in terms of the in-plane principal strains. If B is located between A and C on the Mohr's circle diagram (Fig. 7.61), the maximum shearing strain is equal to the diameter CA of the circle corresponding to a rotation about the b axis, out of the plane of stress.

Concept Application 7.5

As a result of measurements made on the surface of a machine component with strain gages oriented in various ways, it has been established that the principal strains on the free surface are $\epsilon_a = +400 \times 10^{-6}$ in./in. and $\epsilon_b = -50 \times 10^{-6}$ in./in. Knowing that Poisson's ratio for the given material is $\nu = 0.30$, determine (*a*) the maximum in-plane shearing strain, (*b*) the true value of the maximum shearing strain near the surface of the component.

a. Maximum In-Plane Shearing Strain. Draw Mohr's circle through points *A* and *B* corresponding to the given principal strains (Fig. 7.62*a*). The maximum in-plane shearing strain is defined by points *D* and *E* and is equal to the diameter of Mohr's circle:

$$\gamma_{\max\,(\text{in plane})} = 400 \times 10^{-6} + 50 \times 10^{-6} = 450 \times 10^{-6}\,\text{rad}$$

b. Maximum Shearing Strain. Determine the third principal strain ϵ_c. Since a state of plane *stress* is on the surface of the machine component, Eq. (7.59) gives

$$\epsilon_c = -\frac{\nu}{1-\nu}(\epsilon_a + \epsilon_b)$$
$$= -\frac{0.30}{0.70}(400 \times 10^{-6} - 50 \times 10^{-6}) = -150 \times 10^{-6}\,\text{in./in.}$$

Draw Mohr's circles through *A* and *C* and through *B* and *C* (Fig. 7.62*b*), and find that the maximum shearing strain is equal to the diameter of the circle *CA*:

$$\gamma_{\max} = 400 \times 10^{-6} + 150 \times 10^{-6} = 550 \times 10^{-6}\,\text{rad}$$

Note that even though ϵ_a and ϵ_b have opposite signs, the maximum in-plane shearing strain does not represent the true maximum shearing strain.

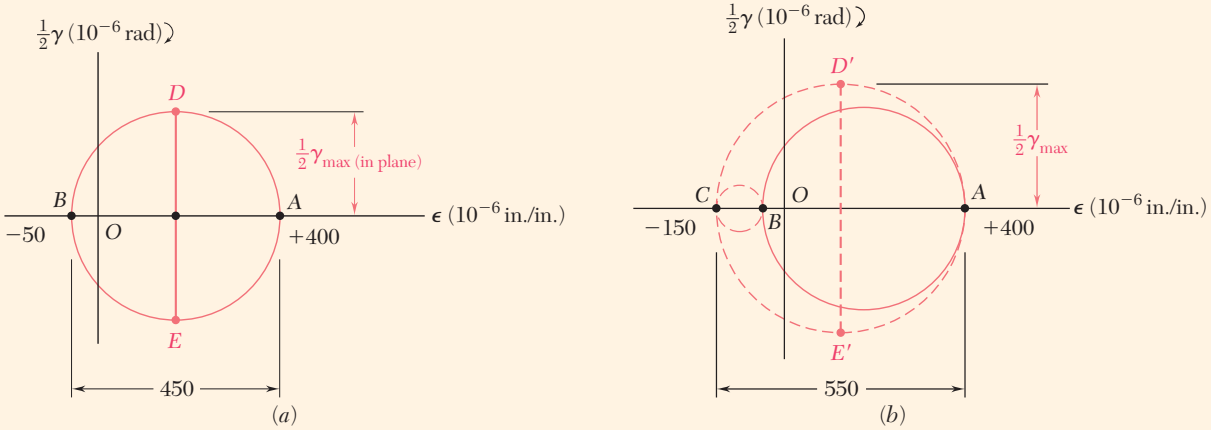


Fig. 7.62 Using Mohr's circle to determine maximum shearing strain. (*a*) Mohr's circle for the plane of the given strains. (*b*) Three-dimensional Mohr's circle for strain.

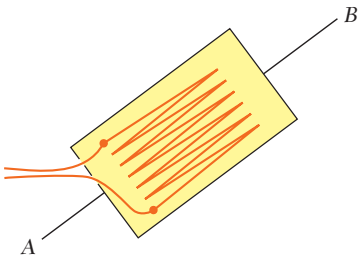


Fig. 7.63 Electrical strain gage.

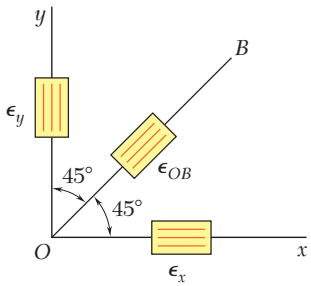


Fig. 7.64 Strain rosette that measures normal strains in direction of *x*, *y*, and bisector *OB*.

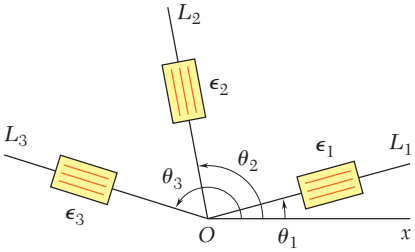


Fig. 7.65 Generalized strain gage rosette arrangement.

*7.9 MEASUREMENTS OF STRAIN; STRAIN ROSETTE

The normal strain can be determined in any given direction on the surface of a structural element or machine component by scribing two gage marks *A* and *B* across a line drawn in the desired direction and measuring the length of the segment *AB* before and after the load has been applied. If *L* is the undeformed length of *AB* and δ its deformation, the normal strain along *AB* is $\epsilon_{AB} = \delta/L$.

A more convenient and accurate method for measuring normal strains is provided by electrical strain gages. A typical electrical strain gage consists of a length of thin wire arranged as shown in Fig. 7.63 and cemented to two pieces of paper. In order to measure the strain ϵ_{AB} of a given material in the direction *AB*, the gage is cemented to the surface of the material with the wire folds running parallel to *AB*. As the material elongates, the wire increases in length and decreases in diameter, causing the electrical resistance of the gage to increase. By measuring the current passing through a properly calibrated gage, the strain ϵ_{AB} can be determined accurately and continuously as the load is increased.

The strain components ϵ_x and ϵ_y can be determined at a given point of the free surface of a material by simply measuring the normal strain along the *x* and *y* axes drawn through that point. Recalling Eq. (7.43), we note that a third measurement of normal strain, made along the bisector *OB* of the angle formed by the *x* and *y* axes, enables us to determine the shearing strain γ_{xy} as well (Fig. 7.64):

$$\gamma_{xy} = 2\epsilon_{OB} - (\epsilon_x + \epsilon_y) \tag{7.43}$$

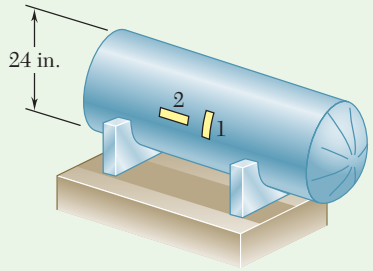
The strain components ϵ_x, ϵ_y, and γ_{xy} at a given point also can be obtained from normal strain measurements made along *any three lines* drawn through that point (Fig. 7.65). Denoting respectively by θ_1, θ_2, and θ_3 the angle each of the three lines forms with the *x* axis, by ϵ_1, ϵ_2, and ϵ_3 the corresponding strain measurements, and substituting into Eq. (7.41), we write the three equations

$$\begin{aligned}
\epsilon_1 &= \epsilon_x \cos^2\theta_1 + \epsilon_y \sin^2\theta_1 + \gamma_{xy} \sin\theta_1 \cos\theta_1 \\
\epsilon_2 &= \epsilon_x \cos^2\theta_2 + \epsilon_y \sin^2\theta_2 + \gamma_{xy} \sin\theta_2 \cos\theta_2 \\
\epsilon_3 &= \epsilon_x \cos^2\theta_3 + \epsilon_y \sin^2\theta_3 + \gamma_{xy} \sin\theta_3 \cos\theta_3
\end{aligned} \tag{7.60}$$

These can be solved simultaneously for ϵ_x, ϵ_y, and γ_{xy}.[†]

The arrangement of strain gages used to measure the three normal strains ϵ_1, ϵ_2, and ϵ_3 is called a *strain rosette*. The rosette used to measure normal strains along the *x* and *y* axes and their bisector is referred to as a 45° rosette (Fig. 7.64). Another rosette frequently used is the 60° rosette (see Sample Prob. 7.7).

[†]It should be noted that the free surface on which the strain measurements are made is in a state of *plane stress*, while Eqs. (7.41) and (7.43) were derived for a state of *plane strain*. However, as observed earlier the normal to the free surface is a principal axis of strain, and the derivations given in Sec. 7.7A remain valid.



Sample Problem 7.6

A cylindrical storage tank used to transport gas under pressure has an inner diameter of 24 in. and a wall thickness of $\frac{3}{4}$ in. Strain gages attached to the surface of the tank in transverse and longitudinal directions indicate strains of 255×10^{-6} and 60×10^{-6} in./in., respectively. Knowing that a torsion test has shown that the modulus of rigidity of the material used in the tank is $G = 11.2 \times 10^{6}$ psi, determine (*a*) the gage pressure inside the tank, (*b*) the principal stresses and the maximum shearing stress in the wall of the tank.

STRATEGY: You can use the given measured strains to plot Mohr's circle for strain, and use this circle to determine the maximum in-plane shearing strain. Applying Hooke's law to obtain the corresponding maximum in-plane shearing stress, you can then determine the gage pressure in the tank through the appropriate thin-walled pressure vessel equation, as well as develop Mohr's circle for stress to determine the principal stresses and the maximum shearing stress.

MODELING and ANALYSIS:

a. Gage Pressure Inside Tank. The given strains are the principal strains at the surface of the tank. Plotting the corresponding points *A* and *B*, draw Mohr's circle for strain (Fig. 1). The maximum in-plane shearing strain is equal to the diameter of the circle.

$$\gamma_{\max\,(\text{in plane})} = \epsilon_1 - \epsilon_2 = 255 \times 10^{-6} - 60 \times 10^{-6} = 195 \times 10^{-6}\,\text{rad}$$

From Hooke's law for shearing stress and strain,

$$\begin{aligned}\tau_{\max\,(\text{in plane})} &= G\gamma_{\max\,(\text{in plane})}\\ &= (11.2 \times 10^{6}\,\text{psi})(195 \times 10^{-6}\,\text{rad})\\ &= 2184\,\text{psi} = 2.184\,\text{ksi}\end{aligned}$$

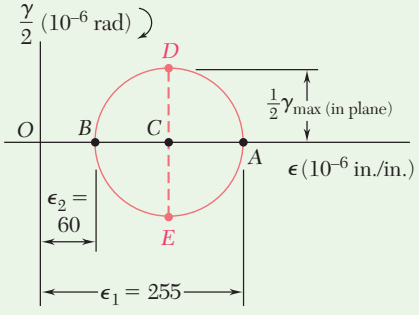


Fig. 1 Mohr's circle for measured strains.

(continued)

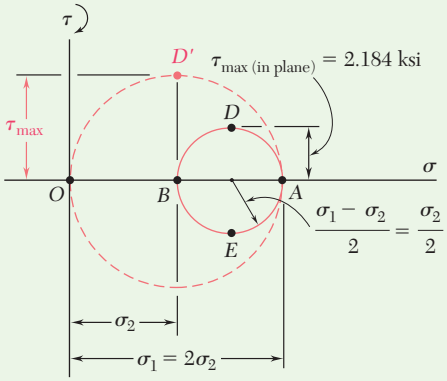


Fig. 2 Three-dimensional Mohr's circles for vessel stress components.

Substituting this and the given data in Eq. (7.33),

$$\tau_{\max\,(\text{in plane})} = \frac{pr}{4t} \qquad 2184 \text{ psi} = \frac{p(12 \text{ in.})}{4(0.75 \text{ in.})}$$

Solving for the gage pressure p,

$$p = 546 \text{ psi}$$

b. Principal Stresses and Maximum Shearing Stress. Recalling that for a thin-walled cylindrical pressure vessel $\sigma_1 = 2\sigma_2$, we draw Mohr's circle for stress (Fig. 2) and obtain

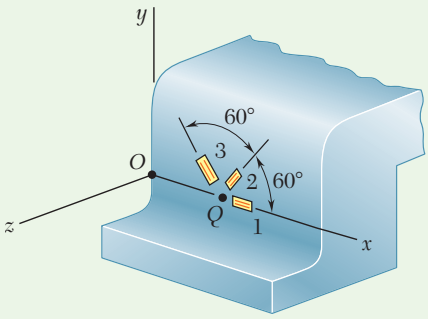
$$\sigma_2 = 2\tau_{\max\,(\text{in plane})} = 2(2.184 \text{ ksi}) = 4.368 \text{ ksi} \qquad \sigma_2 = 4.37 \text{ ksi}$$

$$\sigma_1 = 2\sigma_2 = 2(4.368 \text{ ksi}) \qquad \sigma_1 = 8.74 \text{ ksi}$$

The maximum shearing stress is equal to the radius of the circle of diameter OA and corresponds to a rotation of 45° about a longitudinal axis.

$$\tau_{\max} = \tfrac{1}{2}\sigma_1 = \sigma_2 = 4.368 \text{ ksi} \qquad \tau_{\max} = 4.37 \text{ ksi}$$

Sample Problem 7.7



Using a 60° rosette, the following strains have been measured at point Q on the surface of a steel machine base:

$$\epsilon_1 = 40\,\mu \qquad \epsilon_2 = 980\,\mu \qquad \epsilon_3 = 330\,\mu$$

Using the coordinate axes shown, determine at point Q (*a*) the strain components ϵ_x, ϵ_y, and γ_{xy}, (*b*) the principal strains, (*c*) the maximum shearing strain. (Use $\nu = 0.29$.)

STRATEGY: From the given strain rosette measurements, you can find the strain components ϵ_x, ϵ_y, and γ_{xy} using Eq. (7.60). Using these strains, you can plot Mohr's circle for strain to determine the principal strains and the maximum shearing strain.

MODELING and ANALYSIS:

a. Strain Components ϵ_x, ϵ_y, γ_{xy}. For the coordinate axes shown

$$\theta_1 = 0 \qquad \theta_2 = 60° \qquad \theta_3 = 120°$$

(continued)

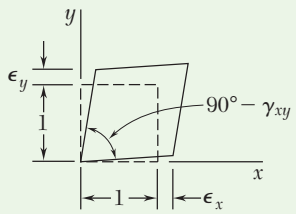


Fig. 1 Undeformed and deformed strain elements at *Q*.

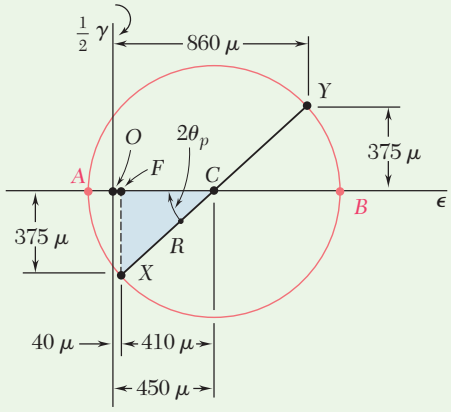


Fig. 2. Mohr's circle used to determine principal strains.

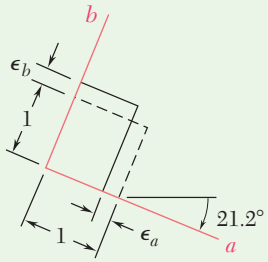


Fig. 3. Undeformed and deformed principal strain element at *Q*.

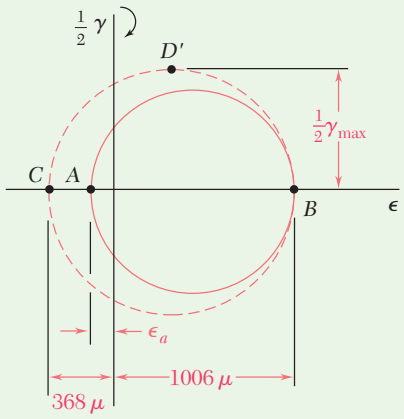


Fig. 4 Three-dimensional Mohr's circles used to determine maximum shearing strain.

Substituting these into Eqs. (7.60), gives

$$\epsilon_1 = \epsilon_x(1) + \epsilon_y(0) + \gamma_{xy}(0)(1)$$
$$\epsilon_2 = \epsilon_x(0.500)^2 + \epsilon_y(0.866)^2 + \gamma_{xy}(0.866)(0.500)$$
$$\epsilon_3 = \epsilon_x(-0.500)^2 + \epsilon_y(0.866)^2 + \gamma_{xy}(0.866)(-0.500)$$

Solving these equations for ϵ_x, ϵ_y, and γ_{xy},

$$\epsilon_x = \epsilon_1 \qquad \epsilon_y = \tfrac{1}{3}(2\epsilon_2 + 2\epsilon_3 - \epsilon_1) \qquad \gamma_{xy} = \frac{\epsilon_2 - \epsilon_3}{0.866}$$

Substituting for ϵ_1, ϵ_2, and ϵ_3,

$$\epsilon_x = 40\,\mu \qquad \epsilon_y = \tfrac{1}{3}[2(980) + 2(330) - 40] \qquad \epsilon_y = +860\,\mu$$
$$\gamma_{xy} = (980 - 330)/0.866 \qquad \gamma_{xy} = 750\,\mu$$

These strains are indicated on the element shown in Fig. 1.

b. Principal Strains. The side of the element associated with ϵ_x rotates counterclockwise; thus, point *X* is plotted below the horizontal axis, as *X*(40, −375). Then *Y*(860, +375) is plotted and Mohr's circle is drawn (Fig. 2).

$$\epsilon_{ave} = \tfrac{1}{2}(860\,\mu + 40\,\mu) = 450\,\mu$$
$$R = \sqrt{(375\,\mu)^2 + (410\,\mu)^2} = 556\,\mu$$
$$\tan 2\theta_p = \frac{375\,\mu}{410\,\mu} \qquad 2\theta_p = 42.4°\downarrow \qquad \theta_p = 21.2°\downarrow$$

Points *A* and *B* correspond to the principal strains,

$$\epsilon_a = \epsilon_{ave} - R = 450\,\mu - 556\,\mu \qquad \epsilon_a = -106\,\mu$$
$$\epsilon_b = \epsilon_{ave} + R = 450\,\mu + 556\,\mu \qquad \epsilon_b = +1006\,\mu$$

These strains are indicated on the element shown in Fig. 3. Since $\sigma_z = 0$ on the surface, Eq. (7.59) is used to find the principal strain ϵ_c:

$$\epsilon_c = -\frac{\nu}{1-\nu}(\epsilon_a + \epsilon_b) = -\frac{0.29}{1 - 0.29}(-106\,\mu + 1006\,\mu) \qquad \epsilon_c = -368\,\mu$$

c. Maximum Shearing Strain. Plotting point *C* and drawing Mohr's circle through points *B* and *C* (Fig. 4), we obtain point *D*′ and write

$$\tfrac{1}{2}\gamma_{max} = \tfrac{1}{2}(1006\,\mu + 368\,\mu) \qquad \gamma_{max} = 1374\,\mu$$

Problems

7.128 through 7.131 For the given state of plane strain, use the method of Sec. 7.7A to determine the state of plane strain associated with axes x' and y' rotated through the given angle θ.

	ϵ_x	ϵ_y	γ_{xy}	θ
7.128 and 7.132	-800μ	$+450\mu$	$+200\mu$	25° ↻
7.129 and 7.133	$+240\mu$	$+160\mu$	$+150\mu$	60° ↻
7.130* and *7.134	-500μ	$+250\mu$	0	15° ↺
7.131 and 7.135	0	$+320\mu$	-100μ	30° ↺

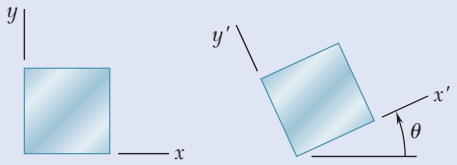


Fig. P7.128 through P7.135

7.132 through 7.135 For the given state of plane strain, use Mohr's circle to determine the state of plane strain associated with axes x' and y' rotated through the given angle θ.

7.136 through 7.139 The following state of strain has been measured on the surface of a thin plate. Knowing that the surface of the plate is unstressed, determine (*a*) the direction and magnitude of the principal strains, (*b*) the maximum in-plane shearing strain, (*c*) the maximum shearing strain. (Use $\nu = \frac{1}{3}$)

	ϵ_x	ϵ_y	γ_{xy}
7.136	-260μ	-60μ	$+480\mu$
7.137	-600μ	-400μ	$+350\mu$
7.138	$+160\mu$	-480μ	-600μ
7.139	$+30\mu$	$+570\mu$	$+720\mu$

7.140 through 7.143 For the given state of plane strain, use Mohr's circle to determine (*a*) the orientation and magnitude of the principal strains, (*b*) the maximum in-plane strain, (*c*) the maximum shearing strain.

	ϵ_x	ϵ_y	γ_{xy}
7.140	$+60\mu$	$+240\mu$	-50μ
7.141	$+400\mu$	$+200\mu$	$+375\mu$
7.142	$+300\mu$	$+60\mu$	$+100\mu$
7.143	-180μ	-260μ	$+315\mu$

7.144 Determine the strain ϵ_x, knowing that the following strains have been determined by use of the rosette shown:

$$\epsilon_1 = +480\mu \qquad \epsilon_2 = -120\mu \qquad \epsilon_3 = +80\mu$$

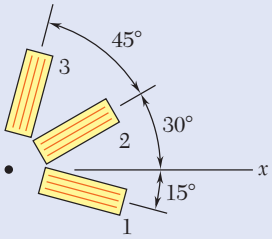


Fig. *P7.144*

7.145 The strains determined by the use of the rosette shown during the test of a machine element are

$$\epsilon_1 = +600\mu \qquad \epsilon_2 = +450\mu \qquad \epsilon_3 = -75\mu$$

Determine (*a*) the in-plane principal strains, (*b*) the in-plane maximum shearing strain.

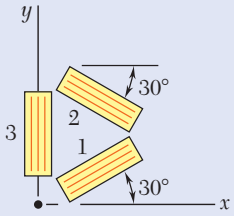


Fig. *P7.145*

7.146 The rosette shown has been used to determine the following strains at a point on the surface of a crane hook:

$$\epsilon_1 = +420 \times 10^{-6} \text{ in./in.} \qquad \epsilon_2 = -45 \times 10^{-6} \text{ in./in.}$$
$$\epsilon_4 = +165 \times 10^{-6} \text{ in./in.}$$

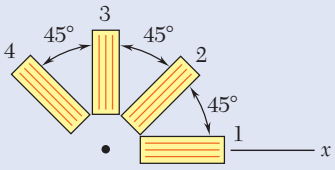


Fig. P7.146

(*a*) What should be the reading of gage 3? (*b*) Determine the principal strains and the maximum in-plane shearing strain.

7.147 Using a 45° rosette, the strains ϵ_1, ϵ_2, and ϵ_3 have been determined at a given point. Using Mohr's circle, show that the principal strains are:

$$\epsilon_{\text{max, min}} = \frac{1}{2}(\epsilon_1 + \epsilon_3) \pm \frac{1}{\sqrt{2}}[(\epsilon_1 - \epsilon_2)^2 + (\epsilon_2 - \epsilon_3)^2]^{\frac{1}{2}}$$

(*Hint:* The shaded triangles are congruent.)

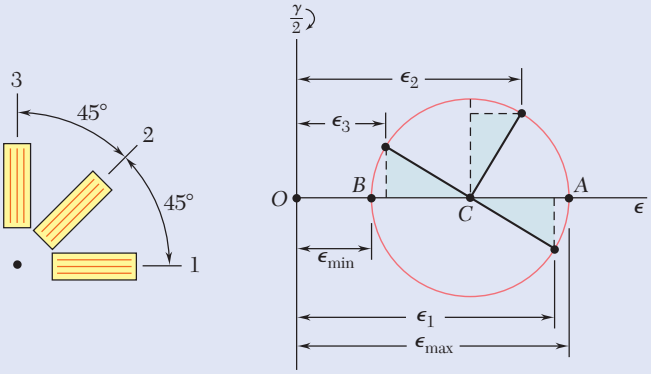


Fig. P7.147

7.148 Show that the sum of the three strain measurements made with a 60° rosette is independent of the orientation of the rosette and equal to

$$\epsilon_1 + \epsilon_2 + \epsilon_3 = 3\epsilon_{avg}$$

where ϵ_{avg} is the abscissa of the center of the corresponding Mohr's circle.

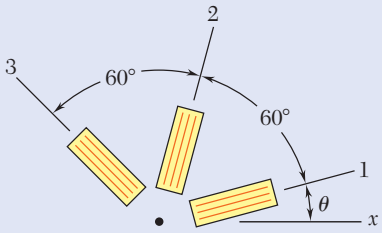


Fig. P7.148

7.149 The strains determined by the use of the rosette attached as shown during the test of a machine element are

$$\epsilon_1 = -93.1 \times 10^{-6} \text{ in./in.} \qquad \epsilon_2 = +385 \times 10^{-6} \text{ in./in.}$$
$$\epsilon_3 = +210 \times 10^{-6} \text{ in./in.}$$

Determine (*a*) the orientation and magnitude of the principal strains in the plane of the rosette, (*b*) the maximum in-plane shearing strain.

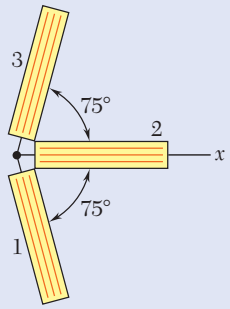


Fig. P7.149

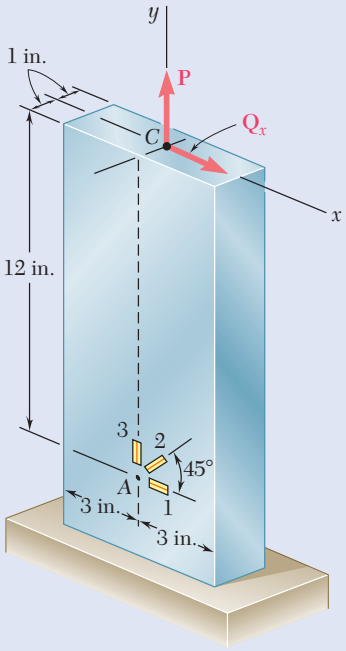


Fig. P7.150

7.150 A centric axial force **P** and a horizontal force $\mathbf{Q}_x$ are both applied at point *C* of the rectangular bar shown. A 45° strain rosette on the surface of the bar at point *A* indicates the following strains:

$$\epsilon_1 = -60 \times 10^{-6} \text{ in./in.} \qquad \epsilon_2 = +240 \times 10^{-6} \text{ in./in.}$$
$$\epsilon_3 = +200 \times 10^{-6} \text{ in./in.}$$

Knowing that $E = 29 \times 10^6$ psi and $\nu = 0.30$, determine the magnitudes of **P** and $\mathbf{Q}_x$.

7.151 Solve Prob. 7.150, assuming that the rosette at point *A* indicates the following strains:

$$\epsilon_1 = -30 \times 10^{-6} \text{ in./in.} \qquad \epsilon_2 = +250 \times 10^{-6} \text{ in./in.}$$
$$\epsilon_3 = +100 \times 10^{-6} \text{ in./in.}$$

7.152 A single strain gage is cemented to a solid 4-in.-diameter steel shaft at an angle $\beta = 25°$ with a line parallel to the axis of the shaft. Knowing that $G = 11.5 \times 10^6$ psi, determine the torque **T** indicated by a gage reading of 300×10^{-6} in./in.

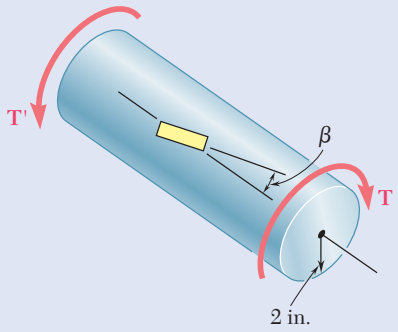


Fig. *P7.152*

7.153 Solve Prob. 7.152, assuming that the gage forms an angle $\beta = 35°$ with a line parallel to the axis of the shaft.

7.154 A single strain gage forming an angle $\beta = 18°$ with a horizontal plane is used to determine the gage pressure in the cylindrical steel tank shown. The cylindrical wall of the tank is 6 mm thick, has a 600-mm inside diameter, and is made of a steel with $E = 200$ GPa and $\nu = 0.30$. Determine the pressure in the tank indicated by a strain gage reading of 280μ.

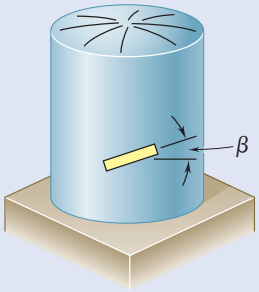


Fig. P7.154

7.155 Solve Prob. 7.154, assuming that the gage forms an angle $\beta = 35°$ with a horizontal plane.

7.156 The given state of plane stress is known to exist on the surface of a machine component. Knowing that $E = 200$ GPa and $G = 77.2$ GPa, determine the direction and magnitude of the three principal strains (*a*) by determining the corresponding state of strain [use Eq. (2.43) and Eq. (2.38)] and then using Mohr's circle for strain, (*b*) by using Mohr's circle for stress to determine the principal planes and principal stresses and then determining the corresponding strains.

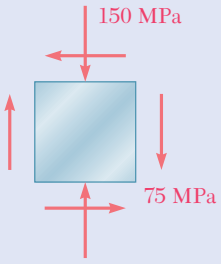


Fig. P7.156

7.157 The following state of strain has been determined on the surface of a cast-iron machine part:

$$\epsilon_x = -720\mu \qquad \epsilon_y = -400\mu \qquad \gamma_{xy} = +660\mu$$

Knowing that $E = 69$ GPa and $G = 28$ GPa, determine the principal planes and principal stresses (*a*) by determining the corresponding state of plane stress [use Eq. (2.36), Eq. (2.43), and the first two equations of Prob. 2.73] and then using Mohr's circle for stress, (*b*) by using Mohr's circle for strain to determine the orientation and magnitude of the principal strains and then determining the corresponding stresses.

Review and Summary

Transformation of Plane Stress

A state of *plane stress* at a given point Q has nonzero values for σ_x, σ_y, and τ_{xy}. The stress components associated with the element are shown in Fig. 7.66*a*. The equations for the components $\sigma_{x'}$, $\sigma_{y'}$, and $\tau_{x'y'}$ associated with that element after being rotated through an angle θ about the z axis (Fig. 7.66*b*) are

$$\sigma_{x'} = \frac{\sigma_x + \sigma_y}{2} + \frac{\sigma_x - \sigma_y}{2}\cos 2\theta + \tau_{xy}\sin 2\theta \tag{7.5}$$

$$\sigma_{y'} = \frac{\sigma_x + \sigma_y}{2} - \frac{\sigma_x - \sigma_y}{2}\cos 2\theta - \tau_{xy}\sin 2\theta \tag{7.7}$$

$$\tau_{x'y'} = -\frac{\sigma_x - \sigma_y}{2}\sin 2\theta + \tau_{xy}\cos 2\theta \tag{7.6}$$

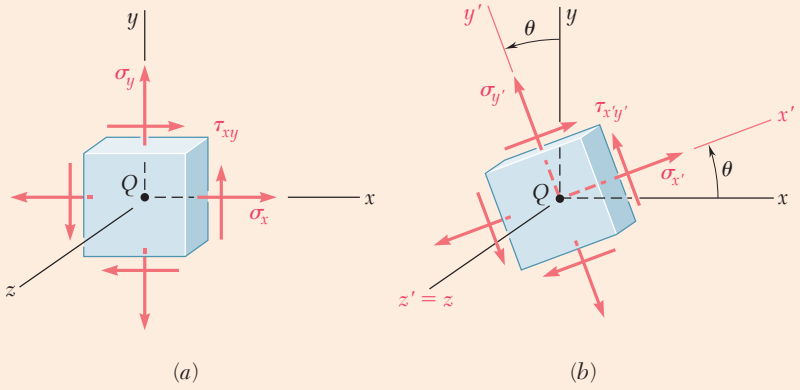


Fig. 7.66 State of plane stress. (*a*) Referred to {*x y z*}. (*b*) Referred to {*x′y′z′*}.

The values θ_p of the angle of rotation that correspond to the maximum and minimum values of the normal stress at point Q are

$$\tan 2\theta_p = \frac{2\tau_{xy}}{\sigma_x - \sigma_y} \tag{7.12}$$

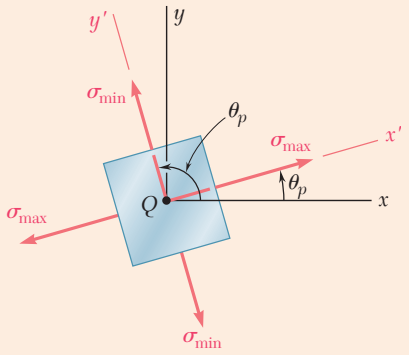


Fig. 7.67 Principal stresses.

Principal Planes and Principal Stresses

The two values obtained for θ_p are 90° apart (Fig. 7.67) and define the *principal planes of stress* at point Q. The corresponding values of the normal stress are called the *principal stresses* at Q:

$$\sigma_{\max,\,\min} = \frac{\sigma_x + \sigma_y}{2} \pm \sqrt{\left(\frac{\sigma_x - \sigma_y}{2}\right)^2 + \tau_{xy}^2} \tag{7.14}$$

The corresponding shearing stress is zero.

Maximum In-Plane Shearing Stress

The angle θ for the largest value of the shearing stress θ_s is found using

$$\tan 2\theta_s = -\frac{\sigma_x - \sigma_y}{2\tau_{xy}} \tag{7.15}$$

The two values obtained for θ_s are 90° apart (Fig. 7.68). However, the planes of maximum shearing stress are at 45° to the principal planes. The maximum value of the shearing stress *in the plane of stress is*

$$\tau_{\max} = \sqrt{\left(\frac{\sigma_x - \sigma_y}{2}\right)^2 + \tau_{xy}^2} \tag{7.16}$$

and the corresponding value of the normal stresses is

$$\sigma' = \sigma_{\text{ave}} = \frac{\sigma_x + \sigma_y}{2} \tag{7.17}$$

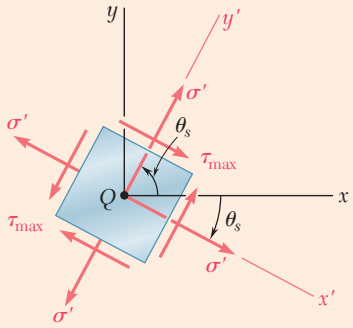


Fig. 7.68 Maximum shearing stress.

Mohr's Circle for Stress

Mohr's circle provides an alternative method for the analysis of the transformation of plane stress based on simple geometric considerations. Given the state of stress shown in the left element in Fig. 7.69*a*, point *X* of coordinates σ_x, $-\tau_{xy}$ and point *Y* of coordinates σ_y, $+\tau_{xy}$ are plotted in Fig. 7.69*b*. Drawing the circle of diameter *XY* provides Mohr's circle. The abscissas of the points of intersection *A* and *B* of the circle with the horizontal axis represent the principal stresses, and the angle of rotation bringing the diameter *XY* into *AB* is twice the angle θ_p defining the principal planes, as shown in the right element of Fig. 7.69*a*. The diameter *DE* defines the maximum shearing stress and the orientation of the corresponding plane (Fig. 7.70).

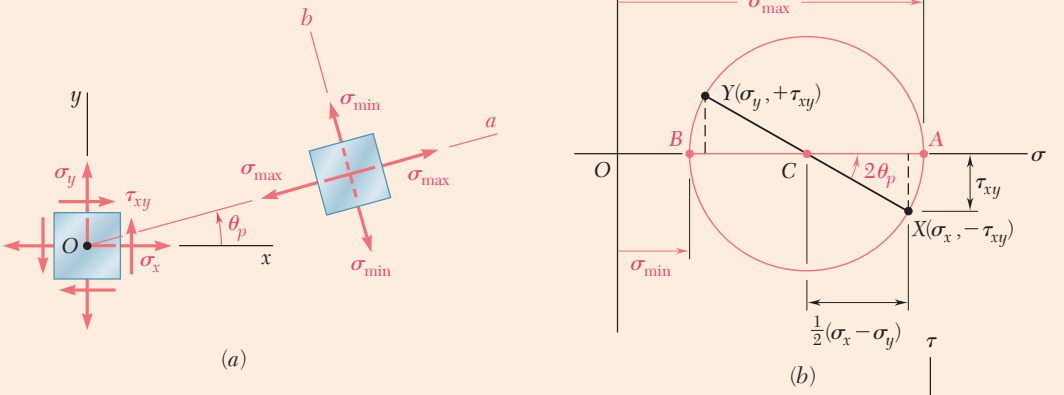


Fig. 7.69 (*a*) Plane stress element, and the orientation of principal planes. (*b*) Corresponding Mohr's circle.

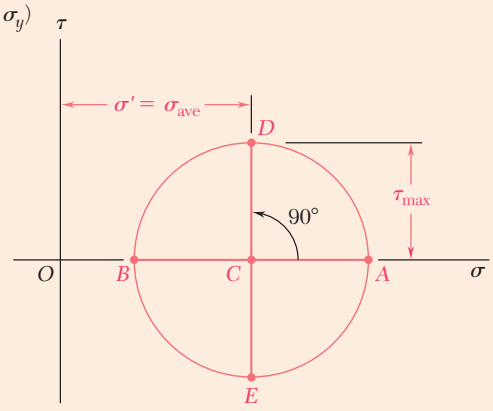


Fig. 7.70 Maximum shearing stress is oriented ±45° from principal directions.

General State of Stress

A *general state of stress* is characterized by six stress components, where the normal stress on a plane of arbitrary orientation can be expressed as a quadratic form of the direction cosines of the normal to that plane. This proves the existence of three *principal axes of stress* and three *principal stresses* at any given point. Rotating a small cubic element about each of the three principal axes was used to draw the corresponding Mohr's circles that yield the values of σ_{max}, σ_{min}, and τ_{max} (Fig. 7.71). In the case of

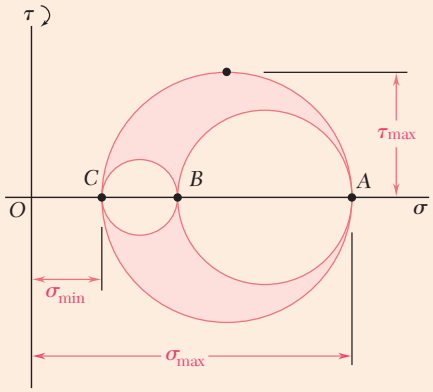


Fig. 7.71 Three-dimensional Mohr's circles for general state of stress.

plane stress when the x and y axes are selected in the plane of stress, point C coincides with the origin O. If A and B are located on opposite sides of O, the maximum shearing stress is equal to the maximum in-plane shearing stress. If A and B are located on the same side of O, this is not the case. For instance if $\sigma_a > \sigma_b > 0$, the maximum shearing stress is equal to $\frac{1}{2}\sigma_a$ and corresponds to a rotation out of the plane of stress (Fig. 7.72).

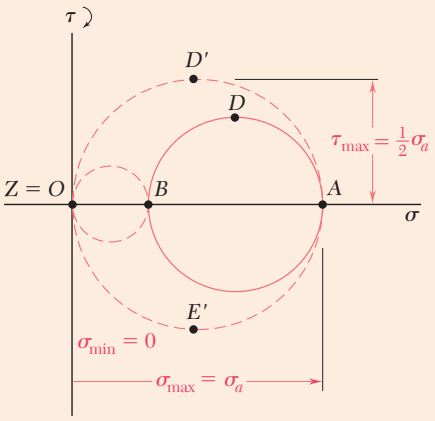


Fig. 7.72 Three-dimensional Mohr's circles for plane stress having two positive principal stresses.

Yield Criteria for Ductile Materials

To predict whether a structural or machine component will fail at some critical point due to yield in the material, the principal stresses σ_a and σ_b at that point for the given loading condition are determined. The point of coordinates σ_a and σ_b is plotted, and if this point falls within a certain area, the component is safe. If it falls outside, the component will fail. The area used with the maximum-shearing-stress criterion is shown in Fig. 7.73, and the area used with the maximum-distortion-energy criterion in Fig. 7.74. Both areas depend upon the value of the yield strength σ_Y of the material.

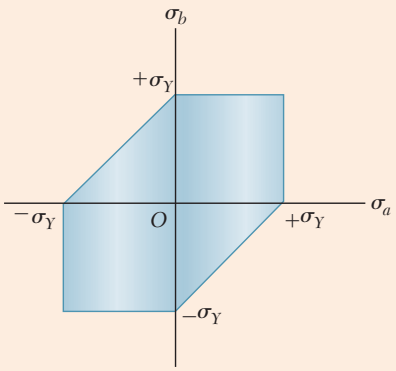


Fig. 7.73 Tresca's hexagon for maximum shearing-stress criterion.

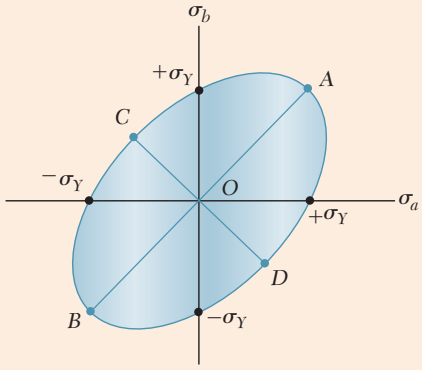


Fig. 7.74 Von Mises surface based on maximum-distortion-energy criterion.

Fracture Criteria for Brittle Materials

The most commonly used method to predict failure of brittle materials is the fracture-based *Mohr's criterion*, which uses the results of various tests for a given material. The shaded area shown in Fig. 7.75 is used when the ultimate strengths σ_{UT} and σ_{UC} have been determined, respectively, from a tension and a compression test. The principal stresses σ_a and σ_b are determined at a given point, and if the corresponding point falls within the shaded area, the component is safe, and if it falls outside, the component will rupture.

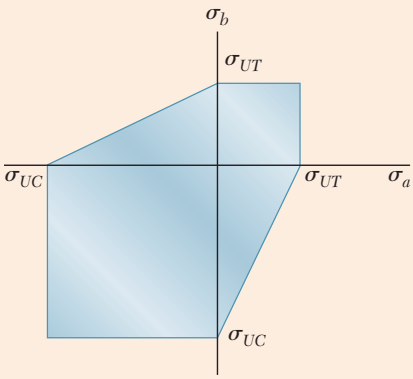


Fig. 7.75 Simplified Mohr's criterion for brittle materials.

Cylindrical Pressure Vessels

The stresses in *thin-walled pressure vessels* and equations relating to the stresses in the walls and the *gage pressure* p in the fluid were discussed. For a *cylindrical vessel* of inside radius r and thickness t (Fig. 7.76), the *hoop stress* σ_1 and the *longitudinal stress* σ_2 are

$$\sigma_1 = \frac{pr}{t} \qquad \sigma_2 = \frac{pr}{2t} \tag{7.30, 7.31}$$

The *maximum shearing* stress occurs out of the plane of stress and is

$$\tau_{\max} = \sigma_2 = \frac{pr}{2t} \tag{7.34}$$

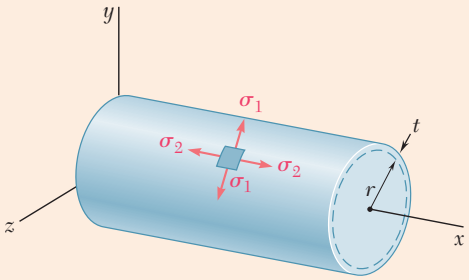


Fig. 7.76 Pressurized cylindrical vessel.

Spherical Pressure Vessels

For a *spherical vessel* of inside radius r and thickness t (Fig. 7.77), the two principal stresses are equal:

$$\sigma_1 = \sigma_2 = \frac{pr}{2t} \tag{7.36}$$

Again, the *maximum shearing* stress occurs out of the plane of stress and is

$$\tau_{\max} = \tfrac{1}{2}\sigma_1 = \frac{pr}{4t} \tag{7.37}$$

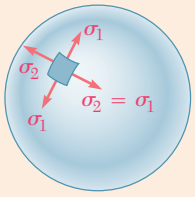


Fig. 7.77 Pressurized spherical vessel.

Transformation of Plane Strain

The last part of the chapter was devoted to the *transformation of strain.* We discussed the transformation of *plane strain* and introduced *Mohr's circle for plane strain.* The discussion was similar to the corresponding discussion of the transformation of stress, except that, where the shearing stress τ was used, we now used $\frac{1}{2}\gamma$, that is, *half the shearing strain.* The formulas obtained for the transformation of strain under a rotation of axes through an angle θ were

$$\epsilon_{x'} = \frac{\epsilon_x + \epsilon_y}{2} + \frac{\epsilon_x - \epsilon_y}{2}\cos 2\theta + \frac{\gamma_{xy}}{2}\sin 2\theta \tag{7.44}$$

$$\epsilon_{y'} = \frac{\epsilon_x + \epsilon_y}{2} - \frac{\epsilon_x - \epsilon_y}{2}\cos 2\theta - \frac{\gamma_{xy}}{2}\sin 2\theta \tag{7.45}$$

$$\gamma_{x'y'} = -(\epsilon_x - \epsilon_y)\sin 2\theta + \gamma_{xy}\cos 2\theta \tag{7.49}$$

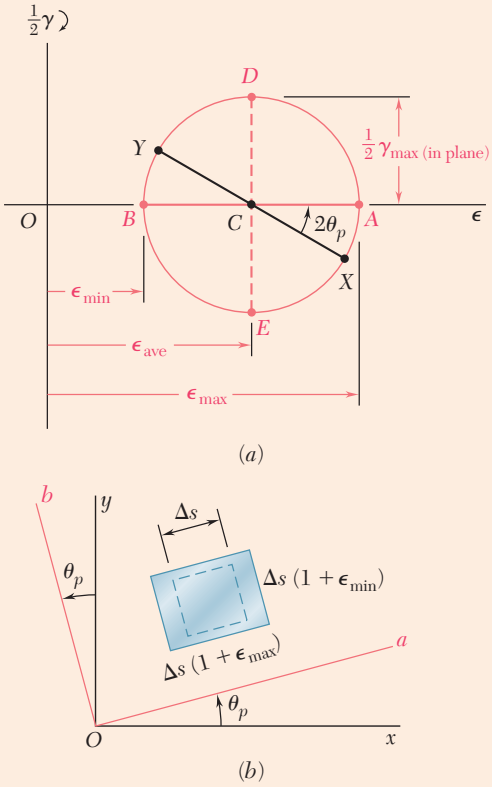


Fig. 7.78 (*a*) Mohr's circle for plane strain, showing principal strains and maximum in-plane shearing strain. (*b*) Strain element oriented to principal directions.

Mohr's Circle for Strain

Using Mohr's circle for strain (Fig. 7.78), the relationships defining the angle of rotation θ_p corresponding to the *principal axes of strain* and the values of the *principal strains* ϵ_{max} and ϵ_{min} are

$$\tan 2\theta_p = \frac{\gamma_{xy}}{\epsilon_x - \epsilon_y} \tag{7.52}$$

$$\epsilon_{max} = \epsilon_{ave} + R \qquad \text{and} \qquad \epsilon_{min} = \epsilon_{ave} - R \tag{7.51}$$

where

$$\epsilon_{ave} = \frac{\epsilon_x + \epsilon_y}{2} \qquad \text{and} \qquad R = \sqrt{\left(\frac{\epsilon_x - \epsilon_y}{2}\right)^2 + \left(\frac{\gamma_{xy}}{2}\right)^2} \tag{7.50}$$

The *maximum shearing strain* for a rotation in the plane of strain is

$$\gamma_{max\,(in\ plane)} = 2R = \sqrt{(\epsilon_x - \epsilon_y)^2 + \gamma_{xy}^2} \tag{7.53}$$

In *plane stress*, the principal strain ϵ_c in a direction perpendicular to the plane of stress is expressed in terms of the in-plane principal strains ϵ_a and ϵ_b:

$$\epsilon_c = -\frac{\nu}{1 - \nu}(\epsilon_a + \epsilon_b) \tag{7.59}$$

Strain Gages and Strain Rosette

Strain gages are used to measure the normal strain on the surface of a structural element or machine component. A *strain rosette* consists of three gages aligned along lines forming angles θ_1, θ_2, and θ_3 with the x axis (Fig. 7.79). The relationships among the measurements ϵ_1, ϵ_2, ϵ_3 of the gages and the components ϵ_x, ϵ_y, γ_{xy} characterizing the state of strain at that point are

$$\begin{aligned}
\epsilon_1 &= \epsilon_x \cos^2\theta_1 + \epsilon_y \sin^2\theta_1 + \gamma_{xy} \sin\theta_1 \cos\theta_1 \\
\epsilon_2 &= \epsilon_x \cos^2\theta_2 + \epsilon_y \sin^2\theta_2 + \gamma_{xy} \sin\theta_2 \cos\theta_2 \\
\epsilon_3 &= \epsilon_x \cos^2\theta_3 + \epsilon_y \sin^2\theta_3 + \gamma_{xy} \sin\theta_3 \cos\theta_3
\end{aligned} \tag{7.60}$$

These equations can be solved for ϵ_x, ϵ_y, and γ_{xy} once ϵ_1, ϵ_2, and ϵ_3 have been determined.

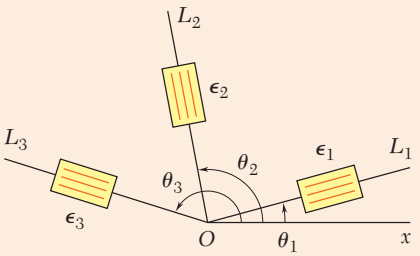


Fig. 7.79 Generalized strain gage rosette arrangement.

Review Problems

7.158 A steel pipe of 12-in. outer diameter is fabricated from $\frac{1}{4}$-in.-thick plate by welding along a helix that forms an angle of 22.5° with a plane perpendicular to the axis of the pipe. Knowing that a 40-kip axial force **P** and an 80-kip·in. torque **T,** each directed as shown, are applied to the pipe, determine the normal and in-plane shearing stresses in directions, respectively, normal and tangential to the weld.

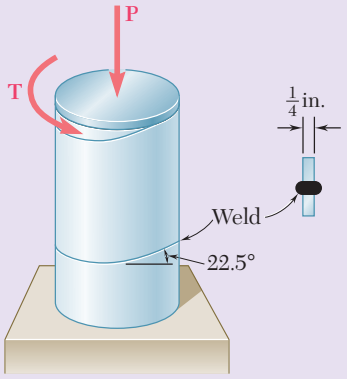


Fig. P7.158

7.159 Two steel plates of uniform cross section 10 × 80 mm are welded together as shown. Knowing that centric 100-kN forces are applied to the welded plates and that $\beta = 25°$, determine (*a*) the in-plane shearing stress parallel to the weld, (*b*) the normal stress perpendicular to the weld.

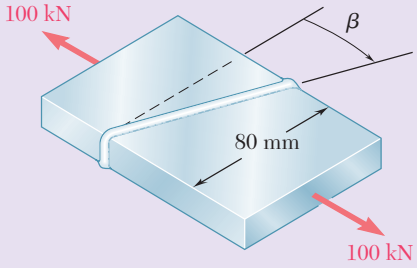


Fig. P7.159 and *P7.160*

7.160 Two steel plates of uniform cross section 10 × 80 mm are welded together as shown. Knowing that centric 100-kN forces are applied to the welded plates and that the in-plane shearing stress parallel to the weld is 30 MPa, determine (*a*) the angle β, (*b*) the corresponding normal stress perpendicular to the weld.

7.161 Determine the principal planes and the principal stresses for the state of plane stress resulting from the superposition of the two states of stress shown.

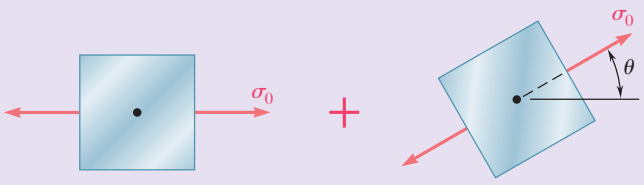


Fig. P7.161

7.162 For the state of stress shown, determine the maximum shearing stress when (*a*) $\sigma_z = +4$ ksi, (*b*) $\sigma_z = -4$ ksi, (*c*) $\sigma_z = 0$.

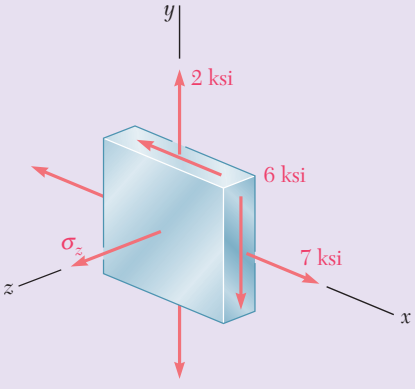


Fig. *P7.162*

7.163 For the state of stress shown, determine the value of τ_{xy} for which the maximum shearing stress is (*a*) 60 MPa, (*b*) 78 MPa.

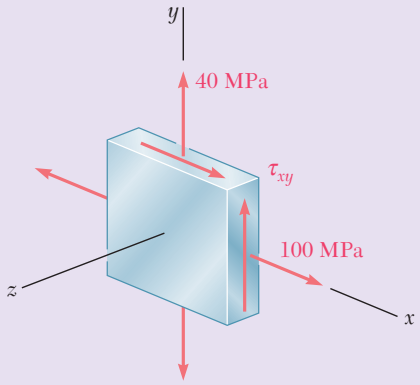


Fig. P7.163

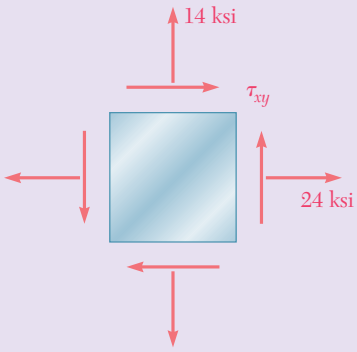


Fig. P7.164

7.164 The state of plane stress shown occurs in a machine component made of a steel with $\sigma_Y = 30$ ksi. Using the maximum-distortion-energy criterion, determine whether yield will occur when (*a*) $\tau_{xy} = 6$ ksi, (*b*) $\tau_{xy} = 12$ ksi, (*c*) $\tau_{xy} = 14$ ksi. If yield does not occur, determine the corresponding factor of safety.

7.165 The compressed-air tank *AB* has an inner diameter of 450 mm and a uniform wall thickness of 6 mm. Knowing that the gage pressure inside the tank is 1.2 MPa, determine the maximum normal stress and the maximum in-plane shearing stress at point *a* on the top of the tank.

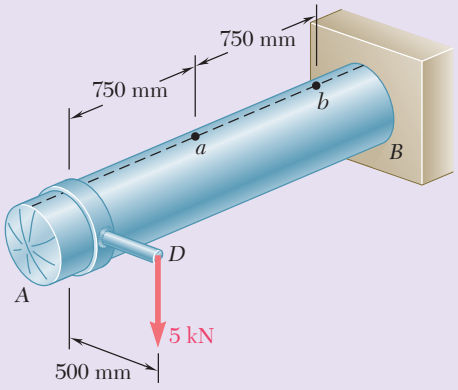


Fig. P7.165

7.166 For the compressed-air tank and loading of Prob. 7.165, determine the maximum normal stress and the maximum in-plane shearing stress at point *b* on the top of the tank.

7.167 The brass pipe AD is fitted with a jacket used to apply a hydrostatic pressure of 500 psi to portion BC of the pipe. Knowing that the pressure inside the pipe is 100 psi, determine the maximum normal stress in the pipe.

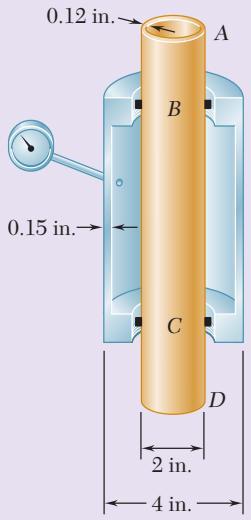


Fig. P7.167

7.168 For the assembly of Prob. 7.167, determine the normal stress in the jacket (*a*) in a direction perpendicular to the longitudinal axis of the jacket, (*b*) in a direction parallel to that axis.

7.169 Determine the largest in-plane normal strain, knowing that the following strains have been obtained by the use of the rosette shown:

$$\epsilon_1 = -50 \times 10^{-6} \text{ in./in.} \qquad \epsilon_2 = +360 \times 10^{-6} \text{ in./in.}$$
$$\epsilon_3 = +315 \times 10^{-6} \text{ in./in.}$$

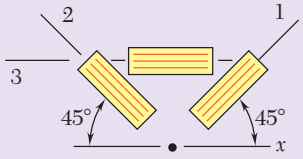


Fig. P7.169

Computer Problems

The following problems are to be solved with a computer.

7.C1 A state of plane stress is defined by the stress components σ_x, σ_y, and τ_{xy} associated with the element shown in Fig. P7.C1*a*. (*a*) Write a computer program that can be used to calculate the stress components $\sigma_{x'}$, $\sigma_{y'}$, and $\tau_{x'y'}$ associated with the element after it has rotated through an angle θ about the z axis (Fig. P.7C1*b*). (*b*) Use this program to solve Probs. 7.13 through 7.16.

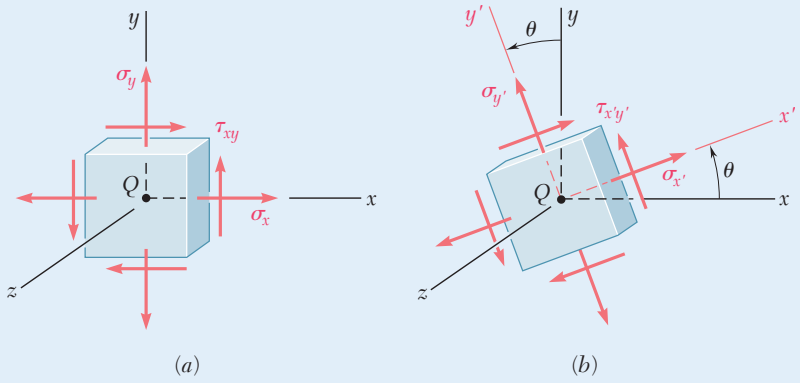


Fig. P7.C1

7.C2 A state of plane stress is defined by the stress components σ_x, σ_y, and τ_{xy} associated with the element shown in Fig. P7.C1*a*. (*a*) Write a computer program that can be used to calculate the principal axes, the principal stresses, the maximum in-plane shearing stress, and the maximum shearing stress. (*b*) Use this program to solve Probs. 7.5, 7.9, 7.68, and 7.69.

7.C3 (*a*) Write a computer program that, for a given state of plane stress and a given yield strength of a ductile material, can be used to determine whether the material will yield. The program should use both the maximum-shearing-stress criterion and the maximum-distortion-energy criterion. It should also print the values of the principal stresses and, if the material does not yield, calculate the factor of safety. (*b*) Use this program to solve Probs. 7.81, 7.82, and 7.164.

7.C4 (*a*) Write a computer program based on Mohr's fracture criterion for brittle materials that, for a given state of plane stress and given values of the ultimate stress of the material in tension and compression, can be used to determine whether rupture will occur. The program should also print the values of the principal stresses. (*b*) Use this program to solve Probs. 7.91 and 7.92 and to check the answers to Probs. 7.93 and 7.94.

7.C5 A state of plane strain is defined by the strain components ϵ_x, ϵ_y, and γ_{xy} associated with the x and y axes. (*a*) Write a computer program that can be used to calculate the strain components $\epsilon_{x'}$, $\epsilon_{y'}$, and $\gamma_{x'y'}$ associated with the frame of reference $x'y'$ obtained by rotating the x and y axes through an angle θ. (*b*) Use this program to solve Probs. 7.129 and 7.131.

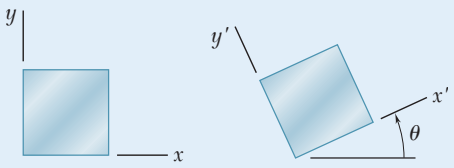


Fig. P7.C5

7.C6 A state of strain is defined by the strain components ϵ_x, ϵ_y, and γ_{xy} associated with the x and y axes. (*a*) Write a computer program that can be used to determine the orientation and magnitude of the principal strains, the maximum in-plane shearing strain, and the maximum shearing strain. (*b*) Use this program to solve Probs. 7.136 through 7.139.

7.C7 A state of plane strain is defined by the strain components ϵ_x, ϵ_y, and γ_{xy} measured at a point. (*a*) Write a computer program that can be used to determine the orientation and magnitude of the principal strains, the maximum in-plane shearing strain, and the magnitude of the shearing strain. (*b*) Use this program to solve Probs. 7.140 through 7.143.

7.C8 A rosette consisting of three gages forming angles of θ_1, θ_2, and θ_3 with the x axis is attached to the free surface of a machine component made of a material with a given Poisson's ratio ν. (*a*) Write a computer program that, for given readings ϵ_1, ϵ_2, and ϵ_3 of the gages, can be used to calculate the strain components associated with the x and y axes and to determine the orientation and magnitude of the three principal strains, the maximum in-plane shearing strain, and the maximum shearing strain. (*b*) Use this program to solve Probs. 7.144, 7.145, 7.146, and 7.169.





8

Principal Stresses under a Given Loading

Due to gravity and wind load, the signpost support column is subjected simultaneously to compression, bending, and torsion. This chapter will examine the stresses resulting from such combined loadings.

Objectives

In this chapter, you will:

- **Describe** how stress components vary throughout a beam.
- **Identify** key stress analysis locations in an I-shaped beam.
- **Design** transmission shafts subject to transverse loads and torques.
- **Describe** the stresses throughout a member arising from combined loads.

Introduction
8.1 PRINCIPAL STRESSES IN A BEAM
8.2 DESIGN OF TRANSMISSION SHAFTS
8.3 STRESSES UNDER COMBINED LOADS

Introduction

In the first part of this chapter, you will apply to the design of beams and shafts the knowledge that you acquired in Chap. 7 on the transformation of stresses. In the second part of the chapter, you will learn how to determine the principal stresses in structural members and machine elements under given loading conditions.

The maximum normal stress σ_m that occurs in a beam under a transverse load (Fig. 8.1*a*) and whether this value exceeds the allowable stress σ_{all} for the given material has been studied in Chap. 5. If the allowable stress is exceeded, the design of the beam is not acceptable. While the danger for a brittle material is actually to fail in tension, the danger for a ductile material is to fail in shear (Fig. 8.1*b*). Thus, a situation where $\sigma_m > \sigma_{all}$ indicates that $|M|_{max}$ is too large for the cross section selected,

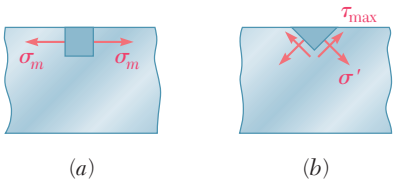


Fig. 8.1 Stress elements where normal stress is maximum in a transversely-loaded beam. (*a*) Element showing maximum normal stress. (*b*) Element showing corresponding maximum shearing stress.

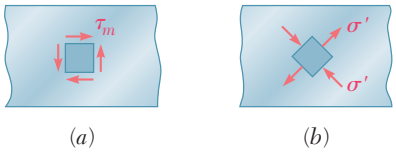


Fig. 8.2 Stress elements where shearing stress is maximum in a transversely-loaded beam. (*a*) Element showing maximum shearing stress. (*b*) Element showing corresponding maximum normal stress.

but it does not provide any information on the actual mechanism of failure. Similarly, $\tau_m > \tau_{all}$ indicates that $|V|_{max}$ is too large for the cross section selected. While the danger for a ductile material is actually to fail in shear (Fig. 8.2*a*), the danger for a brittle material is to fail in tension under the principal stresses (Fig. 8.2*b*). The distribution of the principal stresses in a beam is discussed in Sec. 8.1.

Depending on the shape of the beam's cross section and the value of the shear V in the critical section where $|M| = |M|_{max}$, the largest value of the normal stress may not necessarily occur at the top or bottom, but at some other point within the section. In Sec. 8.1, a combination of large values of σ_x and τ_{xy} near the junction of the web and the flanges of a W- or S-beam can result in a value of the principal stress σ_{max} (Fig. 8.3) that is larger than the value of σ_m on the surface of the beam.

Section 8.2 covers the design of transmission shafts subjected to transverse loads and torques. The effects of both normal stresses due to bending and shearing stresses due to torsion are discussed.

In Sec. 8.3, the stresses are determined at a given point K of a body of arbitrary shape subjected to combined loading. First, the given load is

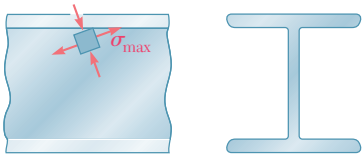


Fig. 8.3 Principal stress element at the junction of a flange and web in an I-shaped beam.

reduced to forces and couples in the section containing K. Next, the normal and shearing stresses at K are calculated. Finally, the principal planes, principal stresses, and maximum shearing stress are found, using one of the methods for transformation of stresses (Chap. 7).

8.1 PRINCIPAL STRESSES IN A BEAM

Consider a prismatic beam AB subjected to some arbitrary transverse loads (Fig. 8.4). The shear and bending moment in a section through a

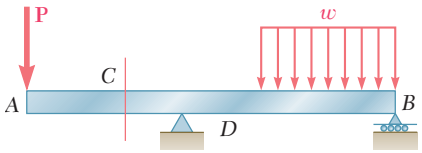


Fig. 8.4 Transversely loaded prismatic beam.

given point C are denoted by V and M, respectively. Recall from Chaps. 5 and 6 that, within the elastic limit, the stresses on a small element with faces perpendicular to the x and y axes reduce to the normal stresses $\sigma_m = Mc/I$ if the element is at the free surface of the beam and to the shearing stresses $\tau_m = VQ/It$ if the element is at the neutral surface (Fig. 8.5).

At any other point of the cross section, an element is subjected simultaneously to the normal stresses

$$\sigma_x = -\frac{My}{I} \tag{8.1}$$

where y is the distance from the neutral surface and I is the centroidal moment of inertia of the section, and to the shearing stresses

$$\tau_{xy} = -\frac{VQ}{It} \tag{8.2}$$

where Q is the first moment about the neutral axis of the portion of the cross-sectional area located above the point where the stresses are computed, and t is the width of the cross section at that point. Either of the methods of analysis presented in Chap. 7 can be used to obtain the principal stresses at any point of the cross section (Fig. 8.6).

The following question now arises: can the maximum normal stress $\sigma_{\max}$ at some point within the cross section be larger than $\sigma_m = Mc/I$ at the surface of the beam? If it can, then determining the largest normal stress in the beam involves more than the computation of $|M|_{\max}$ and the use of Eq. (8.1). An answer to this question is obtained by investigating the distribution of the principal stresses in a narrow rectangular cantilever beam subjected to a concentrated load **P** at its free end (Fig. 8.7). Recall from Sec. 6.2 that the normal and shearing stresses at a distance x from the load **P** and at a distance y above the neutral surface are given, respectively, by Eqs. (6.13) and (6.12). Since the moment of inertia of the cross section is

$$I = \frac{bh^3}{12} = \frac{(bh)(2c)^2}{12} = \frac{Ac^2}{3}$$

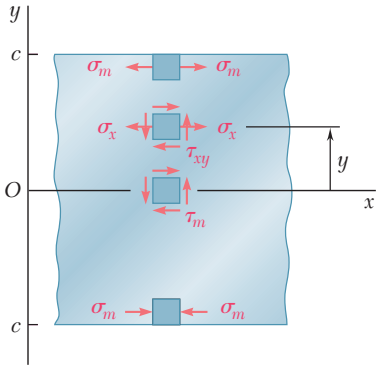


Fig. 8.5 Stress elements at selected points of a beam.

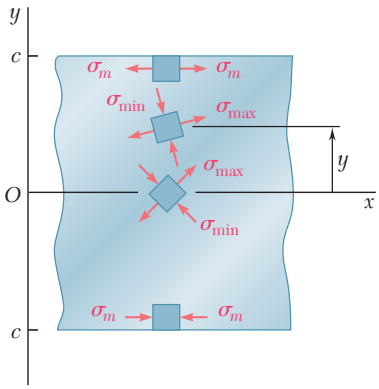


Fig. 8.6 Principal stress elements at selected points of a beam.

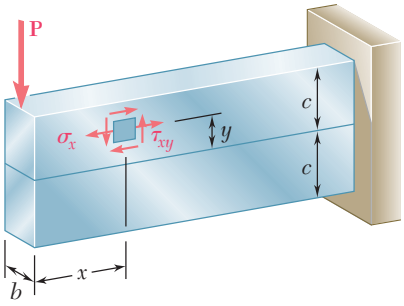


Fig. 8.7 Narrow rectangular cantilever beam supporting a single concentrated load.

where A is the cross-sectional area and c the half-depth of the beam,

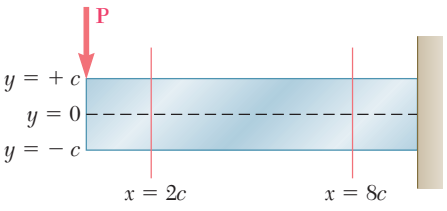
$$\sigma_x = \frac{Pxy}{I} = \frac{Pxy}{\frac{1}{3}Ac^2} = 3\frac{P}{A}\frac{xy}{c^2} \tag{8.3}$$

and

$$\tau_{xy} = \frac{3}{2}\frac{P}{A}\left(1 - \frac{y^2}{c^2}\right) \tag{8.4}$$

Using the methods of Sec. 7.1B or Sec. 7.2, $\sigma_{\max}$ can be determined at any point of the beam. Figure 8.8 shows the results of the computation of the ratios $\sigma_{\max}/\sigma_m$ and $\sigma_{\min}/\sigma_m$ in two sections of the beam, corresponding respectively to $x = 2c$ and $x = 8c$. In each section, these ratios have been determined at 11 different points, and the orientation of the principal axes has been indicated at each point.†

It is clear that $\sigma_{\max}$ is smaller than σ_m in both of the two sections in Fig. 8.8. If it does exceed σ_m elsewhere, it is in sections close to load **P**, where σ_m is small compared to τ_m.‡ But for sections close to load **P**, Saint-Venant's principle does not apply, and Eqs. (8.3) and (8.4) cease to be



	$x = 2c$		$x = 8c$	
y/c	$\sigma_{\min}/\sigma_m$	$\sigma_{\max}/\sigma_m$	$\sigma_{\min}/\sigma_m$	$\sigma_{\max}/\sigma_m$
1.0	0	1.000	0	1.000
0.8	−0.010	0.810	−0.001	0.801
0.6	−0.040	0.640	−0.003	0.603
0.4	−0.090	0.490	−0.007	0.407
0.2	−0.160	0.360	−0.017	0.217
0	−0.250	0.250	−0.063	0.063
− 0.2	−0.360	0.160	−0.217	0.017
− 0.4	−0.490	0.090	−0.407	0.007
− 0.6	−0.640	0.040	−0.603	0.003
− 0.8	−0.810	0.010	−0.801	0.001
− 1.0	−1.000	0	−1.000	0

Fig. 8.8 Distribution of principal stresses in two transverse sections of a rectangular cantilever beam supporting a single concentrated load.

†See Prob. 8.C2, which refers to a program that can be written to obtain the results in Fig. 8.8.

‡As will be verified in Prob. 8.C2, $\sigma_{\max}$ exceeds σ_m if $x \leq 0.544c$.

valid—except in the very unlikely case of a load distributed parabolically over the end section (see. Sec. 6.2), where advanced methods of analysis are used to account for the effect of stress concentrations. It can thus be concluded that, for beams of rectangular cross section, and within the scope of the theory presented in this text, the maximum normal stress can be obtained from Eq. (8.1).

In Fig. 8.8, the directions of the principal axes are found at 11 points in both of the sections considered. If this analysis is extended to a larger number of sections and points in each section, it possible to draw two orthogonal systems of curves on the side of the beam (Fig. 8.9). One

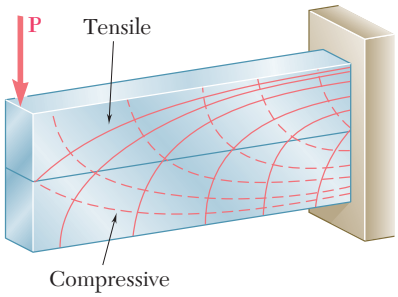


Fig. 8.9 Stress trajectories in a rectangular cantilevered beam supporting a single concentrated load.

system consists of curves tangent to the principal axes corresponding to $\sigma_{\max}$ and the other to $\sigma_{\min}$. These curves are known as the *stress trajectories*. A trajectory of the first group (solid lines) defines the direction of the largest tensile stress at each of its points, while the second group (dashed lines) defines the direction of the largest compressive stress.[†]

The conclusion we have reached for beams of rectangular cross section, that the maximum normal stress in the beam can be obtained from Eq. (8.1), remains valid for many beams of nonrectangular cross section. However, when the width of the cross section varies so that large shearing stresses τ_{xy} occur at points close to the surface of the beam (where σ_x is also large), the principal stress $\sigma_{\max}$ may be larger than σ_m at such points. This is a distinct possibility when selecting W-beams or S-beams, where we should calculate the principal stress $\sigma_{\max}$ at the junctions b and d of the web with the flanges of the beam (Fig. 8.10). This is done by determining σ_x and τ_{xy} at that point from Eqs. (8.1) and (8.2), and by using either of the methods of analysis in Chap. 7 to obtain $\sigma_{\max}$ (see Sample Prob. 8.1). An alternative procedure for selecting an acceptable section uses the approximation $\tau_{\max} = V/A_{\text{web}}$ [Eq. (6.11)]. This leads to a slightly larger and conservative value of the principal stress $\sigma_{\max}$ at the junction of the web with the flanges of the beam (see Sample Prob. 8.2).

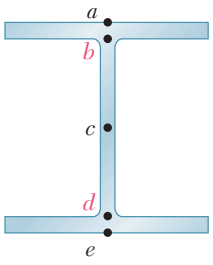


Fig. 8.10 Key stress analysis locations in I-shaped beams.

[†]A brittle material, such as concrete, fails in tension along planes that are perpendicular to the tensile-stress trajectories. Thus, to be effective, steel reinforcing bars should be placed so that they intersect these planes. On the other hand, stiffeners attached to the web of a plate girder are effective in preventing buckling only if they intersect planes perpendicular to the compressive-stress trajectories.

8.2 DESIGN OF TRANSMISSION SHAFTS

The design of transmission shafts in Sec. 3.4 considered only the stresses due to torques exerted on the shafts. However, if the power is transferred to and from the shaft by means of gears or sprocket wheels (Fig. 8.11*a*), the forces on the gear teeth or sprockets are equivalent to force-couple systems applied at the centers of the corresponding cross sections (Fig. 8.11*b*). This means that the shaft is subjected to both a transverse and a torsional load.

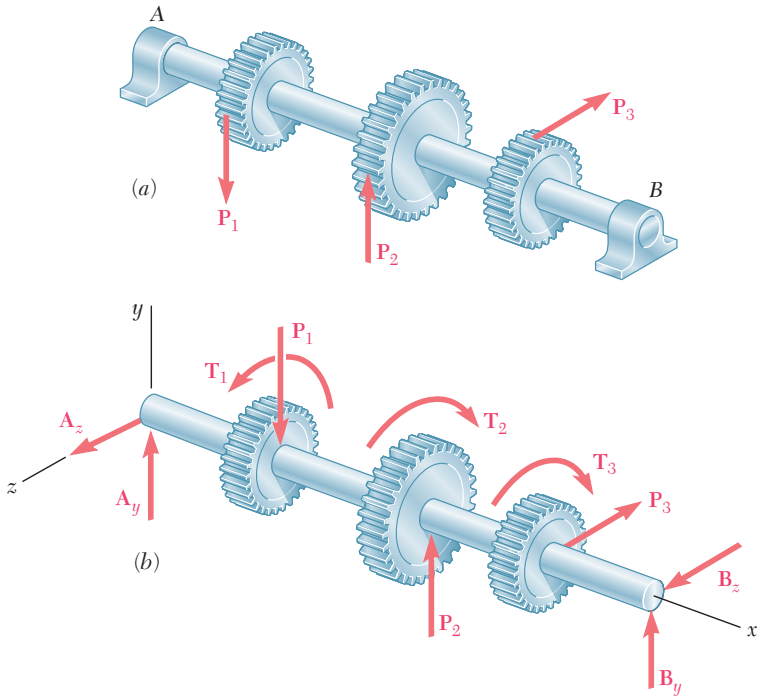


Fig. 8.11 Loadings on gear-shaft systems. (*a*) Forces applied to gear teeth. (*b*) Free-body diagram of shaft, with gear forces replaced by equivalent force-couple systems applied to shaft.

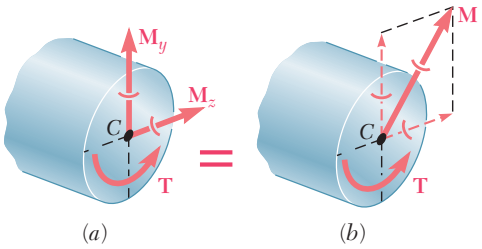


Fig. 8.12 (*a*) Torque and bending couples acting on shaft cross section. (*b*) Bending couples replaced by their resultant **M**.

The shearing stresses produced in the shaft by the transverse loads are usually much smaller than those produced by the torques and will be neglected in this analysis.[†] However, the normal stresses due to transverse loads may be quite large, and their contribution to the maximum shearing stress $\tau_{\max}$ should be taken into account.

Consider the cross section of the shaft at some point *C*. The torque **T** and the bending couples $\mathbf{M}_y$ and $\mathbf{M}_z$ acting in a horizontal and a vertical plane are represented by the couple vectors shown (Fig. 8.12*a*). Since any diameter of the section is a principal axis of inertia for the section, we can replace $\mathbf{M}_y$ and $\mathbf{M}_z$ by their resultant **M** (Fig. 8.12*b*) in order to compute the normal stresses σ_x. Thus σ_x is maximum at the end of the diameter

[†]For an application where the shearing stresses produced by the transverse loads must be considered, see Probs. 8.21 and 8.22.

perpendicular to the vector representing **M** (Fig. 8.13). Recalling that the values of the normal stresses at that point are $\sigma_m = Mc/I$ and zero and the shearing stress is $\tau_m = Tc/J$, plot the corresponding values as points X and Y on a Mohr's circle diagram (Fig. 8.14). The maximum shearing stress is found to be

$$\tau_{\max} = R = \sqrt{\left(\frac{\sigma_m}{2}\right)^2 + (\tau_m)^2} = \sqrt{\left(\frac{Mc}{2I}\right)^2 + \left(\frac{Tc}{J}\right)^2}$$

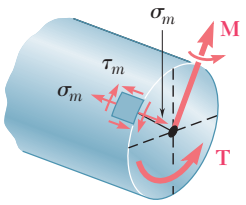


Fig. 8.13 Maximum stress element.

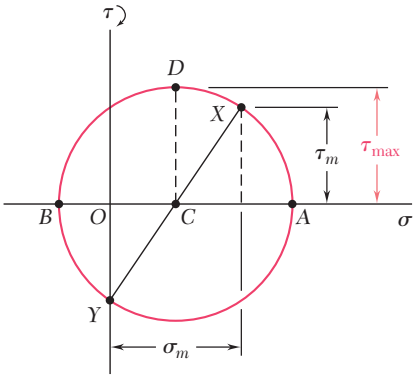


Fig. 8.14 Mohr's circle for shaft loading.

Recalling that $2I = J$ for a circular or annular cross section,

$$\tau_{\max} = \frac{c}{J}\sqrt{M^2 + T^2} \tag{8.5}$$

It follows that the minimum allowable value of the ratio J/c for the cross section of the shaft is

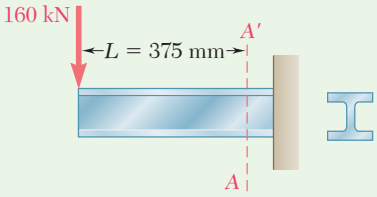
$$\frac{J}{c} = \frac{\left(\sqrt{M^2 + T^2}\right)_{\max}}{\tau_{\text{all}}} \tag{8.6}$$

where the numerator in the right-hand member represents the maximum value of $\sqrt{M^2 + T^2}$ in the shaft and τ_{all} is the allowable shearing stress. Expressing the bending moment M in terms of its components in the two coordinate planes, we obtain:

$$\frac{J}{c} = \frac{\left(\sqrt{M_y^2 + M_z^2 + T^2}\right)_{\max}}{\tau_{\text{all}}} \tag{8.7}$$

Equations (8.6) and (8.7) can be used to design both solid and hollow circular shafts and should be compared to Eq. (3.21), which was obtained under the assumption of torsional loading only.

The maximum value of $\sqrt{M_y^2 + M_z^2 + T^2}$ is easier to find if both bending-moment diagrams corresponding to M_y and M_z and a third diagram representing the values of T along the shaft are drawn (see Sample Prob. 8.3).



Sample Problem 8.1

A 160-kN force is applied as shown at the end of a W200 × 52 rolled-steel beam. Neglecting the effect of fillets and of stress concentrations, determine whether the normal stresses in the beam satisfy a design specification that they be equal to or less than 150 MPa at section *A*–*A*′.

STRATEGY: To determine the maximum normal stress, you should perform a beam stress analysis at the surface of the flange as well as at the junction of the web and flange. A Mohr's circle analysis will also be necessary at the web-flange junction to determine this maximum normal stress.

MODELING and ANALYSIS:

Shear and Bending Moment. Referring to Fig. 1, at section *A*–*A*′, we have

$$M_A = (160\text{ kN})(0.375\text{ m}) = 60\text{ kN·m}$$
$$V_A = 160\text{ kN}$$

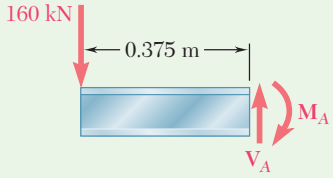


Fig. 1 Free-body diagram of beam, with section at *A*–*A*′

Normal Stresses on Transverse Plane. Referring to the table of *Properties of Rolled-Steel Shapes* in Appendix C to obtain the data shown, determine the stresses σ_a and σ_b (Fig. 2).

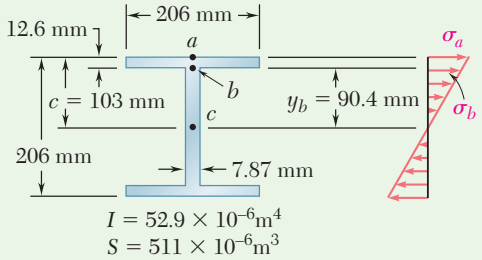


Fig. 2 Cross-section dimensions and normal stress distribution.

At point *a*,

$$\sigma_a = \frac{M_A}{S} = \frac{60\text{ kN·m}}{511 \times 10^{-6}\text{ m}^3} = 117.4\text{ MPa}$$

At point *b*,

$$\sigma_b = \sigma_a \frac{y_b}{c} = (117.4\text{ MPa})\frac{90.4\text{ mm}}{103\text{ mm}} = 103.0\text{ MPa}$$

(continued)

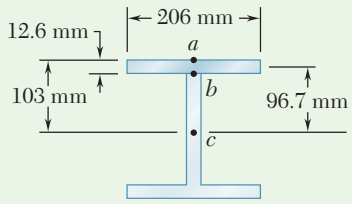


Fig. 3 Dimensions to evaluate Q at point b.

Note that all normal stresses on the transverse plane are less than 150 MPa.

Shearing Stresses on Transverse Plane. Referring to Fig. 3, we obtain the data necessary to evaluate Q and then determine the stresses τ_a and τ_b.

At point a,

$$Q = 0 \qquad \tau_a = 0$$

At point b,

$$Q = (206 \times 12.6)(96.7) = 251.0 \times 10^3\,\text{mm}^3 = 251.0 \times 10^{-6}\,\text{m}^3$$

$$\tau_b = \frac{V_A Q}{It} = \frac{(160\,\text{kN})(251.0 \times 10^{-6}\,\text{m}^3)}{(52.9 \times 10^{-6}\,\text{m}^4)(0.00787\,\text{m})} = 96.5\,\text{MPa}$$

Principal Stress at Point *b*. The state of stress at point b consists of the normal stress $\sigma_b = 103.0$ MPa and the shearing stress $\tau_b = 96.5$ MPa. Draw Mohr's circle (Fig. 4) and find

$$\sigma_{\max} = \frac{1}{2}\sigma_b + R = \frac{1}{2}\sigma_b + \sqrt{\left(\frac{1}{2}\sigma_b\right)^2 + \tau_b^2}$$

$$= \frac{103.0}{2} + \sqrt{\left(\frac{103.0}{2}\right)^2 + (96.5)^2}$$

$$\sigma_{\max} = 160.9\,\text{MPa}$$

The specification, $\sigma_{\max} \le 150$ MPa, is *not* satisfied ◀

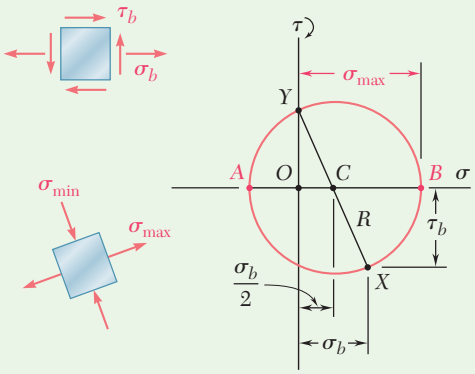


Fig. 4 Stress element for coordinate and principal orientations at point b; Mohr's circle for point b.

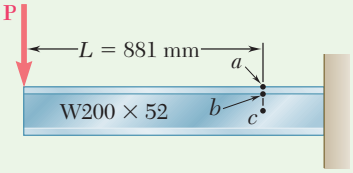
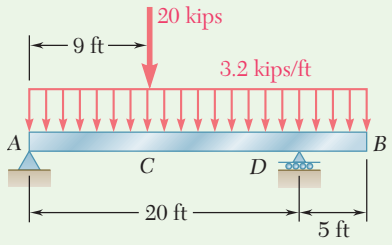


Fig. 5 Condition where maximum principal stress at point a begins to exceed that at point b.

REFLECT and THINK: For this beam and loading, the principal stress at point b is 36% larger than the normal stress at point a. For $L \ge 881$ mm (Fig. 5), the maximum normal stress would occur at point a.

(continued)

Sample Problem 8.2



The overhanging beam AB supports a uniformly distributed load of 3.2 kips/ft and a concentrated load of 20 kips at C. Knowing that the grade of steel to be used has $\sigma_{all} = 24$ ksi and $\tau_{all} = 14.5$ ksi, select the wide-flange shape that should be used.

STRATEGY: Draw the shear and bending-moment diagrams to determine their maximum values. From the maximum bending moment, you can find the required section modulus and use this to select the lightest available wide-flange shape. You can then check to ensure that the maximum shearing stress in the web and the maximum principal stress at the web-flange junction do not exceed the given allowable stresses.

MODELING and ANALYSIS:

Reactions at *A* and *D*. Draw the free-body diagram (Fig. 1) of the beam. From the equilibrium equations $\Sigma M_D = 0$ and $\Sigma M_A = 0$, the values of R_A and R_D are as shown.

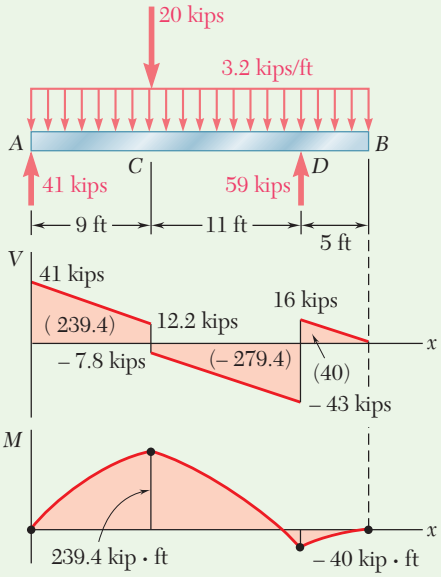


Fig. 1 Free-body diagram of beam; shear and bending moment diagrams.

Shear and Bending-Moment Diagrams. Using the methods discussed in Secs. 5.1 and 5.2, draw the diagrams (Fig. 1) and observe that

$$|M|_{max} = 239.4 \text{ kip·ft} = 2873 \text{ kip·in.} \qquad |V|_{max} = 43 \text{ kips}$$

Section Modulus. For $|M|_{max} = 2873$ kip·in. and $\sigma_{all} = 24$ ksi, the minimum acceptable section modulus of the rolled-steel shape is

$$S_{min} = \frac{|M|_{max}}{\sigma_{all}} = \frac{2873 \text{ kip·in.}}{24 \text{ ksi}} = 119.7 \text{ in}^3$$

Selection of Wide-Flange Shape. Choose from the table of *Properties of Rolled-Steel Shapes* in Appendix C the lightest shapes of a given depth that have a section modulus larger than S_{min}.

Shape	S (in^3)
W24 × 68	154
W21 × 62	127
W18 × 76	146
W16 × 77	134
W14 × 82	123
W12 × 96	131

The lightest shape available is W21 × 62 ◀

(continued)

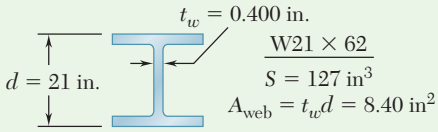


Fig. 2 I-shape cross section properties.

Shearing Stress. For the beam design, assume that the maximum shear is uniformly distributed over the web area of a W21 × 62 (Fig. 2). Write

$$\tau_m = \frac{V_{\max}}{A_{\text{web}}} = \frac{43 \text{ kips}}{8.40 \text{ in}^2} = 5.12 \text{ ksi} < 14.5 \text{ ksi} \qquad \text{(OK)}$$

Principal Stress at Point *b*. The maximum principal stress at point b in the critical section where M is maximum should not exceed $\sigma_{\text{all}} = 24$ ksi. Referring to Fig. 3, we write

$$\sigma_a = \frac{M_{\max}}{S} = \frac{2873 \text{ kip·in.}}{127 \text{ in}^3} = 22.6 \text{ ksi}$$

$$\sigma_b = \sigma_a \frac{y_b}{c} = (22.6 \text{ ksi}) \frac{9.88 \text{ in.}}{10.50 \text{ in.}} = 21.3 \text{ ksi}$$

Conservatively, $\tau_b = \dfrac{V}{A_{\text{web}}} = \dfrac{12.2 \text{ kips}}{8.40 \text{ in}^2} = 1.45 \text{ ksi}$

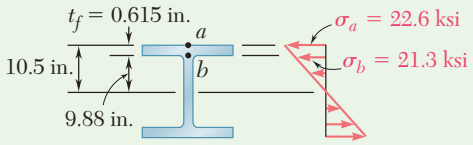


Fig. 3 Key stress analysis locations and normal stress distribution.

Draw Mohr's circle (Fig. 4) and find

$$\sigma_{\max} = \tfrac{1}{2}\sigma_b + R = \frac{21.3 \text{ ksi}}{2} + \sqrt{\left(\frac{21.3 \text{ ksi}}{2}\right)^2 + (1.45 \text{ ksi})^2}$$

$$\sigma_{\max} = 21.4 \text{ ksi} \le 24 \text{ ksi} \quad \text{(OK)}$$

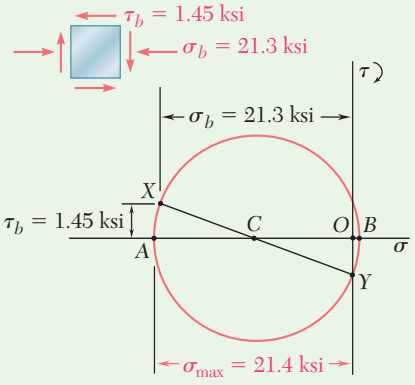
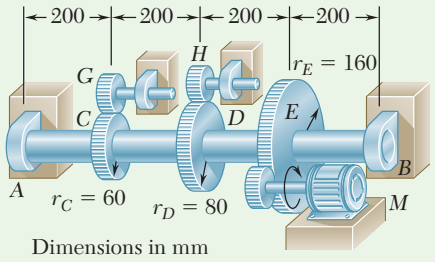


Fig. 4 Stress element at point *b* and Mohr's circle for point *b*.

Sample Problem 8.3



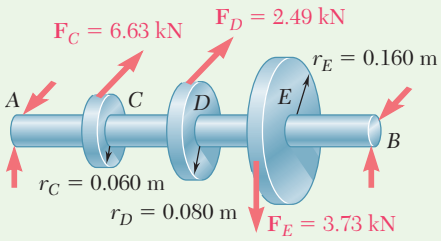


Fig. 1 Free-body diagram of shaft *AB* and its gears.

The solid shaft *AB* rotates at 480 rpm and transmits 30 kW from the motor *M* to machine tools connected to gears *G* and *H*; 20 kW is taken off at gear *G* and 10 kW at gear *H*. Knowing that $\tau_{all} = 50$ MPa, determine the smallest permissible diameter for shaft *AB*.

STRATEGY: After determining the forces and couples exerted on the shaft, you can obtain its bending-moment and torque diagrams. Using these diagrams to aid in identifying the critical transverse section, you can then determine the required shaft diameter.

MODELING:

Draw the free-body diagram of the shaft and gears (Fig. 1). Observing that $f = 480$ rpm $= 8$ Hz, the torque exerted on gear *E* is

$$T_E = \frac{P}{2\pi f} = \frac{30\text{ kW}}{2\pi(8\text{ Hz})} = 597\text{ N·m}$$

The corresponding tangential force acting on the gear is

$$F_E = \frac{T_E}{r_E} = \frac{597\text{ N·m}}{0.16\text{ m}} = 3.73\text{ kN}$$

A similar analysis of gears *C* and *D* yields

$$T_C = \frac{20\text{ kW}}{2\pi(8\text{ Hz})} = 398\text{ N·m} \qquad F_C = 6.63\text{ kN}$$

$$T_D = \frac{10\text{ kW}}{2\pi(8\text{ Hz})} = 199\text{ N·m} \qquad F_D = 2.49\text{ kN}$$

Now replace the forces on the gears by equivalent force-couple systems as shown in Fig. 2.

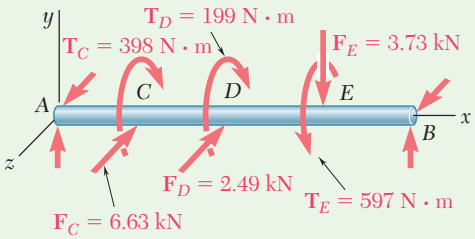


Fig. 2 Free-body diagram of shaft *AB*, with gear forces replaced by equivalent force-couple systems.

(continued)

ANALYSIS:

Bending-Moment and Torque Diagrams (Fig. 3)

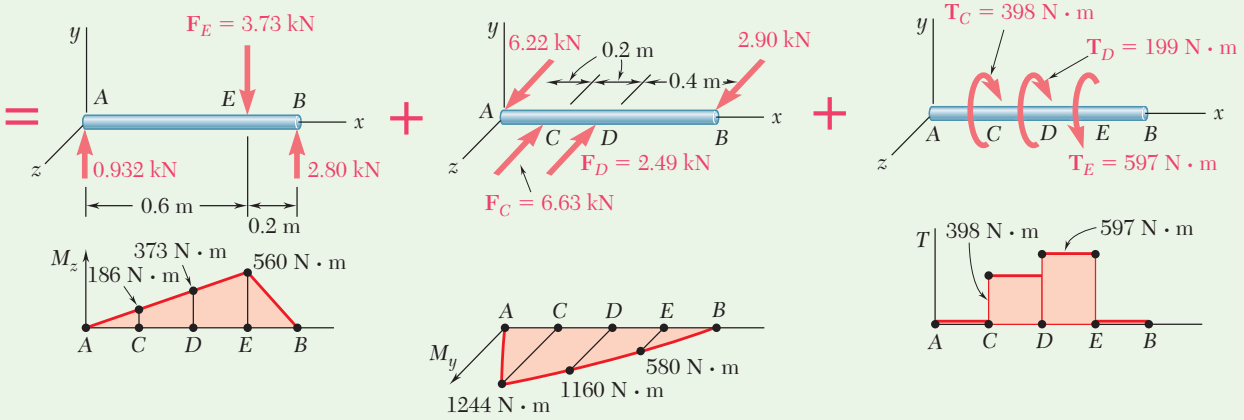


Fig. 3 Analysis of free-body diagram of shaft *AB* alone with equivalent force-couple loads is equivalent to superposition of bending moments from vertical loads, horizontal loads, and applied torques.

Critical Transverse Section. By computing $\sqrt{M_y^2 + M_z^2 + T^2}$ at all potentially critical sections (Fig. 4), the maximum value occurs just to the right of *D*:

$$\sqrt{M_y^2 + M_z^2 + T^2}_{\max} = \sqrt{(1160)^2 + (373)^2 + (597)^2} = 1357\ \text{N·m}$$

Diameter of Shaft. For $\tau_{\text{all}} = 50$ MPa, Eq. (7.32) yields

$$\frac{J}{c} = \frac{\sqrt{M_y^2 + M_z^2 + T^2}_{\max}}{\tau_{\text{all}}} = \frac{1357\ \text{N·m}}{50\ \text{MPa}} = 27.14 \times 10^{-6}\ \text{m}^3$$

For a solid circular shaft of radius *c*,

$$\frac{J}{c} = \frac{\pi}{2} c^3 = 27.14 \times 10^{-6} \qquad c = 0.02585\ \text{m} = 25.85\ \text{mm}$$

$$\text{Diameter} = 2c = 51.7\ \text{mm}$$

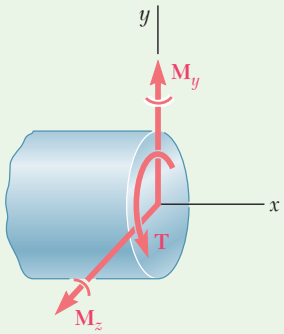


Fig. 4 Bending moment components and torque at critical section.

Problems

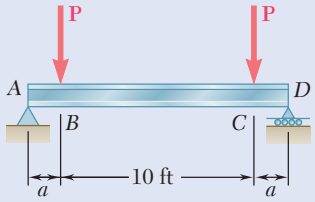


Fig. P8.1

8.1 A W10 × 39 rolled-steel beam supports a load **P** as shown. Knowing that $P = 45$ kips, $a = 10$ in., and $\sigma_{all} = 18$ ksi, determine (*a*) the maximum value of the normal stress σ_m in the beam, (*b*) the maximum value of the principal stress σ_{max} at the junction of the flange and web, (*c*) whether the specified shape is acceptable as far as these two stresses are concerned.

8.2 Solve Prob. 8.1, assuming that $P = 22.5$ kips and $a = 20$ in.

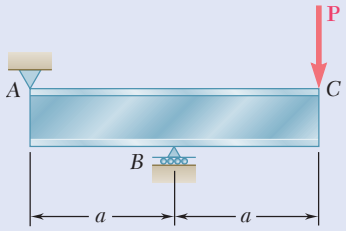


Fig. P8.3

8.3 An overhanging W920 × 449 rolled-steel beam supports a load **P** as shown. Knowing that $P = 700$ kN, $a = 2.5$ m, and $\sigma_{all} = 100$ MPa, determine (*a*) the maximum value of the normal stress σ_m in the beam, (*b*) the maximum value of the principal stress σ_{max} at the junction of the flange and web, (*c*) whether the specified shape is acceptable as far as these two stresses are concerned.

8.4 Solve Prob. 8.3, assuming that $P = 850$ kN and $a = 2.0$ m.

8.5 and 8.6 (*a*) Knowing that $\sigma_{all} = 160$ MPa and $\tau_{all} = 100$ MPa, select the most economical metric wide-flange shape that should be used to support the loading shown. (*b*) Determine the values to be expected for σ_m, τ_m, and the principal stress σ_{max} at the junction of a flange and the web of the selected beam.

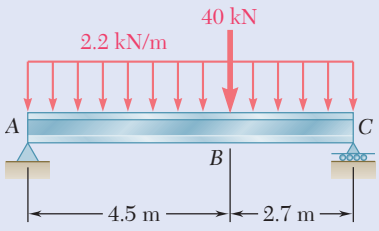


Fig. P8.5

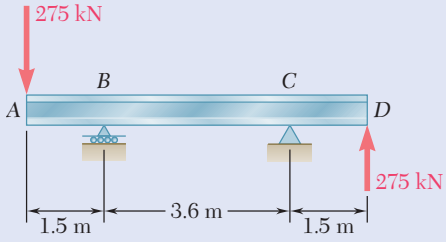


Fig. P8.6

8.7* and *8.8 (*a*) Knowing that $\sigma_{all} = 24$ ksi and $\tau_{all} = 14.5$ ksi, select the most economical wide-flange shape that should be used to support the loading shown. (*b*) Determine the values to be expected for σ_m, τ_m, and the principal stress σ_{max} at the junction of a flange and the web of the selected beam.

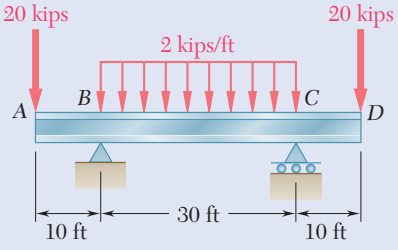


Fig. *P8.7*

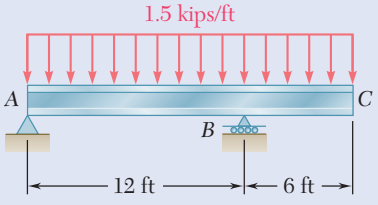


Fig. *P8.8*

8.9 through 8.14 Each of the following problems refers to a rolled-steel shape selected in a problem of Chap. 5 to support a given loading at a minimal cost while satisfying the requirement $\sigma_m \leq \sigma_{all}$. For the selected design, determine (*a*) the actual value of σ_m in the beam, (*b*) the maximum value of the principal stress σ_{max} at the junction of a flange and the web.

8.9 Loading of Prob. 5.73 and selected W530 × 92 shape.

8.10 Loading of Prob. 5.74 and selected W250 × 28.4 shape.

8.11 Loading of Prob. 5.75 and selected S12 × 31.8 shape.

8.12 Loading of Prob. 5.76 and selected S15 × 42.9 shape.

8.13 Loading of Prob. 5.77 and selected S510 × 98.2 shape.

8.14 Loading of Prob. 5.78 and selected S460 × 81.4 shape.

8.15 Determine the smallest allowable diameter of the solid shaft *ABCD*, knowing that $\tau_{all} = 60$ MPa and that the radius of disk *B* is $r = 80$ mm.

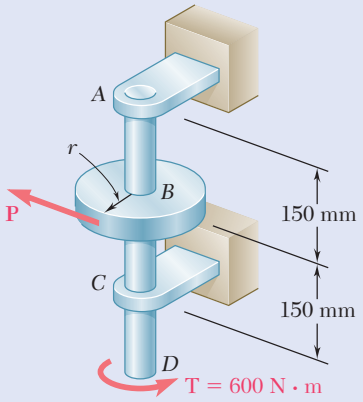


Fig. P8.15 and *P8.16*

8.16 Determine the smallest allowable diameter of the solid shaft *ABCD*, knowing that $\tau_{all} = 60$ MPa and that the radius of disk *B* is $r = 120$ mm.

8.17 Using the notation of Sec. 8.2 and neglecting the effect of shearing stresses caused by transverse loads, show that the maximum normal stress in a circular shaft can be expressed as follows:

$$\sigma_{max} = \frac{c}{J}\left[(M_y^2 + M_z^2)^{\frac{1}{2}} + (M_y^2 + M_z^2 + T^2)^{\frac{1}{2}}\right]_{max}$$

8.18 The 4-kN force is parallel to the *x* axis, and the force **Q** is parallel to the *z* axis. The shaft *AD* is hollow. Knowing that the inner diameter is half the outer diameter and that $\tau_{all} = 60$ MPa, determine the smallest permissible outer diameter of the shaft.

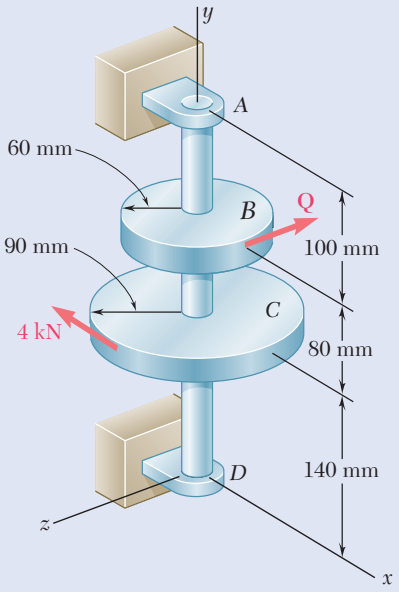


Fig. *P8.18*

8.19 The vertical force $\mathbf{P}_1$ and the horizontal force $\mathbf{P}_2$ are applied as shown to disks welded to the solid shaft *AD*. Knowing that the diameter of the shaft is 1.75 in. and that $\tau_{all} = 8$ ksi, determine the largest permissible magnitude of the force $\mathbf{P}_2$.

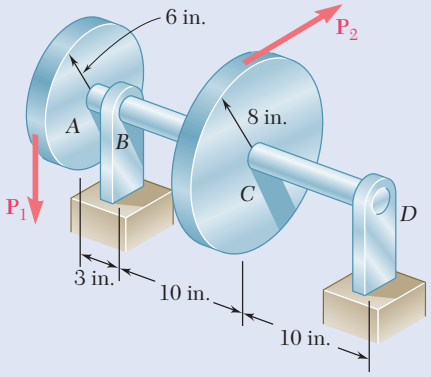


Fig. P8.19

8.20 The two 500-lb forces are vertical and the force **P** is parallel to the *z* axis. Knowing that $\tau_{all} = 8$ ksi, determine the smallest permissible diameter of the solid shaft *AE*.

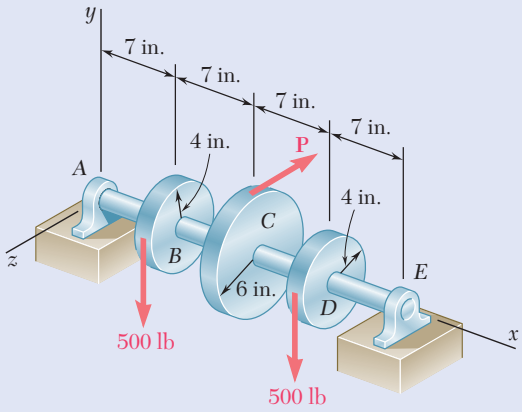


Fig. P8.20

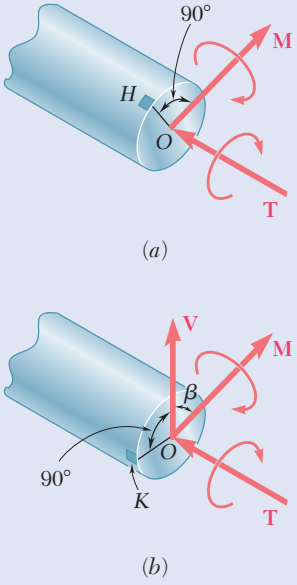


Fig. P8.21

8.21 It was stated in Sec. 8.2 that the shearing stresses produced in a shaft by the transverse loads are usually much smaller than those produced by the torques. In the preceding problems their effect was ignored, and it was assumed that the maximum shearing stress in a given section occurred at point *H* (Fig. P8.21*a*) and was equal to the expression obtained in Eq. (8.5), namely,

$$\tau_H = \frac{c}{J}\sqrt{M^2 + T^2}$$

Show that the maximum shearing stress at point *K* (Fig. P8.21*b*), where the effect of the shear *V* is greatest, can be expressed as

$$\tau_K = \frac{c}{J}\sqrt{(M\cos\beta)^2 + \left(\frac{2}{3}cV + T\right)^2}$$

where β is the angle between the vectors **V** and **M**. It is clear that the effect of the shear *V* cannot be ignored when $\tau_K \geq \tau_H$. (*Hint:* Only the component of **M** along **V** contributes to the shearing stress at *K*.)

8.22 Assuming that the magnitudes of the forces applied to disks A and C of Prob. 8.19 are, respectively, $P_1 = 1080$ lb and $P_2 = 810$ lb, and using the expressions given in Prob. 8.21, determine the values of τ_H and τ_K in a section (a) just to the left of B, (b) just to the left of C.

8.23 The solid shaft AB rotates at 600 rpm and transmits 80 kW from the motor M to a machine tool connected to gear F. Knowing that $\tau_{all} = 60$ MPa, determine the smallest permissible diameter of shaft AB.

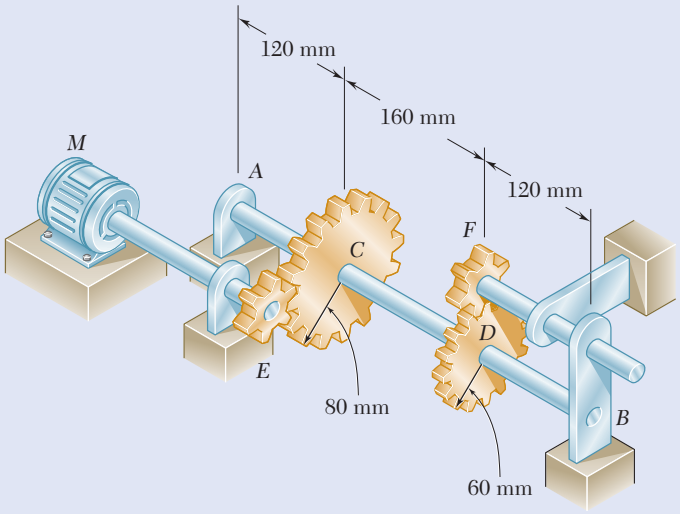


Fig. P8.23

8.24 Solve Prob. 8.23, assuming that shaft AB rotates at 720 rpm.

8.25 The solid shafts ABC and DEF and the gears shown are used to transmit 20 hp from the motor M to a machine tool connected to shaft DEF. Knowing that the motor rotates at 240 rpm and that $\tau_{all} = 7.5$ ksi, determine the smallest permissible diameter of (a) shaft ABC, (b) shaft DEF.

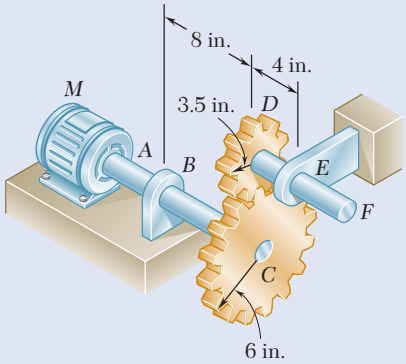


Fig. *P8.25*

8.26 Solve Prob. 8.25, assuming that the motor rotates at 360 rpm.

8.27 The solid shaft *ABC* and the gears shown are used to transmit 10 kW from the motor *M* to a machine tool connected to gear *D*. Knowing that the motor rotates at 240 rpm and that $\tau_{all} = 60$ MPa, determine the smallest permissible diameter of shaft *ABC*.

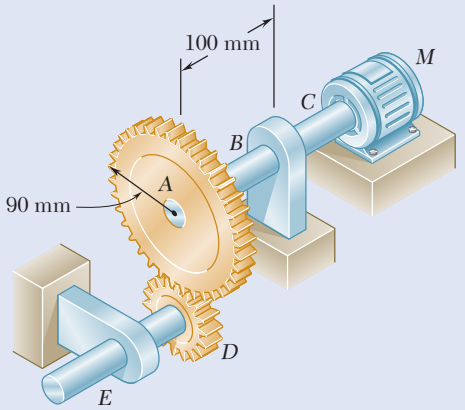


Fig. P8.27

8.28 Assuming that shaft *ABC* of Prob. 8.27 is hollow and has an outer diameter of 50 mm, determine the largest permissible inner diameter of the shaft.

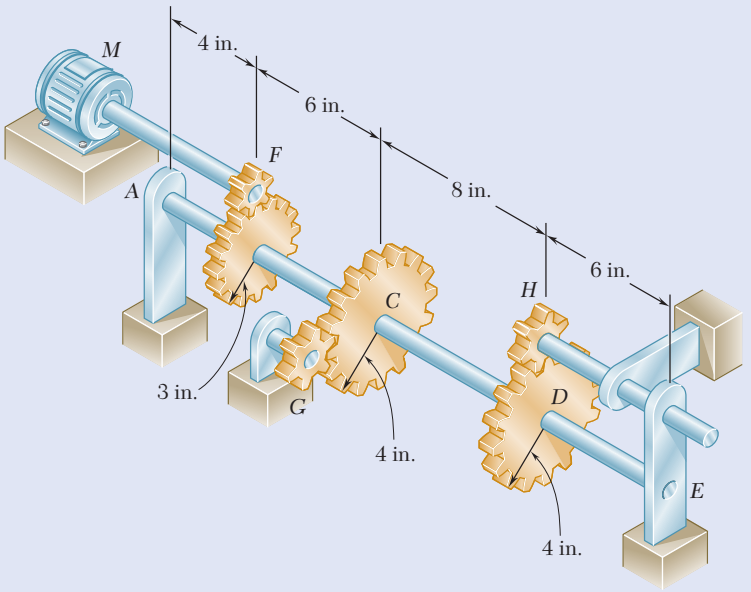


Fig. P8.29

8.29 The solid shaft *AE* rotates at 600 rpm and transmits 60 hp from the motor *M* to machine tools connected to gears *G* and *H*. Knowing that $\tau_{all} = 8$ ksi and that 40 hp is taken off at gear *G* and 20 hp is taken off at gear *H*, determine the smallest permissible diameter of shaft *AE*.

8.30 Solve Prob. 8.29, assuming that 30 hp is taken off at gear *G* and 30 hp is taken off at gear *H*.

8.3 STRESSES UNDER COMBINED LOADS

In Chaps. 1 and 2 you learned to determine the stresses caused by a centric axial load. In Chap. 3, you analyzed the distribution of stresses in a cylindrical member subjected to a twisting couple. In Chap. 4, you determined the stresses caused by bending couples and, in Chaps. 5 and 6, the stresses produced by transverse loads. As you will see presently, you can combine the knowledge you have acquired to determine the stresses in slender structural members or machine components under fairly general loading conditions. For example, the bent member *ABDE* of circular cross section is subjected to several forces (Fig. 8.15). In order to determine the stresses at points *H* or *K*, we first pass a section through these points and determine the force-couple system at the centroid *C* of the section that is required to maintain the equilibrium of portion *ABC*.† This system represents the internal forces in the section and consists of three force components and three couple vectors that are assumed to be directed as shown in Fig. 8.16.

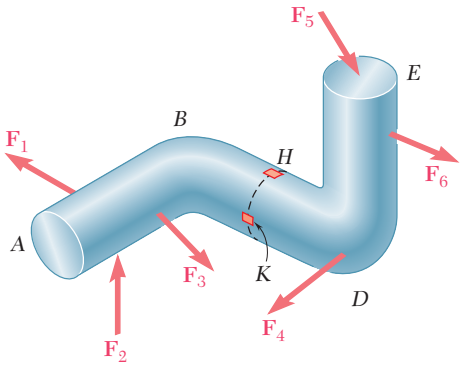


Fig. 8.15 Member *ABDE* subjected to several forces.

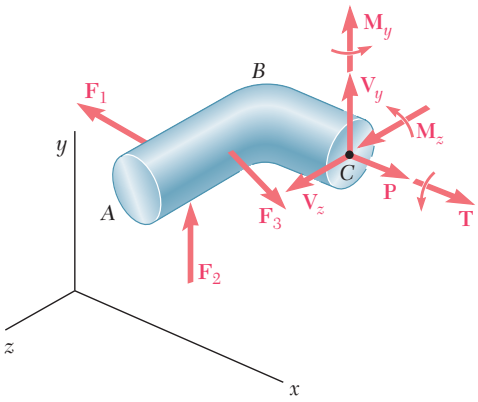


Fig. 8.16 Free-body diagram of segment *ABC* to determine the internal forces and couples at cross section *C*.

Force **P** is a centric axial force that produces normal stresses in the section. The couple vectors $\mathbf{M}_y$ and $\mathbf{M}_z$ cause the member to bend and also produce normal stresses in the section. These have been grouped in Fig. 8.17*a*, and the sums σ_x of the normal stresses produced at points *H* and *K* are shown in Fig. 8.18*a*. These stresses can be determined as shown in Sec. 4.9.

On the other hand, the twisting couple **T** and the shearing forces $\mathbf{V}_y$ and $\mathbf{V}_z$ as shown in Fig. 8.17*b* produce shearing stresses in the section. The sums τ_{xy} and τ_{xz} of the components of the shearing stresses produced at points *H* and *K* are shown in Fig. 8.18*b* and can be determined as indicated

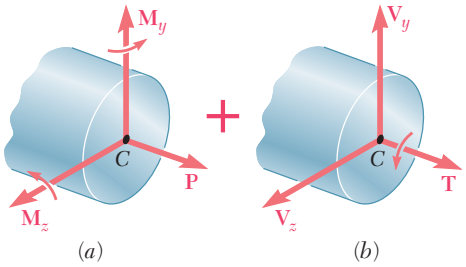


Fig. 8.17 Internal forces and couple vectors separated into (*a*) those causing normal stresses and (*b*) those causing shearing stresses.

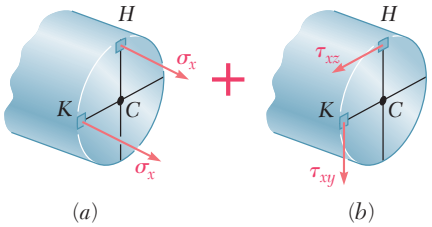


Fig. 8.18 Normal and shearing stresses at points *H* and *K*.

†The force-couple system at *C* can also be defined as *equivalent to the forces acting on the portion of the member located to the right of the section* (see Concept Application 8.1).

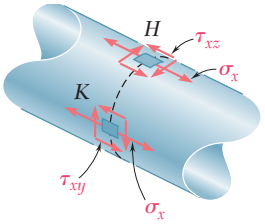


Fig. 8.19 Elements at points *H* and *K* showing combined stresses.

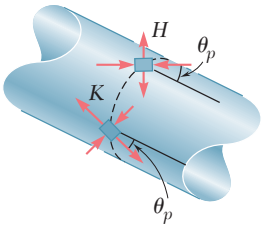


Fig. 8.20 Elements at points *H* and *K* showing principal stresses.

in Secs. 3.1C and 6.1B.[†] The normal and shearing stresses shown in parts *a* and *b* are now combined and displayed at points *H* and *K* on the surface of the member (Fig. 8.19).

The principal stresses and the orientation of the principal planes at points *H* and *K* are determined from σ_x, τ_{xy}, and τ_{xz} at each of these points by one of the methods presented in Chap. 7 (Fig. 8.20). The maximum shearing stress at each of these points and the corresponding planes can be found in a similar way.

The results in this section are valid only if the conditions of applicability of the superposition principle (Sec. 2.5) and of Saint-Venant's principle (Sec. 2.10) are met:

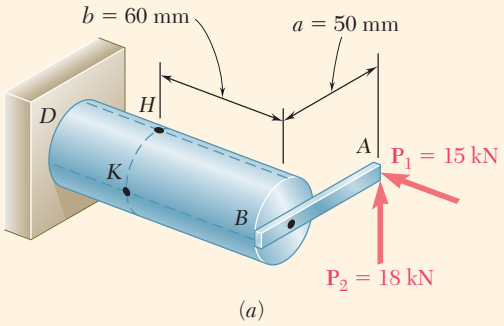
1. The stresses involved must not exceed the proportional limit of the material.
2. The deformations due to one of the loadings must not affect the determination of the stresses due to the others.
3. The section used in your analysis must not be too close to the points of application of the given forces.

The first of these requirements shows that the method presented here cannot be applied to plastic deformations.

[†]Note that your present knowledge allows you to determine the effect of the twisting couple **T** only in circular shafts, members with a rectangular cross section (Sec. 3.9), or thin-walled hollow members (Sec. 3.10).

Concept Application 8.1

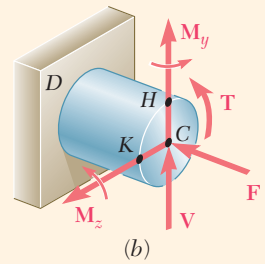
Two forces $\mathbf{P}_1$ and $\mathbf{P}_2$, with a magnitude of $P_1 = 15$ kN and $P_2 = 18$ kN, are applied as shown in Fig. 8.21a to the end *A* of bar *AB*, which is welded to a cylindrical member *BD* of radius $c = 20$ mm. Knowing that the distance from *A* to the axis of member *BD* is $a = 50$ mm and assuming that all stresses remain below the proportional limit of the material, determine (*a*) the normal and shearing stresses at point *K* of the transverse section of member *BD* located at a distance $b = 60$ mm from end *B*, (*b*) the principal axes and principal stresses at *K*, and (*c*) the maximum shearing stress at *K*.



(*a*)

Fig. 8.21 Cylindrical member under combined loading. (*a*) Dimensions and loading.

(continued)



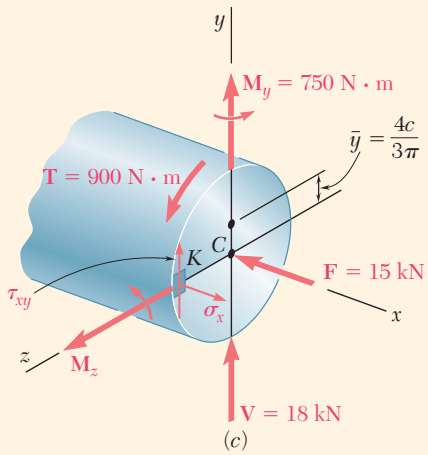


Fig. 8.21 (*Cont.*) (*b*) Internal forces and couples at section containing points *H* and *K*. (*c*) Values of forces and couples that produce stresses at point *K*, as well as the dimension needed to compute the first moment of area.

Internal Forces in Given Section. Replace the forces $\mathbf{P}_1$ and $\mathbf{P}_2$ by an equivalent system of forces and couples applied at the center *C* of the section containing point *K* (Fig. 8.21*b*). This system represents the internal forces in the section and consists of the following forces and couples:

1. A centric axial force **F** equal to the force $\mathbf{P}_1$ with the magnitude
$$F = P_1 = 15\text{ kN}$$
2. A shearing force **V** equal to the force $\mathbf{P}_2$ with the magnitude
$$V = P_2 = 18\text{ kN}$$
3. A twisting couple **T** of torque *T* equal to the moment of $\mathbf{P}_2$ about the axis of member *BD*:
$$T = P_2a = (18\text{ kN})(50\text{ mm}) = 900\text{ N·m}$$
4. A bending couple $\mathbf{M}_y$ of moment M_y equal to the moment of $\mathbf{P}_1$ about a vertical axis through *C*:
$$M_y = P_1a = (15\text{ kN})(50\text{ mm}) = 750\text{ N·m}$$
5. A bending couple $\mathbf{M}_z$ of moment M_z equal to the moment of $\mathbf{P}_2$ about a transverse, horizontal axis through *C*:
$$M_z = P_2b = (18\text{ kN})(60\text{ mm}) = 1080\text{ N·m}$$

The results are shown in Fig. 8.21c.

a. Normal and Shearing Stresses at Point *K*. Each of the forces and couples shown in Fig. 8.21*c* produce a normal or shear stress at point *K*. Compute each of these stresses seperately and then add the normal stresses and add the shearing stresses.

Geometric Properties of the Section For the given data, we have

$$A = \pi c^2 = \pi(0.020\text{ m})^2 = 1.257 \times 10^{-3}\text{ m}^2$$
$$I_y = I_z = \tfrac{1}{4}\pi c^4 = \tfrac{1}{4}\pi(0.020\text{ m})^4 = 125.7 \times 10^{-9}\text{ m}^4$$
$$J_C = \tfrac{1}{2}\pi c^4 = \tfrac{1}{2}\pi(0.020\text{ m})^4 = 251.3 \times 10^{-9}\text{ m}^4$$

Also determine the first moment *Q* and the width *t* of the area of the cross section located above the *z* axis. Recall that $\bar{y} = 4c/3\pi$ for a semicircle of radius *c*, giving

$$Q = A'\bar{y} = \left(\frac{1}{2}\pi c^2\right)\left(\frac{4c}{3\pi}\right) = \frac{2}{3}c^3 = \frac{2}{3}(0.020\text{ m})^3$$
$$= 5.33 \times 10^{-6}\text{ m}^3$$

and

$$t = 2c = 2(0.020\text{ m}) = 0.040\text{ m}$$

(continued)

Normal Stresses. Normal stresses are produced at K by the centric force $\mathbf{F}$ and the bending couple $\mathbf{M}_y$. However, the couple $\mathbf{M}_z$ does not produce any stress at K, since K is located on the neutral axis corresponding to that couple. Determining each sign from Fig. 8.21*c* gives

$$\sigma_x = -\frac{F}{A} + \frac{M_y c}{I_y} = -11.9\text{ MPa} + \frac{(750\text{ N·m})(0.020\text{ m})}{125.7 \times 10^{-9}\text{ m}^4}$$

$$= -11.9\text{ MPa} + 119.3\text{ MPa}$$

$$\sigma_x = +107.4\text{ MPa}$$

Shearing Stresses. The shearing stress $(\tau_{xy})_V$ is due to the vertical shear $\mathbf{V}$, and the shearing stress $(\tau_{xy})_{\text{twist}}$ is caused by the torque $\mathbf{T}$. Using the values for Q, t, I_z, and J_C,

$$(\tau_{xy})_V = +\frac{VQ}{I_z t} = +\frac{(18 \times 10^3\text{ N})(5.33 \times 10^{-6}\text{ m}^3)}{(125.7 \times 10^{-9}\text{ m}^4)(0.040\text{ m})}$$

$$= +19.1\text{ MPa}$$

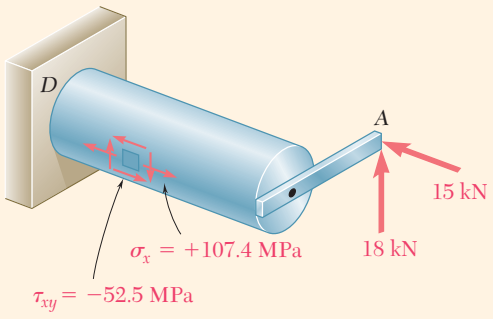
$$(\tau_{xy})_{\text{twist}} = -\frac{Tc}{J_C} = -\frac{(900\text{ N·m})\,(0.020\text{ m})}{251.3 \times 10^{-9}\text{ m}^4} = -71.6\text{ MPa}$$

Adding these provides τ_{xy} at point K.

$$\tau_{xy} = (\tau_{xy})_V + (\tau_{xy})_{\text{twist}} = +19.1\text{ MPa} - 71.6\text{ MPa}$$

$$\tau_{xy} = -52.5\text{ MPa}$$

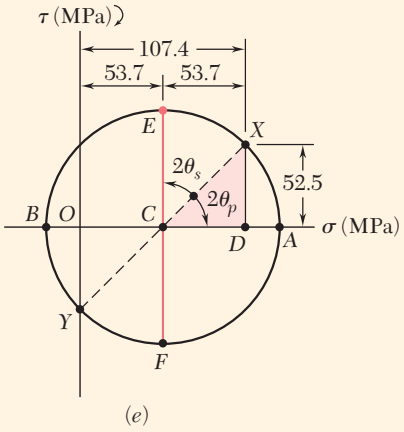
In Fig. 8.21*d*, the normal stress σ_x and the shearing stresses τ_{xy} are acting on a square element located at K on the surface of the cylindrical member. Note that shearing stresses acting on the longitudinal sides of the element also are included.



(*d*)

Fig. 8.21 (*Cont.*) (*d*) Element showing combined stresses at point *K*.

(continued)



(e)

Fig. 8.21 (*Cont.*) (*e*) Mohr's circle for stresses at point *K*.

b. Principal Planes and Principal Stresses at Point *K*. Either of the two methods from Chap. 7 can be used to determine the principal planes and principal stresses at *K*. Selecting Mohr's circle, plot point *X* with coordinates $\sigma_x = +107.4$ MPa and $-\tau_{xy} = +52.5$ MPa and point *Y* with coordinates $\sigma_y = 0$ and $+\tau_{xy} = -52.5$ MPa and draw the circle with the diameter *XY* (Fig. 8.21*e*). Observing that

$$OC = CD = \tfrac{1}{2}(107.4) = 53.7 \text{ MPa} \qquad DX = 52.5 \text{ MPa}$$

we determine the orientation of the principal planes:

$$\tan 2\theta_p = \frac{DX}{CD} = \frac{52.5}{53.7} = 0.97765 \qquad 2\theta_p = 44.4^\circ \downarrow$$
$$\theta_p = 22.2^\circ \downarrow$$

The radius of the circle is

$$R = \sqrt{(53.7)^2 + (52.5)^2} = 75.1 \text{ MPa}$$

and the principal stresses are

$$\sigma_{\max} = OC + R = 53.7 + 75.1 = 128.8 \text{ MPa}$$
$$\sigma_{\min} = OC - R = 53.7 - 75.1 = -21.4 \text{ MPa}$$

The results are shown in Fig. 8.21*f*.

c. Maximum Shearing Stress at Point *K*. This stress corresponds to points *E* and *F* in Fig. 8.21*e*.

$$\tau_{\max} = CE = R = 75.1 \text{ MPa}$$

Observing that $2\theta_s = 90^\circ - 2\theta_p = 90^\circ - 44.4^\circ = 45.6^\circ$, the planes of maximum shearing stress form an angle $\theta_s = 22.8^\circ \curvearrowleft$ with the horizontal. The corresponding element is shown in Fig. 8.21*g*. Note that the normal stresses acting on this element are represented by *OC* in Fig. 8.21*e* and are equal to +53.7 MPa.

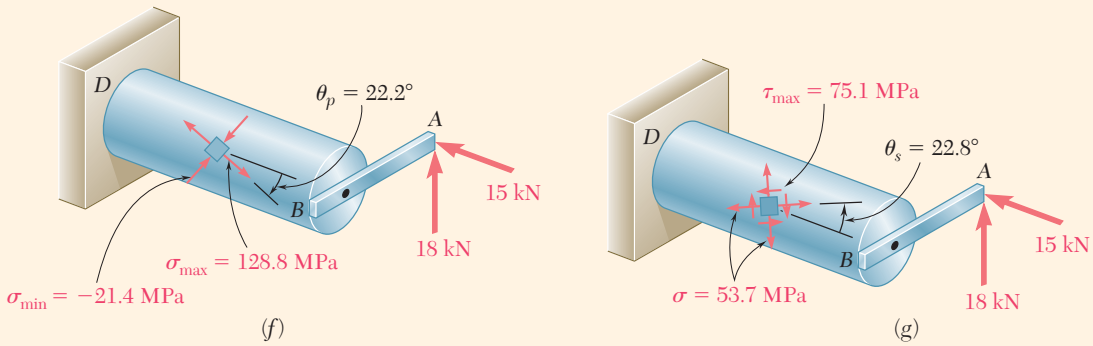
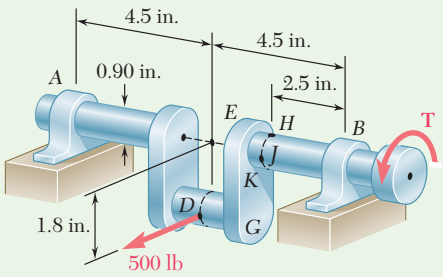


Fig. 8.21 (*Cont.*) (*f*) Principal stress element at point *K*. (*g*) Maximum shearing stress element at point *K*.



Sample Problem 8.4

A horizontal 500-lb force acts at point D of crankshaft AB held in static equilibrium by a twisting couple **T** and reactions at A and B. Knowing that the bearings are self-aligning and exert no couples on the shaft, determine the normal and shearing stresses at points H, J, K, and L located at the ends of the vertical and horizontal diameters of a transverse section located 2.5 in. to the left of bearing B.

STRATEGY: Begin by determining the internal forces and couples acting on the transverse section containing the points of interest, and then evaluate the stresses at these points due to each internal action. Combining these results will provide the total state of stress at each point.

MODELING:

Draw the free-body diagram of the crankshaft (Fig. 1). Find A = B = 250 lb

$$+\circlearrowleft \Sigma M_x = 0: \qquad -(500\text{ lb})(1.8\text{ in.}) + T = 0 \qquad T = 900\text{ lb}\cdot\text{in.}$$

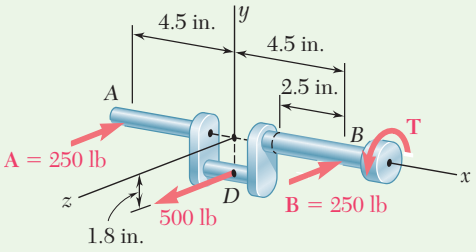


Fig. 1 Free-body diagram of crankshaft.

ANALYSIS:

Internal Forces in Transverse Section. Replace reaction **B** and the twisting couple **T** by an equivalent force-couple system at the center C of the transverse section containing H, J, K, and L. (Fig. 2.)

$$V = B = 250\text{ lb} \qquad T = 900\text{ lb}\cdot\text{in.}$$

$$M_y = (250\text{ lb})(2.5\text{ in.}) = 625\text{ lb}\cdot\text{in.}$$

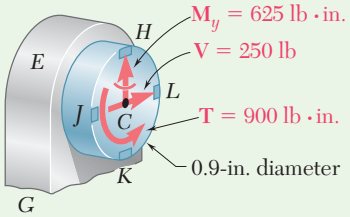


Fig. 2 Resultant force-couple system at section containing points H, J, K, and L.

(continued)

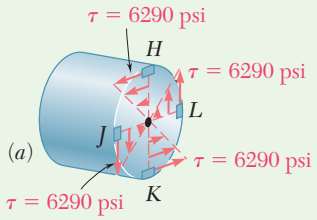


Fig. 3 Shearing stresses resulting from torque *T*.

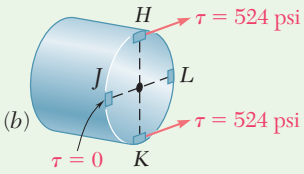


Fig. 4 Shearing stresses resulting from shearing force *V*.

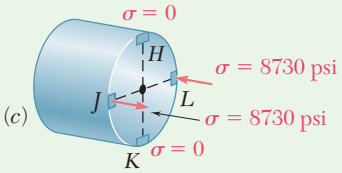


Fig. 5 Normal stresses resulting from bending couple M_y.

The geometric properties of the 0.9-in.-diameter section are

$$A = \pi(0.45\text{ in.})^2 = 0.636\text{ in}^2 \quad I = \tfrac{1}{4}\pi(0.45\text{ in.})^4 = 32.2 \times 10^{-3}\text{ in}^4$$
$$J = \tfrac{1}{2}\pi(0.45\text{ in.})^4 = 64.4 \times 10^{-3}\text{ in}^4$$

Stresses Produced by Twisting Couple T. Using Eq. (3.10), determine the shearing stresses at points *H*, *J*, *K*, and *L* and show them in Fig. 3.

$$\tau = \frac{Tc}{J} = \frac{(900\text{ lb·in.})(0.45\text{ in.})}{64.4 \times 10^{-3}\text{in}^4} = 6290\text{ psi}$$

Stresses Produced by Shearing Force V. The shearing force **V** produces no shearing stresses at points *J* and *L*. At points *H* and *K*, compute *Q* for a semicircle about a vertical diameter and then determine the shearing stress produced by the shear force $V = 250$ lb. These stresses are shown in Fig. 4.

$$Q = \left(\frac{1}{2}\pi c^2\right)\left(\frac{4c}{3\pi}\right) = \frac{2}{3}c^3 = \frac{2}{3}(0.45\text{ in.})^3 = 60.7 \times 10^{-3}\text{ in}^3$$

$$\tau = \frac{VQ}{It} = \frac{(250\text{ lb})(60.7 \times 10^{-3}\text{ in}^3)}{(32.2 \times 10^{-3}\text{ in}^4)(0.9\text{ in.})} = 524\text{ psi}$$

Stresses Produced by the Bending Couple M_y. Since the bending couple $\mathbf{M}_y$ acts in a horizontal plane, it produces no stresses at *H* and *K*. Use Eq. (4.15) to determine the normal stresses at points *J* and *L* and show them in Fig. 5.

$$\sigma = \frac{|M_y|c}{I} = \frac{(625\text{ lb·in.})(0.45\text{ in.})}{32.2 \times 10^{-3}\text{ in}^4} = 8730\text{ psi}$$

Summary. Add the stresses shown to obtain the total normal and shearing stresses at points *H*, *J*, *K*, and *L* (Fig. 6).

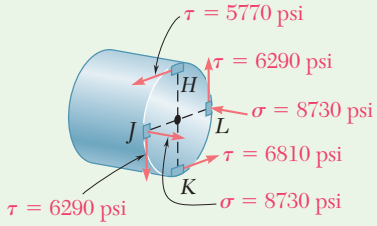
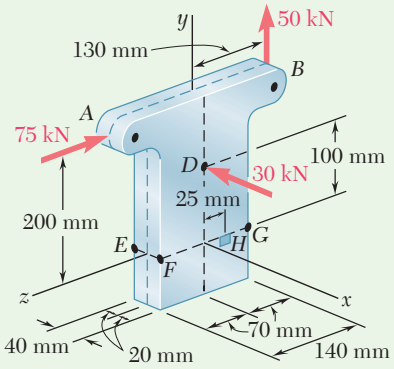


Fig. 6 Stress components at points *H*, *J*, *K*, and *L* from combining all loads.

Sample Problem 8.5



Three forces are applied as shown at points A, B, and D of a short steel post. Knowing that the horizontal cross section of the post is a 40 × 140-mm rectangle, determine the principal stresses, principal planes, and maximum shearing stress at point H.

STRATEGY: Begin by determining the forces and couples acting on the section containing the point of interest, and then use these to calculate the normal and shearing stresses acting at the point. Using Mohr's circle, these stresses can then be transformed to obtain the principal stresses, principal planes, and maximim shearing stress.

MODELING and ANALYSIS:

Internal Forces in Section *EFG*. Replace the three applied forces by an equivalent force-couple system at the center C of the rectangular section EFG (Fig. 1).

$$V_x = -30\text{ kN} \qquad P = 50\text{ kN} \qquad V_z = -75\text{ kN}$$

$$M_x = (50\text{ kN})(0.130\text{ m}) - (75\text{ kN})(0.200\text{ m}) = -8.5\text{ kN·m}$$

$$M_y = 0 \qquad M_z = (30\text{ kN})(0.100\text{ m}) = 3\text{ kN·m}$$

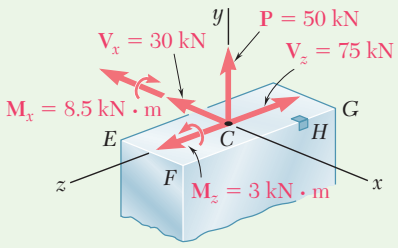


Fig. 1 Equivalent force-couple system at section containing points E, F, G, and H.

Note that there is no twisting couple about the y axis. The geometric properties of the rectangular section are

$$A = (0.040\text{ m})(0.140\text{ m}) = 5.6 \times 10^{-3}\text{ m}^2$$

$$I_x = \tfrac{1}{12}(0.040\text{ m})(0.140\text{ m})^3 = 9.15 \times 10^{-6}\text{ m}^4$$

$$I_z = \tfrac{1}{12}(0.140\text{ m})(0.040\text{ m})^3 = 0.747 \times 10^{-6}\text{ m}^4$$

(continued)

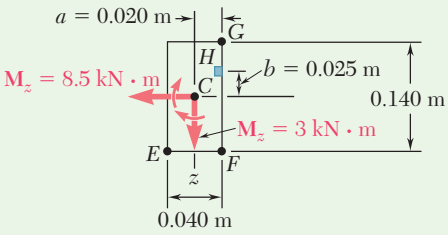


Fig. 2 Dimensions and bending couples used to determine normal stresses.

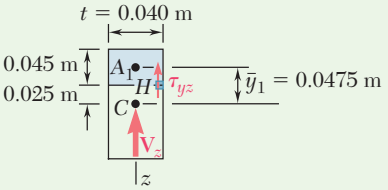


Fig. 3 Dimensions and shearing force used to determine the transverse shearing stress.

Normal Stress at *H*. The normal stresses σ_y are produced by the centric force **P** and by the bending couples $\mathbf{M}_x$ and $\mathbf{M}_z$. The sign of each stress is determined by carefully examining the force-couple system at C (Fig. 2).

$$\sigma_y = +\frac{P}{A} + \frac{|M_z|a}{I_z} - \frac{|M_x|b}{I_x}$$

$$= \frac{50\text{ kN}}{5.6 \times 10^{-3}\text{ m}^2} + \frac{(3\text{ kN·m})(0.020\text{ m})}{0.747 \times 10^{-6}\text{ m}^4} - \frac{(8.5\text{ kN·m})(0.025\text{ m})}{9.15 \times 10^{-6}\text{ m}^4}$$

$$\sigma_y = 8.93\text{ MPa} + 80.3\text{ MPa} - 23.2\text{ MPa} \qquad \sigma_y = 66.0\text{ MPa}$$

Shearing Stress at *H*. Considering the shearing force $\mathbf{V}_x$, we note that $Q = 0$ with respect to the z axis, since H is on the edge of the cross section. Thus, $\mathbf{V}_x$ produces no shearing stress at H. The shearing force $\mathbf{V}_z$ does produce a shearing stress at H (Fig. 3).

$$Q = A_1\bar{y}_1 = [(0.040\text{ m})(0.045\text{ m})](0.0475\text{ m}) = 85.5 \times 10^{-6}\text{ m}^3$$

$$\tau_{yz} = \frac{V_z Q}{I_x t} = \frac{(75\text{ kN})(85.5 \times 10^{-6}\text{ m}^3)}{(9.15 \times 10^{-6}\text{ m}^4)(0.040\text{ m})} \qquad \tau_{yz} = 17.52\text{ MPa}$$

Principal Stresses, Principal Planes, and Maximum Shearing Stress at *H*. Draw Mohr's circle for the stresses at point H (Fig. 4).

$$\tan 2\theta_p = \frac{17.52}{33.0} \qquad 2\theta_p = 27.96° \qquad \theta_p = 13.98°$$

$$R = \sqrt{(33.0)^2 + (17.52)^2} = 37.4\text{ MPa} \qquad \tau_{\max} = 37.4\text{ MPa}$$

$$\sigma_{\max} = OA = OC + R = 33.0 + 37.4 \qquad \sigma_{\max} = 70.4\text{ MPa}$$

$$\sigma_{\min} = OB = OC - R = 33.0 - 37.4 \qquad \sigma_{\min} = -7.4\text{ MPa}$$

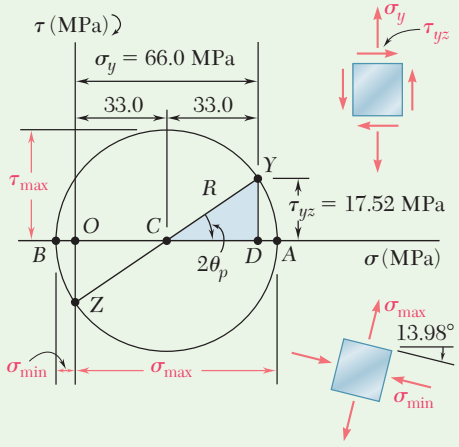


Fig. 4 Mohr's circle at point H used for finding principal stresses and maximum shearing stress and their orientation.

Problems

8.31 Two 1.2-kip forces are applied to an L-shaped machine element *AB* as shown. Determine the normal and shearing stresses at (*a*) point *a*, (*b*) point *b*, (*c*) point *c*.

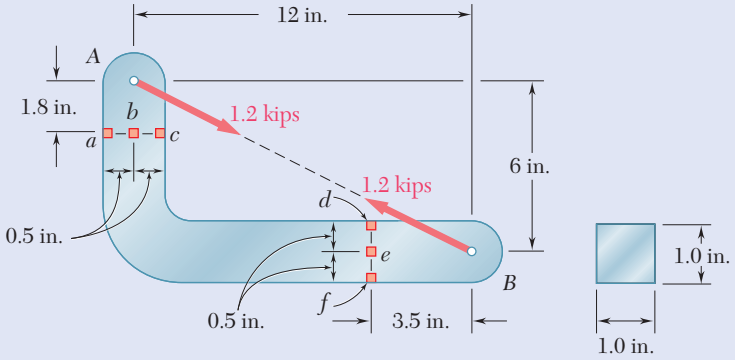


Fig. P8.31 and P8.32

8.32 Two 1.2-kip forces are applied to an L-shaped machine element *AB* as shown. Determine the normal and shearing stresses at (*a*) point *d*, (*b*) point *e*, (*c*) point *f*.

8.33 The cantilever beam *AB* has a rectangular cross section of 150 × 200 mm. Knowing that the tension in the cable *BD* is 10.4 kN and neglecting the weight of the beam, determine the normal and shearing stresses at the three points indicated.

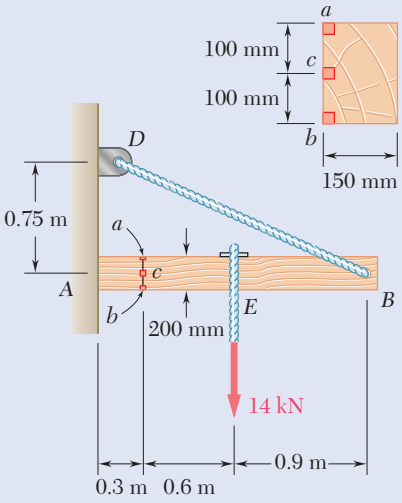


Fig. *P8.33*

8.34 through 8.36 Member *AB* has a uniform rectangular cross section of 10 × 24 mm. For the loading shown, determine the normal and shearing stresses at (*a*) point *H*, (*b*) point *K*.

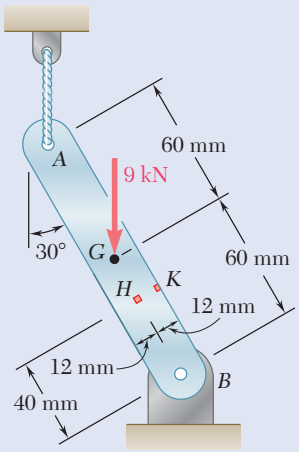


Fig. *P8.34*

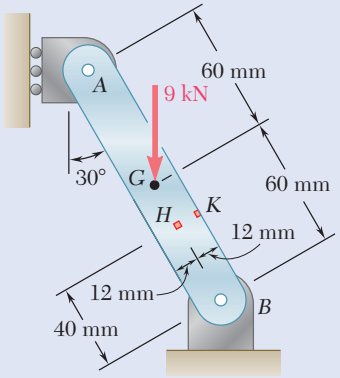


Fig. P8.35

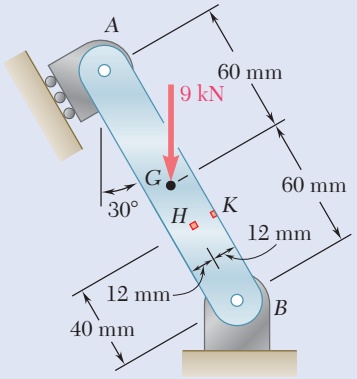


Fig. P8.36

8.37 A 1.5-kip force and a 9-kip·in. couple are applied at the top of the 2.5-in.-diameter cast-iron post shown. Determine the normal and shearing stresses at (*a*) point *H*, (*b*) point *K*.

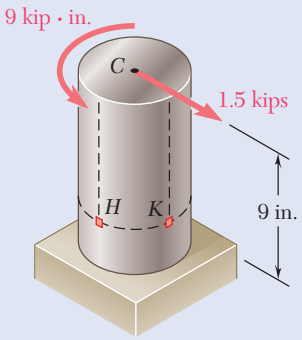


Fig. P8.37

8.38 Two forces are applied to the pipe *AB* as shown. Knowing that the pipe has inner and outer diameters equal to 35 and 42 mm, respectively, determine the normal and shearing stresses at (*a*) point *a*, (*b*) point *b*.

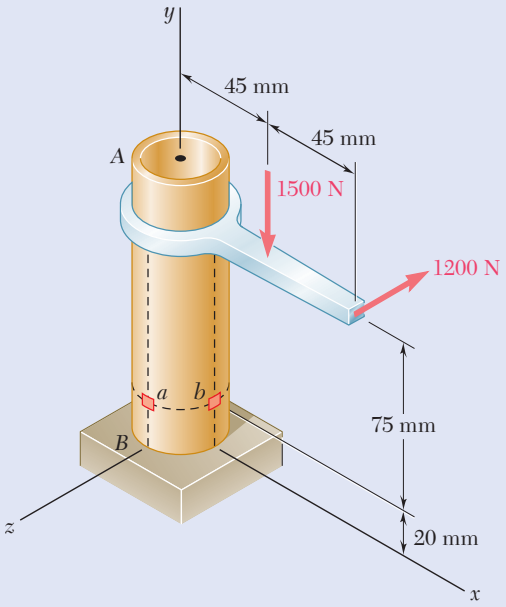


Fig. P8.38

8.39 Several forces are applied to the pipe assembly shown. Knowing that the pipe has inner and outer diameters equal to 1.61 in. and 1.90 in., respectively, determine the normal and shearing stresses at (*a*) point *H*, (*b*) point *K*.

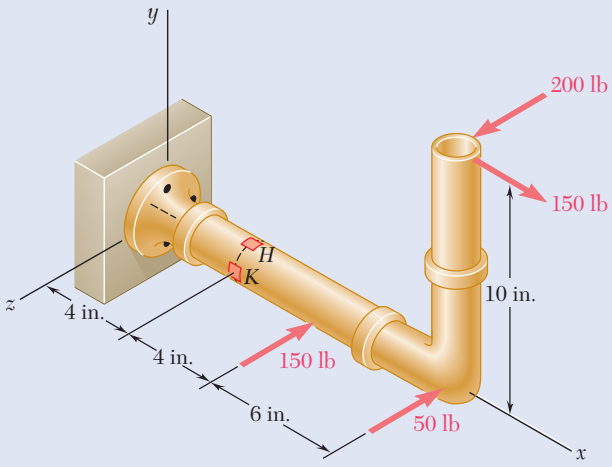


Fig. P8.39

8.40 The steel pile *AB* has a 100-mm outer diameter and an 8-mm wall thickness. Knowing that the tension in the cable is 40 kN, determine the normal and shearing stresses at point *H*.

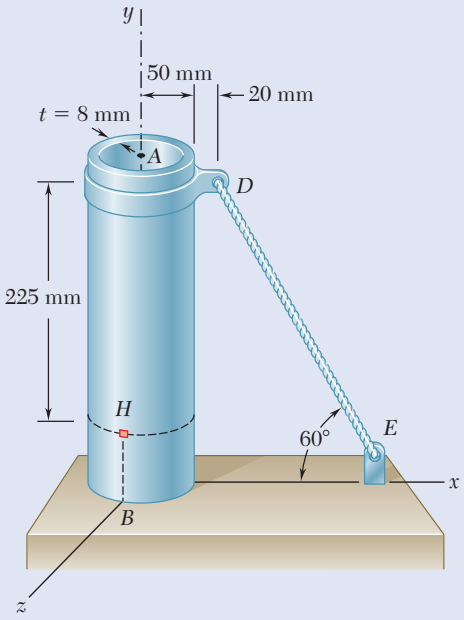


Fig. P8.40

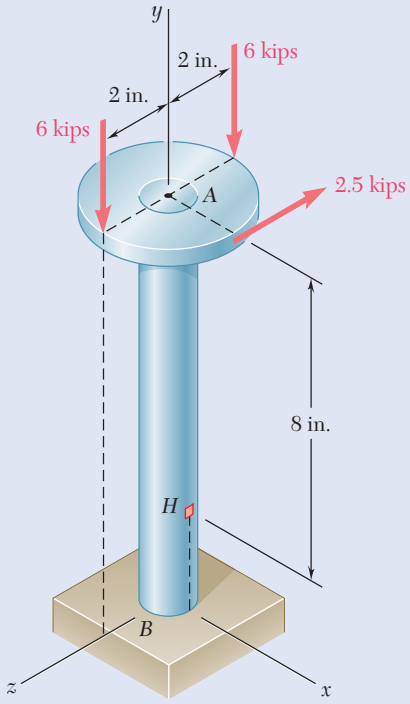


Fig. *P8.41*

8.41 Three forces are applied to a 4-in.-diameter plate that is attached to the solid 1.8-in.-diameter shaft *AB*. At point *H*, determine (*a*) the principal stresses and principal planes, (*b*) the maximum shearing stress.

8.42 The steel pipe *AB* has a 72-mm outer diameter and a 5-mm wall thickness. Knowing that the arm *CDE* is rigidly attached to the pipe, determine the principal stresses, principal planes, and the maximum shearing stress at point *H*.

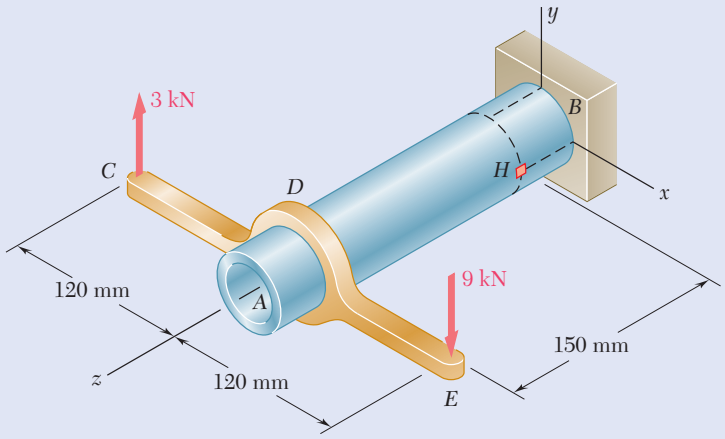


Fig. P8.42

8.43 A 13-kN force is applied as shown to the 60-mm-diameter cast-iron post *ABD*. At point *H*, determine (*a*) the principal stresses and principal planes, (*b*) the maximum shearing stress.

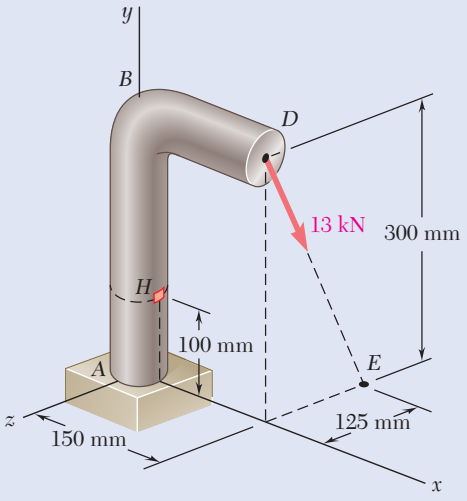


Fig. P8.43

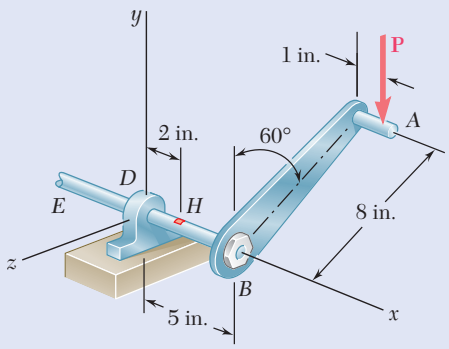


Fig. *P8.44*

8.44 A vertical force **P** of magnitude 60 lb is applied to the crank at point *A*. Knowing that the shaft *BDE* has a diameter of 0.75 in., determine the principal stresses and the maximum shearing stress at point *H* located at the top of the shaft, 2 in. to the right of support *D*.

8.45 Three forces are applied to the bar shown. Determine the normal and shearing stresses at (*a*) point *a*, (*b*) point *b*, (*c*) point *c*.

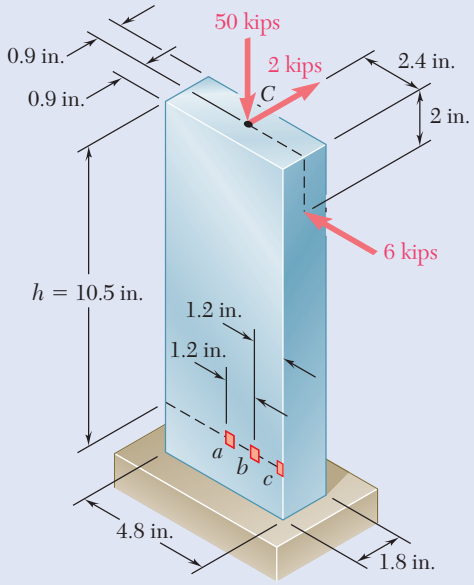


Fig. *P8.45*

8.46 Solve Prob. 8.45, assuming that $h = 12$ in.

8.47 Three forces are applied to the bar shown. Determine the normal and shearing stresses at (*a*) point *a*, (*b*) point *b*, (*c*) point *c*.

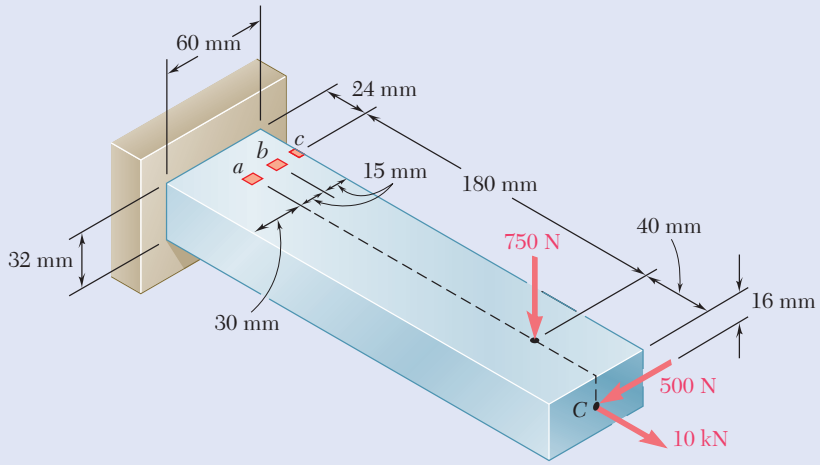


Fig. P8.47

8.48 Solve Prob. 8.47, assuming that the 750-N force is directed vertically upward.

8.49 Two forces are applied to the small post *BD* as shown. Knowing that the vertical portion of the post has a cross section of 1.5 × 2.4 in., determine the principal stresses, principal planes, and maximum shearing stress at point *H*.

8.50 Solve Prob. 8.49, assuming that the magnitude of the 6000-lb force is reduced to 1500 lb.

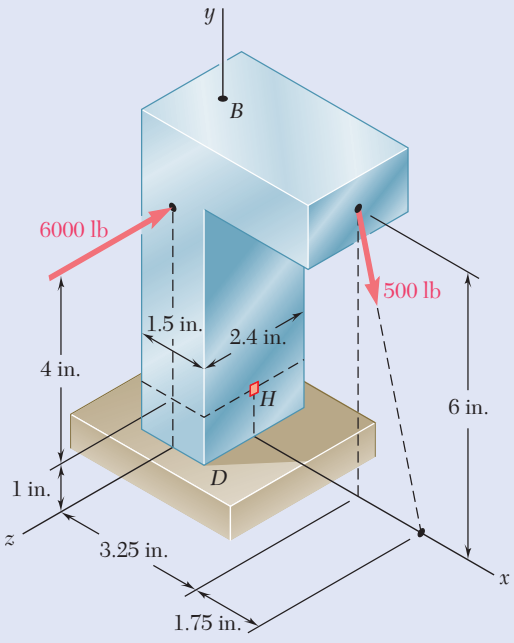


Fig. P8.49

8.51 Three forces are applied to the machine component *ABD* as shown. Knowing that the cross section containing point *H* is a 20 × 40-mm rectangle, determine the principal stresses and the maximum shearing stress at point *H*.

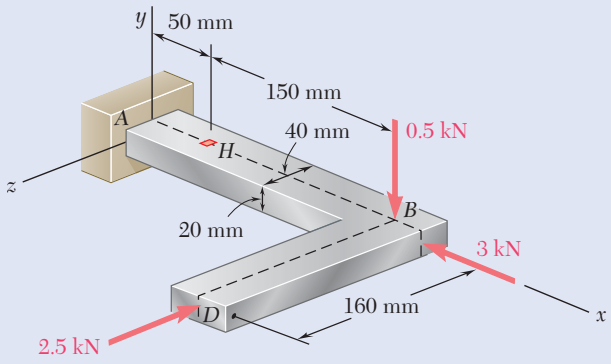


Fig. P8.51

8.52 Solve Prob. 8.51, assuming that the magnitude of the 2.5-kN force is increased to 10 kN.

8.53 Three steel plates, each 13 mm thick, are welded together to form a cantilever beam. For the loading shown, determine the normal and shearing stresses at points *a* and *b*.

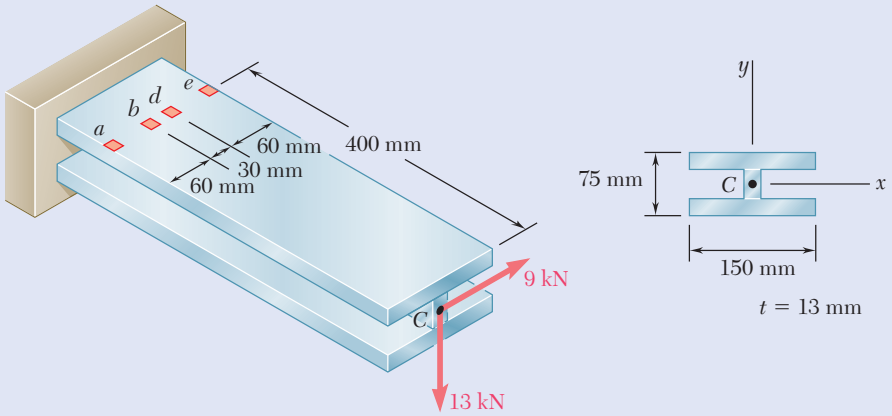


Fig. P8.53 and *P8.54*

8.54 Three steel plates, each 13 mm thick, are welded together to form a cantilever beam. For the loading shown, determine the normal and shearing stresses at points *d* and *e*.

8.55 Two forces $\mathbf{P}_1$ and $\mathbf{P}_2$ are applied as shown in directions perpendicular to the longitudinal axis of a W310 × 60 beam. Knowing that $\mathbf{P}_1 = 25$ kN and $\mathbf{P}_2 = 24$ kN, determine the principal stresses and the maximum shearing stress at point *a*.

8.56 Two forces $\mathbf{P}_1$ and $\mathbf{P}_2$ are applied as shown in directions perpendicular to the longitudinal axis of a W310 × 60 beam. Knowing that $\mathbf{P}_1 = 25$ kN and $\mathbf{P}_2 = 24$ kN, determine the principal stresses and the maximum shearing stress at point *b*.

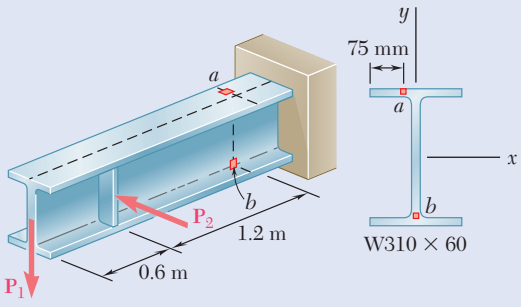


Fig. P8.55 and *P8.56*

8.57 Four forces are applied to a W8 × 28 rolled-steel beam as shown. Determine the principal stresses and maximum shearing stress at point *a*.

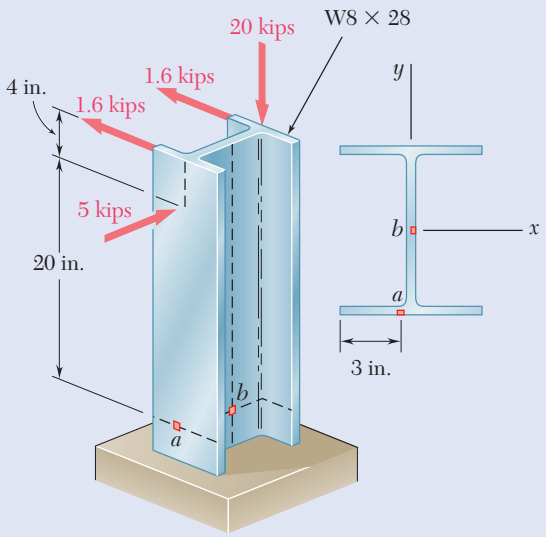


Fig. P8.57 and P8.58

8.58 Four forces are applied to a W8 × 28 rolled-steel beam as shown. Determine the principal stresses and maximum shearing stress at point *b*.

8.59 A force **P** is applied to a cantilever beam by means of a cable attached to a bolt located at the center of the free end of the beam. Knowing that **P** acts in a direction perpendicular to the longitudinal axis of the beam, determine (*a*) the normal stress at point *a* in terms of *P*, *b*, *h*, *l*, and β, (*b*) the values of β for which the normal stress at *a* is zero.

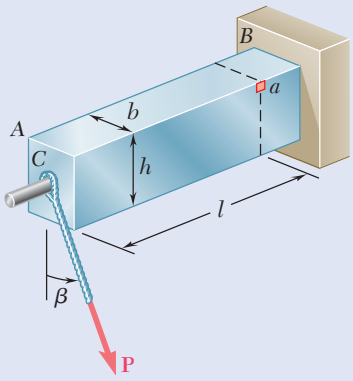


Fig. *P8.59*

8.60 A vertical force **P** is applied at the center of the free end of cantilever beam *AB*. (*a*) If the beam is installed with the web vertical ($\beta = 0$) and with its longitudinal axis *AB* horizontal, determine the magnitude of the force **P** for which the normal stress at point *a* is +120 MPa. (*b*) Solve part *a*, assuming that the beam is installed with $\beta = 3°$.

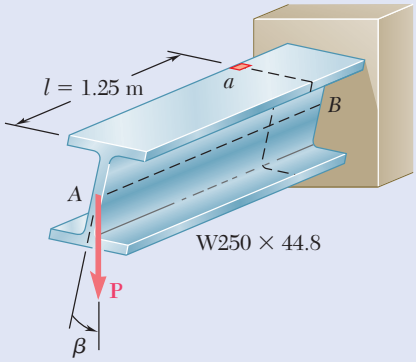


Fig. P8.60

***8.61** A 5-kN force **P** is applied to a wire that is wrapped around bar *AB* as shown. Knowing that the cross section of the bar is a square of side $d = 40$ mm, determine the principal stresses and the maximum shearing stress at point *a*.

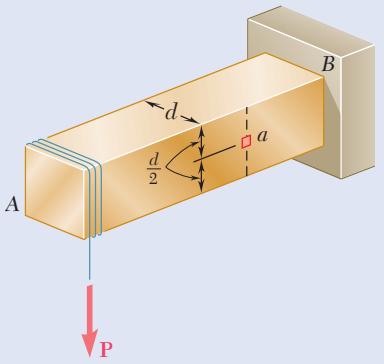


Fig. P8.61

***8.62** Knowing that the structural tube shown has a uniform wall thickness of 0.3 in., determine the principal stresses, principal planes, and maximum shearing stress at (*a*) point *H*, (*b*) point *K*.

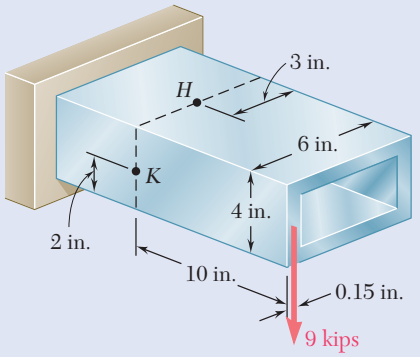


Fig. P8.62

***8.63** The structural tube shown has a uniform wall thickness of 0.3 in. Knowing that the 15-kip load is applied 0.15 in. above the base of the tube, determine the shearing stress at (*a*) point *a*, (*b*) point *b*.

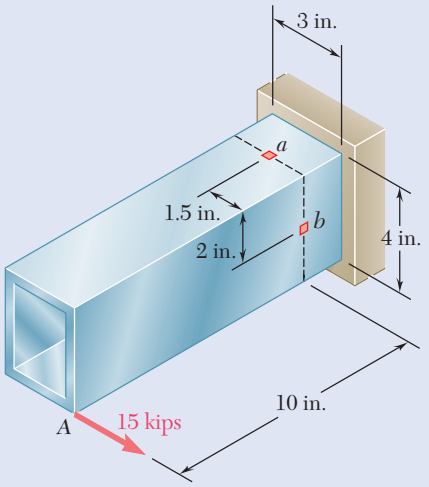


Fig. *P8.63*

***8.64** For the tube and loading of Prob. 8.63, determine the principal stresses and the maximum shearing stress at point *b*.

Review and Summary

Normal and Shearing Stresses in a Beam

The two fundamental relationships for the normal stress σ_x and the shearing stress τ_{xy} at any given point of a cross section of a prismatic beam are

$$\sigma_x = -\frac{My}{I} \tag{8.1}$$

and

$$\tau_{xy} = -\frac{VQ}{It} \tag{8.2}$$

where V = shear in the section
M = bending moment in the section
y = distance of the point from the neutral surface
I = centroidal moment of inertia of the cross section
Q = first moment about the neutral axis of the portion of the cross section located above the given point
t = width of the cross section at the given point

Principal Planes and Principal Stresses in a Beam

Using one of the methods of Ch. 7 for the transformation of stresses, the principal planes and principal stresses were obtained at various points (Fig. 8.22).

We investigated the distribution of principal stresses in a narrow rectangular cantilever beam subjected to a concentrated load **P** at its free end, and found that in any given transverse section—except close to the point of application of the load—the maximum principal stress $\sigma_{\max}$ did not exceed the determination of the maximum normal stress σ_m occurring at the surface of the beam.

While this is true for many beams of nonrectangular cross section, it may not hold for W-beams or S-beams, where $\sigma_{\max}$ at the junctions b and d of the web with the flanges of the beam (Fig. 8.23) may exceed the value of σ_m occurring at points a and e. Therefore, the design of a rolled-steel beam should include the determination of the maximum principal stress at these points.

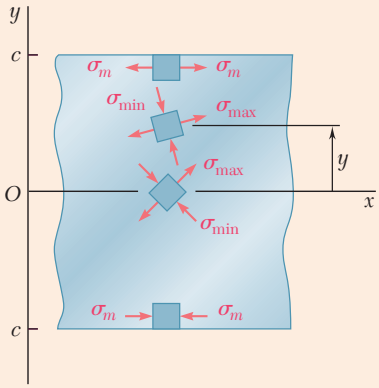


Fig. 8.22 Principal stress elements at selected points of beam.

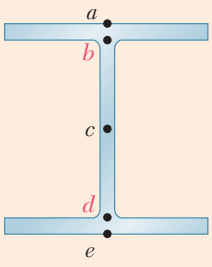


Fig. 8.23 Key locations for determination of principal stresses in I-shaped beams.

Design of Transmission Shafts Under Transverse Loads

The design of *transmission shafts* subjected to *transverse loads* and torques should include consideration of both the normal stresses due to the bending moment M and the shearing stresses due to the torque T. At any given transverse section of a cylindrical shaft (either solid or hollow), the minimum allowable value of the ratio J/c for the cross section is:

$$\frac{J}{c} = \frac{\left(\sqrt{M^2 + T^2}\right)_{\max}}{\tau_{\text{all}}} \tag{8.6}$$

Stresses Under General Loading Conditions

In preceding chapters, you learned to determine the stresses in prismatic members caused by axial loadings (Chaps. 1 and 2), torsion (Chap. 3), bending (Chap. 4), and transverse loadings (Chaps. 5 and 6). In the second part of this chapter (Sec. 8.3), we combined this knowledge to determine stresses under more general loading conditions.

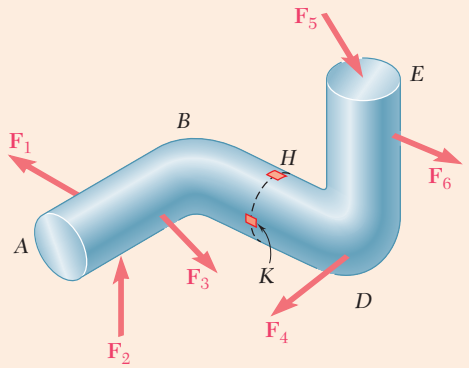


Fig. 8.24 Member *ABCD* subjected to several loads.

For instance, to determine the stresses at point H or K of the bent member shown in Fig. 8.24, a section is passed through these points and the applied loads are replaced by an equivalent force-couple system at the centroid C of the section (Fig. 8.25). The normal and shearing stresses produced at H or K by each of the forces and couples applied at C are determined and then combined to obtain the resulting normal stress σ_x and the resulting shearing stresses τ_{xy} and τ_{xz} at H or K. The principal stresses, the orientation of the principal planes, and the maximum shearing stress at point H or K are then determined using one of the methods presented in Chap. 7.

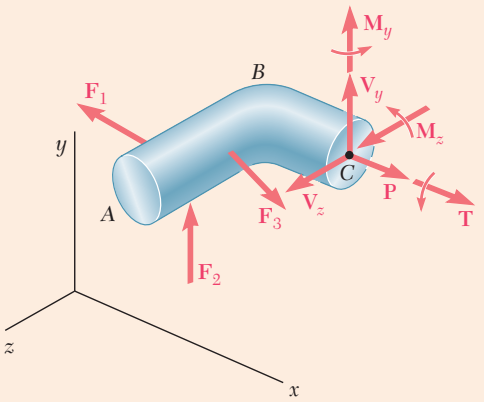


Fig. 8.25 Free-body diagram of segment *ABC* to determine the internal forces and couples at cross section *C*.

Review Problems

8.65 (*a*) Knowing that $\sigma_{all} = 24$ ksi and $\tau_{all} = 14.5$ ksi, select the most economical wide-flange shape that should be used to support the loading shown. (*b*) Determine the values to be expected for σ_m, τ_m, and the principal stress σ_{max} at the junction of a flange and the web of the selected beam.

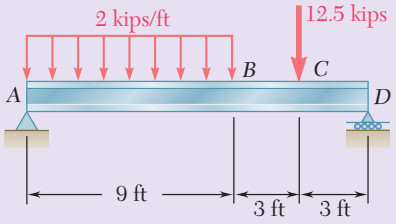


Fig. P8.65

8.66 Neglecting the effect of fillets and of stress concentrations, determine the smallest permissible diameters of the solid rods *BC* and *CD*. Use $\tau_{all} = 60$ MPa.

8.67 Knowing that rods *BC* and *CD* are of diameter 24 mm and 36 mm, respectively, determine the maximum shearing stress in each rod. Neglect the effect of fillets and of stress concentrations.

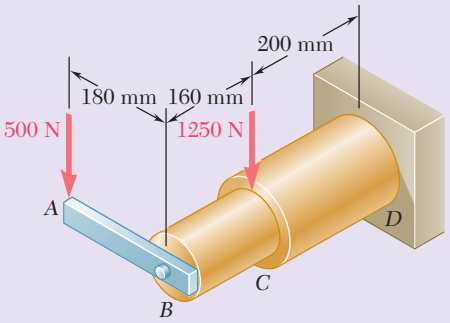


Fig. P8.66 and *P8.67*

8.68 The solid shaft *AB* rotates at 450 rpm and transmits 20 kW from the motor *M* to machine tools connected to gears *F* and *G*. Knowing that $\tau_{all} = 55$ MPa and assuming that 8 kW is taken off at gear *F* and 12 kW is taken off at gear *G*, determine the smallest permissible diameter of shaft *AB*.

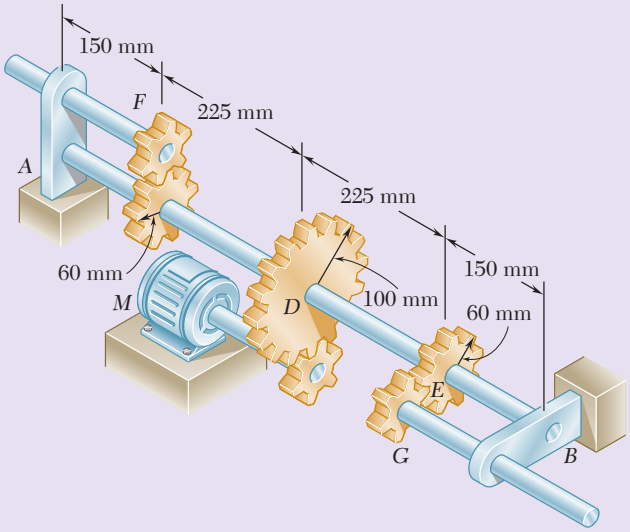


Fig. P8.68

8.69 A 6-kip force is applied to the machine element AB as shown. Knowing that the uniform thickness of the element is 0.8 in., determine the normal and shearing stresses at (a) point a, (b) point b, (c) point c.

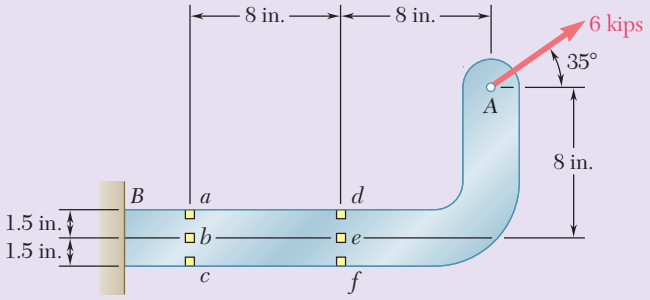


Fig. P8.69

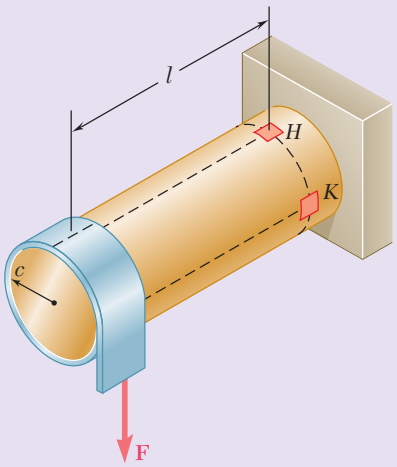


Fig. *P8.70*

8.70 A thin strap is wrapped around a solid rod of radius $c = 20$ mm as shown. Knowing that $l = 100$ mm and $F = 5$ kN, determine the normal and shearing stresses at (a) point H, (b) point K.

8.71 A close-coiled spring is made of a circular wire of radius r that is formed into a helix of radius R. Determine the maximum shearing stress produced by the two equal and opposite forces **P** and **P′**. (*Hint:* First determine the shear **V** and the torque **T** in a transverse cross section.)

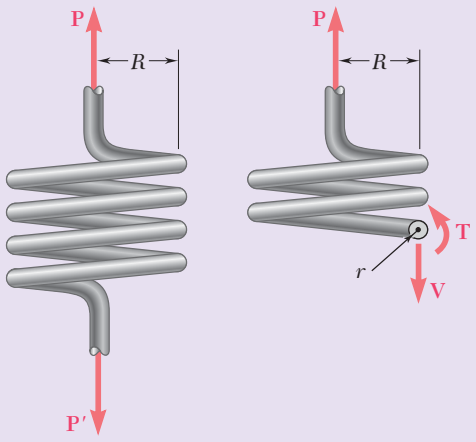


Fig. P8.71

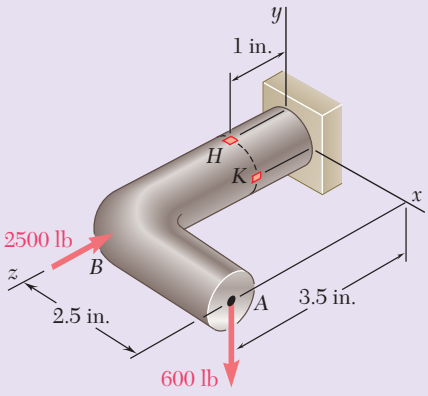


Fig. *P8.72*

8.72 Forces are applied at points A and B of the solid cast-iron bracket shown. Knowing that the bracket has a diameter of 0.8 in., determine the principal stresses and the maximum shearing stress at (a) point H, (b) point K.

8.73 Knowing that the bracket AB has a uniform thickness of $\frac{5}{8}$ in., determine (a) the principal planes and principal stresses at point K, (b) the maximum shearing stress at point K.

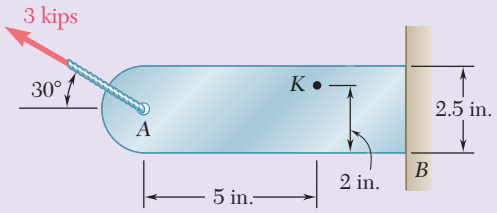


Fig. P8.73

8.74 For the post and loading shown, determine the principal stresses, principal planes, and maximum shearing stress at point H.

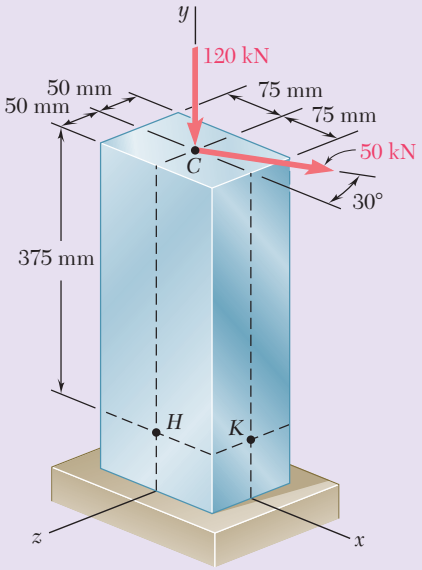


Fig. P8.74

8.75 Knowing that the structural tube shown has a uniform wall thickness of 0.25 in., determine the normal and shearing stresses at the three points indicated.

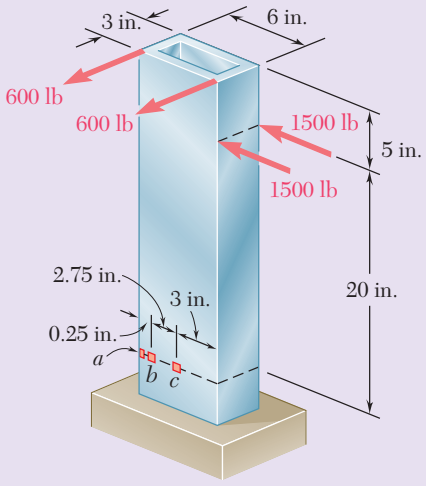


Fig. P8.75

8.76 The cantilever beam AB will be installed so that the 60-mm side forms an angle β between 0 and 90° with the vertical. Knowing that the 600-N vertical force is applied at the center of the free end of the beam, determine the normal stress at point a when (a) $\beta = 0$, (b) $\beta = 90°$. (c) Also, determine the value of β for which the normal stress at point a is a maximum and the corresponding value of that stress.

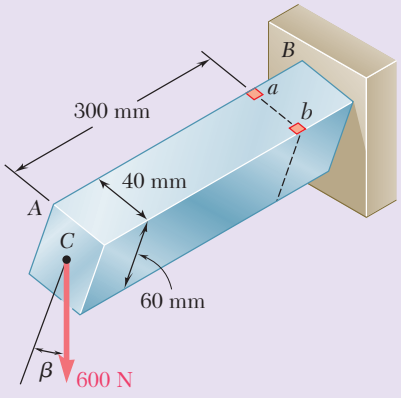


Fig. P8.76

Computer Problems

The following problems are designed to be solved with a computer.

8.C1 Let us assume that the shear V and the bending moment M have been determined in a given section of a rolled-steel beam. Write a computer program to calculate in that section, from the data available in Appendix C, (a) the maximum normal stress σ_m, (b) the principal stress $\sigma_{\max}$ at the junction of a flange and the web. Use this program to solve parts a and b of the following problems:

(1) Prob. 8.1 (Use $V = 45$ kips and $M = 450$ kip·in.)
(2) Prob. 8.2 (Use $V = 22.5$ kips and $M = 450$ kip·in.)
(3) Prob. 8.3 (Use $V = 700$ kN and $M = 1750$ kN·m)
(4) Prob. 8.4 (Use $V = 850$ kN and $M = 1700$ kN·m)

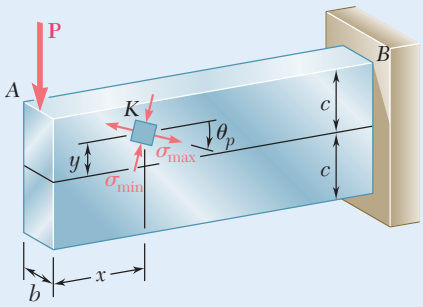


Fig. P8.C2

8.C2 A cantilever beam AB with a rectangular cross section of width b and depth $2c$ supports a single concentrated load $\mathbf{P}$ at its end A. Write a computer program to calculate, for any values of x/c and y/c, (a) the ratios $\sigma_{\max}/\sigma_m$ and $\sigma_{\min}/\sigma_m$, where $\sigma_{\max}$ and $\sigma_{\min}$ are the principal stresses at point $K(x, y)$ and σ_m the maximum normal stress in the same transverse section, (b) the angle θ_p that the principal planes at K form with a transverse and a horizontal plane through K. Use this program to check the values shown in Fig. 8.8 and to verify that $\sigma_{\max}$ exceeds σ_m if $x \leq 0.544c$, as indicated in the second footnote on page 560.

8.C3 Disks $D_1, D_2, \ldots, D_n$ are attached as shown in Fig. 8.C3 to the solid shaft AB of length L, uniform diameter d, and allowable shearing stress τ_{all}. Forces $\mathbf{P}_1, \mathbf{P}_2, \ldots, \mathbf{P}_n$ of known magnitude (except for one of them) are applied to the disks, either at the top or bottom of its vertical diameter, or at the left or right end of its horizontal diameter. Denoting by r_i the radius of disk D_i and by c_i its distance from the support at A, write a computer program to calculate (a) the magnitude of the unknown force $\mathbf{P}_i$, (b) the smallest permissible value of the diameter d of shaft AB. Use this program to solve Prob. 8.18.

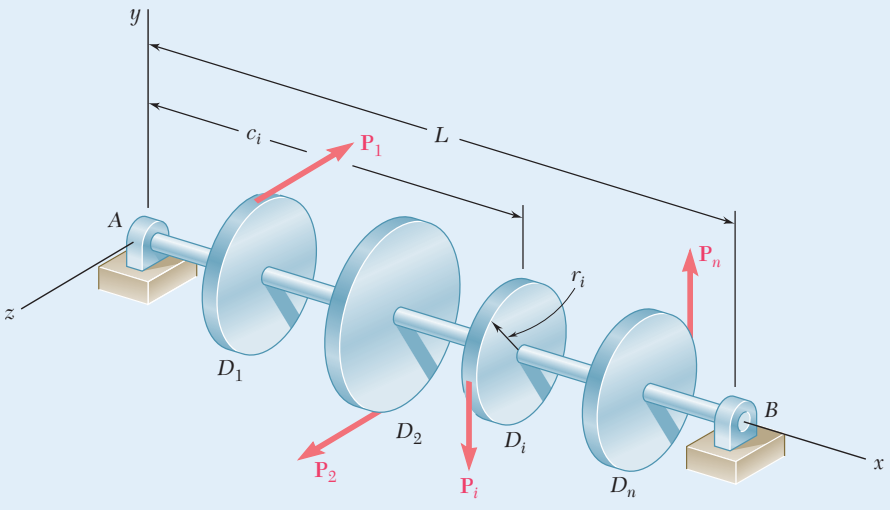


Fig. P8.C3

8.C4 The solid shaft AB of length L, uniform diameter d, and allowable shearing stress τ_{all} rotates at a given speed expressed in rpm (Fig. 8.C4). Gears G_1, G_2, . . . , G_n are attached to the shaft and each of these gears meshes with another gear (not shown), either at the top or bottom of its vertical diameter, or at the left or right end of its horizontal diameter. One of these gears is connected to a motor and the rest of them to various machine tools. Denoting by r_i the radius of disk G_i, by c_i its distance from the support at A, and by P_i the power transmitted to that gear (+ sign) or taken off that gear (−sign), write a computer program to calculate the smallest permissible value of the diameter d of shaft AB. Use this program to solve Probs. 8.27 and 8.68.

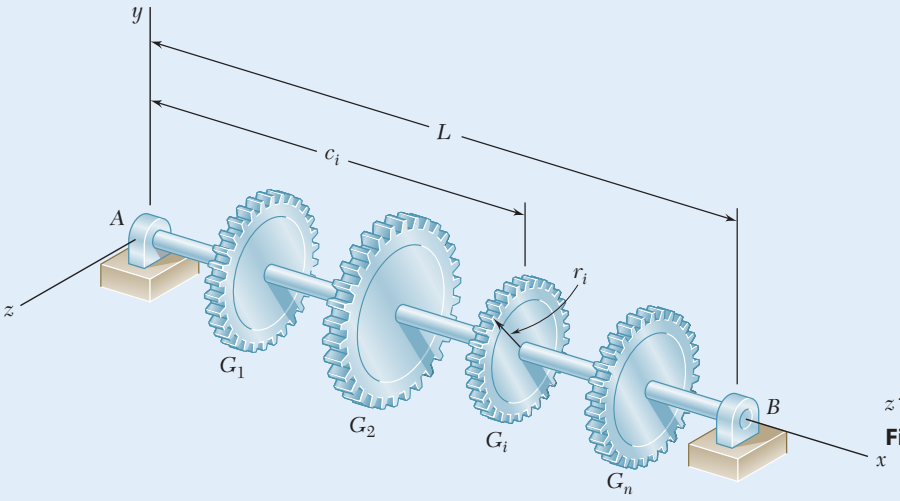


Fig. P8.C4

8.C5 Write a computer program that can be used to calculate the normal and shearing stresses at points with given coordinates y and z located on the surface of a machine part having a rectangular cross section. The internal forces are known to be equivalent to the force-couple system shown. Write the program so that the loads and dimensions can be expressed in either SI or U.S. customary units. Use this program to solve (*a*) Prob. 8.45*b*, (*b*) Prob. 8.47*a*.

8.C6 Member AB has a rectangular cross section of 10 × 24 mm. For the loading shown, write a computer program that can be used to determine the normal and shearing stresses at points H and K for values of d from 0 to 120 mm, using 15-mm increments. Use this program to solve Prob. 8.35.

***8.C7** The structural tube shown has a uniform wall thickness of 0.3 in. A 9-kip force is applied at a bar (not shown) that is welded to the end of the tube. Write a computer program that can be used to determine, for any given value of c, the principal stresses, principal planes, and maximum shearing stress at point H for values of d from −3 in. to 3 in., using one-inch increments. Use this program to solve Prob. 8.62*a*.

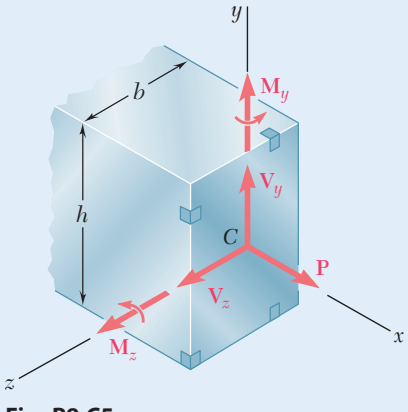


Fig. P8.C5

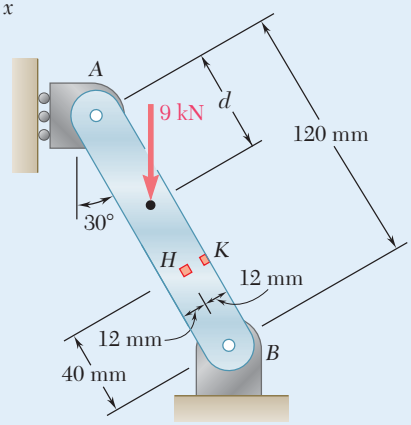


Fig. P8.C6

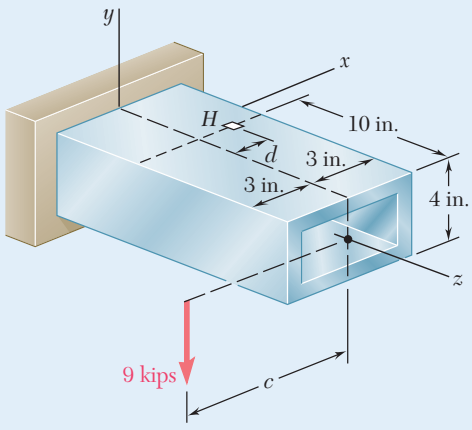
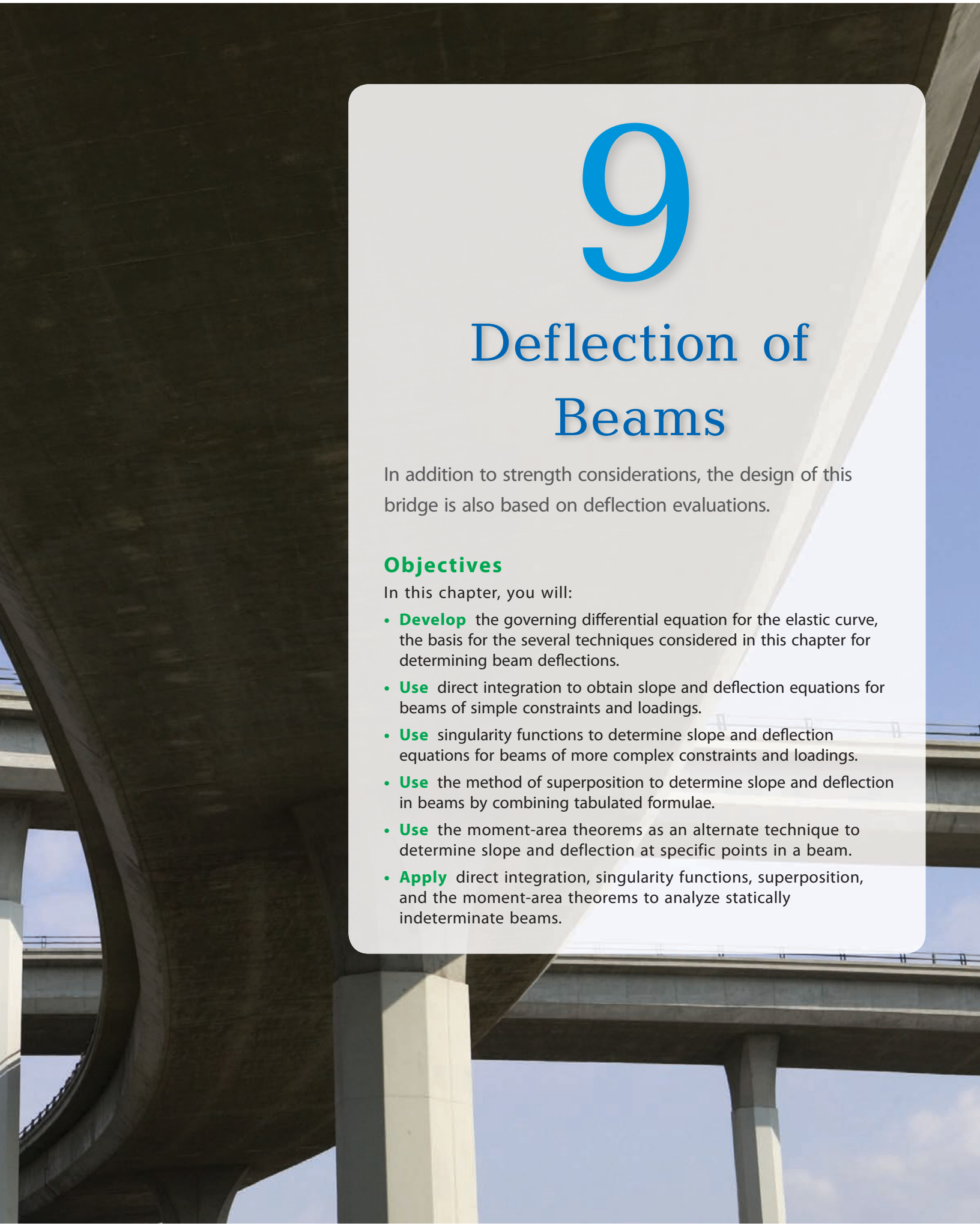


Fig. P8.C7





9

Deflection of Beams

In addition to strength considerations, the design of this bridge is also based on deflection evaluations.

Objectives

In this chapter, you will:

- **Develop** the governing differential equation for the elastic curve, the basis for the several techniques considered in this chapter for determining beam deflections.
- **Use** direct integration to obtain slope and deflection equations for beams of simple constraints and loadings.
- **Use** singularity functions to determine slope and deflection equations for beams of more complex constraints and loadings.
- **Use** the method of superposition to determine slope and deflection in beams by combining tabulated formulae.
- **Use** the moment-area theorems as an alternate technique to determine slope and deflection at specific points in a beam.
- **Apply** direct integration, singularity functions, superposition, and the moment-area theorems to analyze statically indeterminate beams.

Introduction
9.1 DEFORMATION UNDER TRANSVERSE LOADING
9.1A Equation of the Elastic Curve
*9.1B Determination of the Elastic Curve from the Load Distribution
9.2 STATICALLY INDETERMINATE BEAMS
*9.3 SINGULARITY FUNCTIONS TO DETERMINE SLOPE AND DEFLECTION
9.4 METHOD OF SUPERPOSITION
9.4A Statically Determinate Beams
9.4B Statically Indeterminate Beams
*9.5 MOMENT-AREA THEOREMS
*9.5A General Principles
*9.5B Cantilever Beams and Beams with Symmetric Loadings
*9.5C Bending-Moment Diagrams by Parts
*9.6 MOMENT-AREA THEOREMS APPLIED TO BEAMS WITH UNSYMMETRIC LOADINGS
*9.6A General Principles
*9.6B Maximum Deflection
*9.6C Statically Indeterminate Beams

Introduction

In the preceding chapter we learned to design beams for strength. This chapter discusses another aspect in the design of beams: the determination of the *deflection*. The *maximum deflection* of a beam under a given load is of particular interest, since the design specifications of a beam will generally include a maximum allowable value for its deflection. A knowledge of deflections is also required to analyze *indeterminate beams*, in which the number of reactions at the supports exceeds the number of equilibrium equations available to determine unknowns.

Recall from Sec. 4.2 that a prismatic beam subjected to pure bending is bent into a circular arc and, within the elastic range, the curvature of the neutral surface is

$$\frac{1}{\rho} = \frac{M}{EI} \tag{4.21}$$

where M is the bending moment, E is the modulus of elasticity, and I is the moment of inertia of the cross section about its neutral axis.

When a beam is subjected to a transverse loading, Eq. (4.21) remains valid for any transverse section, provided that Saint-Venant's principle applies. However, both the bending moment and the curvature of the neutral surface vary from section to section. Denoting by x the distance from the left end of the beam, we write

$$\frac{1}{\rho} = \frac{M(x)}{EI} \tag{9.1}$$

Knowing the curvature at various points of the beam will help us to draw some general conclusions about the deformation of the beam under loading (Sec. 9.1).

To determine the slope and deflection of the beam at any given point, the second-order linear differential equation, which governs the *elastic curve* characterizing the shape of the deformed beam (Sec. 9.1A), is given as

$$\frac{d^2y}{dx^2} = \frac{M(x)}{EI}$$

If the bending moment can be represented for all values of x by a single function $M(x)$, as shown in Fig. 9.1, the slope $\theta = dy/dx$ and the

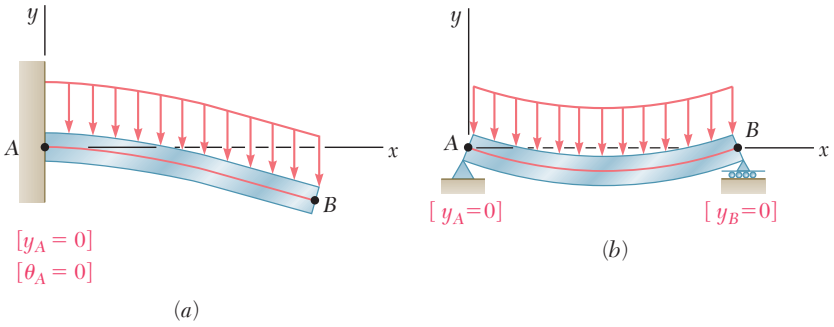


Fig. 9.1 Situations where bending moment can be expressed by a single function $M(x)$. (*a*) Uniformly-loaded cantilever beam. (*b*) Uniformly-loaded simply supported beam.

deflection y at any point of the beam can be obtained through two successive integrations. The two constants of integration introduced in the process are determined from the boundary conditions.

However, if different analytical functions are required to represent the bending moment in various portions of the beam, different differential equations are also required, leading to different functions defining the elastic curve in various portions of the beam. For the beam and loading of Fig. 9.2, for example, two differential equations are

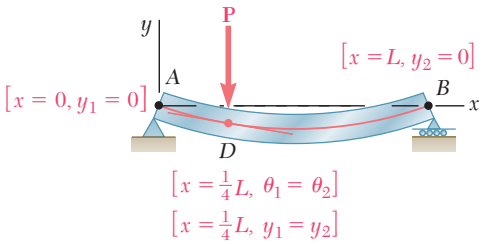


Fig. 9.2 Situation where two sets of equations are required.

required: one for the portion AD and the other for the portion DB. The first equation yields functions θ_1 and y_1, and the second functions θ_2 and y_2. Altogether, four constants of integration must be determined; two will be obtained with the deflection being zero at A and B, and the other two by expressing that the portions AD and DB have the same slope and the same deflection at D.

Sec. 9.1B shows that, in a beam supporting a distributed load $w(x)$, the elastic curve can be obtained directly from $w(x)$ through four successive integrations. The constants introduced in this process are determined from the boundary values of V, M, θ, and y.

Section 9.2 discusses *statically indeterminate beams* where the reactions at the supports involve four or more unknowns. The three equilibrium equations must be supplemented with equations obtained from the boundary conditions that are imposed by the supports.

Determining the elastic curve when several functions are required for the bending moment M can be quite complex, since it requires matching slopes and deflections at every transition point. Section 9.3 uses *singularity functions* to simplify the determination of θ and y at any point of the beam.

The *method of superposition* consists of separately determining and then adding the slope and deflection caused by the various loads applied to a beam (Sec. 9.4). This procedure can be facilitated by the use of the table in Appendix D, which gives the slopes and deflections of beams for various loadings and types of support.

In Sec. 9.5, certain geometric properties of the elastic curve are used to determine the deflection and slope of a beam at a given point. Instead of expressing the bending moment as a function $M(x)$ and integrating it analytically, a diagram representing a variation of M/EI over the length of the beam is drawn, and two moment-area theorems are derived. The *first moment-area theorem* enables the calculation of the angle between the tangents to the beam at two different points. The *second moment-area theorem* is used to calculate the vertical distance from a point on the beam to a tangent through a second point.

The moment-area theorems are used in Sec. 9.5B to determine the slope and deflection at selected points of cantilever beams and beams with symmetric loads. Section 9.5C shows that the areas and moments of areas defined by the M/EI diagram can be determined more easily if we draw the *bending-moment diagram by parts*. This method is particularly effective for *beams of variable cross section*.

Beams with unsymmetric loads and overhanging beams are considered in Sec. 9.6A. Since in beams with unsymmetric loads the maximum deflection does not occur at the center of a beam, Sec. 9.6B shows how to locate the point where the tangent is horizontal in order to determine the *maximum deflection*. Section 9.6C is devoted to the solution of problems involving *statically indeterminate beams*.

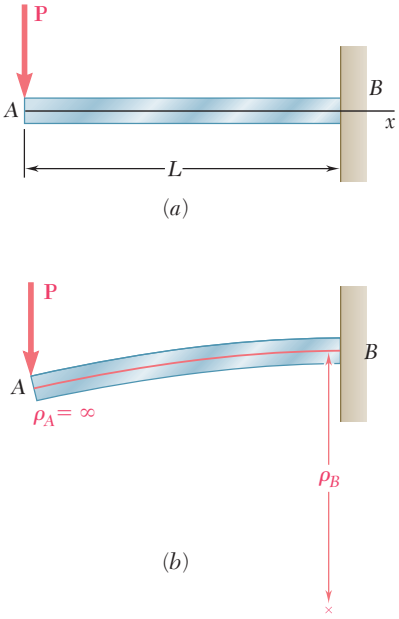


Fig. 9.3 (*a*) Cantilever beam with concentrated load. (*b*) Deformed beam showing curvature at ends.

9.1 DEFORMATION UNDER TRANSVERSE LOADING

Recall that Eq. (4.21) relates the curvature of the neutral surface to the bending moment in a beam in pure bending. This equation is valid for any given transverse section of a beam subjected to a transverse loading, provided that Saint-Venant's principle applies. However, both the bending moment and the curvature of the neutral surface vary from section to section. Denoting by x the distance of the section from the left end of the beam,

$$\frac{1}{\rho} = \frac{M(x)}{EI} \tag{9.1}$$

Consider, for example, a cantilever beam AB of length L subjected to a concentrated load $\mathbf{P}$ at its free end A (Fig. 9.3*a*). We have $M(x) = -Px$, and substituting into Eq. (9.1) gives

$$\frac{1}{\rho} = -\frac{Px}{EI}$$

which shows that the curvature of the neutral surface varies linearly with x from zero at A, where ρ_A itself is infinite, to $-PL/EI$ at B, where $|\rho_B| = EI/PL$ (Fig. 9.3*b*).

Now consider the overhanging beam AD of Fig. 9.4*a* that supports two concentrated loads. From the free-body diagram of the beam (Fig. 9.4*b*), the reactions at the supports are $R_A = 1$ kN and $R_C = 5$ kN. The corresponding

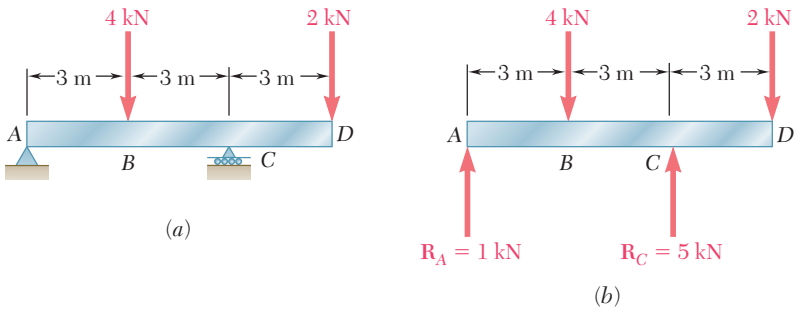


Fig. 9.4 (*a*) Overhanging beam with two concentrated loads. (*b*) Free-body diagram showing reaction forces.

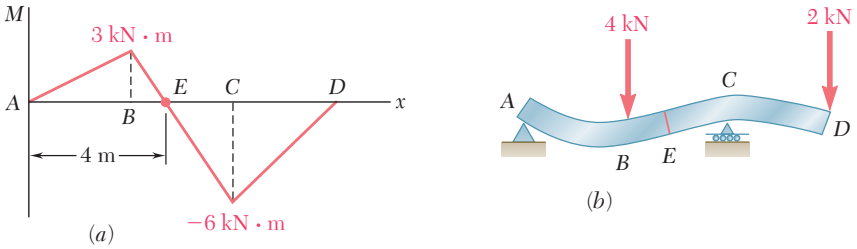


Fig. 9.5 Beam of Fig. 9.4. (*a*) Bending-moment diagram. (*b*) Deformed shape.

bending-moment diagram is shown in Fig. 9.5*a*. Note from the diagram that M and the curvature of the beam are both zero at each end and at a point E located at $x = 4$ m. Between A and E, the bending moment is positive, and the beam is concave upward. Between E and D, the bending moment is negative and the beam is concave downward (Fig. 9.5*b*). The largest value of the curvature (i.e., the smallest value of the radius of curvature) occurs at support C, where $|M|$ is maximum.

The shape of the deformed beam is obtained from the information about its curvature. However, the analysis and design of a beam usually requires more precise information on the *deflection* and the *slope* at various points. Of particular importance is the maximum deflection of the beam. Equation (9.1) will be used in the next section to find the relationship between the deflection y measured at a given point Q on the axis of the beam and the distance x of that point from some fixed origin (Fig. 9.6). This relationship is the equation of the *elastic curve*, into which the axis of the beam is transformed under the given load (Fig. 9.6*b*).†

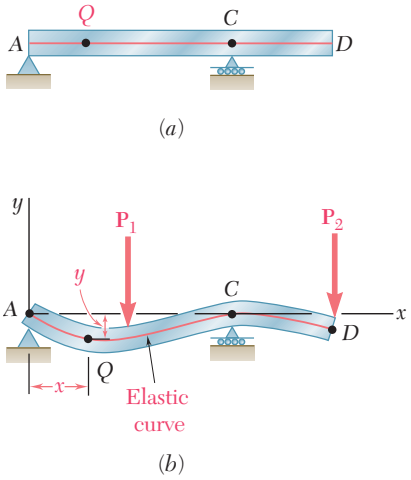


Fig. 9.6 Beam of Fig. 9.4. (*a*) Undeformed. (*b*) Deformed.

9.1A Equation of The Elastic Curve

Recall from elementary calculus that the curvature of a plane curve at a point $Q(x,y)$ is

$$\frac{1}{\rho} = \frac{\dfrac{d^2y}{dx^2}}{\left[1 + \left(\dfrac{dy}{dx}\right)^2\right]^{3/2}} \tag{9.2}$$

where dy/dx and d^2y/dx^2 are the first and second derivatives of the function $y(x)$ represented by that curve. For the elastic curve of a beam, however, the slope dy/dx is very small, and its square is negligible compared to unity. Therefore,

$$\frac{1}{\rho} = \frac{d^2y}{dx^2} \tag{9.3}$$

Substituting for $1/\rho$ from Eq. (9.3) into Eq. (9.1),

$$\frac{d^2y}{dx^2} = \frac{M(x)}{EI} \tag{9.4}$$

This equation is a second-order linear differential equation; it is the governing differential equation for the elastic curve.

†In this chapter, y represents a vertical displacement. It was used in previous chapters to represent the distance of a given point in a transverse section from the neutral axis of that section.

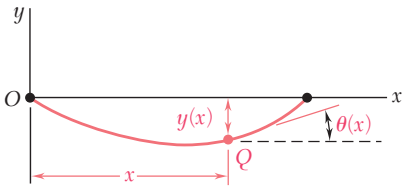


Fig. 9.7 Slope $\theta(x)$ of tangent to the elastic curve.

The product EI is called the *flexural rigidity,* and if it varies along the beam, as in the case of a beam of varying depth, it must be expressed as a function of x before integrating Eq. (9.4). However, for a prismatic beam, the flexural rigidity is constant. Multiply both members of Eq. (9.4) by EI and integrate in x to obtain

$$EI\frac{dy}{dx} = \int_0^x M(x)\,dx + C_1 \tag{9.5a}$$

where C_1 is a constant of integration. Denoting by $\theta(x)$ the angle, measured in radians, that the tangent to the elastic curve at Q forms with the horizontal (Fig. 9.7), and recalling that this angle is very small,

$$\frac{dy}{dx} = \tan\theta \simeq \theta(x)$$

Thus, Eq. (9.5a) in the alternative form is

$$EI\,\theta(x) = \int_0^x M(x)\,dx + C_1 \tag{9.5b}$$

Integrating Eq. (9.5) in x,

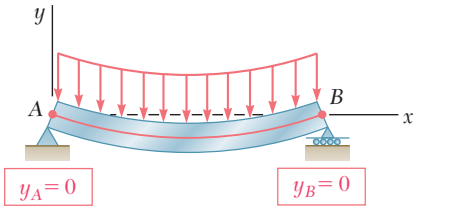
$$EI\,y = \int_0^x \left[\int_0^x M(x)\,dx + C_1\right]dx + C_2$$

$$EI\,y = \int_0^x dx \int_0^x M(x)\,dx + C_1x + C_2 \tag{9.6}$$

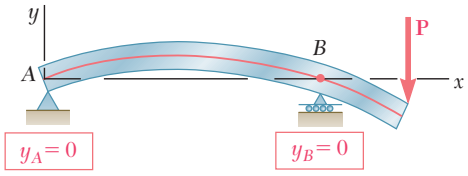
where C_2 is a second constant and where the first term in the right-hand member represents the function of x obtained by integrating the bending moment $M(x)$ twice in x. Although the constants C_1 and C_2 are as yet undetermined, Eq. (9.6) defines the deflection of the beam at any given point Q, and Eqs. (9.5a) or (9.5b) similarly define the slope of the beam at Q.

The constants C_1 and C_2 are determined from the *boundary conditions* or, more precisely, from the conditions imposed on the beam by its supports. Limiting this analysis to *statically determinate beams,* which are supported so that the reactions at the supports can be obtained by the methods of statics, only three types of beams need to be considered here (Fig. 9.8): (*a*) the *simply supported beam,* (*b*) the *overhanging beam,* and (*c*) the *cantilever beam.*

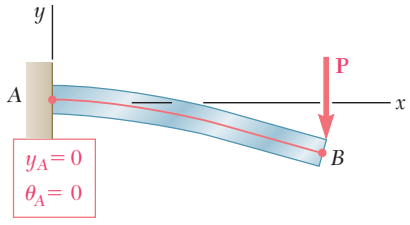
In Figs. 9.8*a* and *b*, the supports consist of a pin and bracket at A and a roller at B and require that the deflection be zero at each of these points. Letting $x = x_A$, $y = y_A = 0$ in Eq. (9.6) and then setting $x = x_B$, $y = y_B = 0$ in the same equation, two equations are obtained that can be solved for C_1 and C_2. For the cantilever beam (Fig. 9.8*c*), both the deflection and the slope at A must be zero. Letting $x = x_A$, $y = y_A = 0$ in Eq. (9.6) and $x = x_A$, $\theta = \theta_A = 0$ in Eq. (9.5b), two equations are again obtained that can be solved for C_1 and C_2.



(*a*) Simply supported beam



(*b*) Overhanging beam



(*c*) Cantilever beam

Fig. 9.8 Known boundary conditions for statically determinate beams.

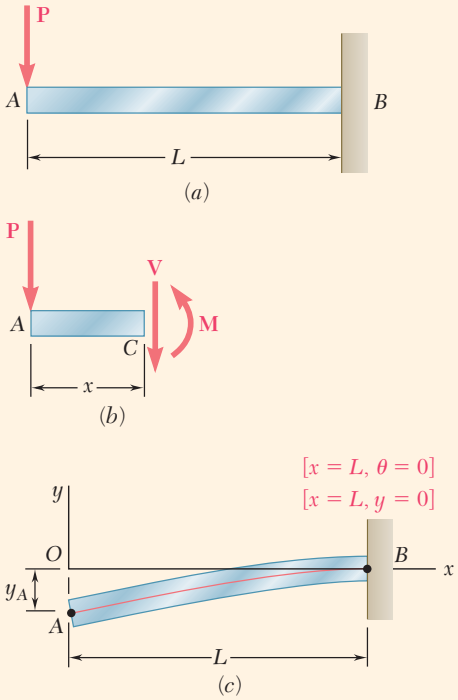


Fig. 9.9 (*a*) Cantilever beam with end load. (*b*) Free-body diagram of section *AC*. (*c*) Deformed shape and boundary conditions.

Concept Application 9.1

The cantilever beam *AB* is of uniform cross section and carries a load **P** at its free end A (Fig. 9.9a). Determine the equation of the elastic curve and the deflection and slope at *A*.

Using the free-body diagram of the portion *AC* of the beam (Fig. 9.9*b*), where *C* is located at a distance *x* from end *A*,

$$M = -Px \tag{1}$$

Substituting for *M* into Eq. (9.4) and multiplying both members by the constant *EI* gives

$$EI\frac{d^2y}{dx^2} = -Px$$

Integrating in *x*,

$$EI\frac{dy}{dx} = -\tfrac{1}{2}Px^2 + C_1 \tag{2}$$

Now observe the fixed end *B* where $x = L$ and $\theta = dy/dx = 0$ (Fig. 9.9c). Substituting these values into Eq. (2) and solving for C_1 gives

$$C_1 = \tfrac{1}{2}PL^2$$

which we carry back into Eq. (2):

$$EI\frac{dy}{dx} = -\tfrac{1}{2}Px^2 + \tfrac{1}{2}PL^2 \tag{3}$$

Integrating both members of Eq. (3),

$$EI\,y = -\tfrac{1}{6}Px^3 + \tfrac{1}{2}PL^2x + C_2 \tag{4}$$

But at *B*, $x = L$, $y = 0$. Substituting into Eq. (4),

$$0 = -\tfrac{1}{6}PL^3 + \tfrac{1}{2}PL^3 + C_2$$
$$C_2 = -\tfrac{1}{3}PL^3$$

Carrying the value of C_2 back into Eq. (4), the equation of the elastic curve is

$$EI\,y = -\tfrac{1}{6}Px^3 + \tfrac{1}{2}PL^2x - \tfrac{1}{3}PL^3$$

or

$$y = \frac{P}{6EI}(-x^3 + 3L^2x - 2L^3) \tag{5}$$

The deflection and slope at *A* are obtained by letting $x = 0$ in Eqs. (3) and (5).

$$y_A = -\frac{PL^3}{3EI} \quad \text{and} \quad \theta_A = \left(\frac{dy}{dx}\right)_A = \frac{PL^2}{2EI}$$

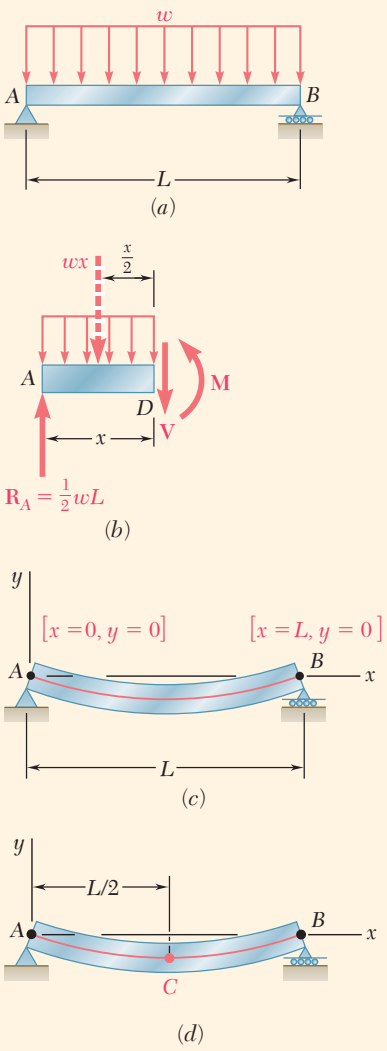


Fig. 9.10 (*a*) Simply supported beam with a uniformly distributed load. (*b*) Free-body diagram of segment *AD*. (*c*) Boundary conditions. (*d*) Point of maximum deflection.

Concept Application 9.2

The simply supported prismatic beam *AB* carries a uniformly distributed load w per unit length (Fig. 9.10*a*). Determine the equation of the elastic curve and the maximum deflection of the beam.

Draw the free-body diagram of the portion *AD* of the beam (Fig. 9.10*b*) and take moments about *D* for

$$M = \tfrac{1}{2}wLx - \tfrac{1}{2}wx^2 \tag{1}$$

Substituting for M into Eq. (9.4) and multiplying both members of this equation by the constant EI gives

$$EI\frac{d^2y}{dx^2} = -\frac{1}{2}wx^2 + \frac{1}{2}wLx \tag{2}$$

Integrating twice in x,

$$EI\frac{dy}{dx} = -\frac{1}{6}wx^3 + \frac{1}{4}wLx^2 + C_1 \tag{3}$$

$$EIy = -\frac{1}{24}wx^4 + \frac{1}{12}wLx^3 + C_1x + C_2 \tag{4}$$

Observing that $y = 0$ at both ends of the beam (Fig. 9.10*c*), let $x = 0$ and $y = 0$ in Eq. (4) and obtain $C_2 = 0$. Then make $x = L$ and $y = 0$ in the same equation, so

$$0 = -\tfrac{1}{24}wL^4 + \tfrac{1}{12}wL^4 + C_1L$$

$$C_1 = -\tfrac{1}{24}wL^3$$

Carrying the values of C_1 and C_2 back into Eq. (9.4), the elastic curve is

$$EIy = -\tfrac{1}{24}wx^4 + \tfrac{1}{12}wLx^3 - \tfrac{1}{24}wL^3x$$

or

$$y = \frac{w}{24EI}(-x^4 + 2Lx^3 - L^3x) \tag{5}$$

Substituting the value for C_1 into Eq. (3), we check that the slope of the beam is zero for $x = L/2$ and thus that the elastic curve has a minimum at the midpoint *C* (Fig. 9.10*d*). Letting $x = L/2$ in Eq. (5),

$$y_C = \frac{w}{24EI}\left(-\frac{L^4}{16} + 2L\frac{L^3}{8} - L^3\frac{L}{2}\right) = -\frac{5wL^4}{384EI}$$

The maximum deflection (the maximum absolute value) is

$$|y|_{\max} = \frac{5wL^4}{384EI}$$

In both concept applications considered so far, only one free-body diagram was required to determine the bending moment in the beam. As a result, a single function of x was used to represent M throughout the beam. However, concentrated loads, reactions at supports, or discontinuities in a distributed load make it necessary to divide the beam into several portions and to represent the bending moment by a different function $M(x)$ in each. As an example, Photo 9.1 shows an elevated roadway supported by beams, which in turn are subjected to concentrated loads from vehicles crossing the bridge. Each of the functions $M(x)$ leads to a different expression for the slope $\theta(x)$ and the deflection $y(x)$. Since each expression must contain two constants of integration, a large number of constants will have to be determined. As shown in the following concept application, the required additional boundary conditions can be obtained by observing that, while the shear and bending moment can be discontinuous at several points in a beam, the *deflection* and the *slope* of the beam *cannot be discontinuous* at any point.



Photo 9.1 A different function $M(x)$ is required in each portion of the beams when a vehicle crosses the bridge.

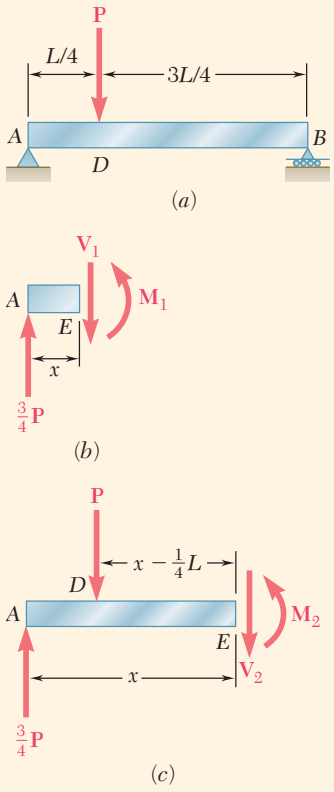


Fig. 9.11 (*a*) Simply supported beam with transverse load *P*. (*b*) Free-body diagram of portion *AE* to find moment left of load *P*. (*c*) Free-body diagram of portion *AE* to find moment right of load *P*.

Concept Application 9.3

For the prismatic beam and load shown (Fig. 9.11*a*), determine the slope and deflection at point *D*.

Divide the beam into two portions, *AD* and *DB*, and determine the function $y(x)$ that defines the elastic curve for each of these portions.

1. From *A* to *D* ($x < L/4$). Draw the free-body diagram of a portion of beam *AE* of length $x < L/4$ (Fig. 9.11*b*). Take moments about *E* to obtain

$$M_1 = \frac{3P}{4}x \tag{1}$$

and recalling Eq. (9.4), we write

$$EI\frac{d^2y_1}{dx^2} = \frac{3}{4}Px \tag{2}$$

where $y_1(x)$ is the function that defines the elastic curve *for portion AD of the beam*. Integrating in x,

$$EI\,\theta_1 = EI\frac{dy_1}{dx} = \frac{3}{8}Px^2 + C_1 \tag{3}$$

$$EI\,y_1 = \frac{1}{8}Px^3 + C_1x + C_2 \tag{4}$$

2. From *D* to *B* ($x > L/4$). Now draw the free-body diagram of a portion of beam *AE* of the length $x > L/4$ (Fig. 9.11*c*) and write

$$M_2 = \frac{3P}{4}x - P\left(x - \frac{L}{4}\right) \tag{5}$$

(continued)

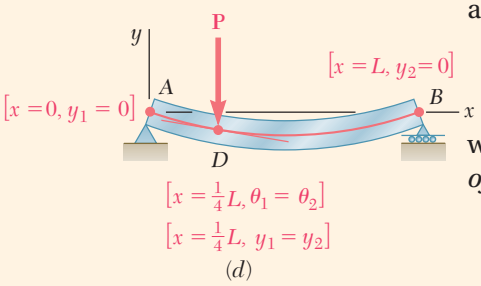


Fig. 9.11 (*cont.*) (*d*) Boundary conditions.

and recalling Eq. (9.4) and rearranging terms, we have

$$EI\frac{d^2y_2}{dx^2} = -\frac{1}{4}Px + \frac{1}{4}PL \tag{6}$$

where $y_2(x)$ is the function that defines the elastic curve *for portion DB of the beam*. Integrating in x,

$$EI\,\theta_2 = EI\frac{dy_2}{dx} = -\frac{1}{8}Px^2 + \frac{1}{4}PLx + C_3 \tag{7}$$

$$EI\,y_2 = -\frac{1}{24}Px^3 + \frac{1}{8}PLx^2 + C_3x + C_4 \tag{8}$$

Determination of the Constants of Integration. The conditions satisfied by the constants of integration are summarized in Fig. 9.11*d*. At the support A, where the deflection is defined by Eq. (4), $x = 0$ and $y_1 = 0$. At the support B, where the deflection is defined by Eq. (8), $x = L$ and $y_2 = 0$. Also, the fact that there can be no sudden change in deflection or in slope at point D requires that $y_1 = y_2$ and $\theta_1 = \theta_2$ when $x = L/4$. Therefore,

$[x = 0, y_1 = 0]$, Eq. (4): $\quad 0 = C_2$ **(9)**

$[x = L, y_2 = 0]$, Eq. (8): $\quad 0 = \frac{1}{12}PL^3 + C_3L + C_4$ **(10)**

$[x = L/4, \theta_1 = \theta_2]$, Eqs. (3) and (7):

$$\frac{3}{128}PL^2 + C_1 = \frac{7}{128}PL^2 + C_3 \tag{11}$$

$[x = L/4, y_1 = y_2]$, Eqs. (4) and (8):

$$\frac{PL^3}{512} + C_1\frac{L}{4} = \frac{11PL^3}{1536} + C_3\frac{L}{4} + C_4 \tag{12}$$

Solving these equations simultaneously,

$$C_1 = -\frac{7PL^2}{128}, \quad C_2 = 0, \quad C_3 = -\frac{11PL^2}{128}, \quad C_4 = \frac{PL^3}{384}$$

Substituting for C_1 and C_2 into Eqs. (3) and (4), $x \le L/4$ is

$$EI\,\theta_1 = \frac{3}{8}Px^2 - \frac{7PL^2}{128} \tag{13}$$

$$EI\,y_1 = \frac{1}{8}Px^3 - \frac{7PL^2}{128}x \tag{14}$$

Letting $x = L/4$ in each of these equations, the slope and deflection at point D are

$$\theta_D = -\frac{PL^2}{32EI} \quad \text{and} \quad y_D = -\frac{3PL^3}{256EI}$$

Note that since $\theta_D \neq 0$, the deflection at D is *not* the maximum deflection of the beam.

*9.1B Determination of the Elastic Curve from the Load Distribution

Section. 9.1A showed that the equation of the elastic curve can be obtained by integrating twice the differential equation

$$\frac{d^2y}{dx^2} = \frac{M(x)}{EI} \tag{9.4}$$

where $M(x)$ is the bending moment in the beam. Now recall from Sec. 5.2 that, when a beam supports a distributed load $w(x)$, we have $dM/dx = V$ and $dV/dx = -w$ at any point of the beam. Differentiating both members of Eq. (9.4) with respect to x and assuming EI to be constant,

$$\frac{d^3y}{dx^3} = \frac{1}{EI}\frac{dM}{dx} = \frac{V(x)}{EI} \tag{9.7}$$

and differentiating again,

$$\frac{d^4y}{dx^4} = \frac{1}{EI}\frac{dV}{dx} = -\frac{w(x)}{EI}$$

Thus, when a prismatic beam supports a distributed load $w(x)$, its elastic curve is governed by the fourth-order linear differential equation

$$\frac{d^4y}{dx^4} = -\frac{w(x)}{EI} \tag{9.8}$$

Multiply both members of Eq. (9.8) by the constant EI and integrate four times to obtain

$$\begin{aligned}
EI\frac{d^4y}{dx^4} &= -w(x)\\
EI\frac{d^3y}{dx^3} &= V(x) = -\int w(x)\,dx + C_1\\
EI\frac{d^2y}{dx^2} &= M(x) = -\int dx \int w(x)\,dx + C_1x + C_2\\
EI\frac{dy}{dx} &= EI\,\theta(x) = -\int dx \int dx \int w(x)\,dx + \frac{1}{2}C_1x^2 + C_2x + C_3\\
EIy(x) &= -\int dx \int dx \int dx \int w(x)\,dx + \frac{1}{6}C_1x^3 + \frac{1}{2}C_2x^2 + C_3x + C_4
\end{aligned} \tag{9.9}$$

The four constants of integration are determined from the boundary conditions. These conditions include (*a*) the conditions imposed on the deflection or slope of the beam by its supports (see. Sec. 9.1A) and (*b*) the condition that V and M be zero at the free end of a cantilever beam or that M be zero at both ends of a simply supported beam (see. Sec. 5.2). This has been illustrated in Fig. 9.12.

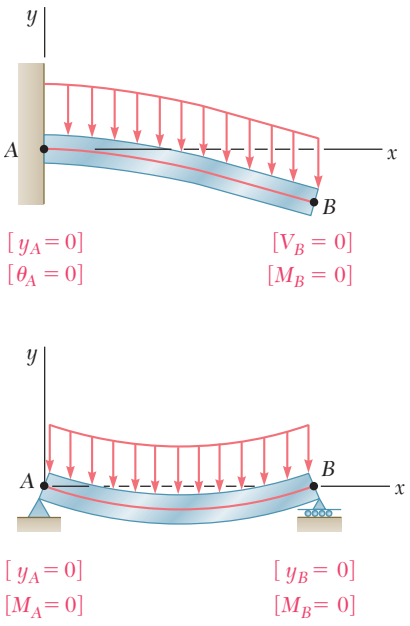


Fig. 9.12 Boundary conditions for (*a*) cantilever beam (*b*) simply supported beam.

This method can be used effectively with cantilever or simply supported beams carrying a distributed load. In the case of overhanging beams, the reactions at the supports cause discontinuities in the shear (i.e., in the third derivative of y,), and different functions are required to define the elastic curve over the entire beam.

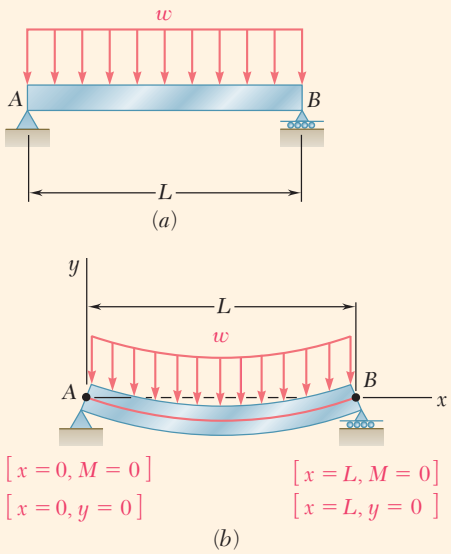


Fig. 9.13 (*a*) Simply supported beam with a uniformly distributed load. (*b*) Boundary conditions.

Concept Application 9.4

The simply supported prismatic beam AB carries a uniformly distributed load w per unit length (Fig. 9.13*a*). Determine the equation of the elastic curve and the maximum deflection of the beam. (This is the same beam and load as in Concept Application 9.2.)

Since w = constant, the first three of Eqs. (9.9) yield

$$EI\frac{d^4y}{dx^4} = -w$$

$$EI\frac{d^3y}{dx^3} = V(x) = -wx + C_1$$

$$EI\frac{d^2y}{dx^2} = M(x) = -\frac{1}{2}wx^2 + C_1x + C_2 \qquad \textbf{(1)}$$

Noting that the boundary conditions require that $M = 0$ at both ends of the beam (Fig. 9.13*b*), let $x = 0$ and $M = 0$ in Eq. (1) and obtain $C_2 = 0$. Then make $x = L$ and $M = 0$ in the same equation and obtain $C_1 = \frac{1}{2}wL$.

Carry the values of C_1 and C_2 back into Eq. (1) and integrate twice to obtain

$$EI\frac{d^2y}{dx^2} = -\frac{1}{2}wx^2 + \frac{1}{2}wLx$$

$$EI\frac{dy}{dx} = -\frac{1}{6}wx^3 + \frac{1}{4}wLx^2 + C_3$$

$$EIy = -\frac{1}{24}wx^4 + \frac{1}{12}wLx^3 + C_3x + C_4 \qquad \textbf{(2)}$$

But the boundary conditions also require that $y = 0$ at both ends of the beam. Letting $x = 0$ and $y = 0$ in Eq. (2), $C_4 = 0$. Letting $x = L$ and $y = 0$ in the same equation gives

$$0 = -\tfrac{1}{24}wL^4 + \tfrac{1}{12}wL^4 + C_3L$$
$$C_3 = -\tfrac{1}{24}wL^3$$

Carrying the values of C_3 and C_4 back into Eq. (2) and dividing both members by EI, the equation of the elastic curve is

$$y = \frac{w}{24EI}(-x^4 + 2Lx^3 - L^3x) \qquad \textbf{(3)}$$

The maximum deflection is obtained by making $x = L/2$ in Eq. (3).

$$|y|_{\max} = \frac{5wL^4}{384EI}$$

9.2 STATICALLY INDETERMINATE BEAMS

In the preceding sections, our analysis was limited to statically determinate beams. Now consider the prismatic beam AB (Fig. 9.14*a*), which has a fixed end at A and is supported by a roller at B. Drawing the free-body diagram of the beam (Fig. 9.14*b*), the reactions involve four unknowns, with only three equilibrium equations:

$$\Sigma F_x = 0 \quad \Sigma F_y = 0 \quad \Sigma M_A = 0 \tag{9.10}$$

Since only A_x can be determined from these equations, the beam is *statically indeterminate.*

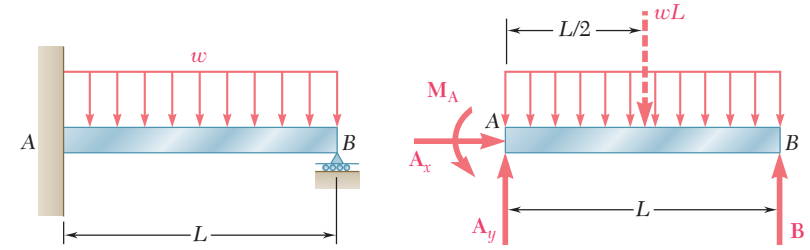


Fig. 9.14 (*a*) Statically indeterminate beam with a uniformly distributed load. (*b*) Free-body diagram with four unknown reactions.

Recall from Chaps. 2 and 3 that, in a statically indeterminate problem, the reactions can be obtained by considering the *deformations* of the structure. Therefore, we proceed with the computation of the slope and deformation along the beam. Following the method used in Sec. 9.1A, the bending moment $M(x)$ at any given point AB is expressed in terms of the distance x from A, the given load, and the unknown reactions. Integrating in x, expressions for θ and y are found. These contain two additional unknowns: the constants of integration C_1 and C_2. Altogether, six equations are available to determine the reactions and constants C_1 and C_2; they are the three equilibrium equations of Eq. (9.10) and the three equations expressing that the boundary conditions are satisfied (i.e., that the slope and deflection at A are zero and that the deflection at B is zero (Fig. 9.15)). Thus, the reactions at the supports can be determined, and the equation of the elastic curve can be obtained.

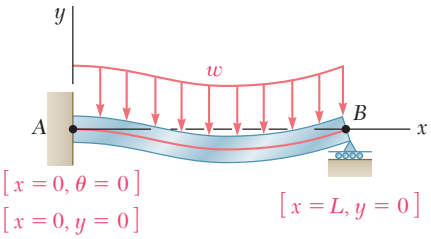


Fig. 9.15 Boundary conditions for beam of Fig. 9.14.

Concept Application 9.5

Determine the reactions at the supports for the prismatic beam of Fig. 9.14*a*.

Equilibrium Equations. From the free-body diagram of Fig. 9.14*b*,

$$\stackrel{+}{\rightarrow} \Sigma F_x = 0: \quad A_x = 0$$

$$+\uparrow \Sigma F_y = 0: \quad A_y + B - wL = 0 \tag{1}$$

$$+\circlearrowleft \Sigma M_A = 0: \quad M_A + BL - \tfrac{1}{2}wL^2 = 0$$

(continued)

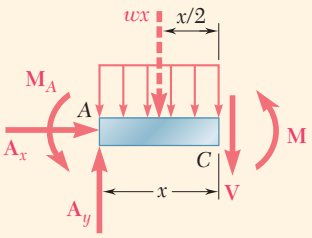


Fig. 9.16 Free-body diagram of beam portion *AC*.

Equation of Elastic Curve. Draw the free-body diagram of a portion of beam *AC* (Fig. 9.16) to obtain

$$+\circlearrowleft \Sigma M_C = 0: \qquad M + \tfrac{1}{2}wx^2 + M_A - A_y x = 0 \tag{2}$$

Solving Eq. (2) for M and carrying into Eq. (9.4),

$$EI\frac{d^2y}{dx^2} = -\frac{1}{2}wx^2 + A_y x - M_A$$

Integrating in x gives

$$EI\,\theta = EI\frac{dy}{dx} = -\frac{1}{6}wx^3 + \frac{1}{2}A_y x^2 - M_A x + C_1 \tag{3}$$

$$EI\,y = -\frac{1}{24}wx^4 + \frac{1}{6}A_y x^3 - \frac{1}{2}M_A x^2 + C_1 x + C_2 \tag{4}$$

Referring to the boundary conditions indicated in Fig. 9.15, $x = 0$, $\theta = 0$ in Eq. (3), $x = 0$, $y = 0$ in Eq. (4), and conclude that $C_1 = C_2 = 0$. Thus, Eq. (4) is rewritten as

$$EI\,y = -\tfrac{1}{24}wx^4 + \tfrac{1}{6}A_y x^3 - \tfrac{1}{2}M_A x^2 \tag{5}$$

But the third boundary condition requires that $y = 0$ for $x = L$. Carrying these values into Eq. (5),

$$0 = -\tfrac{1}{24}wL^4 + \tfrac{1}{6}A_y L^3 - \tfrac{1}{2}M_A L^2$$

or

$$3M_A - A_y L + \tfrac{1}{4}wL^2 = 0 \tag{6}$$

Solving this equation simultaneously with the three equilibrium equations of Eq. (1), the reactions at the supports are

$$A_x = 0 \qquad A_y = \tfrac{5}{8}wL \qquad M_A = \tfrac{1}{8}wL^2 \qquad B = \tfrac{3}{8}wL$$

In the previous Concept Application, there was one redundant reaction (i.e., one more than could be determined from the equilibrium equations alone). The corresponding beam is *statically indeterminate to the first degree*. Another example of a beam indeterminate to the first degree is provided in Sample Prob. 9.3. If the beam supports are such that two reactions are redundant (Fig. 9.17*a*), the beam is *indeterminate to the second degree*. While there are now five unknown reactions (Fig. 9.17*b*), four equations can be obtained from the boundary conditions (Fig. 9.17*c*). Thus, seven equations are available to determine the five reactions and the two constants of integration.

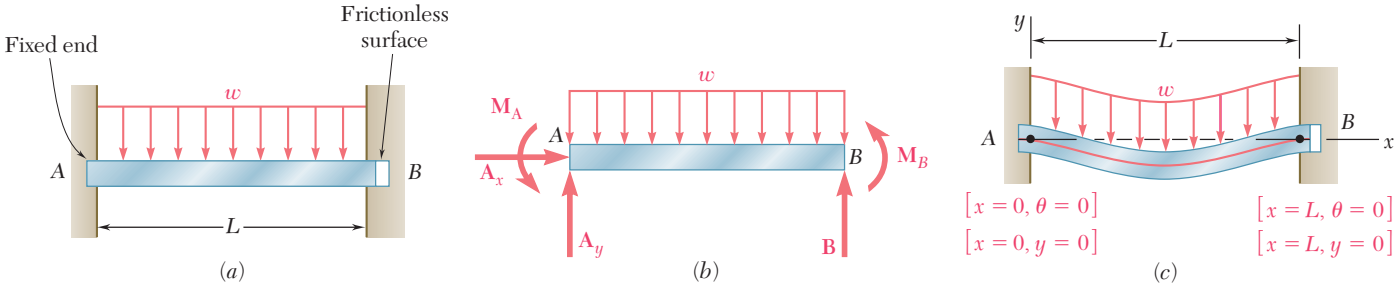
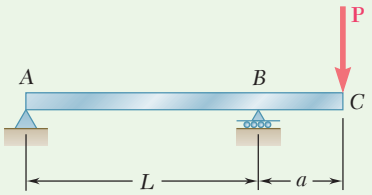


Fig. 9.17 (*a*) Beam statically indeterminate to the second degree. (*b*) Free-body diagram. (*c*) Boundary conditions.



Sample Problem 9.1

The overhanging steel beam *ABC* carries a concentrated load **P** at end *C*. For portion *AB* of the beam, (*a*) derive the equation of the elastic curve, (*b*) determine the maximum deflection, (*c*) evaluate $y_{\max}$ for the following data:

W14 × 68	$I = 722\ \text{in}^4$	$E = 29 \times 10^6\ \text{psi}$
$P = 50\ \text{kips}$	$L = 15\ \text{ft} = 180\ \text{in.}$	$a = 4\ \text{ft} = 48\ \text{in.}$

STRATEGY: You should begin by determining the bending-moment equation for the portion of interest. Substituting this into the differential equation of the elastic curve, integrating twice, and applying the boundary conditions, you can then obtain the equation of the elastic curve. Use this equation to find the desired deflections.

MODELING: Using the free-body diagram of the entire beam (Fig. 1) gives the reactions: $\mathbf{R}_A = Pa/L \downarrow$ $\mathbf{R}_B = P(1 + a/L) \uparrow$. The free-body diagram of the portion of beam *AD* of length *x* (Fig. 1) gives

$$M = -P\frac{a}{L}x \qquad (0 < x < L)$$

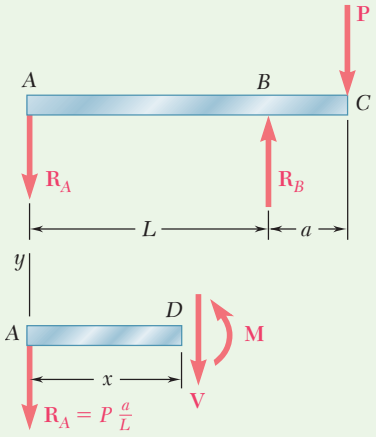


Fig. 1 Free-body diagrams of beam and portion *AD*.

ANALYSIS:

Differential Equation of the Elastic Curve. Using Eq. (9.4) gives

$$EI\frac{d^2y}{dx^2} = -P\frac{a}{L}x$$

Noting that the flexural rigidity *EI* is constant, integrate twice and find

$$EI\frac{dy}{dx} = -\frac{1}{2}P\frac{a}{L}x^2 + C_1 \qquad \textbf{(1)}$$

$$EI\,y = -\frac{1}{6}P\frac{a}{L}x^3 + C_1x + C_2 \qquad \textbf{(2)}$$

(continued)

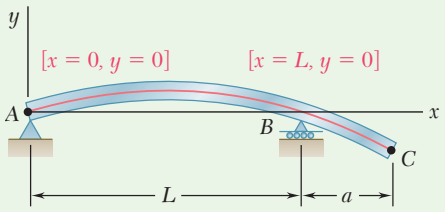


Fig. 2 Boundary conditions.

Determination of Constants. For the boundary conditions shown (Fig. 2),

$[x = 0, y = 0]$: From Eq. (2), $C_2 = 0$

$[x = L, y = 0]$: Again using Eq. (2),

$$EI(0) = -\frac{1}{6}P\frac{a}{L}L^3 + C_1L \qquad C_1 = +\frac{1}{6}PaL$$

a. Equation of the Elastic Curve. Substituting for C_1 and C_2 into Eqs. (1) and (2),

$$EI\frac{dy}{dx} = -\frac{1}{2}P\frac{a}{L}x^2 + \frac{1}{6}PaL \qquad \frac{dy}{dx} = \frac{PaL}{6EI}\left[1 - 3\left(\frac{x}{L}\right)^2\right] \qquad \textbf{(3)}$$

$$EI\,y = -\frac{1}{6}P\frac{a}{L}x^3 + \frac{1}{6}PaLx \qquad y = \frac{PaL^2}{6EI}\left[\frac{x}{L} - \left(\frac{x}{L}\right)^3\right] \qquad \textbf{(4)}$$

b. Maximum Deflection in Portion *AB*. The maximum deflection $y_{\max}$ occurs at point E where the slope of the elastic curve is zero (Fig. 3). Setting $dy/dx = 0$ in Eq. (3), the abscissa x_m of point E is

$$0 = \frac{PaL}{6EI}\left[1 - 3\left(\frac{x_m}{L}\right)^2\right] \qquad x_m = \frac{L}{\sqrt{3}} = 0.577L$$

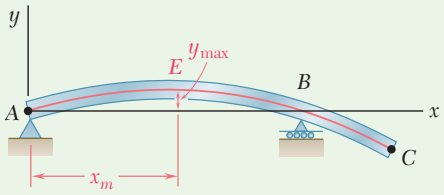


Fig. 3 Deformed elastic curve with location of maximum deflection.

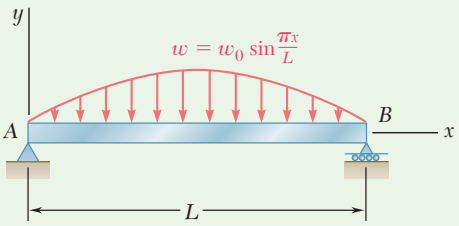
Substitute $x_m/L = 0.577$ into Eq. (4):

$$y_{\max} = \frac{PaL^2}{6EI}[(0.577) - (0.577)^3] \qquad y_{\max} = 0.0642\frac{PaL^2}{EI}$$

c. Evaluation of y_{max}. For the data given, the value of $y_{\max}$ is

$$y_{\max} = 0.0642\frac{(50\text{ kips})(48\text{ in.})(180\text{ in.})^2}{(29 \times 10^6\text{ psi})(722\text{ in}^4)} \qquad y_{\max} = 0.238\text{ in.}$$

REFLECT and THINK: Because the maximum deflection is positive, it is upward. As a check, we see that this is consistent with the deflected shape anticipated for this loading (Fig. 3).



Sample Problem 9.2

For the beam and loading shown determine (*a*) the equation of the elastic curve, (*b*) the slope at end *A*, (*c*) the maximum deflection.

STRATEGY: Determine the elastic curve directly from the load distribution using Eq. (9.8), applying the appropriate boundary conditions. Use this equation to find the desired slope and deflection.

MODELING and ANALYSIS:

Differential Equation of the Elastic Curve. From Eq. (9.8),

$$EI\frac{d^4y}{dx^4} = -w(x) = -w_0 \sin\frac{\pi x}{L} \tag{1}$$

Integrate Eq. (1) twice:

$$EI\frac{d^3y}{dx^3} = V = +w_0\frac{L}{\pi}\cos\frac{\pi x}{L} + C_1 \tag{2}$$

$$EI\frac{d^2y}{dx^2} = M = +w_0\frac{L^2}{\pi^2}\sin\frac{\pi x}{L} + C_1x + C_2 \tag{3}$$

Boundary Conditions: Refer to Fig. 1.

$[x = 0, M = 0]$: From Eq. (3), $C_2 = 0$

$[x = L, M = 0]$: Again using Eq. (3),

$$0 = w_0\frac{L^2}{\pi^2}\sin\pi + C_1L \quad C_1 = 0$$

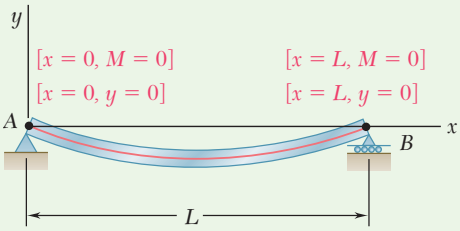


Fig. 1 Boundary conditions.

Thus,

$$EI\frac{d^2y}{dx^2} = +w_0\frac{L^2}{\pi^2}\sin\frac{\pi x}{L} \tag{4}$$

Integrate Eq. (4) twice:

$$EI\frac{dy}{dx} = EI\,\theta = -w_0\frac{L^3}{\pi^3}\cos\frac{\pi x}{L} + C_3 \tag{5}$$

$$EI\,y = -w_0\frac{L^4}{\pi^4}\sin\frac{\pi x}{L} + C_3x + C_4 \tag{6}$$

Boundary Conditions: Refer to Fig. 1.

$[x = 0, y = 0]$: Using Eq. (6), $C_4 = 0$

$[x = L, y = 0]$: Again using Eq. (6), $C_3 = 0$

(continued)

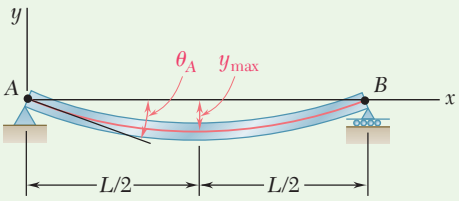


Fig. 2 Deformed elastic curve showing slope at *A* and maximum deflection.

a. Equation of Elastic Curve.

$$EIy = -w_0\frac{L^4}{\pi^4}\sin\frac{\pi x}{L}$$

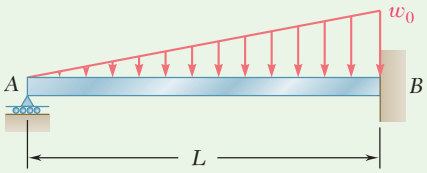
b. Slope at End A. Refer to Fig. 2. For $x = 0$,

$$EI\,\theta_A = -w_0\frac{L^3}{\pi^3}\cos 0 \qquad \theta_A = \frac{w_0L^3}{\pi^3EI}\curvearrowright$$

c. Maximum Deflection. Referring to Fig. 2, for $x = \frac{1}{2}L$,

$$ELy_{\max} = -w_0\frac{L^4}{\pi^4}\sin\frac{\pi}{2} \qquad y_{\max} = \frac{w_0L^4}{\pi^4EI}\downarrow$$

REFLECT and THINK: As a check, we observe that the directions of the slope at end *A* and the maximum deflection are consistent with the deflected shape anticipated for this loading (Fig. 1).



Sample Problem 9.3

For the uniform beam *AB* (*a*) determine the reaction at *A*, (*b*) derive the equation of the elastic curve, (*c*) determine the slope at *A*. (Note that the beam is statically indeterminate to the first degree.)

STRATEGY: The beam is statically indeterminate to the first degree. Treating the reaction at *A* as the redundant, write the bending-moment equation as a function of this redundant reaction and the existing load. After substituting the bending-moment equation into the differential equation of the elastic curve, integrating twice, and applying the boundary conditions, the reaction can be determined. Use the equation for the elastic curve to find the desired slope.

MODELING: Using the free body shown in Fig. 1, obtain the bending moment diagram:

$$+\circlearrowleft\Sigma M_D = 0: \qquad R_Ax - \frac{1}{2}\left(\frac{w_0x^2}{L}\right)\frac{x}{3} - M = 0 \qquad M = R_Ax - \frac{w_0x^3}{6L}$$

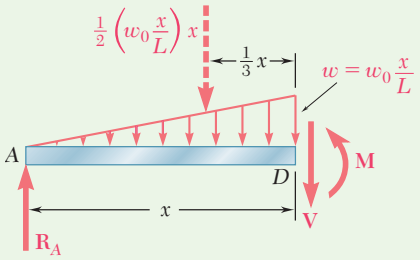


Fig. 1 Free-body diagram of portion *AD* of beam.

(continued)

ANALYSIS:

Differential Equation of the Elastic Curve. Use Eq. (9.4) for

$$EI\frac{d^2y}{dx^2} = R_A x - \frac{w_0 x^3}{6L}$$

Noting that the flexural rigidity EI is constant, integrate twice and find

$$EI\frac{dy}{dx} = EI\,\theta = \frac{1}{2}R_A x^2 - \frac{w_0 x^4}{24L} + C_1 \tag{1}$$

$$EI\,y = \frac{1}{6}R_A x^3 - \frac{w_0 x^5}{120L} + C_1 x + C_2 \tag{2}$$

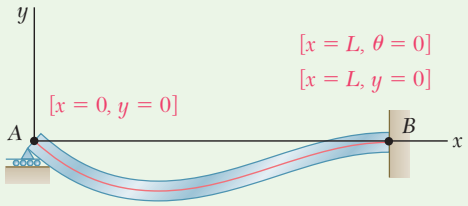


Fig. 2 Boundary conditions.

Boundary Conditions. The three boundary conditions that must be satisfied are shown in Fig. 2.

$$[x = 0, y = 0]: \quad C_2 = 0 \tag{3}$$

$$[x = L, \theta = 0]: \quad \frac{1}{2}R_A L^2 - \frac{w_0 L^3}{24} + C_1 = 0 \tag{4}$$

$$[x = L, y = 0]: \quad \frac{1}{6}R_A L^3 - \frac{w_0 L^4}{120} + C_1 L + C_2 = 0 \tag{5}$$

a. Reaction at *A*. Multiplying Eq. (4) by L, subtracting Eq. (5) member by member from the equation obtained, and noting that $C_2 = 0$, give

$$\tfrac{1}{3}R_A L^3 - \tfrac{1}{30}w_0 L^4 = 0 \qquad \mathbf{R}_A = \tfrac{1}{10}w_0 L \uparrow$$

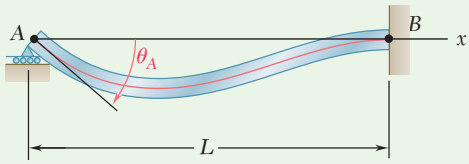


Fig. 3 Deformed elastic curve showing slope at A.

The reaction is independent of E and I. Substituting $R_A = \frac{1}{10}w_0 L$ into Eq. (4),

$$\tfrac{1}{2}(\tfrac{1}{10}w_0 L)L^2 - \tfrac{1}{24}w_0 L^3 + C_1 = 0 \qquad C_1 = -\tfrac{1}{120}w_0 L^3$$

b. Equation of the Elastic Curve. Substituting for R_A, C_1, and C_2 into Eq. (2),

$$EI\,y = \frac{1}{6}\left(\frac{1}{10}w_0 L\right)x^3 - \frac{w_0 x^5}{120L} - \left(\frac{1}{120}w_0 L^3\right)x$$

$$y = \frac{w_0}{120EIL}(-x^5 + 2L^2x^3 - L^4x)$$

c. Slope at A (Fig. 3). Differentiate the equation of the elastic curve with respect to x:

$$\theta = \frac{dy}{dx} = \frac{w_0}{120EIL}(-5x^4 + 6L^2x^2 - L^4)$$

Making $x = 0$, $\qquad \theta_A = -\dfrac{w_0 L^3}{120EI} \qquad \theta_A = \dfrac{w_0 L^3}{120EI}\circlearrowright$

Problems

In the following problems assume that the flexural rigidity *EI* of each beam is constant.

9.1 through 9.4 For the loading shown, determine (*a*) the equation of the elastic curve for the cantilever beam *AB*, (*b*) the deflection at the free end, (*c*) the slope at the free end.

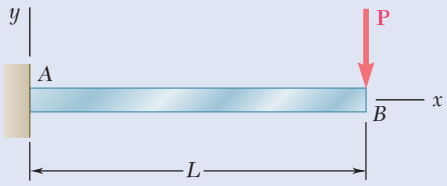


Fig. P9.1

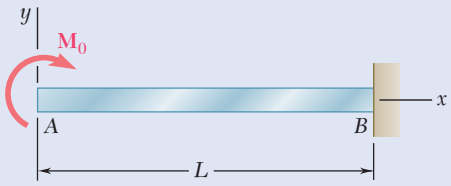


Fig. P9.2

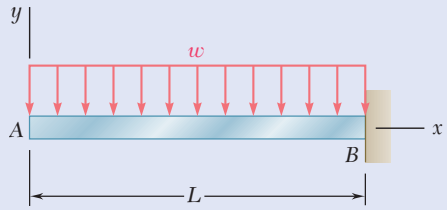


Fig. P9.3

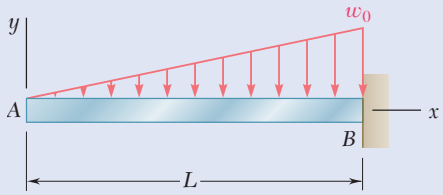


Fig. P9.4

9.5 and 9.6 For the cantilever beam and loading shown, determine (*a*) the equation of the elastic curve for portion *AB* of the beam, (*b*) the deflection at *B*, (*c*) the slope at *B*.

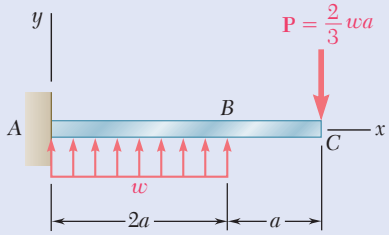


Fig. P9.5

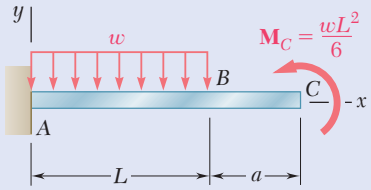


Fig. *P9.6*

9.7 For the beam and loading shown, determine (*a*) the equation of the elastic curve for portion *AB* of the beam, (*b*) the deflection at midspan, (*c*) the slope at *B*.

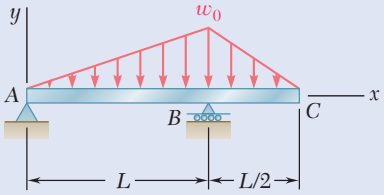


Fig. P9.7

9.8 For the beam and loading shown, determine (*a*) the equation of the elastic curve for portion *AB* of the beam, (*b*) the slope at *A*, (*c*) the slope at *B*.

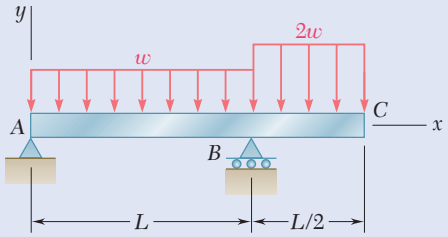


Fig. *P9.8*

9.9 Knowing that beam *AB* is a W10 × 33 rolled shape and that $w_0 = 3$ kips/ft, $L = 12$ ft, and $E = 29 \times 10^6$ psi, determine (*a*) the slope at *A*, (*b*) the deflection at *C*.

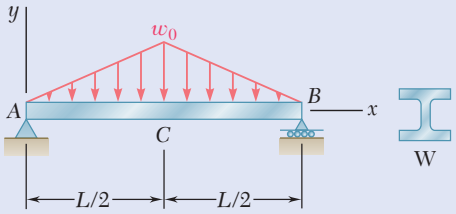


Fig. P9.9

9.10 Knowing that beam *AB* is an S200 × 34 rolled shape and that $P = 60$ kN, $L = 2$ m, and $E = 200$ GPa, determine (*a*) the slope at *A*, (*b*) the deflection at *C*.

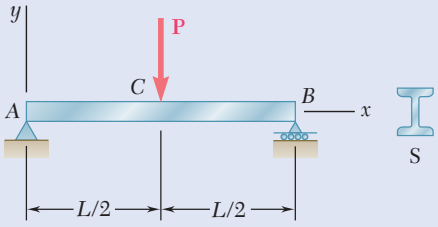


Fig. P9.10

9.11 For the beam and loading shown, (*a*) express the magnitude and location of the maximum deflection in terms of w_0, *L*, *E*, and *I*. (*b*) Calculate the value of the maximum deflection, assuming that beam *AB* is a W18 × 50 rolled shape and that $w_0 = 4.5$ kips/ft, $L = 18$ ft, and $E = 29 \times 10^6$ psi.

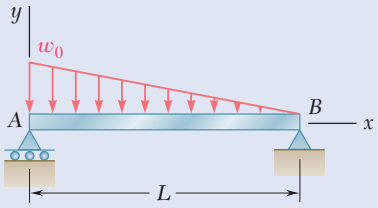


Fig. P9.11

9.12 (*a*) Determine the location and magnitude of the maximum absolute deflection in *AB* between *A* and the center of the beam. (*b*) Assuming that beam *AB* is a W460 × 113, $M_0 = 224$ kN·m, and $E = 200$ GPa, determine the maximum allowable length *L* of the beam if the maximum deflection is not to exceed 1.2 mm.

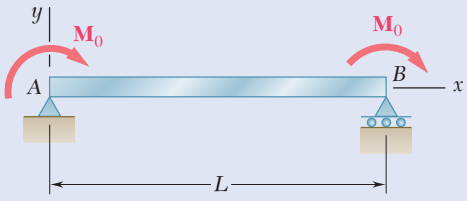


Fig. P9.12

9.13 For the beam and loading shown, determine the deflection at point *C*. Use $E = 29 \times 10^6$ psi.

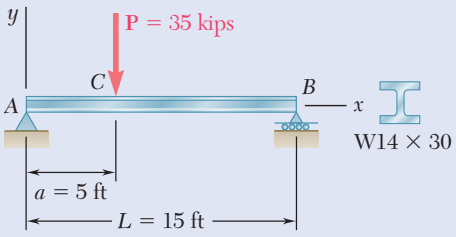


Fig. P9.13

9.14 Knowing that beam AE is a W360 × 101 rolled shape and that $M_0 = 310$ kN·m, $L = 2.4$ m, $a = 0.5$ m, and $E = 200$ GPa, determine (*a*) the equation of the elastic curve for portion BD, (*b*) the deflection at point C.

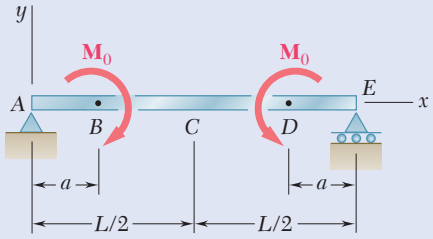


Fig. P9.14

9.15 For the beam and loading shown, knowing that $a = 2$ m, $w = 50$ kN/m, and $E = 200$ GPa, determine (*a*) the slope at support A, (*b*) the deflection at point C.

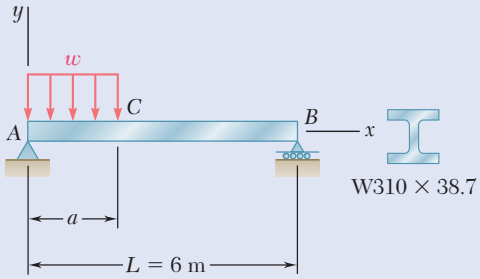


Fig. P9.15

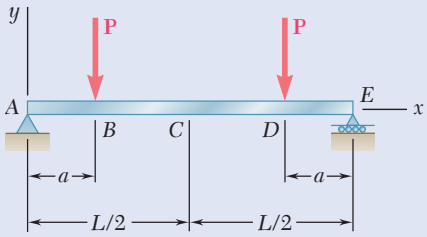


Fig. P9.16

9.16 Knowing that beam AE is an S200 × 27.4 rolled shape and that $P = 17.5$ kN, $L = 2.5$ m, $a = 0.8$ m, and $E = 200$ GPa, determine (*a*) the equation of the elastic curve for portion BD, (*b*) the deflection at the center C of the beam.

9.17 For the beam and loading shown, determine (*a*) the equation of the elastic curve, (*b*) the deflection at the free end.

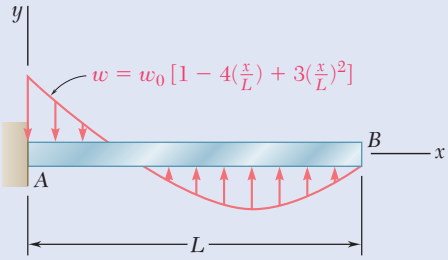


Fig. P9.17

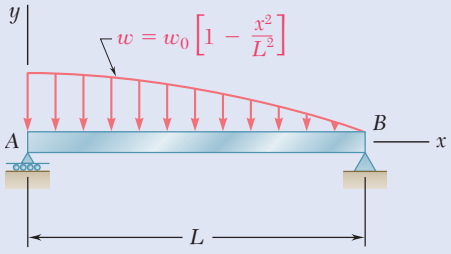


Fig. P9.18

9.18 For the beam and loading shown, determine (*a*) the equation of the elastic curve, (*b*) the slope at end A, (*c*) the deflection at the midpoint of the span.

9.19 through 9.22 For the beam and loading shown, determine the reaction at the roller support.

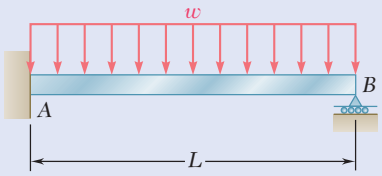


Fig. P9.19

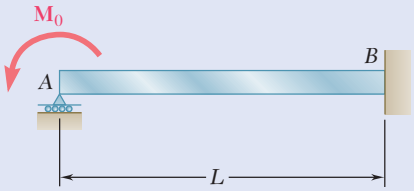


Fig. P9.20

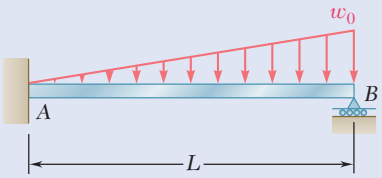


Fig. *P9.21*

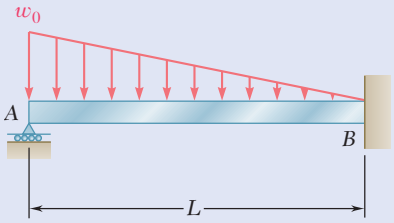


Fig. *P9.22*

9.23 For the beam shown, determine the reaction at the roller support when $w_0 = 6$ kips/ft.

9.24 For the beam shown, determine the reaction at the roller support when $w_0 = 15$ kN/m.

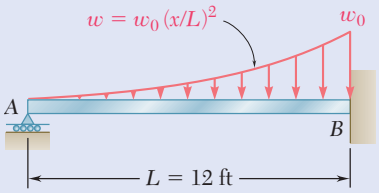


Fig. P9.23

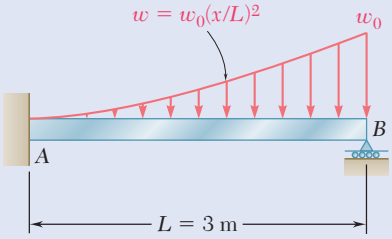


Fig. P9.24

9.25 through 9.28 Determine the reaction at the roller support and draw the bending moment diagram for the beam and loading shown.

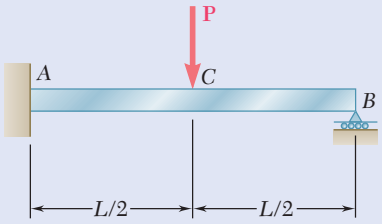


Fig. P9.25

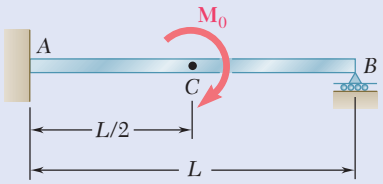


Fig. P9.26

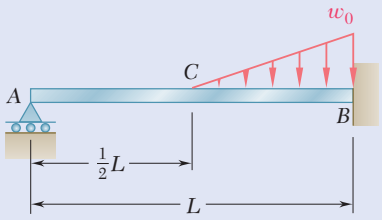


Fig. P9.27

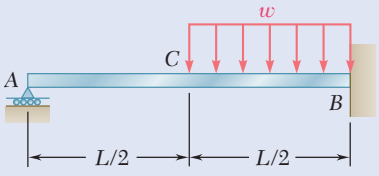


Fig. P9.28

9.29 and 9.30 Determine the reaction at the roller support and the deflection at point *C*.

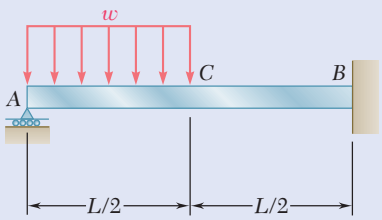


Fig. P9.29

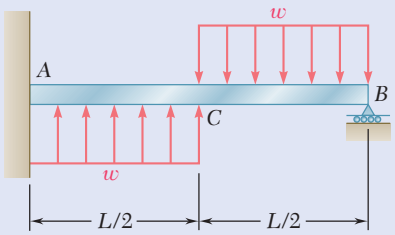


Fig. P9.30

9.31 and 9.32 Determine the reaction at the roller support and the deflection at point *D* if *a* is equal to *L*/3.

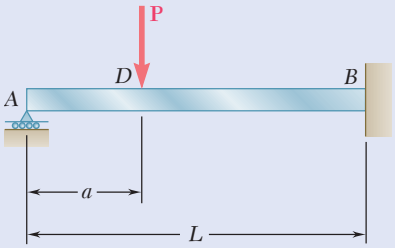


Fig. P9.31

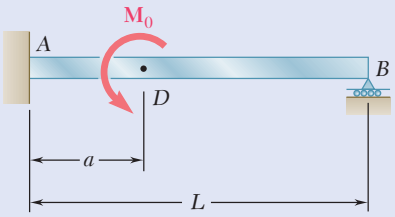


Fig. P9.32

9.33 and 9.34 Determine the reaction at *A* and draw the bending moment diagram for the beam and loading shown.

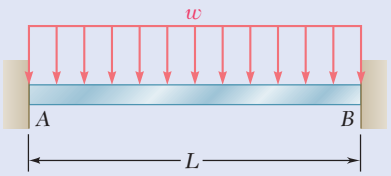


Fig. P9.33

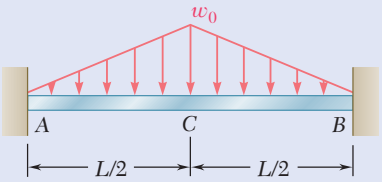


Fig. P9.34

*9.3 SINGULARITY FUNCTIONS TO DETERMINE SLOPE AND DEFLECTION

The integration method provides a convenient and effective way of determining the slope and deflection at any point of a prismatic beam, *as long as the bending moment can be represented by a single analytical function* $M(x)$. However, when the loading of the beam needs two different functions to represent the bending moment over the entire length, as in Concept Application 9.3 (Fig. 9.11*a*), four constants of integration are required. An equal number of equations, expressing continuity conditions at point D as well as boundary conditions at supports A and B, must be used to determine these constants. If three or more functions are needed for the bending moment, additional constants and a corresponding number of additional equations are required, resulting in rather lengthy computations. Such is the case for the beam shown in Photo 9.2. This section simplifies computations in situations like this through the use of the singularity functions discussed in Sec. 5.4.



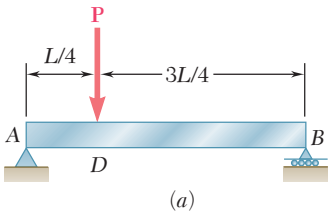
Photo 9.2 In this roof structure, each of the open-web joists applies a concentrated load to the beam that supports it.

Consider again the beam and loading of Concept Application 9.3 (Fig. 9.11) and draw the free-body diagram of that beam (Fig. 9.18). Use the appropriate singularity function (Sec. 5.4) to represent the contribution to the shear of the concentrated load **P**, and write

$$V(x) = \frac{3P}{4} - P\langle x - \tfrac{1}{4}L\rangle^0$$

Integrate in x and recall from Sec. 5.4 that, in the absence of any concentrated couple, the expression for the bending moment does not contain a constant term, so

$$M(x) = \frac{3P}{4}x - P\langle x - \tfrac{1}{4}L\rangle \qquad \textbf{(9.11)}$$



(*a*)

Fig. 9.11 (*repeated*) Simply supported beam with transverse load ***P***.

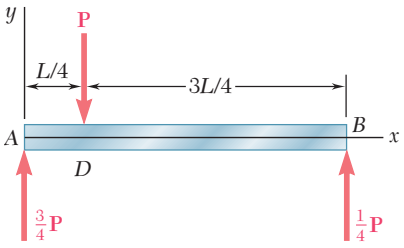


Fig. 9.18 Free-body diagram for beam of Fig. 9.11.

Substituting for $M(x)$ from Eq. (9.11) into Eq. (9.4),

$$EI\frac{d^2y}{dx^2} = \frac{3P}{4}x - P\langle x - \tfrac{1}{4}L\rangle \tag{9.12}$$

and, integrating in x,

$$EI\,\theta = EI\frac{dy}{dx} = \frac{3}{8}Px^2 - \frac{1}{2}P\langle x - \tfrac{1}{4}L\rangle^2 + C_1 \tag{9.13}$$

$$EI\,y = \frac{1}{8}Px^3 - \frac{1}{6}P\langle x - \tfrac{1}{4}L\rangle^3 + C_1x + C_2 \tag{9.14}^{\dagger}$$

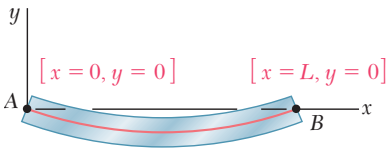


Fig. 9.19 Boundary conditions for beam of Fig. 9.11.

The constants C_1 and C_2 can be determined from the boundary conditions shown in Fig. 9.19. Letting $x = 0$, $y = 0$ in Eq. (9.14),

$$0 = 0 - \frac{1}{6}P\langle 0 - \tfrac{1}{4}L\rangle^3 + 0 + C_2$$

which reduces to $C_2 = 0$, since any bracket containing a negative quantity is equal to zero. Letting now $x = L$, $y = 0$, and $C_2 = 0$ in Eq. (9.14),

$$0 = \frac{1}{8}PL^3 - \frac{1}{6}P\langle \tfrac{3}{4}L\rangle^3 + C_1L$$

Since the quantity between brackets is positive, the brackets can be replaced by ordinary parentheses. Solving for C_1 gives

$$C_1 = -\frac{7PL^2}{128}$$

The expressions obtained for the constants C_1 and C_2 are the same found in Concept Application 9.3. But the need for additional constants C_3 and C_4 has been eliminated, and the equations expressing that the slope and the deflection are continuous at point D are not needed.

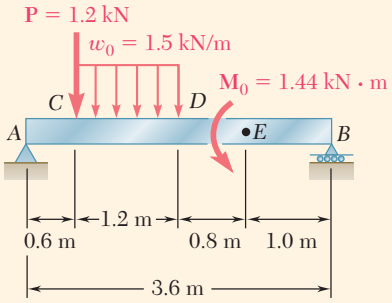
†The continuity conditions for the slope and deflection at D are "built-in" in Eqs. (9.13) and (9.14). Indeed, the difference between the expressions for the slope θ_1 in AD and the slope θ_2 in DB is represented by the term $-\frac{1}{2}P\langle x - \frac{1}{4}L\rangle^2$ in Eq. (9.13), and this term is equal to zero at D. Similarly, the difference between the expressions for the deflection y_1 in AD and the deflection y_2 in DB is represented by $-\frac{1}{6}P\langle x - \frac{1}{4}L\rangle^3$ in Eq. (9.14), and this term is also equal to zero at D.

Concept Application 9.6

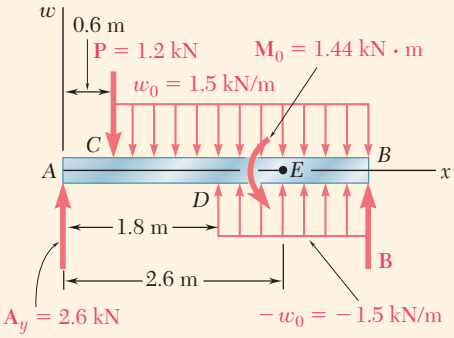
For the beam and loading shown (Fig. 9.20*a*) and using singularity functions, (*a*) express the slope and deflection as functions of the distance x from the support at A, (*b*) determine the deflection at the midpoint D. Use $E = 200$ GPa and $I = 6.87 \times 10^{-6}$ m^4.

(*a*) The beam is loaded and supported in the same manner as the beam of Concept Application 5.5. Recall that the distributed load was

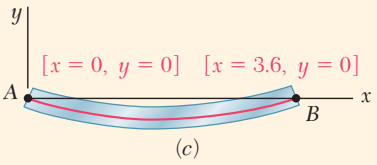
(continued)



(*a*)



(*b*)



(*c*)

Fig. 9.20 (*a*) Simply supported beam with multiple loads. (*b*) Free-body diagram of beam showing equivalent loading system. (*c*) Boundary conditions.

replaced by the two equivalent open-ended loads shown in Fig. 9.20*b*. The expressions for the shear and bending moment are

$$V(x) = -1.5\langle x - 0.6\rangle^1 + 1.5\langle x - 1.8\rangle^1 + 2.6 - 1.2\langle x - 0.6\rangle^0$$

$$M(x) = -0.75\langle x - 0.6\rangle^2 + 0.75\langle x - 1.8\rangle^2 + 2.6x - 1.2\langle x - 0.6\rangle^1 - 1.44\langle x - 2.6\rangle^0$$

Integrating the last expression twice,

$$EI\theta = -0.25\langle x - 0.6\rangle^3 + 0.25\langle x - 1.8\rangle^3 + 1.3x^2 - 0.6\langle x - 0.6\rangle^2 - 1.44\langle x - 2.6\rangle^1 + C_1 \qquad \textbf{(1)}$$

$$EIy = -0.0625\langle x - 0.6\rangle^4 + 0.0625\langle x - 1.8\rangle^4 + 0.4333x^3 - 0.2\langle x - 0.6\rangle^3 - 0.72\langle x - 2.6\rangle^2 + C_1x + C_2 \qquad \textbf{(2)}$$

The constants C_1 and C_2 can be determined from the boundary conditions shown in Fig. 9.20*c*. Letting $x = 0$, $y = 0$ in Eq. (2) and noting that all the brackets contain negative quantities and, therefore, are equal to zero, we conclude that $C_2 = 0$. Letting $x = 3.6$, $y = 0$, and $C_2 = 0$ in Eq. (2) gives

$$0 = -0.0625\langle 3.0\rangle^4 + 0.0625\langle 1.8\rangle^4 + 0.4333(3.6)^3 - 0.2\langle 3.0\rangle^3 - 0.72\langle 1.0\rangle^2 + C_1(3.6) + 0$$

Since all the quantities between brackets are positive, the brackets can be replaced by ordinary parentheses. Solving for C_1, we find $C_1 = -2.692$.

(*b*) Substituting for C_1 and C_2 into Eq. (2) and making $x = x_D = 1.8$ m, we find that the deflection at point D is defined by the relation

$$EIy_D = -0.0625\langle 1.2\rangle^4 + 0.0625\langle 0\rangle^4 + 0.4333(1.8)^3 - 0.2\langle 1.2\rangle^3 - 0.72\langle -0.8\rangle^2 - 2.692(1.8)$$

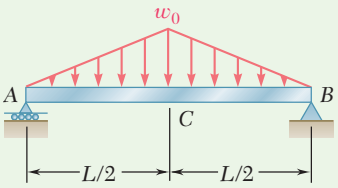
The last bracket contains a negative quantity and, therefore, is equal to zero. All the other brackets contain positive quantities and can be replaced by ordinary parentheses.

$$EIy_D = -0.0625(1.2)^4 + 0.0625(0)^4 + 0.4333(1.8)^3 - 0.2(1.2)^3 - 0 - 2.692(1.8) = -2.794$$

Recalling the given numerical values of E and I,

$$(200\text{ GPa})(6.87 \times 10^{-6}\text{ m}^4)y_D = -2.794\text{ kN·m}^3$$

$$y_D = -13.64 \times 10^{-3}\text{ m} = -2.03\text{ mm}$$



Sample Problem 9.4

For the prismatic beam and loading shown, determine (*a*) the equation of the elastic curve, (*b*) the slope at *A*, (*c*) the maximum deflection.

STRATEGY: You can begin by determining the bending-moment equation of the beam, using a singularity function for any transition in loading. Substituting this into the differential equation of the elastic curve, integrating twice, and applying the boundary conditions, you can then obtain the equation of the elastic curve. Use this equation to find the desired slope and deflection.

MODELING: The equation defining the bending moment of the beam was obtained in Sample Prob. 5.9. Using the modified loading diagram shown in Fig. 1, we had [Eq. (3)]:

$$M(x) = -\frac{w_0}{3L}x^3 + \frac{2w_0}{3L}\langle x - \tfrac{1}{2}L\rangle^3 + \tfrac{1}{4}w_0Lx$$

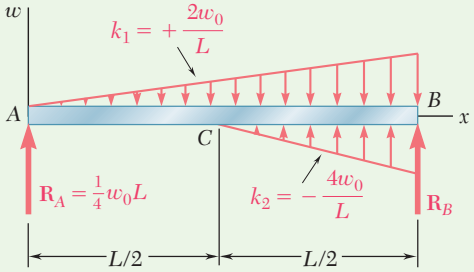


Fig. 1 Free-body diagram showing modified loading.

ANALYSIS:

a. Equation of the Elastic Curve. Using Eq. (9.4),

$$EI\frac{d^2y}{dx^2} = -\frac{w_0}{3L}x^3 + \frac{2w_0}{3L}\langle x - \tfrac{1}{2}L\rangle^3 + \tfrac{1}{4}w_0Lx \qquad \textbf{(1)}$$

and, integrating twice in *x*,

$$EI\,\theta = -\frac{w_0}{12L}x^4 + \frac{w_0}{6L}\langle x - \tfrac{1}{2}L\rangle^4 + \frac{w_0L}{8}x^2 + C_1 \qquad \textbf{(2)}$$

$$EI\,y = -\frac{w_0}{60L}x^5 + \frac{w_0}{30L}\langle x - \tfrac{1}{2}L\rangle^5 + \frac{w_0L}{24}x^3 + C_1x + C_2 \qquad \textbf{(3)}$$

(continued)

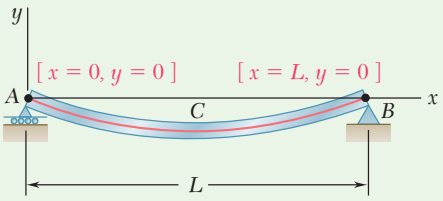


Fig. 2 Boundary conditions.

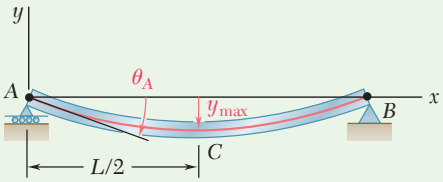


Fig. 3 Deformed elastic curve showing slope at *A* and maximum deflection at *C*.

Boundary Conditions. Referring to Fig. 2,

$[x = 0, y = 0]$: Using Eq. (3) and noting that each bracket $\langle\ \rangle$ contains a negative quantity and is equal to zero, $C_2 = 0$.

$[x = L, y = 0]$: Again using Eq. (3),

$$0 = -\frac{w_0 L^4}{60} + \frac{w_0}{30L}\left(\frac{L}{2}\right)^5 + \frac{w_0 L^4}{24} + C_1 L \qquad C_1 = -\frac{5}{192} w_0 L^3$$

Substituting C_1 and C_2 into Eqs. (2) and (3),

$$EI\,\theta = -\frac{w_0}{12L}x^4 + \frac{w_0}{6L}\langle x - \tfrac{1}{2}L\rangle^4 + \frac{w_0 L}{8}x^2 - \frac{5}{192}w_0 L^3 \qquad \textbf{(4)}$$

$$EI\,y = -\frac{w_0}{60L}x^5 + \frac{w_0}{30L}\langle x - \tfrac{1}{2}L\rangle^5 + \frac{w_0 L}{24}x^3 - \frac{5}{192}w_0 L^3 x \qquad \textbf{(5)}$$

b. Slope at A (Fig. 3). Substituting $x = 0$ into Eq. (4),

$$EI\,\theta_A = -\frac{5}{192}w_0 L^3 \qquad \theta_A = \frac{5w_0 L^3}{192EI}\curvearrowright$$

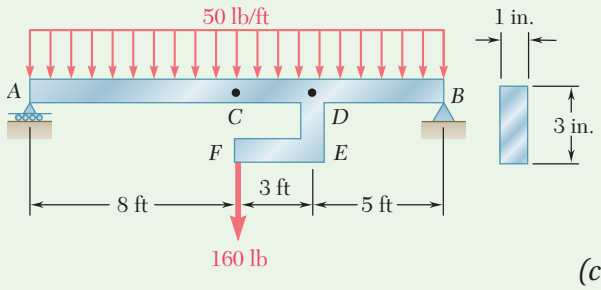
c. Maximum Deflection (Fig. 3). Because of the symmetry of the supports and loading, the maximum deflection occurs at point C where $x = \frac{1}{2}L$. Substituting into Eq. (5),

$$EI\,y_{\max} = w_0 L^4\left[-\frac{1}{60(32)} + 0 + \frac{1}{24(8)} - \frac{5}{192(2)}\right] = -\frac{w_0 L^4}{120}$$

$$y_{\max} = \frac{w_0 L^4}{120EI}\downarrow$$

Sample Problem 9.5

The rigid bar *DEF* is welded at point *D* to the uniform steel beam *AB*. For the loading shown, determine (*a*) the equation of the elastic curve of the beam, (*b*) the deflection at the midpoint *C* of the beam. Use $E = 29 \times 10^6$ psi.



(continued)

STRATEGY: Begin by determining the bending-moment equation of the beam *ADB*, using a singularity function for any transition in loading. Substituting this into the differential equation of the elastic curve, integrating twice, and applying the boundary conditions, you can then obtain the equation of the elastic curve. Use this equation to find the desired deflection.

MODELING: The equation defining the bending moment of the beam was obtained in Sample Prob. 5.10. Using the modified loading diagram shown in Fig. 1 and expressing x in feet, [Eq. (3)] is

$$M(x) = -25x^2 + 480x - 160\langle x - 11\rangle^1 - 480\langle x - 11\rangle^0 \quad \text{lb·ft}$$

ANALYSIS:

a. Equation of the Elastic Curve. Using Eq. (9.4),

$$EI(d^2y/dx^2) = -25x^2 + 480x - 160\langle x - 11\rangle^1 - 480\langle x - 11\rangle^0 \quad \text{lb·ft} \quad \textbf{(1)}$$

and, integrating twice in x,

$$EI\,\theta = -8.333x^3 + 240x^2 - 80\langle x - 11\rangle^2 - 480\langle x - 11\rangle^1 + C_1 \quad \text{lb·ft}^2 \quad \textbf{(2)}$$

$$EI\,y = -2.083x^4 + 80x^3 - 26.67\langle x - 11\rangle^3 - 240\langle x - 11\rangle^2 + C_1x + C_2 \quad \text{lb·ft}^3 \quad \textbf{(3a)}$$

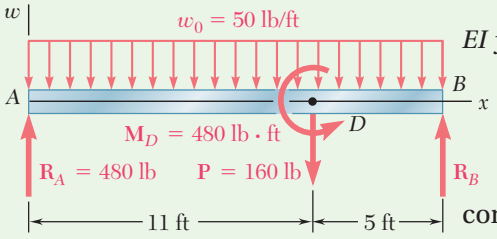


Fig. 1 Free-body diagram of showing equivalent force-couple system.

Boundary Conditions. Referring to Fig. 2,

$[x = 0, y = 0]$: Using Eq. (3) and noting that each bracket $\langle\ \rangle$ contains a negative quantity and, thus, is equal to zero, we find $C_2 = 0$.

$[x = 16\text{ ft}, y = 0]$: Again using Eq. (3), each bracket contains a positive quantity and can be replaced by a parenthesis:

$$0 = -2.083(16)^4 + 80(16)^3 - 26.67(5)^3 - 240(5)^2 + C_1(16)$$

$$C_1 = -11.36 \times 10^3$$

Substituting the values found for C_1 and C_2 into Eq. (3) gives

$$EI\,y = -2.083x^4 + 80x^3 - 26.67\langle x - 11\rangle^3 - 240\langle x - 11\rangle^2 - 11.36 \times 10^3x \quad \text{lb·ft}^3 \quad \textbf{(3b)}$$

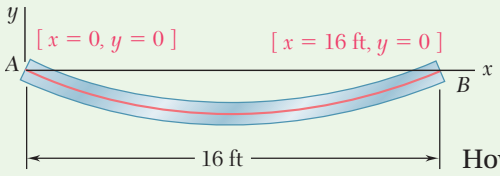


Fig. 2 Boundary conditions.

To determine EI, recall that $E = 29 \times 10^6$ psi and compute

$$I = \tfrac{1}{12}bh^3 = \tfrac{1}{12}(1\text{ in.})(3\text{ in.})^3 = 2.25\text{ in}^4$$

$$EI = (29 \times 10^6\text{ psi})(2.25\text{ in}^4) = 65.25 \times 10^6\text{ lb·in}^2$$

However, since all previous computations have been carried out with feet as the unit of length,

$$EI = (65.25 \times 10^6\text{ lb·in}^2)(1\text{ ft}/12\text{ in.})^2 = 453.1 \times 10^3\text{ lb·ft}^2$$

(continued)

b. Deflection at Midpoint C. (Fig. 3). Making $x = 8$ ft in Eq. (3b),

$$EI\,y_C = -2.083(8)^4 + 80(8)^3 - 26.67\langle -3\rangle^3 - 240\langle -3\rangle^2 - 11.36 \times 10^3(8)$$

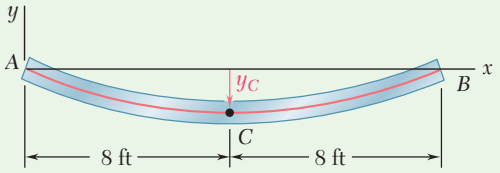


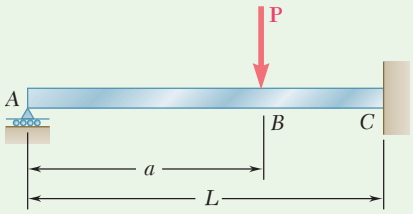
Fig. 3 Deformed elastic curve showing displacement at midpoint *C*.

Noting that each bracket is equal to zero and substituting for EI its numerical value gives

$$(453.1 \times 10^3 \text{ lb·ft}^2)\,y_C = -58.45 \times 10^3 \text{ lb·ft}^3$$

and solving for y_C: $y_C = -0.1290$ ft $y_C = -1.548$ in. ◀

REFLECT and THINK: Note that the deflection obtained at midpoint *C* is *not* the maximum deflection.



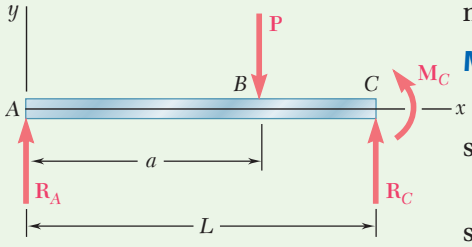


Fig. 1 Free-body diagram.

Sample Problem 9.6

For the uniform beam *ABC*, (*a*) express the reaction at *A* in terms of *P*, *L*, *a*, *E*, and *I*, (*b*) determine the reaction at *A* and the deflection under the load when $a = L/2$.

STRATEGY: The beam is statically indeterminate to the first degree. Using singularity functions, you can write the bending-moment equation for the beam, including the unknown reaction at *A* as part of the expression. After substituting this equation into the differential equation of the elastic curve, integrating twice, and applying the boundary conditions, the reaction at *A* can be determined, followed by the determination of the desired deflection.

MODELING:

Reactions. For the given vertical load **P** the reactions are as shown in Fig. 1. We note that they are statically indeterminate.

Shear and Bending Moment. Using a step function to represent the contribution of **P** to the shear,

$$V(x) = R_A - P\langle x - a\rangle^0$$

Integrating in x, the bending moment is

$$M(x) = R_A x - P\langle x - a\rangle^1$$

(continued)

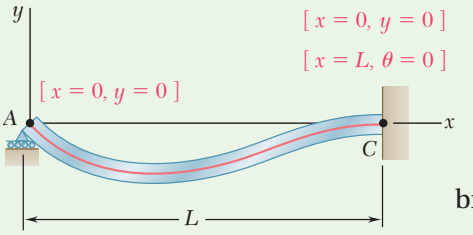


Fig. 2 Boundary conditions.

ANALYSIS:

Equation of the Elastic Curve. Using Eq. (9.4),

$$EI\frac{d^2y}{dx^2} = R_A x - P\langle x - a\rangle^1$$

Integrating twice in x,

$$EI\frac{dy}{dx} = EI\,\theta = \frac{1}{2}R_A x^2 - \frac{1}{2}P\langle x - a\rangle^2 + C_1$$

$$EI\,y = \frac{1}{6}R_A x^3 - \frac{1}{6}P\langle x - a\rangle^3 + C_1 x + C_2$$

Boundary Conditions Referring to Fig. 2 and noting that the bracket $\langle x - a\rangle$ is equal to zero for $x = 0$ and to $(L - a)$ for $x = L$,

$$[x = 0, y = 0]: \quad C_2 = 0 \tag{1}$$

$$[x = L, \theta = 0]: \quad \tfrac{1}{2}R_A L^2 - \tfrac{1}{2}P(L - a)^2 + C_1 = 0 \tag{2}$$

$$[x = L, y = 0]: \quad \tfrac{1}{6}R_A L^3 - \tfrac{1}{6}P(L - a)^3 + C_1 L + C_2 = 0 \tag{3}$$

a. Reaction at *A*. Multiplying Eq. (2) by L, subtracting Eq. (3) member by member from the equation, and noting that $C_2 = 0$, we obtain

$$\frac{1}{3}R_A L^3 - \frac{1}{6}P(L - a)^2[3L - (L - a)] = 0$$

$$\mathbf{R}_A = P\left(1 - \frac{a}{L}\right)^2\left(1 + \frac{a}{2L}\right)\uparrow \quad \blacktriangleleft$$

The reaction is independent of E and I.

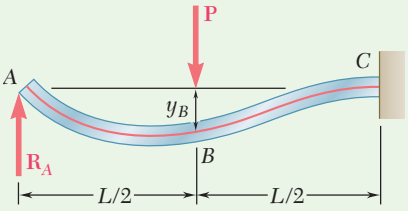


Fig. 3 Deformed elastic curve showing deflection at *B*.

b. Reaction at *A* and Deflection at *B* when $a = \frac{1}{2}L$ (Fig. 3). Making $a = \frac{1}{2}L$ in the expression obtained for R_A,

$$R_A = P(1 - \tfrac{1}{2})^2(1 + \tfrac{1}{4}) = 5P/16 \qquad \mathbf{R}_A = \frac{5}{16}P\uparrow \quad \blacktriangleleft$$

Substituting $a = L/2$ and $R_A = 5P/16$ into Eq. (2) and solving for C_1, $C_1 = -PL^2/32$. Making $x = L/2$, $C_1 = -PL^2/32$, and $C_2 = 0$ in the expression obtained for y,

$$y_B = -\frac{7PL^3}{768EI} \qquad y_B = \frac{7PL^3}{768EI}\downarrow \quad \blacktriangleleft$$

REFLECT and THINK: Note that the deflection obtained at B is *not* the maximum deflection.

Problems

Use singularity functions to solve the following problems and assume that the flexural rigidity *EI* of each beam is constant.

9.35 and 9.36 For the beam and loading shown, determine (*a*) the equation of the elastic curve, (*b*) the slope at end *A*, (*c*) the deflection at point *C*.

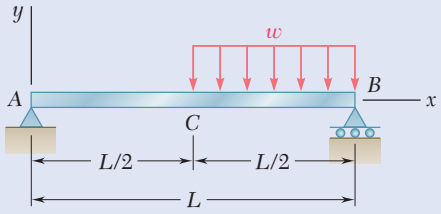


Fig. P9.35

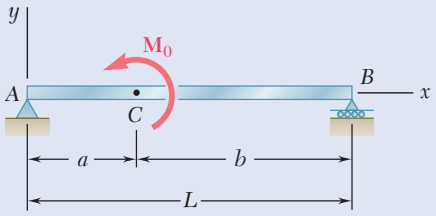


Fig. P9.36

9.37 and 9.38 For the beam and loading shown, determine the deflection at (*a*) point *B*, (*b*) point *C*, (*c*) point *D*.

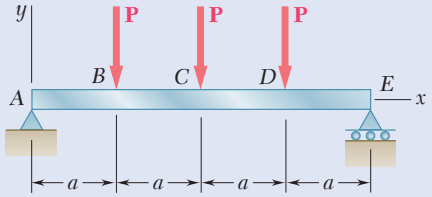


Fig. P9.37

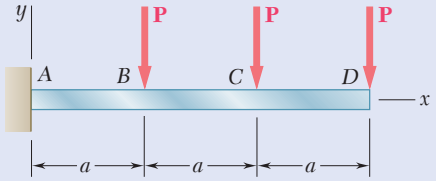


Fig. P9.38

9.39* and *9.40 For the beam and loading shown, determine (*a*) the deflection at end *A*, (*b*) the deflection at point *C*, (*c*) the slope at end *D*.

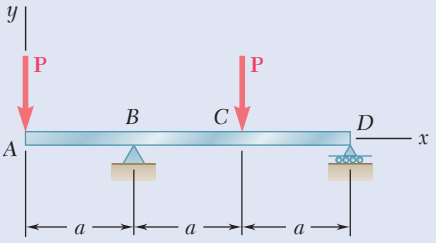


Fig. *P9.39*

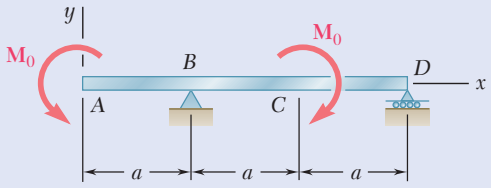


Fig. *P9.40*

9.41 and *9.42* For the beam and loading shown, determine (*a*) the equation of the elastic curve, (*b*) the deflection at the midpoint *C*.

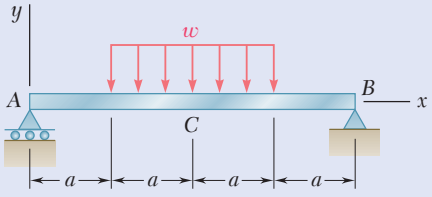


Fig. P9.41

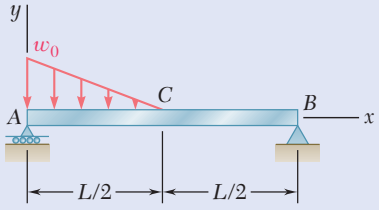


Fig. *P9.42*

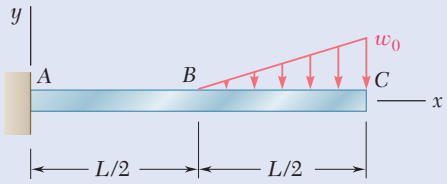


Fig. P9.43

9.43 For the beam and loading shown, determine (*a*) the equation of the elastic curve, (*b*) the deflection at point *B*, (*c*) the deflection at point *C*.

9.44 For the beam and loading shown, determine (*a*) the equation of the elastic curve, (*b*) the deflection at point *B*, (*c*) the deflection at point *D*.

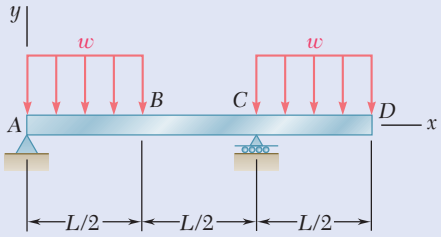


Fig. P9.44

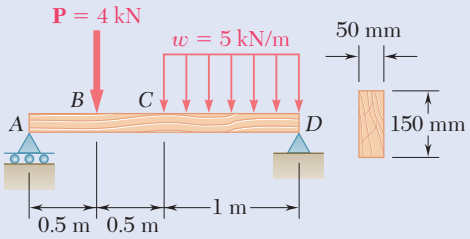


Fig. P9.45

9.45 For the timber beam and loading shown, determine (*a*) the slope at end *A*, (*b*) the deflection at the midpoint *C*. Use $E = 12$ GPa.

9.46 For the beam and loading shown, determine (*a*) the slope at end *A*, (*b*) the deflection at point *B*. Use $E = 29 \times 10^6$ psi.

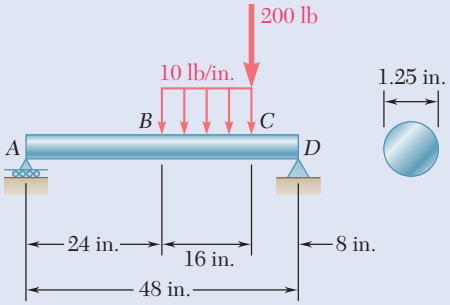


Fig. P9.46

9.47 For the beam and loading shown, determine (*a*) the slope at end *A*, (*b*) the deflection at point *C*. Use $E = 29 \times 10^6$ psi.

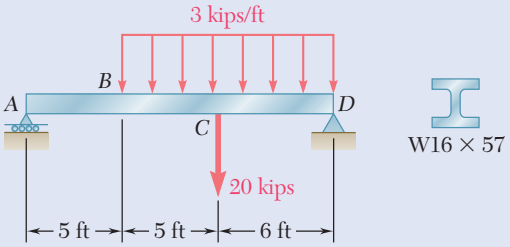


Fig. *P9.47*

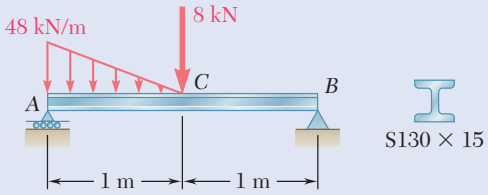


Fig. P9.48

9.48 For the beam and loading shown, determine (*a*) the slope at end *A*, (*b*) the deflection at the midpoint *C*. Use $E = 200$ GPa.

9.49 and 9.50 For the beam and loading shown, determine (*a*) the reaction at the roller support, (*b*) the deflection at point *C*.

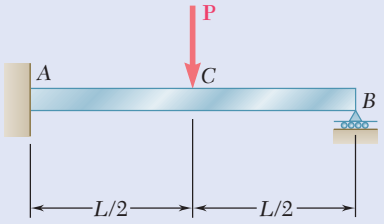


Fig. P9.49

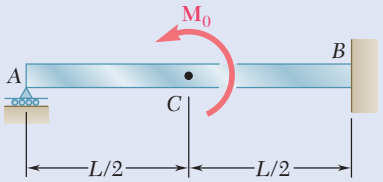


Fig. P9.50

9.51 and *9.52* For the beam and loading shown, determine (*a*) the reaction at the roller support, (*b*) the deflection at point *B*.

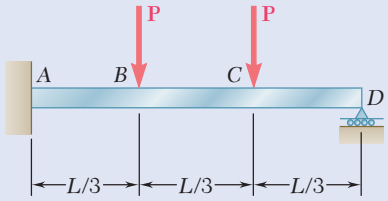


Fig. P9.51

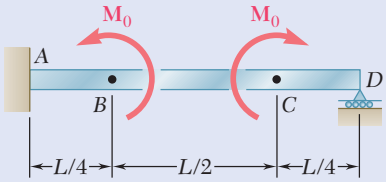


Fig. *P9.52*

9.53 For the beam and loading shown, determine (*a*) the reaction at point *C*, (*b*) the deflection at point *B*. Use $E = 200$ GPa.

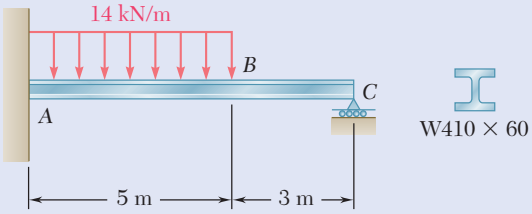


Fig. P9.53

9.54 For the beam shown and knowing that $P = 40$ kN, determine (*a*) the reaction at point *E*, (*b*) the deflection at point *C*. Use $E = 200$ GPa.

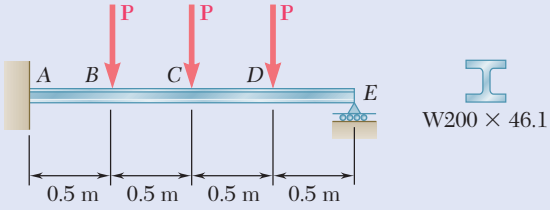


Fig. P9.54

9.55 and 9.56 For the beam and loading shown, determine (*a*) the reaction at point *A*, (*b*) the deflection at point *C*. Use $E = 29 \times 10^6$ psi.

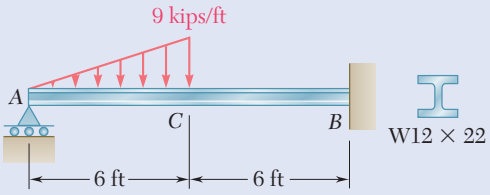


Fig. *P9.55*

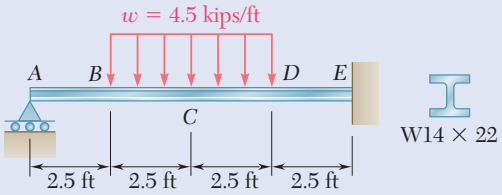


Fig. P9.56

9.57 For the beam and loading shown, determine (*a*) the reaction at point *A*, (*b*) the deflection at point *D*.

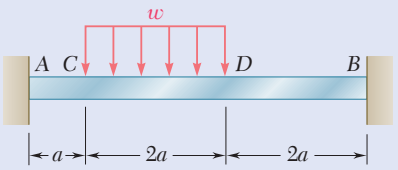


Fig. P9.57

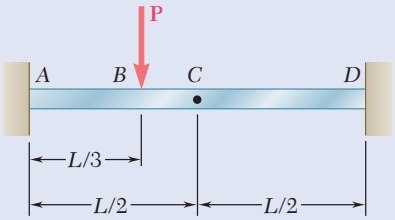


Fig. P9.58

9.58 For the beam and loading shown, determine (*a*) the reaction at point *A*, (*b*) the deflection at midpoint *C*.

9.59 through 9.62 For the beam and loading indicated, determine the magnitude and location of the largest downward deflection.

9.59 Beam and loading of Prob. 9.45.

9.60 Beam and loading of Prob. 9.46.

9.61 Beam and loading of Prob. 9.47.

9.62 Beam and loading of Prob. 9.48.

9.63 The rigid bars *BF* and *DH* are welded to the rolled-steel beam *AE* as shown. Determine for the loading shown (*a*) the deflection at point *B*, (*b*) the deflection at midpoint *C* of the beam. Use $E = 200$ GPa.

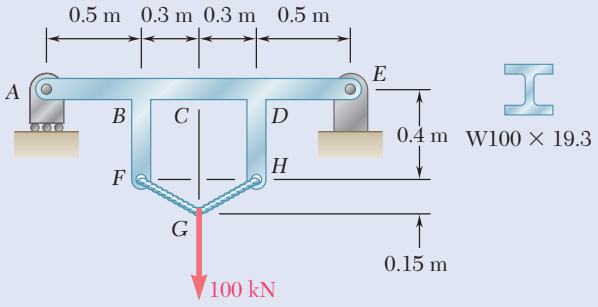


Fig. *P9.63*

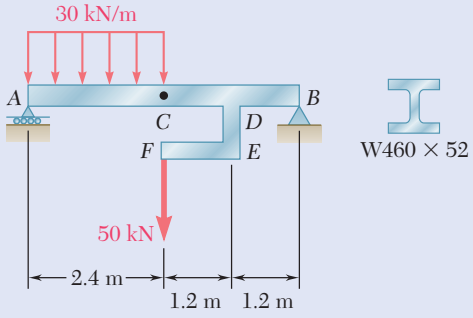


Fig. *P9.64*

9.64 The rigid bar *DEF* is welded at point *D* to the rolled-steel beam *AB*. For the loading shown, determine (*a*) the slope at point *A*, (*b*) the deflection at midpoint *C* of the beam. Use $E = 200$ GPa.

9.4 METHOD OF SUPERPOSITION

9.4A Statically Determinate Beams

When a beam is subjected to several concentrated or distributed loads, it is convenient to compute separately the slope and deflection caused by each of the given loads. The slope and deflection due to the combined loads are obtained by applying the principle of superposition (Sec. 2.5) and adding the values of the slope or deflection corresponding to the various loads.

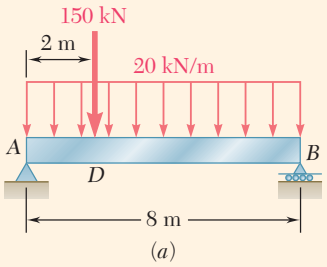


Fig. 9.21 (*a*) Simply supported beam having distributed and concentrated loads.

Concept Application 9.7

Determine the slope and deflection at D for the beam and loading shown (Fig. 9.21*a*), knowing that the flexural rigidity of the beam is $EI = 100\ \text{MN}\cdot\text{m}^2$.

The slope and deflection at any point of the beam can be obtained by superposing the slopes and deflections caused by the concentrated load and by the distributed load (Fig. 9.21*b*).

Since the concentrated load in Fig. 9.21*c* is applied at quarter span, the results for the beam and loading of Concept Application 9.3 can be used to write

$$(\theta_D)_P = -\frac{PL^2}{32EI} = -\frac{(150 \times 10^3)(8)^2}{32(100 \times 10^6)} = -3 \times 10^{-3}\ \text{rad}$$

$$(y_D)_P = -\frac{3PL^3}{256EI} = -\frac{3(150 \times 10^3)(8)^3}{256(100 \times 10^6)} = -9 \times 10^{-3}\ \text{m}$$

$$= -9\ \text{mm}$$

On the other hand, recalling the equation of the elastic curve obtained for a uniformly distributed load in Concept Application 9.2, the deflection in Fig. 9.21*d* is

$$y = \frac{w}{24EI}(-x^4 + 2Lx^3 - L^3x) \qquad \textbf{(1)}$$

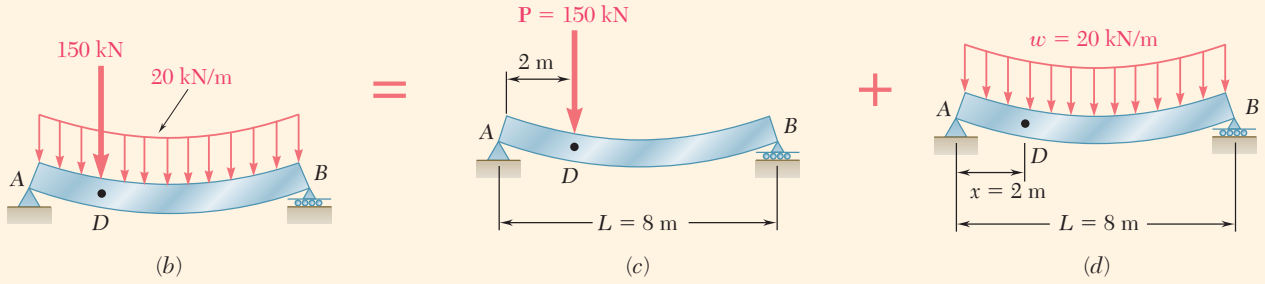


Fig. 9.21 (*b*) The beam's loading can be obtained by superposing deflections due to (*c*) the concentrated load and (*d*) the distributed load.

Differentiating with respect to x gives

$$\theta = \frac{dy}{dx} = \frac{w}{24EI}(-4x^3 + 6Lx^2 - L^3) \qquad \textbf{(2)}$$

(continued)

Making $w = 20$ kN/m, $x = 2$ m, and $L = 8$ m in Eqs. (1) and (2), we obtain

$$(\theta_D)_w = \frac{20 \times 10^3}{24(100 \times 10^6)}(-352) = -2.93 \times 10^{-3}\,\text{rad}$$

$$(y_D)_w = \frac{20 \times 10^3}{24(100 \times 10^6)}(-912) = -7.60 \times 10^{-3}\,\text{m}$$

$$= -7.60\,\text{mm}$$

Combining the slopes and deflections produced by the concentrated and the distributed loads,

$$\theta_D = (\theta_D)_P + (\theta_D)_w = -3 \times 10^{-3} - 2.93 \times 10^{-3}$$

$$= -5.93 \times 10^{-3}\,\text{rad}$$

$$y_D = (y_D)_P + (y_D)_w = -9\,\text{mm} - 7.60\,\text{mm} = -16.60\,\text{mm}$$

To facilitate the work of practicing engineers, most structural and mechanical engineering handbooks include tables giving the deflections and slopes of beams for various loadings and types of support. Such a table is found in Appendix D. The slope and deflection of the beam of Fig. 9.21*a* could have been determined from that table. Indeed, using the information given under cases 5 and 6, we could have expressed the deflection of the beam for any value $x \le L/4$. Taking the derivative of the expression obtained in this way would have yielded the slope of the beam over the same interval. We also note that the slope at both ends of the beam can be obtained by simply adding the corresponding values given in the table. However, the maximum deflection of the beam of Fig. 9.21*a* *cannot* be obtained by adding the maximum deflections of cases 5 and 6, since these deflections occur at different points of the beam.[†]



Photo 9.3 The continuous beams supporting this highway overpass have three supports and are thus statically indeterminate.

9.4B Statically Indeterminate Beams

We often find it convenient to use the method of superposition to determine the reactions at the supports of a statically indeterminate beam. Considering a beam indeterminate to the first degree, such as the beam shown in Photo 9.3, we can use the approach described in Sec. 9.2. We designate one of the reactions as redundant and eliminate or modify accordingly the corresponding support. The redundant reaction is then treated as an unknown load that, together with the other loads, must produce deformations compatible with the original supports. The slope or deflection at the point where the support has been modified or eliminated is obtained by computing the deformations caused by both the given loads and the redundant reaction and by superposing the results. Once the reactions at the supports are found, the slope and deflection can be determined.

[†]An approximate value of the maximum deflection of the beam can be obtained by plotting the values of y corresponding to various values of x. The determination of the exact location and magnitude of the maximum deflection would require setting equal to zero the expression obtained for the slope of the beam and solving this equation for x.

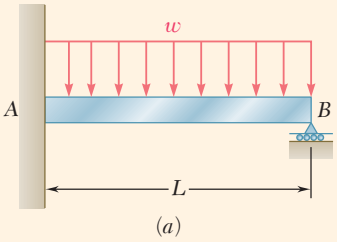


Fig. 9.22 (*a*) Statically indeterminate beam with a uniformly distributed load.

Concept Application 9.8

Determine the reactions at the supports for the prismatic beam and loading shown in Fig. 9.22*a*. (This is the same beam and loading as in Concept Application 9.5.)

We consider the reaction at B as redundant and release the beam from the support. The reaction $\mathbf{R}_B$ is now considered as an unknown load (Fig. 9.22*b*) and will be determined from the condition that the deflection of the beam at B must be zero. The solution is carried out by considering separately the deflection $(y_B)_w$ caused at B by the uniformly distributed load w (Fig. 9.22*c*) and the deflection $(y_B)_R$ produced at the same point by the redundant reaction $\mathbf{R}_B$ (Fig. 9.22*d*).

From the table of Appendix D (cases 2 and 1),

$$(y_B)_w = -\frac{wL^4}{8EI} \qquad (y_B)_R = +\frac{R_B L^3}{3EI}$$

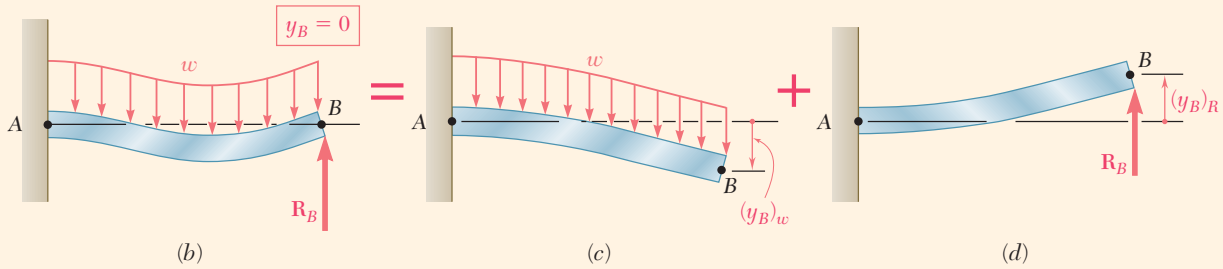


Fig. 9.22 (*b*) Analyze the indeterminate beam by superposing two determinate cantilever beams, subjected to (*c*) a uniformly distributed load, (*d*) the redundant reaction.

Writing that the deflection at B is the sum of these two quantities and that it must be zero,

$$y_B = (y_B)_w + (y_B)_R = 0$$

$$y_B = -\frac{wL^4}{8EI} + \frac{R_B L^3}{3EI} = 0$$

and, solving for R_B, $\qquad R_B = \frac{3}{8}wL \qquad \mathbf{R}_B = \frac{3}{8}wL \uparrow$

Drawing the free-body diagram of the beam (Fig. 9.22*e*) and writing the corresponding equilibrium equations,

$+\uparrow \Sigma F_y = 0$: $\qquad R_A + R_B - wL = 0$ **(1)**

$$R_A = wL - R_B = wL - \tfrac{3}{8}wL = \tfrac{5}{8}wL$$

$$\mathbf{R}_A = \tfrac{5}{8}wL \uparrow$$

$+\circlearrowleft \Sigma M_A = 0$: $\qquad M_A + R_B L - (wL)(\tfrac{1}{2}L) = 0$ **(2)**

$$M_A = \tfrac{1}{2}wL^2 - R_B L = \tfrac{1}{2}wL^2 - \tfrac{3}{8}wL^2 = \tfrac{1}{8}wL^2$$

$$\mathbf{M}_A = \tfrac{1}{8}wL^2 \circlearrowleft$$

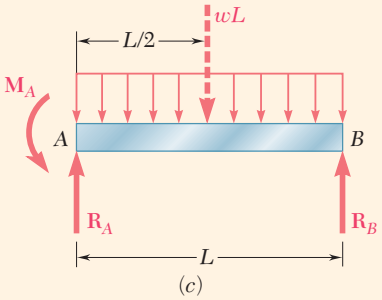
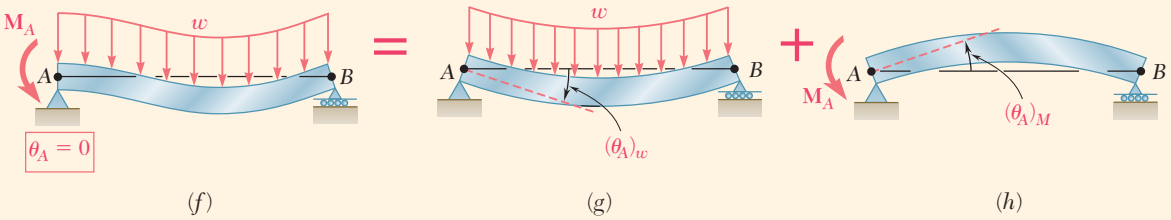


Fig. 9.22 (*e*) Free-body diagram of indeterminate beam.

(continued)

Alternative Solution. We may consider the couple exerted at the fixed end A as redundant and replace the fixed end by a pin-and-bracket support. The couple $\mathbf{M}_A$ is now considered as an unknown load (Fig. 9.22f) and will be determined from the condition that the slope of the beam at A must be zero. The solution is carried out by considering separately the slope $(\theta_A)_w$ caused at A by the uniformly distributed load w (Fig. 9.22g) and the slope $(\theta_A)_M$ produced at the same point by the unknown couple $\mathbf{M}_A$ (Fig 9.22h).



(f) (g) (h)

Fig. 9.22 (f) Analyze the indeterminate beam by superposing two determinate simply supported beams, subjected to (g) a uniformly distributed load, (h) the redundant reaction.

Using the table of Appendix D (cases 6 and 7) and noting that A and B must be interchanged in case 7,

$$(\theta_A)_w = -\frac{wL^3}{24EI} \qquad (\theta_A)_M = \frac{M_A L}{3EI}$$

Writing that the slope at A is the sum of these two quantities and that it must be zero gives

$$\theta_A = (\theta_A)_w + (\theta_A)_M = 0$$

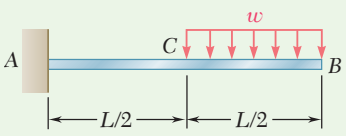
$$\theta_A = -\frac{wL^3}{25EI} + \frac{M_A L}{3EI} = 0$$

where M_A is

$$M_A = \tfrac{1}{8}wL^2 \qquad \mathbf{M}_A = \tfrac{1}{8}wL^2 \curvearrowleft$$

The values of R_A and R_B are found by using the equilibrium equations (1) and (2).

The beam considered in the preceding Concept Application was indeterminate to the first degree. In the case of a beam indeterminate to the second degree (see Sec. 9.2), two reactions must be designated as redundant, and the corresponding supports must be eliminated or modified accordingly. The redundant reactions are then treated as unknown loads that, simultaneously and together with the other loads, must produce deformations that are compatible with the original supports. (See Sample Prob. 9.9.)



Sample Problem 9.7

For the beam and loading shown, determine the slope and deflection at point *B*.

STRATEGY: Using the method of superposition, you can model the given problem using a summation of beam load cases for which deflection formulae are readily available.

MODELING: Through the principle of superposition, the given loading can be obtained by superposing the loadings shown in the following picture equation of Fig. 1. The beam *AB* is the same in each part of the figure.

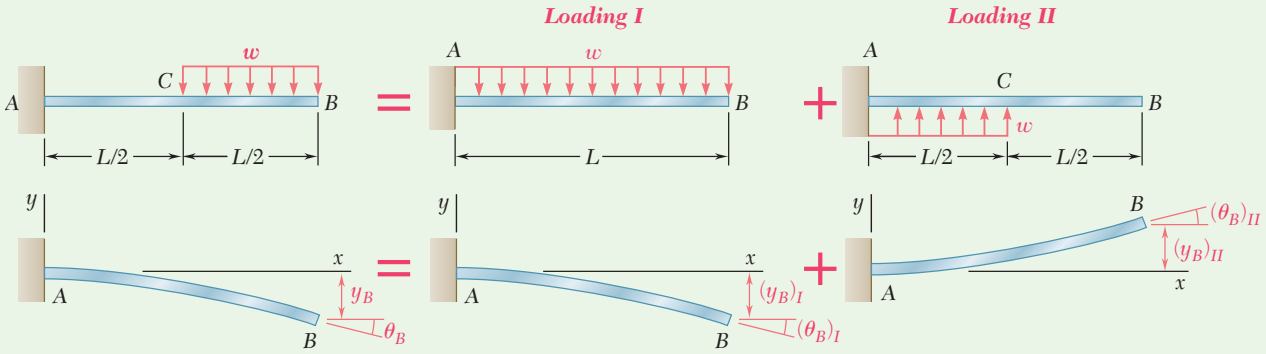


Fig. 1 Actual loading is equivalent to the superposition of two distributed loads.

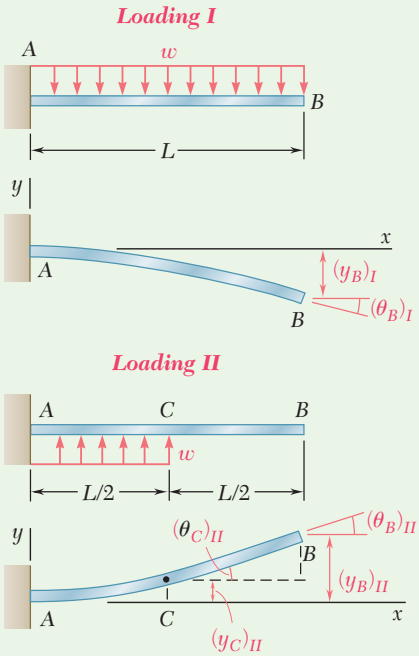


Fig. 2 Deformation details of the superposed loadings I and II.

ANALYSIS: For each of the loadings I and II (detailed further in Fig. 2), determine the slope and deflection at *B* by using the table of *Beam Deflections and Slopes* in Appendix D.

Loading I

$$(\theta_B)_I = -\frac{wL^3}{6EI} \qquad (y_B)_I = -\frac{wL^4}{8EI}$$

Loading II

$$(\theta_C)_{II} = +\frac{w(L/2)^3}{6EI} = +\frac{wL^3}{48EI} \qquad (y_C)_{II} = +\frac{w(L/2)^4}{8EI} = +\frac{wL^4}{128EI}$$

(continued)

In portion *CB*, the bending moment for loading II is zero. Thus, the elastic curve is a straight line.

$$(\theta_B)_{II} = (\theta_C)_{II} = +\frac{wL^3}{48EI} \qquad (y_B)_{II} = (y_C)_{II} + (\theta_C)_{II}\left(\frac{L}{2}\right)$$

$$= \frac{wL^4}{128EI} + \frac{wL^3}{48EI}\left(\frac{L}{2}\right) = +\frac{7wL^4}{384EI}$$

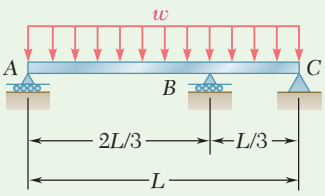
Slope at Point *B*

$$\theta_B = (\theta_B)_I + (\theta_B)_{II} = -\frac{wL^3}{6EI} + \frac{wL^3}{48EI} = -\frac{7wL^3}{48EI} \quad \theta_B = \frac{7wL^3}{48EI} \curvearrowleft$$

Deflection at *B*

$$y_B = (y_B)_I + (y_B)_{II} = -\frac{wL^4}{8EI} + \frac{7wL^4}{384EI} = -\frac{41wL^4}{384EI} \qquad y_B = \frac{41wL^4}{384EI} \downarrow$$

REFLECT and THINK: Note that the formulae for one beam case can sometimes be extended to obtain the desired deflection of another case, as you saw here for loading II.



Sample Problem 9.8

For the uniform beam and loading shown, determine (*a*) the reaction at each support, (*b*) the slope at end *A*.

STRATEGY: The beam is statically indeterminate to the first degree. Strategically selecting the reaction at *B* as the redundant, you can use the method of superposition to model the given problem by using a summation of load cases for which deflection formulae are readily available.

MODELING: The reaction $\mathbf{R}_B$ is selected as redundant and considered as an unknown load. Applying the principle of superposition, the deflections due to the distributed load and to the reaction $\mathbf{R}_B$ are considered separately as shown in Fig. 1.

(continued)

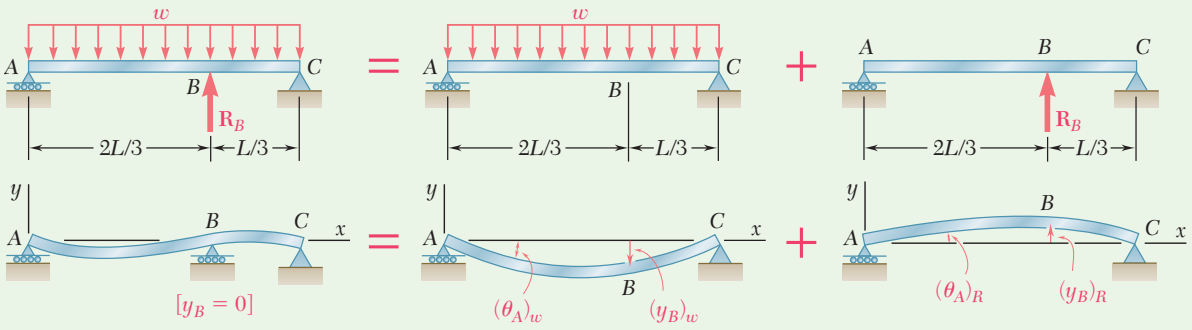


Fig. 1 Indeterminate beam modeled as superposition of two determinate simply supported beams with reaction at *B* chosen as redundant.

ANALYSIS: For each loading case, the deflection at point *B* is found by using the table of *Beam Deflections* and Slopes in Appendix D.

Distributed Loading. Use case 6, Appendix D:

$$y = -\frac{w}{24EI}(x^4 - 2Lx^3 + L^3x)$$

At point *B*, $x = \frac{2}{3}L$:

$$(y_B)_w = -\frac{w}{24EI}\left[\left(\frac{2}{3}L\right)^4 - 2L\left(\frac{2}{3}L\right)^3 + L^3\left(\frac{2}{3}L\right)\right] = -0.01132\frac{wL^4}{EI}$$

Redundant Reaction Loading. From case 5, Appendix D, with $a = \frac{2}{3}L$ and $b = \frac{1}{3}L$,

$$(y_B)_R = -\frac{Pa^2b^2}{3EIL} = +\frac{R_B}{3EIL}\left(\frac{2}{3}L\right)^2\left(\frac{L}{3}\right)^2 = 0.01646\frac{R_BL^3}{EI}$$

a. Reactions at Supports. Recalling that $y_B = 0$,

$$y_B = (y_B)_w + (y_B)_R$$

$$0 = -0.01132\frac{wL^4}{EI} + 0.01646\frac{R_BL^3}{EI} \qquad \mathbf{R}_B = 0.688wL \uparrow \blacktriangleleft$$

Since the reaction R_B is now known, use the methods of statics to determine the other reactions (Fig. 2):

$$\mathbf{R}_A = 0.271wL \uparrow \quad \mathbf{R}_C = 0.0413wL \uparrow \blacktriangleleft$$

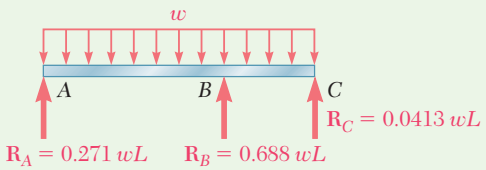


Fig. 2 Free-body diagram of beam with calculated reactions.

(continued)

b. Slope at End *A*. Referring again to Appendix D,

Distributed Loading. $(\theta_A)_w = -\dfrac{wL^3}{24EI} = -0.04167\dfrac{wL^3}{EI}$

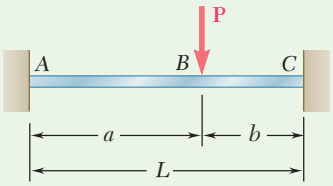
Redundant Reaction Loading. For $P = -R_B = -0.688wL$ and $b = \frac{1}{3}L$,

$$(\theta_A)_R = -\frac{Pb(L^2 - b^2)}{6EIL} = +\frac{0.688wL}{6EIL}\left(\frac{L}{3}\right)\left[L^2 - \left(\frac{L}{3}\right)^2\right] \qquad (\theta_A)_R = 0.03398\frac{wL^3}{EI}$$

Finally, $\theta_A = (\theta_A)_w + (\theta_A)_R$

$$\theta_A = -0.04167\frac{wL^3}{EI} + 0.03398\frac{wL^3}{EI} = -0.00769\frac{wL^3}{EI}$$

$$\theta_A = 0.00769\frac{wL^3}{EI} \curvearrowright$$



Sample Problem 9.9

For the beam and loading shown, determine the reaction at the fixed support *C*.

STRATEGY: The beam is statically indeterminate to the second degree. Strategically selecting the reactions at *C* as redundants, you can use the method of superposition and model the given problem by using a summation of load cases for which deflection formulae are readily available.

MODELING: Assuming the axial force in the beam to be zero, the beam *ABC* is indeterminate to the second degree, and we choose two reaction components as redundants: the vertical force $\mathbf{R}_C$ and the couple $\mathbf{M}_C$. The deformations caused by the given load **P**, the force $\mathbf{R}_C$, and the couple $\mathbf{M}_C$ are considered separately, as shown in Fig. 1.

ANALYSIS: For each load, the slope and deflection at point *C* is found by using the table of *Beam Deflections and Slopes* in Appendix D.

Load P. For this load, portion *BC* of the beam is straight.

$$(\theta_C)_P = (\theta_B)_P = -\frac{Pa^2}{2EI} \qquad (y_C)_P = (y_B)_P + (\theta_B)_P b$$

$$= -\frac{Pa^3}{3EI} - \frac{Pa^2}{2EI}b = -\frac{Pa^2}{6EI}(2a + 3b)$$

(continued)

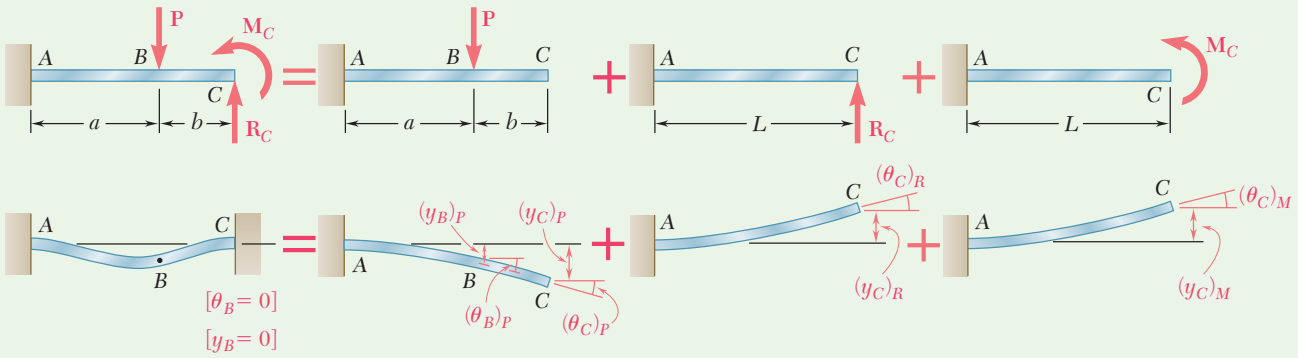


Fig. 1 Indeterminate beam modeled as the superposition of three determinate cases, including one for each of the two redundant reactions.

Force R_C

$$(\theta_C)_R = +\frac{R_C L^2}{2EI} \qquad (y_C)_R = +\frac{R_C L^3}{3EI}$$

Couple M_C

$$(\theta_C)_M = +\frac{M_C L}{EI} \qquad (y_C)_M = +\frac{M_C L^2}{2EI}$$

Boundary Conditions. At end C, the slope and deflection must be zero:

$$[x = L, \theta_C = 0]: \quad \theta_C = (\theta_C)_P + (\theta_C)_R + (\theta_C)_M$$

$$0 = -\frac{Pa^2}{2EI} + \frac{R_C L^2}{2EI} + \frac{M_C L}{EI} \tag{1}$$

$$[x = L, y_C = 0]: \quad y_C = (y_C)_P + (y_C)_R + (y_C)_M$$

$$0 = -\frac{Pa^2}{6EI}(2a + 3b) + \frac{R_C L^3}{3EI} + \frac{M_C L^2}{2EI} \tag{2}$$

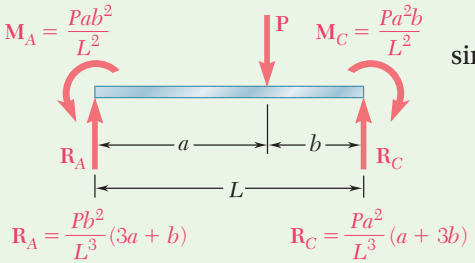


Fig. 2 Free-body diagram showing the reaction results.

Reaction Components at C. Solve Eqs. (1) and (2) simultaneously:

$$R_C = +\frac{Pa^2}{L^3}(a + 3b) \qquad \mathbf{R}_C = \frac{Pa^2}{L^3}(a + 3b) \uparrow$$

$$M_C = -\frac{Pa^2 b}{L^2} \qquad \mathbf{M}_C = \frac{Pa^2 b}{L^2} \circlearrowleft$$

The methods of statics are used to determine the reaction at A, shown in Fig. 2.

REFLECT and THINK: Note that an alternate strategy that could have been used in this particular problem is to treat the couple reactions at the ends as redundant. The application of superposition would then have involved a simply-supported beam, for which deflection formulae are also readily available.

Problems

Use the method of superposition to solve the following problems and assume that the flexural rigidity *EI* of each beam is constant.

9.65 through 9.68 For the cantilever beam and loading shown, determine the slope and deflection at the free end.

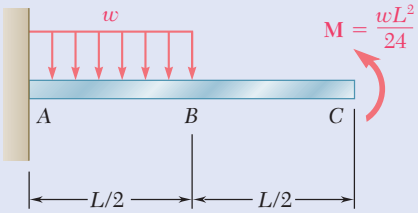


Fig. P9. 65

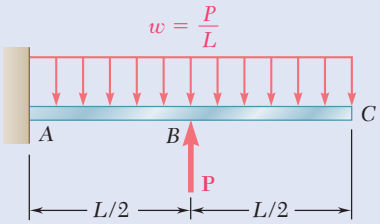


Fig. P9. 66

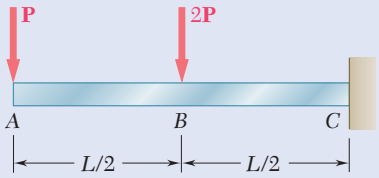


Fig. P9.67

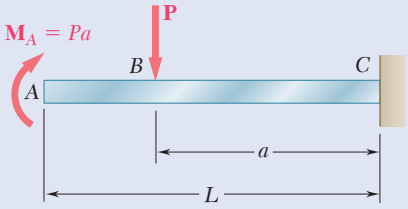


Fig. P9.68

9.69 through 9.72 For the beam and loading shown, determine (*a*) the deflection at point *C*, (*b*) the slope at end *A*.

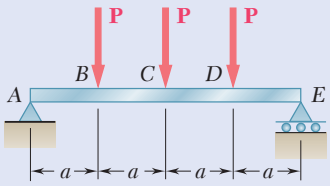


Fig. *P9.69*

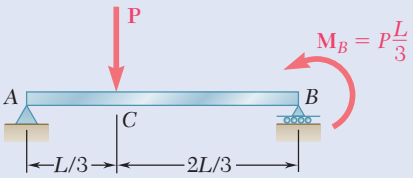


Fig. *P9.70*

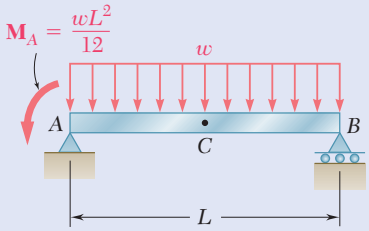


Fig. P9.71

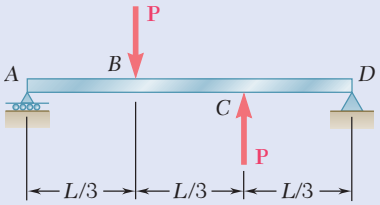


Fig. P9.72

9.73 For the cantilever beam and loading shown, determine the slope and deflection at end C. Use $E = 200$ GPa.

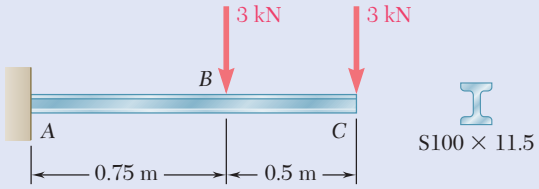


Fig. P9.73 and *P9.74*

9.74 For the cantilever beam and loading shown, determine the slope and deflection at point B. Use $E = 200$ GPa.

9.75 For the cantilever beam and loading shown, determine the slope and deflection at end A. Use $E = 29 \times 10^6$ psi.

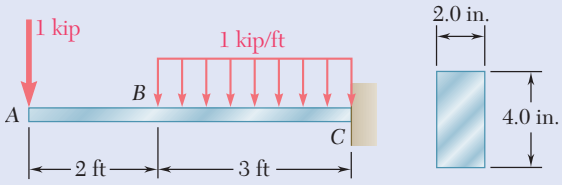


Fig. P9.75 and P9.76

9.76 For the cantilever beam and loading shown, determine the slope and deflection at point B. Use $E = 29 \times 10^6$ psi.

9.77 and *9.78* For the beam and loading shown, determine (a) the slope at end A, (b) the deflection at point C. Use $E = 200$ GPa.

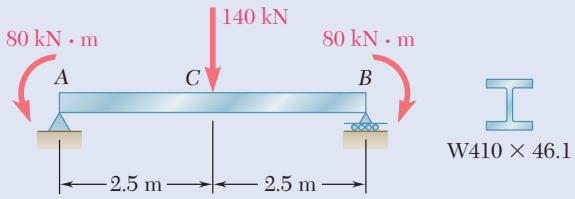


Fig. P9.77

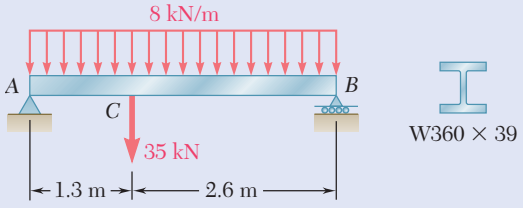


Fig. *P9.78*

9.79 and 9.80 For the uniform beam shown, determine (a) the reaction at A, (b) the reaction at B.

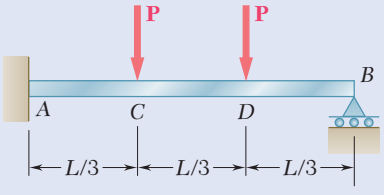


Fig. P9.79

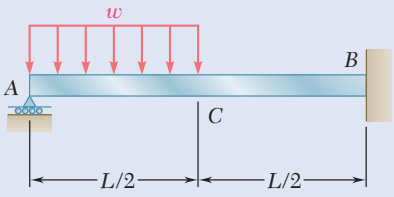


Fig. P9.80

9.81 and 9.82 For the uniform beam shown, determine the reaction at each of the three supports.

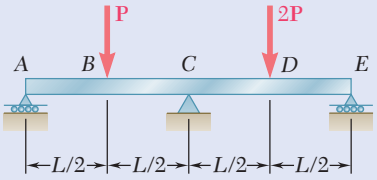


Fig. P9.81

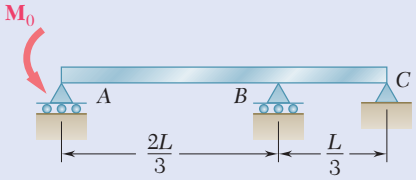


Fig. P9.82

9.83 and 9.84 For the beam shown, determine the reaction at B.

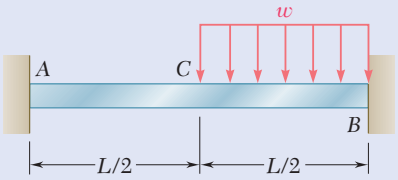


Fig. P9.83

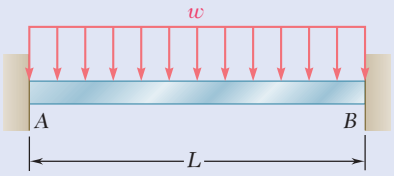


Fig. P9.84

9.85 Beam DE rests on the cantilever beam AC as shown. Knowing that a square rod of side 10 mm is used for each beam, determine the deflection at end C if the 25-N · m couple is applied (a) to end E of the beam DE, (b) to end C of the beam AC. Use $E = 200$ GPa.

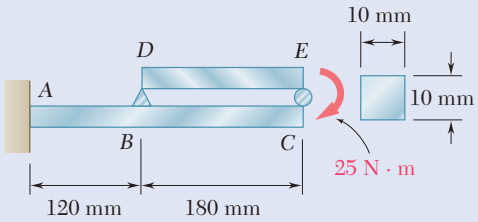


Fig. P9.85

9.86 Beam AD rests on beam EF as shown. Knowing that a W12 × 26 rolled-steel shape is used for each beam, determine for the loading shown the deflection at points B and C. Use $E = 29 \times 10^6$ psi.

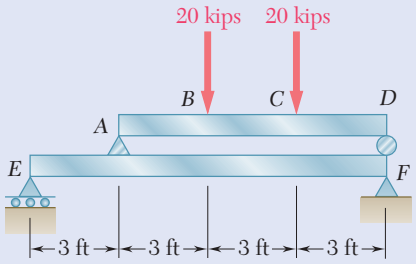


Fig. P9.86

9.87 The two beams shown have the same cross section and are joined by a hinge at C. For the loading shown, determine (a) the slope at point A, (b) the deflection at point B. Use $E = 29 \times 10^6$ psi.

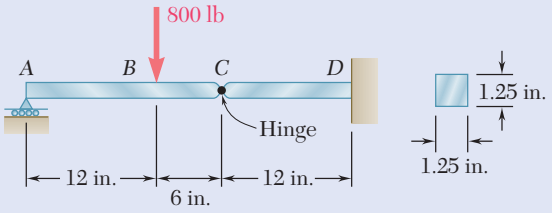


Fig. P9.87

9.88 A central beam BD is joined at hinges to two cantilever beams AB and DE. All beams have the cross section shown. For the loading shown, determine the largest w so that the deflection at C does not exceed 3 mm. Use $E = 200$ GPa.

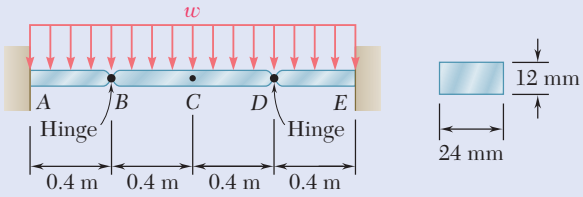


Fig. P9.88

9.89 For the loading shown, and knowing that beams AB and DE have the same flexural rigidity, determine the reaction (a) at B, (b) at E.

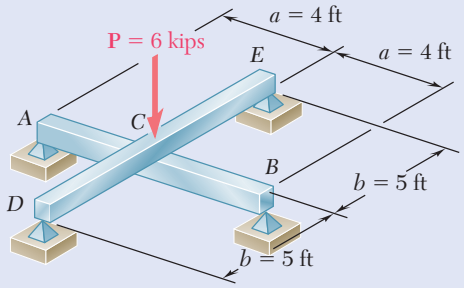


Fig. *P9.89*

9.90 Before the load **P** was applied, a gap, $\delta_0 = 0.5$ mm, existed between the cantilever beam AC and the support at B. Knowing that $E = 200$ GPa, determine the magnitude of **P** for which the deflection at C is 1 mm.

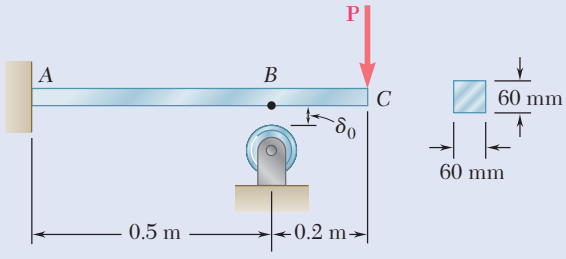


Fig. P9.90

9.91 Knowing that the rod *ABC* and the wire *BD* are both made of steel, determine (*a*) the deflection at *B*, (*b*) the reaction at *A*. Use $E = 200$ GPa.

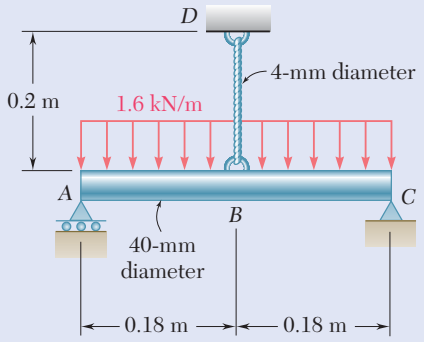


Fig. P9.91

9.92 Before the 2-kip/ft load is applied, a gap, $\delta_0 = 0.8$ in., exists between the W16 × 40 beam and the support at *C*. Knowing that $E = 29 \times 10^6$ psi, determine the reaction at each support after the uniformly distributed load is applied.

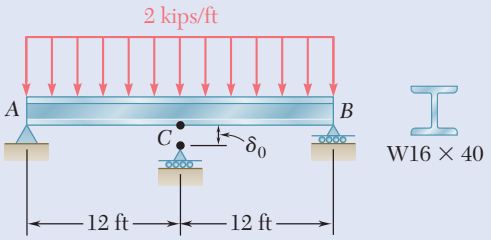


Fig. *P9.92*

9.93 A $\frac{7}{8}$-in.-diameter rod *BC* is attached to the lever *AB* and to the fixed support at *C*. Lever *AB* has a uniform cross section $\frac{3}{8}$ in. thick and 1 in. deep. For the loading shown, determine the deflection of point *A*. Use $E = 29 \times 10^6$ psi and $G = 11.2 \times 10^6$ psi.

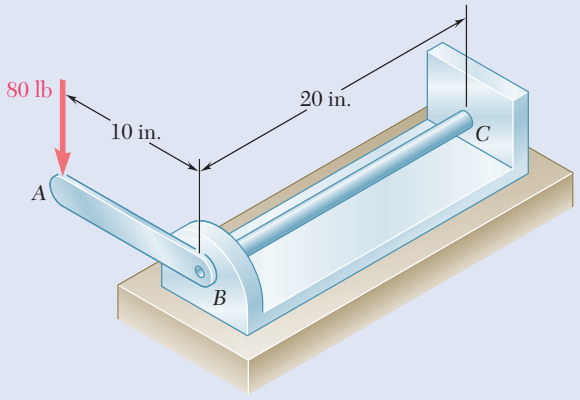


Fig. P9.93

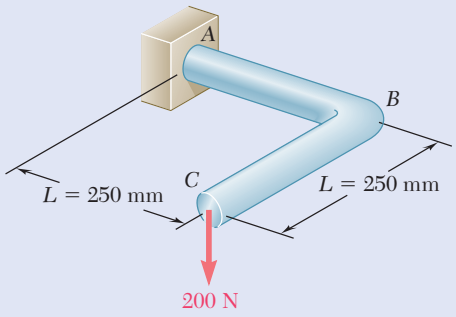


Fig. P9.94

9.94 A 16-mm-diameter rod has been bent into the shape shown. Determine the deflection of end *C* after the 200-N force is applied. Use $E = 200$ GPa and $G = 80$ GPa.

*9.5 MOMENT-AREA THEOREMS

*9.5A General Principles

In Sec. 9.1 through Sec. 9.3 we used a mathematical method based on the integration of a differential equation to determine the deflection and slope of a beam at any given point. The bending moment was expressed as a function $M(x)$ of the distance x measured along the beam, and two successive integrations led to the functions $\theta(x)$ and $y(x)$ representing, respectively, the slope and deflection at any point of the beam. In this section you will see how geometric properties of the elastic curve can be used to determine the deflection and slope of a beam at a specific point (Photo 9.4).



Photo 9.4 The maximum deflection of each beam supporting the floors of a building should be taken into account in the design process.

First Moment-Area Theorem. Consider a beam AB subjected to some arbitrary loading (Fig. 9.23*a*). Draw the diagram representing the variation along the beam of M/EI obtained by dividing the bending moment M by the flexural rigidity EI (Fig. 9.23*b*). Except for a difference in the scales of ordinates, this diagram is the same as the bending-moment diagram if the flexural rigidity of the beam is constant.

Recalling Eq. (9.4) and that $dy/dx = \theta$,

$$\frac{d\theta}{dx} = \frac{d^2y}{dx^2} = \frac{M}{EI}$$

or

$$d\theta = \frac{M}{EI}\,dx \qquad \textbf{(9.15)}^{\dagger}$$

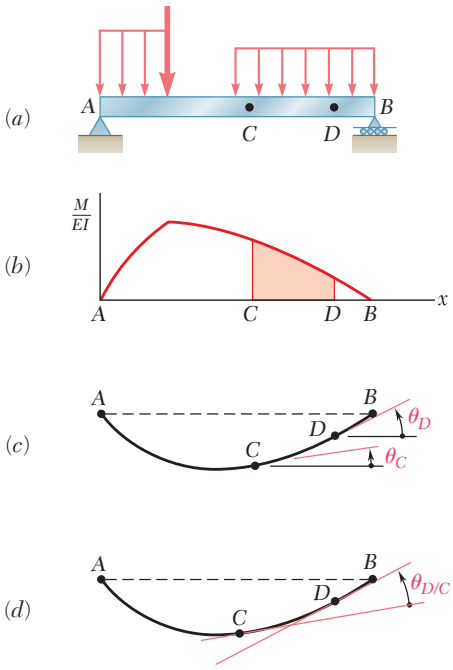


Fig. 9.23 First moment-area theorem. (*a*) Beam subjected to arbitrary load. (*b*) Plot of *M/EI* curve. (*c*) Elastic curve showing slope at *C* and *D*. (*d*) Elastic curve showing slope at *D* with respect to *C*.

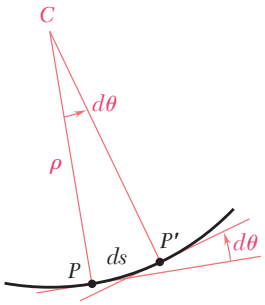


Fig. 9.24 Geometry of the elastic curve used to define the slope at point *P′* with respect to *P*.

†This relationship also can be determined by noting that the angle $d\theta$ formed by the tangents to the elastic curve at P and P' (Fig. 9.24) is also the angle formed by the corresponding normals to that curve. Thus $d\theta = ds/\rho$, where ds is the length of the arc PP' and ρ is the radius of curvature at P. Substituting for $1/\rho$ from Eq. (4.21) and noting that since the slope at P is very small, ds is equal in first approximation to the horizontal distance dx between P and P', we will again obtain Eq. (9.15).

Next consider two arbitrary points C and D on the beam and integrate both members of Eq. (9.15) from C to D:

$$\int_{\theta_C}^{\theta_D} d\theta = \int_{x_C}^{x_D} \frac{M}{EI}\, dx$$

or

$$\theta_D - \theta_C = \int_{x_C}^{x_D} \frac{M}{EI}\, dx \tag{9.16}$$

where θ_C and θ_D indicate the slope at C and D (Fig. 9.24*c*). But the right-hand member of Eq. (9.16) represents the area under the M/EI diagram between C and D, while the left-hand member is the angle between the tangents to the elastic curve at C and D (Fig. 9.23*d*). This angle is given as

$$\theta_{D/C} = \text{area under } M/EI \text{ diagram between } C \text{ and } D \tag{9.17}$$

This is the *first moment-area theorem*.

Note that $\theta_{D/C}$ and the area under the M/EI diagram have the same sign. This positive area (i.e., located above the x axis) corresponds to a counterclockwise rotation of the tangent to the elastic curve moving from C to D, and a negative area corresponds to a clockwise rotation.

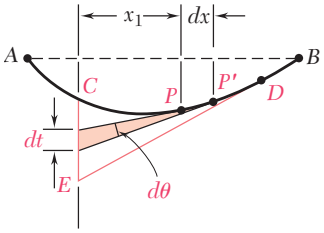


Fig. 9.25 Geometry used to determine the tangential deviation of C with respect to D.

Second Moment-Area Theorem. Now consider two points P and P' located between C and D at a distance dx from each other (Fig. 9.25). The tangents to the elastic curve drawn at P and P' intercept a segment with a length dt on the vertical through point C. Since the slope θ at P and the angle $d\theta$ formed by the tangents at P and P' are both small quantities, dt is assumed to be equal to the arc of the circle of radius x_1 subtending the angle $d\theta$. Therefore,

$$dt = x_1\, d\theta$$

or substituting for $d\theta$ from Eq. (9.15),

$$dt = x_1 \frac{M}{EI}\, dx \tag{9.18}$$

Now integrate Eq. (9.18) from C to D. As point P describes the elastic curve from C to D, the tangent at P sweeps the vertical through C from C to E. Thus, the integral of the left-hand member is equal to the vertical distance from C to the tangent at D. This distance is denoted by $t_{C/D}$ and is called the *tangential deviation of C with respect to D*. Therefore,

$$t_{C/D} = \int_{x_C}^{x_D} x_1 \frac{M}{EI}\, dx \tag{9.19}$$

Observe that $(M/EI)\,dx$ represents an element of area under the (M/EI) diagram, and $x_1\,(M/EI)\,dx$ is the first moment of that element with respect to a vertical axis through C (Fig. 9.26). The right-hand member in Eq. (9.19) represents the first moment with respect to that axis of the area located under the M/EI diagram between C and D.

We can, therefore, state the *second moment-area theorem* as follows: *The tangential deviation $t_{C/D}$ of C with respect to D is equal to the first moment with respect to a vertical axis through C of the area under the (M/EI) diagram between C and D.*

Recalling that the first moment of an area with respect to an axis is equal to the product of the area and the distance from its centroid to that axis, the second moment-area theorem is expressed as:

$$t_{C/D} = (\text{area between } C \text{ and } D)\,\bar{x}_1 \tag{9.20}$$

where the area refers to the area under the M/EI diagram and where $\bar{x}_1$ is the distance from the centroid of the area to the vertical axis through C (Fig. 9.27*a*).

Remember to distinguish between the tangential deviation of C with respect to D ($t_{C/D}$) and the tangential deviation of D with respect to C ($t_{D/C}$). The tangential deviation $t_{D/C}$ represents the vertical distance from D to the tangent to the elastic curve at C and is obtained by multiplying the area under the (M/EI) diagram by the distance $\bar{x}_2$ from its centroid to the vertical axis through D (Fig. 9.27*b*):

$$t_{D/C} = (\text{area between } C \text{ and } D)\,\bar{x}_2 \tag{9.21}$$

Note that if an area under the M/EI diagram is located above the x axis, its first moment with respect to a vertical axis is positive. If it is located below the x axis, its first moment is negative. As shown in Figure 9.27, a point with a *positive* tangential deviation is located *above* the corresponding tangent. A point with a *negative* tangential deviation is located *below* that tangent.

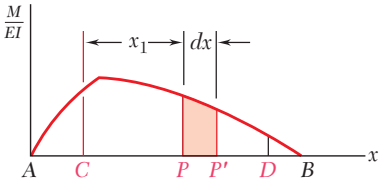


Fig. 9.26 The expression $x_1(M/EI)dx$ is the first moment of the shaded area with respect to C.

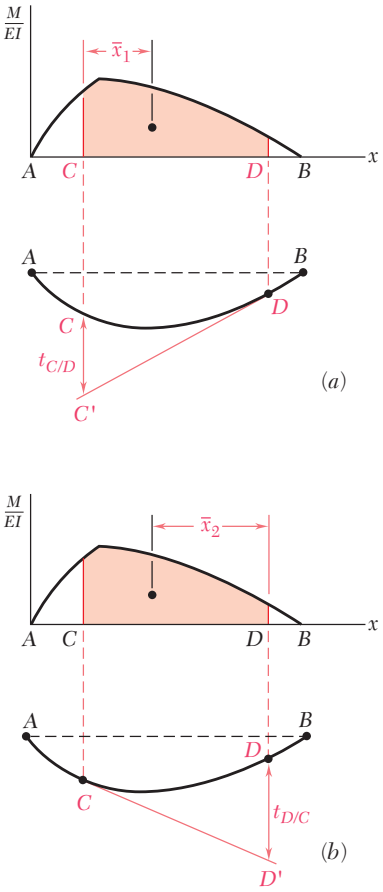
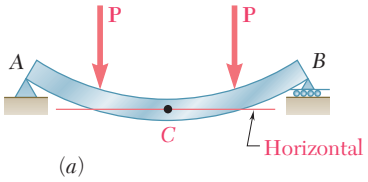


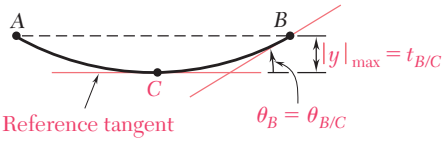
Fig. 9.27 Second moment-area theorem illustrated. (*a*) Evaluating $t_{C/D}$. (*b*) Evaluating $t_{D/C}$.

*9.5B Cantilever Beams and Beams with Symmetric Loadings

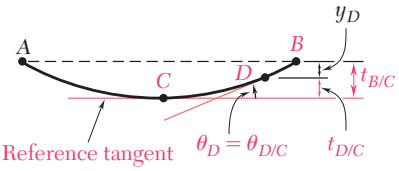
Recall that the first moment-area theorem defines the angle $\theta_{D/C}$ *between* the tangents at two points C and D of the elastic curve. The angle θ_D that the tangent at D forms with the horizontal (i.e., the slope at D) can be obtained only if the slope at C is known. Similarly, the second moment-area theorem defines the vertical distance of one point of the elastic curve from the tangent at another point. Therefore, the tangential deviation $t_{D/C}$ helps to locate point D only if the tangent at C is known. Thus, the two moment-area theorems can be applied effectively to determine slopes and deflections only if a certain *reference tangent* to the elastic curve has been determined.



(a)



(b)



(c)

Fig. 9.29 Application of moment-area method to simply supported beams with symmetric loads. (*a*) Beam and loads. (*b*) Maximum deflection and slope at point *B*. (*c*) Deflection and slope at arbitrary point *D*.

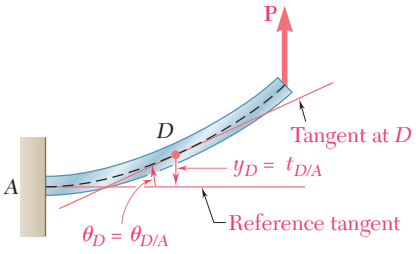
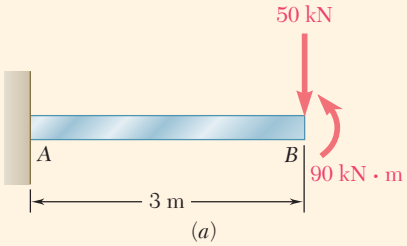


Fig. 9.28 Application of moment-area method to cantilever beams.

In *cantilever beams* (Fig. 9.28), the tangent to the elastic curve at the fixed end A is known and can be used as the reference tangent. Since $\theta_A = 0$, the slope of the beam at any point D is $\theta_D = \theta_{D/A}$ and can be obtained using the first moment-area theorem. On the other hand, the deflection y_D of point D is equal to the tangential deviation $t_{D/A}$ measured from the horizontal reference tangent at A and can be obtained using the second moment-area theorem.

In a simply supported beam AB with a *symmetric load* (Fig. 9.29*a*) or an overhanging symmetric beam with a symmetric load (see Sample Prob. 9.11), the tangent at the center C of the beam must be horizontal (by reason of symmetry) and can be used as the reference tangent (Fig. 9.29*b*). Since $\theta_C = 0$, the slope at the support B is $\theta_B = \theta_{B/C}$ and can be obtained using the first moment-area theorem. Also, $|y|_{max}$ is equal to the tangential deviation $t_{B/C}$ and can be obtained with the second moment-area theorem. The slope at any other point D of the beam (Fig. 9.29*c*) is found in a similar way, and the deflection at D is $y_D = t_{D/C} - t_{B/C}$.



(a)

Fig. 9.30 (*a*) Cantilevered beam with end loads.

Concept Application 9.9

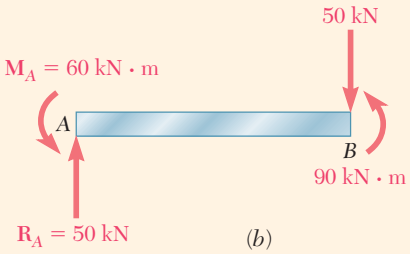
Determine the slope and deflection at end B of the prismatic cantilever beam AB when it is loaded as shown (Fig. 9.30*a*), knowing that the flexural rigidity of the beam is $EI = 10\ \text{MN}\cdot\text{m}^2$.

Draw the free-body diagram of the beam (Fig. 9.30*b*). Summing vertical components and moments about A, the reaction at the fixed end A consists of a 50 kN upward vertical force $\mathbf{R}_A$ and a 60 kN·m counterclockwise couple $\mathbf{M}_A$. Next, draw the bending-moment diagram (Fig. 9.30*c*) and determine from similar triangles the distance x_D from end A to point D of the beam where $M = 0$:

$$\frac{x_D}{60} = \frac{3 - x_D}{90} = \frac{3}{150} \qquad x_D = 1.2\ \text{m}$$

Dividing the values obtained for M by the flexural rigidity EI, draw the M/EI diagram (Fig. 9.30*d*) and compute the areas corresponding respectively to the segments AD and DB, assigning a positive sign to

(continued)



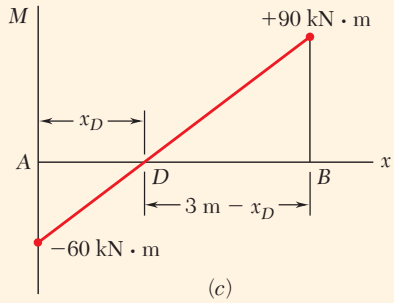


Fig. 9.30 (*b*) Free-body diagram with reactions. (*c*) Moment diagram.

the area located above the x axis and a negative sign to the area located below that axis. Use the first moment-area theorem to obtain

$$\begin{aligned}\theta_{B/A} &= \theta_B - \theta_A = \text{area from } A \text{ to } B = A_1 + A_2\\ &= -\tfrac{1}{2}(1.2\text{ m})(6 \times 10^{-3}\text{ m}^{-1}) + \tfrac{1}{2}(1.8\text{ m})(9 \times 10^{-3}\text{ m}^{-1})\\ &= -3.6 \times 10^{-3} + 8.1 \times 10^{-3}\\ &= +4.5 \times 10^{-3}\text{ rad}\end{aligned}$$

and, since $\theta_A = 0$,

$$\theta_B = +4.5 \times 10^{-3}\text{ rad}$$

Using the second moment-area theorem, the tangential deviation $t_{B/A}$ is equal to the first moment about a vertical axis through B of the total area between A and B. The moment of each partial area is the product of that area and the distance from its centroid to the axis through B:

$$\begin{aligned}t_{B/A} &= A_1(2.6\text{ m}) + A_2(0.6\text{ m})\\ &= (-3.6 \times 10^{-3})(2.6\text{ m}) + (8.1 \times 10^{-3})(0.6\text{ m})\\ &= -9.36\text{ mm} + 4.86\text{ mm} = -4.50\text{ mm}\end{aligned}$$

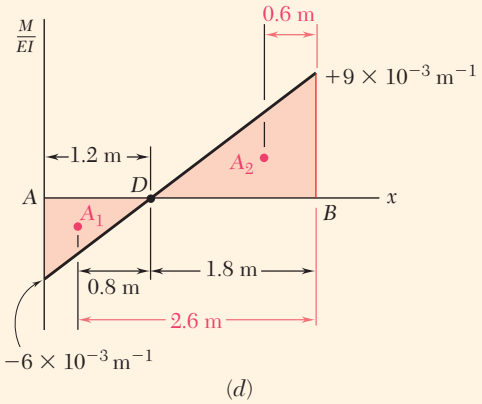


Fig. 9.30 (*d*) Plot of *M/EI* showing locations of area centroids.

Since the reference tangent at A is horizontal, the deflection at B is equal to $t_{B/A}$, so

$$y_B = t_{B/A} = -4.50\text{ mm}$$

The deflected beam is shown in Fig. 9.30*e*.

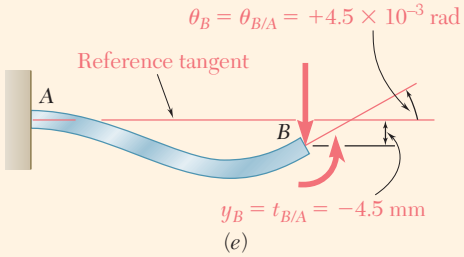


Fig. 9.30 (*e*) Deflected beam showing slope and deflection results at end *B*.

*9.5C Bending-Moment Diagrams by Parts

In many applications, the angle $\theta_{D/C}$ and the tangential deviation $t_{D/C}$ are easier to determine if the effect of each load is evaluated independently. A separate M/EI diagram is drawn for each load, and angle $\theta_{D/C}$ is obtained by adding the areas under the various diagrams. Similarly, the tangential deviation $t_{D/C}$ is obtained by adding the first moments of these areas about a vertical axis through D. A bending-moment or M/EI diagram plotted this way is said to be *drawn by parts*.

When an M/EI diagram is drawn by parts, the areas defined consist of simple geometric shapes, such as rectangles, triangles, and parabolic spandrels. The areas and centroids of some of these shapes are shown in Fig. 9.31.

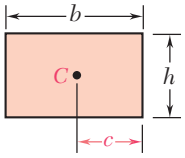
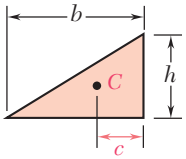
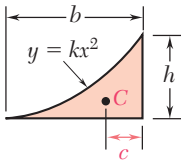
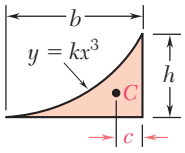
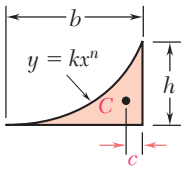
Shape		Area	c
Rectangle		bh	$\frac{b}{2}$
Triangle		$\frac{bh}{2}$	$\frac{b}{3}$
Parabolic spandrel		$\frac{bh}{3}$	$\frac{b}{4}$
Cubic spandrel		$\frac{bh}{4}$	$\frac{b}{5}$
General spandrel		$\frac{bh}{n+1}$	$\frac{b}{n+2}$

Fig. 9.31 Areas and centroids of common shapes.

Concept Application 9.10

Determine the slope and deflection at end B of the prismatic beam of Concept Application 9.9, drawing the bending-moment diagram by parts.

The given load is replaced by the two equivalent loads shown in Fig. 9.32*a*, and the corresponding bending-moment and M/EI diagrams are drawn from right to left, starting at the free end B.

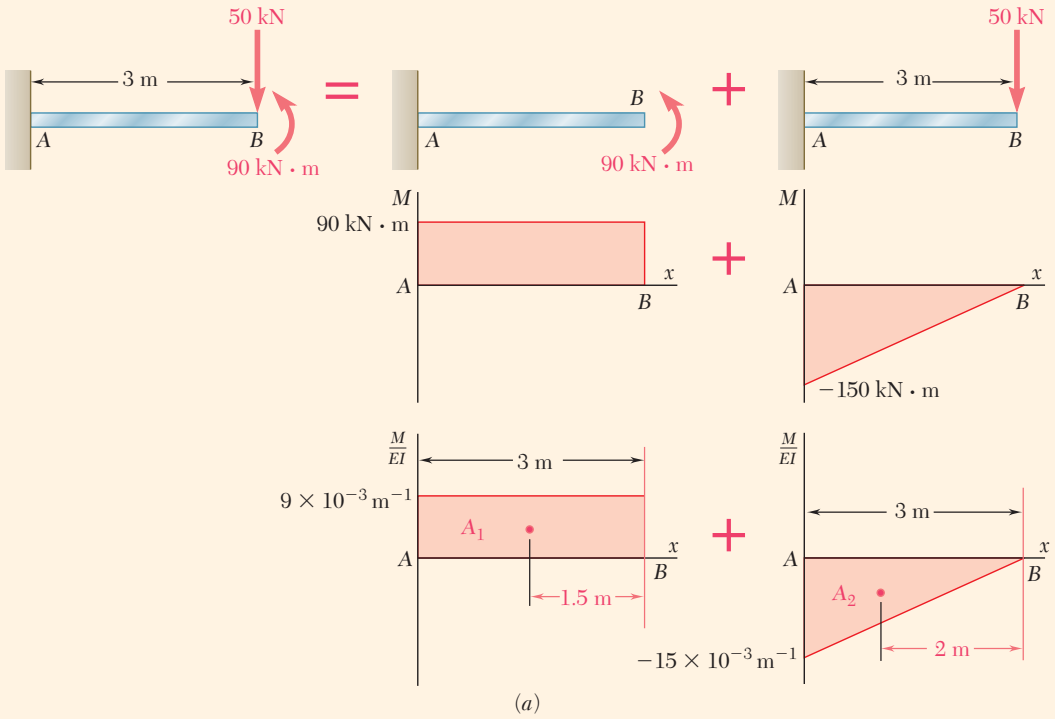


Fig. 9.32 (*a*) Superposition of loads and their resulting bending-moment and *M/EI* diagrams.

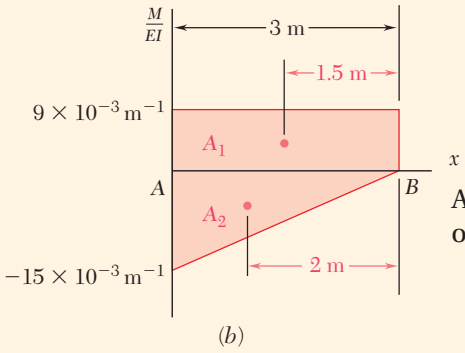


Fig. 9.32 *M/EI* diagrams combined into a single drawing.

Applying the first moment-area theorem and recalling that $\theta_A = 0$

$$\theta_B = \theta_{B/A} = A_1 + A_2$$
$$= (9 \times 10^{-3}\,\text{m}^{-1})(3\,\text{m}) - \tfrac{1}{2}(15 \times 10^{-3}\,\text{m}^{-1})(3\,\text{m})$$
$$= 27 \times 10^{-3} - 22.5 \times 10^{-3} = 4.5 \times 10^{-3}\,\text{rad}$$

Applying the second moment-area theorem, compute the first moment of each area about a vertical axis through B and write

$$y_B = t_{B/A} = A_1(1.5\,\text{m}) + A_2(2\,\text{m})$$
$$= (27 \times 10^{-3})(1.5\,\text{m}) - (22.5 \times 10^{-3})(2\,\text{m})$$
$$= 40.5\,\text{mm} - 45\,\text{mm} = -4.5\,\text{mm}$$

It practice, it is convenient to combine the two portions of the M/EI diagram into a single drawing (Fig. 9.32*b*).

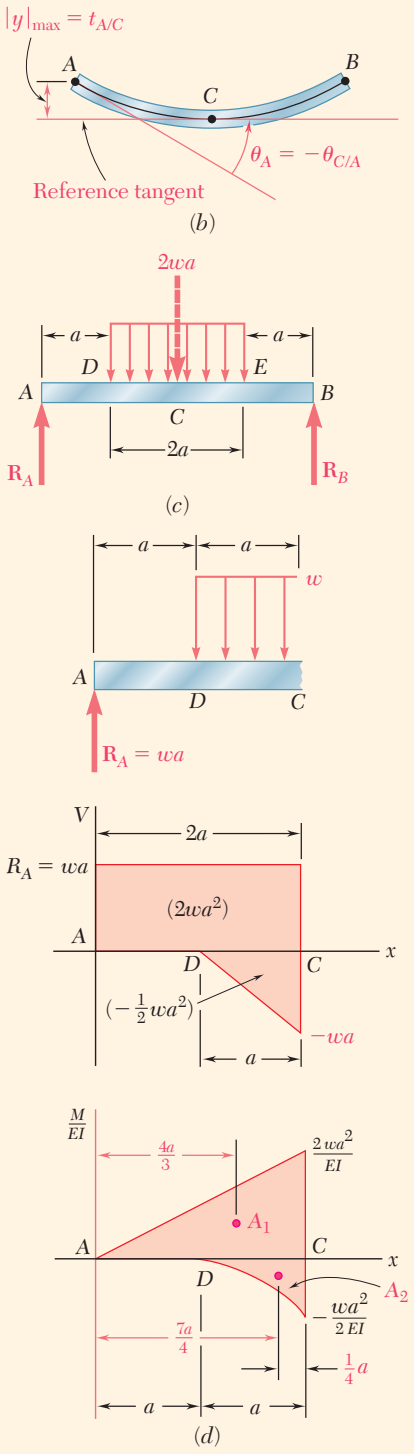


Fig. 9.33 (*b*) Elastic curve with maximum deflection and slope at point *A* shown. (*c*) Free-body diagram of the beam. (*d*) Shear and *M*/*EI* diagrams for the left half of the beam.

Concept Application 9.11

For the prismatic beam *AB* and the loading shown in Fig. 9.33*a*, determine the slope at a support and the maximum deflection.

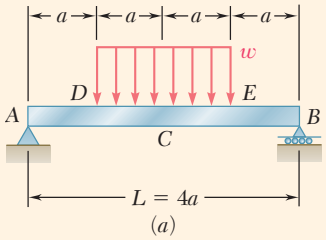


Fig. 9.33 (*a*) Simply supported beam with symmetric distributed loading.

Sketch the deflected beam (Fig. 9.33*b*). Since the tangent at the center *C* of the beam is horizontal, it is used as the reference tangent, and $|y|_{max} = t_{A/C}$. But since $\theta_C = 0$,

$$\theta_{C/A} = \theta_C - \theta_A = -\theta_A \qquad \text{or} \qquad \theta_A = -\theta_{C/A}$$

The free-body diagram of the beam (Fig. 9.33*c*) shows

$$R_A = R_B = wa$$

Next, the shear and bending-moment diagrams are drawn for portion *AC* of the beam. These diagrams are drawn by parts, considering the effects of the reaction $\mathbf{R}_A$ and of the distributed load separately. However, for convenience the two parts of each diagram have been plotted together in Fig. 9.33*d*. Recall that when the distributed load is uniform, the corresponding parts of the shear and bending-moment diagrams are, respectively, linear and parabolic. The area and centroid of the triangle and of the parabolic spandrel are obtained by referring to Fig. 9.31. The areas of the triangle and spandrel are

$$A_1 = \frac{1}{2}(2a)\left(\frac{2wa^2}{EI}\right) = \frac{2wa^3}{EI}$$

and

$$A_2 = -\frac{1}{3}(a)\left(\frac{wa^2}{2EI}\right) = -\frac{wa^3}{6EI}$$

Applying the first moment-area theorem,

$$\theta_{C/A} = A_1 + A_2 = \frac{2wa^3}{EI} - \frac{wa^3}{6EI} = \frac{11wa^3}{6EI}$$

Recall from Figs. 9.33*a* and *b* that $a = \frac{1}{4}L$ and $\theta_A = -\theta_{C/A}$, making

$$\theta_A = -\frac{11wa^3}{6EI} = -\frac{11wL^3}{384EI}$$

Applying the second moment-area theorem

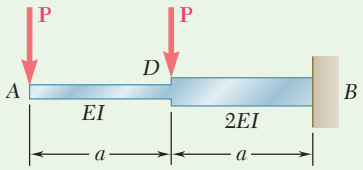
$$t_{A/C} = A_1\frac{4a}{3} + A_2\frac{7a}{4} = \left(\frac{2wa^3}{EI}\right)\frac{4a}{3} + \left(-\frac{wa^3}{6EI}\right)\frac{7a}{4} = \frac{19wa^4}{8EI}$$

and

$$|y|_{max} = t_{A/C} = \frac{19wa^4}{8EI} = \frac{19wL^4}{2048EI}$$

Sample Problem 9.10

Prismatic rods *AD* and *DB* are welded together to form the cantilever beam *ADB*. Knowing that the flexural rigidity is *EI* in portion *AD* of the beam and 2*EI* in portion *DB*, determine the slope and deflection at end *A* for the loading shown.



STRATEGY: To apply the moment-area theorems, you should first obtain the *M/EI* diagram for the beam. For a cantilever beam, it is convenient to place the reference tangent at the fixed end, since it is known to be horizontal.

MODELING and ANALYSIS:

(M/EI) Diagram. Referring to Fig. 1, draw the bending-moment diagram for the beam and then obtain the *M/EI* diagram by dividing the value of *M* at each point of the beam by the corresponding value of the flexural rigidity.

Reference Tangent. Referring to Fig. 2, choose the horizontal tangent at the fixed end *B* as the reference tangent. Since $\theta_B = 0$ and $y_B = 0$,

$$\theta_A = -\theta_{B/A} \quad y_A = t_{A/B}$$

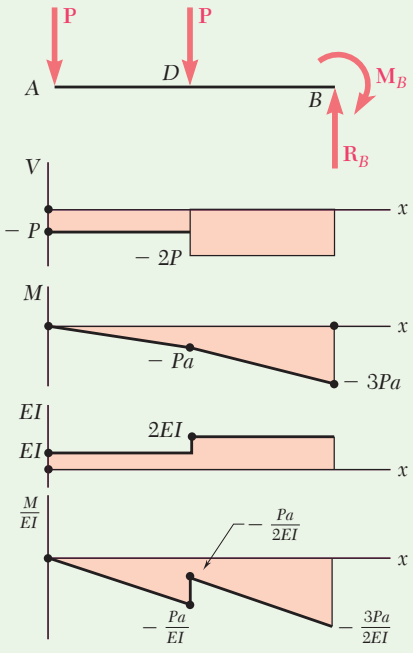


Fig. 1 Free-body diagram and construction of the *M/EI* diagram.

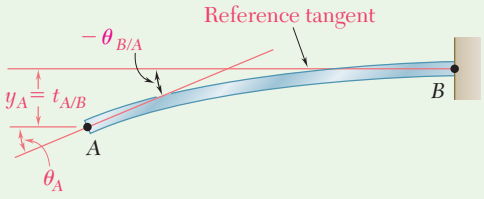


Fig. 2 Slope and deflection at end *A* related to reference tangent at fixed end *B*.

(continued)

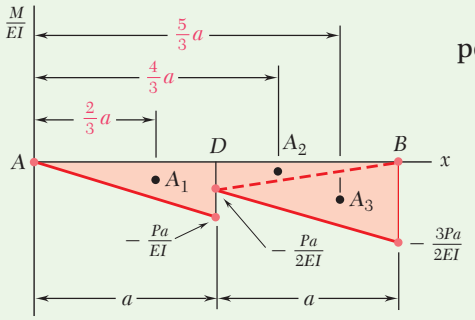


Fig. 3 Areas and centroids of moment-area diagram used to find slope and deflection.

Slope at *A*. Divide the *M/EI* diagram into the three triangular portions shown in Fig. 3.

$$A_1 = -\frac{1}{2}\frac{Pa}{EI}a = -\frac{Pa^2}{2EI}$$

$$A_2 = -\frac{1}{2}\frac{Pa}{2EI}a = -\frac{Pa^2}{4EI}$$

$$A_3 = -\frac{1}{2}\frac{3Pa}{2EI}a = -\frac{3Pa^2}{4EI}$$

Using the first moment-area theorem,

$$\theta_{B/A} = A_1 + A_2 + A_3 = -\frac{Pa^2}{2EI} - \frac{Pa^2}{4EI} - \frac{3Pa^2}{4EI} = -\frac{3Pa^2}{2EI}$$

$$\theta_A = -\theta_{B/A} = +\frac{3Pa^2}{2EI} \qquad \theta_A = \frac{3Pa^2}{2EI}\measuredangle$$

Deflection at *A*. Using the second moment-area theorem,

$$y_A = t_{A/B} = A_1\left(\frac{2}{3}a\right) + A_2\left(\frac{4}{3}a\right) + A_3\left(\frac{5}{3}a\right)$$

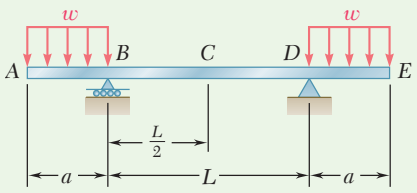
$$= \left(-\frac{Pa^2}{2EI}\right)\frac{2a}{3} + \left(-\frac{Pa^2}{4EI}\right)\frac{4a}{3} + \left(-\frac{3Pa^2}{4EI}\right)\frac{5a}{3}$$

$$y_A = -\frac{23Pa^3}{12EI} \qquad y_A = \frac{23Pa^3}{12EI}\downarrow$$

REFLECT and THINK: This example demonstrates that the moment-area theorems can be just as easily used for nonprismatic beams as for prismatic beams.

Sample Problem 9.11

For the prismatic beam and loading shown, determine the slope and deflection at end *E*.



STRATEGY: To apply the moment-area theorems, you should first obtain the *M/EI* diagram for the beam. Due to the symmetry of both the beam and its loading, it is convenient to place the reference tangent at the mid-point since it is known to be horizontal.

(continued)

MODELING and ANALYSIS:

***M/EI* Diagram.** From a free-body diagram of the beam (Fig. 1), determine the reactions and then draw the shear and bending-moment diagrams. Since the flexural rigidity of the beam is constant, divide each value of M by EI and obtain the M/EI diagram shown.

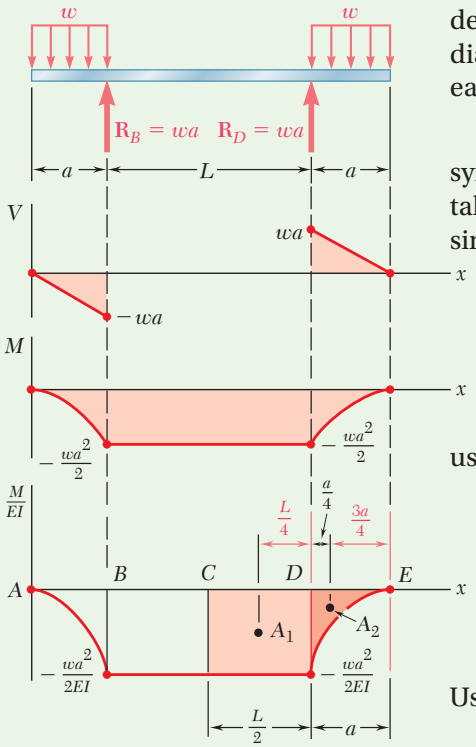


Fig. 1 Free-body diagram and construction of the moment-area diagram.

Reference Tangent. In Fig. 2, since the beam and its loads are symmetric with respect to the midpoint C, the tangent at C is horizontal and can be used as the reference tangent. Referring to Fig. 2 and since $\theta_C = 0$,

$$\theta_E = \theta_C + \theta_{E/C} = \theta_{E/C} \tag{1}$$

$$y_E = t_{E/C} - t_{D/C} \tag{2}$$

Slope at *E*. Referring to the M/EI diagram shown in Fig. 1 and using the first moment-area theorem,

$$A_1 = -\frac{wa^2}{2EI}\left(\frac{L}{2}\right) = -\frac{wa^2L}{4EI}$$

$$A_2 = -\frac{1}{3}\left(\frac{wa^2}{2EI}\right)(a) = -\frac{wa^3}{6EI}$$

Using Eq. (1),

$$\theta_E = \theta_{E/C} = A_1 + A_2 = -\frac{wa^2L}{4EI} - \frac{wa^3}{6EI}$$

$$\theta_E = -\frac{wa^2}{12EI}(3L + 2a) \qquad \theta_E = \frac{wa^2}{12EI}(3L + 2a) \curvearrowright$$

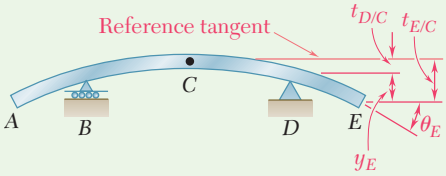


Fig. 2 Due to symmetry, reference tangent at midpoint C is horizontal. Shown are the slope and deflection at end E related to this reference tangent.

Deflection at *E*. Use the second moment-area theorem to write

$$t_{D/C} = A_1\frac{L}{4} = \left(-\frac{wa^2L}{4EI}\right)\frac{L}{4} = -\frac{wa^2L^2}{16EI}$$

$$t_{E/C} = A_1\left(a + \frac{L}{4}\right) + A_2\left(\frac{3a}{4}\right)$$

$$= \left(-\frac{wa^2L}{4EI}\right)\left(a + \frac{L}{4}\right) + \left(-\frac{wa^3}{6EI}\right)\left(\frac{3a}{4}\right)$$

$$= -\frac{wa^3L}{4EI} - \frac{wa^2L^2}{16EI} - \frac{wa^4}{8EI}$$

Use Eq. (2) to obtain

$$y_E = t_{E/C} - t_{D/C} = -\frac{wa^3L}{4EI} - \frac{wa^4}{8EI}$$

$$y_E = -\frac{wa^3}{8EI}(2L + a) \qquad y_E = \frac{wa^3}{8EI}(2L + a) \downarrow$$

Problems

Use the moment-area method to solve the following problems.

9.95 through 9.98 For the uniform cantilever beam and loading shown, determine (*a*) the slope at the free end, (*b*) the deflection at the free end.

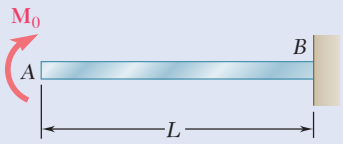


Fig. P9.95

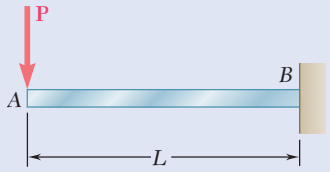


Fig. P9.96

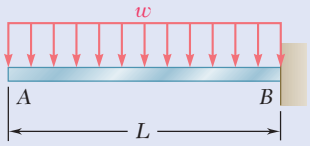


Fig. P9.97

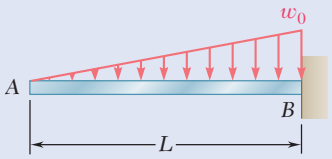


Fig. P9.98

9.99* and *9.100 For the uniform cantilever beam and loading shown, determine the slope and deflection at (*a*) point *B*, (*b*) point *C*.

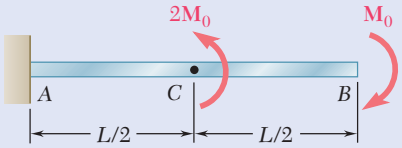


Fig. *P9.99*

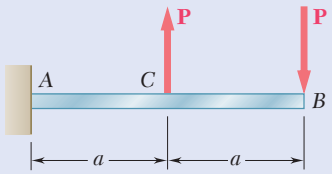


Fig. *P9.100*

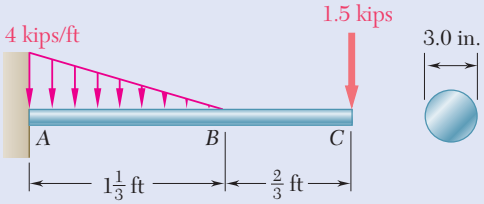


Fig. P9.101

9.101 For the cantilever beam and loading shown, determine (*a*) the slope at point *C*, (*b*) the deflection at point *C*. Use $E = 29 \times 10^6$ psi.

9.102 For the cantilever beam and loading shown, determine (*a*) the slope at point *A*, (*b*) the deflection at point *A*. Use $E = 200$ GPa.

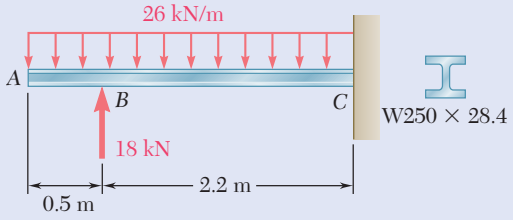


Fig. P9.102

9.103 Two C6 × 8.2 channels are welded back to back and loaded as shown. Knowing that $E = 29 \times 10^6$ psi, determine (*a*) the slope at point *D*, (*b*) the deflection at point *D*.

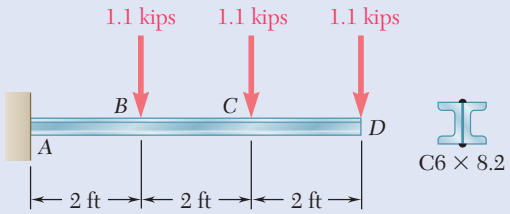


Fig. P9.103

9.104 For the cantilever beam and loading shown, determine (*a*) the slope at point *A*, (*b*) the deflection at point *A*. Use $E = 200$ GPa.

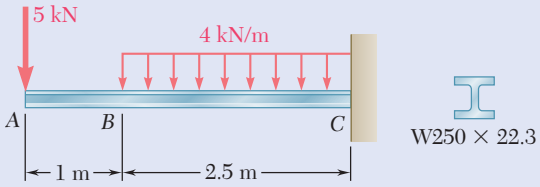


Fig. P9.104

9.105 For the cantilever beam and loading shown, determine (*a*) the slope at point *A*, (*b*) the deflection at point *A*.

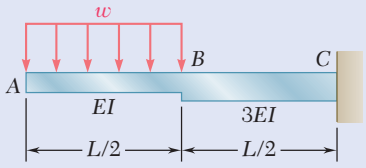


Fig. P9.105

9.106 For the cantilever beam and loading shown, determine the deflection and slope at end *A* caused by the moment $\mathbf{M}_0$.

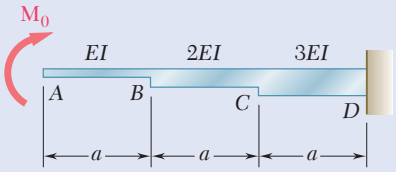


Fig. P9.106

9.107 Two cover plates are welded to the rolled-steel beam as shown. Using $E = 200$ GPa, determine (*a*) the slope at end *A*, (*b*) the deflection at end *A*.

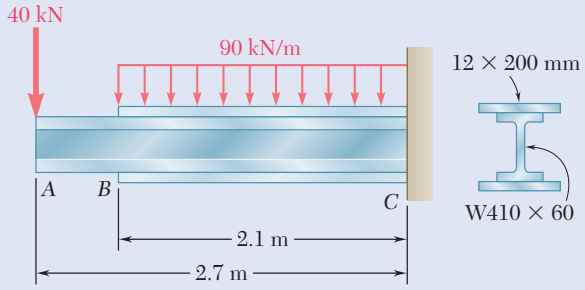


Fig. P9.107

9.108 Two cover plates are welded to the rolled-steel beam as shown. Using $E = 29 \times 10^6$ psi, determine (*a*) the slope at end *C*, (*b*) the deflection at end *C*.

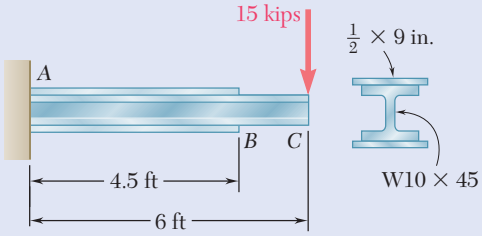


Fig. *P9.108*

9.109 through 9.114 For the prismatic beam and loading shown, determine (*a*) the slope at end *A*, (*b*) the deflection at the center *C* of the beam.

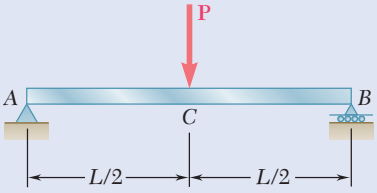


Fig. P9.109

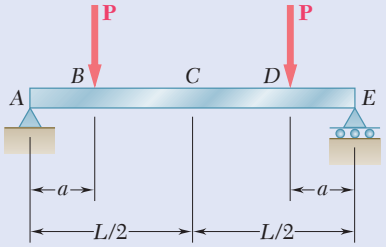


Fig. P9.110

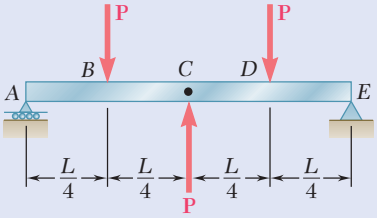


Fig. P9.111

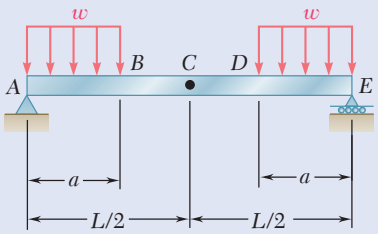


Fig. P9.112

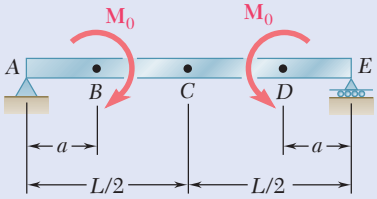


Fig. P9.113

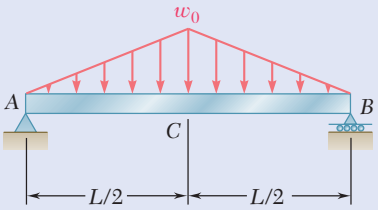


Fig. *P9.114*

9.115 and 9.116 For the beam and loading shown, determine (*a*) the slope at end *A*, (*b*) the deflection at the center *C* of the beam.

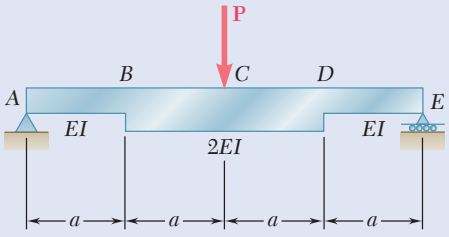


Fig. P9.115

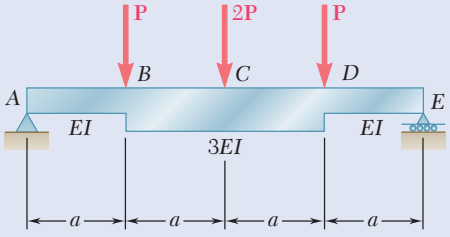


Fig. *P9.116*

9.117 Knowing that the magnitude of the load **P** is 7 kips, determine (*a*) the slope at end *A*, (*b*) the deflection at end *A*, (*c*) the deflection at midpoint *C* of the beam. Use $E = 29 \times 10^6$ psi.

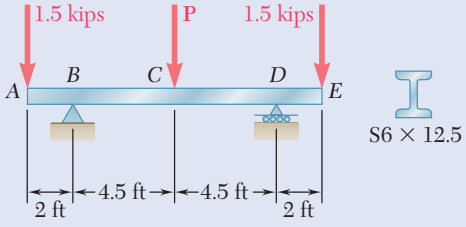
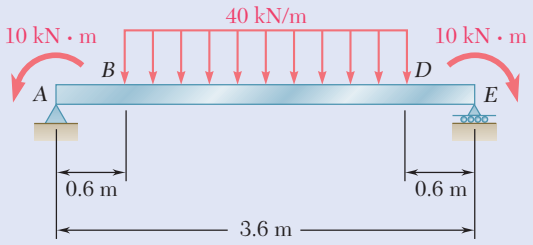


Fig. *P9.117*

9.118 and 9.119 For the beam and loading shown, determine (*a*) the slope at end *A*, (*b*) the deflection at the midpoint of the beam. Use $E = 200$ GPa.



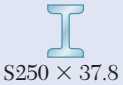


Fig. P9.118

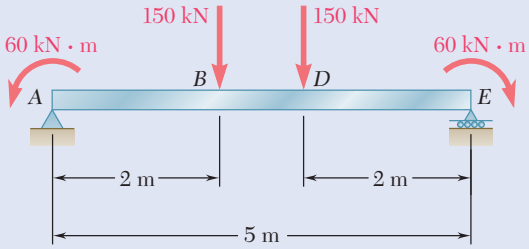




Fig. P9.119

9.120 For the beam and loading shown and knowing that $w = 8$ kN/m, determine (*a*) the slope at end *A*, (*b*) the deflection at midpoint *C*. Use $E = 200$ GPa.

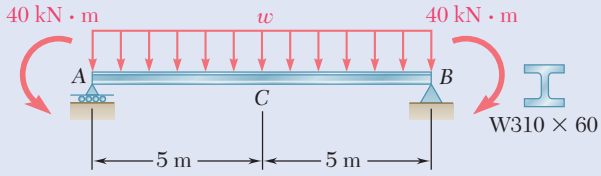


Fig. P9.120

***9.121** For the beam and loading of Prob. 9.117, determine (*a*) the load **P** for which the deflection is zero at the midpoint *C* of the beam, (*b*) the corresponding deflection at end *A*. Use $E = 29 \times 10^6$ psi.

9.122 For the beam and loading of Prob. 9.120, determine the value of *w* for which the deflection is zero at the midpoint *C* of the beam. Use $E = 200$ GPa.

***9.123** A uniform rod *AE* is to be supported at two points *B* and *D*. Determine the distance *a* for which the slope at ends *A* and *E* is zero.

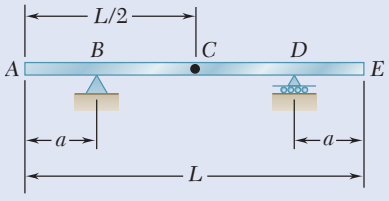


Fig. P9.123 and P9.124

***9.124** A uniform rod *AE* is to be supported at two points *B* and *D*. Determine the distance *a* from the ends of the rod to the points of support, if the downward deflections of points *A*, *C*, and *E* are to be equal.

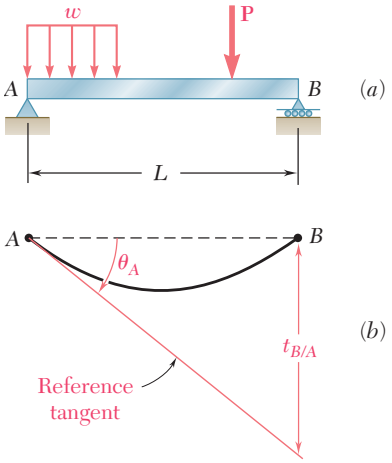


Fig. 9.34 (*a*) Unsymmetric loading. (*b*) Application of moment-area method to find slope at point *A*.

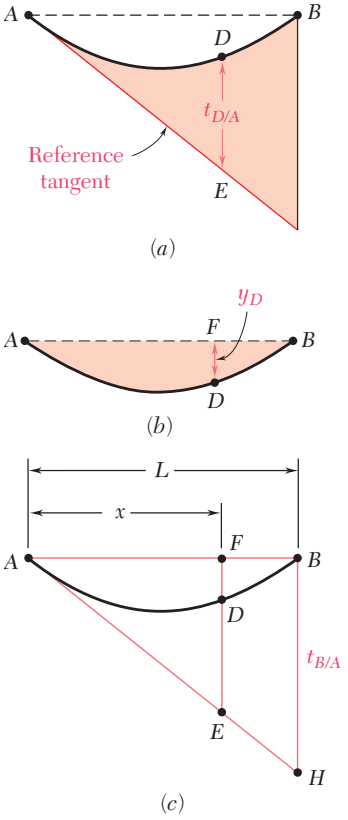


Fig. 9.36 (*a*) Tangential deviation of point *D* with respect to point *A*. (*b*) Deflection of point *D*. (*c*) Knowing *HB* through $t_{B/A}$, *EF* can be found by similar triangles.

*9.6 MOMENT-AREA THEOREMS APPLIED TO BEAMS WITH UNSYMMETRIC LOADINGS

*9.6A General Principles

When a simply supported or overhanging beam carries a symmetric load, the tangent at the center *C* of the beam is horizontal and can be used as the reference tangent (Sec. 9.6). When a simply supported or overhanging beam carries an unsymmetric load, it is not always possible to determine by inspection the point of the beam where the tangent is horizontal. Other means must be used to locate a reference tangent (i.e., a tangent of known slope for applying either of the two moment-area theorems).

It is usually convenient to select the reference tangent at one of the beam supports. For example, considering the tangent at the support *A* of the simply supported beam *AB* (Fig. 9.34), its slope can be determined by computing the tangential deviation $t_{B/A}$ of the support *B* with respect to *A* and dividing $t_{B/A}$ by the distance *L* between the supports. Recalling that the tangential deviation of a point located above the tangent is positive,

$$\theta_A = -\frac{t_{B/A}}{L} \tag{9.22}$$

Once the slope of the reference tangent has been found, the slope θ_D of the beam at any point *D* (Fig. 9.35) can be determined by using the first moment-area theorem to obtain $\theta_{D/A}$, and then writing:

$$\theta_D = \theta_A + \theta_{D/A} \tag{9.23}$$

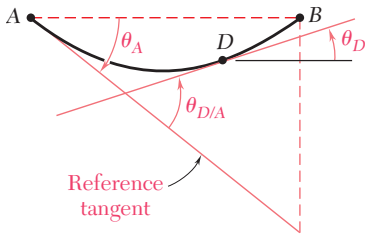


Fig. 9.35 Finding the tangential deviation between supports provides a convenient reference tangent for evaluating slopes.

The tangential deviation $t_{D/A}$ of *D* with respect to the support *A* can be obtained from the second moment-area theorem. Note that $t_{D/A}$ is equal to segment *ED* (Fig. 9.36*a*) and represents the vertical distance *D* *from the reference tangent*. On the other hand, the deflection y_D of point *D* represents the vertical distance of *D* *from the horizontal line AB* (Fig. 9.36*b*). Since y_D is equal in magnitude to the segment *FD*, it can be expressed as the difference between *EF* and *ED* (Fig. 9.36*c*). Observing from the similar triangles *AFE* and *ABH* that

$$\frac{EF}{x} = \frac{HB}{L} \qquad \text{or} \qquad EF = \frac{x}{L}t_{B/A}$$

and recalling the sign conventions used for deflections and tangential deviations,

$$y_D = ED - EF = t_{D/A} - \frac{x}{L}t_{B/A} \tag{9.24}$$

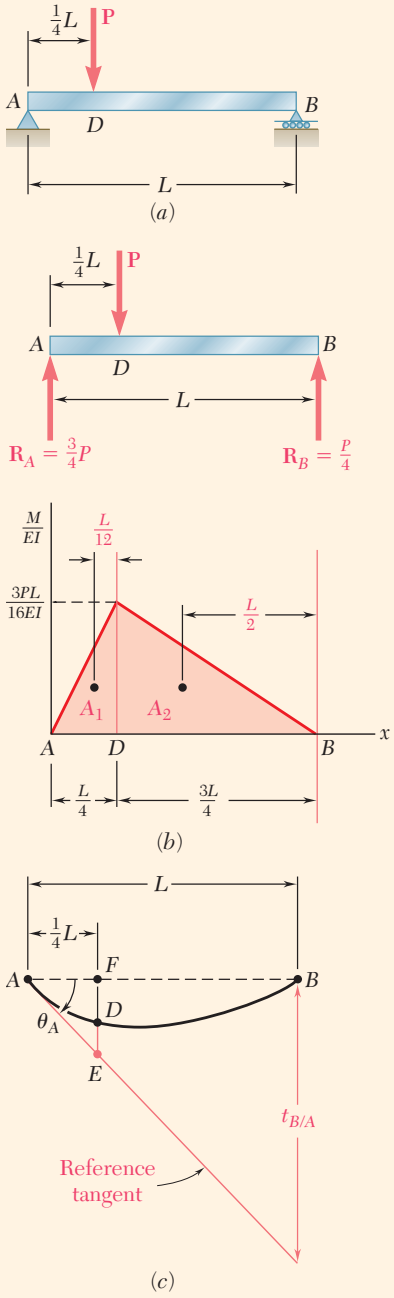


Fig. 9.37 (*a*) Simply supported beam with unsymmetric load. (*b*) Free-body diagram and *M/EI* diagram. (*c*) Reference tangent and geometry to determine slope and deflection at point *D*.

Concept Application 9.12

For the prismatic beam and loading shown (Fig. 9.37*a*), determine the slope and deflection at point *D*.

Reference Tangent at Support A. Compute the reactions at the supports and draw the M/EI diagram (Fig. 9.37*b*). The tangential deviation $t_{B/A}$ of support B with respect to support A is found by applying the second moment-area theorem and computing the moments about a vertical axis through B of the areas A_1 and A_2.

$$A_1 = \frac{1}{2}\frac{L}{4}\frac{3PL}{16EI} = \frac{3PL^2}{128EI} \qquad A_2 = \frac{1}{2}\frac{3L}{4}\frac{3PL}{16EI} = \frac{9PL^2}{128EI}$$

$$t_{B/A} = A_1\left(\frac{L}{12} + \frac{3L}{4}\right) + A_2\left(\frac{L}{2}\right)$$

$$= \frac{3PL^2}{128EI}\frac{10L}{12} + \frac{9PL^2}{128EI}\frac{L}{2} = \frac{7PL^3}{128EI}$$

The slope of the reference tangent at A (Fig. 9.37*c*) is

$$\theta_A = -\frac{t_{B/A}}{L} = -\frac{7PL^2}{128EI}$$

Slope at D. Applying the first moment-area theorem from A to D,

$$\theta_{D/A} = A_1 = \frac{3PL^2}{128EI}$$

Thus, the slope at D is

$$\theta_D = \theta_A + \theta_{D/A} = -\frac{7PL^2}{128EI} + \frac{3PL^2}{128EI} = -\frac{PL^2}{32EI}$$

Deflection at D. The tangential deviation $DE = t_{D/A}$ is found by computing the moment of the area A_1 about a vertical axis through D:

$$DE = t_{D/A} = A_1\left(\frac{L}{12}\right) = \frac{3PL^2}{128EI}\frac{L}{12} = \frac{PL^3}{512EI}$$

The deflection at D is equal to the difference between the segments DE and EF (Fig. 9.37*c*). Thus,

$$y_D = DE - EF = t_{D/A} - \tfrac{1}{4}t_{B/A}$$

$$= \frac{PL^3}{512EI} - \frac{1}{4}\frac{7PL^3}{128EI}$$

$$y_D = -\frac{3PL^3}{256EI} = -0.01172PL^3/EI$$

*9.6B Maximum Deflection

When a simply supported or overhanging beam carries an unsymmetric load, the maximum deflection generally does not occur at the center of the beam. As shown in Photo 9.5, the bridge is loaded by the truck at each axle location. To determine the maximum deflection of such a beam, it is first necessary to locate point K of the beam where the tangent is horizontal. The deflection at that point is the maximum deflection.



Photo 9.5 The deflections of the beams used for the bridge must be reviewed for different possible positions of the truck.

This analysis must begin by determining a reference tangent at one of the supports. If support A is selected, the slope θ_A of the tangent at A is obtained by computing the tangential deviation $t_{B/A}$ of support B with respect to A and dividing that quantity by the distance L between the two supports.

Since the slope θ_K at point K is zero (Fig. 9.38*a*),

$$\theta_{K/A} = \theta_K - \theta_A = 0 - \theta_A = -\theta_A$$

Recalling the first moment-area theorem, point K can be found from the M/EI diagram knowing that $\theta_{K/A} = -\theta_A$ (Fig. 9.38*b*).

Observing that the maximum deflection $|y|_{\max}$ is equal to the tangential deviation $t_{A/K}$ of support A with respect to K (Fig. 9.38*a*), $|y|_{\max}$ is found by computing the first moment with respect to the vertical axis through A of the area between A and K (Fig. 9.38*b*).

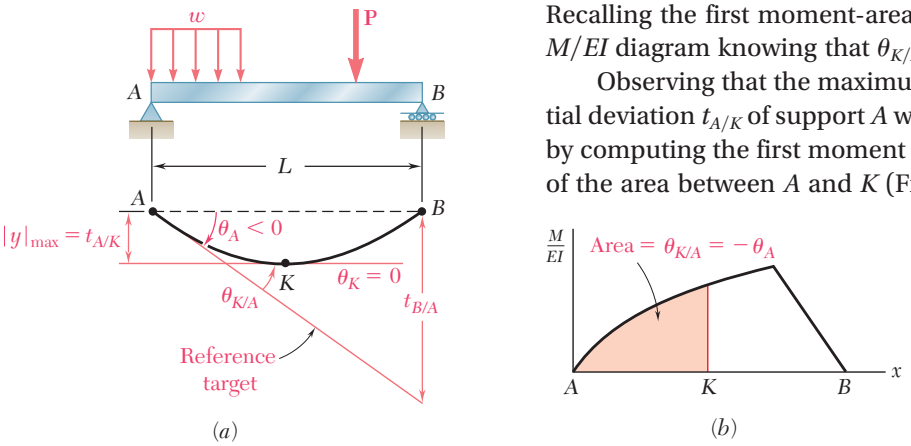


Fig. 9.38 Determination of maximum deflection using moment-area method. (*a*) The maximum deflection occurs at a point K where $\theta_K = 0$, which is where $\theta_{K/A} = -\theta_A$. (*b*) With point K so located, the maximum deflection is equal to the first moment of the shaded area with respect to A.

Concept Application 9.13

Determine the maximum deflection of the beam of Concept Application 9.12. The free-body diagram is shown in Fig. 9.39*a*.

Determination of Point K Where Slope Is Zero. Recall that the slope at point D, where the load is applied, is negative. It follows that point K, where the slope is zero, is located between D and the support B (Fig. 9.39*b*). Our computations are simplified if the slope at K is related to the slope at B, rather than to the slope at A.

Since the slope at A has already been determined in Concept Application 9.12, the slope at B is obtained by

$$\theta_B = \theta_A + \theta_{B/A} = \theta_A + A_1 + A_2$$

$$\theta_B = -\frac{7PL^2}{128EI} + \frac{3PL^2}{128EI} + \frac{9PL^2}{128EI} = \frac{5PL^2}{128EI}$$

Observing that the bending moment at a distance u from end B is $M = \frac{1}{4}Pu$ (Fig. 9.39*c*), the area A' located between K and B under the M/EI diagram (Fig. 9.39*d*) is expressed as

$$A' = \frac{1}{2}\frac{Pu}{4EI}u = \frac{Pu^2}{8EI}$$

Use the first moment-area theorem to obtain

$$\theta_{B/K} = \theta_B - \theta_K = A'$$

and since $\theta_K = 0$, $\qquad \theta_B = A'$

Substituting the values obtained for θ_B and A',

$$\frac{5PL^2}{128EI} = \frac{Pu^2}{8EI}$$

and solving for u,

$$u = \frac{\sqrt{5}}{4}L = 0.559L$$

Thus, the distance from the support A to point K is

$$AK = L - 0.559L = 0.441L$$

Maximum Deflection. The maximum deflection $|y|_{\max}$ is equal to the tangential deviation $t_{B/K}$ and thus to the first moment of area A' about a vertical axis through B (Fig. 9.39*d*).

$$|y|_{max} = t_{B/K} = A'\left(\frac{2u}{3}\right) = \frac{Pu^2}{8EI}\left(\frac{2u}{3}\right) = \frac{Pu^3}{12EI}$$

Substituting the value obtained for u,

$$|y|_{\max} = \frac{P}{12EI}\left(\frac{\sqrt{5}}{4}L\right)^3 = 0.01456PL^3/EI$$

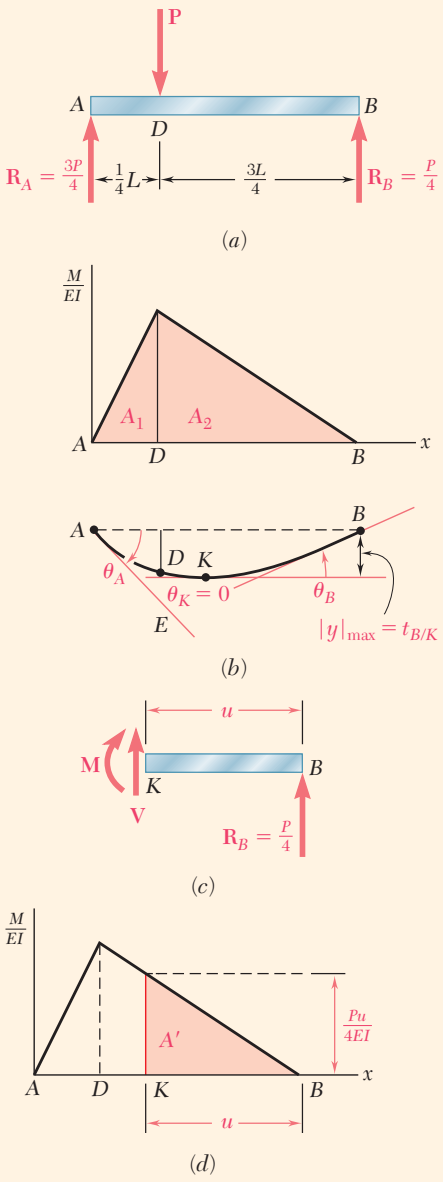


Fig. 9.39 (*a*) Free-body diagram. (*b*) *M*/*EI* diagram and geometry to determine the maximum deflection. (*c*) Free-body diagram of portion *KB*. (*d*) Maximum deflection is the first moment of the shaded area with respect to *B*.

*9.6C Statically Indeterminate Beams

Reactions at the supports of a statically indeterminate beam can be determined using the moment-area method in much the same way that was described in Sec. 9.4. For a beam indeterminate to the first degree, one of the reactions is designated as redundant, and the corresponding support is eliminated or modified accordingly. The redundant reaction is then treated as an unknown load, which, together with the other loads, must produce deformations that are compatible with the original supports. This compatibility condition is usually expressed by writing that the tangential deviation of one support with respect to another either is zero or has a predetermined value.

Two separate free-body diagrams of the beam are drawn. One shows *the given loads and the corresponding reactions* at the supports that have not been eliminated; the other shows *the redundant reaction and the corresponding reactions* at the same supports (see Concept Application 9.14). An M/EI diagram is drawn for each of the two loadings, and the desired tangential deviations are obtained using the second moment-area theorem. Superposing the results, we obtain the required compatibility condition needed to determine the redundant reaction. The other reactions are obtained from the free-body diagram of beam.

Once the reactions at the supports are found, the slope and deflection are obtained using the moment-area method at any other point of the beam.

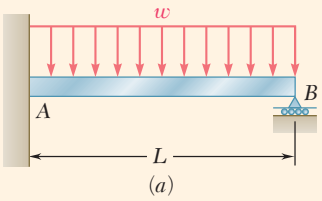


Fig. 9.40 (*a*) Statically indeterminate beam with a uniformly distributed load.

Concept Application 9.14

Determine the reaction at the supports for the prismatic beam and loading shown (Fig. 9.40*a*).

Consider the couple exerted at the fixed end A as redundant and replace the fixed end by a pin-and-bracket support. Couple $\mathbf{M}_A$ is now considered to be an unknown load (Fig. 9.40*b*) and will be determined from the condition that the tangent to the beam at A must be horizontal. Thus, this tangent must pass through the support B, and the tangential deviation $t_{B/A}$ of B with respect to A must be zero. The solution is

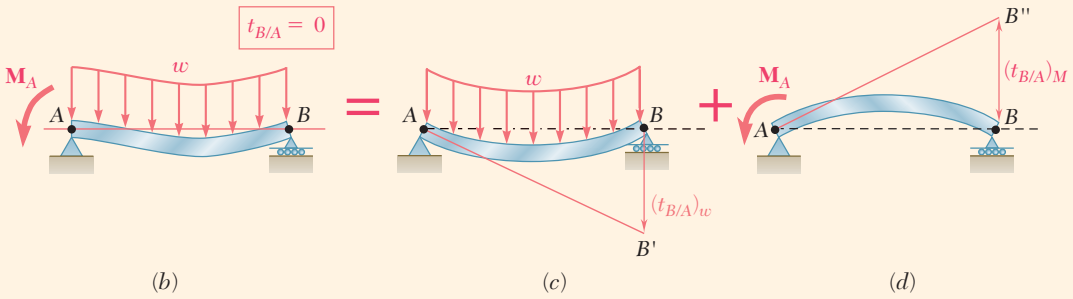


Fig. 9.40 (*b*) Analyze the indeterminate beam by superposing two determinate simply supported beams, subjected to (*c*) a uniformly distributed load, (*d*) the redundant reaction.

(continued)

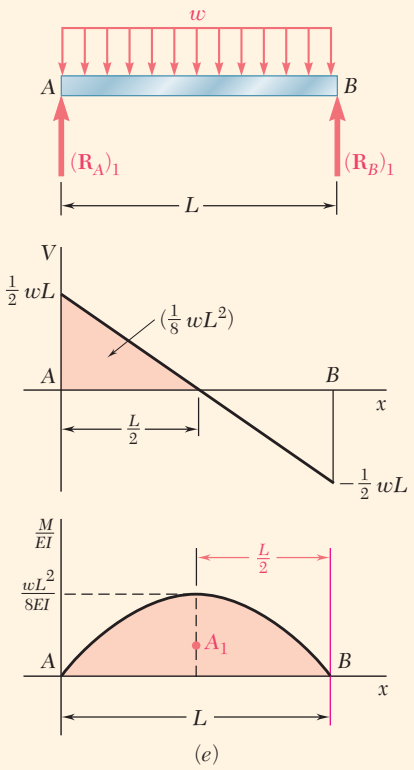


Fig. 9.40 (*e*) Free-body diagram of beam with distributed load, shear diagram, and *M*/*EI* diagram.

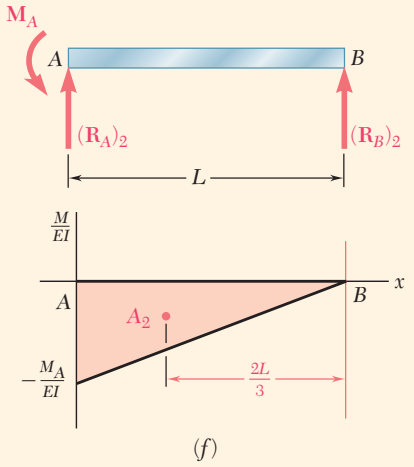


Fig. 9.40 (*f*) Free-body diagram of beam with redundant couple and *M*/*EI* diagram.

carried out by computing separately the tangential deviation $(t_{B/A})_w$ caused by the uniformly distributed load w (Fig. 9.40*c*) and the tangential deviation $(t_{B/A})_M$ produced by the unknown couple $\mathbf{M}_A$ (Fig. 9.40*d*).

Using the free-body diagram of the beam under the known distributed load w (Fig. 9.40*e*), determine the corresponding reactions at the supports A and B.

$$(\mathbf{R}_A)_1 = (\mathbf{R}_B)_1 = \tfrac{1}{2}wL \uparrow \qquad \textbf{(1)}$$

Now draw the corresponding shear and *M*/*EI* diagrams (Fig. 9.40*e*). Observing that *M*/*EI* is represented by an arc of parabola and recalling the formula $A = \frac{2}{3}bh$ for the area under a parabola, the first moment of this area about a vertical axis through B is

$$(t_{B/A})_w = A_1\left(\frac{L}{2}\right) = \left(\frac{2}{3}L\frac{wL^2}{8EI}\right)\left(\frac{L}{2}\right) = \frac{wL^4}{24EI} \qquad \textbf{(2)}$$

Using the free-body diagram of the beam when it is subjected to the unknown couple $\mathbf{M}_A$ (Fig. 9.40*f*), the corresponding reactions at A and B are

$$(\mathbf{R}_A)_2 = \frac{M_A}{L} \uparrow \qquad (\mathbf{R}_B)_2 = \frac{M_A}{L} \downarrow \qquad \textbf{(3)}$$

Drawing the corresponding *M*/*EI* diagram (Fig. 9.40*f*), the second moment-area theorem is applied to obtain

$$(t_{B/A})_M = A_2\left(\frac{2L}{3}\right) = \left(-\frac{1}{2}L\frac{M_A}{EI}\right)\left(\frac{2L}{3}\right) = -\frac{M_AL^2}{3EI} \qquad \textbf{(4)}$$

Combining the results obtained in Eqs. (2) and (4) and expressing that the resulting tangential deviation $t_{B/A}$ must be zero (Fig. 9.40*b, c, d*),

$$t_{B/A} = (t_{B/A})_w + (t_{B/A})_M = 0$$

$$\frac{wL^4}{24EI} - \frac{M_AL^2}{3EI} = 0$$

and solving for M_A,

$$M_A = +\tfrac{1}{8}wL^2 \qquad \mathbf{M}_A = \tfrac{1}{8}wL^2 \curvearrowleft$$

Substituting for M_A into Eq. (3), and recalling Eq. (1), the values of R_A and R_B are

$$R_A = (R_A)_1 + (R_A)_2 = \tfrac{1}{2}wL + \tfrac{1}{8}wL = \tfrac{5}{8}wL$$
$$R_B = (R_B)_1 + (R_B)_2 = \tfrac{1}{2}wL - \tfrac{1}{8}wL = \tfrac{3}{8}wL$$

In Concept Application 9.14, there was a single redundant reaction (i.e., the beam was *statically indeterminate to the first degree*). The *moment-area theorems* also can be used when there are additional redundant reactions, but it is necessary to write additional equations. Thus, for a beam that is *statically indeterminate to the second degree*, it would be necessary to select two redundant reactions and write two equations considering the *deformations* of the structure involved.

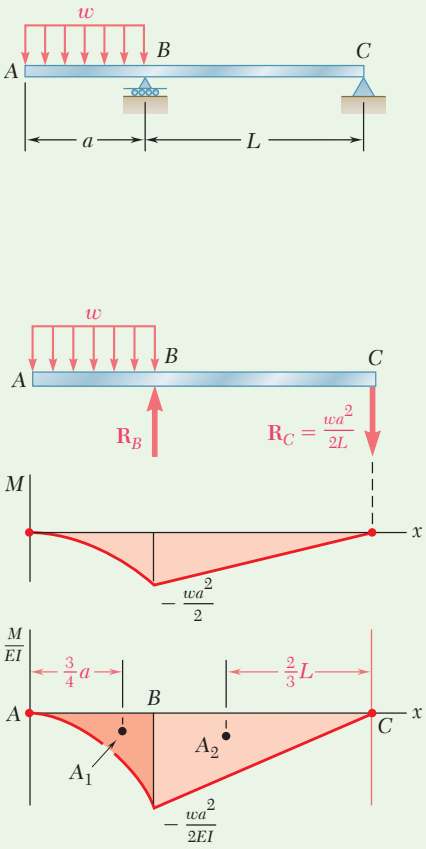


Fig. 1 Free-body, moment, and *M/EI* diagrams.

Sample Problem 9.12

For the beam and loading shown, (*a*) determine the deflection at end *A*, (*b*) evaluate y_A for the following data:

W 10 × 33: $I = 171$ in^4 E $= 29 \times 10^6$ psi
$a = 3$ ft $= 36$ in. $L = 5.5$ ft $= 66$ in.
$w = 13.5$ kips/ft $= 1125$ lb/in.

STRATEGY: To apply the moment-area theorems, you should first obtain the *M/EI* diagram for the beam. Then, by placing the reference tangent at a support, you can evaluate the tangential deviations at other strategic points that, through simple geometry, will enable the determination of the desired deflection.

MODELING and ANALYSIS:

***M/EI* Diagram.** Referring to Fig. 1, draw the bending-moment diagram. Since the flexural rigidity *EI* is constant, the *M/EI* diagram is as shown, which consists of a parabolic spandrel of area A_1 and a triangle of area A_2.

$$A_1 = \frac{1}{3}\left(-\frac{wa^2}{2EI}\right)a = -\frac{wa^3}{6EI}$$

$$A_2 = \frac{1}{2}\left(-\frac{wa^2}{2EI}\right)L = -\frac{wa^2L}{4EI}$$

Reference Tangent at *B*. The reference tangent is drawn at point *B* in Fig. 2. Using the second moment-area theorem, the tangential deviation of *C* with respect to *B* is

$$t_{C/B} = A_2\frac{2L}{3} = \left(-\frac{wa^2L}{4EI}\right)\frac{2L}{3} = -\frac{wa^2L^2}{6EI}$$

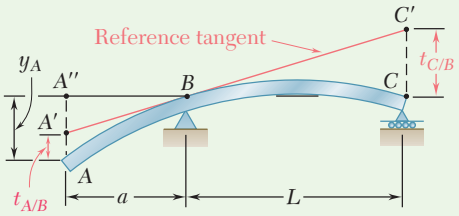


Fig. 2 Reference tangent and geometry to determine deflection at *A*.

From the similar triangles $A''A'B$ and $CC'B$,

$$A''A' = t_{C/B}\left(\frac{a}{L}\right) = -\frac{wa^2L^2}{6EI}\left(\frac{a}{L}\right) = -\frac{wa^3L}{6EI}$$

Again using the second moment-area theorem,

$$t_{A/B} = A_1\frac{3a}{4} = \left(-\frac{wa^3}{6EI}\right)\frac{3a}{4} = -\frac{wa^4}{8EI}$$

(continued)

a. Deflection at End *A*

$$y_A = A''A' + t_{A/B} = -\frac{wa^3L}{6EI} - \frac{wa^4}{8EI} = -\frac{wa^4}{8EI}\left(\frac{4}{3}\frac{L}{a} + 1\right)$$

$$y_A = \frac{wa^4}{8EI}\left(1 + \frac{4}{3}\frac{L}{a}\right)\downarrow \quad \blacktriangleleft$$

b. Evaluation of y_A.

Substituting the data,

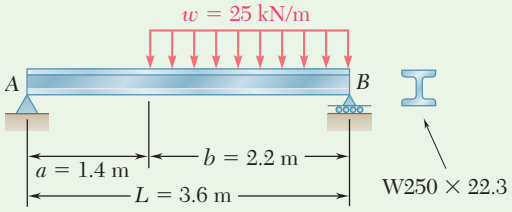
$$y_A = \frac{(1125\ \text{lb/in.})(36\ \text{in.})^4}{8(29 \times 10^6\ \text{lb/in}^2)(171\ \text{in}^4)}\left(1 + \frac{4}{3}\frac{66\ \text{in.}}{36\ \text{in.}}\right)$$

$$y_A = 0.1641\ \text{in.}\downarrow \quad \blacktriangleleft$$

REFLECT and THINK: Note that an equally effective alternate strategy would be to draw a reference tangent at point *C*.

Sample Problem 9.13

For the beam and loading shown, determine the magnitude and location of the largest deflection. Use $E = 200$ GPa.



STRATEGY: To apply the moment-area theorems, you should first obtain the *M/EI* diagram for the beam. Then, by placing the reference tangent at a support, you can evaluate the tangential deviation at the other support that, through simple geometry and the further application of the moment-area theorems, will enable the determination of the maximum deflection.

MODELING: Use the free-body diagram of the entire beam in Fig. 1 to obtain

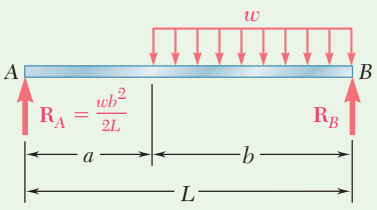


Fig. 1 Free-body diagram.

$$\mathbf{R}_A = 16.81\ \text{kN}\uparrow \qquad \mathbf{R}_B = 38.2\ \text{kN}\uparrow$$

(continued)

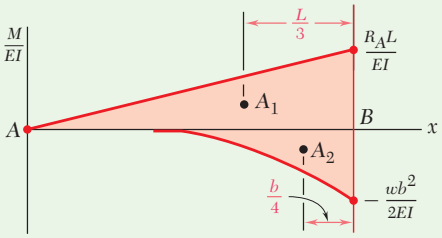


Fig. 2 Parts of *M/EI* diagram with centroid locations.

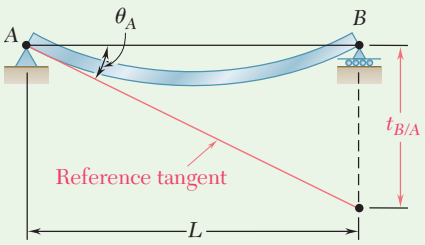


Fig. 3 Determination of θ_A through tangential deviation $t_{B/A}$.

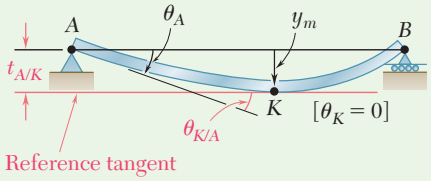


Fig. 4 Geometry to determine maximum deflection.

ANALYSIS:

***M/EI* Diagram.** Draw the *M/EI* diagram by parts (Fig. 2), considering the effects of the reaction $\mathbf{R}_A$ and of the distributed load separately. The areas of the triangle and of the spandrel are

$$A_1 = \frac{1}{2}\frac{R_A L}{EI}L = \frac{R_A L^2}{2EI} \qquad A_2 = \frac{1}{3}\left(-\frac{wb^2}{2EI}\right)b = -\frac{wb^3}{6EI}$$

Reference Tangent. As seen in Fig. 3, the tangent to the beam at support *A* is chosen as the reference tangent. Using the second moment-area theorem, the tangential deviation $t_{B/A}$ of support *B* with respect to support *A* is

$$t_{B/A} = A_1\frac{L}{3} + A_2\frac{b}{4} = \left(\frac{R_A L^2}{2EI}\right)\frac{L}{3} + \left(-\frac{wb^3}{6EI}\right)\frac{b}{4} = \frac{R_A L^3}{6EI} - \frac{wb^4}{24EI}$$

Slope at *A*

$$\theta_A = -\frac{t_{B/A}}{L} = -\left(\frac{R_A L^2}{6EI} - \frac{wb^4}{24EIL}\right) \tag{1}$$

Largest Deflection. As seen in Fig. 4, the largest deflection occurs at point *K*, where the slope of the beam is zero. Using Fig. 5, write

$$\theta_K = \theta_A + \theta_{K/A} = 0 \tag{2}$$

But

$$\theta_{K/A} = A_3 + A_4 = \frac{R_A x_m^2}{2EI} - \frac{w}{6EI}(x_m - a)^3 \tag{3}$$

Substitute for θ_A and $\theta_{K/A}$ from Eqs. (1) and (3) into Eq. (2):

$$-\left(\frac{R_A L^2}{6EI} - \frac{wb^4}{24EIL}\right) + \left[\frac{R_A x_m^2}{2EI} - \frac{w}{6EI}(x_m - a)^3\right] = 0$$

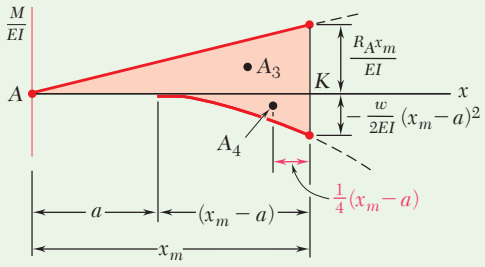


Fig. 5 *M/EI* diagram between Point *A* and the location of maximum deflection, point *K*.

(continued)

Substituting the numerical data gives

$$-29.53\frac{10^3}{EI} + 8.405x_m^2\frac{10^3}{EI} - 4.167(x_m - 1.4)^3\frac{10^3}{EI} = 0$$

Solving by trial and error for x_m, $x_m = 1.890$ m ◀

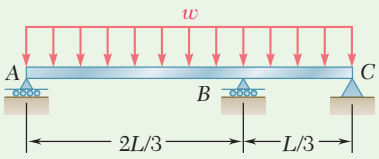
Computing the moments of A_3 and A_4 about a vertical axis through A gives

$$|y|_m = t_{A/K} = A_3\frac{2x_m}{3} + A_4\left[a + \frac{3}{4}(x_m - a)\right]$$

$$= \frac{R_A x_m^3}{3EI} - \frac{wa}{6EI}(x_m - a)^3 - \frac{w}{8EI}(x_m - a)^4$$

Using the given data, $R_A = 16.81$ kN, and $I = 28.7 \times 10^{-6}$ m^4,

$y_m = 6.44$ mm↓ ◀



Sample Problem 9.14

For the uniform beam and loading shown, determine the reaction at B.

STRATEGY: Applying the superposition concept, you can model this statically indeterminate problem as a summation of the displacements for the given load and the redundant load cases. The redundant reaction can then be found by noting that a displacement associated with the two cases must be consistent with the geometry of the original beam.

MODELING: The beam is indeterminate to the first degree. Referring to Fig. 1, the reaction $\mathbf{R}_B$ is chosen as redundant, and the distributed load and redundant reaction load are considered separately.

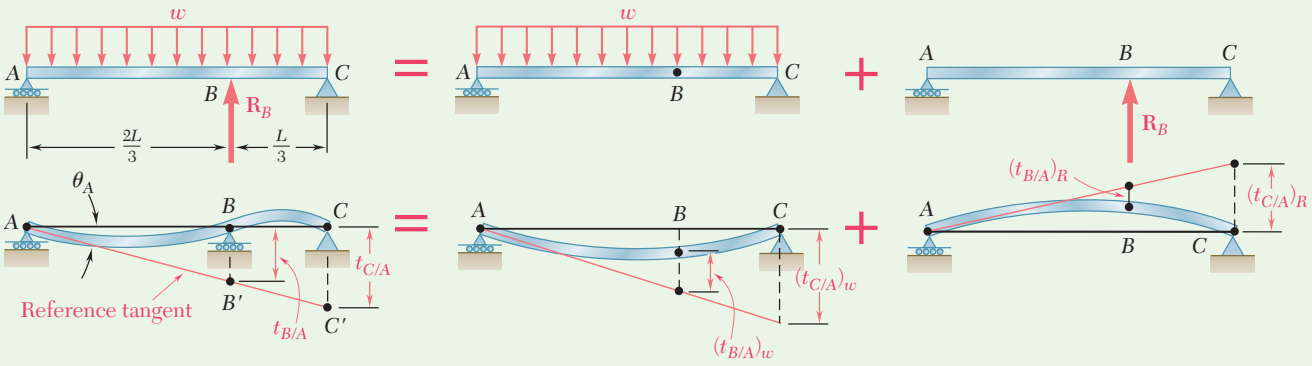


Fig. 1 Indeterminate beam modeled as superposition of two determinate beams with reaction at B chosen as redundant.

(continued)

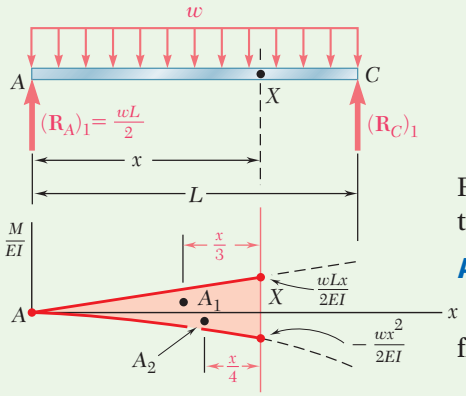


Fig. 2 Free-body and *M/EI* diagrams for beam with distributed load.

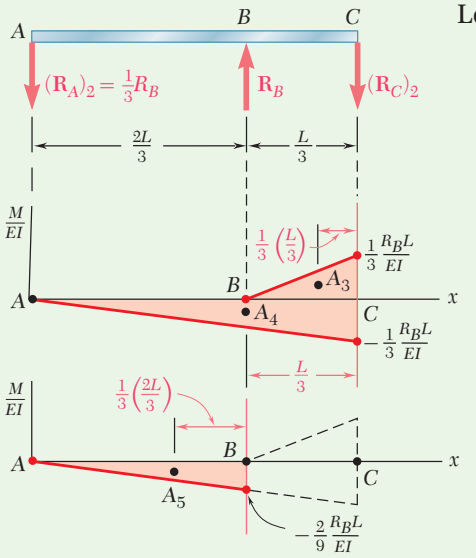


Fig. 3 Free-body and *M/EI* diagrams for beam with redundant reaction.

Next the tangent at A is selected as the reference tangent. From the similar triangles ABB' and ACC',

$$\frac{t_{C/A}}{L} = \frac{t_{B/A}}{\frac{2}{3}L} \qquad t_{C/A} = \frac{3}{2}t_{B/A} \tag{1}$$

For each loading, we draw the *M/EI* diagram and then determine the tangential deviations of B and C with respect to A.

ANALYSIS:

Distributed Loading (Fig. 2). Considering the *M/EI* diagram from end A to an arbitrary point X,

$$(t_{X/A})_w = A_1\frac{x}{3} + A_2\frac{x}{4} = \left(\frac{1}{2}\frac{wLx}{2EI}x\right)\frac{x}{3} + \left(-\frac{1}{3}\frac{wx^2}{2EI}x\right)\frac{x}{4} = \frac{wx^3}{24EI}(2L - x)$$

Letting $x = L$ and $x = \frac{2}{3}L$,

$$(t_{C/A})_w = \frac{wL^4}{24EI} \qquad (t_{B/A})_w = \frac{4}{243}\frac{wL^4}{EI}$$

Redundant Reaction Loading (Fig. 3).

$$(t_{C/A})_R = A_3\frac{L}{9} + A_4\frac{L}{3} = \left(\frac{1}{2}\frac{R_BL}{3EI}\frac{L}{3}\right)\frac{L}{9} + \left(-\frac{1}{2}\frac{R_BL}{3EI}L\right)\frac{L}{3} = -\frac{4}{81}\frac{R_BL^3}{EI}$$

$$(t_{B/A})_R = A_5\frac{2L}{9} = \left[-\frac{1}{2}\frac{2R_BL}{9EI}\left(\frac{2L}{3}\right)\right]\frac{2L}{9} = -\frac{4}{243}\frac{R_BL^3}{EI}$$

Combined Loading. Adding the results gives

$$t_{C/A} = \frac{wL^4}{24EI} - \frac{4}{81}\frac{R_BL^3}{EI} \qquad t_{B/A} = \frac{4}{243}\frac{(wL^4 - R_BL^3)}{EI}$$

Reaction at *B*. Substituting for $t_{C/A}$ and $t_{B/A}$ into Eq. (1),

$$\left(\frac{wL^4}{24EI} - \frac{4}{81}\frac{R_BL^3}{EI}\right) = \frac{3}{2}\left[\frac{4}{243}\frac{(wL^4 - R_BL^3)}{EI}\right]$$

$$R_B = 0.6875wL \qquad R_B = 0.688wL \uparrow \blacktriangleleft$$

REFLECT and THINK: Note that an alternate strategy would be to determine the deflections at B for the given load and the redundant reaction and to set the sum equal to zero.

Problems

Use the moment-area method to solve the following problems.

9.125 through 9.128 For the prismatic beam and loading shown, determine (*a*) the deflection at point *D*, (*b*) the slope at end *A*.

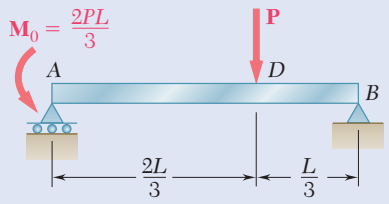


Fig. P9.125

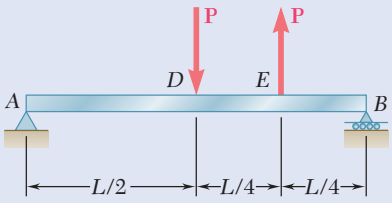


Fig. P9.126

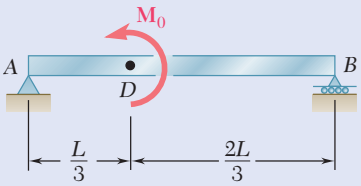


Fig. *P9.127*

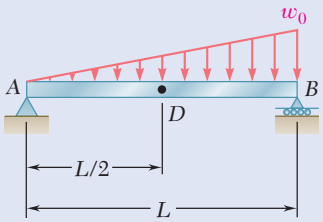


Fig. P9.128

9.129 and 9.130 For the beam and loading shown, determine (*a*) the slope at end *A*, (*b*) the deflection at point *D*. Use $E = 200$ GPa.

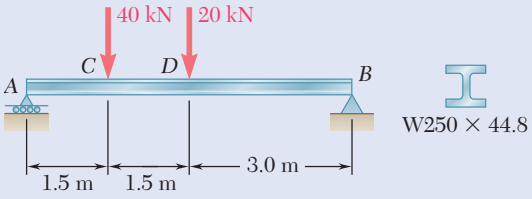


Fig. P9.129

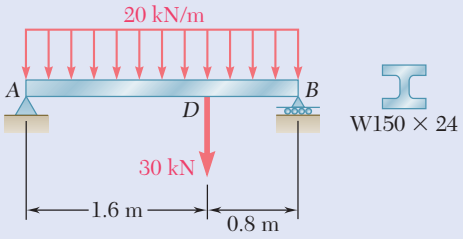


Fig. P9.130

9.131 For the timber beam and loading shown, determine (*a*) the slope at point *A*, (*b*) the deflection at point *C*. Use $E = 1.7 \times 10^6$ psi.

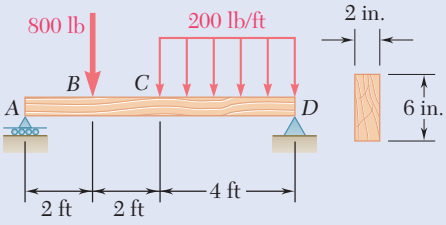


Fig. *P9.131*

9.132 For the beam and loading shown, determine (*a*) the slope at point *A*, (*b*) the deflection at point *E*. Use $E = 29 \times 10^6$ psi.

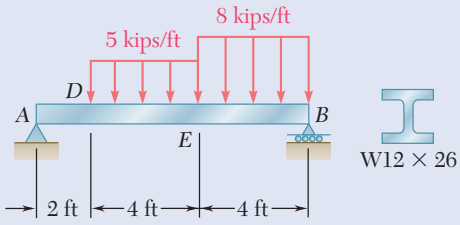


Fig. P9.132

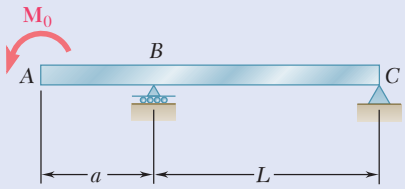


Fig. P9.133

9.133 For the beam and loading shown, determine (*a*) the slope at point *A*, (*b*) the deflection at point *A*.

9.134 For the beam and loading shown, determine (*a*) the slope at point *A*, (*b*) the deflection at point *D*.

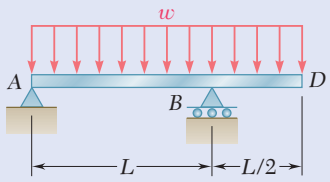


Fig. *P9.134*

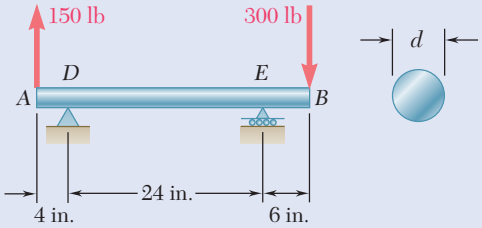


Fig. P9.135

9.135 Knowing that the beam *AB* is made of a solid steel rod of diameter $d = 0.75$ in., determine for the loading shown (*a*) the slope at point *D*, (*b*) the deflection at point *A*. Use $E = 29 \times 10^6$ psi.

9.136 Knowing that the beam *AD* is made of a solid steel bar, determine (*a*) the slope at point *B*, (*b*) the deflection at point *A*. Use $E = 200$ GPa.

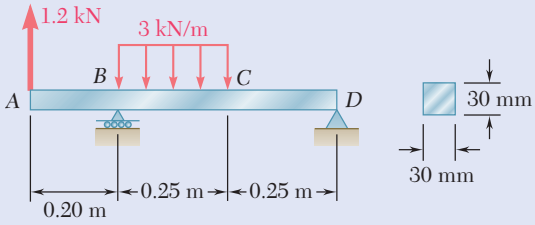


Fig. P9.136

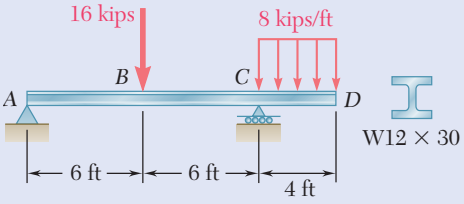


Fig. P9.137

9.137 For the beam and loading shown, determine (*a*) the slope at point *C*, (*b*) the deflection at point *D*. Use $E = 29 \times 10^6$ psi.

9.138 For the beam and loading shown, determine (*a*) the slope at point *B*, (*b*) the deflection at point *D*. Use $E = 200$ GPa.

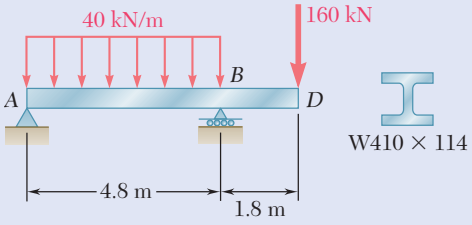


Fig. *P9.138*

9.139 For the beam and loading shown, determine (*a*) the slope at end *A*, (*b*) the slope at end *B*, (*c*) the deflection at the midpoint *C*.

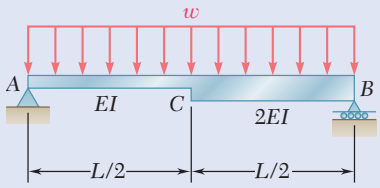


Fig. P9.139

9.140 For the beam and loading shown, determine the deflection (*a*) at point *D*, (*b*) at point *E*.

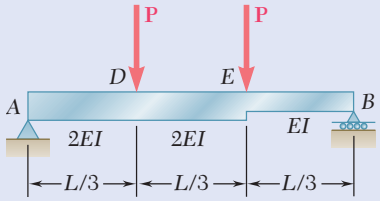


Fig. P9.140

***9.141* through 9.144** For the beam and loading shown, determine the magnitude and location of the largest downward deflection.

9.141 Beam and loading of Prob. 9.126
9.142 Beam and loading of Prob. 9.128
9.143 Beam and loading of Prob. 9.129
9.144 Beam and loading of Prob. 9.132

9.145 For the beam and loading of Prob. 9.135, determine the largest upward deflection in span *DE*.

9.146 For the beam and loading of Prob. 9.138, determine the largest upward deflection in span *AB*.

9.147 through 9.150 For the beam and loading shown, determine the reaction at the roller support.

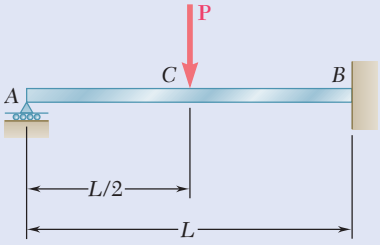


Fig. P9.147

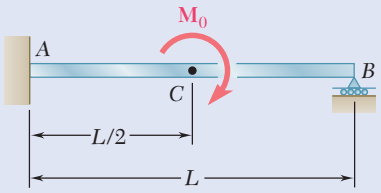


Fig. P9.148

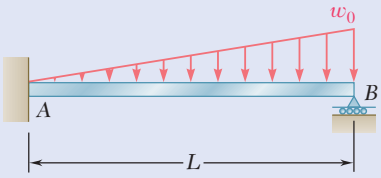


Fig. *P9.149*

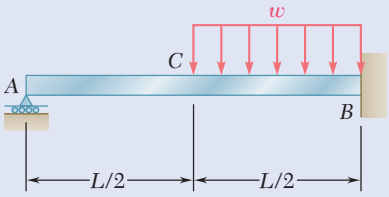


Fig. P9.150

9.151 and 9.152 For the beam and loading shown, determine the reaction at each support.

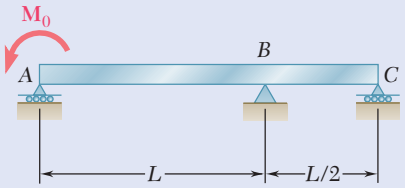


Fig. *P9.151*

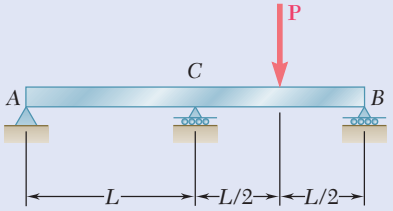


Fig. P9.152

9.153 A hydraulic jack can be used to raise point B of the cantilever beam ABC. The beam was originally straight, horizontal, and unloaded. A 20-kN load was then applied at point C, causing this point to move down. Determine (a) how much point B should be raised to return point C to its original position, (b) the final value of the reaction at B. Use $E = 200$ GPa.

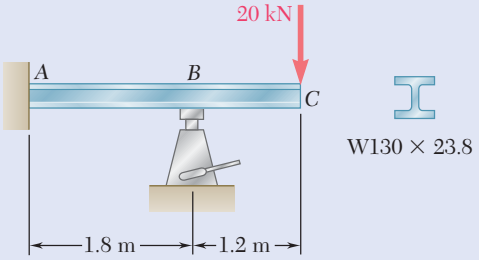


Fig. P9.153

9.154 Determine the reaction at the roller support and draw the bending-moment diagram for the beam and loading shown.

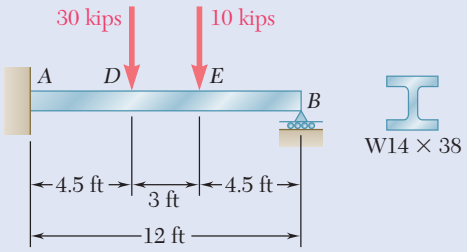


Fig. P9.154

9.155 For the beam and loading shown, determine the spring constant k for which the force in the spring is equal to one-third of the total load on the beam.

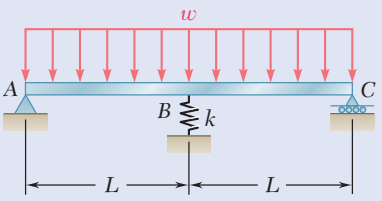


Fig. P9.155 and P9.156

9.156 For the beam and loading shown, determine the spring constant k for which the bending moment at B is $M_B = -wL^2/10$.

Review and Summary

Two approaches were used in this chapter to determine the slopes and deflections of beams under transverse loadings. A mathematical method based on the method of integration of a differential equation was used to get the slopes and deflections at any point along the beam. Then the *moment-area method* was used to find the slopes and deflections at a given point along the beam. Particular emphasis was placed on the computation of the maximum deflection of a beam under a given loading. These methods also were used to determine support reactions and deflections of *indeterminate beams*, where the number of reactions at the supports exceeds the number of equilibrium equations available to determine these unknowns.

Deformation Under Transverse Loading

The relationship of the curvature $1/\rho$ of the neutral surface and the bending moment M in a prismatic beam in pure bending can be applied to a beam under a transverse loading, but in this case both M and $1/\rho$ vary from section to section. Using the distance x from the left end of the beam,

$$\frac{1}{\rho} = \frac{M(x)}{EI} \tag{9.1}$$

This equation enables us to determine the radius of curvature of the neutral surface for any value of x and to draw some general conclusions regarding the shape of the deformed beam.

A relationship was found between the deflection y of a beam, measured at a given point Q, and the distance x of that point from some fixed origin (Fig. 9.41). The resulting equation defines the *elastic curve* of a beam. Expressing the curvature $1/\rho$ in terms of the derivatives of the function $y(x)$ and substituting into Eq. (9.1), we obtained the second-order linear differential equation

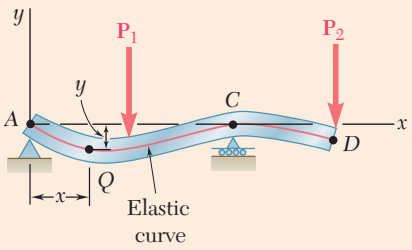


Fig. 9.41 Elastic curve for beam with transverse loads.

$$\frac{d^2y}{dx^2} = \frac{M(x)}{EI} \tag{9.4}$$

Integrating this equation twice, the expressions defining the slope $\theta(x) = dy/dx$ and the deflection $y(x)$ were obtained:

$$EI\frac{dy}{dx} = \int_0^x M(x)\,dx + C_1 \tag{9.5}$$

$$EI\,y = \int_0^x dx \int_0^x M(x)\,dx + C_1x + C_2 \tag{9.6}$$

The product EI is known as the *flexural rigidity* of the beam. Two constants of integration C_1 and C_2 can be determined from the *boundary*

conditions imposed on the beam by its supports (Fig. 9.42). The maximum deflection can be obtained by first determining the value of x for which the slope is zero and then computing the corresponding value of y.

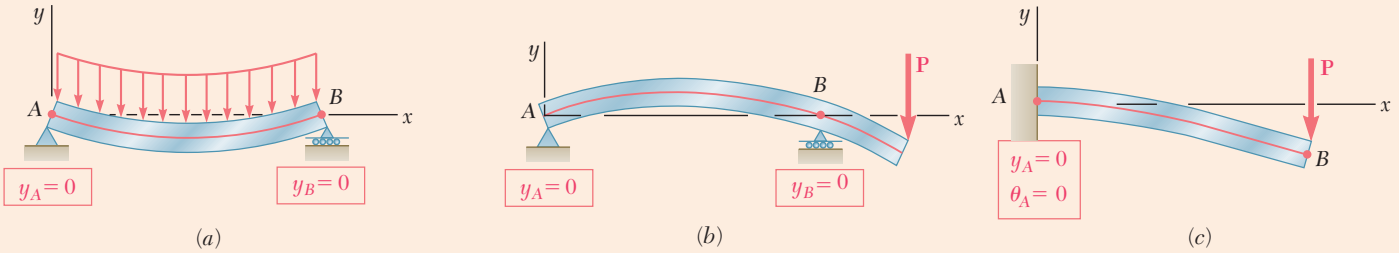


Fig. 9.42 Known boundary conditions for statically determinate beams. **(*a*)** Simply supported beam. **(*b*)** Overhanging beam. **(*c*)** Cantilever beam.

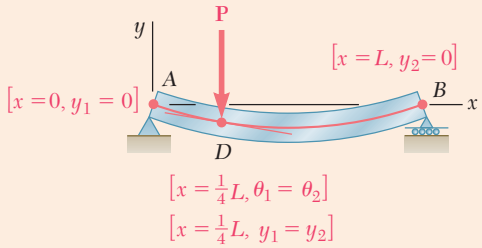


Fig. 9.43 Simply supported beam and boundary conditions, where two sets of functions are required due to the discontinuity in load at point *D*.

Elastic Curve Defined by Different Functions

When the load requires different analytical functions to represent the bending moment in various portions of the beam, multiple differential equations are required to represent the slope $\theta(x)$ and the deflection $y(x)$. For the beam and load considered in Fig. 9.43, two differential equations are required: one for the portion of beam AD and the other for the portion DB. The first equation yields the functions θ_1 and y_1, and the second the functions θ_2 and y_2. Altogether, four constants of integration must be determined: two by writing that the deflections at A and B are zero and two by expressing that the portions of beam AD and DB have the same slope and the same deflection at D.

For a beam supporting a distributed load $w(x)$, the elastic curve can be determined directly from $w(x)$ through four integrations yielding V, M, θ, and y (in that order). For the cantilever beam of Fig. 9.44*a* and the simply supported beam of Fig. 9.44*b*, four constants of integration can be determined from the four boundary conditions.

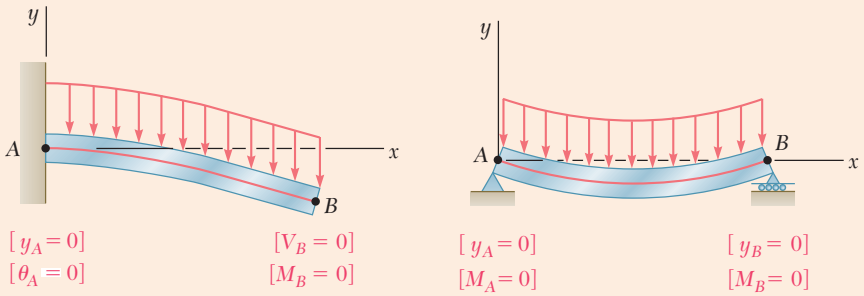


Fig. 9.44 Boundary conditions for beams carrying a distributed load. **(*a*)** Cantilever beam. **(*b*)** Simply supported beam.

Statically Indeterminate Beams

Statically indeterminate beams are supported such that the reactions at the supports involve four or more unknowns. Since only three equilibrium equations are available to determine these unknowns, they are supplemented with equations obtained from the boundary conditions imposed

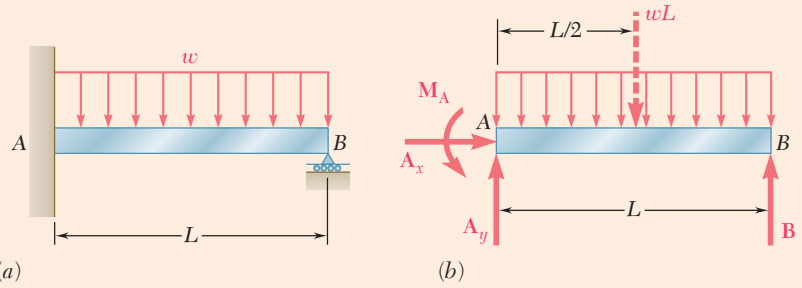


Fig. 9.45 (*a*) Statically indeterminate beam with a uniformly distributed load. (*b*) Free-body diagram with four unknown reactions.

by the supports. For the beam of Fig 9.45, the reactions at the supports involve four unknowns: M_A, A_x, A_y, and B. This beam is *indeterminate to the first degree*. (If five unknowns are involved, the beam is indeterminate to the *second degree*.) Expressing the bending moment $M(x)$ in terms of the four unknowns and integrating twice, the slope $\theta(x)$ and the deflection $y(x)$ are determined in terms of the same unknowns and the constants of integration C_1 and C_2. The six unknowns are obtained by solving the three equilibrium equations for the free body of Fig. 9.45*b* and the three equations expressing that $\theta = 0$, $y = 0$ for $x = 0$, and that $y = 0$ for $x = L$ (Fig. 9.46) simultaneously.

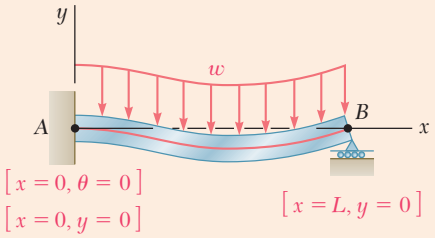


Fig. 9.46 Boundary conditions for beam of Fig. 9.45.

Use of Singularity Functions

The integration method provides an effective way to determine the slope and deflection at any point of a prismatic beam, as long as the bending moment M can be represented by a single analytical function. However, when several functions are required to represent M over the entire length of the beam, the use of *singularity functions* considerably simplifies the determination of θ and y at any point of the beam. Considering the beam of Fig. 9.47 and drawing its free-body diagram (Fig. 9.48), the shear at any point of the beam is

$$V(x) = \frac{3P}{4} - P\langle x - \tfrac{1}{4}L\rangle^0$$

where the step function $\langle x - \frac{1}{4}L\rangle^0$ is equal to zero when the quantity inside the brackets $\langle\ \ \rangle$ is negative and otherwise is equal to one. Integrating three times,

$$M(x) = \frac{3P}{4}x - P\langle x - \tfrac{1}{4}L\rangle \qquad \textbf{(9.11)}$$

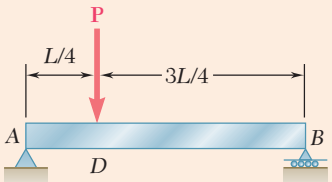


Fig. 9.47 Simply supported beam with concentrated load.

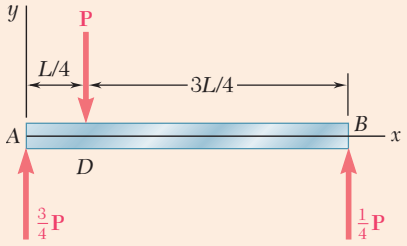


Fig. 9.48 Free-body diagram for beam of Fig. 9.47.

$$EI\,\theta = EI\frac{dy}{dx} = \tfrac{3}{8}Px^2 - \tfrac{1}{2}P\langle x - \tfrac{1}{4}L\rangle^2 + C_1 \qquad \textbf{(9.13)}$$

$$EI\,y = \tfrac{1}{8}Px^3 - \tfrac{1}{6}P\langle x - \tfrac{1}{4}L\rangle^3 + C_1x + C_2 \qquad \textbf{(9.14)}$$

where the brackets $\langle\ \ \rangle$ should be replaced by zero when the quantity inside is negative and by parentheses otherwise. Constants C_1 and C_2 are determined from the boundary conditions shown in Fig. 9.49.

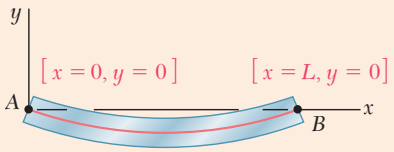


Fig. 9.49 Boundary conditions for simply supported beam.

Method of Superposition

The *method of superposition* separately determines and then adds the slope and deflection caused by the various loads applied to a beam. This procedure is made easier using the table of Appendix D, which gives the slopes and deflections of beams for various loadings and types of support.

Statically Indeterminate Beams by Superposition

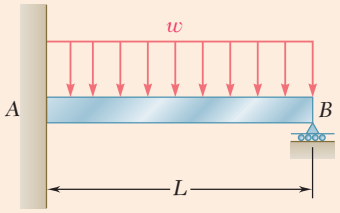


Fig. 9.50 Indeterminate beam with uniformly distributed load.

The method of superposition can be effective for analyzing *statically indeterminate beams.* For example, the beam of Fig. 9.50 involves four unknown reactions and is indeterminate to the *first degree;* the reaction at B is chosen as *redundant,* and the beam is released from that support. Treating the reaction $\mathbf{R}_B$ as an unknown load and considering the deflections caused at B by the given distributed load and by $\mathbf{R}_B$ separately, the sum of these deflections is zero (Fig. 9.51). For a beam indeterminate to the *second degree* (i.e., with reactions at the supports involving five unknowns), two reactions are redundant, and the corresponding supports must be eliminated or modified accordingly.

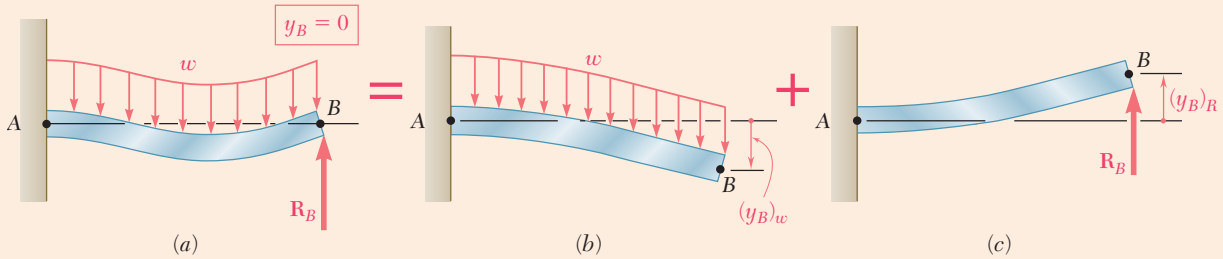


Fig. 9.51 (*a*) Analyze indeterminate beam by superposing two determinate beams, with (*b*) a uniformly distributed load, (*c*) the redundant reaction.

First Moment-Area Theorem

Deflections and slopes of beams can also be determined using the *moment-area method.* The *moment-area theorems* were developed by drawing a diagram representing the variation along the beam of the

quantity M/EI, which is obtained by dividing the bending moment M by the flexural rigidity EI (Fig. 9.52). The *first moment-area theorem* is stated as: *The area under the (M/EI) diagram between two points is equal to the angle between the tangents to the elastic curve drawn at these points.* Considering tangents at C and D,

$$\theta_{D/C} = \text{area under } (M/EI) \text{ diagram between } C \text{ and } D \qquad \textbf{(9.17)}$$

Second Moment-Area Theorem

Again using the M/EI diagram and a sketch of the deflected beam (Fig. 9.53), a tangent at point D is drawn and the vertical distance $t_{C/D}$, which is called the tangential deviation of C with respect to D, is considered. The *second moment-area theorem* is stated as: *The tangential deviation $t_{C/D}$ of C with respect to D is equal to the first moment with respect to a vertical axis through C of the area under the M/EI diagram between C and D.* It is important to distinguish between the tangential deviation of C with respect to D (Fig. 9.53*a*), which is

$$t_{C/D} = (\text{area between } C \text{ and } D)\,\bar{x}_1 \qquad \textbf{(9.20)}$$

and the tangential deviation of D with respect to C (Fig. 9.53*b*), which is

$$t_{D/C} = (\text{area between } C \text{ and } D)\,\bar{x}_2 \qquad \textbf{(9.21)}$$

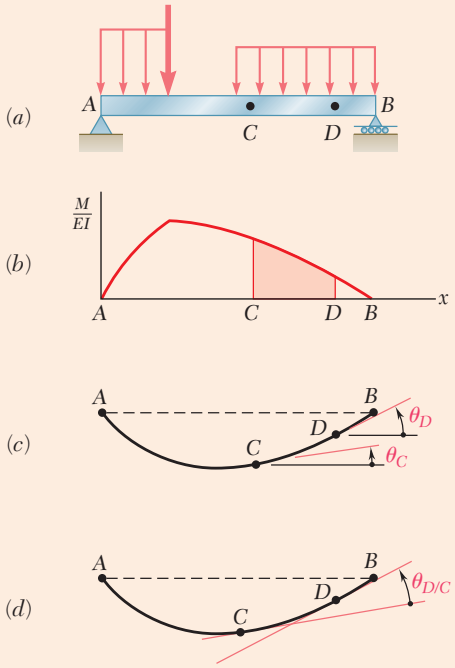


Fig. 9.52 First moment-area theorem Illustrated. (*a*) Beam subjected to arbitrary load. (*b*) *M/EI* diagram. (*c*) Elastic curve showing slope at *C* and *D*. (*d*) Elastic curve showing slope at *D* with respect to *C*.

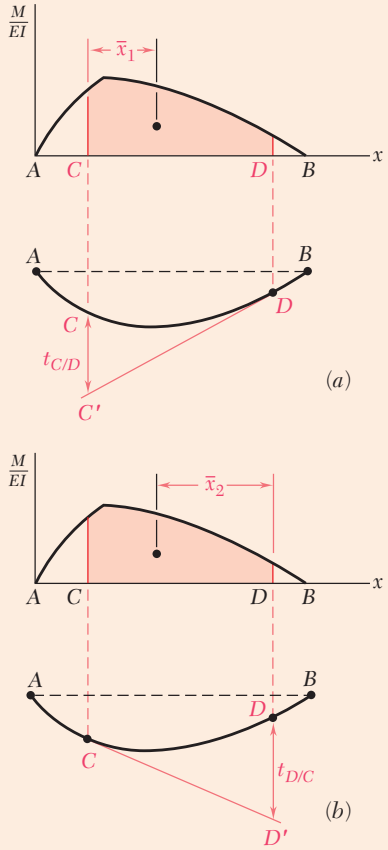


Fig. 9.53 Second moment-area theorem illustrated. (*a*) Evaluating $t_{C/D}$. (*b*) Evaluating $t_{D/C}$.

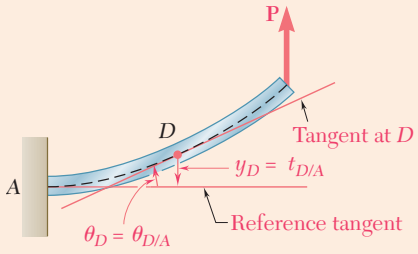


Fig. 9.54 Application of moment-area method to cantilever beams.

Cantilever Beams

Beams with Symmetric Loadings

To determine the slope and deflection at points of *cantilever* beams, the tangent at the fixed support is horizontal (Fig. 9.54). For *symmetrically loaded beams*, the tangent is horizontal at the midpoint C of the beam (Fig. 9.55). Using the horizontal tangent as a *reference tangent,* slopes and deflections are determined by using, respectively, the first and second moment-area theorems. To find a deflection that is not a tangential deviation (Fig. 9.55*c*), it is first necessary to determine which tangential deviations can be combined to obtain the desired deflection.

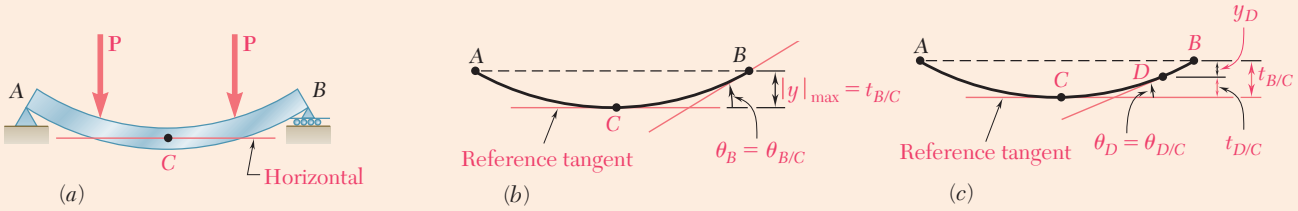


Fig. 9.55 Application of moment-area method to simply supported beams with symmetric loadings. (*a*) Beam and loadings. (*b*) Maximum deflection and slope at point *B*. (*c*) Deflection and slope at arbitrary point *D*.

Bending-Moment Diagram by Parts

In many cases, the application of the moment-area theorems is simplified if the effect of each load is considered separately. To do this, we draw the M/EI *diagram by parts* with a separate M/EI diagram for each load. The areas and the moments of areas under the several diagrams are added to determine slopes and tangential deviations for the original beam and loading.

Unsymmetric Loadings

The moment-area method is also used to analyze beams with *unsymmetric loadings.* Observing that the location of a horizontal tangent is usually not obvious, a reference tangent is selected at one of the beam supports, since the slope of that tangent is easily determined. For the beam and loading shown in Fig. 9.56, the slope of the tangent at A is obtained by computing the tangential deviation $t_{B/A}$ and dividing it by the distance L between supports A and B. Then, using both moment-area theorems and simple geometry, the slope and deflection are determined at any point of the beam.

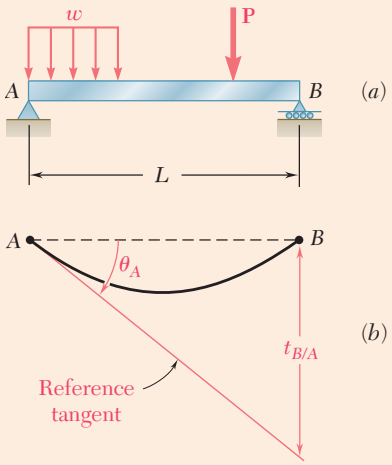


Fig. 9.56 Application of moment-area method to unsymmetrically loaded beam establishes a reference tangent at a support.

Maximum Deflection

The *maximum deflection* of an unsymmetrically loaded beam generally does not occur at midspan. The approach indicated in the preceding paragraph was used to determine point K where the maximum deflection occurs and the magnitude of that deflection. Observing that the slope at K is zero (Fig. 9.57), $\theta_{K/A} = -\theta_A$. Recalling the first moment-area theorem, the location of K is found by determining an area under the M/EI diagram equal to $\theta_{K/A}$. The maximum deflection is then obtained by computing the tangential deviation $t_{A/K}$.

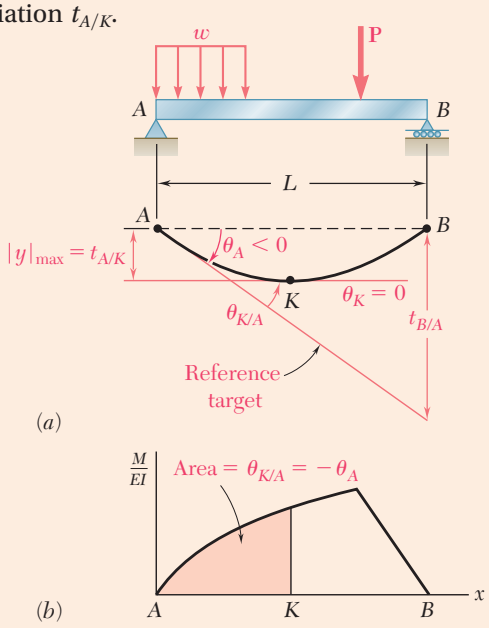


Fig. 9.57 Determination of maximum deflection using moment-area method.

Statically Indeterminate Beams

The moment-area method can be used for the analysis of *statically indeterminate beams*. Since the reactions for the beam and loading shown in Fig. 9.58 cannot be determined by statics alone, one of the reactions of the beam is designated as redundant ($\mathbf{M}_A$ in Fig. 9.59*a*), and the redundant reaction is considered to be an unknown load. The tangential deviation of B with respect to A is considered separately for the distributed load (Fig. 9.59*b*) and for the redundant reaction (Fig. 9.59*c*). Expressing that under the combined action of the distributed load and of the couple $\mathbf{M}_A$ the tangential deviation of B with respect to A must be zero,

$$t_{B/A} = (t_{B/A})_w + (t_{B/A})_M = 0$$

From this equation, the magnitude of the redundant reaction $\mathbf{M}_A$ can be found.

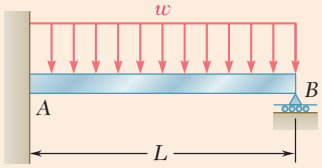


Fig. 9.58 Statically indeterminate beam.

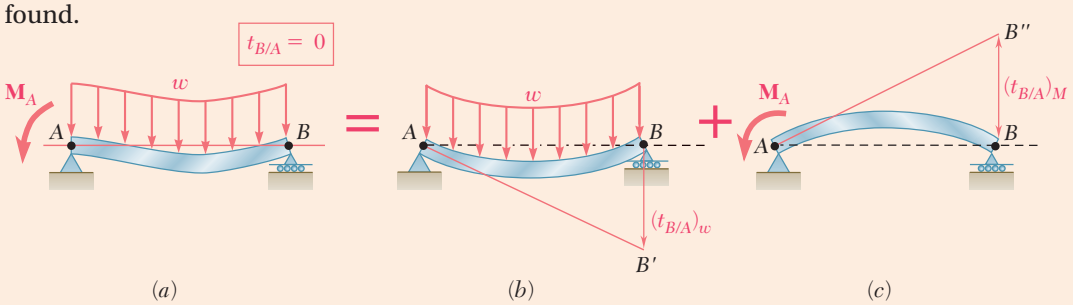


Fig. 9.59 Modeling the indeterminate beam as the superposition of two determinate cases.

Review Problems

9.157 For the loading shown, determine (*a*) the equation of the elastic curve for the cantilever beam *AB*, (*b*) the deflection at the free end, (*c*) the slope at the free end.

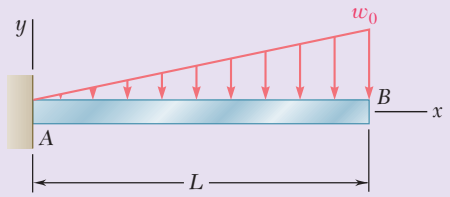


Fig. P9.157

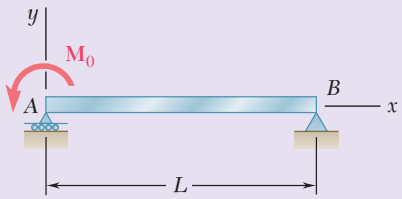


Fig. P9.158

9.158 (*a*) Determine the location and magnitude of the maximum deflection of beam *AB*. (*b*) Assuming that beam *AB* is a W360 × 64, $L = 3.5$ m, and $E = 200$ GPa, calculate the maximum allowable value of the applied moment $\mathbf{M}_0$ if the maximum deflection is not to exceed 1 mm.

9.159 For the beam and loading shown, determine (*a*) the equation of the elastic curve, (*b*) the slope at end *A*, (*c*) the deflection at the midpoint of the span.

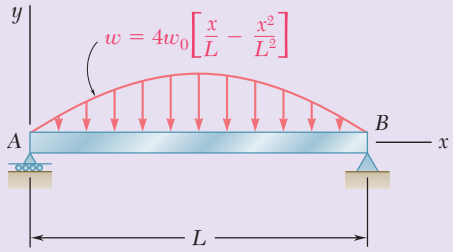


Fig. P9.159

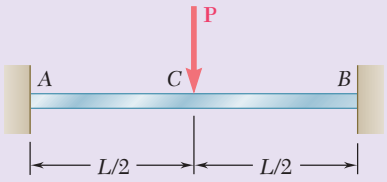


Fig. P9.160

9.160 Determine the reaction at *A* and draw the bending moment diagram for the beam and loading shown.

9.161 For the beam and loading shown, determine (*a*) the slope at end *A*, (*b*) the deflection at point *C*. Use $E = 200$ GPa.

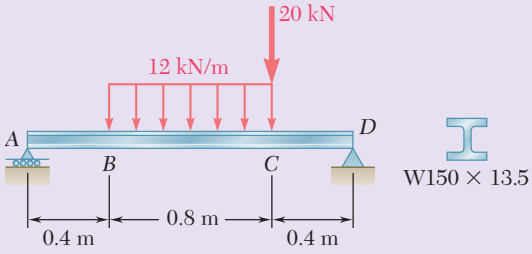


Fig. P9.161

9.162 For the beam and loading shown, determine (*a*) the reaction at point *C*, (*b*) the deflection at point *B*. Use $E = 29 \times 10^6$ psi.

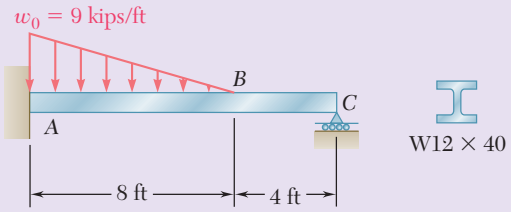


Fig. *P9.162*

9.163 Beam *CE* rests on beam *AB* as shown. Knowing that a W10 × 30 rolled-steel shape is used for each beam, determine for the loading shown the deflection at point *D*. Use $E = 29 \times 10^6$ psi.

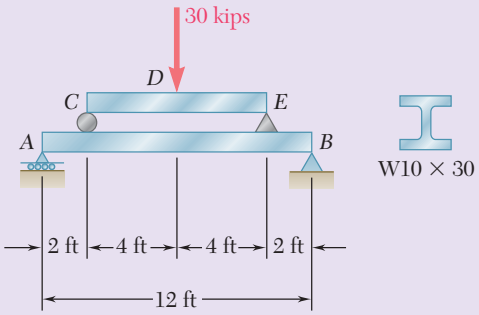


Fig. P9.163

9.164 The cantilever beam *BC* is attached to the steel cable *AB* as shown. Knowing that the cable is initially taut, determine the tension in the cable caused by the distributed load shown. Use $E = 200$ GPa.

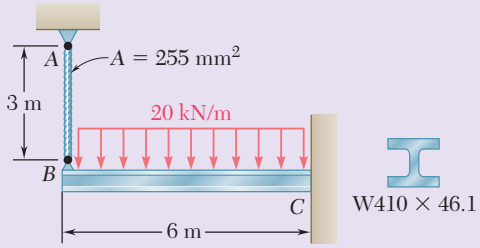


Fig. *P9.164*

9.165 For the cantilever beam and loading shown, determine (*a*) the slope at point *A*, (*b*) the deflection at point *A*. Use $E = 200$ GPa.

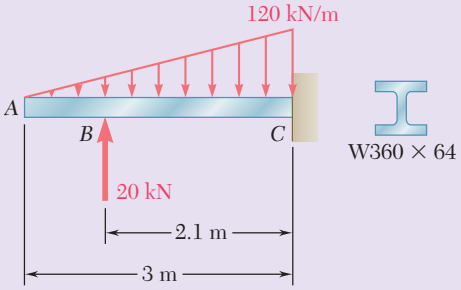


Fig. P9.165

9.166 Knowing that $P = 4$ kips, determine (*a*) the slope at end *A*, (*b*) the deflection at the midpoint *C* of the beam. Use $E = 29 \times 10^6$ psi.

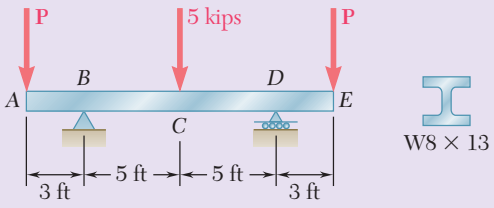


Fig. P9.166

9.167 For the beam and loading shown, determine (*a*) the slope at point *A*, (*b*) the deflection at point *D*.

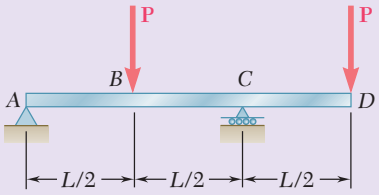


Fig. *P9.167*

9.168 Determine the reaction at the roller support and draw the bending-moment diagram for the beam and loading shown.

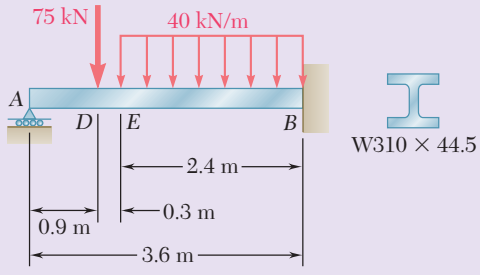


Fig. P9.168

Computer Problems

The following problems are designed to be solved with a computer.

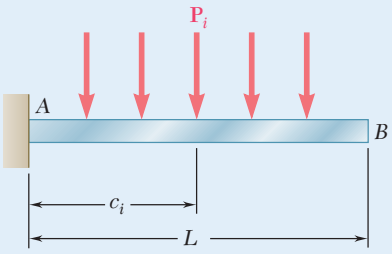


Fig. P9.C1

9.C1 Several concentrated loads can be applied to the cantilever beam *AB*. Write a computer program to calculate the slope and deflection of beam *AB* from $x = 0$ to $x = L$, using given increments Δx. Apply this program with increments $\Delta x = 50$ mm to the beam and loading of Prob. 9.73 and Prob. 9.74.

9.C2 The 22-ft beam *AB* consists of a W21 × 62 rolled-steel shape and supports a 3.5-kip/ft distributed load as shown. Write a computer program and use it to calculate for values of *a* from 0 to 22 ft, using 1-ft increments, (*a*) the slope and deflection at *D*, (*b*) the location and magnitude of the maximum deflection. Use $E = 29 \times 10^6$ psi.

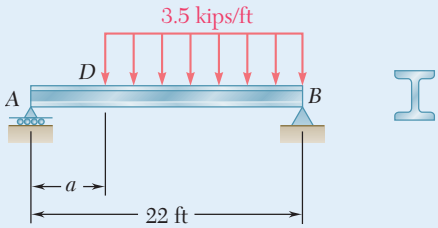


Fig. P9.C2

9.C3 The cantilever beam *AB* carries the distributed loads shown. Write a computer program to calculate the slope and deflection of beam *AB* from $x = 0$ to $x = L$ using given increments Δx. Apply this program with increments $\Delta x = 100$ mm, assuming that $L = 2.4$ m, $w = 36$ kN/m, and (*a*) $a = 0.6$ m, (*b*) $a = 1.2$ m, (*c*) $a = 1.8$ m. Use $E = 200$ GPa.

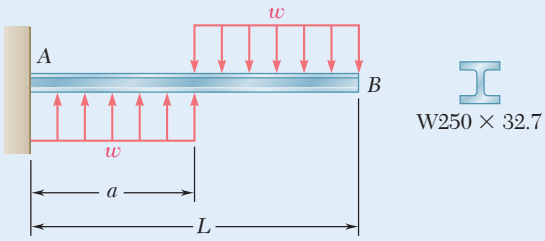


Fig. P9.C3

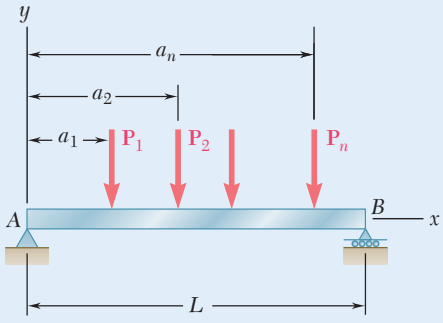


Fig. P9.C4

9.C4 The simple beam *AB* is of constant flexural rigidity *EI* and carries several concentrated loads as shown. Using the *Method of Integration*, write a computer program that can be used to calculate the slope and deflection at points along the beam from $x = 0$ to $x = L$ using given increments Δx. Apply this program to the beam and loading of (*a*) Prob. 9.13 with $\Delta x = 1$ ft, (*b*) Prob. 9.16 with $\Delta x = 0.05$ m, (*c*) Prob. 9.129 with $\Delta x = 0.25$ m.

9.C5 The supports of beam AB consist of a fixed support at end A and a roller support located at point D. Write a computer program that can be used to calculate the slope and deflection at the free end of the beam for values of a from 0 to L using given increments Δa. Apply this program to calculate the slope and deflection at point B for each of the following cases:

	L	ΔL	w	E	Shape
(a)	12 ft	0.5 ft	1.6 k/ft	29×10^6 psi	W16 × 57
(b)	3 m	0.2 m	18 kN/m	200 GPa	W460 × 113

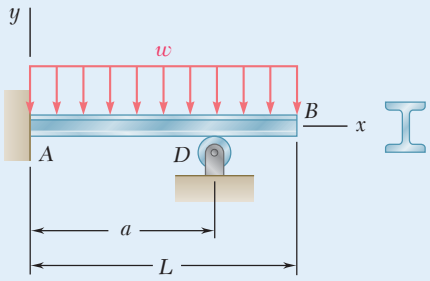


Fig. P9.C5

9.C6 For the beam and loading shown, use the *Moment-Area Method* to write a computer program to calculate the slope and deflection at points along the beam from $x = 0$ to $x = L$ using given increments Δx. Apply this program to calculate the slope and deflection at each concentrated load for the beam of (a) Prob. 9.77 with $\Delta x = 0.5$ m, (b) Prob. 9.119 with $\Delta x = 0.5$ m.

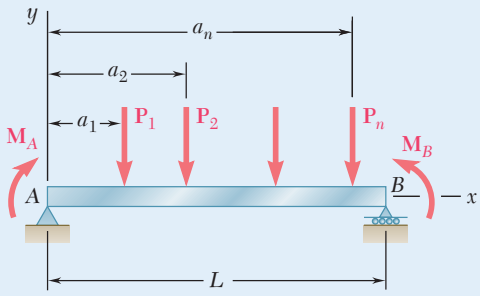


Fig. P9.C6

9.C7 Two 52-kN loads are maintained 2.5 m apart as they are moved slowly across beam AB. Write a computer program to calculate the deflection at the midpoint C of the beam for values of x from 0 to 9 m, using 0.5-m increments. Use $E = 200$ GPa.

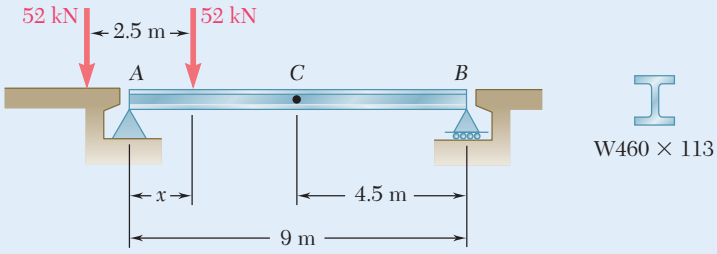


Fig. P9.C7

9.C8 A uniformly distributed load w and several distributed loads P_i may be applied to beam AB. Write a computer program to determine the reaction at the roller support and apply this program to the beam and loading of (a) Prob. 9.53a, (b) Prob. 9.154.

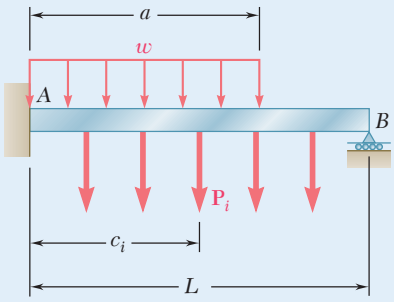
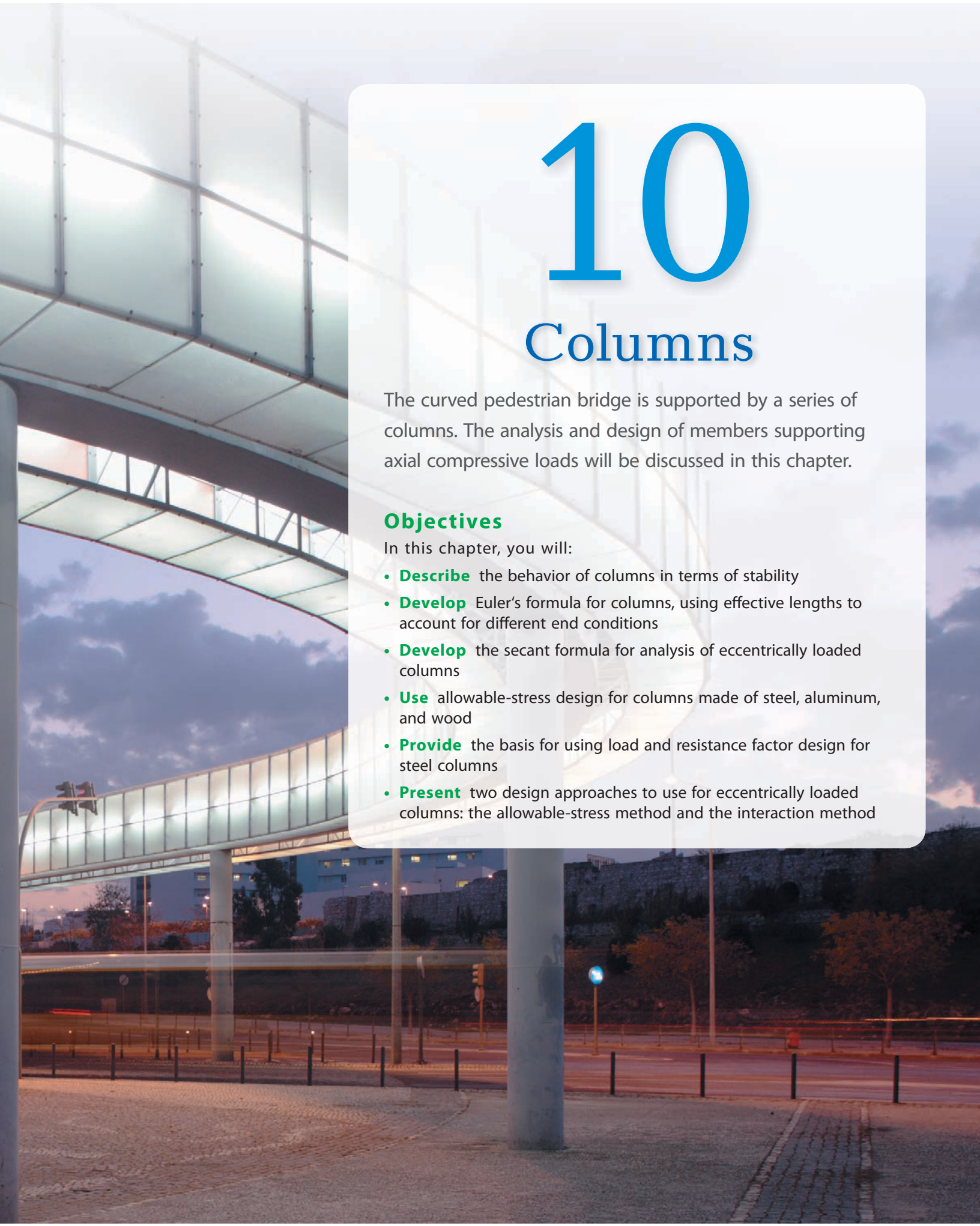


Fig. P9.C8





10 Columns

The curved pedestrian bridge is supported by a series of columns. The analysis and design of members supporting axial compressive loads will be discussed in this chapter.

Objectives

In this chapter, you will:

- **Describe** the behavior of columns in terms of stability
- **Develop** Euler's formula for columns, using effective lengths to account for different end conditions
- **Develop** the secant formula for analysis of eccentrically loaded columns
- **Use** allowable-stress design for columns made of steel, aluminum, and wood
- **Provide** the basis for using load and resistance factor design for steel columns
- **Present** two design approaches to use for eccentrically loaded columns: the allowable-stress method and the interaction method

Introduction
10.1 STABILITY OF STRUCTURES
10.1A Euler's Formula for Pin-Ended Columns
10.1B Euler's Formula for Columns with Other End Conditions
*10.2 ECCENTRIC LOADING AND THE SECANT FORMULA
10.3 CENTRIC LOAD DESIGN
10.3A Allowable Stress Design
10.3B Load and Resistance Factor Design
10.4 ECCENTRIC LOAD DESIGN

Introduction

In the preceding chapters, we had two primary concerns: (1) the strength of the structure, i.e., its ability to support a specified load without experiencing excessive stress; (2) the ability of the structure to support a specified load without undergoing unacceptable deformations. This chapter is concerned with the stability of the structure (its ability to support a given load without experiencing a sudden change in configuration). This discussion is focused on columns, that is, the analysis and design of vertical prismatic members supporting axial loads.

In Sec. 10.1, the stability of a simplified model is discussed, where the column consists of two rigid rods connected by a pin and a spring and supports a load **P.** If its equilibrium is disturbed, this system will return to its original equilibrium position as long as P does not exceed a certain value P_{cr}, called the *critical load.* This is a *stable* system. However, if $P > P_{cr}$, the system moves away from its original position and settles in a new position of equilibrium. This system is said to be *unstable.*

In Sec. 10.1A, the *stability of elastic columns* considers a pin-ended column subjected to a centric axial load. *Euler's formula* for the critical load of the column is derived, and the corresponding critical normal stress in the column is determined. Applying a factor of safety to the critical load, we obtain the allowable load that can be safely applied to a pin-ended column.

In Sec. 10.1B, the analysis of the stability of columns with different end conditions is considered by learning how to determine the *effective length* of a column.

Columns supporting eccentric axial loads are discussed in Sec. 10.2. These columns have transverse deflections for all magnitudes of the load. An equation for the maximum deflection under a given load is developed and used to determine the maximum normal stress in the column. Finally, the *secant formula* relating the average and maximum stresses in a column is developed.

In the first sections of the chapter, each column is assumed to be a straight, homogeneous prism. In the last part of the chapter, real columns are designed and analyzed using empirical formulas set forth by professional organizations. In Sec. 10.3A, design equations are presented for the allowable stress in columns made of steel, aluminum, or wood that are subjected to a centric load. Section 10.3B describes an alternative approach for steel columns, the load and resistance factor design method. The design of columns under an eccentric axial load is covered in Sec. 10.4.

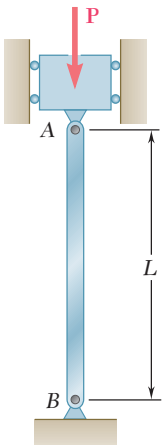


Fig. 10.1 Pinned-ended axially loaded column.

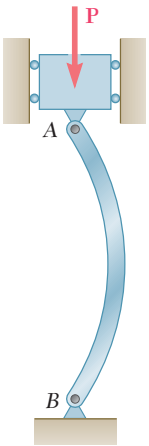


Fig. 10.2 Buckled pin-ended column.

10.1 STABILITY OF STRUCTURES

Consider the design of a column AB of length L to support a given load **P** (Fig. 10.1). The column is pin-connected at both ends, and **P** is a centric axial load. If the cross-sectional area A is selected so that the value $\sigma = P/A$ of the stress on a transverse section is less than the allowable stress σ_{all} for the material used and the deformation $\delta = PL/AE$ falls within the given specifications, we might conclude that the column has been properly designed. However, it may happen that as the load is applied, the column *buckles* (Fig. 10.2). Instead of remaining straight, it suddenly



Photo 10.1 Laboratory test showing a buckled column.

becomes sharply curved such as shown in Photo 10.1. Clearly, a column that buckles under the load it is to support is not properly designed.

Before getting into the actual discussion of the stability of elastic columns, some insight will be gained on the problem by considering a simplified model consisting of two rigid rods AC and BC connected at C by a pin and a torsional spring of constant K (Fig. 10.3).

If the two rods and forces **P** and **P′** are perfectly aligned, the system will remain in the position of equilibrium shown in Fig.10.4*a* as long as it is not disturbed. But suppose we move C slightly to the right so that each rod forms a small angle $\Delta\theta$ with the vertical (Fig. 10.4*b*). Will the system return to its original equilibrium position, or will it move further away? In the first case, the system is *stable;* in the second, it is *unstable*.

To determine whether the two-rod system is stable or unstable, consider the forces acting on rod AC (Fig. 10.5). These forces consist of the couple formed by **P** and **P′** of moment $P(L/2)\sin\Delta\theta$, which tends to move the rod away from the vertical, and the couple **M** exerted by the spring, which tends to bring the rod back into its original vertical position. Since the angle of deflection of the spring is $2\ \Delta\theta$, the moment of couple **M** is $M = K(2\ \Delta\theta)$. If the moment of the second couple is larger than the moment of the first couple, the system tends to return to its original equilibrium position; the system is stable. If the moment of the first couple is larger than the moment of the second couple, the system tends to move

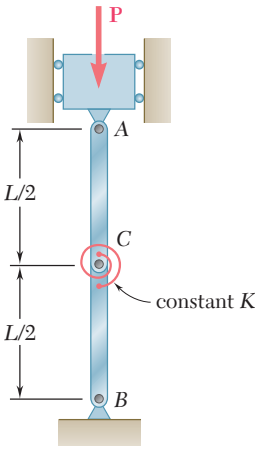


Fig. 10.3 Model column made of two rigid rods joined by a torsional spring at *C*.

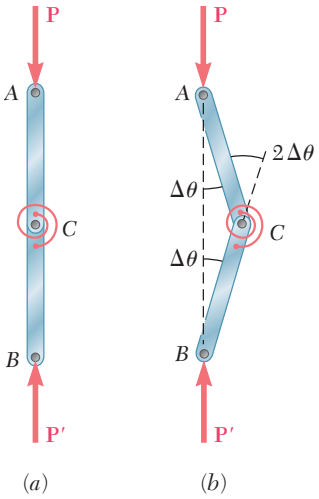


Fig. 10.4 Free-body diagram of model column (*a*) perfectly aligned (*b*) point *C* moved slightly out of alignment.

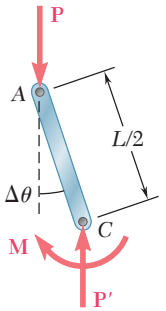


Fig. 10.5 Free-body diagram of rod *AC* in unaligned position.

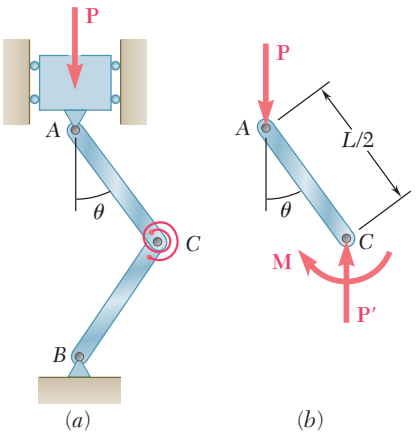


Fig. 10.6 (*a*) Model column in buckled position, (*b*) free-body diagram of rod *AC*.

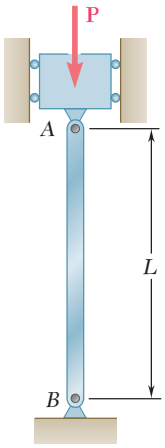


Fig. 10.1 (repeated).

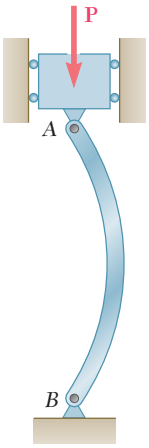


Fig. 10.2 (repeated).

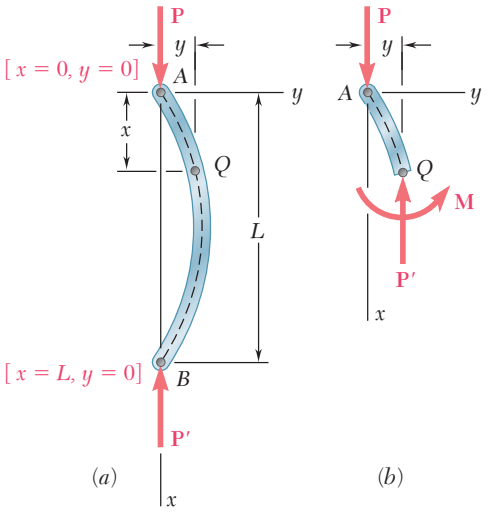


Fig. 10.7 Free-body diagrams of (*a*) buckled column and (*b*) portion *AQ*.

away from its original equilibrium position; the system is unstable. The load when the two couples balance each other is called the *critical load,* P_{cr}, which is given as

$$P_{cr}(L/2)\sin\Delta\theta = K(2\Delta\theta) \tag{10.1}$$

or since $\sin\Delta\theta \approx \Delta\theta$, when the displacement of C is very small (at the immediate onset of buckling),

$$P_{cr} = 4K/L \tag{10.2}$$

Clearly, the system is stable for $P < P_{cr}$ and unstable for $P > P_{cr}$.

Assume that a load $P > P_{cr}$ has been applied to the two rods of Fig. 10.3 and the system has been disturbed. Since $P > P_{cr}$, the system will move further away from the vertical and, after some oscillations, will settle into a new equilibrium position (Fig. 10.6*a*). Considering the equilibrium of the free body AC (Fig. 10.6*b*), an equation similar to Eq. (10.1) but involving the finite angle θ, is

$$P(L/2)\sin\theta = K(2\theta)$$

or

$$\frac{PL}{4K} = \frac{\theta}{\sin\theta} \tag{10.3}$$

The value of θ corresponding to the equilibrium position in Fig. 10.6 is obtained by solving Eq. (10.3) by trial and error. But for any positive value of θ, $\sin\theta < \theta$. Thus, Eq. (10.3) yields a value of θ different from zero only when the left-hand member of the equation is larger than one. Recalling Eq. (10.2), this is true only if $P > P_{cr}$. But, if $P < P_{cr}$, the second equilibrium position shown in Fig. 10.6 would not exist, and the only possible equilibrium position would be the one corresponding to $\theta = 0$. Thus, for $P < P_{cr}$, the position where $\theta = 0$ must be stable.

This observation applies to structures and mechanical systems in general and is used in the next section for the stability of elastic columns.

10.1A Euler's Formula for Pin-Ended Columns

Returning to the column AB considered in the preceding section (Fig. 10.1), we propose to determine the critical value of the load **P,** i.e., the value P_{cr} of the load for which the position shown in Fig. 10.1 ceases to be stable. If $P > P_{cr}$, the slightest misalignment or disturbance will cause the column to buckle into a curved shape, as shown in Fig. 10.2.

This approach determines the conditions under which the configuration of Fig. 10.2 is possible. Since a column is like a beam placed in a vertical position and subjected to an axial load, we proceed as in Chap. 9 and denote by x the distance from end A of the column to a point Q of its elastic curve and by y the deflection of that point (Fig. 10.7*a*). The x axis is vertical and directed downward, and the y axis is horizontal and directed to the right. Considering the equilibrium of the free body AQ (Fig. 10.7*b*),

the bending moment at Q is $M = -Py$. Substituting this value for M in Eq. (9.4) gives

$$\frac{d^2y}{dx^2} = \frac{M}{EI} = -\frac{P}{EI}y \tag{10.4}$$

or transposing the last term,

$$\frac{d^2y}{dx^2} + \frac{P}{EI}y = 0 \tag{10.5}$$

This equation is a linear, homogeneous differential equation of the second order with constant coefficients. Setting

$$p^2 = \frac{P}{EI} \tag{10.6}$$

Eq. (10.5) is rewritten as

$$\frac{d^2y}{dx^2} + p^2y = 0 \tag{10.7}$$

which is the same as the differential equation for simple harmonic motion, except the independent variable is now the distance x instead of the time t. The general solution of Eq. (10.7) is

$$y = A \sin px + B \cos px \tag{10.8}$$

and is easily checked by calculating d^2y/dx^2 and substituting for y and d^2y/dx^2 into Eq. (10.7).

Recalling the boundary conditions that must be satisfied at ends A and B of the column (Fig. 10.7*a*), make $x = 0$, $y = 0$ in Eq. (10.8), and find that $B = 0$. Substituting $x = L$, $y = 0$, obtain

$$A \sin pL = 0 \tag{10.9}$$

This equation is satisfied if either $A = 0$ or $\sin pL = 0$. If the first of these conditions is satisfied, Eq. (10.8) reduces to $y = 0$ and the column is straight (Fig. 10.1). For the second condition to be satisfied, $pL = n\pi$, or substituting for p from (10.6) and solving for P,

$$P = \frac{n^2\pi^2EI}{L^2} \tag{10.10}$$

The smallest value of P defined by Eq. (10.10) is that corresponding to $n = 1$. Thus,

$$P_{\text{cr}} = \frac{\pi^2EI}{L^2} \tag{10.11a}$$

This expression is known as *Euler's formula,* after the Swiss mathematician Leonhard Euler (1707–1783). Substituting this expression for P into Eq. (10.6), the value for p into Eq. (10.8), and recalling that $B = 0$,

$$y = A \sin \frac{\pi x}{L} \tag{10.12}$$

which is the equation of the elastic curve after the column has buckled (Fig. 10.2). Note that the maximum deflection $y_m = A$ is indeterminate.

This is because the differential Eq. (10.5) is a linearized approximation of the governing differential equation for the elastic curve.†

If $P < P_{cr}$, the condition $\sin pL = 0$ cannot be satisfied, and the solution of Eq. (10.12) does not exist. Then we must have $A = 0$, and the only possible configuration for the column is a straight one. Thus, for $P < P_{cr}$ the straight configuration of Fig. 10.1 is stable.

In a column with a circular or square cross section, the moment of inertia I is the same about any centroidal axis, and the column is as likely to buckle in one plane as another (except for the restraints that can be imposed by the end connections). For other cross-sectional shapes, the critical load should be found by making $I = I_{min}$ in Eq. (10.11a). If it occurs, buckling will take place in a plane perpendicular to the corresponding principal axis of inertia.

The stress corresponding to the critical load is the *critical stress* σ_{cr}. Recalling Eq. (10.11a) and setting $I = Ar^2$, where A is the cross-sectional area and r its radius of gyration gives

$$\sigma_{cr} = \frac{P_{cr}}{A} = \frac{\pi^2 EAr^2}{AL^2}$$

or

$$\sigma_{cr} = \frac{\pi^2 E}{(L/r)^2} \qquad \textbf{(10.13a)}$$

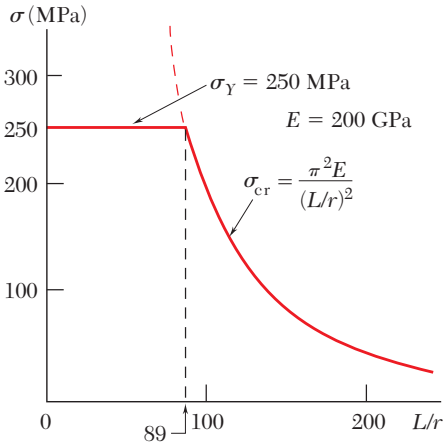


Fig. 10.8 Plot of critical stress.

The quantity L/r is the *slenderness ratio* of the column. The minimum value of the radius of gyration r should be used to obtain the slenderness ratio and the critical stress in a column.

Equation (10.13a) shows that the critical stress is proportional to the modulus of elasticity of the material and inversely proportional to the square of the slenderness ratio of the column. The plot of σ_{cr} versus L/r is shown in Fig. 10.8 for structural steel, assuming $E = 200$ GPa and $\sigma_Y = 250$ MPa. Keep in mind that no factor of safety has been used in plotting σ_{cr}. Also, if σ_{cr} obtained from Eq. (10.13a) or from the curve of Fig. 10.8 is larger than the yield strength σ_Y, this value is of no interest, since the column will yield in compression and cease to be elastic before it has a chance to buckle.

The analysis of the behavior of a column has been based on the assumption of a perfectly aligned centric load. In practice, this is seldom the case, and in Sec. 10.2, the effect of eccentric loading is taken into account. This approach leads to a smoother transition from the buckling failure of long, slender columns to the compression failure of short, stubby columns. It also provides a more realistic view of the relationship between the slenderness ratio of a column and the load that causes it to fail.

†Recall that $d^2y/dx^2 = M/EI$ was obtained in Sec. 9.1A by assuming that the slope dy/dx of the beam could be neglected and that the exact expression in Eq. (9.3) for the curvature of the beam could be replaced by $1/\rho = d^2y/dx^2$.

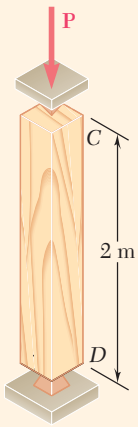


Fig. 10.9 Pin-ended wood column of square cross section.

Concept Application 10.1

A 2-m-long pin-ended column with a square cross section is to be made of wood (Fig 10.9). Assuming $E = 13$ GPa, $\sigma_{all} = 12$ MPa, and using a factor of safety of 2.5 to calculate Euler's critical load for buckling, determine the size of the cross section if the column is to safely support (*a*) a 100-kN load, (*b*) a 200-kN load.

a. For the 100-kN Load. Use the given factor of safety to obtain

$$P_{cr} = 2.5(100\text{ kN}) = 250\text{ kN} \qquad L = 2\text{ m} \qquad E = 13\text{ GPa}$$

Use Euler's formula, Eq. (10.11a), and solve for I:

$$I = \frac{P_{cr}L^2}{\pi^2 E} = \frac{(250 \times 10^3\text{ N})(2\text{ m})^2}{\pi^2(13 \times 10^9\text{ Pa})} = 7.794 \times 10^{-6}\text{ m}^4$$

Recalling that, for a square of side a, $I = a^4/12$, write

$$\frac{a^4}{12} = 7.794 \times 10^{-6}\text{ m}^4 \qquad a = 98.3\text{ mm} \approx 100\text{ mm}$$

Check the value of the normal stress in the column:

$$\sigma = \frac{P}{A} = \frac{100\text{ kN}}{(0.100\text{ m})^2} = 10\text{ MPa}$$

Since σ is smaller than the allowable stress, a 100 × 100-mm cross section is acceptable.

b. For the 200-kN Load. Solve Eq. (10.11a) again for I, but make $P_{cr} = 2.5(200) = 500$ kN to obtain

$$I = 15.588 \times 10^{-6}\text{ m}^4$$

$$\frac{a^4}{12} = 15.588 \times 10^{-6} \qquad a = 116.95\text{ mm}$$

The value of the normal stress is

$$\sigma = \frac{P}{A} = \frac{200\text{ kN}}{(0.11695\text{ m})^2} = 14.62\text{ MPa}$$

Since this is larger than the allowable stress, the dimension obtained is not acceptable, and the cross section must be selected on the basis of its resistance to compression.

$$A = \frac{P}{\sigma_{all}} = \frac{200\text{ kN}}{12\text{ MPa}} = 16.67 \times 10^{-3}\text{ m}^2$$

$$a^2 = 16.67 \times 10^{-3}\text{ m}^2 \qquad a = 129.1\text{ mm}$$

A 130 × 130-mm cross section is acceptable.

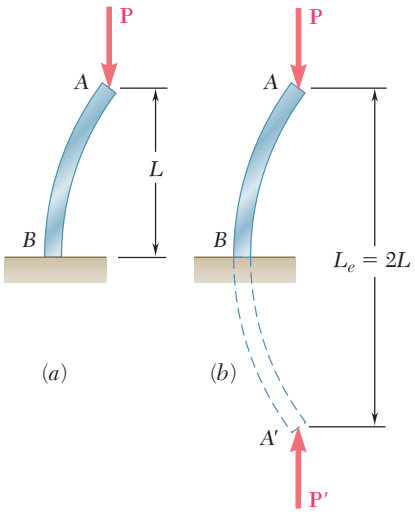


Fig. 10.10 Effective length of a fixed-free column of length L is equivalent to a pin-ended column of length $2L$.

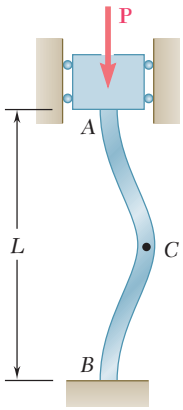


Fig. 10.11 Column with fixed ends.

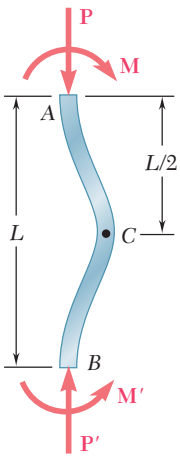


Fig. 10.12 Free-body diagram of buckled fixed-ended column.

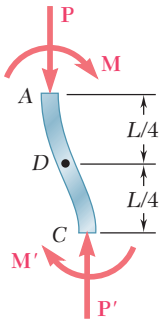


Fig. 10.13 Free-body diagram of upper half of fixed-ended column.

10.1B Euler's Formula for Columns with Other End Conditions

Euler's formula (10.11) was derived in the preceding section for a column that was pin-connected at both ends. Now the critical load P_{cr} will be determined for columns with different end conditions.

A column with one free end A supporting a load **P** and one fixed end B (Fig. 10.10*a*) behaves as the upper half of a pin-connected column (Fig. 10.10*b*). The critical load for the column of Fig. 10.10*a* is thus the same as for the pin-ended column of Fig. 10.10*b* and can be obtained from Euler's formula Eq. (10.11a) by using a column length equal to twice the actual length L. We say that the *effective length* L_e of the column of Fig. 10.10 is equal to $2L$, and substitute $L_e = 2L$ in Euler's formula:

$$P_{cr} = \frac{\pi^2 EI}{L_e^2} \tag{10.11b}$$

The critical stress is

$$\sigma_{cr} = \frac{\pi^2 E}{(L_e/r)^2} \tag{10.13b}$$

The quantity L_e/r is called the *effective slenderness ratio* of the column and for Fig. 10.10*a* is equal to $2L/r$.

Now consider a column with two fixed ends A and B supporting a load **P** (Fig. 10.11). The symmetry of the supports and the load about a horizontal axis through the midpoint C requires that the shear at C and the horizontal components of the reactions at A and B be zero (Fig. 10.12a). Thus, the restraints imposed on the upper half AC of the column by the support at A and by the lower half CB are identical (Fig. 10.13). Portion AC must be symmetric about its midpoint D, and this point must be a point of inflection where the bending moment is zero. The bending moment at the midpoint E of the lower half of the column also must be zero (Fig. 10.14*a*). Since the bending moment at the ends of a pin-ended column is zero, portion DE of the column in Fig. 10.13*a* must behave like a pin-ended column (Fig. 10.14*b*). Thus, the effective length of a column with two fixed ends is $L_e = L/2$.

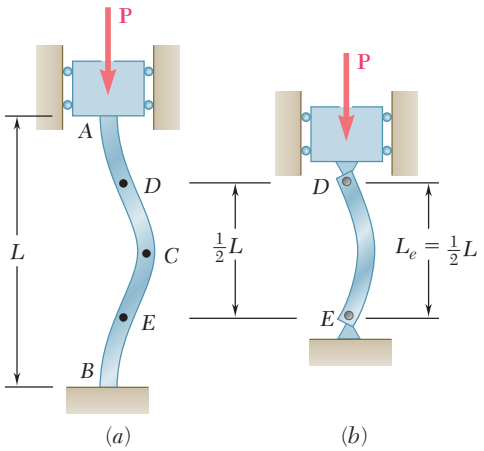


Fig. 10.14 Effective length of a fixed-ended column of length L is equivalent to a pin-ended column of length $L/2$.

In a column with one fixed end B and one pin-connected end A supporting a load **P** (Fig. 10.15), the differential equation of the elastic curve must be solved to determine the effective length. From the free-body diagram of the entire column (Fig. 10.16), a transverse force **V** is exerted at end A, in addition to the axial load **P**, and **V** is statically indeterminate. Considering the free-body diagram of a portion AQ of the column (Fig. 10.17), the bending moment at Q is

$$M = -Py - Vx$$

Substituting this value into Eq. (9.4) of Sec. 9.1A,

$$\frac{d^2y}{dx^2} = \frac{M}{EI} = -\frac{P}{EI}y - \frac{V}{EI}x$$

Transposing the term containing y and setting

$$p^2 = \frac{P}{EI} \tag{10.6}$$

as in Sec. 10.1A gives

$$\frac{d^2y}{dx^2} + p^2y = -\frac{V}{EI}x \tag{10.14}$$

This is a linear, nonhomogeneous differential equation of the second order with constant coefficients. Observing that the left-hand members of Eqs. (10.7) and (10.14) are identical, the general solution of Eq. (10.14) can be obtained by adding a particular solution of Eq. (10.14) to the solution of Eq. (10.8) obtained for Eq. (10.7). Such a particular solution is

$$y = -\frac{V}{p^2EI}x$$

or recalling Eq. (10.6),

$$y = -\frac{V}{P}x \tag{10.15}$$

Adding the solutions of Eq. (10.8) and (10.15), the general solution of Eq. (10.14) is

$$y = A\sin px + B\cos px - \frac{V}{P}x \tag{10.16}$$

The constants A and B and the magnitude V of the unknown transverse force **V** are obtained from the boundary conditions in Fig. (10.16). Making $x = 0$, $y = 0$ in Eq. (10.16), $B = 0$. Making $x = L$, $y = 0$, gives

$$A\sin pL = \frac{V}{P}L \tag{10.17}$$

Taking the derivative of Eq. (10.16), with $B = 0$,

$$\frac{dy}{dx} = Ap\cos px - \frac{V}{P}$$

and making $x = L$, $dy/dx = 0$,

$$Ap\cos pL = \frac{V}{P} \tag{10.18}$$

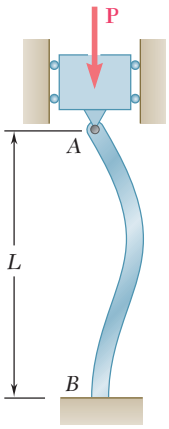


Fig. 10.15 Column with fixed-pinned end conditions.

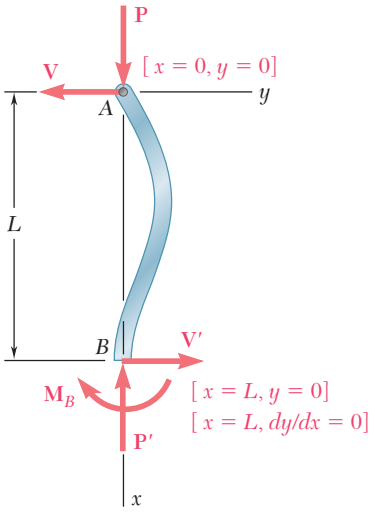


Fig. 10.16 Free-body diagram of buckled fixed-pinned column.

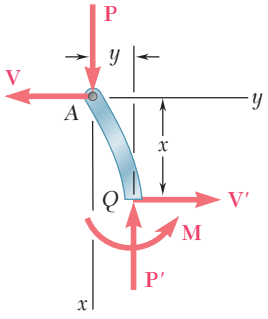


Fig. 10.17 Free-body diagram of portion AQ of buckled fixed-pinned column.

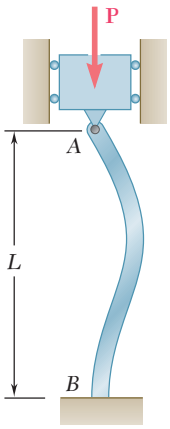


Fig. 10.15 (repeated).

Dividing Eq. (10.17) by Eq. (10.18) member by member, a solution like Eq. (10.16) can exist only if

$$\tan pL = pL \tag{10.19}$$

Solving this equation by trial and error, the smallest value of pL that satisfies Eq. (10.19) is

$$pL = 4.4934 \tag{10.20}$$

Carrying the value of p from Eq. (10.20) into Eq. (10.6) and solving for P, the critical load for the column of Fig. 10.15 is

$$P_{\text{cr}} = \frac{20.19EI}{L^2} \tag{10.21}$$

The effective length of the column is obtained by equating the right-hand members of Eqs. (10.11b) and (10.21):

$$\frac{\pi^2 EI}{L_e^2} = \frac{20.19EI}{L^2}$$

Solving for L_e, the effective length of a column with one fixed end and one pin-connected end is $L_e = 0.699L \approx 0.7L$.

The effective lengths corresponding to the various end conditions are shown in Fig. 10.18.

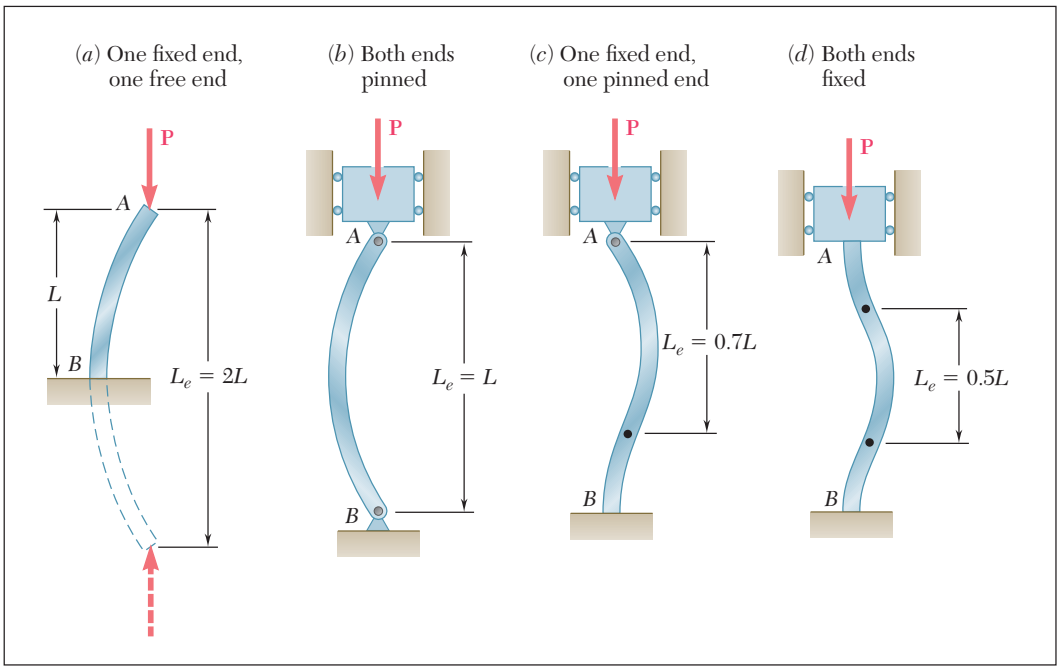
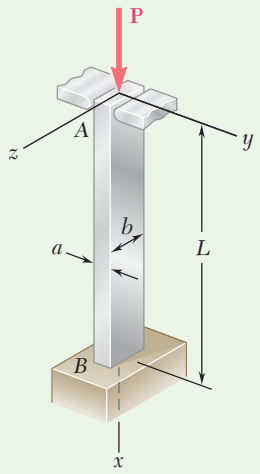


Fig. 10.18 Effective length of column for various end conditions.

Sample Problem 10.1



An aluminum column with a length of L and a rectangular cross section has a fixed end B and supports a centric load at A. Two smooth and rounded fixed plates restrain end A from moving in one of the vertical planes of symmetry of the column but allow it to move in the other plane. (a) Determine the ratio a/b of the two sides of the cross section corresponding to the most efficient design against buckling. (b) Design the most efficient cross section for the column, knowing that $L = 20$ in., $E = 10.1 \times 10^6$ psi, $P = 5$ kips, and a factor of safety of 2.5 is required.

STRATEGY: The most efficient design is that for which the critical stresses corresponding to the two possible buckling modes are equal. This occurs if the two critical stresses obtained from Eq. (10.13b) are the same. Thus for this problem, the two effective slenderness ratios in this equation must be equal to solve part a. Use Fig. 10.18 to determine the effective lengths. The design data can then be used with Eq. (10.13b) to size the cross section for part b.

MODELING:

Buckling in *xy* Plane. Referring to Fig. 10.18c, the effective length of the column with respect to buckling in this plane is $L_e = 0.7L$. The radius of gyration r_z of the cross section is obtained by

$$I_z = \tfrac{1}{12}ba^3 \quad A = ab$$

and since $I_z = Ar_z^2$,

$$r_z^2 = \frac{I_z}{A} = \frac{\frac{1}{12}ba^3}{ab} = \frac{a^2}{12} \qquad r_z = a/\sqrt{12}$$

The effective slenderness ratio of the column with respect to buckling in the xy plane is

$$\frac{L_e}{r_z} = \frac{0.7L}{a/\sqrt{12}} \tag{1}$$

Buckling in *xz* Plane. Referring to Fig. 10.18a, the effective length of the column with respect to buckling in this plane is $L_e = 2L$, and the corresponding radius of gyration is $r_y = b/\sqrt{12}$. Thus,

$$\frac{L_e}{r_y} = \frac{2L}{b/\sqrt{12}} \tag{2}$$

(continued)

ANALYSIS:

a. Most Efficient Design. The most efficient design is when the critical stresses corresponding to the two possible modes of buckling are equal. Referring to Eq. (10.13b), this is the case if the two values obtained above for the effective slenderness ratio are equal.

$$\frac{0.7L}{a/\sqrt{12}} = \frac{2L}{b/\sqrt{12}}$$

and solving for the ratio a/b,

$$\frac{a}{b} = \frac{0.7}{2} \qquad \frac{a}{b} = 0.35 \blacktriangleleft$$

b. Design for Given Data. Since $F.S. = 2.5$ is required,

$$P_{cr} = (F.S.)P = (2.5)(5 \text{ kips}) = 12.5 \text{ kips}$$

Using $a = 0.35b$,

$$A = ab = 0.35b^2 \quad \text{and} \quad \sigma_{cr} = \frac{P_{cr}}{A} = \frac{12{,}500 \text{ lb}}{0.35b^2}$$

Making $L = 20$ in. in Eq. (2), $L_e/r_y = 138.6/b$. Substituting for E, L_e/r, and σ_{cr} into Eq. (10.13b) gives

$$\sigma_{cr} = \frac{\pi^2 E}{(L_e/r)^2} \qquad \frac{12{,}500 \text{ lb}}{0.35b^2} = \frac{\pi^2(10.1 \times 10^6 \text{ psi})}{(138.6/b)^2}$$

$$b = 1.620 \text{ in.} \qquad a = 0.35b = 0.567 \text{ in.} \blacktriangleleft$$

REFLECT and THINK: The calculated critical Euler buckling stress can never be taken to exceed the yield strength of the material. In this problem, you can readily determine that the critical stress $\sigma_{cr} = 13.6$ ksi; though the specific alloy was not given, this stress is less than the tensile yield strength σ_y values for all aluminum alloys listed in Appendix B.

Problems

10.1 Knowing that the spring at A is of constant k and that the bar AB is rigid, determine the critical load P_{cr}.

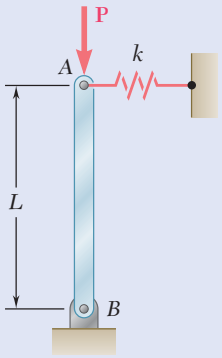


Fig. P10.1

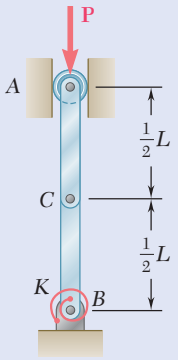


Fig. P10.2

10.2 Two rigid bars AC and BC are connected by a pin at C as shown. Knowing that the torsional spring at B is of constant K, determine the critical load P_{cr} for the system.

10.3 and 10.4 Two rigid bars AC and BC are connected as shown to a spring of constant k. Knowing that the spring can act in either tension or compression, determine the critical load P_{cr} for the system.

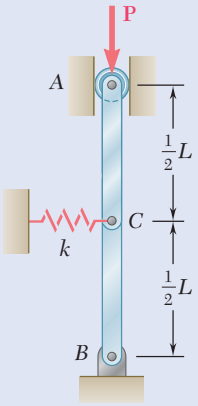


Fig. P10.3

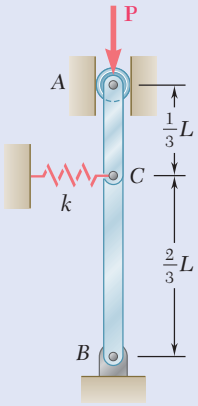


Fig. P10.4

10.5 The steel rod BC is attached to the rigid bar AB and to the fixed support at C. Knowing that $G = 11.2 \times 10^6$ psi, determine the diameter of rod BC for which the critical load P_{cr} of the system is 80 lb.

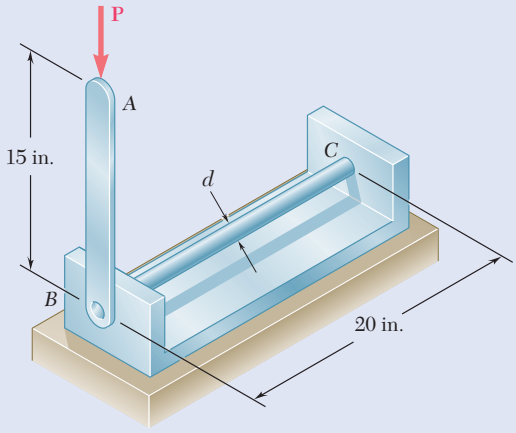


Fig. *P10.5*

10.6 The rigid rod AB is attached to a hinge at A and to two springs, each of constant $k = 2$ kips/in., that can act in either tension or compression. Knowing that $h = 2$ ft, determine the critical load.

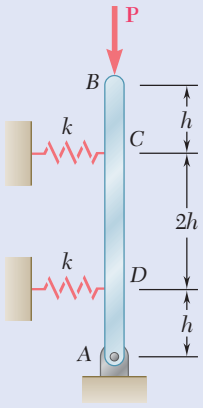


Fig. P10.6

10.7 The rigid bar AD is attached to two springs of constant k and is in equilibrium in the position shown. Knowing that the equal and opposite loads P and P′ remain horizontal, determine the magnitude P_{cr} of the critical load for the system.

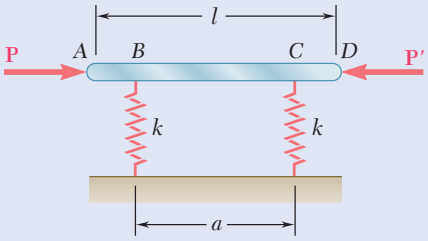


Fig. P10.7

10.8 A frame consists of four L-shaped members connected by four torsional springs, each of constant K. Knowing that equal loads **P** are applied at points A and D as shown, determine the critical value P_{cr} of the loads applied to the frame.

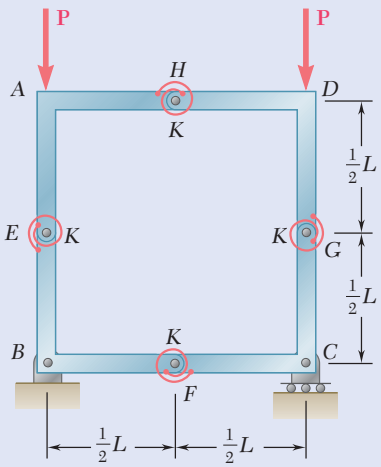


Fig. *P10.8*

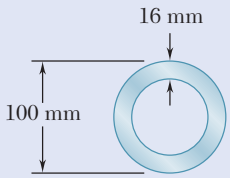


Fig. P10.9

10.9 Determine the critical load of a pin-ended steel tube that is 5 m long and has a 100-mm outer diameter and a 16-mm wall thickness. Use $E = 200$ GPa.

10.10 Determine the critical load of a pin-ended wooden stick that is 3 ft long and has a $\frac{3}{16} \times 1\frac{1}{4}$-in. rectangular cross section. Use $E = 1.6 \times 10^6$ psi.

10.11 A column of effective length L can be made by gluing together identical planks in either of the arrangements shown. Determine the ratio of the critical load using the arrangement a to the critical load using the arrangement b.

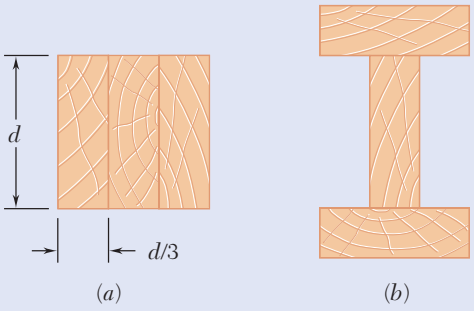


Fig. P10.11

10.12 A compression member of 1.5-m effective length consists of a solid 30-mm-diameter brass rod. In order to reduce the weight of the member by 25%, the solid rod is replaced by a hollow rod of the cross section shown. Determine (*a*) the percent reduction in the critical load, (*b*) the value of the critical load for the hollow rod. Use $E = 200$ GPa.

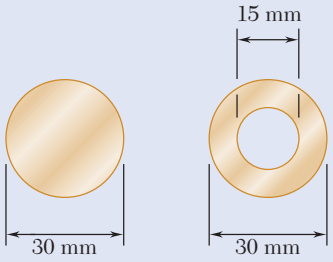


Fig. *P10.12*

10.13 Determine the radius of the round strut so that the round and square struts have the same cross-sectional area and compute the critical load of each strut. Use $E = 200$ GPa.

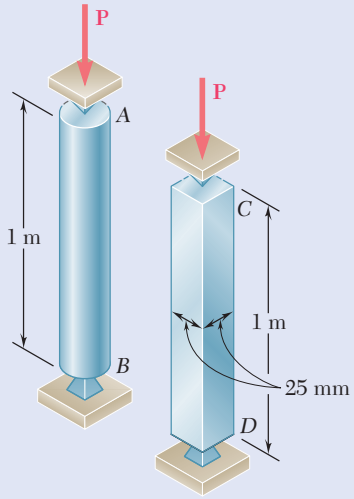


Fig. P10.13 and *P10.14*

10.14 Determine (*a*) the critical load for the square strut, (*b*) the radius of the round strut for which both struts have the same critical load. (*c*) Express the cross-sectional area of the square strut as a percentage of the cross-sectional area of the round strut. Use $E = 200$ GPa.

10.15 A column with the cross section shown has a 13.5-ft effective length. Using a factor of safety equal to 2.8, determine the allowable centric load that can be applied to the column. Use $E = 29 \times 10^6$ psi.

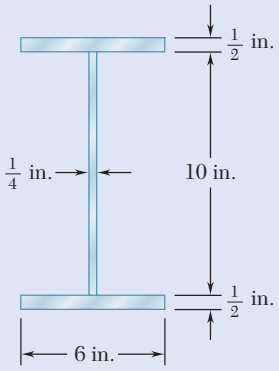
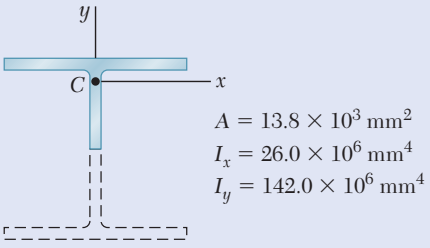


Fig. P10.15

10.16 A column is made from half of a W360 × 216 rolled-steel shape, with the geometric properties as shown. Using a factor of safety equal to 2.6, determine the allowable centric load if the effective length of the column is 6.5 m. Use $E = 200$ GPa.



$A = 13.8 \times 10^3$ mm^2
$I_x = 26.0 \times 10^6$ mm^4
$I_y = 142.0 \times 10^6$ mm^4

Fig. P10.16

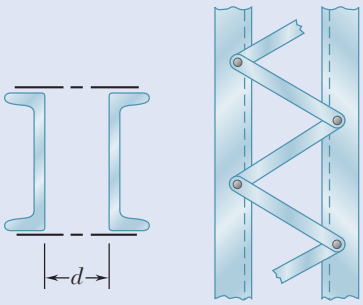


Fig. *P10.18*

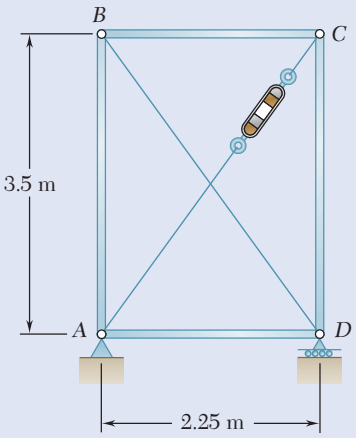


Fig. *P10.20*

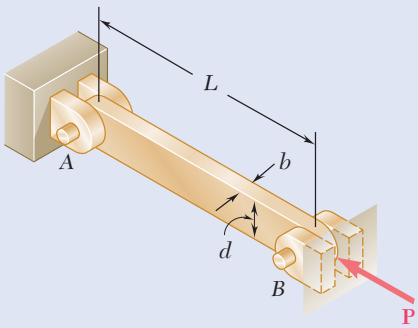


Fig. P10.21

10.17 A column of 22-ft effective length is made by welding two 9 × 0.5-in. plates to a W8 × 35 as shown. Determine the allowable centric load if a factor of safety of 2.3 is required. Use $E = 29 \times 10^6$ psi.

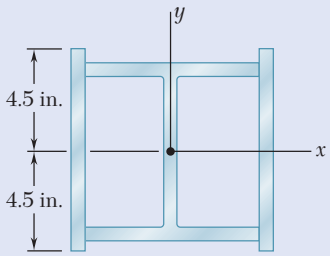


Fig. P10.17

10.18 A single compression member of 8.2-m effective length is obtained by connecting two C200 × 17.1 steel channels with lacing bars as shown. Knowing that the factor of safety is 1.85, determine the allowable centric load for the member. Use $E = 200$ GPa and $d = 100$ mm.

10.19 Knowing that $P = 5.2$ kN, determine the factor of safety for the structure shown. Use $E = 200$ GPa and consider only buckling in the plane of the structure.

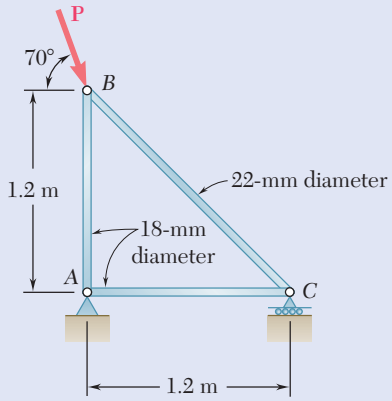


Fig. P10.19

10.20 Members *AB* and *CD* are 30-mm-diameter steel rods, and members *BC* and *AD* are 22-mm-diameter steel rods. When the turnbuckle is tightened, the diagonal member *AC* is put in tension. Knowing that a factor of safety with respect to buckling of 2.75 is required, determine the largest allowable tension in *AC*. Use $E = 200$ GPa and consider only buckling in the plane of the structure.

10.21 The uniform brass bar *AB* has a rectangular cross section and is supported by pins and brackets as shown. Each end of the bar can rotate freely about a horizontal axis through the pin, but rotation about a vertical axis is prevented by the brackets. (*a*) Determine the ratio b/d for which the factor of safety is the same about the horizontal and vertical axes. (*b*) Determine the factor of safety if $P = 1.8$ kips, $L = 7$ ft, $d = 1.5$ in., and $E = 29 \times 10^6$ psi.

10.22 A 1-in.-square aluminum strut is maintained in the position shown by a pin support at A and by sets of rollers at B and C that prevent rotation of the strut in the plane of the figure. Knowing that $L_{AB} = 3$ ft, determine (a) the largest values of L_{BC} and L_{CD} that can be used if the allowable load **P** is to be as large as possible, (b) the magnitude of the corresponding allowable load. Consider only buckling in the plane of the figure and use $E = 10.4 \times 10^6$ psi.

10.23 A 1-in.-square aluminum strut is maintained in the position shown by a pin support at A and by sets of rollers at B and C that prevent rotation of the strut in the plane of the figure. Knowing that $L_{AB} = 3$ ft, $L_{BC} = 4$ ft, and $L_{CD} = 1$ ft, determine the allowable load **P** using a factor of safety with respect to buckling of 3.2. Consider only buckling in the plane of the figure and use $E = 10.4 \times 10^6$ psi.

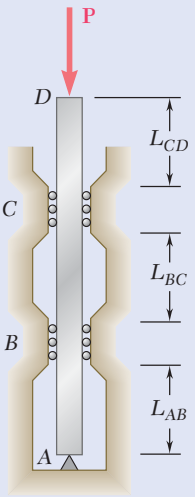


Fig. P10.22 and *P10.23*

10.24 Column ABC has a uniform rectangular cross section with $b = 12$ mm and $d = 22$ mm. The column is braced in the xz plane at its midpoint C and carries a centric load **P** of magnitude 3.8 kN. Knowing that a factor of safety of 3.2 is required, determine the largest allowable length L. Use $E = 200$ GPa.

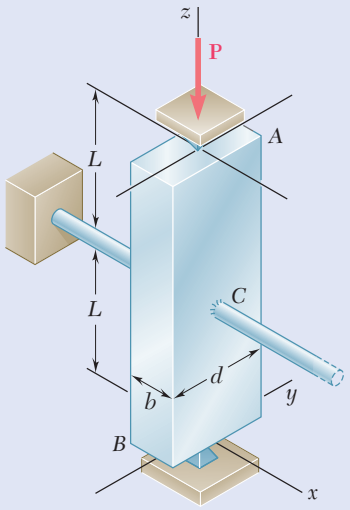


Fig. P10.24 and P10.25

10.25 Column ABC has a uniform rectangular cross section and is braced in the xz plane at its midpoint C. (a) Determine the ratio b/d for which the factor of safety is the same with respect to buckling in the xz and yz planes. (b) Using the ratio found in part a, design the cross section of the column so that the factor of safety will be 3.0 when $P = 4.4$ kN, $L = 1$ m, and $E = 200$ GPa.

10.26 Column AB carries a centric load **P** of magnitude 15 kips. Cables BC and BD are taut and prevent motion of point B in the xz plane. Using Euler's formula and a factor of safety of 2.2, and neglecting the tension in the cables, determine the maximum allowable length L. Use $E = 29 \times 10^6$ psi.

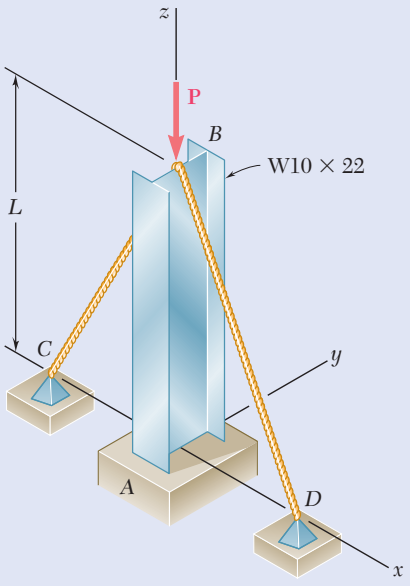


Fig. *P10.26*

10.27 Each of the five struts shown consists of a solid steel rod. (*a*) Knowing that the strut of Fig. (1) is of a 20-mm diameter, determine the factor of safety with respect to buckling for the loading shown. (*b*) Determine the diameter of each of the other struts for which the factor of safety is the same as the factor of safety obtained in part *a*. Use $E = 200$ GPa.

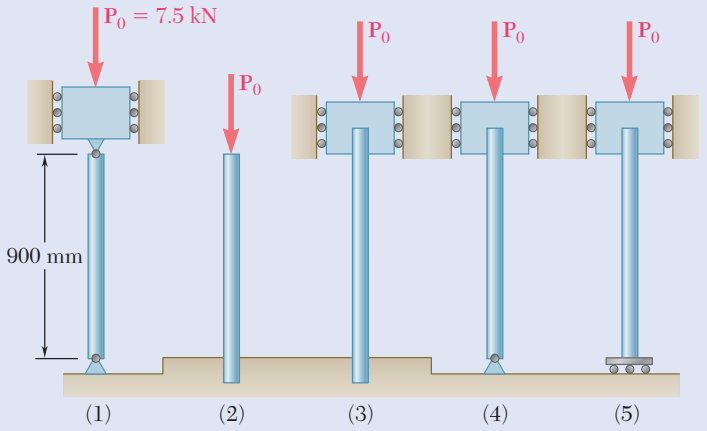


Fig. P10.27

10.28 A rigid block of mass m can be supported in each of the four ways shown. Each column consists of an aluminum tube that has a 44-mm outer diameter and a 4-mm wall thickness. Using $E = 70$ GPa and a factor of safety of 2.8, determine the allowable mass for each support condition.

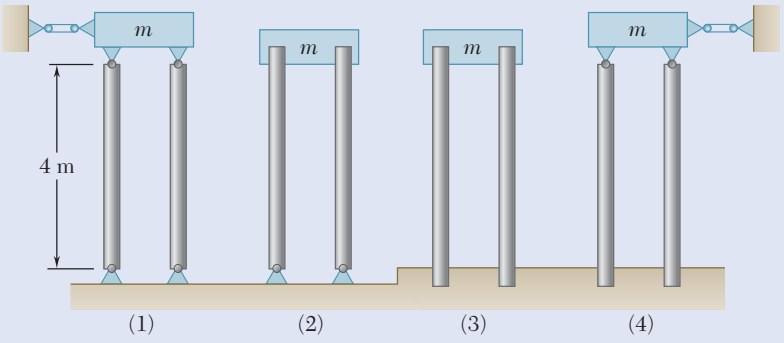


Fig. P10.28

*10.2 ECCENTRIC LOADING AND THE SECANT FORMULA

In this section, column buckling is approached by observing that the load **P** applied to a column is never perfectly centric. The eccentricity of the load is the distance between the line of action **P** and the axis of the column (Fig. 10.19*a*). The given eccentric load is replaced by a centric force **P** and a couple $\mathbf{M}_A$ of moment $M_A = Pe$ (Fig. 10.19*b*). Regardless of how small the

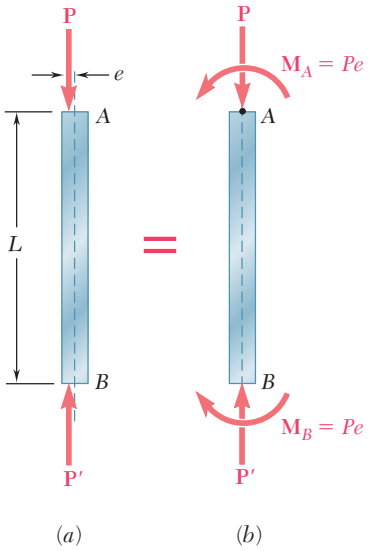


Fig. 10.19 (*a*) Column with an eccentric load (*b*) modeled as a column with an equivalent centric force-couple load.

load **P** and the eccentricity e are, the couple $\mathbf{M}_A$ will cause some bending of the column (Fig. 10.20). As the eccentric load increases, both the couple $\mathbf{M}_A$ and the axial force **P** increase, and both cause the column to bend further. Viewed in this way, buckling is not a question of determining how long the column can remain straight and stable under an increasing load, but how much the column can be permitted to bend if the allowable stress is not exceeded and the deflection $y_{\max}$ is not excessive.

We first write and solve the differential equation of the elastic curve, proceeding in the same manner as we did earlier in Secs. 10.1A and B. Drawing the free-body diagram of a portion AQ of the column and choosing the coordinate axes as shown (Fig. 10.21), we find that the bending moment at Q is

$$M = -Py - M_A = -Py - Pe \tag{10.22}$$

Substituting the value of M into Eq. (9.4) gives

$$\frac{d^2y}{dx^2} = \frac{M}{EI} = -\frac{P}{EI}y - \frac{Pe}{EI}$$

Transposing the term containing y and setting

$$p^2 = \frac{P}{EI} \tag{10.6}$$

as done earlier gives

$$\frac{d^2y}{dx^2} + p^2y = -p^2e \tag{10.23}$$

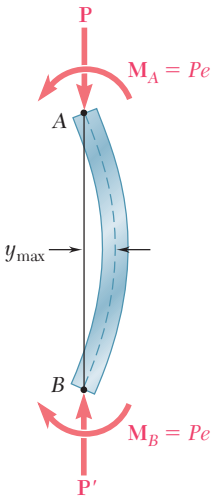


Fig. 10.20 Free-body diagram of an eccentrically loaded column.

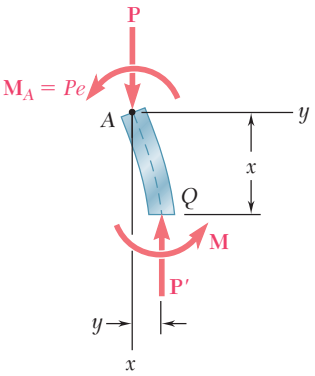


Fig. 10.21 Free-body diagram of portion AQ of an eccentrically loaded column.

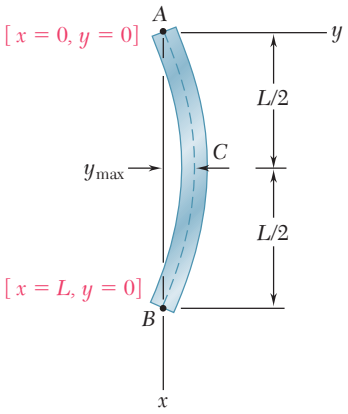


Fig. 10.22 Boundary conditions for an eccentrically loaded column.

Since the left-hand member of Eq. (10.23) is the same as Eq. (10.7), the general solution of Eq. (10.23) is rewritten as

$$y = A \sin px + B \cos px - e \tag{10.24}$$

where the last term is a particular solution.

Constants A and B are obtained from the boundary conditions shown in Fig. 10.22. Making $x = 0$, $y = 0$ in Eq. (10.24), we have

$$B = e$$

Making $x = L$, $y = 0$ gives

$$A \sin pL = e(1 - \cos pL) \tag{10.25}$$

Recalling that

$$\sin pL = 2 \sin \frac{pL}{2} \cos \frac{pL}{2}$$

and

$$1 - \cos pL = 2 \sin^2 \frac{pL}{2}$$

and substituting into Eq. (10.25) after reductions gives

$$A = e \tan \frac{pL}{2}$$

Substituting for A and B into Eq. (10.24), the equation of the elastic curve is

$$y = e\left(\tan \frac{pL}{2} \sin px + \cos px - 1\right) \tag{10.26}$$

The maximum deflection is obtained by setting $x = L/2$ in Eq. (10.26).

$$y_{\max} = e\left(\tan \frac{pL}{2} \sin \frac{pL}{2} + \cos \frac{pL}{2} - 1\right)$$

$$= e\left(\frac{\sin^2 \frac{pL}{2} + \cos^2 \frac{pL}{2}}{\cos \frac{pL}{2}} - 1\right)$$

$$y_{\max} = e\left(\sec \frac{pL}{2} - 1\right) \tag{10.27}$$

Recalling Eq. (10.6), we have

$$y_{\max} = e\left[\sec\left(\sqrt{\frac{P}{EI}} \frac{L}{2}\right) - 1\right] \tag{10.28}$$

The expression obtained indicates that $y_{\max}$ becomes infinite when

$$\sqrt{\frac{P}{EI}} \frac{L}{2} = \frac{\pi}{2} \tag{10.29}$$

While the deflection does not actually become infinite, it nevertheless becomes unacceptably large, and P should not be allowed to reach the critical value which satisfies Eq. (10.29). Solving Eq. (10.29) for P,

$$P_{cr} = \frac{\pi^2 EI}{L^2} \tag{10.30}$$

which also was obtained in Sec. 10.1A for a column under a centric load. Solving Eq. (10.30) for EI and substituting into Eq. (10.28), the maximum deflection in the alternative form is

$$y_{max} = e\left(\sec\frac{\pi}{2}\sqrt{\frac{P}{P_{cr}}} - 1\right) \tag{10.31}$$

The maximum stress σ_{max} occurs in the section of the column where the bending moment is maximum (i.e., the transverse section through the midpoint C) and can be obtained by adding the normal stresses due to the axial force and the bending couple exerted on that section (see Sec. 4.7). Thus,

$$\sigma_{max} = \frac{P}{A} + \frac{M_{max}c}{I} \tag{10.32}$$

From the free-body diagram of portion AC (Fig. 10.23),

$$M_{max} = Py_{max} + M_A = P(y_{max} + e)$$

Substituting this into Eq. (10.32) and recalling that $I = Ar^2$,

$$\sigma_{max} = \frac{P}{A}\left[1 + \frac{(y_{max} + e)c}{r^2}\right] \tag{10.33}$$

Substituting the value obtained in Eq. (10.28) for y_{max}:

$$\sigma_{max} = \frac{P}{A}\left[1 + \frac{ec}{r^2}\sec\left(\sqrt{\frac{P}{EI}}\frac{L}{2}\right)\right] \tag{10.34}$$

An alternative form of σ_{max} is obtained by substituting from (10.31) into Eq. (10.33) for y_{max}. Thus,

$$\sigma_{max} = \frac{P}{A}\left(1 + \frac{ec}{r^2}\sec\frac{\pi}{2}\sqrt{\frac{P}{P_{cr}}}\right) \tag{10.35}$$

This equation can be used with any end conditions, as long as the appropriate value is used for the critical load (see Sec. 10.1B).

Since σ_{max} does not vary linearly with load P, the principle of superposition does not apply to the determination of stress due to the simultaneous application of several loads. The resultant load must be computed first, and then Eqs. (10.34) or (10.35) can be used to find the corresponding stress. For the same reason, any given factor of safety should be applied to the load—not to the stress—when using the *second formula*.

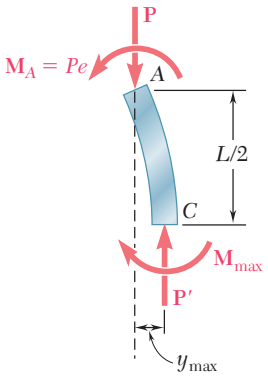


Fig. 10.23 Free-body diagram of upper half of eccentrically loaded column.

Making $I = Ar^2$ in Eq. (10.34) and solving for the ratio P/A in front of the bracket gives

$$\frac{P}{A} = \frac{\sigma_{\max}}{1 + \dfrac{ec}{r^2}\sec\left(\dfrac{1}{2}\sqrt{\dfrac{P}{EA}}\dfrac{L_e}{r}\right)} \tag{10.36}$$

where the effective length is applied for various end conditions. This equation is *the secant formula*. It defines the force per unit area, P/A, that causes a specified maximum stress $\sigma_{\max}$ in a column with a given effective slenderness ratio L_e/r for a ratio ec/r^2, where e is the eccentricity of the applied load. Since P/A appears in both members, it is necessary to solve a transcendental equation by trial and error to obtain the value of P/A corresponding to a given column and loading condition.

Equation (10.36) is used to draw the curves shown in Fig. 10.24*a* and *b* for a steel column, assuming the values of E and σ_Y shown. These curves make it possible to determine the load per unit area P/A, which causes the column to yield for given values of the ratios L_e/r and ec/r^2.

For small values of L_e/r, the secant is almost equal to 1 in Eq. (10.36), and thus P/A can be assumed equal to

$$\frac{P}{A} = \frac{\sigma_{\max}}{1 + \dfrac{ec}{r^2}} \tag{10.37}$$

This value can be obtained by neglecting the effect of the lateral deflection of the column and using the method of Sec. 4.8. On the other hand, Fig. 10.24 shows that, for large values of L_e/r, the curves corresponding to the ratio ec/r^2 get very close to Euler's curve given in Eq. (10.13b). Thus, the effect of the eccentricity of the load on P/A becomes negligible. The secant formula is mainly used for intermediate values of L_e/r. However, to use it effectively, the eccentricity e of the load should be known, but unfortunately, this quantity is seldom known with any degree of precision.

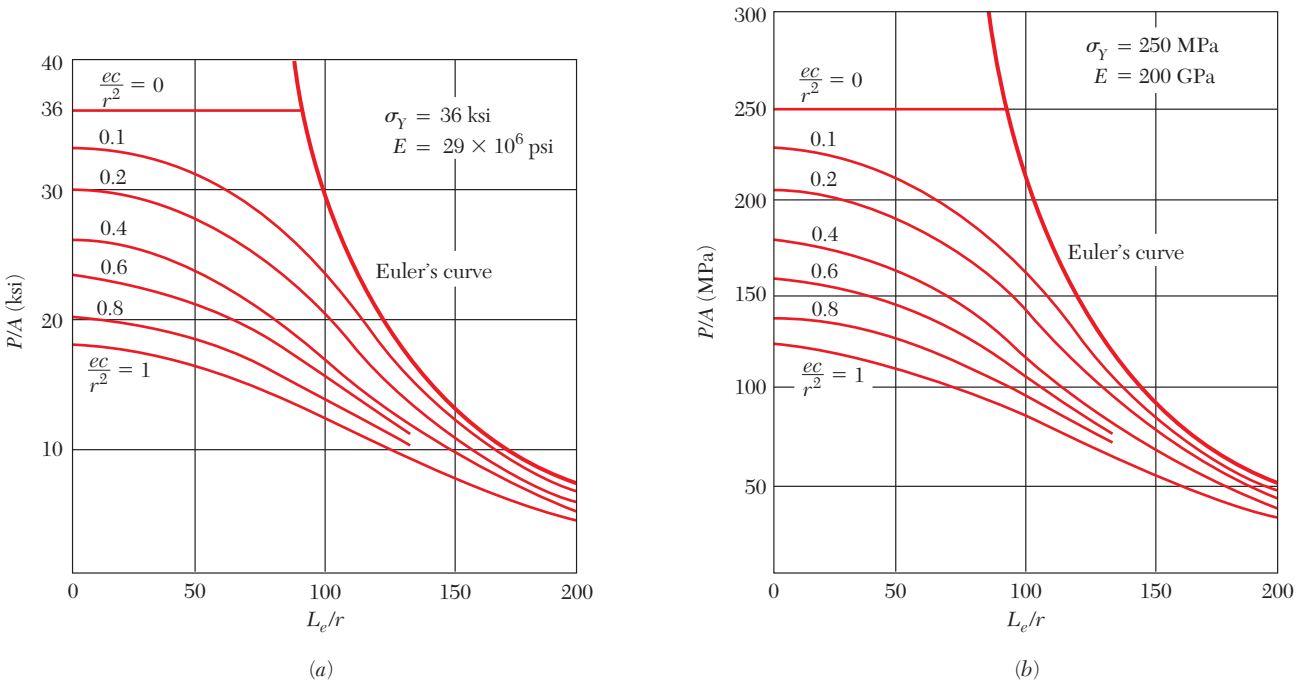
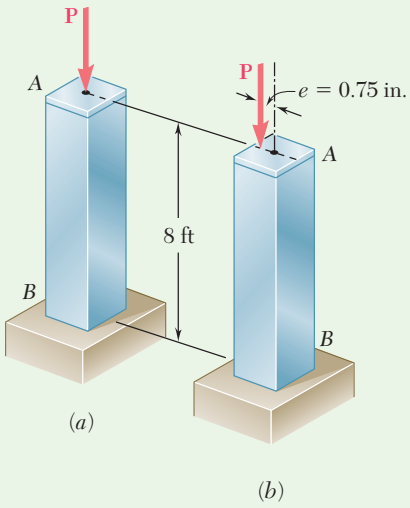
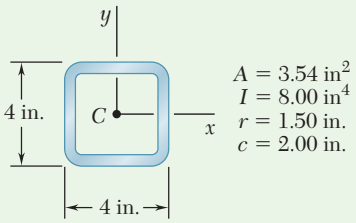


Fig. 10.24 Secant formula plots for buckling in eccentrically loaded columns. (*a*) U.S. customary units. (*b*) Metric units.



Sample Problem 10.2

The uniform column AB consists of an 8-ft section of structural tubing with the cross section shown. (*a*) Using Euler's formula and a factor of safety of 2, determine the allowable centric load for the column and the corresponding normal stress. (*b*) Assuming that the allowable load found in part *a* is applied at a point 0.75 in. from the geometric axis of the column, determine the horizontal deflection of the top of the column and the maximum normal stress in the column. Use $E = 29 \times 10^6$ psi.



STRATEGY: For part *a*, use the factor of safety with Euler's formula to determine the allowable centric load. For part *b*, use Eqs. (10.31) and (10.35) to find the horizontal deflection and maximum normal stress in the column, respectively.

MODELING:

Effective Length. Since the column has one end fixed and one end free, its effective length is

$$L_e = 2(8\text{ ft}) = 16\text{ ft} = 192\text{ in.}$$

Critical Load. Using Euler's formula,

$$P_{cr} = \frac{\pi^2 EI}{L_e^2} = \frac{\pi^2(29 \times 10^6\text{ psi})(8.00\text{ in}^4)}{(192\text{ in.})^2} \qquad P_{cr} = 62.1\text{ kips}$$

ANALYSIS:

a. Allowable Load and Stress. For a factor of safety of 2,

$$P_{all} = \frac{P_{cr}}{F.S.} = \frac{62.1\text{ kips}}{2} \qquad P_{all} = 31.1\text{ kips}$$

and

$$\sigma = \frac{P_{all}}{A} = \frac{31.1\text{ kips}}{3.54\text{ in}^2} \qquad \sigma = 8.79\text{ ksi}$$

(continued)

b. Eccentric Load (Fig. 1). Observe that column AB and its load are identical to the upper half of the column of Fig. 10.20, which was used for the secant formulas. Thus, the formulas of Sec. 10.2 apply directly here. Recalling that $P_{all}/P_{cr} = \frac{1}{2}$ and using Eq. (10.31), the horizontal deflection of point A is

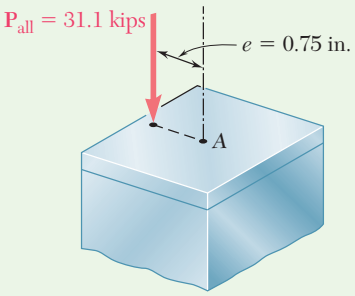


Fig. 1 Allowable load applied at assumed eccentricity.

$$y_m = e\left[\sec\left(\frac{\pi}{2}\sqrt{\frac{P}{P_{cr}}}\right) - 1\right] = (0.75\text{ in.})\left[\sec\left(\frac{\pi}{2\sqrt{2}}\right) - 1\right]$$

$$= (0.75\text{ in.})(2.252 - 1) \qquad y_m = 0.939\text{ in.}$$

This result is illustrated in Fig. 2.

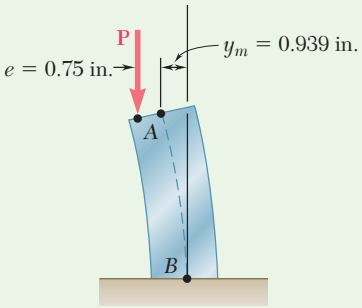


Fig. 2 Deflection of eccentrically loaded column.

The maximum normal stress is obtained from Eq. (10.35) as

$$\sigma_m = \frac{P}{A}\left[1 + \frac{ec}{r^2}\sec\left(\frac{\pi}{2}\sqrt{\frac{P}{P_{cr}}}\right)\right]$$

$$= \frac{31.1\text{ kips}}{3.54\text{ in}^2}\left[1 + \frac{(0.75\text{ in.})(2\text{ in.})}{(1.50\text{ in.})^2}\sec\left(\frac{\pi}{2\sqrt{2}}\right)\right]$$

$$= (8.79\text{ ksi})[1 + 0.667(2.252)] \qquad \sigma_m = 22.0\text{ ksi}$$

Problems

10.29 An axial load **P** = 15 kN is applied at point *D* that is 4 mm from the geometric axis of the square aluminum bar *BC*. Using *E* = 70 GPa, determine (*a*) the horizontal deflection of end *C*, (*b*) the maximum stress in the column.

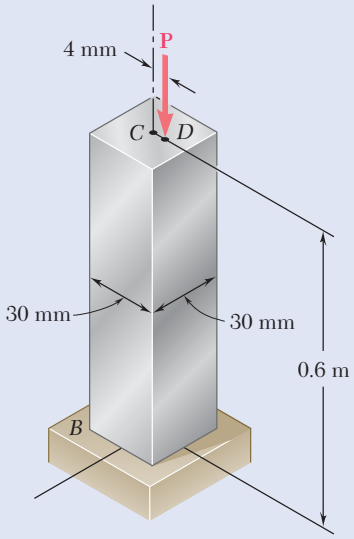


Fig. P10.29

10.30 An axial load **P** is applied to the 32-mm-diameter steel rod *AB* as shown. For *P* = 37 kN and *e* = 1.2 mm, determine (*a*) the deflection at the midpoint *C* of the rod, (*b*) the maximum stress in the rod. Use *E* = 200 GPa.

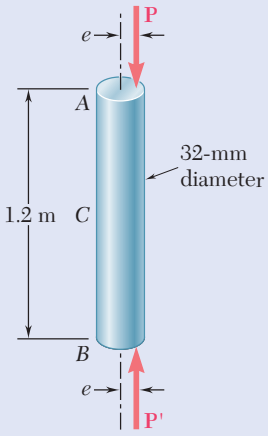


Fig. P10.30

10.31 The line of action of the 310-kN axial load is parallel to the geometric axis of the column *AB* and intersects the *x* axis at *x* = *e*. Using *E* = 200 GPa, determine (*a*) the eccentricity *e* when the deflection of the midpoint *C* of the column is 9 mm, (*b*) the maximum stress in the column.

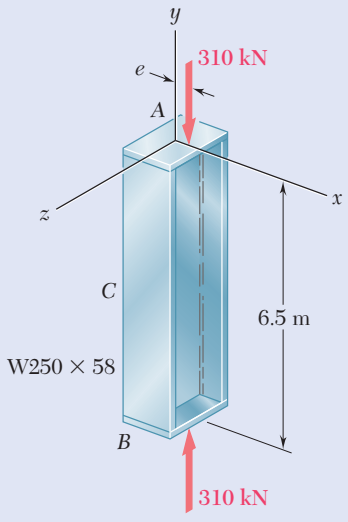


Fig. *P10.31*

10.32 An axial load **P** is applied to the 1.375-in. diameter steel rod *AB* as shown. When $P = 21$ kips, it is observed that the horizontal deflection at midpoint *C* is 0.03 in. Using $E = 29 \times 10^6$ psi, determine (*a*) the eccentricity *e* of the load, (*b*) the maximum stress in the rod.

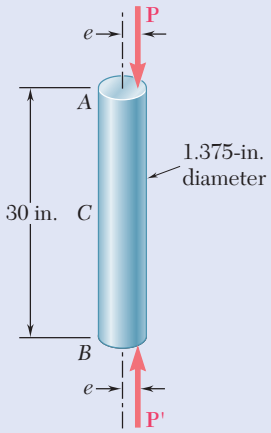


Fig. P10.32

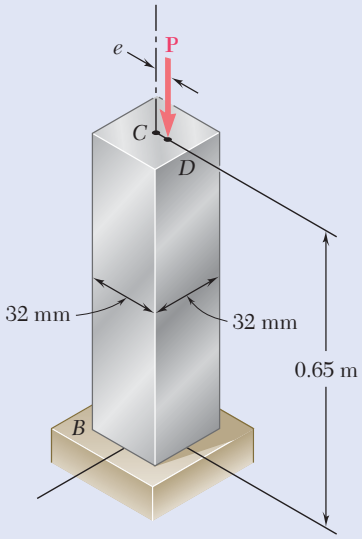


Fig. *P10.33*

10.33 An axial load **P** is applied to the 32-mm-square aluminum bar *BC* as shown. When $P = 24$ kN, the horizontal deflection at end *C* is 4 mm. Using $E = 70$ GPa, determine (*a*) the eccentricity *e* of the load, (*b*) the maximum stress in the bar.

10.34 The axial load **P** is applied at a point located on the *x* axis at a distance *e* from the geometric axis of the rolled-steel column *BC*. When $P = 82$ kips, the horizontal deflection of the top of the column is 0.20 in. Using $E = 29 \times 10^6$ psi, determine (*a*) the eccentricity *e* of the load, (*b*) the maximum stress in the column.

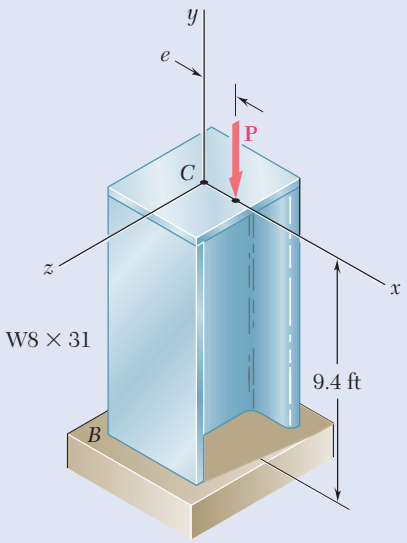


Fig. P10.34

10.35 An axial load **P** is applied at point D that is 0.25 in. from the geometric axis of the square aluminum bar BC. Using $E = 10.1 \times 10^6$ psi, determine (a) the load **P** for which the horizontal deflection of end C is 0.50 in., (b) the corresponding maximum stress in the column.

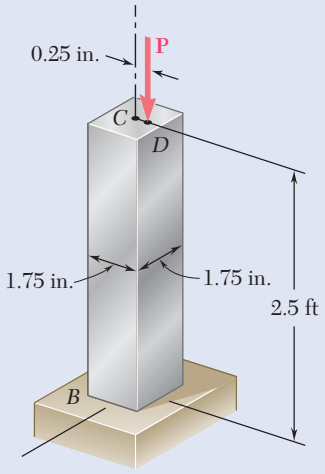


Fig. P10.35

10.36 A brass pipe having the cross section shown has an axial load **P** applied 5 mm from its geometric axis. Using $E = 120$ GPa, determine (a) the load **P** for which the horizontal deflection at the midpoint C is 5 mm, (b) the corresponding maximum stress in the column.

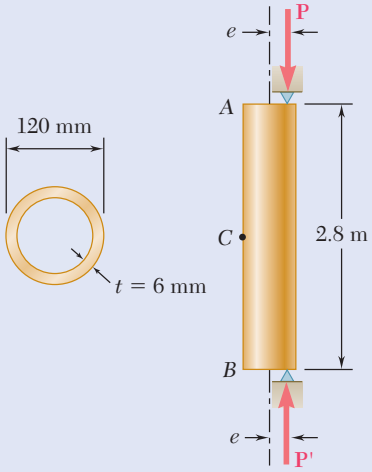


Fig. P10.36

10.37 Solve Prob. 10.36, assuming that the axial load **P** is applied 10 mm from the geometric axis of the column.

10.38 The line of action of the axial load **P** is parallel to the geometric axis of the column AB and intersects the x axis at $x = 0.8$ in. Using $E = 29 \times 10^6$ psi, determine (a) the load **P** for which the horizontal deflection at the end C is 0.5 in., (b) the corresponding maximum stress in the column.

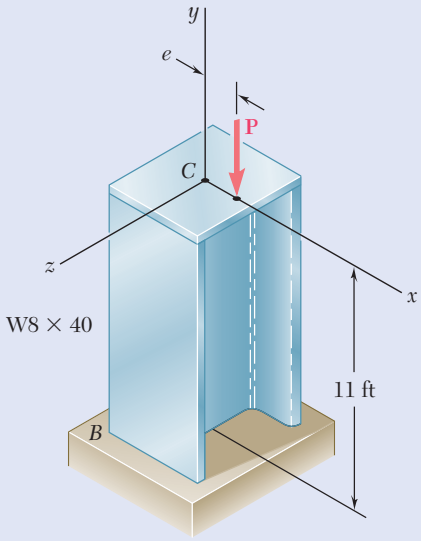


Fig. *P10.38*

10.39 The line of action of the axial load **P** is parallel to the geometric axis of the column and applied at a point located on the x axis at a distance $e = 12$ mm from the geometric axis of the W310 × 60 rolled-steel column BC. Assuming that $L = 7.0$ m and using $E = 200$ GPa, determine (a) the load **P** for which the horizontal deflection of the midpoint C of the column is 15 mm, (b) the corresponding maximum stress in the column.

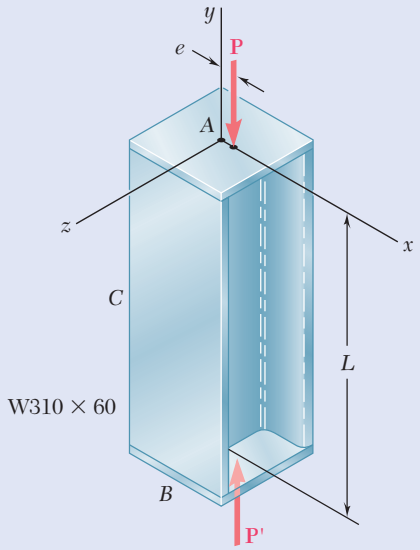


Fig. P10.39

10.40 Solve Prob. 10.39, assuming that L is 9.0 m.

10.41 The steel bar AB has a $\frac{3}{8} \times \frac{3}{8}$-in. square cross section and is held by pins that are a fixed distance apart and are located at a distance $e = 0.03$ in. from the geometric axis of the bar. Knowing that at temperature T_0 the pins are in contact with the bar and that the force in the bar is zero, determine the increase in temperature for which the bar will just make contact with point C if $d = 0.01$ in. Use $E = 29 \times 10^6$ psi and a coefficient of thermal expansion $\alpha = 6.5 \times 10^{-6}$/°F.

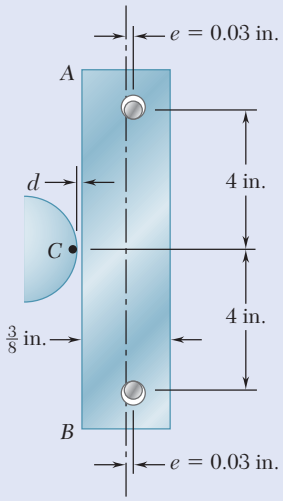


Fig. P10.41

10.42 For the bar of Prob. 10.41, determine the required distance d for which the bar will just make contact with point C when the temperature increases by 120 °F.

10.43 A 3.5-m-long steel tube having the cross section and properties shown is used as a column. For the grade of steel used $\sigma_Y = 250$ MPa and $E = 200$ GPa. Knowing that a factor of safety of 2.6 with respect to permanent deformation is required, determine the allowable load **P** when the eccentricity e is (a) 15 mm, (b) 7.5 mm. (*Hint:* Since the factor of safety must be applied to the load **P**, not to the stress, use Fig. 10.24 to determine P_Y).

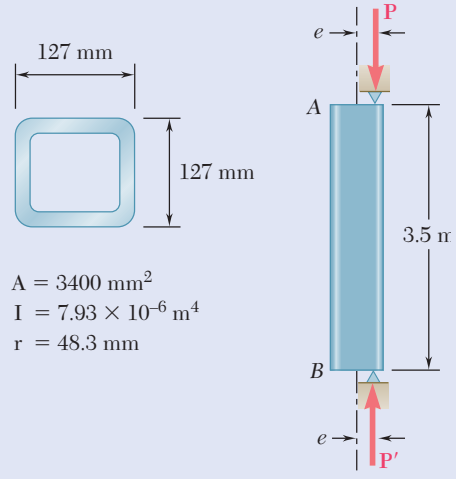


Fig. P10.43

10.44 Solve Prob. 10.43, assuming that the length of the tube is increased to 5 m.

10.45 An axial load **P** is applied to the W8 × 28 rolled-steel column *BC* that is free at its top *C* and fixed at its base *B*. Knowing that the eccentricity of the load is $e = 0.6$ in. and that for the grade of steel used $\sigma_Y = 36$ ksi and $E = 29 \times 10^6$ psi, determine (*a*) the magnitude of *P* of the allowable load when a factor of safety of 2.5 with respect to permanent deformation is required, (*b*) the ratio of the load found in part *a* to the magnitude of the allowable centric load for the column. (See hint of Prob. 10.43.)

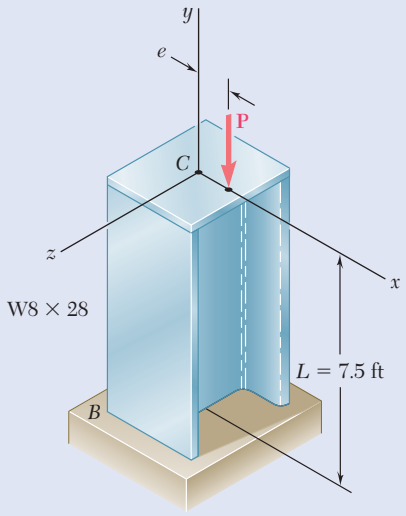


Fig. 10.45 and *10.46*

10.46 An axial load **P** of magnitude 50 kips is applied at a point located on the *x* axis at a distance $e = 0.25$ in. from the geometric axis of the W8 × 28 rolled-steel column *BC*. Knowing that the column is free at its top *C* and fixed at its base *B* and that $\sigma_Y = 36$ ksi and $E = 29 \times 10^6$ psi, determine the factor of safety with respect to yield. (See hint of Prob. 10.43.)

10.47 A 100-kN axial load **P** is applied to the W150 × 18 rolled-steel column *BC* that is free at its top *C* and fixed at its base *B*. Knowing that the eccentricity of the load is $e = 6$ mm, determine the largest permissible length *L* if the allowable stress in the column is 80 MPa. Use $E = 200$ GPa.

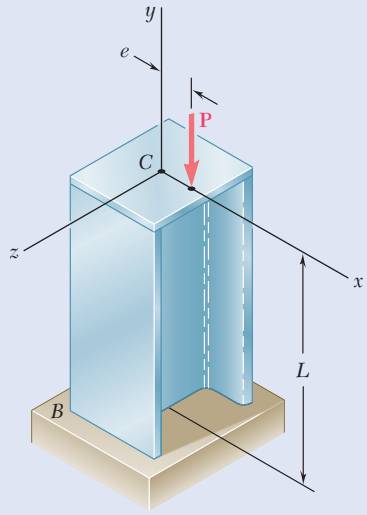


Fig. 10.47

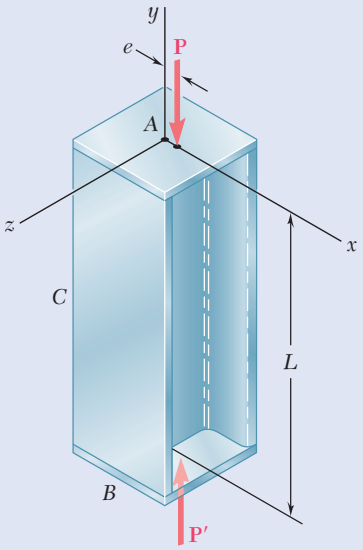


Fig. 10.49

10.48 A 26-kip axial load **P** is applied to a W6 × 12 rolled-steel column *BC* that is free at its top *C* and fixed at its base *B*. Knowing that the eccentricity of the load is $e = 0.25$ in., determine the largest permissible length *L* if the allowable stress in the column is 14 ksi. Use $E = 29 \times 10^6$ psi.

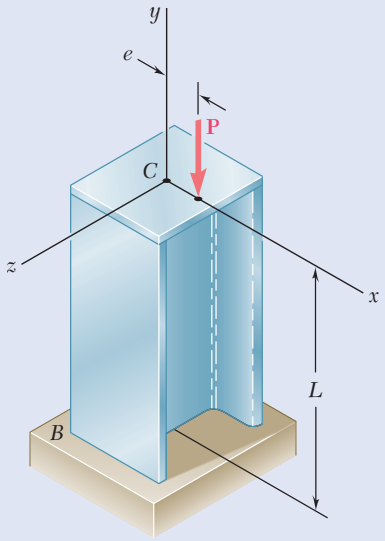


Fig. **10.48**

10.49 Axial loads of magnitude $P = 135$ kips are applied parallel to the geometric axis of the W10 × 54 rolled-steel column *AB* and intersect the *x* axis at a distance *e* from the geometric axis. Knowing that $\sigma_{all} = 12$ ksi and $E = 29 \times 10^6$ psi, determine the largest permissible length *L* when (*a*) $e = 0.25$ in., (*b*) $e = 0.5$ in.

10.50 Axial loads of magnitude $P = 84$ kN are applied parallel to the geometric axis of the W200 × 22.5 rolled-steel column *AB* and intersect the *x* axis at a distance *e* from the geometric axis. Knowing that $\sigma_{all} = 75$ MPa and $E = 200$ GPa, determine the largest permissible length *L* when (*a*) $e = 5$ mm, (*b*) $e = 12$ mm.

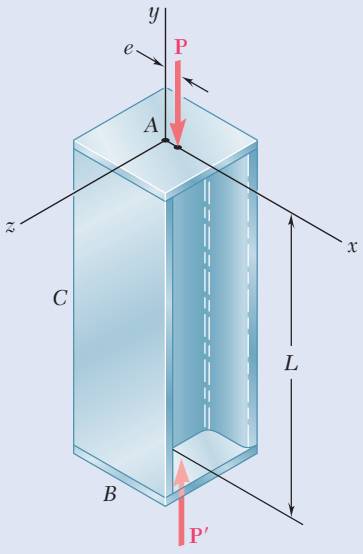


Fig. 10.50

10.51 An axial load of magnitude $P = 220$ kN is applied at a point located on the x axis at a distance $e = 6$ mm from the geometric axis of the wide-flange column BC. Knowing that $E = 200$ GPa, choose the lightest W200 shape that can be used if $\sigma_{all} = 120$ MPa.

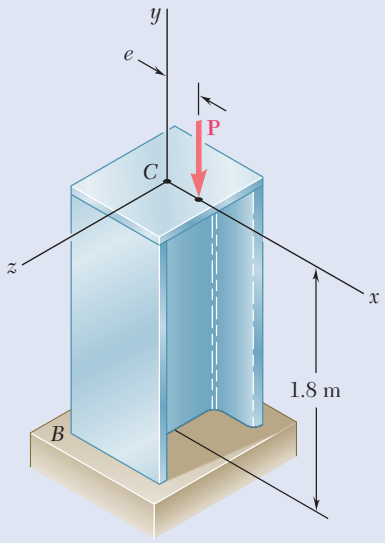


Fig. 10.51

10.52 Solve Prob. 10.51, assuming that the magnitude of the axial load is $P = 345$ kN.

10.53 A 12-kip axial load is applied with an eccentricity $e = 0.375$ in. to the circular steel rod BC that is free at its top C and fixed at its base B. Knowing that the stock of rods available for use have diameters in increments of $\frac{1}{8}$ in. from 1.5 in. to 3.0 in., determine the lightest rod that can be used if $\sigma_{all} = 15$ ksi. Use $E = 29 \times 10^6$ psi.

10.54 Solve Prob. 10.53, assuming that the 12-kip axial load will be applied to the rod with an eccentricity $e = \frac{1}{2}d$.

10.55 Axial loads of magnitude $P = 175$ kN are applied parallel to the geometric axis of a W250 × 44.8 rolled-steel column AB and intersect the x axis at a distance $e = 12$ mm from its geometric axis. Knowing that $\sigma_Y = 250$ MPa and $E = 200$ GPa, determine the factor of safety with respect to yield. (*Hint:* Since the factor of safety must be applied to the load **P**, not to the stresses, use Fig. 10.24 to determine P_Y.)

10.56 Solve Prob. 10.55, assuming that $e = 16$ mm and $P = 155$ kN.

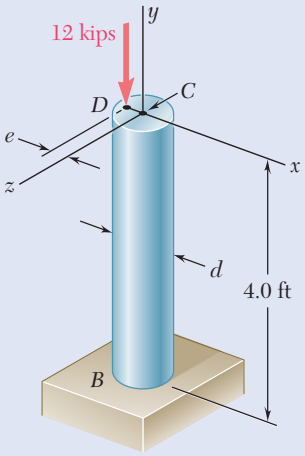


Fig. 10.53

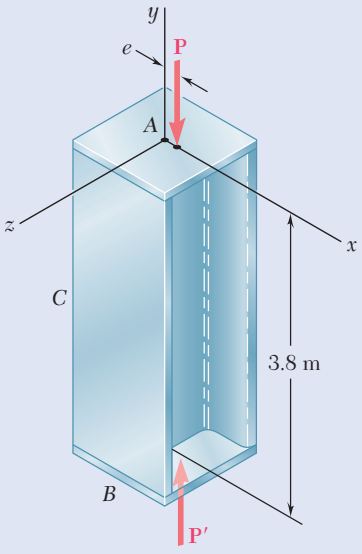


Fig. *10.55*

10.3 CENTRIC LOAD DESIGN

The preceding sections determined the critical load of a column by using Euler's formula and investigated the deformations and stresses in eccentrically loaded columns by using the secant formula. In each case, all stresses remained below the proportional limit, and the column was initially a straight, homogeneous prism. Real columns fall short of such an idealization, and in practice the design of columns is based on empirical formulas that reflect the results of numerous laboratory tests.

Over the last century, many steel columns have been tested by applying to them a centric axial load and increasing the load until failure occurred. The results of such tests are represented in Fig. 10.25 where a point has been plotted with its ordinate equal to the normal stress σ_{cr} at failure and its abscissa is equal to the corresponding effective slenderness ratio L_e/r. Although there is considerable scatter in the test results, regions corresponding to three types of failure can be observed.

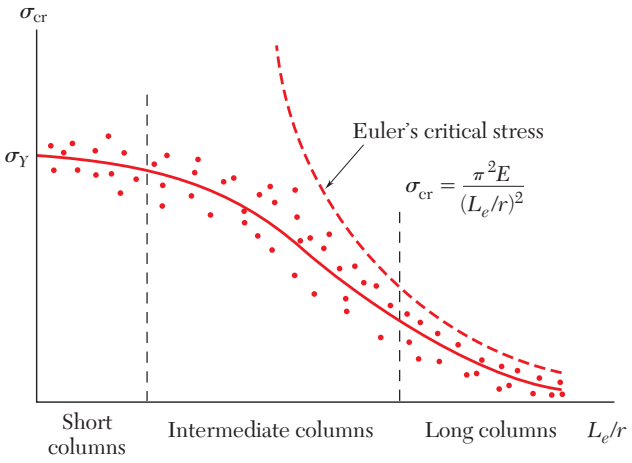


Fig. 10.25 Plot of test data for steel columns.

- For long columns, where L_e/r is large, failure is closely predicted by Euler's formula, and the value of σ_{cr} depends on the modulus of elasticity E of the steel used—but not on its yield strength σ_Y.
- For very short columns and compression blocks, failure essentially occurs as a result of yield, and $\sigma_{cr} \approx \sigma_Y$.
- For columns of intermediate length, failure is dependent on both σ_Y and E. In this range, column failure is an extremely complex phenomenon, and test data is used extensively to guide the development of specifications and design formulas.

Empirical formulas for an allowable or critical stress given in terms of the effective slenderness ratio were first introduced over a century ago. Since then, they have undergone a process of refinement and improvement. Typical empirical formulas used to approximate test data are shown

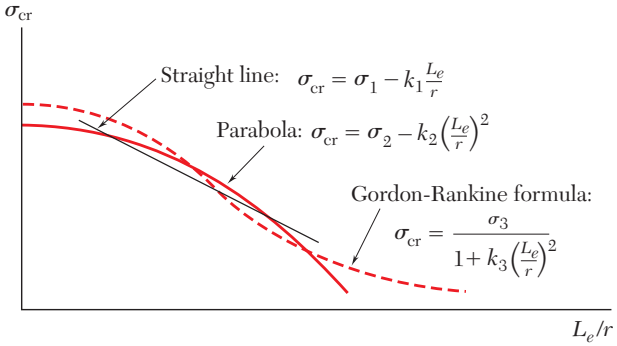


Fig. 10.26 Plots of empirical formulas for critical stresses.

in Fig. 10.26. It is not always possible to use a single formula for all values of L_e/r. Most design specifications use different formulas—each with a definite range of applicability. In each case we must check that the equation used is applicable for the value of L_e/r for the column involved. Furthermore, it must determined whether the equation provides the critical stress for the column, to which the appropriate factor of safety must be applied, or if it provides an allowable stress.

Photo 10.2 shows examples of columns that are designed using such design specification formulas. The design formulas for three different materials using *Allowable Stress Design* are presented next, followed by formulas for the design of steel columns based on *Load and Resistance Factor Design*.†



(*a*) (*b*)

Photo 10.2 (*a*) The water tank is supported by steel columns. (*b*) The house under construction is framed with wood columns.

10.3A Allowable Stress Design

Structural Steel. The most commonly used formulas for allowable stress design of steel columns under a centric load are found in the *Specification for Structural Steel Buildings* of the American Institute of Steel Construction.‡ An exponential expression is used to predict σ_{all} for columns of short and intermediate lengths, and an Euler-based

†In specific design formulas, the letter L always refers to the effective length of the column.

‡*Manual of Steel Construction,* 14th ed., American Institute of Steel Construction, Chicago, 2011.

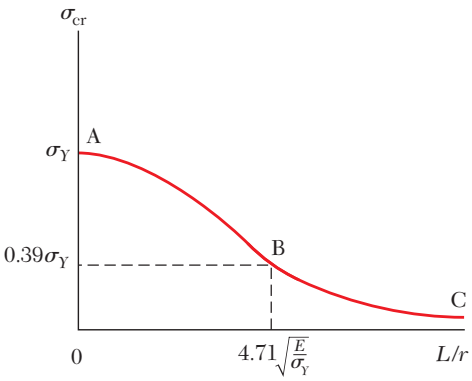


Fig. 10.27 Design curve for columns recommended by the American Institute of Steel Construction.

relation is used for long columns. The design relationships are developed in two steps.

1. A curve representing the variation of σ_{cr} as a function of L/r is obtained (Fig. 10.27). It is important to note that this curve does not incorporate any factor of safety.[§] Portion AB of this curve is

$$\sigma_{cr} = [0.658^{(\sigma_Y/\sigma_e)}]\sigma_Y \tag{10.38}$$

where

$$\sigma_e = \frac{\pi^2 E}{(L/r)^2} \tag{10.39}$$

Portion BC is

$$\sigma_{cr} = 0.877\sigma_e \tag{10.40}$$

When $L/r = 0$, $\sigma_{cr} = \sigma_Y$ in Eq. (10.38). At point B, Eq. (10.38) intersects Eq. (10.40). The slenderness L/r at the junction between the two equations is

$$\frac{L}{r} = 4.71\sqrt{\frac{E}{\sigma_Y}} \tag{10.41}$$

If L/r is smaller than the value from Eq. (10.41), σ_{cr} is determined from Eq. (10.38). If L/r is greater, σ_{cr} is determined from Eq. (10.40). At the slenderness L/r specified in Eq. (10.41), the stress $\sigma_e = 0.44\ \sigma_Y$. Using Eq. (10.40), $\sigma_{cr} = 0.877\ (0.44\ \sigma_Y) = 0.39\ \sigma_Y$.

2. A factor of safety must be used for the final design. The factor of safety given by the specification is 1.67. Thus,

$$\sigma_{all} = \frac{\sigma_{cr}}{1.67} \tag{10.42}$$

These equations can be used with SI or U.S. customary units.

By using Eqs. (10.38), (10.40), (10.41), and (10.42), the allowable axial stress can be determined for a given grade of steel and any given value of L/r. The procedure is to compute L/r at the intersection between the two equations from Eq. (10.41). For smaller given values of L/r, use Eqs. (10.38) and (10.42) to calculate σ_{all}, and if greater, use Eqs. (10.40) and (10.42). Figure 10.28 provides an example of how σ_e varies as a function of L/r for different grades of structural steel.

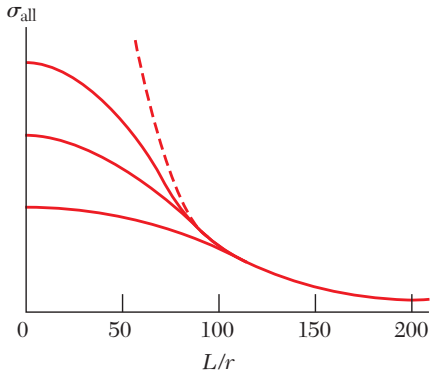


Fig. 10.28 Steel column design curves for different grades of steel.

[§]In the *Specification for Structural Steel Buildings*, the symbol F is used for stresses.

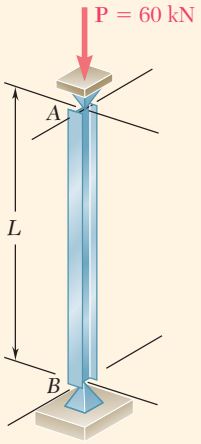


Fig. 10.29 Centrically loaded S100 × 11.5 rolled steel member.

Concept Application 10.2

Determine the longest unsupported length L for which the S100 × 11.5 rolled-steel compression member AB can safely carry the centric load shown (Fig. 10.29). Assume $\sigma_Y = 250$ MPa and $E = 200$ GPa.

From Appendix C, for an S100 × 11.5 shape,

$$A = 1460\,\text{mm}^2 \quad r_x = 41.7\,\text{mm} \quad r_y = 14.6\,\text{mm}$$

If the 60-kN load is to be safely supported,

$$\sigma_{\text{all}} = \frac{P}{A} = \frac{60 \times 10^3\,\text{N}}{1460 \times 10^{-6}\,\text{m}^2} = 41.1 \times 10^6\,\text{Pa}$$

To compute the critical stress σ_{cr}, we start by assuming that L/r is larger than the slenderness specified by Eq. (10.41). We then use Eq. (10.40) with Eq. (10.39) and write

$$\sigma_{\text{cr}} = 0.877\,\sigma_e = 0.877\,\frac{\pi^2 E}{(L/r)^2}$$

$$= 0.877\,\frac{\pi^2(200 \times 10^9\,\text{Pa})}{(L/r)^2} = \frac{1.731 \times 10^{12}\,\text{Pa}}{(L/r)^2}$$

Using this expression in Eq. (10.42),

$$\sigma_{\text{all}} = \frac{\sigma_{\text{cr}}}{1.67} = \frac{1.037 \times 10^{12}\,\text{Pa}}{(L/r)^2}$$

Equating this expression to the required value of σ_{all} gives

$$\frac{1.037 \times 10^{12}\,\text{Pa}}{(L/r)^2} = 41.1 \times 10^6\,\text{Pa} \qquad L/r = 158.8$$

The slenderness ratio from Eq. (10.41) is

$$\frac{L}{r} = 4.71\sqrt{\frac{200 \times 10^9}{250 \times 10^6}} = 133.2$$

Our assumption that L/r is greater than this slenderness ratio is correct. Choosing the smaller of the two radii of gyration:

$$\frac{L}{r_y} = \frac{L}{14.6 \times 10^{-3}\,\text{m}} = 158.8 \qquad L = 2.32\,\text{m}$$

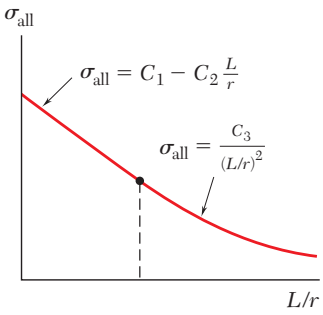


Fig. 10.30 Design curve for columns recommended by the Aluminum Association.

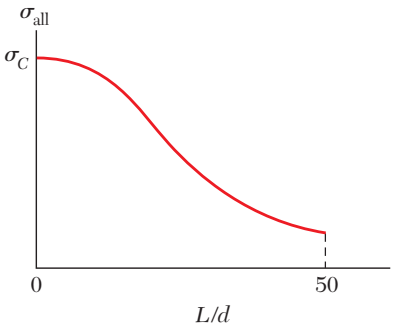


Fig. 10.31 Design curve for columns recommended by the American Forest & Paper Association.

Aluminum. Many aluminum alloys are used in structures and machines. For most columns, the specifications of the Aluminum Association[†] provide two formulas for the allowable stress in columns under centric loading. The variation of σ_{all} with L/r defined by these formulas is shown in Fig. 10.30. For short columns, a linear relationship between σ_{all} and L/r is used. For long columns, an Euler-type equation is used. Specific formulas for the design of buildings and similar structures are given in both SI and U.S. customary units for two commonly used alloys.

Alloy 6061-T6:

$$L/r < 66: \quad \sigma_{all} = [20.3 - 0.127(L/r)] \text{ ksi} \tag{10.43a}$$

$$= [140 - 0.874(L/r)] \text{ MPa} \tag{10.43b}$$

$$L/r \geq 66: \quad \sigma_{all} = \frac{51{,}400 \text{ ksi}}{(L/r)^2} = \frac{354 \times 10^3 \text{ MPa}}{(L/r)^2} \tag{10.44a, b}$$

Alloy 2014-T6:

$$L/r < 55: \quad \sigma_{all} = [30.9 - 0.229(L/r)] \text{ ksi} \tag{10.45a}$$

$$= [213 - 1.577(L/r)] \text{ MPa} \tag{10.45b}$$

$$L/r \geq 55: \quad \sigma_{all} = \frac{55{,}400 \text{ ksi}}{(L/r)^2} = \frac{382 \times 10^3 \text{ MPa}}{(L/r)^2} \tag{10.46a, b}$$

Wood. For the design of wood columns, the specifications of the American Forest & Paper Association[‡] provide a single equation to obtain the allowable stress for short, intermediate, and long columns under centric loading. For a column with a *rectangular* cross section of sides b and d, where $d < b$, the variation of σ_{all} with L/d is shown in Fig. 10.31.

For solid columns made from a single piece of wood or by gluing laminations together, the allowable stress σ_{all} is

$$\sigma_{all} = \sigma_C C_P \tag{10.47}$$

where σ_C is the adjusted allowable stress for compression parallel to the grain.[§] Adjustments for σ_C are included in the specifications to account for different variations (such as in the load duration). The column stability factor C_P accounts for the column length and is defined by

$$C_P = \frac{1 + (\sigma_{CE}/\sigma_C)}{2c} - \sqrt{\left[\frac{1 + (\sigma_{CE}/\sigma_C)}{2c}\right]^2 - \frac{\sigma_{CE}/\sigma_C}{c}} \tag{10.48}$$

The parameter c accounts for the type of column, and it is equal to 0.8 for sawn lumber columns and 0.90 for glued laminated wood columns. The value of σ_{CE} is defined as

$$\sigma_{CE} = \frac{0.822E}{(L/d)^2} \tag{10.49}$$

where E is an adjusted modulus of elasticity for column buckling. Columns in which L/d exceeds 50 are not permitted by the *National Design Specification for Wood Construction*.

[†]*Specifications for Aluminum Structures,* Aluminum Association, Inc., Washington, D.C., 2010.

[‡]*National Design Specification for Wood Construction,* American Forest & Paper Association, American Wood Council, Washington, D.C., 2012.

[§]In the *National Design Specification for Wood Construction,* the symbol F is used for stresses.

Concept Application 10.3

Knowing that column *AB* (Fig. 10.32) has an effective length of 14 ft and must safely carry a 32-kip load, design the column using a square glued laminated cross section. The adjusted modulus of elasticity for the wood is $E = 800 \times 10^3$ psi, and the adjusted allowable stress for compression parallel to the grain is $\sigma_C = 1060$ psi.

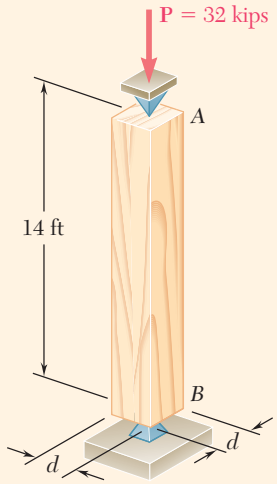


Fig. 10.32 Centrically loaded wood column.

Note that $c = 0.90$ for glued laminated wood columns. Computing the value of σ_{CE}, using Eq. (10.49), gives

$$\sigma_{CE} = \frac{0.822E}{(L/d)^2} = \frac{0.822(800 \times 10^3 \text{ psi})}{(168 \text{ in.}/d)^2} = 23.299d^2 \text{ psi}$$

Equation (10.48) is used to express the column stability factor in terms of d, with $(\sigma_{CE}/\sigma_C) = (23.299d^2/1.060 \times 10^3) = 21.98 \times 10^{-3}\, d^2$,

$$C_P = \frac{1 + (\sigma_{CE}/\sigma_C)}{2c} - \sqrt{\left[\frac{1 + (\sigma_{CE}/\sigma_C)}{2c}\right]^2 - \frac{\sigma_{CE}/\sigma_C}{c}}$$

$$= \frac{1 + 21.98 \times 10^{-3} d^2}{2(0.90)} - \sqrt{\left[\frac{1 + 21.98 \times 10^{-3} d^2}{2(0.90)}\right]^2 - \frac{21.98 \times 10^{-3} d^2}{0.90}}$$

(continued)

Since the column must carry 32 kips, Eq. (10.47) gives

$$\sigma_{\text{all}} = \frac{32 \text{ kips}}{d^2} = \sigma_C C_P = 1.060 C_P$$

Solving this equation for C_P and substituting the value into the previous equation, we obtain

$$\frac{30.19}{d^2} = \frac{1 + 21.98 \times 10^{-3} d^2}{2(0.90)} - \sqrt{\left[\frac{1 + 21.98 \times 10^{-3} d^2}{2(0.90)}\right]^2 - \frac{21.98 \times 10^{-3} d^2}{0.90}}$$

Solving for d by trial and error yields $d = 6.45$ in.

10.3B Load and Resistance Factor Design

***Structural Steel** Section 1.5D gave an alternative method of design based on determining the load when the structure ceases to be useful. Design is based on the inequality given by

$$\gamma_D P_D + \gamma_L P_L \leq \phi P_U \tag{1.27}$$

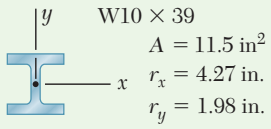
The design of steel columns under a centric load using Load and Resistance Factor Design with the American Institute of Steel Construction Specification is similar to that for the Allowable Stress Design. Using the critical stress σ_{cr}, the ultimate load P_U is

$$P_U = \sigma_{cr} A \tag{10.50}$$

The critical stress σ_{cr} is determined using Eq. (10.41) for the slenderness at the junction between Eqs. (10.38) and Eq. (10.40). If the specified slenderness L/r is smaller than in Eq. (10.41), Eq. (10.38) governs. If it is larger, Eq. (10.40) governs. The equations can be used with SI or U.S. customary units.

By using Eq. (10.50) with Eq. (1.27), it can be determined if the design is acceptable. First calculate the slenderness ratio from Eq. (10.41). For values of L/r smaller than this slenderness, the *ultimate load* P_U used with Eq. (1.27) is obtained from Eq. (10.50), where σ_{cr} is determined from Eq. (10.38). For values of L/r larger than this slenderness, the *ultimate load* P_U is found by using Eq. (10.50) with Eq. (10.40). The Load and Resistance Factor Design Specification of the American Institute of Steel Construction specifies that the *resistance factor* ϕ is 0.90.

Note: The design formulas presented throughout Sec. 10.3 are examples of different design approaches. These equations do not provide all of the requirements needed for many designs, and the student should refer to the appropriate design specifications before attempting actual designs.



Sample Problem 10.3

Column AB consists of a $W10 \times 39$ rolled-steel shape made of a grade of steel for which $\sigma_Y = 36$ ksi and $E = 29 \times 10^6$ psi. Determine the allowable centric load **P** (*a*) if the effective length of the column is 24 ft in all directions, (*b*) if bracing is provided to prevent the movement of the midpoint C in the xz plane. (Assume that the movement of point C in the yz plane is not affected by the bracing.)

STRATEGY: The allowable centric load for part *a* is determined from the governing allowable stress design equation for steel, Eq. (10.38) or Eq. (10.40), based on buckling associated with the axis with a smaller radius of gyration since the effective lengths are the same. In part *b*, it is necessary to determine the effective slenderness ratios for both axes, including the reduced effective length due to the bracing. The larger slenderness ratio governs the design.

MODELING: First compute the slenderness ratio from Eq. (10.41) corresponding to the given yield strength $\sigma_Y = 36$ ksi.

$$\frac{L}{r} = 4.71\sqrt{\frac{29 \times 10^6}{36 \times 10^3}} = 133.7$$

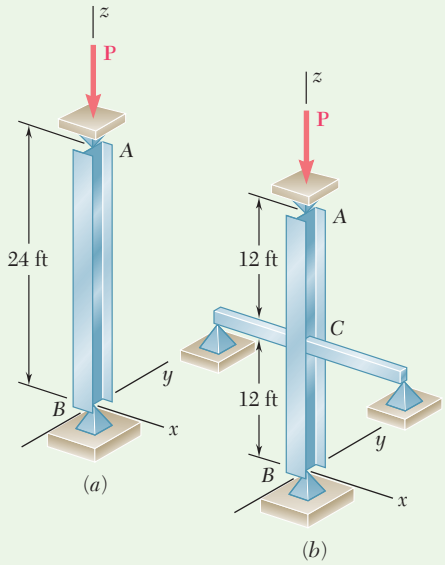


Fig. 1 Centrically loaded column (*a*) unbraced, (*b*) braced.

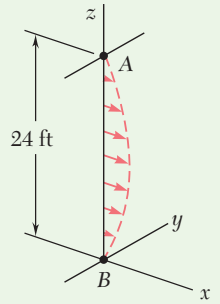


Fig. 2 Buckled shape for unbraced column.

ANALYSIS:

a. Effective Length = 24 ft. The column is shown in Fig. 1*a*. Knowing that $r_y < r_x$, buckling takes place in the xz plane (Fig. 2). For $L = 24$ ft and $r = r_y = 1.98$ in., the slenderness ratio is

$$\frac{L}{r_y} = \frac{(24 \times 12)\text{ in.}}{1.98\text{ in.}} = \frac{288\text{ in.}}{1.98\text{ in.}} = 145.5$$

Since $L/r > 133.7$, Eq. (10.39) in Eq. (10.40) is used to determine

$$\sigma_{cr} = 0.877\sigma_e = 0.877\frac{\pi^2 E}{(L/r)^2} = 0.877\frac{\pi^2(29 \times 10^3\text{ ksi})}{(145.5)^2} = 11.86\text{ ksi}$$

The allowable stress is determined using Eq. (10.42)

$$\sigma_{\text{all}} = \frac{\sigma_{cr}}{1.67} = \frac{11.86\text{ ksi}}{1.67} = 7.10\text{ ksi}$$

and

$$P_{\text{all}} = \sigma_{\text{all}}A = (7.10\text{ ksi})(11.5\text{ in}^2) = 81.7\text{ kips}$$

(continued)

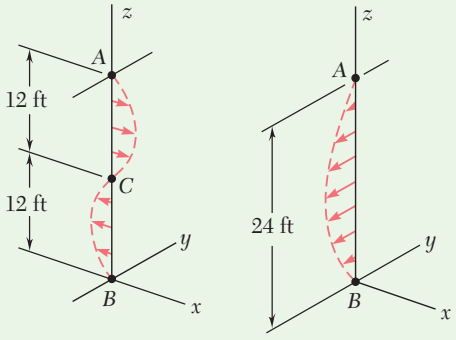
b. Bracing at Midpoint C. The column is shown in Fig. 1*b*. Since bracing prevents movement of point *C* in the *xz* plane but not in the *yz* plane, the slenderness ratio corresponding to buckling in each plane (Fig. 3) is computed to determine which is larger.

xz Plane: Effective length = 12 ft = 144 in., $r = r_y = 1.98$ in.

$$L/r = (144 \text{ in.})/(1.98 \text{ in.}) = 72.7$$

yz Plane: Effective length = 24 ft = 288 in., $r = r_x = 4.27$ in.

$$L/r = (288 \text{ in.})/(4.27 \text{ in.}) = 67.4$$



Buckling in *xz* plane Buckling in *yz* plane

Fig. 3 Buckled shapes for braced column.

Since the larger slenderness ratio corresponds to a smaller allowable load, we choose $L/r = 72.7$. Since this is smaller than $L/r = 133.7$, Eqs. (10.39) and (10.38) are used to determine σ_{cr}:

$$\sigma_e = \frac{\pi^2 E}{(L/r)^2} = \frac{\pi^2(29 \times 10^3 \text{ ksi})}{(72.7)^2} = 54.1 \text{ ksi}$$

$$\sigma_{cr} = \left[0.658^{(\sigma_Y/\sigma_e)}\right] F_Y = \left[0.658^{(36 \text{ ksi}/54.1 \text{ ksi})}\right] 36 \text{ ksi} = 27.3 \text{ ksi}$$

The allowable stress using Eq. (10.42) and the allowable load are

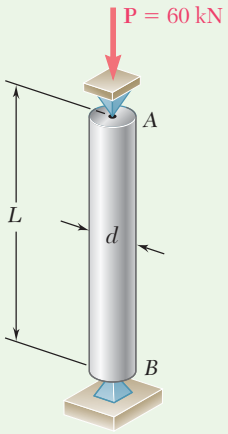
$$\sigma_{\text{all}} = \frac{\sigma_{cr}}{1.67} = \frac{27.3 \text{ ksi}}{1.67} = 16.32 \text{ ksi}$$

$$P_{\text{all}} = \sigma_{\text{all}} A = (16.32 \text{ ksi})(11.5 \text{ in}^2) \qquad P_{\text{all}} = 187.7 \text{ kips} \blacktriangleleft$$

REFLECT and THINK: This sample problem shows the benefit of using bracing to reduce the effective length for buckling about the weak axis when a column has significantly different radii of gyration, which is typical for steel wide-flange columns.

Sample Problem 10.4

Using the aluminum alloy 2014-T6 for the circular rod shown, determine the smallest diameter that can be used to support the centric load $P = 60$ kN if (*a*) $L = 750$ mm, (*b*) $L = 300$ mm.



STRATEGY: Use the aluminum allowable stress equations to design the column, i.e., to determine the smallest diameter that can be used. Since there are two design equations based on L/r, it is first necessary to assume which governs. Then check the assumption.

MODELING: For the cross section of the solid circular rod shown in Fig. 1,

$$I = \frac{\pi}{4}c^4 \qquad A = \pi c^2 \qquad r = \sqrt{\frac{I}{A}} = \sqrt{\frac{\pi c^4/4}{\pi c^2}} = \frac{c}{2}$$

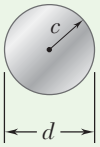


Fig. 1 Cross section of aluminum column.

ANALYSIS:

a. Length of 750 mm. Since the diameter of the rod is not known, L/r must be assumed. Assume that $L/r > 55$ and use Eq. (10.46). For the centric load **P**, $\sigma = P/A$ and write

$$\frac{P}{A} = \sigma_{all} = \frac{382 \times 10^3 \text{ MPa}}{(L/r)^2}$$

(continued)

$$\frac{60 \times 10^3\,\text{N}}{\pi c^2} = \frac{382 \times 10^9\,\text{Pa}}{\left(\dfrac{0.750\,\text{m}}{c/2}\right)^2}$$

$$c^4 = 112.5 \times 10^{-9}\,\text{m}^4 \qquad c = 18.31\,\text{mm}$$

For $c = 18.31$ mm, the slenderness ratio is

$$\frac{L}{r} = \frac{L}{c/2} = \frac{750\,\text{mm}}{(18.31\,\text{mm})/2} = 81.9 > 55$$

The assumption that L/r is greater than 55 is correct. For $L = 750$ mm, the required diameter is

$$d = 2c = 2(18.31\,\text{mm}) \qquad d = 36.6\,\text{mm}$$

b. Length of 300 mm. Assume that $L/r > 55$. Using Eq. (10.46) and following the procedure used in part *a*, $c = 11.58$ mm and $L/r = 51.8$. Since L/r is less than 55, this assumption is wrong. Now assume that $L/r < 55$ and use Eq. (10.45*b*) for the design of this rod.

$$\frac{P}{A} = \sigma_{\text{all}} = \left[213 - 1.577\left(\frac{L}{r}\right)\right]\text{MPa}$$

$$\frac{60 \times 10^3\,\text{N}}{\pi c^2} = \left[213 - 1.577\left(\frac{0.3\,\text{m}}{c/2}\right)\right]10^6\,\text{Pa}$$

$$c = 11.95\,\text{mm}$$

For $c = 11.95$ mm, the slenderness ratio is

$$\frac{L}{r} = \frac{L}{c/2} = \frac{300\,\text{mm}}{(11.95\,\text{mm})/2} = 50.2$$

The second assumption that $L/r < 55$ is correct. For $L = 300$ mm, the required diameter is

$$d = 2c = 2(11.95\,\text{mm}) \qquad d = 23.9\,\text{mm}$$

Problems

10.57 Using allowable stress design, determine the allowable centric load for a column of 6-m effective length that is made from the following rolled-steel shape: (*a*) W200 × 35.9, (*b*) W200 × 86. Use $\sigma_Y = 250$ MPa and $E = 200$ GPa.

10.58 A W8 × 31 rolled-steel shape is used for a column of 21-ft effective length. Using allowable stress design, determine the allowable centric load if the yield strength of the grade of steel used is (*a*) $\sigma_Y = 36$ ksi, (*b*) $\sigma_Y = 50$ ksi. Use $E = 29 \times 10^6$ psi.

10.59 A rectangular structural tube having the cross section shown is used as a column of 5-m effective length. Knowing that $\sigma_Y = 250$ MPa and $E = 200$ GPa, use allowable stress design to determine the largest centric load that can be applied to the steel column.

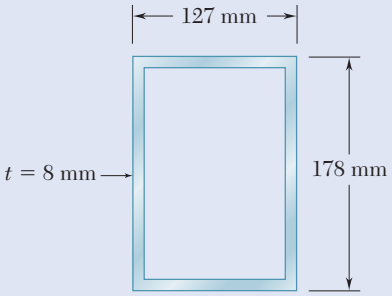


Fig. P10.59

10.60 A column having a 3.5-m effective length is made of sawn lumber with a 114 × 140-mm cross section. Knowing that for the grade of wood used the adjusted allowable stress for compression parallel to the grain is $\sigma_C = 7.6$ MPa and the adjusted modulus $E = 2.8$ GPa, determine the maximum allowable centric load for the column.

10.61 A sawn lumber column with a 7.5 × 5.5-in. cross section has an 18-ft effective length. Knowing that for the grade of wood used the adjusted allowable stress for compression parallel to the grain is $\sigma_C = 1200$ psi and that the adjusted modulus $E = 470 \times 10^3$ psi, determine the maximum allowable centric load for the column.

10.62 Bar *AB* is free at its end *A* and fixed at its base *B*. Determine the allowable centric load **P** if the aluminum alloy is (*a*) 6061-T6, (*b*) 2014-T6.

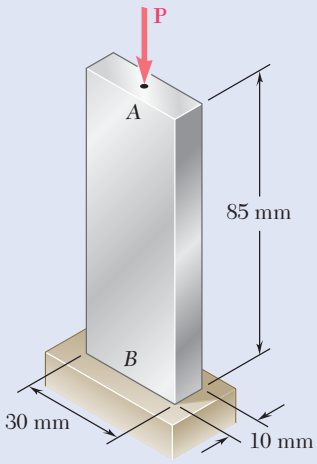


Fig. P10.62

10.63 A compression member has the cross section shown and an effective length of 5 ft. Knowing that the aluminum alloy used is 2014-T6, determine the allowable centric load.

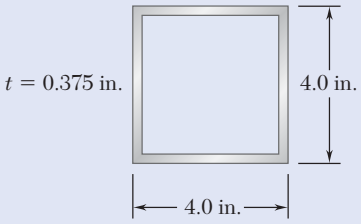


Fig. *P10.63*

10.64 A compression member has the cross section shown and an effective length of 5 ft. Knowing that the aluminum alloy used is 6061-T6, determine the allowable centric load.

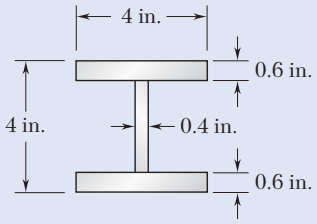


Fig. P10.64



Fig. P10.65

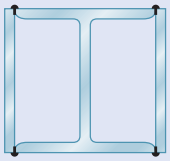


Fig. P10.66

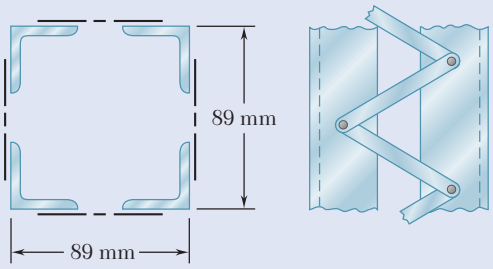


Fig. *P10.67*

10.65 A compression member of 8.2-ft effective length is obtained by bolting together two L5 × 3 × $\frac{1}{2}$-in. steel angles as shown. Using allowable stress design, determine the allowable centric load for the column. Use $\sigma_Y = 36$ ksi and $E = 29 \times 10^6$ psi.

10.66 A compression member of 9-m effective length is obtained by welding two 10-mm-thick steel plates to a W250 × 80 rolled-steel shape as shown. Knowing that $\sigma_Y = 345$ MPa and $E = 200$ GPa and using allowable stress design, determine the allowable centric load for the compression member.

10.67 A column of 6.4-m effective length is obtained by connecting four L89 × 89 × 9.5-mm steel angles with lacing bars as shown. Using allowable stress design, determine the allowable centric load for the column. Use $\sigma_Y = 345$ MPa and $E = 200$ GPa.

10.68 A column of 21-ft effective length is obtained by connecting C10 × 20 steel channels with lacing bars as shown. Using allowable stress design, determine the allowable centric load for the column. Use $\sigma_Y = 36$ ksi and $E = 29 \times 10^6$ psi.

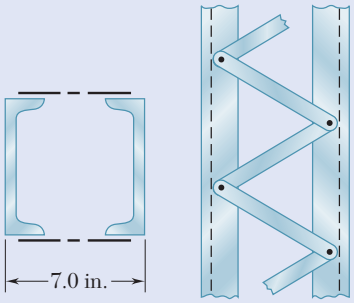


Fig. P10.68

10.69 The glued laminated column shown is made from four planks, each of 38 × 190-mm cross section. Knowing that for the grade of wood used the adjusted allowable stress for compression parallel to the grain is $\sigma_C = 10$ MPa and $E = 12$ GPa, determine the maximum allowable centric load if the effective length of the column is (*a*) 7 m, (*b*) 3 m.

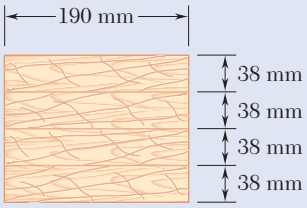


Fig. P10.69

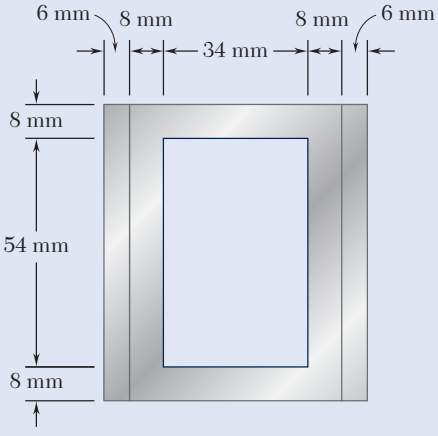


Fig. *P10.70*

10.70 An aluminum structural tube is reinforced by bolting two plates to it as shown for use as a column of 1.7-m effective length. Knowing that all material is aluminum alloy 2014-T6, determine the maximum allowable centric load.

10.71 The glued laminated column shown is free at its top A and fixed at its base B. Using wood that has an adjusted allowable stress for compression parallel to the grain $\sigma_C = 9.2$ MPa and an adjusted modulus of elasticity $E = 5.7$ GPa, determine the smallest cross section that can support a centric load of 62 kN.

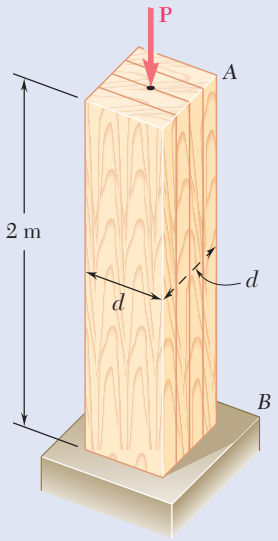


Fig. P10.71

10.72 An 18-kip centric load is applied to a rectangular sawn lumber column of 22-ft effective length. Using lumber for which the adjusted allowable stress for compression parallel to the grain is $\sigma_C = 1050$ psi and the adjusted modulus is $E = 440 \times 10^3$ psi, determine the smallest cross section that can be used. Use $b = 2d$.

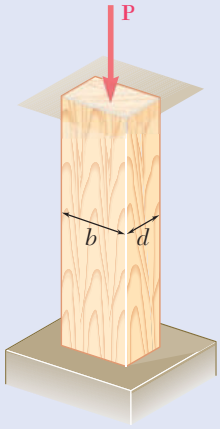


Fig. P10.72

10.73 A laminated column of 2.1-m effective length is to be made by gluing together wood pieces of 25 × 150-mm cross section. Knowing that for the grade of wood used the adjusted allowable stress for compression parallel to the grain is $\sigma_C = 7.7$ MPa and the adjusted modulus is $E = 5.4$ GPa, determine the number of wood pieces that must be used to support the concentric load shown when (*a*) $P = 52$ kN, (*b*) $P = 108$ kN.

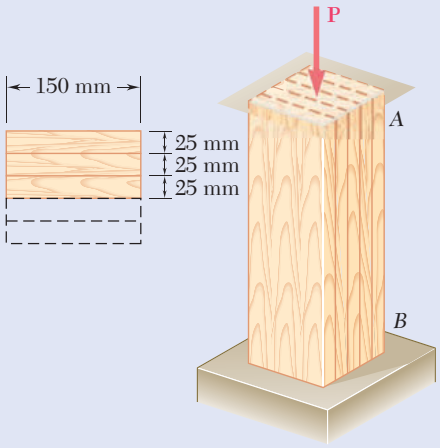


Fig. *P10.73*

10.74 For a rod made of aluminum alloy 2014-T6, select the smallest square cross section that can be used if the rod is to carry a 55-kip centric load.

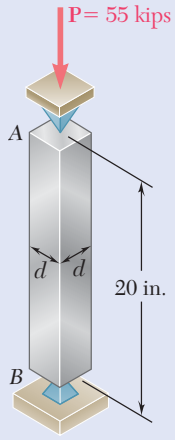


Fig. P10.74

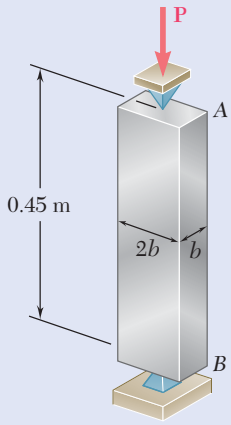


Fig. P10.75

10.75 A 72-kN centric load must be supported by an aluminum column as shown. Using the aluminum alloy 6061-T6, determine the minimum dimension b that can be used.

10.76 An aluminum tube of 90-mm outer diameter is to carry a centric load of 120 kN. Knowing that the stock of tubes available for use are made of alloy 2014-T6 and with wall thicknesses in increments of 3 mm from 6 mm to 15 mm, determine the lightest tube that can be used.

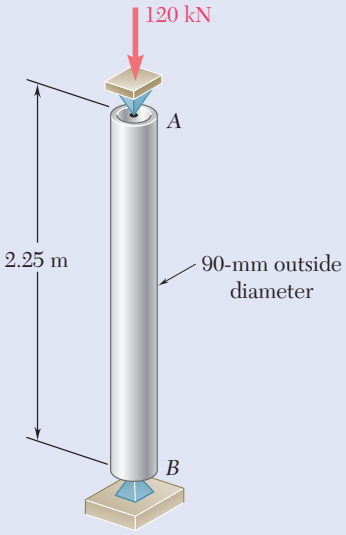


Fig. *P10.76*

10.77 A column of 4.6-m effective length must carry a centric load of 525 kN. Knowing that $\sigma_Y = 345$ MPa and $E = 200$ GPa, use allowable stress design to select the wide-flange shape of 200-mm nominal depth that should be used.

10.78 A column of 22.5-ft effective length must carry a centric load of 288 kips. Using allowable stress design, select the wide-flange shape of 14-in. nominal depth that should be used. Use $\sigma_Y = 50$ ksi and $E = 29 \times 10^6$ psi.

10.79 A column of 17-ft effective length must carry a centric load of 235 kips. Using allowable stress design, select the wide-flange shape of 10-in. nominal depth that should be used. Use $\sigma_Y = 36$ ksi and $E = 29 \times 10^6$ psi.

10.80 A centric load **P** must be supported by the steel bar *AB*. Using allowable stress design, determine the smallest dimension d of the cross section that can be used when (*a*) $P = 108$ kN, (*b*) $P = 166$ kN. Use $\sigma_Y = 250$ MPa and $E = 200$ GPa.

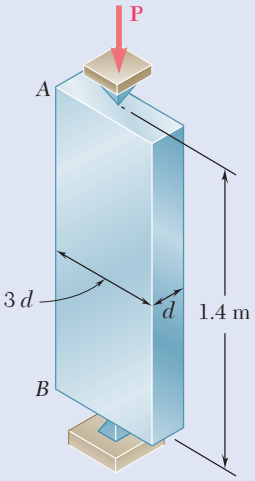


Fig. P10.80

10.81 A square steel tube having the cross section shown is used as a column of 26-ft effective length to carry a centric load of 65 kips. Knowing that the tubes available for use are made with wall thicknesses ranging from $\frac{1}{4}$ in. to $\frac{3}{4}$ in. in increments of $\frac{1}{16}$ in., use allowable stress design to determine the lightest tube that can be used. Use $\sigma_Y = 36$ ksi and $E = 29 \times 10^6$ psi.

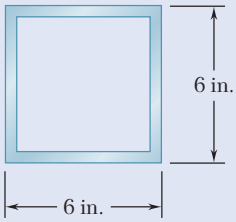


Fig. *P10.81*

10.82 Solve Prob. 10.81, assuming that the effective length of the column is decreased to 20 ft.

10.83 Two 89 × 64-mm angles are bolted together as shown for use as a column of 2.4-m effective length to carry a centric load of 180 kN. Knowing that the angles available have thicknesses of 6.4 mm, 9.5 mm, and 12.7 mm, use allowable stress design to determine the lightest angles that can be used. Use $\sigma_Y = 250$ MPa and $E = 200$ GPa.

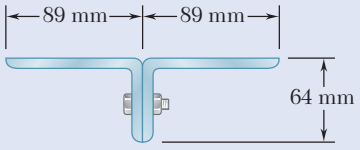


Fig. P10.83

10.84 Two 89 × 64-mm angles are bolted together as shown for use as a column of 2.4-m effective length to carry a centric load of 325 kN. Knowing that the angles available have thicknesses of 6.4 mm, 9.5 mm, and 12.7 mm, use allowable stress design to determine the lightest angles that can be used. Use $\sigma_Y = 250$ MPa and $E = 200$ GPa.

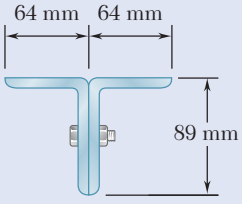


Fig. P10.84

***10.85** A rectangular steel tube having the cross section shown is used as a column of 14.5-ft effective length. Knowing that $\sigma_Y = 36$ ksi and $E = 29 \times 10^6$ psi, use load and resistance factor design to determine the largest centric live load that can be applied if the centric dead load is 54 kips. Use a dead load factor $\gamma_D = 1.2$, a live load factor $\gamma_L = 1.6$ and the resistance factor $\phi = 0.90$.

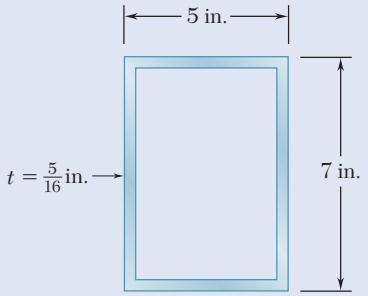


Fig. P10.85

***10.86** A column with a 5.8-m effective length supports a centric load, with ratio of dead to live load equal to 1.35. The dead load factor is $\gamma_D = 1.2$, the live load factor $\gamma_L = 1.6$, and the resistance factor $\phi = 0.90$. Use load and resistance factor design to determine the allowable centric dead and live loads if the column is made of the following rolled-steel shape: (*a*) W250 × 67, (*b*) W360 × 101. Use $\sigma_Y = 345$ MPa and $E = 200$ GPa.

***10.87** A steel column of 5.5-m effective length must carry a centric dead load of 310 kN and a centric live load of 375 kN. Knowing that $\sigma_Y = 250$ MPa and $E = 200$ GPa, use load and resistance factor design to select the wide-flange shape of 310-mm nominal depth that should be used. The dead load factor $\gamma_D = 1.2$, the live load factor $\gamma_L = 1.6$, and the resistance factor $\phi = 0.90$.

***10.88** The steel tube having the cross section shown is used as a column of 15-ft effective length to carry a centric dead load of 51 kips and a centric live load of 58 kips. Knowing that the tubes available for use are made with wall thicknesses in increments of $\frac{1}{16}$ in. from $\frac{3}{16}$ in. to $\frac{3}{8}$ in., use load and resistance factor design to determine the lightest tube that can be used. Use $\sigma_Y = 36$ ksi and $E = 29 \times 10^6$ psi. The dead load factor $\gamma_D = 1.2$, the live load factor $\gamma_L = 1.6$, and the resistance factor $\phi = 0.90$.

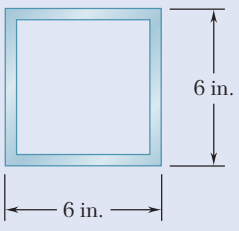


Fig. P10.88

10.4 ECCENTRIC LOAD DESIGN

In this section, the design of columns subjected to an eccentric load is considered. The empirical formulas developed in the preceding section for columns under a centric load can be modified and used when load **P** is applied to the column with a known eccentricity e.

Recall from Sec. 4.7 that an eccentric axial load **P** applied in a plane of symmetry can be replaced by an equivalent system consisting of a centric load **P** and a couple **M** of moment $M = Pe$, where e is the distance from the line of action of the load to the longitudinal axis of the column (Fig. 10.33). The normal stresses exerted on a transverse section of the column are obtained by superposing the stresses due to the centric load **P** and the couple **M** (Fig. 10.34), provided that the section is not too close

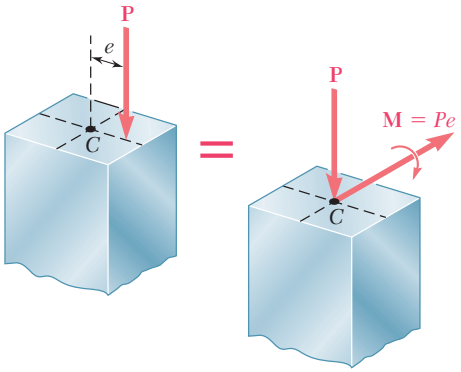


Fig. 10.33 Eccentric axial load replaced with an equivalent centric load and couple.

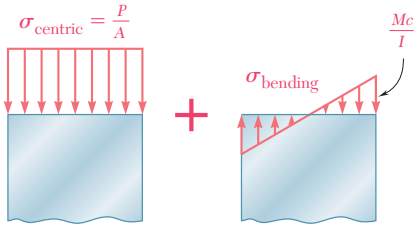


Fig. 10.34 Normal stress of an eccentrically loaded column is the superposition of centric axial and bending stresses.

to either end of the column and as long as the stresses do not exceed the proportional limit of the material. The normal stress due to the eccentric load **P** can be expressed as

$$\sigma = \sigma_{\text{centric}} + \sigma_{\text{bending}} \tag{10.51}$$

The maximum compressive stress in the column is

$$\sigma_{\max} = \frac{P}{A} + \frac{Mc}{I} \tag{10.52}$$

In a properly designed column, the maximum stress given in Eq. (10.52) should not exceed the allowable stress for the column. Two alternative approaches can be used to satisfy this requirement: the *allowable-stress method* and the *interaction method.*

Allowable-Stress Method. This method is based on the assumption that the allowable stress for an eccentrically loaded column is the same as if the column were centrically loaded. Therefore, $\sigma_{\max} \leq \sigma_{\text{all}}$, where σ_{all} is the allowable stress under a centric load. Substituting for $\sigma_{\max}$ from Eq. (10.52) gives

$$\frac{P}{A} + \frac{Mc}{I} \leq \sigma_{\text{all}} \tag{10.53}$$

The allowable stress is determined using the same equations in Sec. 10.3. For a given material, these equations express σ_{all} as a function of the slenderness ratio of the column. Engineering codes require that the largest value of the slenderness ratio of the column be used to determine the allowable stress, whether it corresponds to the actual plane of bending or not. This requirement sometimes results in an overly conservative design.

Concept Application 10.4

A column with a 2-in.-square cross section and 28-in. effective length is made of the aluminum alloy 2014-T6 (Fig. 10.35). Using the allowable-stress method, determine the maximum load P that can be safely supported with an eccentricity of 0.8 in.

Compute the radius of gyration r using the given data:

$$A = (2\text{ in.})^2 = 4\text{ in}^2 \qquad I = \tfrac{1}{12}(2\text{ in.})^4 = 1.333\text{ in}^4$$

$$r = \sqrt{\frac{I}{A}} = \sqrt{\frac{1.333\text{ in}^4}{4\text{ in}^2}} = 0.5774\text{ in.}$$

Next, compute $L/r = (28\text{ in.})/(0.5774\text{ in.}) = 48.50$.

Since $L/r < 55$, use Eq. (10.45a) to determine the allowable stress for the aluminum column subjected to a centric load.

$$\sigma_{all} = [30.9 - 0.229(48.50)] = 19.79\text{ ksi}$$

Now use Eq. (10.53) with $M = Pe$ and $c = \frac{1}{2}(2\text{ in.}) = 1\text{ in.}$ to determine the allowable load:

$$\frac{P}{4\text{ in}^2} + \frac{P(0.8\text{ in.})(1\text{ in.})}{1.333\text{ in}^4} \le 19.79\text{ ksi}$$

$$P \le 23.3\text{ kips}$$

The maximum load that can be safely applied is $P = 23.3$ kips.

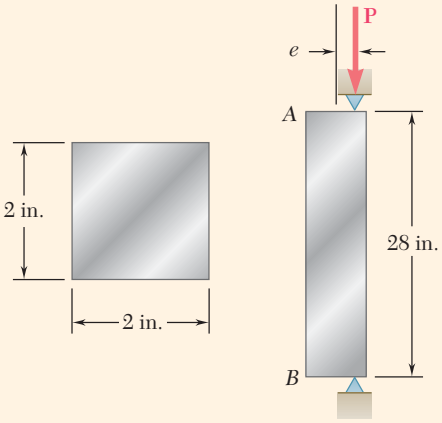


Fig. 10.35 Column subjected to eccentric axial load.

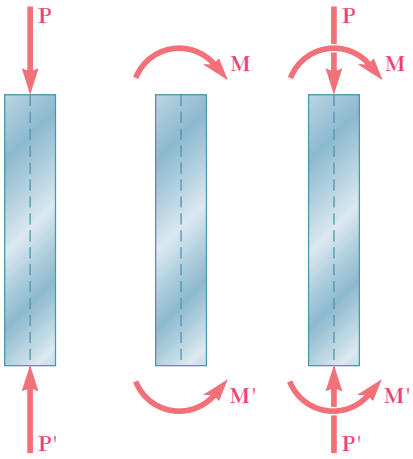


Fig. 10.36 Column subjected to (*a*) centric axial load, (*b*) pure bending, (*c*) eccentric load.

Interaction Method. Recall that the allowable stress for a column subjected to a centric load (Fig. 10.36*a*) is generally smaller than the allowable stress for a column in pure bending (Fig. 10.36*b*), since it takes into account the possibility of buckling. Therefore, when the allowable-stress method is used to design an eccentrically loaded column such that the sum of the stresses due to the centric load **P** and the bending couple **M** (Fig. 10.36*c*) does not exceed the allowable stress for a centrically loaded column, the resulting design is often overly conservative. An improved method of design can be developed by rewriting Eq. (10.53) in the form

$$\frac{P/A}{\sigma_{all}} + \frac{Mc/I}{\sigma_{all}} \le 1 \qquad \textbf{(10.54)}$$

and substituting for σ_{all} in the first and second terms the allowable stresses, that correspond, respectively, to the allowable stresses obtained for the centric load of Fig. 10.36*a* and the pure bending of Fig. 10.36*b*. Thus,

$$\frac{P/A}{(\sigma_{all})_{centric}} + \frac{Mc/I}{(\sigma_{all})_{bending}} \le 1 \qquad \textbf{(10.55)}$$

This is known as an *interaction formula*.

When $M = 0$, the use of Eq. (10.55) results in the design of a centrically loaded column by the method of Sec. 10.3. On the other hand, when $P = 0$, this equation results in the design of a beam in pure bending by the method of Sec. 5.3. When P and M are both different from zero, the interaction formula results in a design that takes into account the capacity of the member to resist bending as well as axial loading. In all cases, $(\sigma_{all})_{centric}$ is determined by using the largest slenderness ratio of the column, regardless of the plane in which bending takes place.[†]

Concept Application 10.5

Use the interaction method to determine the maximum load P that can be safely supported by the column of Concept Application 10.4 with an eccentricity of 0.8 in. The allowable stress in bending is 24 ksi.

The value of $(\sigma_{all})_{centric}$ has been determined and thus

$$(\sigma_{all})_{centric} = 19.79 \text{ ksi} \qquad (\sigma_{all})_{bending} = 24 \text{ ksi}$$

Substituting these values into Eq. (10.55),

$$\frac{P/A}{19.79 \text{ ksi}} + \frac{Mc/I}{24 \text{ ksi}} \le 1.0$$

Use the numerical data from Concept Application 10.4 to write

$$\frac{P/4}{19.79 \text{ ksi}} + \frac{P(0.8)(1.0)/1.333}{24 \text{ ksi}} \le 1.0$$

$$P \le 26.6 \text{ kips}$$

The maximum load that can be safely applied is $P = 26.6$ kips.

When the eccentric load **P** is not applied in a plane of symmetry, it causes bending about both of the principal axes of the cross section of the column. The eccentric load **P** then can be replaced by a centric load **P** and two couples $\mathbf{M}_x$ and $\mathbf{M}_z$, as shown in Fig. 10.37. The interaction formula to be used is

$$\frac{P/A}{(\sigma_{all})_{centric}} + \frac{|M_x|z_{max}/I_x}{(\sigma_{all})_{bending}} + \frac{|M_z|x_{max}/I_z}{(\sigma_{all})_{bending}} \le 1 \qquad \textbf{(10.56)}$$

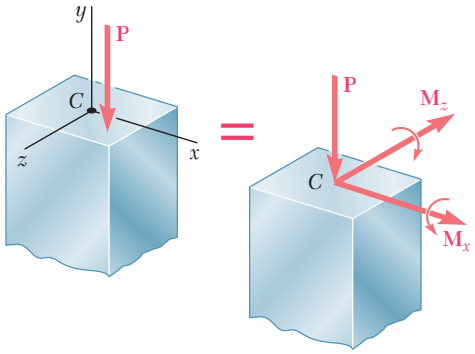
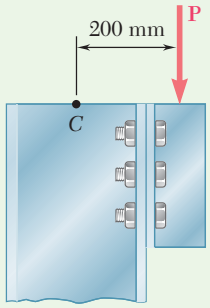


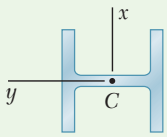
Fig. 10.37 Equivalent centric load and couples for an eccentric axial load causing biaxial bending.

[†]This procedure is required by all major codes for the design of steel, aluminum, and timber compression members. In addition, many specifications call for the use of an additional factor in the second term of Eq. (10.55). This factor takes into account the additional stresses resulting from the deflection of the column due to bending.

Sample Problem 10.5



Using the allowable-stress method, determine the largest load **P** that can be safely carried by a W310 × 74 steel column of 4.5-m effective length. Use $E = 200$ GPa and $\sigma_Y = 250$ MPa.



W310 × 74
$A = 9420 \text{ mm}^2$
$r_x = 132 \text{ mm}$
$r_y = 49.8 \text{ mm}$
$S_x = 1050 \times 10^3 \text{ mm}^3$

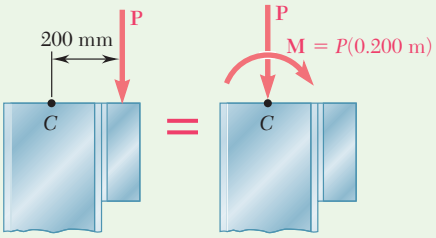


Fig. 1 Eccentric loading replaced by centric force-couple system acting at column's centroid.

STRATEGY: Determine the allowable centric stress for the column, using the governing allowable stress design equation for steel, Eq. (10.38) or Eq. (10.40) with Eq. (10.42). Then use Eq. (10.53) to calculate the load **P**.

MODELING and ANALYSIS:

The largest slenderness ratio of the column is $L/r_y = (4.5 \text{ m})/(0.0498 \text{ m}) = 90.4$. Using Eq. (10.41) with $E = 200$ GPa and $\sigma_Y = 250$ MPa, the slenderness ratio at the junction between the two equations for σ_{cr} is $L/r = 133.2$. Thus, Eqs. (10.38) and (10.39) are used, and $\sigma_{cr} = 162.2$ MPa. Using Eq. (10.42), the allowable stress is

$$(\sigma_{\text{all}})_{\text{centric}} = 162.2/1.67 = 97.1 \text{ MPa}$$

For the given column, replacing the eccentric loading with a centric force-couple system acting at the centroid (Fig. 1), we write

$$\frac{P}{A} = \frac{P}{9.42 \times 10^{-3} \text{ m}^2} \qquad \frac{Mc}{I} = \frac{M}{S} = \frac{P(0.200 \text{ m})}{1.050 \times 10^{-3} \text{ m}^3}$$

Substituting into Eq. (10.53), we obtain

$$\frac{P}{A} + \frac{Mc}{I} \le \sigma_{\text{all}}$$

$$\frac{P}{9.42 \times 10^{-3} \text{ m}^2} + \frac{P(0.200 \text{ m})}{1.050 \times 10^{-3} \text{ m}^3} \le 97.1 \text{ MPa} \qquad P \le 327 \text{ kN}$$

The largest allowable load **P** is **P** = 327 kN ↓ ◀

Sample Problem 10.6

Using the interaction method, solve Sample Prob. 10.5. Assume $(\sigma_{all})_{bending} = 150$ MPa.

STRATEGY: Use the allowable centric stress found in Sample Problem 10.5 to calculate the load **P**.

MODELING and ANALYSIS:

Using Eq. (10.55),

$$\frac{P/A}{(\sigma_{all})_{centric}} + \frac{Mc/I}{(\sigma_{all})_{bending}} \leq 1$$

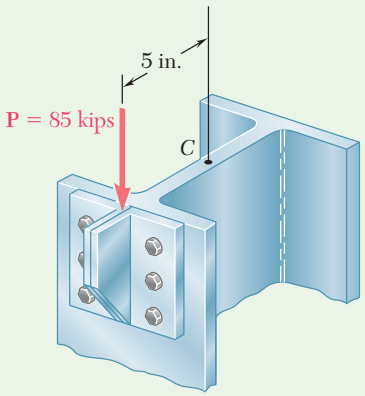
Substituting the allowable bending stress and the allowable centric stress found in Sample Prob. 10.5, as well as the other given data, we obtain

$$\frac{P/(9.42 \times 10^{-3}\,\text{m}^2)}{97.1 \times 10^{6}\,\text{Pa}} + \frac{P(0.200\,\text{m})/(1.050 \times 10^{-3}\,\text{m}^3)}{150 \times 10^{6}\,\text{Pa}} \leq 1$$

$$P \leq 423\,\text{kN}$$

The largest allowable load **P** is $\mathbf{P} = 423\ \text{kN} \downarrow$ ◀

Sample Problem 10.7



A steel column with an effective length of 16 ft is loaded eccentrically as shown. Using the interaction method, select the wide-flange shape of 8-in. nominal depth that should be used. Assume $E = 29 \times 10^6$ psi and $\sigma_Y = 36$ ksi, and use an allowable stress in bending of 22 ksi.

STRATEGY: It is necessary to select the lightest column that satisfies Eq. (l0.55). This involves a trial-and-error process, which can be shortened if the first 8-in. wide-flange shape selected is close to the final solution. This is done by using the allowable-stress method, Eq. (10.53), with an approximate allowable stress.

MODELING and ANALYSIS:

So that we can select a trial section, we use the allowable-stress method with $\sigma_{all} = 22$ ksi and write

$$\sigma_{all} = \frac{P}{A} + \frac{Mc}{I_x} = \frac{P}{A} + \frac{Mc}{Ar_x^2} \qquad \textbf{(1)}$$

(continued)

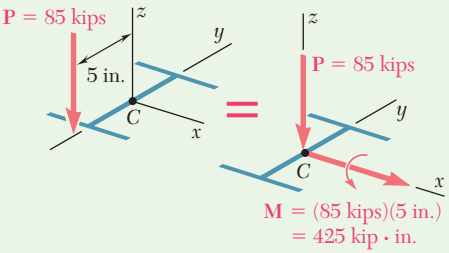
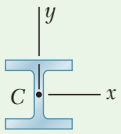
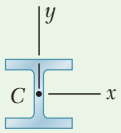


Fig. 1 Eccentric loading replaced by equivalent force-couple at column's centroid.



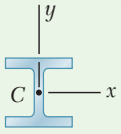
W8 × 35
$A = 10.3\ \text{in}^2$
$r_x = 3.51\ \text{in.}$
$r_y = 2.03\ \text{in.}$
$S_x = 31.2\ \text{in}^3$
$L = 16\ \text{ft} = 192\ \text{in.}$

Fig. 2 Section properties for W8 × 35.



W8 × 48
$A = 14.1\ \text{in}^2$
$r_x = 3.61\ \text{in.}$
$r_y = 2.08\ \text{in.}$
$S_x = 43.2\ \text{in}^3$
$L = 16\ \text{ft} = 192\ \text{in.}$

Fig. 3 Section properties for W8 × 48.



W8 × 40
$A = 11.7\ \text{in}^2$
$r_x = 3.53\ \text{in.}$
$r_y = 2.04\ \text{in.}$
$S_x = 35.5\ \text{in}^3$
$L = 16\ \text{ft} = 192\ \text{in.}$

Fig. 4 Section properties for W8 × 40.

From Appendix C, we observe that for shapes of 8-in. nominal depth $c \approx 4$ in. and $r_x \approx 3.5$ in. Using Fig. 1 and substituting into Eq. (1),

$$22\ \text{ksi} = \frac{85\ \text{kips}}{A} + \frac{(425\ \text{kip·in.})(4\ \text{in.})}{A(3.5\ \text{in.})^2} \qquad A \approx 10.2\ \text{in}^2$$

For a first trial shape, select W8 × 35.

Trial 1: W8 × 35 (Fig. 2). The allowable stresses are

Allowable Bending Stress: (see data) $(\sigma_{\text{all}})_{\text{bending}} = 22\ \text{ksi}$

Allowable Concentric Stress: The largest slenderness ratio of the column is $L/r_y = (192\ \text{in.})/(2.03\ \text{in.}) = 94.6$. Using Eq. (10.41) with $E = 29 \times 10^6$ psi and $\sigma_Y = 36$ ksi, the slenderness ratio at the junction between the two equations for σ_{cr} is $L/r = 133.7$. Thus, use Eqs. (10.38) and (10.39) and find $\sigma_{cr} = 22.5$ ksi. Using Eq. (10.42), the allowable stress is

$$(\sigma_{\text{all}})_{\text{centric}} = 22.5/1.67 = 13.46\ \text{ksi}$$

For the W8 × 35 trial shape,

$$\frac{P}{A} = \frac{85\ \text{kips}}{10.3\ \text{in}^2} = 8.25\ \text{ksi} \qquad \frac{Mc}{I} = \frac{M}{S_x} = \frac{425\ \text{kip·in.}}{31.2\ \text{in}^3} = 13.62\ \text{ksi}$$

With this data, the left-hand member of Eq. (10.55) is

$$\frac{P/A}{(\sigma_{\text{all}})_{\text{centric}}} + \frac{Mc/I}{(\sigma_{\text{all}})_{\text{bending}}} = \frac{8.25\ \text{ksi}}{13.46\ \text{ksi}} + \frac{13.62\ \text{ksi}}{22\ \text{ksi}} = 1.232$$

Since $1.232 > 1.000$, the requirement expressed by the interaction formula is not satisfied. Select a larger trial shape.

Trial 2: W8 × 48 (Fig.3). Following the procedure used in trial 1 gives

$$\frac{L}{r_y} = \frac{192\ \text{in.}}{2.08\ \text{in.}} = 92.3 \qquad (\sigma_{\text{all}})_{\text{centric}} = 13.76\ \text{ksi}$$

$$\frac{P}{A} = \frac{85\ \text{kips}}{14.1\ \text{in}^2} = 6.03\ \text{ksi} \qquad \frac{Mc}{I} = \frac{M}{S_x} = \frac{425\ \text{kip·in.}}{43.2\ \text{in}^3} = 9.84\ \text{ksi}$$

Substituting into Eq. (10.55) gives

$$\frac{P/A}{(\sigma_{\text{all}})_{\text{centric}}} + \frac{Mc/I}{(\sigma_{\text{all}})_{\text{bending}}} = \frac{6.03\ \text{ksi}}{13.76\ \text{ksi}} + \frac{9.82\ \text{ksi}}{22\ \text{ksi}} = 0.885 < 1.000$$

The W8 × 48 shape is satisfactory but may be unnecessarily large.

Trial 3: W8 × 40 (Fig.4). Following the same procedure, the interaction formula is not satisfied.

Selection of Shape. The shape to be used is W8 × 48 ◀

Problems

10.89 An eccentric load is applied at a point 22 mm from the geometric axis of a 60-mm-diameter rod made of a steel for which $\sigma_Y = 250$ MPa and $E = 200$ GPa. Using the allowable-stress method, determine the allowable load **P**.

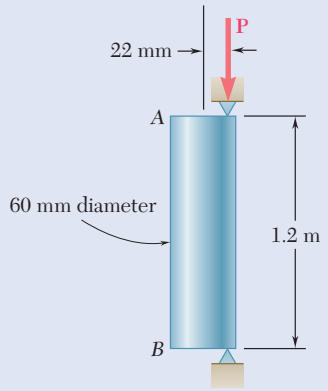


Fig. P10.89

10.90 Solve Prob, 10.89, assuming that the load is applied at a point 40 mm from the geometric axis and that the effective length is 0.9 m.

10.91 A sawn-lumber column of 5.0 × 7.5-in. cross section has an effective length of 8.5 ft. The grade of wood used has an adjusted allowable stress for compression parallel to the grain $\sigma_C = 1180$ psi and an adjusted modulus $E = 440 \times 10^3$ psi. Using the allowable-stress method, determine the largest eccentric load **P** that can be applied when (*a*) $e = 0.5$ in., (*b*) $e = 1.0$ in.

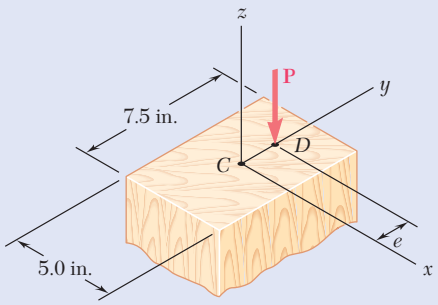


Fig. P10.91

10.92 Solve Prob. 10.91 using the interaction method and an allowable stress in bending of 1300 psi.

10.93 A column of 5.5-m effective length is made of the aluminum alloy 2014-T6 for which the allowable stress in bending is 220 MPa. Using the interaction method, determine the allowable load **P**, knowing that the eccentricity is (*a*) $e = 0$, (*b*) $e = 40$ mm.

10.94 Solve Prob. 10.93, assuming that the effective length of the column is 3.0 m.

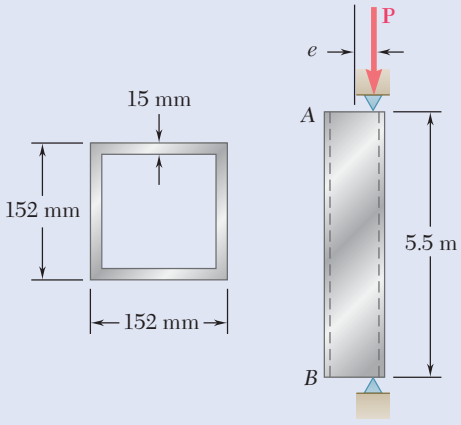


Fig. P10.93

10.95 A steel compression member of 9-ft effective length supports an eccentric load as shown. Using the allowable-stress method, determine the maximum allowable eccentricity e if (a) P = 30 kips, (b) P = 18 kips. Use σ_Y = 36 ksi and $E = 29 \times 10^6$ psi.

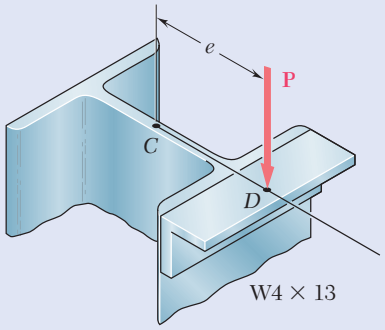


Fig. P10.95

10.96 Solve Prob. 10.95, assuming that the effective length of the column is increased to 12 ft and that (a) P = 20 kips, (b) P = 15 kips.

10.97 Two L4 × 3 × $\frac{3}{8}$-in. steel angles are welded together to form the column AB. An axial load **P** of magnitude 14 kips is applied at point D. Using the allowable-stress method, determine the largest allowable length L. Assume σ_Y = 36 ksi and $E = 29 \times 10^6$ psi.

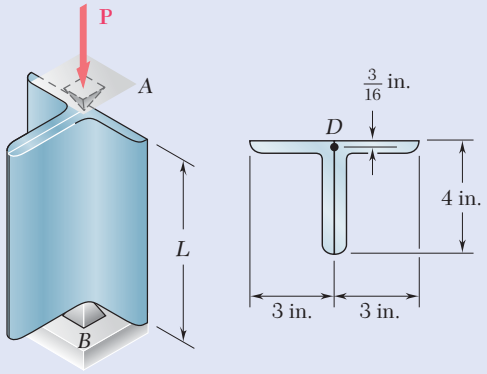


Fig. P10.97

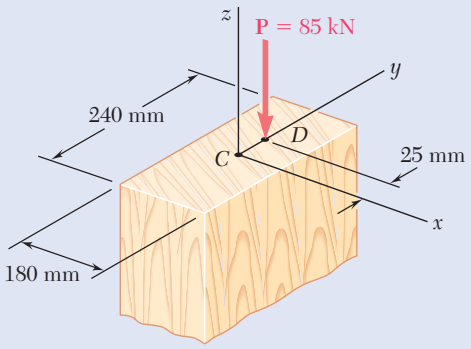


Fig. P10.99

10.98 Solve Prob. 10.97 using the interaction method with P = 18 kips and an allowable stress in bending of 22 ksi.

10.99 A rectangular column is made of a grade of sawn wood that has an adjusted allowable stress for compression parallel to the grain σ_C = 8.3 MPa and an adjusted modulus of elasticity E = 11.1 GPa. Using the allowable-stress method, determine the largest allowable effective length L that can be used.

10.100 Solve Prob. 10.99, assuming that P = 105 kN.

10.101 An eccentric load $P = 48$ kN is applied at a point 20 mm from the geometric axis of a 50-mm-diameter rod made of the aluminum alloy 6061-T6. Using the interaction method and an allowable stress in bending of 145 MPa, determine the largest allowable effective length L that can be used.

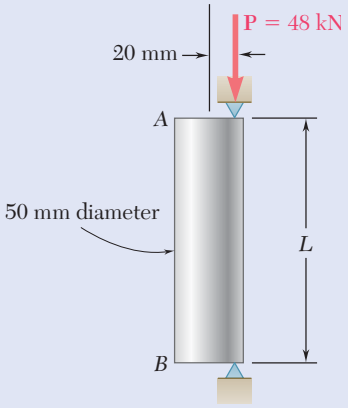


Fig. P10.101

10.102 Solve Prob. 10.101, assuming that the aluminum alloy used is 2014-T6 and that the allowable stress in bending is 180 MPa.

10.103 A compression member made of steel has a 720-mm effective length and must support the 198-kN load **P** as shown. For the material used $\sigma_Y = 250$ MPa and $E = 200$ GPa. Using the interaction method with an allowable bending stress equal to 150 MPa, determine the smallest dimension d of the cross section that can be used.

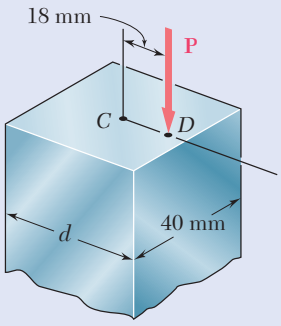


Fig. P10.103

10.104 Solve Prob. 10.103, assuming that the effective length is 1.62 m and that the magnitude of P of the eccentric load is 128 kN.

10.105 A steel tube of 80-mm outer diameter is to carry a 93-kN load **P** with an eccentricity of 20 mm. The tubes available for use are made with wall thicknesses in increments of 3 mm from 6 mm to 15 mm. Using the allowable-stress method, determine the lightest tube that can be used. Assume $E = 200$ GPa and $\sigma_Y = 250$ MPa.

10.106 Solve Prob. 10.105, using the interaction method with $P = 165$ kN, $e = 15$ mm, and an allowable stress in bending of 150 MPa.

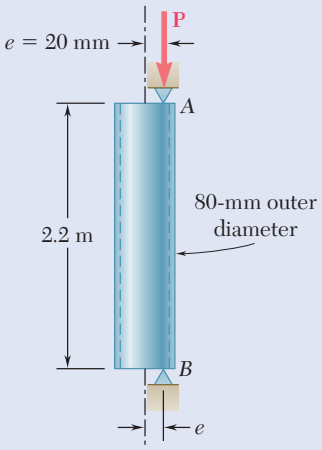


Fig. P10.105

10.107 A sawn lumber column of rectangular cross section has a 2.2-m effective length and supports a 41-kN load as shown. The sizes available for use have b equal to 90 mm, 140 mm, 190 mm, and 240 mm. The grade of wood has an adjusted allowable stress for compression parallel to the grain $\sigma_C = 8.1$ MPa and an adjusted modulus $E = 8.3$ GPa. Using the allowable-stress method, determine the lightest section that can be used.

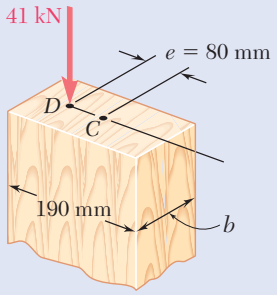


Fig. P10.107

10.108 Solve Prob. 10.107, assuming that $e = 40$ mm.

10.109 A compression member of rectangular cross section has an effective length of 36 in. and is made of the aluminum alloy 2014-T6 for which the allowable stress in bending is 24 ksi. Using the interaction method, determine the smallest dimension d of the cross section that can be used when $e = 0.4$ in.

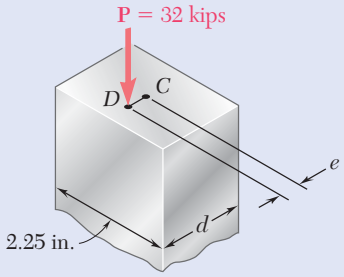


Fig. P10.109

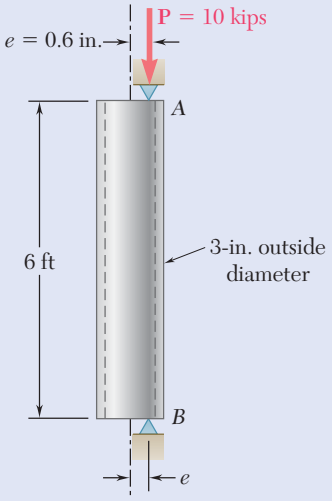


Fig. P10.111

10.110 Solve Prob. 10.109, assuming that $e = 0.2$ in.

10.111 An aluminum tube of 3-in. outside diameter is to carry a load of 10 kips having an eccentricity $e = 0.6$ in. Knowing that the stock of tubes available for use are made of alloy 2014-T6 and have wall thicknesses in increments of $\frac{1}{16}$ in. up to $\frac{1}{2}$ in., determine the lightest tube that can be used. Use the allowable-stress method.

10.112 Solve Prob. 10.111, using the interaction method of design with an allowable stress in bending of 25 ksi.

10.113 A steel column having a 24-ft effective length is loaded eccentrically as shown. Using the allowable-stress method, select the wide-flange shape of 14-in. nominal depth that should be used. Use $\sigma_Y = 36$ ksi and $E = 29 \times 10^6$ psi.

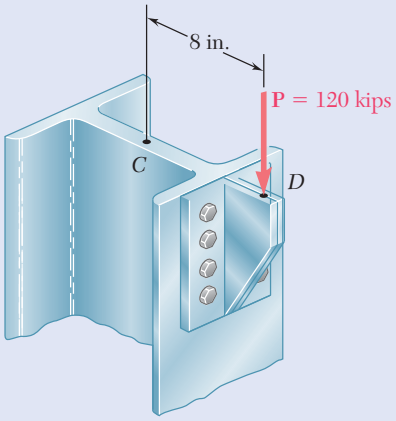


Fig. P10.113

10.114 Solve Prob. 10.113 using the interaction method, assuming that $\sigma_Y = 50$ ksi and the allowable stress in bending is 30 ksi.

10.115 A steel compression member of 5.8-m effective length is to support a 296-kN eccentric load **P**. Using the interaction method, select the wide-flange shape of 200-mm nominal depth that should be used. Use $E = 200$ GPa, $\sigma_Y = 250$ MPa, and $\sigma_{all} = 150$ MPa in bending.

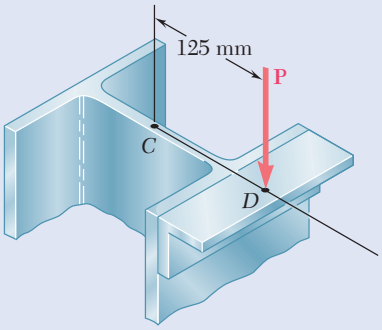


Fig. *P10.115*

10.116 A steel column of 7.2-m effective length is to support an 83-kN eccentric load **P** at a point D, located on the x axis as shown. Using the allowable-stress method, select the wide-flange shape of 250-mm nominal depth that should be used. Use $E = 200$ GPa and $\sigma_Y = 250$ MPa.

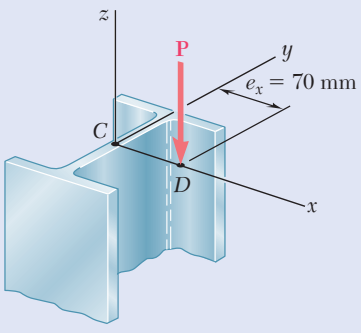


Fig. P10.116

Review and Summary

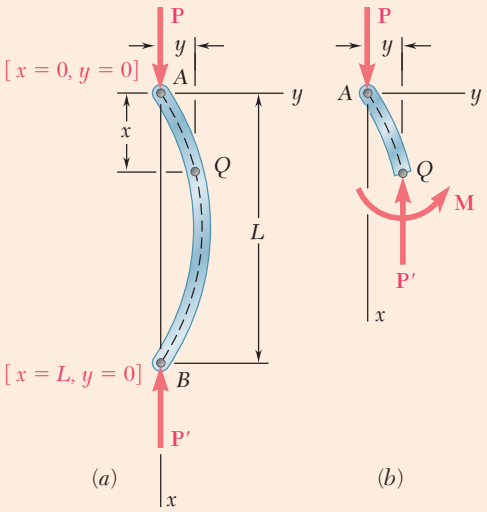


Fig. 10.38 Free-body diagrams of (*a*) buckled column and (*b*) portion *AQ*.

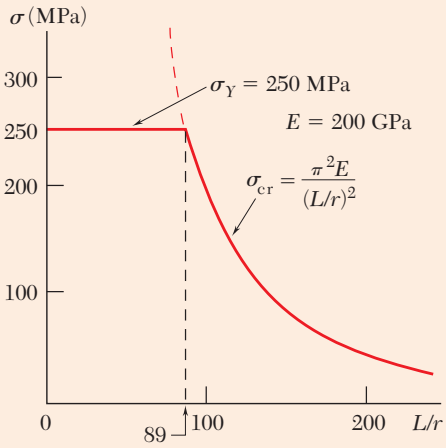


Fig. 10.39 Plot of critical stress.

Critical Load

The design and analysis of columns (i.e., prismatic members supporting axial loads), is based on the determination of the *critical load*. Two equilibrium positions of the column model are possible: the original position with zero transverse deflections and a second position involving deflections that could be quite large. The first equilibrium position is unstable for $P > P_{cr}$ and stable for $P < P_{cr}$, since in the latter case it was the only possible equilibrium position.

We considered a pin-ended column of length L and constant flexural rigidity EI subjected to an axial centric load P. Assuming that the column buckled (Fig. 10.38), the bending moment at point Q is equal to $-Py$. Thus,

$$\frac{d^2y}{dx^2} = \frac{M}{EI} = -\frac{P}{EI}y \tag{10.4}$$

Euler's Formula

Solving this differential equation, subject to the boundary conditions corresponding to a pin-ended column, we determined the smallest load P for which buckling can take place. This load, known as the *critical load* and denoted by P_{cr}, is given by *Euler's formula:*

$$P_{cr} = \frac{\pi^2 EI}{L^2} \tag{10.11a}$$

where L is the length of the column. For this or any larger load, the equilibrium of the column is unstable, and transverse deflections will occur.

Slenderness Ratio

Denoting the cross-sectional area of the column by A and its radius of gyration by r, the critical stress σ_{cr} corresponding to the critical load P_{cr} is

$$\sigma_{cr} = \frac{\pi^2 E}{(L/r)^2} \tag{10.13a}$$

The quantity L/r is the *slenderness ratio*. The critical stress σ_{cr} is plotted as a function of L/r in Fig. 10.39. Since the analysis was based on stresses remaining below the yield strength of the material, the column will fail by yielding when $\sigma_{cr} > \sigma_Y$.

Effective Length

The critical load of columns with various end conditions is written as

$$P_{cr} = \frac{\pi^2 EI}{L_e^2} \tag{10.11b}$$

where L_e is the *effective length* of the column, i.e., the length of an equivalent pin-ended column. The effective lengths of several columns with various end conditions were calculated and shown in Fig. 10.18 on page 700.

Eccentric Axial Load

For a pin-ended column subjected to a load P applied with an eccentricity e, the load can be replaced with a centric axial load and a couple of moment $M_A = Pe$ (Fig. 10.40). The maximum transverse deflection is

$$y_{\max} = e\left[\sec\left(\sqrt{\frac{P}{EI}}\frac{L}{2}\right) - 1\right] \tag{10.28}$$

Secant Formula

The maximum stress in a column supporting an eccentric axial load can be found using the *secant formula:*

$$\frac{P}{A} = \frac{\sigma_{\max}}{1 + \dfrac{ec}{r^2}\sec\left(\dfrac{1}{2}\sqrt{\dfrac{P}{EA}}\dfrac{L_e}{r}\right)} \tag{10.36}$$

This equation can be solved for the force per unit area P/A, which causes a specified maximum stress $\sigma_{\max}$ in a pin-ended or other column of effective slenderness ratio L_e/r.

Design of Real Columns

Since imperfections exist in all columns, the *design of real columns* is done with empirical formulas based on laboratory tests, set forth in specifications and codes issued by professional organizations. For *centrically loaded columns* made of steel, aluminum, or wood, design is based on equations for the allowable stress as a function of the slenderness ratio L/r. For structural steel, the *Load and Resistance Factor Design* method also can be used.

Design of Eccentrically Loaded Columns

Two methods can be used for the design of columns under an *eccentric* load. The first method is the *allowable-stress method.* This conservative method assumes that the allowable stress is the same as if the column were centrically loaded. The allowable-stress method requires that the following inequality to be satisfied:

$$\frac{P}{A} + \frac{Mc}{I} \le \sigma_{\text{all}} \tag{10.53}$$

The second method is the *interaction method,* which is the basis of most modern specifications. In this method, the allowable stress for a centrically loaded column is used for the portion of the total stress due to the axial load, and the allowable stress in bending is used for the stress due to bending. Thus, the inequality to be satisfied is

$$\frac{P/A}{(\sigma_{\text{all}})_{\text{centric}}} + \frac{Mc/I}{(\sigma_{\text{all}})_{\text{bending}}} \le 1 \tag{10.55}$$

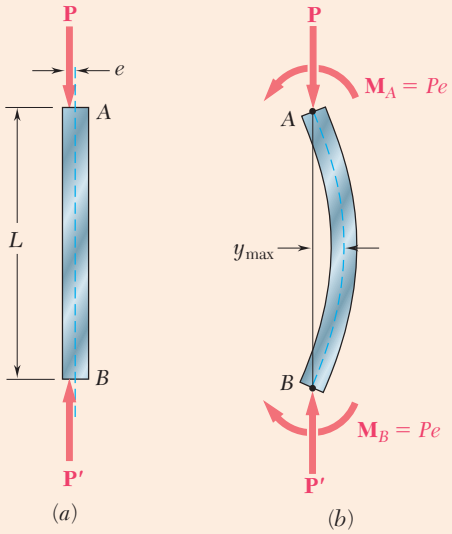


Fig. 10.40 (*a*) Column with an eccentric load (*b*) modeled as a column with an equivalent centric force-couple load.

Review Problems

10.117 Determine (*a*) the critical load for the steel strut, (*b*) the dimension *d* for which the aluminum strut will have the same critical load. (*c*) Express the weight of the aluminum strut as a percent of the weight of the steel strut.

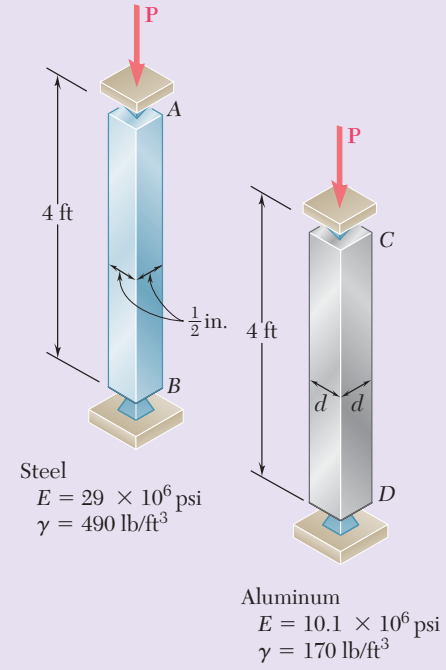


Fig. P10.117

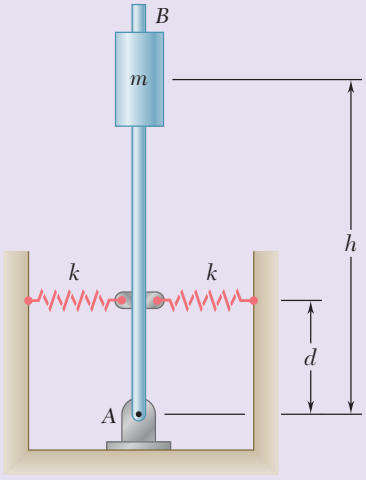


Fig. P10.118

10.118 The rigid rod *AB* is attached to a hinge at *A* and to two springs, each of constant *k*. If $h = 450$ mm, $d = 300$ mm, and $m = 200$ kg, determine the range of values of *k* for which the equilibrium of rod *AB* is stable in the position shown. Each spring can act in either tension or compression.

10.119 A column of 3-m effective length is to be made by welding together two C130 × 13 rolled-steel channels. Using $E = 200$ GPa, determine for each arrangement shown the allowable centric load if a factor of safety of 2.4 is required.

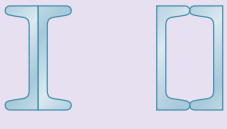


Fig. *P10.119*

10.120 (a) Considering only buckling in the plane of the structure shown and using Euler's formula, determine the value of θ between 0 and 90° for which the allowable magnitude of the load **P** is maximum. (b) Determine the corresponding maximum value of P knowing that a factor of safety of 3.2 is required. Use $E = 29 \times 10^6$ psi.

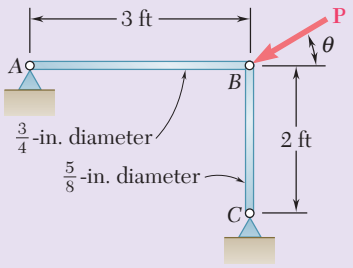


Fig. P10.120

10.121 Member AB consists of a single C130 × 10.4 steel channel of length 2.5 m. Knowing that the pins A and B pass through the centroid of the cross section of the channel, determine the factor of safety for the load shown with respect to buckling in the plane of the figure when $\theta = 30°$. Use $E = 200$ GPa.

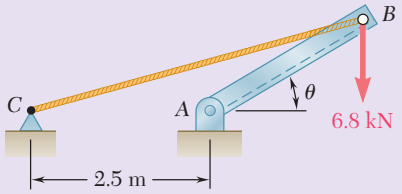


Fig. P10.121

10.122 The line of action of the 75-kip axial load is parallel to the geometric axis of the column AB and intersects the x axis at $x = 0.6$ in. Using $E = 29 \times 10^6$ psi, determine (a) the horizontal deflection of the midpoint C of the column, (b) the maximum stress in the column.

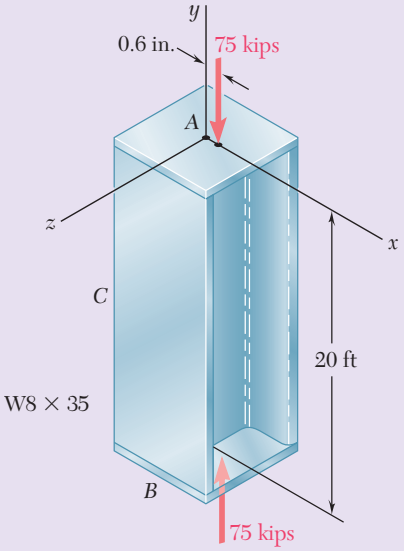


Fig. P10.122

10.123 Supports A and B of the pin-ended column shown are at a fixed distance L from each other. Knowing that at a temperature T_0 the force in the column is zero and that buckling occurs when the temperature is $T_1 = T_0 + \Delta T$, express ΔT in terms of b, L and the coefficient of thermal expansion α.

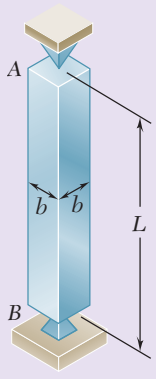


Fig. P10.123

10.124 A column is made from half of a W360 × 216 rolled-steel shape, with the geometric properties as shown. Using allowable stress design, determine the allowable centric load if the effective length of the column is (a) 4.0 m, (b) 6.5 m. Use $\sigma_Y = 345$ MPa and $E = 200$ GPa.

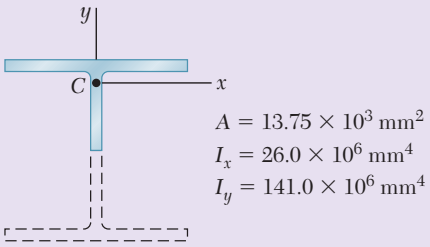


Fig. P10.124

10.125 A rectangular column with a 4.4-m effective length is made of glued laminated wood. Knowing that for the grade of wood used the adjusted allowable-stress for compression parallel to the grain is $\sigma_C = 8.3$ MPa and the adjusted modulus $E = 4.6$ GPa, determine the maximum allowable centric load for the column.

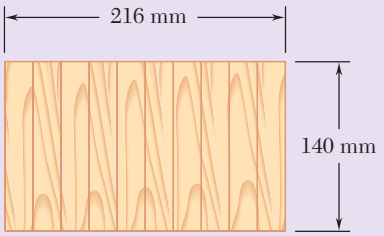


Fig. P10.125

10.126 A column of 4.5-m effective length must carry a centric load of 900 kN. Knowing that $\sigma_Y = 345$ MPa and $E = 200$ GPa, use allowable-stress design to select the wide-flange shape of 250-mm nominal depth that should be used.

10.127 An 11-kip vertical load **P** is applied at the midpoint of one edge of the square cross section of the steel compression member *AB*, which is free at its top *A* and fixed at its base *B*. Knowing that for the grade of steel used $\sigma_Y = 36$ ksi and $E = 29 \times 10^6$ psi and using the allowable-stress method, determine the smallest allowable dimension *d*.

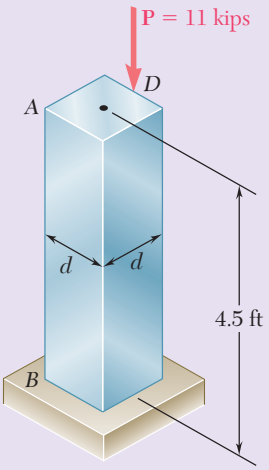


Fig. *P10.127*

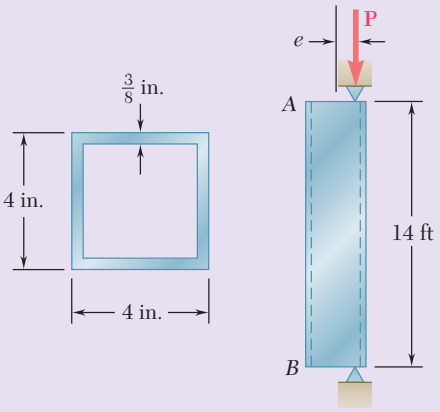


Fig. P10.128

10.128 A column of 14-ft effective length consists of a section of steel tubing having the cross section shown. Using the allowable-stress method, determine the maximum allowable eccentricity *e* if (*a*) $P = 55$ kips, (*b*) $P = 35$ kips. Use $\sigma_Y = 36$ ksi and $E = 29 \times 10^6$ psi.

Computer Problems

The following problems are designed to be solved with a computer.

10.C1 A solid steel rod having an effective length of 500 mm is to be used as a compression strut to carry a centric load **P**. For the grade of steel used, $E = 200$ GPa and $\sigma_Y = 245$ MPa. Knowing that a factor of safety of 2.8 is required and using Euler's formula, write a computer program and use it to calculate the allowable centric load P_{all} for values of the radius of the rod from 6 mm to 24 mm, using 2-mm increments.

10.C2 An aluminum bar is fixed at end A and supported at end B so that it is free to rotate about a horizontal axis through the pin. Rotation about a vertical axis at end B is prevented by the brackets. Knowing that $E = 10.1 \times 10^6$ psi, use Euler's formula with a factor of safety of 2.5 to determine the allowable centric load **P** for values of b from 0.75 in. to 1.5 in., using 0.125-in. increments.

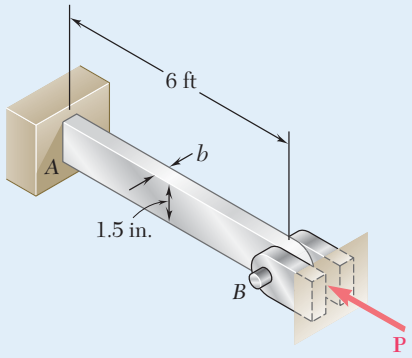


Fig. C10.C2

10.C3 The pin-ended members AB and BC consist of sections of aluminum pipe of 120-mm outer diameter and 10-mm wall thickness. Knowing that a factor of safety of 3.5 is required, determine the mass m of the largest block that can be supported by the cable arrangement shown for values of h from 4 m to 8 m, using 0.25-m increments. Use $E = 70$ GPa and consider only buckling in the plane of the structure.

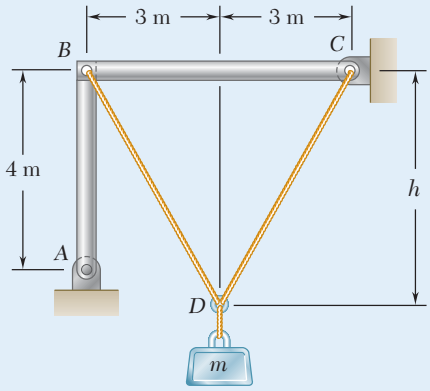


Fig. C10.C3

10.C4 An axial load **P** is applied at a point located on the x axis at a distance $e = 0.5$ in. from the geometric axis of the W8 × 40 rolled-steel column AB. Using $E = 29 \times 10^6$ psi, write a computer program and use it to calculate for values of P from 25 to 75 kips, using 5-kip increments, (a) the horizontal deflection at the midpoint C, (b) the maximum stress in the column.

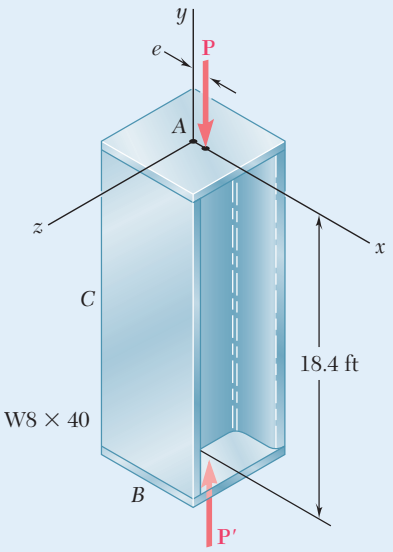


Fig. C10.C4

10.C5 A column of effective length L is made from a rolled-steel shape and carries a centric axial load **P**. The yield strength for the grade of steel used is denoted by σ_Y, the modulus of elasticity by E, the cross-sectional area of the selected shape by A, and its smallest radius of gyration by r. Using the AISC design formulas for allowable stress design, write a computer program that can be used with either SI or U.S. customary units to determine the allowable load **P**. Use this program to solve (a) Prob. 10.57, (b) Prob. 10.58, (c) Prob. 10.124.

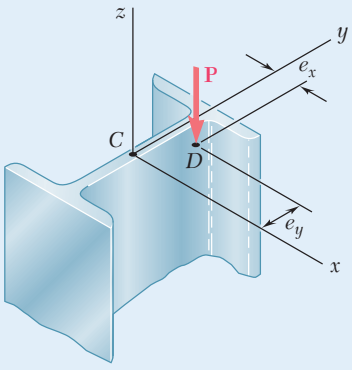
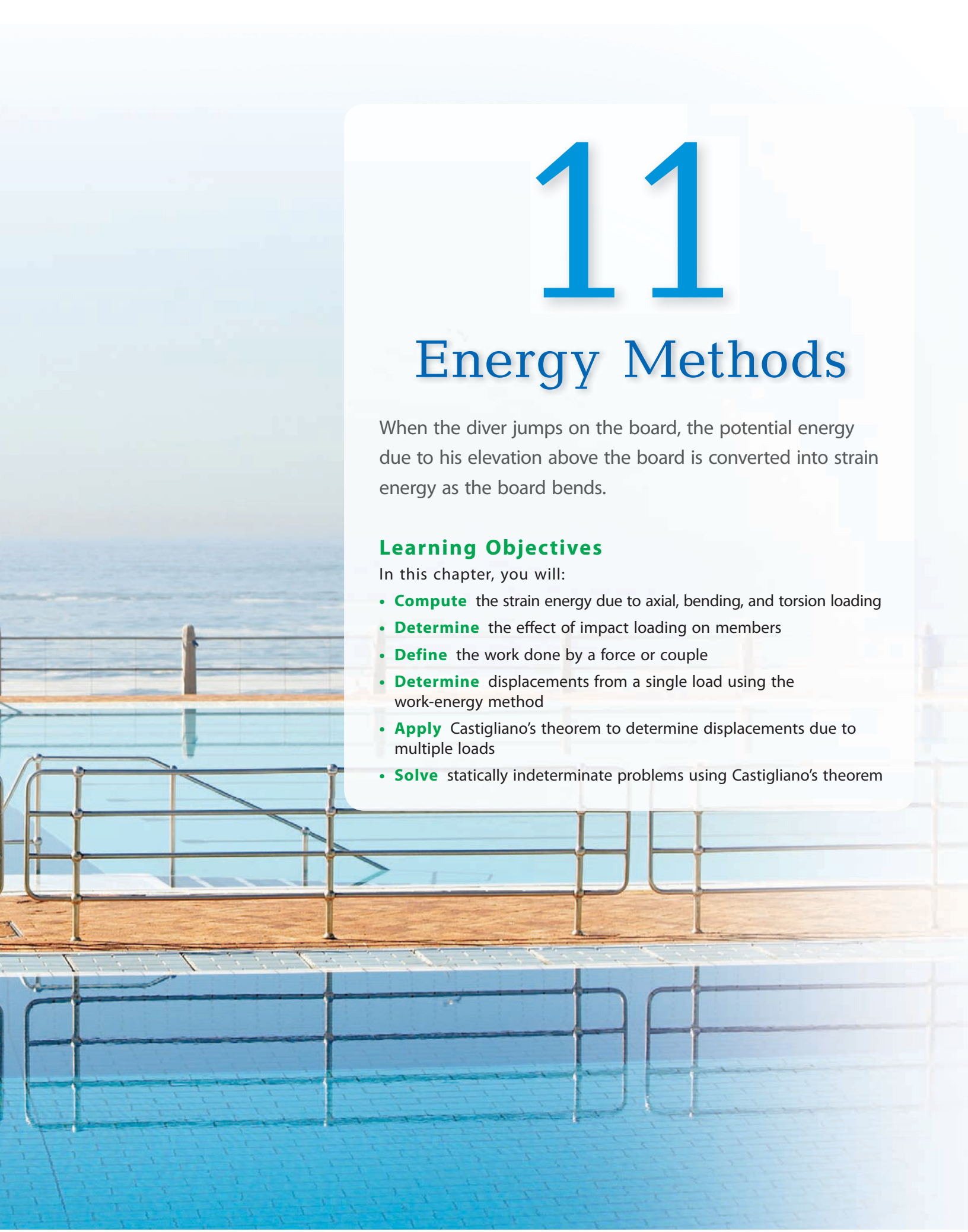


Fig. C10.C6

10.C6 A column of effective length L is made from a rolled-steel shape and is loaded eccentrically as shown. The yield strength of the grade of steel used is denoted by σ_Y, the allowable stress in bending by σ_{all}, the modulus of elasticity by E, the cross-sectional area of the selected shape by A, and its smallest radius of gyration by r. Write a computer program that can be used with either SI or U.S. customary units to determine the allowable load **P**, using either the allowable-stress method or the interaction method. Use this program to check the given answer for (a) Prob. 10.113, (b) Prob. 10.114.

This page intentionally left blank





11

Energy Methods

When the diver jumps on the board, the potential energy due to his elevation above the board is converted into strain energy as the board bends.

Learning Objectives

In this chapter, you will:

- **Compute** the strain energy due to axial, bending, and torsion loading
- **Determine** the effect of impact loading on members
- **Define** the work done by a force or couple
- **Determine** displacements from a single load using the work-energy method
- **Apply** Castigliano's theorem to determine displacements due to multiple loads
- **Solve** statically indeterminate problems using Castigliano's theorem

Introduction

11.1 STRAIN ENERGY
11.1A Strain Energy Concepts
11.1B Strain-Energy Density
11.2 ELASTIC STRAIN ENERGY
11.2A Normal Stresses
11.2B Shearing Stresses
11.3 STRAIN ENERGY FOR A GENERAL STATE OF STRESS
11.4 IMPACT LOADS
11.4A Analysis
11.4B Design
11.5 SINGLE LOADS
11.5A Energy Formulation
11.5B Deflections
*11.6 MULTIPLE LOADS
*11.7 CASTIGLIANO'S THEOREM
*11.8 DEFLECTIONS BY CASTIGLIANO'S THEOREM
*11.9 STATICALLY INDETERMINATE STRUCTURES

Introduction

In the previous chapter we were concerned with the relations existing between forces and deformations under various loading conditions. Our analysis was based on two fundamental concepts, the concept of stress (Chap. 1) and the concept of strain (Chap. 2). A third important concept, the concept of *strain energy,* will now be introduced.

The *strain energy* of a member is the increase in energy associated with the deformation of the member. The strain energy is equal to the work done by a slowly increasing load applied to the member. The *strain-energy density* of a material is the strain energy per unit volume; this it is equal to the area under the stress-strain diagram of the material (Sec. 11.1B). From the stress-strain diagram of a material, two additional properties are the *modulus of toughness* and the *modulus of resilience* of the material.

In Sec. 11.2 the elastic strain energy associated with *normal stresses* is discussed for members under axial loading and in bending. The elastic strain energy associated with shearing stresses (such as in torsional loadings of shafts and in transversely loaded beams) is discussed. Strain energy for a *general state of stress* is considered in Sec. 11.3, where the *maximum-distortion-energy criterion* for yielding is derived.

The effect of *impact loading* on members is considered in Sec. 11.4. The *maximum stress* and the *maximum deflection* caused by a moving mass impacting a member are calculated. Properties that increase the ability of a structure to withstand impact loads effectively are discussed in Sec. 11.4B.

In Sec. 11.5A the elastic strain of a member subjected to a *single concentrated load* is calculated, and in Sec. 11.5B the deflection at the point of application of a single load is determined.

The last portion of the chapter is devoted to the strain energy of structures subjected to *multiple loads* (Sec. 11.6). *Castigliano's theorem* is derived (Sec. 11.7) and used (Sec. 11.8) to determine the deflection at a given point of a structure subjected to several loads. Indeterminate structures are analyzed using Castigliano's theorem (Sec. 11.9).

11.1 STRAIN ENERGY

11.1A Strain Energy Concepts

Consider a rod BC with a length of L and uniform cross-sectional area A that is attached at B to a fixed support and subjected at C to a *slowly increasing* axial load **P** (Fig. 11.1). By plotting the magnitude P of the load against the deformation x of the rod (Sec. 2.1), a load-deformation diagram is obtained (Fig. 11.2) that is characteristic of rod BC.

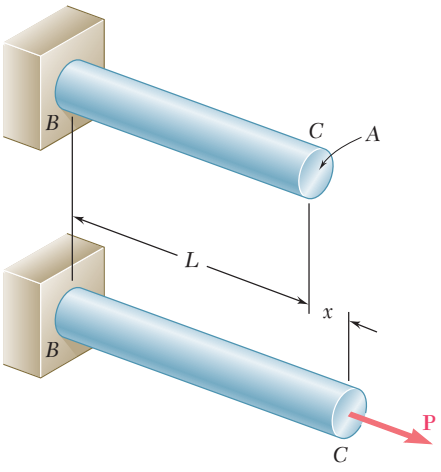


Fig. 11.1 Axially loaded rod

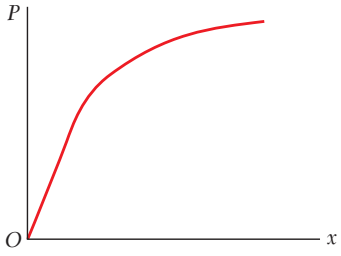


Fig. 11.2 Load-deformation diagram for axial loading.

Now consider the work dU done by the load **P** as the rod elongates by a small amount dx. This *elementary work* is equal to the product of the magnitude P of the load and of the small elongation dx

$$dU = P\,dx \tag{11.1}$$

Note that this equation is equal to the element with an area of width dx located under the load-deformation diagram (Fig. 11.3). The *total work* U done by the load as the rod undergoes a deformation x_1 is

$$U = \int_0^{x_1} P\,dx$$

and is equal to the area under the load-deformation diagram between $x = 0$ and $x = x_1$.

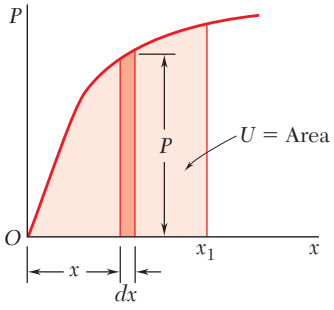


Fig. 11.3 Work due to load **P** is equal to the area under the load-deformation diagram.

The work done by load **P** as it is slowly applied to the rod results in the increase of energy associated with the deformation of the rod. This energy is the *strain energy* of the rod.

$$\text{Strain energy} = U = \int_0^{x_1} P\,dx \tag{11.2}$$

Recall that work and energy should be obtained by multiplying units of length by units of force. So, when SI units are used, work and energy are expressed in N·m, which is called a *joule* (J). When U.S. customary units are used, work and energy are in ft·lb or in in·lb.

For a linear elastic deformation, the portion of the load-deformation diagram involved can be represented by a straight line with equation $P = kx$ (Fig. 11.4). Substituting for P in Eq. (11.2) gives

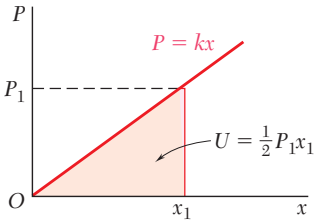


Fig. 11.4 Work due to linear elastic deformation.

$$U = \int_0^{x_1} kx\,dx = \tfrac{1}{2}kx_1^2$$

or

$$U = \tfrac{1}{2}P_1x_1 \tag{11.3}$$

where P_1 is the load corresponding to the deformation x_1.

Strain energy can be used to determine the effects of impact loadings on structures or machine components. For example, a body of mass m moving with a velocity $\mathbf{v}_0$ strikes the end B of a rod AB (Fig. 11.5*a*). Neglecting the inertia of the rod and assuming no dissipation of energy during the impact, the maximum strain energy U_m acquired by the rod (Fig. 11.5*b*) is equal to the original kinetic energy $T = \frac{1}{2}mv_0^2$ of the moving body. If we then determine P_m of the static load (which would have produced the same strain energy in the rod), we can obtain σ_m of the largest stress occurring in the rod by dividing P_m by the cross-sectional area.

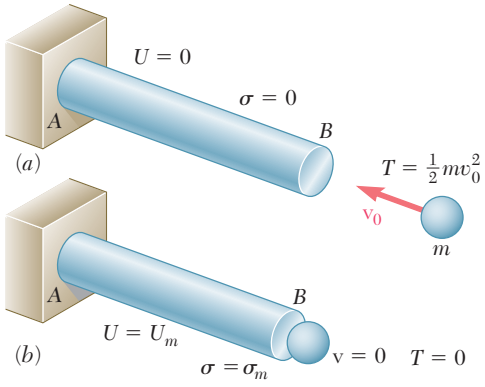


Fig. 11.5 Rod subject to impact loading.

11.1B Strain-Energy Density

As noted in Sec. 2.1, the load-deformation diagram for a rod BC depends upon the length L and the cross-sectional area A. The strain energy U defined by Eq. (11.2), therefore, will also depend on the dimensions of the rod. To eliminate the effect of size and direct attention to the properties of the material, the strain energy per unit volume will be considered. Dividing the strain energy U by the volume $V = AL$ of the rod (Fig. 11.1) and using Eq. (11.2) gives

$$\frac{U}{V} = \int_0^{x_1} \frac{P}{A}\frac{dx}{L}$$

Recalling that P/A represents the normal stress σ_x and x/L the normal strain ϵ_x,

$$\frac{U}{V} = \int_0^{\epsilon_1} \sigma_x \, d\epsilon_x$$

where ϵ_1 denotes the value of the strain corresponding to the elongation x_1. The strain energy per unit volume U/V is called the *strain-energy density,* denoted by u. Therefore,

$$\text{Strain-energy density} = u = \int_0^{\epsilon_1} \sigma_x \, d\epsilon_x \tag{11.4}$$

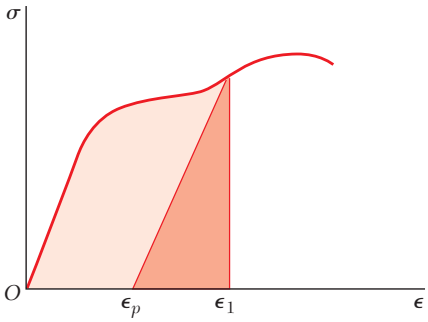


Fig. 11.6 Strain-energy density is the area under the stress-strain curve between $\epsilon_x = 0$ and $\epsilon_x = \epsilon_1$. If loaded into the plastic region, only the energy associated with elastic unloading is recovered.

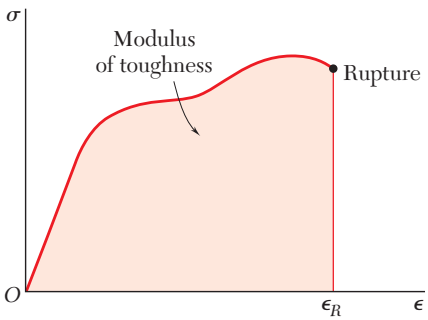


Fig. 11.7 Modulus of toughness is the area under the stress-strain curve to rupture.

The strain-energy density u is expressed in units of energy divided by units of volume. Thus, when SI metric units are used, the strain-energy density is in J/m^3 or its multiples kJ/m^3 and MJ/m^3. When U.S. customary units are used, they are in in·lb/in^3.[†]

Referring to Fig. 11.6, the strain-energy density u is equal to the area under the stress-strain curve, which is measured from $\epsilon_x = 0$ to $\epsilon_x = \epsilon_1$. If the material is unloaded, the stress returns to zero. However, there is a permanent deformation represented by the strain ϵ_p, and only the part of the strain energy per unit volume corresponding to the triangular area is recovered. The remainder of the energy spent deforming the material is dissipated in the form of heat.

The strain-energy density obtained by setting $\epsilon_1 = \epsilon_R$ in Eq. (11.4), where ϵ_R is the strain at rupture, is called the *modulus of toughness* of the material. It is equal to the area under the entire stress-strain diagram (Fig. 11.7) and represents the energy per unit volume required for the material to rupture. The toughness of a material is related to its ductility, as well as its ultimate strength (Sec. 2.1B), and the capacity of a structure

[†]Note that 1 J/m^3 and 1 Pa are both equal to 1 N/m^2, while 1 in.·lb/in^3 and 1 psi are both equal to 1 lb/in^2. Thus, strain-energy density and stress are dimensionally equal and can be expressed in the same units.

to withstand an impact load depends upon the toughness of the material used (Photo 11.1).

If the stress σ_x remains within the proportional limit of the material, Hooke's law applies:

$$\sigma_x = E\epsilon_x \tag{11.5}$$

Substituting for σ_x from Eq. (11.5) into Eq. (11.4) gives

$$u = \int_0^{\epsilon_1} E\epsilon_x \, d\epsilon_x = \frac{E\epsilon_1^2}{2} \tag{11.6}$$

or using Eq. (11.5) to express ϵ_1 in terms of the corresponding stress σ_1 gives

$$u = \frac{\sigma_1^2}{2E} \tag{11.7}$$

The strain-energy density obtained by setting $\sigma_1 = \sigma_Y$ in Eq. (11.7), where σ_Y is the yield strength, is called the *modulus of resilience* of the material, and is denoted by u_Y. So,

$$u_Y = \frac{\sigma_Y^2}{2E} \tag{11.8}$$

The modulus of resilience is equal to the area under the straight-line portion OY of the stress-strain diagram (Fig. 11.8) and represents the energy per unit volume that the material can absorb without yielding. A structure's ability to withstand an impact load without being permanently deformed depends on the resilience of the material used.

Since the modulus of toughness and the modulus of resilience represent characteristic values of the strain-energy density of the material considered, they are both expressed in J/m^3 or its multiples if SI units are used, and in in·lb/in^3 if U.S. customary units are used.[†]



Photo 11.1 The railroad coupler is made of a ductile steel that has a large modulus of toughness.

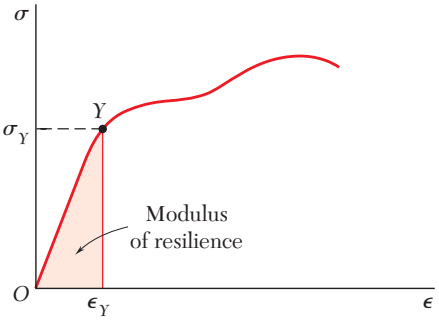


Fig. 11.8 Modulus of resilience is the area under the stress-strain curve to yield.

11.2 ELASTIC STRAIN ENERGY

11.2A Normal Stresses

Since the rod considered in the preceding section was subjected to uniformly distributed stresses σ_x, the strain-energy density was constant throughout the rod and could be defined as the ratio U/V of the strain energy U and the volume V of the rod. In a structural element or machine part with a nonuniform stress distribution, the strain-energy density u can be defined by considering the strain energy of a small element of material of volume ΔV. So,

$$u = \lim_{\Delta V \to 0} \frac{\Delta U}{\Delta V}$$

or

$$u = \frac{dU}{dV} \tag{11.9}$$

[†]Note that the modulus of toughness and the modulus of resilience could be expressed in the same units as stress.

The expression previously obtained for u (Sec. 11.1B) in terms of σ_x and ϵ_x is valid, so

$$u = \int_0^{\epsilon_x} \sigma_x \, d\epsilon_x \tag{11.10}$$

which allows for variations in the stress σ_x, the strain ϵ_x, and the strain-energy density u from point to point.

For values of σ_x within the proportional limit, $\sigma_x = E\epsilon_x$ in Eq. (11.10) and

$$u = \frac{1}{2}E\epsilon_x^2 = \frac{1}{2}\sigma_x\epsilon_x = \frac{1}{2}\frac{\sigma_x^2}{E} \tag{11.11}$$

The strain energy U of a body subjected to uniaxial normal stresses can be obtained by substituting for u from Eq. (11.11) into Eq. (11.9) and integrating both members.

$$U = \int \frac{\sigma_x^2}{2E} dV \tag{11.12}$$

This equation is valid only for elastic deformations and is called the *elastic strain energy* of the body.

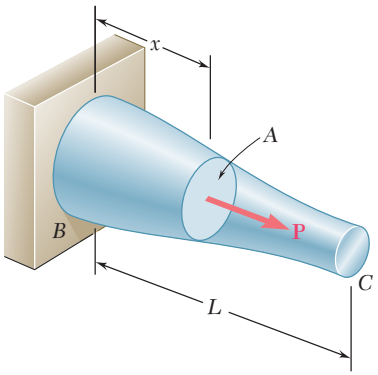


Fig. 11.9 Rod with centric axial load.

Strain Energy under Axial Loading. Recall from Sec. 2.10 that when a rod is subjected to a centric axial load, it can be assumed that the normal stresses σ_x are uniformly distributed in any given cross section. Using the area of the section A located at a distance x from end B of the rod (Fig. 11.9) and the internal force P in that section, we write $\sigma_x = P/A$. Substituting for σ_x into Eq. (11.12) gives

$$U = \int \frac{P^2}{2EA^2} dV$$

or setting $dV = A\,dx$,

$$U = \int_0^L \frac{P^2}{2AE} dx \tag{11.13}$$

For a rod of uniform cross section with equal and opposite forces of magnitude P at its ends (Fig. 11.10), Eq. (11.13) yields

$$U = \frac{P^2 L}{2AE} \tag{11.14}$$

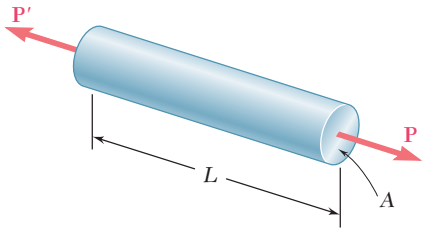


Fig. 11.10 Prismatic rod with centric axial load.

Concept Application 11.1

A rod consists of two portions *BC* and *CD* of the same material, same length, but of different cross sections (Fig. 11.11). Determine the strain energy of the rod when it is subjected to a centric axial load **P**, expressing the result in terms of *P*, *L*, *E*, the cross-sectional area *A* of portion *CD*, and the ratio *n* of the two diameters.

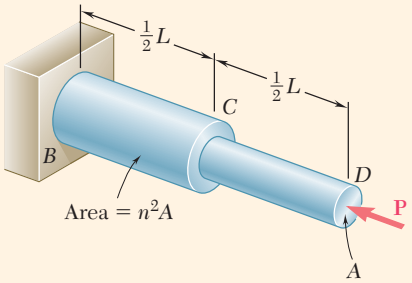


Fig. 11.11 Axially loaded stepped rod.

Use Eq. (11.14) for the strain energy of each of the two portions, and add the expressions obtained:

$$U_n = \frac{P^2(\frac{1}{2}L)}{2AE} + \frac{P^2(\frac{1}{2}L)}{2(n^2A)E} = \frac{P^2L}{4AE}\left(1 + \frac{1}{n^2}\right)$$

or

$$U_n = \frac{1 + n^2}{2n^2}\frac{P^2L}{2AE} \tag{1}$$

Check that, for $n = 1$,

$$U_1 = \frac{P^2L}{2AE}$$

which is the same as Eq. (11.14) for a rod of length *L* and uniform cross section of area *A*. Also note that for $n > 1$, $U_n < U_1$. As an example, when $n = 2$, $U_2 = (\frac{5}{8})U_1$. Since the maximum stress occurs in portion *CD* of the rod and is equal to $\sigma_{\max} = P/A$, then for a given allowable stress, increasing the diameter of portion *BC* of the rod results in a *decrease* of the overall energy-absorbing capacity. Unnecessary changes in cross-sectional area should be avoided in the design of members subjected to loads (such as impact loadings) where the energy-absorbing capacity of the member is critical.

Concept Application 11.2

A load **P** is supported at B by two rods of the same material and of the same uniform cross section of area A (Fig. 11.12*a*). Determine the strain energy of the system.

Using the forces F_{BC} and F_{BD} in members BC and BD and recalling Eq. (11.14), the strain energy of the system is

$$U = \frac{F_{BC}^2(BC)}{2AE} + \frac{F_{BD}^2(BD)}{2AE} \tag{1}$$

From Fig. 11.12*a*,

$$BC = 0.6l \qquad BD = 0.8l$$

From the free-body diagram of pin B and the corresponding force triangle (Fig. 11.12*b*),

$$F_{BC} = +0.6P \qquad F_{BD} = -0.8P$$

Substituting into Eq. (1) gives

$$U = \frac{P^2l[(0.6)^3 + (0.8)^3]}{2AE} = 0.364\frac{P^2l}{AE}$$

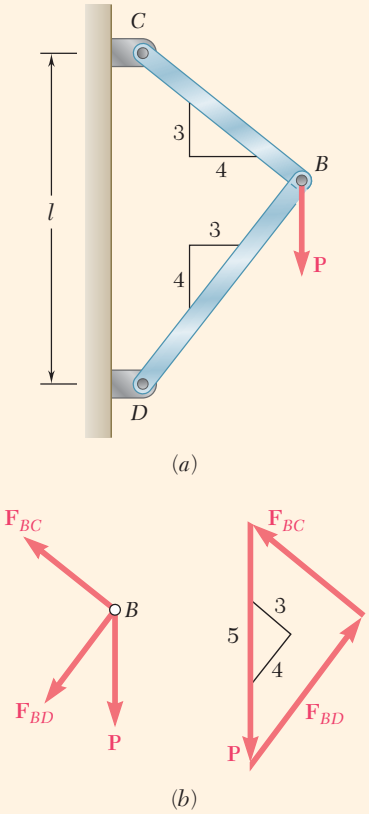


Fig. 11.12 (*a*) Frame *CBD* supporting a vertical force *P*. (*b*) Free-body diagram of joint *B* and corresponding force triangle.

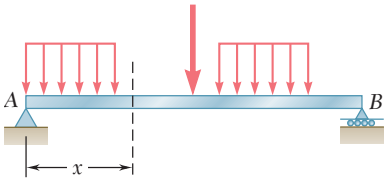


Fig. 11.13 Transversely loaded beam.

Strain Energy in Bending. Consider a beam AB subjected to a given loading (Fig. 11.13), and let M be the bending moment at a distance x from end A. Neglecting the effect of shear and taking into account only the normal stresses $\sigma_x = My/I$, substitute this expression into Eq. (11.12) and write

$$U = \int \frac{\sigma_x^2}{2E}\,dV = \int \frac{M^2y^2}{2EI^2}\,dV$$

Setting $dV = dA\,dx$, where dA represents an element of the cross-sectional area, and recalling that $M^2/2EI^2$ is a function of x alone gives

$$U = \int_0^L \frac{M^2}{2EI^2}\left(\int y^2\,dA\right)dx$$

Recall that the integral within the parentheses represents the moment of inertia I of the cross section about its neutral axis. Thus,

$$U = \int_0^L \frac{M^2}{2EI}\,dx \tag{11.15}$$

Concept Application 11.3

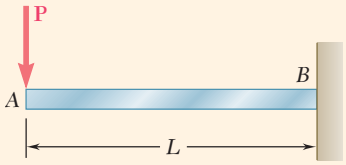


Fig. 11.14 Cantilever beam with load *P*.

Determine the strain energy of the prismatic cantilever beam *AB* (Fig. 11.14), taking into account only the effect of the normal stresses.

The bending moment at a distance x from end A is $M = -Px$. Substitute this expression into Eq. (11.15) to obtain

$$U = \int_0^L \frac{P^2x^2}{2EI}\,dx = \frac{P^2L^3}{6EI}$$

11.2B Shearing Stresses

When a material is subjected to plane shearing stresses τ_{xy}, the strain-energy density at a given point is

$$u = \int_0^{\gamma_{xy}} \tau_{xy}\,d\gamma_{xy} \tag{11.16}$$

where γ_{xy} is the shearing strain corresponding to τ_{xy} (Fig. 11.15*a*). Note that the strain-energy density u is equal to the area under the shearing-stress-strain diagram (Fig. 11.15*b*).

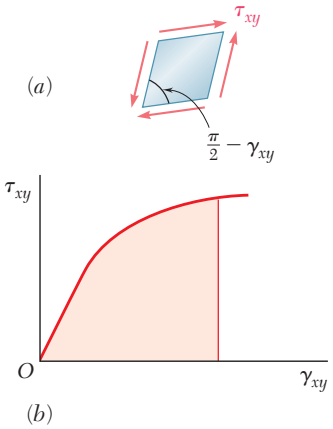


Fig. 11.15 (*a*) Shearing strain corresponding to τ_{xy}. (*b*) Strain-energy density u is the area under the stress-strain diagram.

For values of τ_{xy} within the proportional limit, $\tau_{xy} = G\gamma_{xy}$, where G is the modulus of rigidity of the material. Substituting for τ_{xy} into Eq. (11.16) and integrating gives

$$u = \frac{1}{2}G\gamma_{xy}^2 = \frac{1}{2}\tau_{xy}\gamma_{xy} = \frac{\tau_{xy}^2}{2G} \tag{11.17}$$

The value of the strain energy U of a body subjected to plane shearing stresses can be obtained by recalling from Sec. 11.2A that

$$u = \frac{dU}{dV} \tag{11.9}$$

Substituting for u from Eq. (11.17) into Eq. (11.9) and integrating both members gives

$$U = \int \frac{\tau_{xy}^2}{2G}\,dV \tag{11.18}$$

This equation defines the elastic strain energy associated with the shear deformations of the body. Like the similar expression in Sec. 11.2A for uniaxial normal stresses, it is only valid for elastic deformations.

Strain Energy in Torsion. Consider a shaft *BC* of non-uniform circular cross section with a length of L subjected to one or several twisting couples. Using the polar moment of inertia J of the cross section located

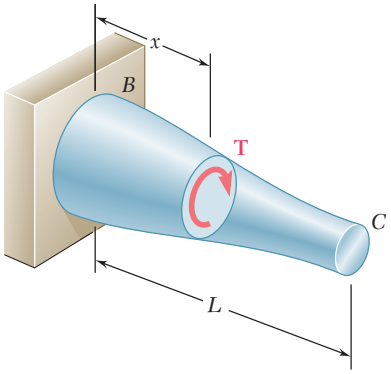


Fig. 11.16 Shaft subject to torque.

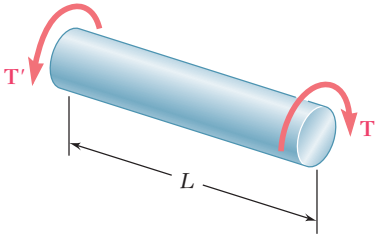


Fig. 11.17 Prismatic shaft subject to torque.

a distance x from B (Fig. 11.16) and the internal torque T, recall that the shearing stresses are $\tau_{xy} = T\rho/J$. Substituting for τ_{xy} into Eq. (11.18),

$$U = \int \frac{\tau_{xy}^2}{2G}\,dV = \int \frac{T^2\rho^2}{2GJ^2}\,dV$$

Set $dV = dA\,dx$, where dA is the element cross-sectional area, and observe that $T^2/2GJ^2$ is a function of x alone to obtain

$$U = \int_0^L \frac{T^2}{2GJ^2}\left(\int \rho^2\,dA\right)dx$$

Recall that the integral within the parentheses represents the polar moment of inertia J of the cross section, giving

$$U = \int_0^L \frac{T^2}{2GJ}\,dx \tag{11.19}$$

For a shaft of uniform cross section subjected at its ends to equal and opposite couples of magnitude T (Fig. 11.17), Eq. (11.19) yields

$$U = \frac{T^2L}{2GJ} \tag{11.20}$$

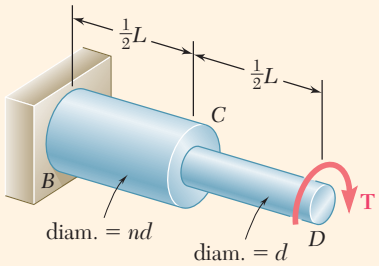


Fig. 11.18 Stepped shaft subject to torque T.

Concept Application 11.4

A circular shaft consists of two portions BC and CD of the same material and length, but of different cross sections (Fig. 11.18). Determine the strain energy of the shaft when it is subjected to a twisting couple **T** at end D. Express the results in terms of T, L, G, the polar moment of inertia J of the smaller cross section, and the ratio n of the two diameters.

Use Eq. (11.20) to compute the strain energy of each of the two portions of shaft, and add the expressions obtained. Note that the polar moment of inertia of portion BC is equal to n^4J giving

$$U_n = \frac{T^2(\frac{1}{2}L)}{2GJ} + \frac{T^2(\frac{1}{2}L)}{2G(n^4J)} = \frac{T^2L}{4GJ}\left(1 + \frac{1}{n^4}\right)$$

or

$$U_n = \frac{1 + n^4}{2n^4}\frac{T^2L}{2GJ} \tag{1}$$

For $n = 1$,

$$U_1 = \frac{T^2L}{2GJ}$$

which is the expression given in Eq. (11.20) for a shaft of length L and uniform cross section. Note that, for $n > 1$, $U_n < U_1$. For example, when $n = 2$, $U_2 = (\frac{17}{32})U_1$. Since the maximum shearing stress occurs in segment CD of the shaft and is proportional to the torque T, increasing the diameter of segment BC results in a *decrease* of the overall energy-absorbing capacity of the shaft.

Strain Energy under Transverse Loading. In Sec. 11.2A an equation for the strain energy of a beam subjected to a transverse loading was obtained. However, in that expression, only the effect of the normal stresses due to bending is taken into account and the effect of the shearing stresses is neglected. In Concept Application 11.5, both types of stresses will be taken into account.

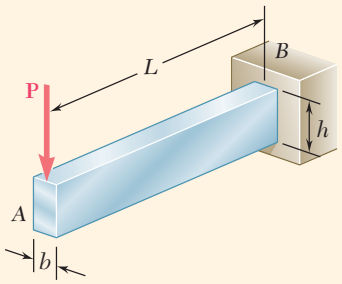


Fig. 11.19 Rectangular cantilever beam with load *P*.

Concept Application 11.5

Determine the strain energy of the rectangular cantilever beam *AB* (Fig. 11.19), taking into account the effect of both normal and shearing stresses.

Recall from Concept Application 11.3 that the strain energy due to the normal stresses σ_x is

$$U_\sigma = \frac{P^2L^3}{6EI}$$

To determine the strain energy U_τ due to the shearing stresses τ_{xyw}, recall Eq. (6.9) and find that, for a beam with a rectangular cross section of width b and depth h,

$$\tau_{xy} = \frac{3}{2}\frac{V}{A}\left(1 - \frac{y^2}{c^2}\right) = \frac{3}{2}\frac{P}{bh}\left(1 - \frac{y^2}{c^2}\right)$$

Substituting for τ_{xy} into Eq. (11.18),

$$U_\tau = \frac{1}{2G}\left(\frac{3}{2}\frac{P}{bh}\right)^2 \int\left(1 - \frac{y^2}{c^2}\right)^2 dV$$

or setting $dV = b\,dy\,dx$, and after reductions,

$$U_\tau = \frac{9P^2}{8Gbh^2}\int_{-c}^{c}\left(1 - 2\frac{y^2}{c^2} + \frac{y^4}{c^4}\right)dy\int_0^L dx$$

Performing integrations and recalling that $c = h/2$,

$$U_\tau = \frac{9P^2L}{8Gbh^2}\left[y - \frac{2}{3}\frac{y^3}{c^2} + \frac{1}{5}\frac{y^5}{c^4}\right]_{-c}^{+c} = \frac{3P^2L}{5Gbh} = \frac{3P^2L}{5GA}$$

The total strain energy of the beam is

$$U = U_\sigma + U_\tau = \frac{P^2L^3}{6EI} + \frac{3P^2L}{5GA}$$

or with $I/A = h^2/12$ and factoring the expression for U_σ,

$$U = \frac{P^2L^3}{6EI}\left(1 + \frac{3Eh^2}{10GL^2}\right) = U_\sigma\left(1 + \frac{3Eh^2}{10GL^2}\right) \qquad \textbf{(1)}$$

Recall from Sec. 2.7 that $G \geq E/3$. Considering the parenthesis, this equation is less than $1 + 0.9(h/L)^2$ and the relative error is less than $0.9(h/L)^2$ when the effect of shear is neglected. For a beam with a ratio h/L less than $\frac{1}{10}$, the percentage error is less than 0.9%. It is therefore customary in engineering practice to neglect the effect of shear to compute the strain energy of shallow beams.

11.3 STRAIN ENERGY FOR A GENERAL STATE OF STRESS

In the preceding sections, we determined the strain energy of a body in a state of uniaxial stress (Sec. 11.2A) and in a state of plane shearing stress (Sec. 11.2B). In a body in a general state of stress characterized by the six stress components σ_x, σ_y, σ_z, τ_{xy}, τ_{yz}, and τ_{zx} (Fig. 2.35), the strain-energy density is obtained by adding the expressions given in Eqs. (11.10) and (11.16), as well as the four other expressions obtained through a permutation of the subscripts.

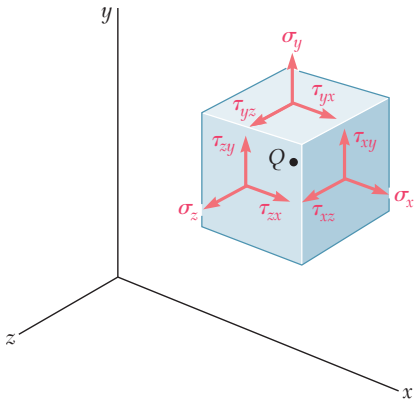


Fig. 2.35 (repeated) Positive stress component at point *Q* for a general state of stress.

In the elastic deformation of an isotropic body, each of the six stress-strain relationships involved is linear, and the strain-energy density is

$$u = \tfrac{1}{2}(\sigma_x\epsilon_x + \sigma_y\epsilon_y + \sigma_z\epsilon_z + \tau_{xy}\gamma_{xy} + \tau_{yz}\gamma_{yz} + \tau_{zx}\gamma_{zx}) \qquad \textbf{(11.21)}$$

Recalling Eq. (2.29) and substituting for the strain components into Eq. (11.21), the most general state of stress at a given point of an elastic isotropic body is

$$u = \frac{1}{2E}[\sigma_x^2 + \sigma_y^2 + \sigma_z^2 - 2\nu(\sigma_x\sigma_y + \sigma_y\sigma_z + \sigma_z\sigma_x)] + \frac{1}{2G}(\tau_{xy}^2 + \tau_{yz}^2 + \tau_{zx}^2) \qquad \textbf{(11.22)}$$

If the principal axes at the given point are used as coordinate axes, the shearing stresses become zero and Eq. (11.22) reduces to

$$u = \frac{1}{2E}[\sigma_a^2 + \sigma_b^2 + \sigma_c^2 - 2\nu(\sigma_a\sigma_b + \sigma_b\sigma_c + \sigma_c\sigma_a)] \qquad \textbf{(11.23)}$$

where σ_a, σ_b, and σ_c are the principal stresses at the given point.

Now recall from Sec. 7.5A that one criterion used to predict whether a given state of stress causes a ductile material to yield is the maximum-distortion-energy criterion, which is based on the energy per unit volume associated with the distortion (or change in shape) of that material.

Separating the strain-energy density u at a given point into two parts, u_v associated with a change in volume of the material at that point and u_d associated with a distortion of the material at the same point,

$$u = u_v + u_d \tag{11.24}$$

In order to determine u_v and u_d, we introduce the *average value* $\overline{\sigma}$ of the principal stresses at the point considered as

$$\overline{\sigma} = \frac{\sigma_a + \sigma_b + \sigma_c}{3} \tag{11.25}$$

and set

$$\sigma_a = \overline{\sigma} + \sigma'_a \qquad \sigma_b = \overline{\sigma} + \sigma'_b \qquad \sigma_c = \overline{\sigma} + \sigma'_c \tag{11.26}$$

Thus, the given state of stress (Fig. 11.20*a*) can be obtained by superposing the states of stress shown in Fig. 11.20*b* and *c*. The state of stress described in Fig. 11.20*b* tends to change the volume of the element but not its shape, since all of the faces of the element are subjected to the same stress $\overline{\sigma}$. On the other hand, it follows from Eqs. (11.25) and (11.26) that

$$\sigma'_a + \sigma'_b + \sigma'_c = 0 \tag{11.27}$$

This indicates that some of the stresses shown in Fig. 11.20*c* are tensile and others compressive. Thus, this state of stress tends to change the shape of the element. However, it does not tend to change its volume. Recall from Eq. (2.22) that the dilatation e (i.e., the change in volume per unit volume) caused by this state of stress is

$$e = \frac{1 - 2\nu}{E}(\sigma'_a + \sigma'_b + \sigma'_c)$$

or $e = 0$ in view of Eq. (11.27). Thus, the portion u_v of the strain-energy density must be associated with the state of stress shown in Fig. 11.20*b*, while the portion u_d must be associated with the state of stress shown in Fig. 11.20*c*.

The portion u_v of the strain-energy density corresponding to a change in volume of the element can be obtained by substituting $\overline{\sigma}$ for each of the principal stresses in Eq. (11.23). Thus,

$$u_v = \frac{1}{2E}[3\overline{\sigma}^2 - 2\nu(3\overline{\sigma}^2)] = \frac{3(1 - 2\nu)}{2E}\overline{\sigma}^2$$

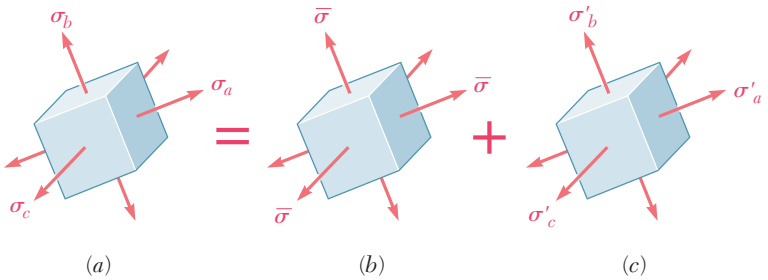


Fig. 11.20 (*a*) Element subject to multiaxial state of stress expressed as the superposition of (*b*) stresses tending to cause volume change, (*c*) stresses tending to cause distortion.

or recalling Eq. (11.25),

$$u_v = \frac{1 - 2\nu}{6E}(\sigma_a + \sigma_b + \sigma_c)^2 \tag{11.28}$$

The portion of the strain-energy density corresponding to the distortion of the element is found by solving Eq. (11.24) for u_d and substituting for u and u_v from Eqs. (11.23) and (11.28), respectively.

$$u_d = u - u_v = \frac{1}{6E}[3(\sigma_a^2 + \sigma_b^2 + \sigma_c^2) - 6\nu(\sigma_a\sigma_b + \sigma_b\sigma_c + \sigma_c\sigma_a) - (1 - 2\nu)(\sigma_a + \sigma_b + \sigma_c)^2]$$

Expanding the square and rearranging terms,

$$u_d = \frac{1 + \nu}{6E}[(\sigma_a^2 - 2\sigma_a\sigma_b + \sigma_b^2) + (\sigma_b^2 - 2\sigma_b\sigma_c + \sigma_c^2) + (\sigma_c^2 - 2\sigma_c\sigma_a + \sigma_a^2)]$$

Noting that each of the parentheses inside the bracket is a perfect square, and recalling from Eq. (2.34) that the coefficient in front of the bracket is equal to $1/12G$, the portion u_d of the strain-energy density (i.e., the distortion energy per unit volume) is

$$u_d = \frac{1}{12G}[(\sigma_a - \sigma_b)^2 + (\sigma_b - \sigma_c)^2 + (\sigma_c - \sigma_a)^2] \tag{11.29}$$

In *plane stress*, assuming that the c axis is perpendicular to the plane of stress, $\sigma_c = 0$ and Eq. (11.29) reduces to

$$u_d = \frac{1}{6G}(\sigma_a^2 - \sigma_a\sigma_b + \sigma_b^2) \tag{11.30}$$

Considering a tensile-test specimen, at yield $\sigma_a = \sigma_Y$, $\sigma_b = 0$, and $(u_d)_Y = \sigma_Y^2/6G$. The maximum-distortion-energy criterion for plane stress indicates that a given state of stress is safe when $u_d < (u_d)_Y$, or by substituting for u_d from Eq. (11.30), it is safe as long as

$$\sigma_a^2 - \sigma_a\sigma_b + \sigma_b^2 < \sigma_Y^2 \tag{7.26}$$

which is the condition in Sec. 7.5A and represented graphically by the ellipse of Fig. 7.32. For a general state of stress, Eq. (11.29) obtained for u_d should be used. The maximum-distortion-energy criterion is then found by the condition:

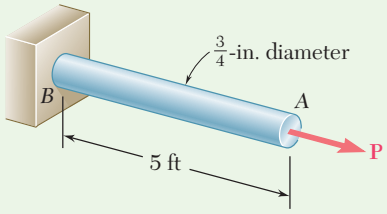
$$(\sigma_a - \sigma_b)^2 + (\sigma_b - \sigma_c)^2 + (\sigma_c - \sigma_a)^2 < 2\sigma_Y^2 \tag{11.31}$$

which indicates that a given state of stress is safe if the point of coordinates σ_a, σ_b, σ_c is located within the surface defined by

$$(\sigma_a - \sigma_b)^2 + (\sigma_b - \sigma_c)^2 + (\sigma_c - \sigma_a)^2 = 2\sigma_Y^2 \tag{11.32}$$

This surface is a circular cylinder with a radius of $\sqrt{2/3}\,\sigma_Y$ and an axis of symmetry forming equal angles with the three principal axes of stress.

Sample Problem 11.1



During a routine manufacturing operation, rod AB must acquire an elastic strain energy of 120 in·lb. Using $E = 29 \times 10^6$ psi, determine the required yield strength of the steel if the factor of safety is 5 with respect to permanent deformation.

STRATEGY: Use the specified factor of safety to determine the required strain-energy density, and then use Eq. (11.8) to determine the yield strength.

MODELING and ANALYSIS:

Factor of Safety. Since a factor of safety of 5 is required, the rod should be designed for a strain energy of

$$U = 5(120 \text{ in·lb}) = 600 \text{ in·lb}$$

Strain-Energy Density. The volume of the rod is

$$V = AL = \frac{\pi}{4}(0.75 \text{ in.})^2(60 \text{ in.}) = 26.5 \text{ in}^3$$

Since the rod has a uniform cross section, the required strain-energy density is

$$u = \frac{U}{V} = \frac{600 \text{ in·lb}}{26.5 \text{ in}^3} = 22.6 \text{ in·lb/in}^3$$

Yield Strength. Recall that the modulus of resilience is equal to the strain-energy density when the maximum stress is equal to σ_Y (Fig. 1). Using Eq. (11.8),

$$u = \frac{\sigma_Y^2}{2E}$$

$$22.6 \text{ in·lb/in}^3 = \frac{\sigma_Y^2}{2(29 \times 10^6 \text{ psi})} \qquad \sigma_Y = 36.2 \text{ ksi}$$

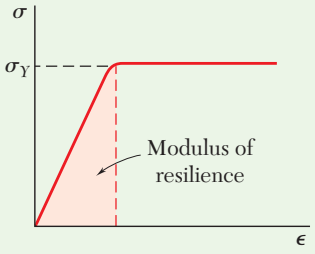
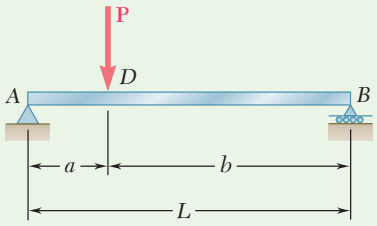


Fig. 1 The modulus of resilience equals the strain-energy density up to yield.

REFLECT and THINK: Since energy loads are not linearly related to the stresses they produce, factors of safety associated with energy loads should be applied to the energy loads and not to the stresses.



Sample Problem 11.2

(*a*) Taking into account only the effect of normal stresses due to bending, determine the strain energy of the prismatic beam *AB* for the loading shown. (*b*) Evaluate the strain energy, knowing that the beam is a W10 × 45, $P = 40$ kips, $L = 12$ ft, $a = 3$ ft, $b = 9$ ft, and $E = 29 \times 10^6$ psi.

STRATEGY: Use a free-body diagram to determine the reactions, and write equations for the moment as a function of the coordinate along the beam. The strain energy required for part *a* is then determined from Eq. (11.15). Use this with the data to numerically evaluate the strain energy for part *b*.

MODELING:

Bending Moment. Using the free-body diagram of the entire beam (Fig. 1), determine the reactions

$$\mathbf{R}_A = \frac{Pb}{L}\uparrow \qquad \mathbf{R}_B = \frac{Pa}{L}\uparrow$$

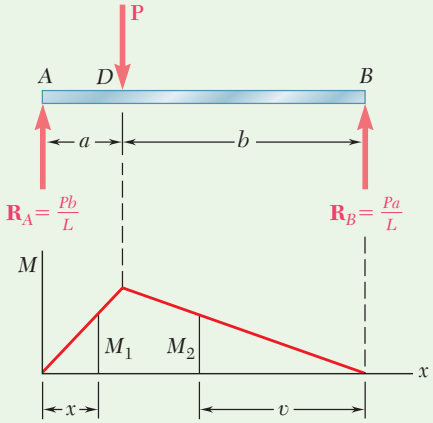


Fig. 1 Free-body and bending-moment diagrams.

Using the free-body diagram in Fig. 2, the bending moment for portion *AD* of the beam is

$$M_1 = \frac{Pb}{L}x$$

From *A* to *D*:

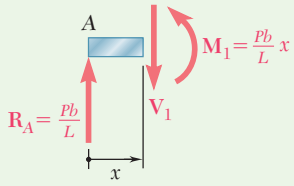


Fig. 2 Free-body diagram, taking a section within portion *AD*.

(continued)

Similarly using the free-body diagram in Fig. 3, the bending moment for portion DB at a distance v from end B is

$$M_2 = \frac{Pa}{L} v$$

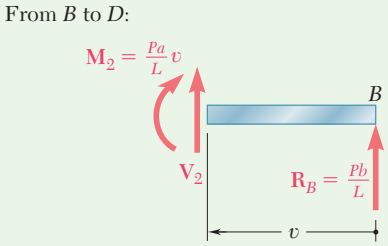


Fig. 3 Free-body diagram, taking a section within portion *DB*.

ANALYSIS:

a. Strain Energy. Since strain energy is a scalar quantity, add the strain energy of segment AD to that of DB to obtain the total strain energy of the beam. Using Eq. (11.15),

$$U = U_{AD} + U_{DB}$$

$$= \int_0^a \frac{M_1^2}{2EI}\,dx + \int_0^b \frac{M_2^2}{2EI}\,dv$$

$$= \frac{1}{2EI}\int_0^a \left(\frac{Pb}{L}x\right)^2 dx + \frac{1}{2EI}\int_0^b \left(\frac{Pa}{L}v\right)^2 dv$$

$$= \frac{1}{2EI}\frac{P^2}{L^2}\left(\frac{b^2a^3}{3} + \frac{a^2b^3}{3}\right) = \frac{P^2a^2b^2}{6EIL^2}(a + b)$$

or since $(a + b) = L$,

$$U = \frac{P^2a^2b^2}{6EIL}$$

b. Evaluation of the Strain Energy. The moment of inertia of a W10 × 45 rolled-steel shape is obtained from Appendix C, and the given data is restated using units of kips and inches.

$P = 40$ kips $\qquad L = 12$ ft $= 144$ in.

$a = 3$ ft $= 36$ in. $\qquad b = 9$ ft $= 108$ in.

$E = 29 \times 10^6$ psi $= 29 \times 10^3$ ksi $\qquad I = 248$ in^4

Substituting into the expression for U,

$$U = \frac{(40 \text{ kips})^2(36 \text{ in.})^2(108 \text{ in.})^2}{6(29 \times 10^3 \text{ ksi})(248 \text{ in}^4)(144 \text{ in.})} \qquad U = 3.89 \text{ in} \cdot \text{kips}$$

Problems

11.1 Determine the modulus of resilience for each of the following grades of structural steel:

(*a*) ASTM A709 Grade 50: $\sigma_Y = 50$ ksi
(*b*) ASTM A913 Grade 65: $\sigma_Y = 65$ ksi
(*c*) ASTM A709 Grade 100: $\sigma_Y = 100$ ksi

11.2 Determine the modulus of resilience for each of the following aluminum alloys:

(*a*) 1100-H14: $E = 70$ GPa: $\sigma_Y = 55$ MPa
(*b*) 2014-T6: $E = 72$ GPa: $\sigma_Y = 220$ MPa
(*c*) 6061-T6: $E = 69$ GPa: $\sigma_Y = 150$ MPa

11.3 Determine the modulus of resilience for each of the following metals:

(*a*) Stainless steel
AISI 302 (annealed): $E = 190$ GPa $\sigma_Y = 260$ MPa
(*b*) Stainless steel
AISI 302 (cold-rolled): $E = 190$ GPa $\sigma_Y = 520$ MPa
(*c*) Malleable cast iron: $E = 165$ GPa $\sigma_Y = 230$ MPa

11.4 Determine the modulus of resilience for each of the following alloys:

(*a*) Titanium: $E = 16.5 \times 10^6$ psi $\sigma_Y = 120$ ksi
(*b*) Magnesium: $E = 6.5 \times 10^6$ psi $\sigma_Y = 29$ ksi
(*c*) Cupronickel (annealed): $E = 20 \times 10^6$ psi $\sigma_Y = 16$ ksi

11.5 The stress-strain diagram shown has been drawn from data obtained during a tensile test of a specimen of structural steel. Using $E = 29 \times 10^6$ psi, determine (*a*) the modulus of resilience of the steel, (*b*) the modulus of toughness of the steel.

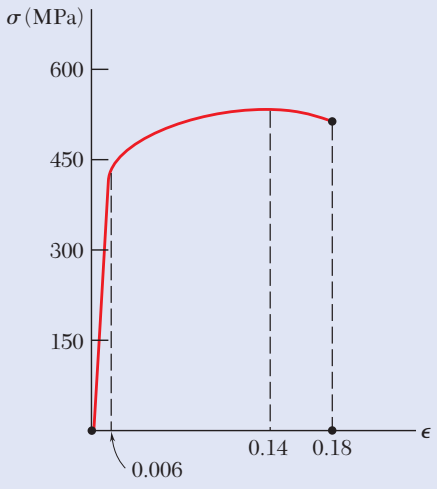


Fig. P11.6

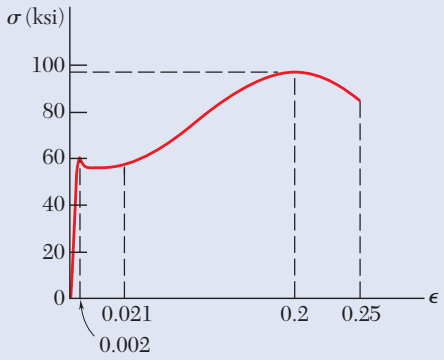


Fig. P11.5

11.6 The stress-strain diagram shown has been drawn from data obtained during a tensile test of an aluminum alloy. Using $E = 72$ GPa, determine (*a*) the modulus of resilience of the alloy, (*b*) the modulus of toughness of the alloy.

11.7 The load-deformation diagram shown has been drawn from data obtained during a tensile test of a specimen of an aluminum alloy. Knowing that the cross-sectional area of the specimen was 600 mm^2 and that the deformation was measured using a 400-mm gage length, determine by approximate means (*a*) the modulus of resilience of the alloy, (*b*) the modulus of toughness of the alloy.

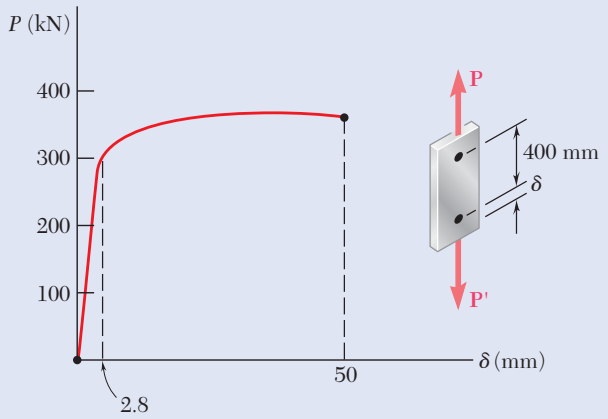


Fig. P11.7

11.8 The load-deformation diagram shown has been drawn from data obtained during a tensile test of a $\frac{5}{8}$-in.-diameter rod of structural steel. Knowing that the deformation was measured using an 18-in. gage length, determine by approximate means (*a*) the modulus of resilience of the steel, (*b*) the modulus of toughness of the steel.

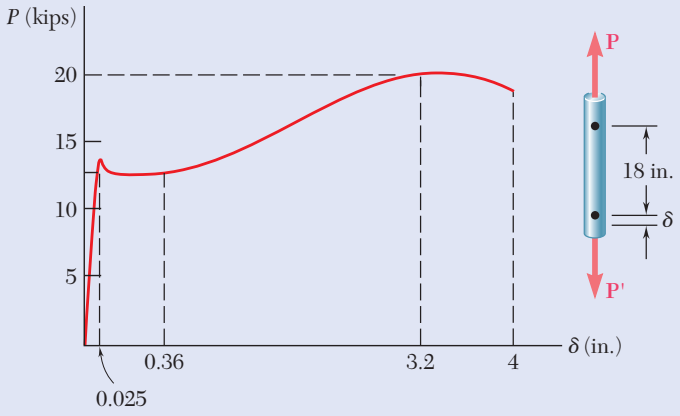


Fig. *P11.8*

11.9 Using $E = 29 \times 10^6$ psi, determine (*a*) the strain energy of the steel rod *ABC* when $P = 8$ kips, (*b*) the corresponding strain energy density in portions *AB* and *BC* of the rod.

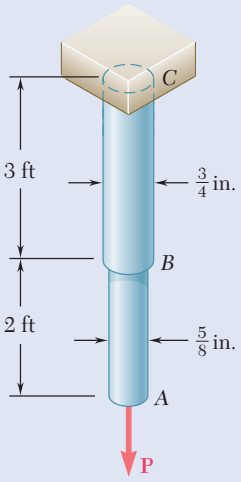


Fig. P11.9

11.10 Using $E = 200$ GPa, determine (a) the strain energy of the steel rod ABC when $P = 25$ kN, (b) the corresponding strain-energy density in portions AB and BC of the rod.

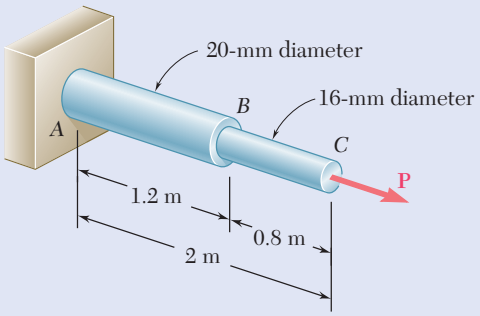


Fig. P11.10

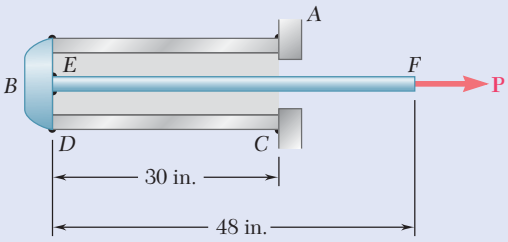


Fig. P11.11

11.11 A 30-in. length of aluminum pipe of cross-sectional area 1.85 in^2 is welded to a fixed support A and to a rigid cap B. The steel rod EF, of 0.75-in. diameter, is welded to cap B. Knowing that the modulus of elasticity is 29×10^6 psi for the steel and 10.6×10^6 psi for the aluminum, determine (a) the total strain energy of the system when P = 8 kips, (b) the corresponding strain-energy density of the pipe CD and in the rod EF.

11.12 A single 6-mm-diameter steel pin B is used to connect the steel strip DE to two aluminum strips, each of 20-mm width and 5-mm thickness. The modulus of elasticity is 200 GPa for the steel and 70 GPa for the aluminum. Knowing that for the pin at B the allowable shearing stress is $\tau_{all} = 85$ MPa, determine, for the loading shown, the maximum strain energy that can be acquired by the assembled strips.

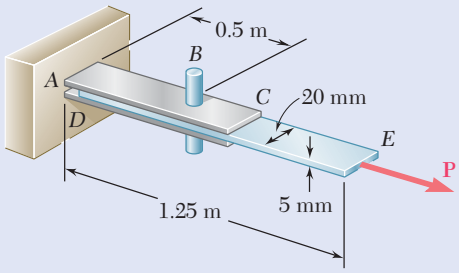


Fig. P11.12

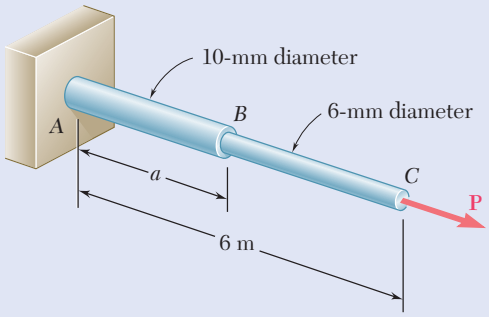


Fig. *P11.13*

11.13 Rods AB and BC are made of a steel for which the yield strength is $\sigma_Y = 300$ MPa and the modulus of elasticity is $E = 200$ GPa. Determine the maximum strain energy that can be acquired by the assembly without causing any permanent deformation when the length a of rod AB is (a) 2 m, (b) 4 m.

11.14 Rod BC is made of a steel for which the yield strength is $\sigma_Y = 300$ MPa and the modulus of elasticity is $E = 200$ GPa. Knowing that a strain energy of 10 J must be acquired by the rod when the axial load **P** is applied, determine the diameter of the rod for which the factor of safety with respect to permanent deformation is six.

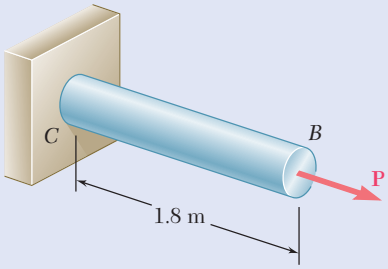


Fig. *P11.14*

11.15 The assembly ABC is made of a steel for which $E = 200$ GPa and $\sigma_Y = 320$ MPa. Knowing that a strain energy of 5 J must be acquired by the assembly as the axial load **P** is applied, determine the factor of safety with respect to permanent deformation when (*a*) $x = 300$ mm, (*b*) $x = 600$ mm.

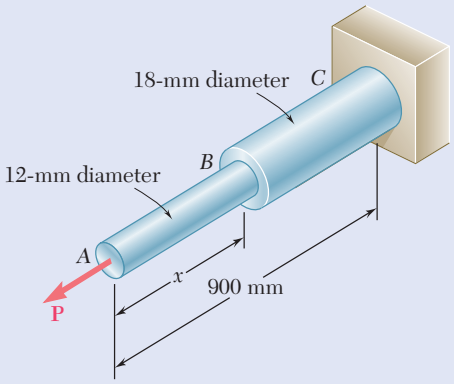


Fig. P11.15

11.16 Show by integration that the strain energy of the tapered rod AB is

$$U = \frac{1}{4}\frac{P^2 L}{EA_{\min}}$$

where $A_{\min}$ is the cross-sectional area at end B.

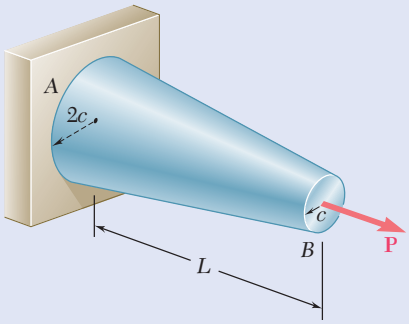


Fig. P11.16

11.17 Using $E = 10.6 \times 10^6$ psi, determine by approximate means the maximum strain energy that can be acquired by the aluminum rod shown if the allowable normal stress is $\sigma_{all} = 22$ ksi.

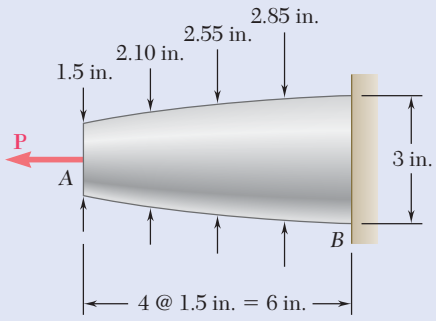


Fig. P11.17

11.18 through 11.21 In the truss shown, all members are made of the same material and have the uniform cross-sectional area indicated. Determine the strain energy of the truss when the load **P** is applied.

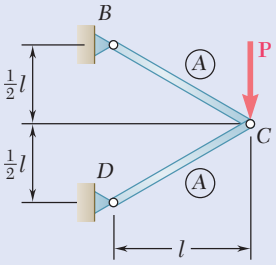


Fig. P11.18

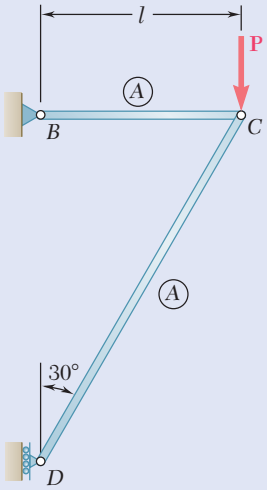


Fig. *P11.19*

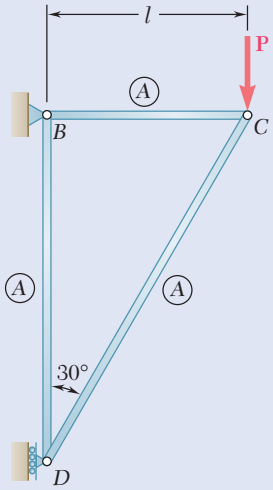


Fig. P11.20

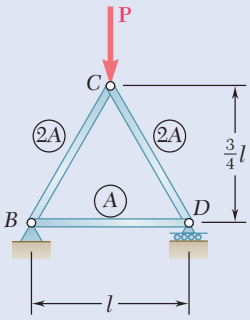


Fig. P11.21

11.22 Each member of the truss shown is made of aluminum and has the cross-sectional area shown. Using $E = 72$ GPa, determine the strain energy of the truss for the loading shown.

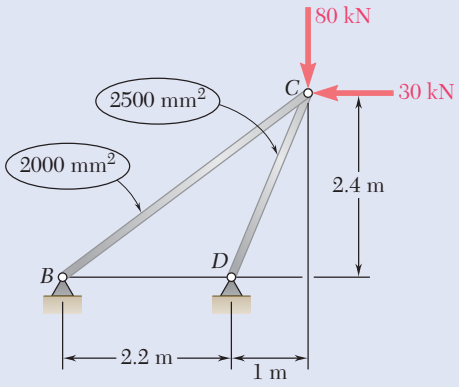


Fig. *P11.22*

11.23 Each member of the truss shown is made of aluminum and has the cross-sectional area shown. Using $E = 10.5 \times 10^6$ psi, determine the strain energy of the truss for the loading shown.

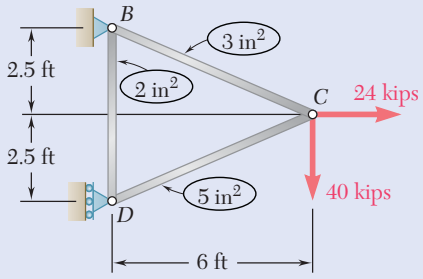


Fig. P11.23

11.24 through 11.27 Taking into account only the effect of normal stresses, determine the strain energy of the prismatic beam *AB* for the loading shown.

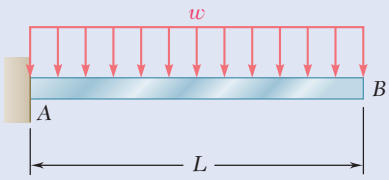


Fig. P11.24

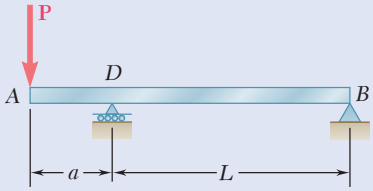


Fig. P11.25

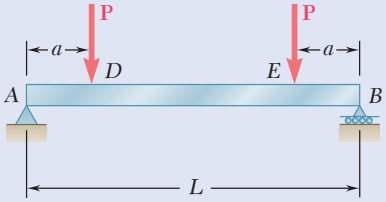


Fig. *P11.26*

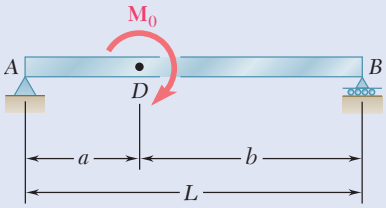


Fig. P11.27

11.28 and *11.29* Using $E = 29 \times 10^6$ psi, determine the strain energy due to bending for the steel beam and loading shown. (Neglect the effect of shearing stresses.)

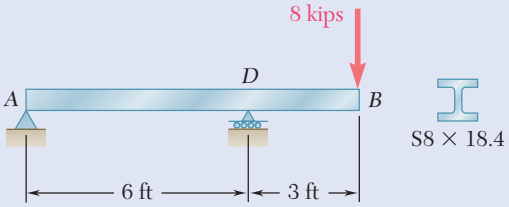


Fig. P11.28

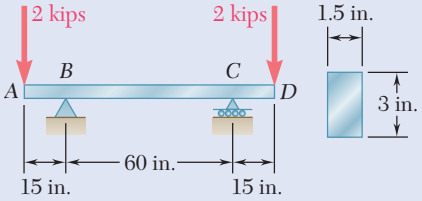


Fig. *P11.29*

11.30 and 11.31 Using $E = 200$ GPa, determine the strain energy due to bending for the steel beam and loading shown. (Neglect the effect of shearing stresses.)

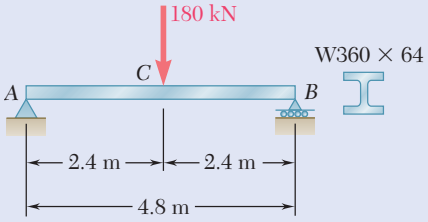


Fig. P11.30

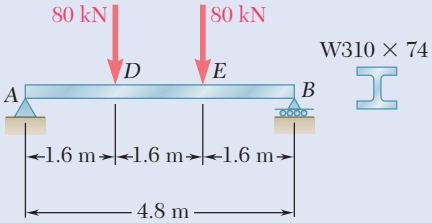


Fig. P11.31

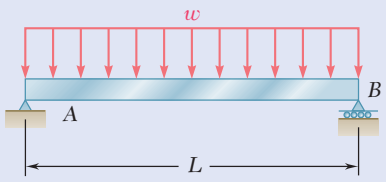


Fig. P11.32

11.32 Assuming that the prismatic beam AB has a rectangular cross section, show that for the given loading the maximum value of the strain-energy density in the beam is

$$u_{\max} = \frac{45}{8}\frac{U}{V}$$

where U is the strain energy of the beam and V is its volume.

11.33 In the assembly shown, torques $\mathbf{T}_A$ and $\mathbf{T}_B$ are exerted on disks A and B, respectively. Knowing that both shafts are solid and made of aluminum ($G = 73$ GPa), determine the total strain energy acquired by the assembly.

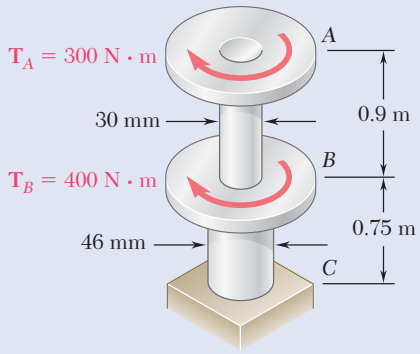


Fig. P11.33

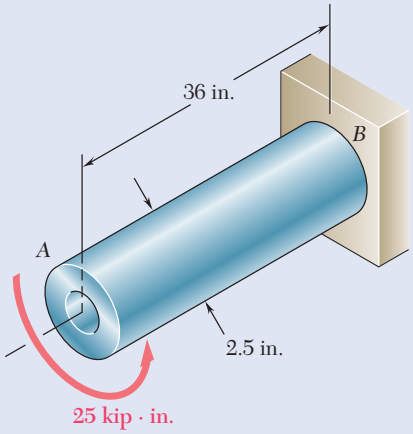


Fig. *P11.34*

11.34 The design specifications for the steel shaft AB require that the shaft acquire a strain energy of 400 in · lb as the 25-kip · in. torque is applied. Using $G = 11.2 \times 10^6$ psi, determine (*a*) the largest inner diameter of the shaft that can be used, (*b*) the corresponding maximum shearing stress in the shaft.

11.35 Show by integration that the strain energy in the tapered rod AB is

$$U = \frac{7}{48}\frac{T^2 L}{G J_{\min}}$$

where $J_{\min}$ is the polar moment of inertia of the rod at end B.

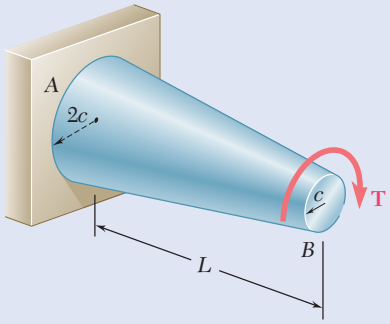


Fig. P11.35

11.36 The state of stress shown occurs in a machine component made of a brass for which $\sigma_Y = 160$ MPa. Using the maximum-distortion-energy criterion, determine the range of values of σ_z for which yield does not occur.

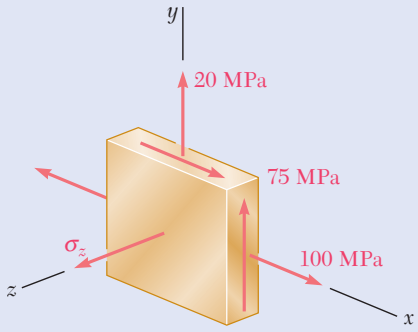


Fig. *P11.36* and P11.37

11.37 The state of stress shown occurs in a machine component made of a brass for which $\sigma_Y = 160$ MPa. Using the maximum-distortion-energy criterion, determine whether yield occurs when (*a*) $\sigma_z = +45$ MPa, (*b*) $\sigma_z = -45$ MPa.

11.38 The state of stress shown occurs in a machine component made of a grade of steel for which $\sigma_Y = 65$ ksi. Using the maximum-distortion-energy criterion, determine the range of values of σ_y for which the factor of safety associated with the yield strength is equal to or larger than 2.2.

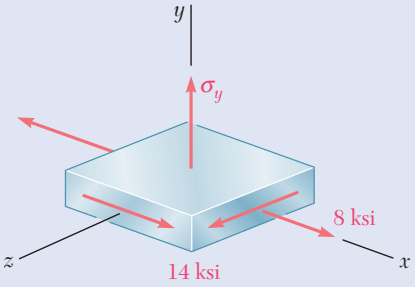


Fig. *P11.38* and P11.39

11.39 The state of stress shown occurs in a machine component made of a grade of steel for which $\sigma_Y = 65$ ksi. Using the maximum-distortion-energy criterion, determine the factor of safety associated with the yield strength when (*a*) $\sigma_y = +16$ ksi, (*b*) $\sigma_y = -16$ ksi.

11.40 Determine the strain energy of the prismatic beam *AB*, taking into account the effect of both normal and shearing stresses.

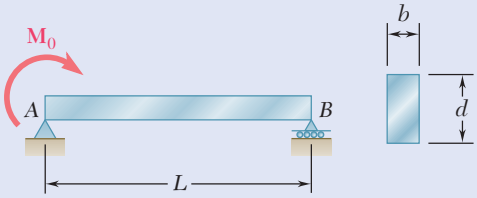


Fig. P11.40

***11.41** A vibration isolation support is made by bonding a rod *A*, of radius R_1, and a tube *B*, of inner radius R_2, to a hollow rubber cylinder. Denoting by *G* the modulus of rigidity of the rubber, determine the strain energy of the hollow rubber cylinder for the loading shown.

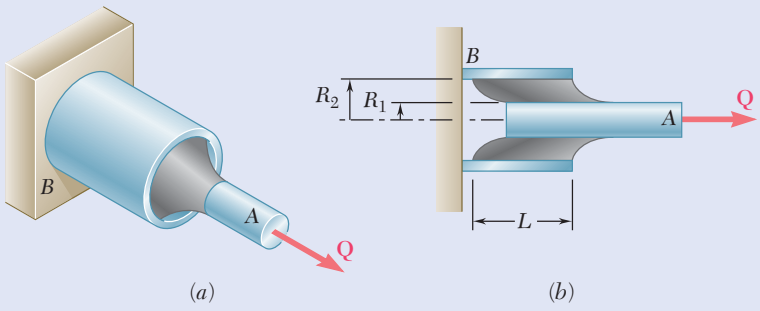


Fig. P11.41

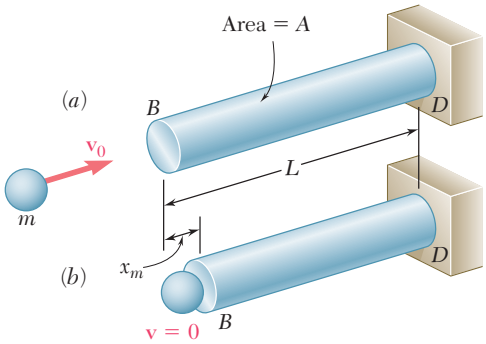


Fig. 11.21 Rod subject to impact loading.

11.4 IMPACT LOADS

11.4A Analysis

Consider a rod BD with an uniform cross section that is hit at end B by a body of mass m moving with a velocity $\mathbf{v}_0$ (Fig. 11.21*a*). As the rod deforms under the impact (Fig. 11.21*b*), stresses develop within the rod and reach a maximum value σ_m. After vibrating for a while, the rod comes to rest, and all stresses disappear. Such a sequence of events is called *impact loading* (Photo 11.2).

Several assumptions are made to determine the maximum value σ_m of the stress at a given point of a structure subjected to an impact load.

First, the kinetic energy $T = \frac{1}{2}mv_0^2$ of the striking body is assumed to be transferred entirely to the structure. Thus, the strain energy U_m corresponding to the maximum deformation x_m is

$$U_m = \tfrac{1}{2}mv_0^2 \tag{11.33}$$

This assumption leads to the following requirements.

1. No energy should be dissipated during the impact.
2. The striking body should not bounce off the structure and retain part of its energy. This, in turn, necessitates that the inertia of the structure be negligible, compared to the inertia of the striking body.



Photo 11.2 Steam alternately lifts a weight inside the pile driver and then propels it downward. This delivers a large impact load to the pile that is being driven into the ground.

In practice, neither of these requirements is satisfied, and only part of the kinetic energy of the striking body is actually transferred to the structure. Thus, assuming that all of the kinetic energy of the striking body is transferred to the structure leads to a conservative design.

The stress-strain diagram obtained from a static test of the material is also assumed to be valid under impact loads. So, for an elastic deformation of the structure, the maximum value of the strain energy is

$$U_m = \int \frac{\sigma_m^2}{2E}\,dV \tag{11.34}$$

For the uniform rod in Fig. 11.21, the maximum stress σ_m has the same value throughout the rod, and $U_m = \sigma_m^2\, V/2E$. Solving for σ_m and substituting for U_m from Eq. (11.33) gives

$$\sigma_m = \sqrt{\frac{2U_m E}{V}} = \sqrt{\frac{mv_0^2 E}{V}} \tag{11.35}$$

Note from this equation that selecting a rod with a large volume V and a low modulus of elasticity E results in a smaller value of the maximum stress σ_m for a given impact load.

In most problems, the distribution of stresses in the structure is not uniform, and Eq. (11.35) does not apply. It is then convenient to determine the static load $\mathbf{P}_m$ that produces the same strain energy as the impact load and compute from P_m the corresponding value σ_m of the largest stress in the structure.

Concept Application 11.6

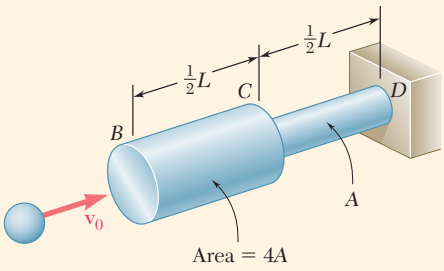


Fig. 11.22 Stepped rod impacted by a body of mass *m*.

A body of mass m moving with a velocity $\mathbf{v}_0$ hits the end B of the nonuniform rod BCD (Fig. 11.22). Knowing that the diameter of segment BC is twice the diameter of portion CD, determine the maximum value σ_m of the stress in the rod.

Making $n = 2$ in Eq. (1) from Concept Application 11.1, when rod BCD is subjected to a static load P_m, its strain energy is

$$U_m = \frac{5P_m^2 L}{16AE} \tag{1}$$

where A is the cross-sectional area of segment CD. Solving Eq. (1) for P_m, the static load that produces the same strain energy as the given impact load is

$$P_m = \sqrt{\frac{16}{5}\frac{U_m AE}{L}}$$

where U_m is given by Eq. (11.33). The largest stress occurs in segment CD. Dividing P_m by the area A of that portion,

$$\sigma_m = \frac{P_m}{A} = \sqrt{\frac{16}{5}\frac{U_m E}{AL}} \tag{2}$$

or substituting for U_m from Eq. (11.33) gives

$$\sigma_m = \sqrt{\frac{8}{5}\frac{mv_0^2 E}{AL}} = 1.265\sqrt{\frac{mv_0^2 E}{AL}}$$

Comparing this with the value obtained for σ_m in the uniform rod of Fig. 11.21 and making $V = AL$ in Eq. (11.35), note that the maximum stress in the rod of variable cross section is 26.5% larger than in the lighter uniform rod. Thus, as in our discussion of Concept Application 11.1, increasing the diameter of segment BC results in a *decrease* of the energy-absorbing capacity of the rod.

Concept Application 11.7

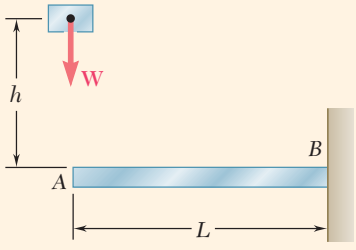


Fig. 11.23 Weight *W* falling on cantilever beam.

A block of weight W is dropped from a height h onto the free end of the cantilever beam AB (Fig. 11.23). Determine the maximum value of the stress in the beam.

As it falls through the distance h, the potential energy Wh of the block is transformed into kinetic energy. As a result of the impact, the kinetic energy is transformed into strain energy. Therefore,

$$U_m = Wh \tag{1}$$

(continued)

The total distance the block drops is actually $h + y_m$, where y_m is the maximum deflection of the end of the beam. Thus, a more accurate expression for U_m (see Sample Prob. 11.3) is

$$U_m = W(h + y_m) \tag{2}$$

However, when $h \gg y_m$, y_m may be neglected, and thus Eq. (1) applies.

Recalling the equation for the strain energy of the cantilever beam AB in Concept Application 11.3, which was based on neglecting the effect of shear,

$$U_m = \frac{P_m^2 L^3}{6EI}$$

Solving this equation for P_m, the static force that produces the same strain energy in the beam is

$$P_m = \sqrt{\frac{6U_m EI}{L^3}} \tag{3}$$

The maximum stress σ_m occurs at the fixed end B and is

$$\sigma_m = \frac{|M|c}{I} = \frac{P_m Lc}{I}$$

Substituting for P_m from Eq. (3),

$$\sigma_m = \sqrt{\frac{6U_m E}{L(I/c^2)}} \tag{4}$$

or recalling Eq. (1),

$$\sigma_m = \sqrt{\frac{6WhE}{L(I/c^2)}}$$

11.4B Design

Now compare the values from the preceding section for the maximum stress σ_m: (*a*) in the rod of uniform cross section of shown in Fig. 11.21, (*b*) in the rod of variable cross section of Concept Application 11.6, and (*c*) in the cantilever beam of Concept Application 11.7, assuming that the last has a circular cross section with a radius of c.

(*a*) Equation (11.35) shows that, if U_m is the amount of energy transferred to the rod as a result of the impact loading, the maximum stress in the rod of uniform cross section is

$$\sigma_m = \sqrt{\frac{2U_m E}{V}} \tag{11.36a}$$

where V is the volume of the rod.

(*b*) Considering the rod of Concept Application 11.6 and observing that the volume of the rod is

$$V = 4A(L/2) + A(L/2) = 5AL/2$$

substitute $AL = 2V/5$ into Eq. (2) of Concept Application 11.6 and write

$$\sigma_m = \sqrt{\frac{8U_m E}{V}} \tag{11.36b}$$

(*c*) Finally, recalling that $I = \frac{1}{4}\pi c^4$ for a beam of circular cross section,

$$L(I/c^2) = L(\tfrac{1}{4}\pi c^4/c^2) = \tfrac{1}{4}(\pi c^2 L) = \tfrac{1}{4}V$$

where V is the volume of the beam. Substituting into Eq. (4) of Concept Application 11.7, the maximum stress in the cantilever beam is

$$\sigma_m = \sqrt{\frac{24U_m E}{V}} \tag{11.36c}$$

In each case, the maximum stress σ_m is proportional to the square root of the modulus of elasticity of the material and inversely proportional to the square root of the volume of the member. Assuming that all three members have the same volume and are of the same material, we note that for a given value of the absorbed energy, the uniform rod experiences the lowest maximum stress and the cantilever beam the highest.

This is explained by the fact that the distribution of stresses is uniform in case *a*, and the strain energy is uniformly distributed throughout the rod. In case *b*, on the other hand, the stresses in segment *BC* of the rod are only 25% as large as the stresses in segment *CD*. This uneven distribution of the stresses and strain energy results in a maximum stress σ_m that is twice as large as the corresponding stress in the uniform rod. Finally, in case *c*, where the cantilever beam is subjected to a transverse impact load, the stresses vary linearly along the beam as well as through a transverse section. This uneven distribution of strain energy causes the maximum stress σ_m to be 3.46 times larger than in the same member loaded axially (as in case *a*).

The properties discussed in this section are quite general and can be observed in all types of structures subject to impact loads. Thus, a structural member designed to most effectively withstand an impact load should

1. Have a large volume.
2. Be made of a material with a low modulus of elasticity and a high yield strength.
3. Be shaped so that the stresses are distributed as evenly as possible throughout the member.

11.5 SINGLE LOADS

11.5A Energy Formulation

The concept of strain energy introduced at the beginning of this chapter considered the work done by an axial load **P** applied to the end of a rod of uniform cross section (Fig. 11.1). The strain energy of the rod for an elongation x_1 was defined as the work of the load **P** as it is slowly increased from 0 to P_1 corresponding to x_1. Thus,

$$\text{Strain energy} = U = \int_0^{x_1} P\,dx \tag{11.2}$$

For an elastic deformation, the work of load **P** and the strain energy of the rod is

$$U = \tfrac{1}{2}P_1x_1 \tag{11.3}$$

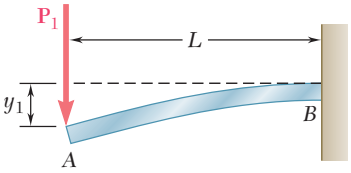


Fig. 11.24 Cantilever beam with load $\mathbf{P}_1$.

The strain energy of structural members under various load conditions was determined in Sec. 11.2 using the strain-energy density u at every point of the member and integrating u over the entire member.

When a structure or member is subjected to a *single concentrated load,* Eq. (11.3) can be used to evaluate its elastic strain energy, provided that the relationship between the load and the resulting deformation is known. For instance, the cantilever beam of Concept Application 11.3 (Fig. 11.24) has

$$U = \tfrac{1}{2}P_1y_1$$

and substituting the value from the table of *Beam Deflections and Slopes* of Appendix D for y_1 gives

$$U = \frac{1}{2}P_1\left(\frac{P_1L^3}{3EI}\right) = \frac{P_1^2L^3}{6EI} \tag{11.37}$$

A similar approach can be used to determine the strain energy of a structure or member subjected to a *single couple.* Recall that the elementary work of a couple of moment M is $M\,d\theta$, where $d\theta$ is a small angle. Since M and θ are linearly related, the elastic strain energy of a cantilever beam AB subjected to a single couple $\mathbf{M}_1$ at its end A (Fig. 11.25) is

$$U = \int_0^{\theta_1} M\,d\theta = \tfrac{1}{2}M_1\theta_1 \tag{11.38}$$

where θ_1 is the slope of the beam at A. Substituting the value obtained from Appendix D for θ_1 gives

$$U = \frac{1}{2}M_1\left(\frac{M_1L}{EI}\right) = \frac{M_1^2L}{2EI} \tag{11.39}$$

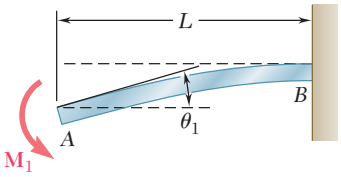


Fig. 11.25 Cantilever beam with couple $\mathbf{M}_1$.

Likewise, the elastic strain energy of a uniform circular shaft AB with a length of L subjected at its end B to a single torque $\mathbf{T}_1$ (Fig. 11.26) is

$$U = \int_0^{\phi_1} T\,d\phi = \tfrac{1}{2}T_1\phi_1 \qquad \textbf{(11.40)}$$

Substituting for the angle of twist ϕ_1 from Eq. (3.15) gives

$$U = \frac{1}{2}T_1\left(\frac{T_1L}{JG}\right) = \frac{T_1^2L}{2JG}$$

The method presented in this section may simplify the solution of many impact-loading problems. In Concept Application 11.8, the crash of an automobile into a barrier (Photo 11.3) is analyzed by using a simplified model consisting of a block and a simple beam.

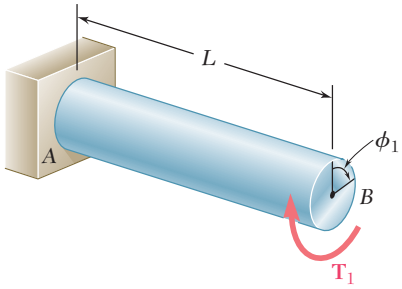
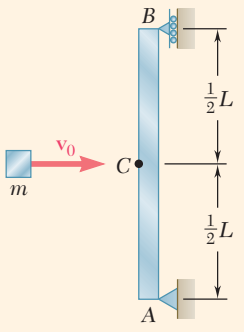


Fig. 11.26 Cantilevered shaft with torque $\mathbf{T}_1$.



Photo 11.3 As the automobile crashed into the barrier, considerable energy is dissipated as heat during the permanent deformation of the automobile and the barrier.



(*a*)

Fig. 11.27 (*a*) Simply supported beam having block propelled into its midpoint.

Concept Application 11.8

A block of mass m moving with a velocity $\mathbf{v}_0$ hits the prismatic member AB squarely at its midpoint C (Fig. 11.27*a*). Determine (*a*) the equivalent static load P_m, (*b*) the maximum stress σ_m in the member, and (*c*) the maximum deflection x_m at point C.

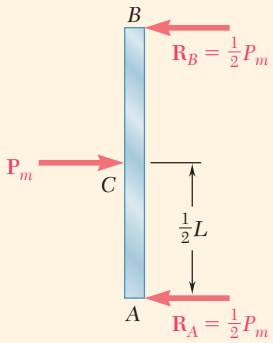
a. Equivalent Static Load. The maximum strain energy of the member is equal to the kinetic energy of the block before impact.

$$U_m = \tfrac{1}{2}mv_0^2 \qquad \textbf{(1)}$$

On the other hand, U_m can be given as the work of the equivalent horizontal static load as it is slowly applied at the midpoint C

$$U_m = \tfrac{1}{2}P_m x_m \qquad \textbf{(2)}$$

(continued)



(*b*)

Fig. 11.27 (continued) (*b*) Free-body diagram of beam.

where x_m is the deflection of C corresponding to the static load P_m. From the table of *Beam Deflections and Slopes* of Appendix D,

$$x_m = \frac{P_m L^3}{48EI} \tag{3}$$

Substituting for x_m from Eq. (3) into Eq. (2),

$$U_m = \frac{1}{2}\frac{P_m^2 L^3}{48EI}$$

Solving for P_m and recalling Eq. (1), the static load equivalent to the given impact loading is

$$P_m = \sqrt{\frac{96U_m EI}{L^3}} = \sqrt{\frac{48mv_0^2\, EI}{L^3}} \tag{4}$$

b. Maximum Stress. Drawing the free-body diagram of the member (Fig. 11.27*b*), the maximum value of the bending moment occurs at C and is $M_{\max} = P_m L/4$. The maximum stress occurs in a transverse section through C and is equal to

$$\sigma_m = \frac{M_{\max} c}{I} = \frac{P_m L c}{4I}$$

Substituting for P_m from Eq. (4),

$$\sigma_m = \sqrt{\frac{3mv_0^2\, EI}{L(I/c)^2}}$$

c. Maximum Deflection. Substituting into Eq. (3) the expression obtained for P_m in Eq. (4):

$$x_m = \frac{L^3}{48EI}\sqrt{\frac{48mv_0^2\, EI}{L^3}} = \sqrt{\frac{mv_0^2 L^3}{48EI}}$$

11.5B Deflections

The preceding section showed that, if the deflection x_1 of a structure or member under a single concentrated load $\mathbf{P}_1$ is known, the corresponding strain energy U is

$$U = \tfrac{1}{2}P_1 x_1 \tag{11.3}$$

A similar equation for the strain energy of a structural member under a single couple $\mathbf{M}_1$ is

$$U = \tfrac{1}{2}M_1\theta_1 \tag{11.38}$$

If the strain energy U of a structure or member subjected to a single concentrated load $\mathbf{P}_1$ or couple $\mathbf{M}_1$ is known, Eq. (11.3) or (11.38) can be used to determine the corresponding deflection x_1 or angle θ_1. In order to find the deflection under a single load applied to a structure with several components, rather than use one of the methods of Chap. 9, it is often easier to first compute the strain energy of the structure by integrating the

strain-energy density over its various parts, as was done in Sec. 11.2, and then use either Eq. (11.3) or Eq. (11.38) for the desired deflection. Similarly, the angle of twist ϕ_1 of a composite shaft can be obtained by integrating the strain-energy density over various parts of the shaft and solving Eq. (11.40) for ϕ_1.

The method in this section can be used *only if the given structure is subjected to a single concentrated load or couple.* The strain energy of a structure subjected to several loads *cannot* be determined by computing the work of each load as if applied independently to the structure (see Sec. 11.6). Even if it is possible to determine the strain energy of the structure in this manner, only one equation is available for the deflections corresponding to various loads. In Secs. 11.7 and 11.8, another method based on the concept of strain energy is developed that can be used to find the deflection or slope at a given point—even when that structure is subjected to several concentrated loads, distributed loads, or couples simultaneously.

Concept Application 11.9

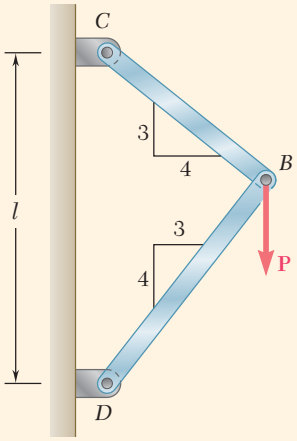


Fig. 11.28 Frame *CBD* with vertical load **P**.

A load **P** is supported at B by two uniform rods of the same cross-sectional area A (Fig. 11.28). Determine the vertical deflection of point B.

The strain energy of the system under the given load was determined in Concept Application 11.2. Equating U to the work of the load, write

$$U = 0.364\frac{P^2l}{AE} = \frac{1}{2}Py_B$$

and solving for the vertical deflection of B,

$$y_B = 0.728\frac{Pl}{AE}$$

Remark. Once the forces in the two rods have been obtained (see Concept Application 11.2), the deformations $\delta_{B/C}$ and $\delta_{B/D}$ can be obtained using the method in Chap. 2. However, determining the vertical deflection of point B from these deformations requires a careful geometric analysis of the various displacements. The strain-energy method used here makes such an analysis unnecessary.

Concept Application 11.10

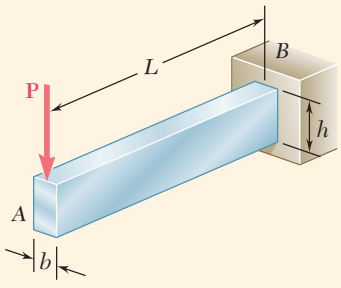


Fig. 11.29 Cantilevered rectangular beam with load **P**.

Determine the deflection of end A of the cantilever beam AB (Fig. 11.29), taking into account the effect of (*a*) the normal stresses only, (*b*) the normal and shearing stresses.

a. Effect of Normal Stresses. The work of the force **P** as it is slowly applied to A is

$$U = \tfrac{1}{2}Py_A$$

(continued)

Substituting for U the strain energy of the beam in Concept Application 11.3, where only the effect of the normal stresses was considered, write

$$\frac{P^2L^3}{6EI} = \frac{1}{2}Py_A$$

and solving for y_A,

$$y_A = \frac{PL^3}{3EI}$$

b. Effect of Normal and Shearing Stresses. Now substitute for U the expression for the total strain energy of the beam obtained in Concept Application 11.5, where the effects of both the normal and shearing stresses were taken into account. Thus,

$$\frac{P^2L^3}{6EI}\left(1 + \frac{3Eh^2}{10GL^2}\right) = \frac{1}{2}Py_A$$

and solving for y_A,

$$y_A = \frac{PL^3}{3EI}\left(1 + \frac{3Eh^2}{10GL^2}\right)$$

Note that the relative error when the effect of shear is neglected is the same as that obtained in Concept Application 11.5, (i.e., less than $0.9(h/L)^2$). This is less than 0.9% for a beam with a ratio h/L less than $\frac{1}{10}$.

Concept Application 11.11

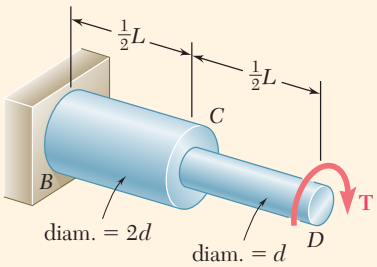


Fig. 11.30 Stepped shaft *BCD* with torque **T**.

A torque **T** is applied at the end D of shaft BCD (Fig. 11.30). Knowing that both portions of the shaft are of the same material and length, but that the diameter of BC is twice the diameter of CD, determine the angle of twist for the entire shaft.

In Concept Application 11.4, the strain energy of a similar shaft was determined by breaking the shaft into its component parts BC and CD. Making $n = 2$ in Eq. (1) of that Concept Application gives

$$U = \frac{17}{32}\frac{T^2L}{2GJ}$$

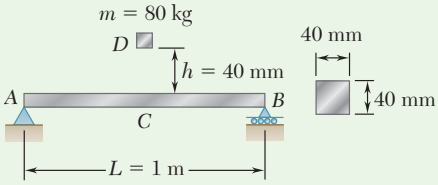
where G is the modulus of rigidity of the material and J is the polar moment of inertia of segment CD. Making U equal to the work of the torque as it is slowly applied to end D and recalling Eq. (11.40), write

$$\frac{17}{32}\frac{T^2L}{2GJ} = \frac{1}{2}T\phi_{D/B}$$

and solving for the angle of twist $\phi_{D/B}$,

$$\phi_{D/B} = \frac{17TL}{32GJ}$$

Sample Problem 11.3



The block D of mass m is released from rest and falls a distance h before it strikes the midpoint C of the aluminum beam AB. Using $E = 73$ GPa, determine (a) the maximum deflection of point C, (b) the maximum stress in the beam.

STRATEGY: Calculate the strain energy of the beam in terms of the deflection and equate this to the work done by the block. This then can be used with the data to solve part a. Using the relation between the applied load and deflection (Appendix D), obtain the equivalent static load and use this to get the normal stress due to bending.

MODELING:

Principle of Work and Energy. The block is released from rest (Fig. 1, position *1*). Note that in this position both the kinetic and strain energy are zero. In position *2* (Fig. 1), where the maximum deflection y_m occurs, the kinetic energy is also zero. Use to the table of *Beam Deflections and Slopes* in Appendix D to find the expression for y_m shown in Fig. 2. The strain energy of the beam in position *2* is

$$U_2 = \frac{1}{2}P_m y_m = \frac{1}{2}\frac{48EI}{L^3}y_m^2 \qquad U_2 = \frac{24EI}{L^3}y_m^2$$

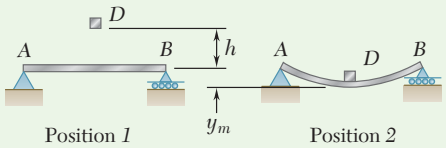


Fig. 1 Block released from rest (position *1*) and maximum deflection of beam (position *2*).

The work done by the weight **W** of the block is $W(h + y_m)$. Equating the strain energy of the beam to the work done by **W** gives

$$\frac{24EI}{L^3}y_m^2 = W(h + y_m) \qquad \textbf{(1)}$$

ANALYSIS:

a. Maximum Deflection of Point C. From the given data,

$$EI = (73 \times 10^9\ \text{Pa})\tfrac{1}{12}(0.04\ \text{m})^4 = 15.573 \times 10^3\ \text{N·m}^2$$

$$L = 1\ \text{m} \qquad h = 0.040\ \text{m} \qquad W = mg = (80\ \text{kg})(9.81\ \text{m/s}^2) = 784.8\ \text{N}$$

Substituting W into Eq. (1), we obtain a quadratic equation that can be solved for the deflection:

$$(373.8 \times 10^3)y_m^2 - 784.8y_m - 31.39 = 0 \qquad y_m = 10.27\ \text{mm} \blacktriangleleft$$

(continued)

From Appendix D

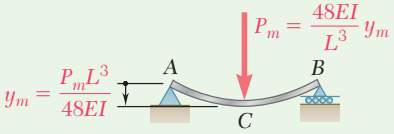


Fig. 2 Equivalent static force to cause deflection y_m.

b. Maximum Stress. The value of P_m (Fig. 2) is

$$P_m = \frac{48EI}{L^3} y_m = \frac{48(15.573 \times 10^3 \text{ N·m})}{(1 \text{ m})^3}(0.01027 \text{ m}) \qquad P_m = 7677 \text{ N}$$

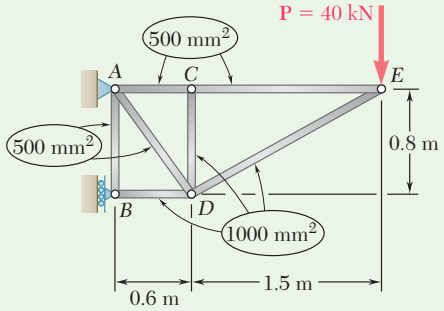
Recalling that $\sigma_m = M_{\max} c/I$ and $M_{\max} = \frac{1}{4} P_m L$, write

$$\sigma_m = \frac{(\frac{1}{4} P_m L)c}{I} = \frac{\frac{1}{4}(7677 \text{ N})(1 \text{ m})(0.020 \text{ m})}{\frac{1}{12}(0.040 \text{ m})^4} \qquad \sigma_m = 179.9 \text{ MPa}$$

REFLECT and THINK: An approximation for the work done by the weight of the block is obtained by omitting y_m from the expression for the work and from the right-hand member of Eq. (1), as was done in Concept Application 11.7. If this approximation is used here, $y_m = 9.16$ mm, and the error is 10.8%. However, if an 8-kg block is dropped from a height of 400 mm (producing the same value for Wh), omitting y_m from the right-hand member of Eq. (1) results in an error of only 1.2%.

Sample Problem 11.4

Members of the truss shown consist of sections of aluminum pipe with the cross-sectional areas indicated. Using $E = 73$ GPa, determine the vertical deflection of point E caused by load **P**.



STRATEGY: Draw a free-body diagram of the truss to determine the reactions and then use free-body diagrams at each joint to find the member forces. Eq. (11.14) can then be used to determine the strain energy in each member. Equate the total strain energy in the members to the work done by the load **P** to determine the vertical deflection at the load.

MODELING:

Axial Forces in Truss Members. The reactions are found by using the free-body diagram of the entire truss (Fig. 1*a*). Consider the equilibrium of joints E, C, D, and B in sequence (Fig. 1*b* through 1*e*). At each joint, determine the forces indicated by dashed lines. At joint B, the equation $\Sigma F_x = 0$ provides a check of the computations.

(continued)

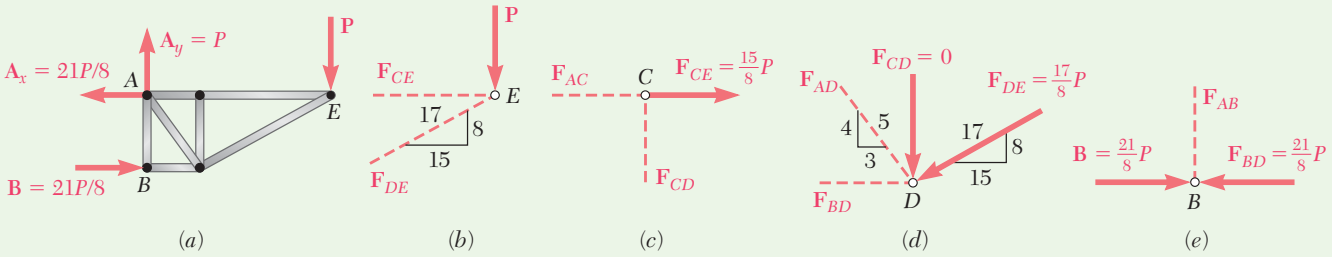


Fig. 1 (*a*) Free-body diagram of truss. (*b-e*) Force diagrams at joints.

$\Sigma F_y = 0$: $F_{DE} = -\frac{17}{8}P$ $\quad \Sigma F_x = 0$: $F_{AC} = +\frac{15}{8}P$ $\quad \Sigma F_y = 0$: $F_{AD} = +\frac{5}{4}P$ $\quad \Sigma F_y = 0$: $F_{AB} = 0$

$\Sigma F_x = 0$: $F_{CE} = +\frac{15}{8}P$ $\quad \Sigma F_y = 0$: $F_{CD} = 0$ $\quad \Sigma F_x = 0$: $F_{BD} = -\frac{21}{8}P$ $\quad \Sigma F_x = 0$: (Checks)

ANALYSIS:

Strain Energy. Noting that E is the same for all members, the strain energy of the truss is

$$U = \sum \frac{F_i^2 L_i}{2A_i E} = \frac{1}{2E} \sum \frac{F_i^2 L_i}{A_i} \tag{1}$$

where F_i is the force in a given member indicated in the following table and where the summation is extended over all members of the truss.

Member	F_i	L_i, m	A_i, m^2	$\frac{F_i^2 L_i}{A_i}$
AB	0	0.8	500×10^{-6}	0
AC	$+15P/8$	0.6	500×10^{-6}	$4\,219P^2$
AD	$+5P/4$	1.0	500×10^{-6}	$3\,125P^2$
BD	$-21P/8$	0.6	1000×10^{-6}	$4\,134P^2$
CD	0	0.8	1000×10^{-6}	0
CE	$+15P/8$	1.5	500×10^{-6}	$10\,547P^2$
DE	$-17P/8$	1.7	1000×10^{-6}	$7\,677P^2$

$$\sum \frac{F_i^2 L_i}{A_i} = 29\,700P^2$$

Returning to Eq. (1),

$$U = (1/2E)(29.7 \times 10^3 P^2).$$

Principle of Work-Energy. The work done by the load **P** as it is gradually applied is $\frac{1}{2} P y_E$. Equating the work done by **P** to the strain energy U and recalling that $E = 73$ GPa and $P = 40$ kN,

$$\frac{1}{2} P y_E = U \qquad \frac{1}{2} P y_E = \frac{1}{2E}(29.7 \times 10^3 P^2)$$

$$y_E = \frac{1}{E}(29.7 \times 10^3 P) = \frac{(29.7 \times 10^3)(40 \times 10^3)}{73 \times 10^9}$$

$$y_E = 16.27 \times 10^{-3}\,\text{m} \qquad y_E = 16.27\ \text{mm}\downarrow \quad \blacktriangleleft$$

Problems

11.42 A 5-kg collar D moves along the uniform rod AB and has a speed $v_0 = 6$ m/s when it strikes a small plate attached to end A of the rod. Using $E = 200$ GPa and knowing that the allowable stress in the rod is 250 MPa, determine the smallest diameter that can be used for the rod.

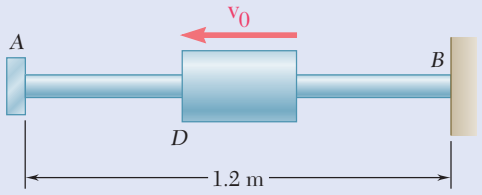


Fig. P11.42

11.43 The 18-lb cylindrical block E has a horizontal velocity v_0 when it strikes squarely the yoke BD that is attached to the $\frac{7}{8}$-in.-diameter rods AB and CD. Knowing that the rods are made of a steel for which $\sigma_Y = 50$ ksi and $E = 29 \times 10^6$ psi, determine the maximum allowable speed v_0 if the rods are not to be permanently deformed.

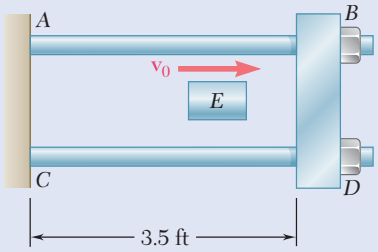


Fig. P11.43 and P11.44

11.44 The cylindrical block E has a speed $v_0 = 16$ ft/s when it strikes squarely the yoke BD that is attached to the $\frac{7}{8}$-in.-diameter rods AB and CD. Knowing that the rods are made of a steel for which $\sigma_Y = 50$ ksi and $E = 29 \times 10^6$ psi, determine the weight of block E for which the factor of safety is five with respect to permanent deformation of the rods.

11.45 The 35-kg collar D is released from rest in the position shown and is stopped by a plate attached at end C of the vertical rod ABC. Knowing that $E = 200$ GPa for both portions of the rod, determine the distance h for which the maximum stress in the rod is 250 MPa.

11.46 The 15-kg collar D is released from rest in the position shown and is stopped by a plate attached at end C of the vertical rod ABC. Knowing that $E = 200$ GPa for both portions of the rod, determine (*a*) the maximum deflection of end C, (*b*) the equivalent static load, (*c*) the maximum stress that occurs in the rod.

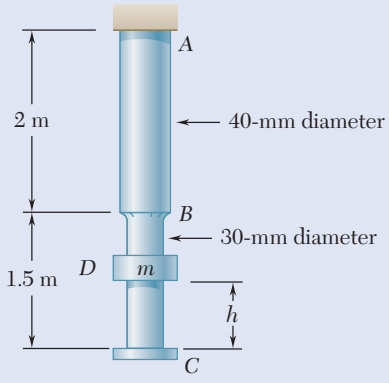


Fig. P11.45 and P11.46

11.47 The 48-kg collar G is released from rest in the position shown and is stopped by plate BDF that is attached to the 20-mm-diameter steel rod CD and to the 15-mm-diameter steel rods AB and EF. Knowing that for the grade of steel used $\sigma_{all} = 180$ MPa and $E = 200$ GPa, determine the largest allowable distance h.

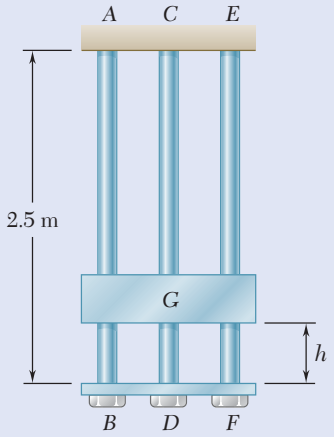


Fig. *P11.47*

11.48 A 25-lb block C moving horizontally with at velocity $\mathbf{v}_0$ hits the post AB squarely as shown. Using $E = 29 \times 10^6$ psi, determine the largest speed v_0 for which the maximum normal stress in the post does not exceed 18 ksi.

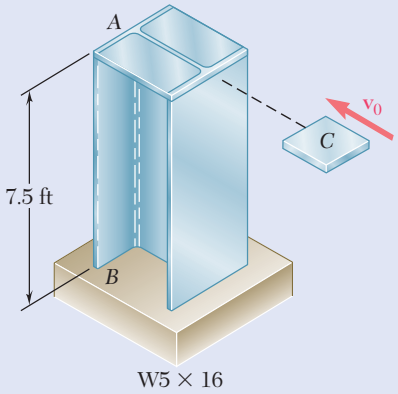


Fig. P11.48

11.49 Solve Prob. 11.48, assuming that the post AB has been rotated 90° about its longitudinal axis.

11.50 An aluminum tube having the cross section shown is struck squarely in its midsection by a 6-kg block moving horizontally with a speed of 2 m/s. Using $E = 70$ GPa, determine (a) the equivalent static load, (b) the maximum stress in the beam, (c) the maximum deflection at the midpoint C of the beam.

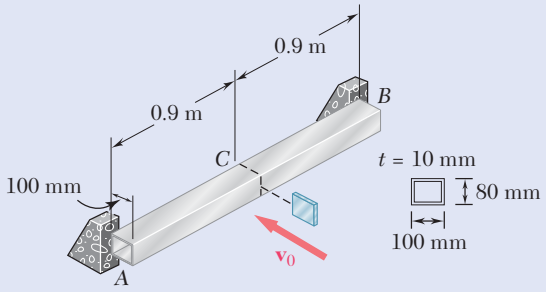


Fig. P11.50

11.51 Solve Prob. 11.50, assuming that the tube has been replaced by a solid aluminum bar with the same outside dimensions as the tube.

11.52 The 2-kg block D is dropped from the position shown onto the end of a 16-mm-diameter rod. Knowing that $E = 200$ GPa, determine (a) the maximum deflection of end A, (b) the maximum bending moment in the rod, (c) the maximum normal stress in the rod.

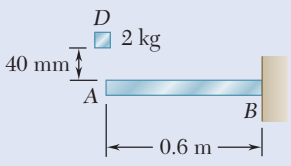


Fig. P11.52

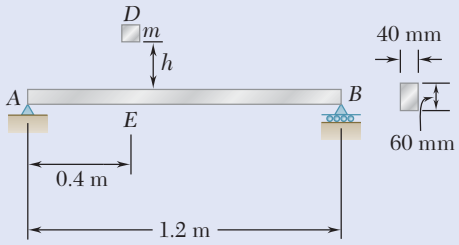


Fig. P11.53

11.53 The 10-kg block D is dropped from a height $h = 450$ mm onto the aluminum beam AB. Knowing that $E = 70$ GPa, determine (a) the maximum deflection of point E, (b) the maximum stress in the beam.

11.54 The 4-lb block D is dropped from the position shown onto the end of a $\frac{5}{8}$-in.-diameter rod. Knowing that $E = 29 \times 10^6$ psi, determine (a) the maximum deflection at point A, (b) the maximum bending moment in the rod, (c) the maximum normal stress in the rod.

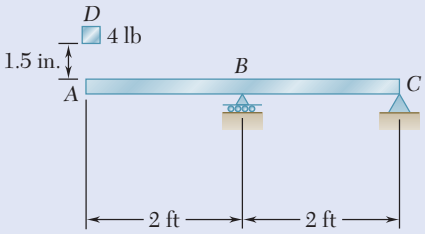


Fig. P11.54

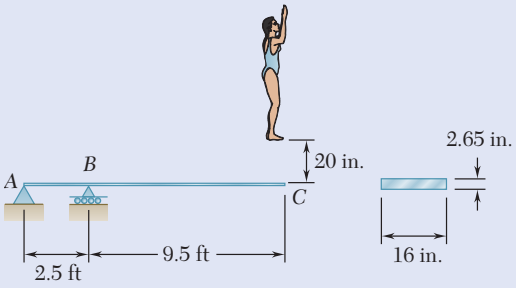


Fig. *P11.55*

11.55 A 160-lb diver jumps from a height of 20 in. onto end C of a diving board having the uniform cross section shown. Assuming that the diver's legs remain rigid and using $E = 1.8 \times 10^6$ psi, determine (a) the maximum deflection at point C, (b) the maximum normal stress in the board, (c) the equivalent static load.

11.56 A block of weight W is dropped from a height h onto the horizontal beam AB and hits it at point D. (a) Show that the maximum deflection y_m at point D can be expressed as

$$y_m = y_{st}\left(1 + \sqrt{1 + \frac{2h}{y_{st}}}\right)$$

where y_{st} represents the deflection at D caused by a static load W applied at that point and where the quantity in parenthesis is referred to as the *impact factor*. (b) Compute the impact factor for the beam of Prob. 11.52.

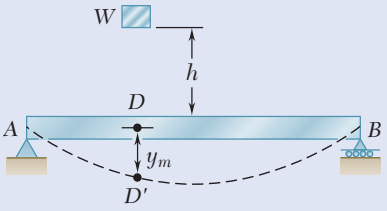


Fig. P11.56 and P11.57

11.57 A block of weight W is dropped from a height h onto the horizontal beam AB and hits point D. (a) Denoting by y_m the exact value of the maximum deflection at D and by y'_m the value obtained by neglecting the effect of this deflection on the change in potential energy of the block, show that the absolute value of the relative error is $(y'_m - y_m)/y_m$, never exceeding $y'_m/2h$. (b) Check the result obtained in part a by solving part a of Prob. 11.52 without taking y_m into account when determining the change in potential energy of the load, and comparing the answer obtained in this way with the exact answer to that problem.

11.58 and 11.59 Using the method of work and energy, determine the deflection at point D caused by the load $\mathbf{P}$.

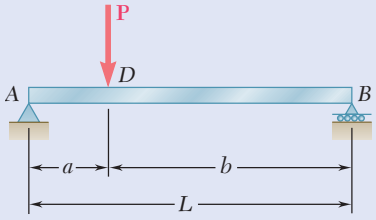


Fig. P11.58

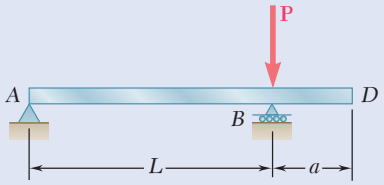


Fig. P11.59

***11.60* and 11.61** Using the method of work and energy, determine the slope at point D caused by the couple $\mathbf{M}_0$.

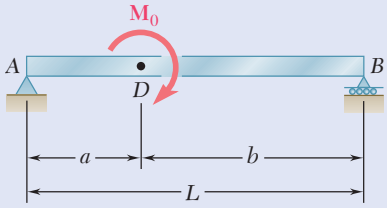


Fig. *P11.60*

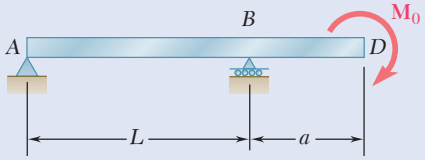


Fig. P11.61

11.62 and 11.63 Using the method of work and energy, determine the deflection at point C caused by the load $\mathbf{P}$.

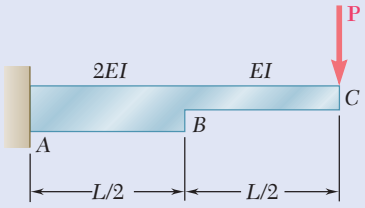


Fig. P11.62

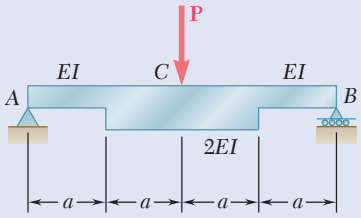


Fig. P11.63

11.64 Using the method of work and energy, determine the slope at point B caused by the couple $\mathbf{M}_0$.

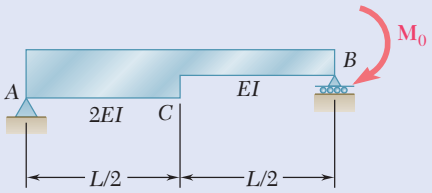


Fig. *P11.64*

11.65 Using the method of work and energy, determine the slope at point D caused by the couple $\mathbf{M}_0$.

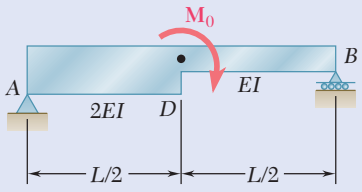


Fig. P11.65

11.66 The 20-mm diameter steel rod BC is attached to the lever AB and to the fixed support C. The uniform steel lever is 10 mm thick and 30 mm deep. Using the method of work and energy, determine the deflection of point A when $L = 600$ mm. Use $E = 200$ GPa and $G = 77.2$ GPa.

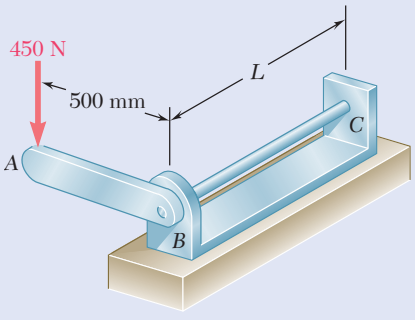


Fig. P11.66

11.67 Torques of the same magnitude T are applied to the steel shafts AB and CD. Using the method of work and energy, determine the length L of the hollow portion of shaft CD for which the angle of twist at C is equal to 1.25 times the angle of twist at A.

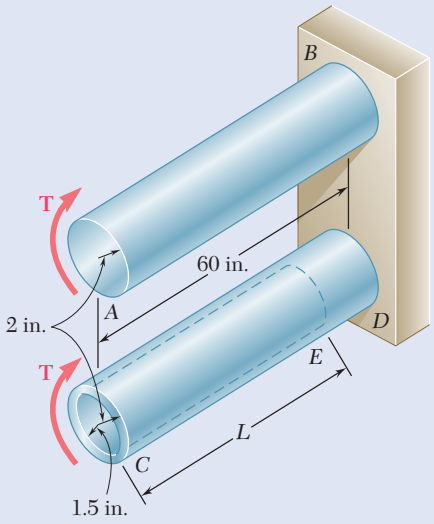


Fig. P11.67

11.68 Two steel shafts, each of 0.75-in.-diameter, are connected by the gears shown. Knowing that $G = 11.2 \times 10^6$ psi and that shaft DF is fixed at F, determine the angle through which end A rotates when a 750-lb·in. torque is applied at A. (Neglect the strain energy due to the bending of the shafts.)

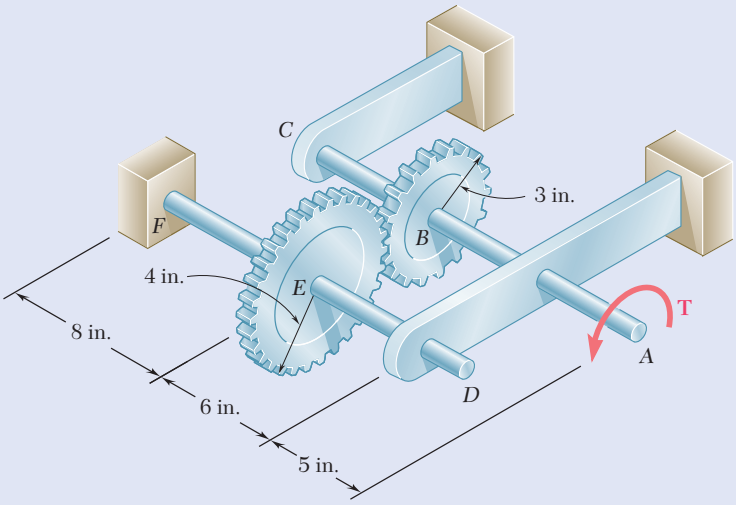


Fig. P11.68

11.69 The 20-mm-diameter steel rod CD is welded to the 20-mm-diameter steel shaft AB as shown. End C of rod CD is touching the rigid surface shown when a couple $\mathbf{T}_B$ is applied to a disk attached to shaft AB. Knowing that the bearings are self aligning and exert no couples on the shaft, determine the angle of rotation of the disk when $T_B = 400$ N·m. Use $E = 200$ GPa and $G = 77.2$ GPa. (Consider the strain energy due to both bending and twisting in shaft AB and to bending in arm CD.)

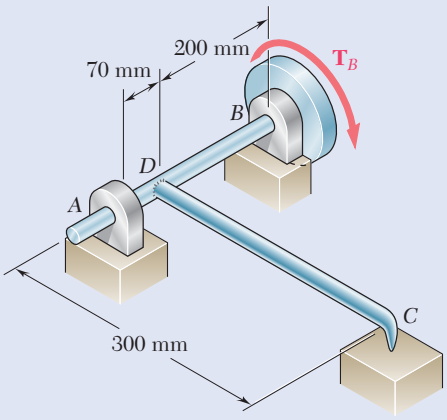


Fig. *P11.69*

11.70 The thin-walled hollow cylindrical member AB has a noncircular cross section of nonuniform thickness. Using the expression given in Eq. (3.50) of Sec. 3.10 and the expression for the strain-energy density given in Eq. (11.17), show that the angle of twist of member AB is

$$\phi = \frac{TL}{4\mathfrak{A}^2 G} \oint \frac{ds}{t}$$

where ds is the length of a small element of the wall cross section and $\mathfrak{A}$ is the area enclosed by center line of the wall cross section.

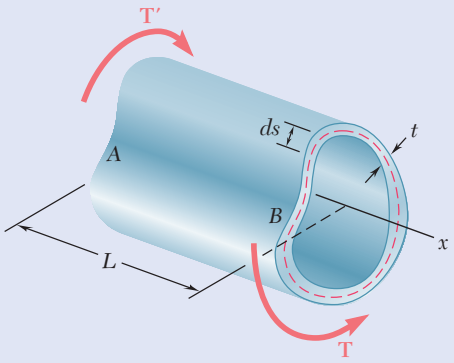


Fig. P11.70

***11.71* and 11.72** Each member of the truss shown has a uniform cross-sectional area A. Using the method of work and energy, determine the horizontal deflection of the point of application of the load **P**.

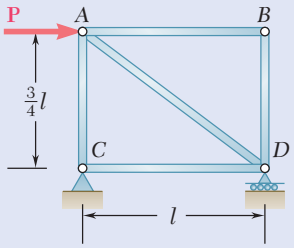


Fig. *P11.71*

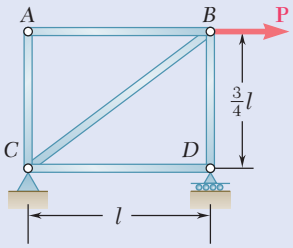


Fig. P11.72

11.73 Each member of the truss shown is made of steel and has a uniform cross-sectional area of 5 in^2. Using $E = 29 \times 10^6$ psi, determine the vertical deflection of joint B caused by the application of the 20-kip load.

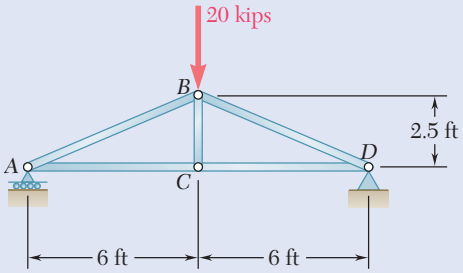


Fig. P11.73

11.74 Each member of the truss shown is made of steel. The cross-sectional area of member BC is 800 mm^2, and for all other members the cross-sectional area is 400 mm^2. Using $E = 200$ GPa, determine the deflection of point D caused by the 60-kN load.

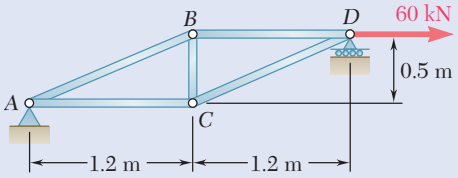


Fig. *P11.74*

11.75 Each member of the truss shown is made of steel and has a cross-sectional area of 5 in^2. Using E = 29×10^6 psi, determine the vertical deflection of point C caused by the 15-kip load.

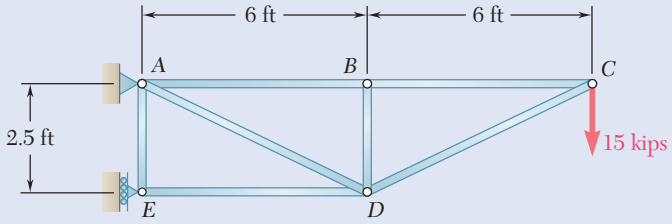


Fig. P11.75

11.76 The steel rod BC has a 24-mm diameter and the steel cable $ABDCA$ has a 12-mm diameter. Using $E = 200$ GPa, determine the deflection of joint D caused by the 12-kN load.

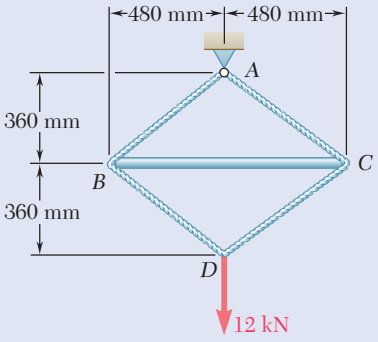


Fig. P11.76

*11.6 WORK AND ENERGY UNDER MULTIPLE LOADS

In this section, the strain energy of a structure subjected to several loads is considered and expressed in terms of the loads and resulting deflections.

Consider an elastic beam AB subjected to two concentrated loads $\mathbf{P}_1$ and $\mathbf{P}_2$. The strain energy of the beam is equal to the work of $\mathbf{P}_1$ and $\mathbf{P}_2$ as they are slowly applied to the beam at C_1 and C_2, respectively (Fig. 11.31). However, in order to evaluate this work, the deflections x_1 and x_2 must be expressed in terms of the loads $\mathbf{P}_1$ and $\mathbf{P}_2$.

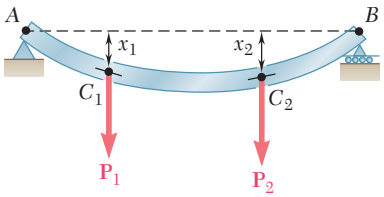


Fig. 11.31 Beam with multiple loads.

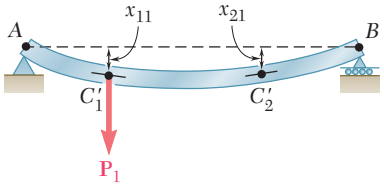


Fig. 11.32 Beam deflections at C_1 and C_2 due to single load $\mathbf{P}_1$.

Assume that only $\mathbf{P}_1$ is applied to the beam (Fig. 11.32). Both C_1 and C_2 are deflected, and their deflections are proportional to the load P_1. Denoting these deflections by x_{11} and x_{21}, respectively, write

$$x_{11} = \alpha_{11}P_1 \qquad x_{21} = \alpha_{21}P_1 \tag{11.41}$$

where α_{11} and α_{21} are constants called *influence coefficients*. These constants represent the deflections of C_1 and C_2 when a unit load is applied at C_1 and are characteristics of the beam.

Now assume that only $\mathbf{P}_2$ is applied to the beam (Fig. 11.33). The resulting deflections of C_1 and C_2 are denoted by x_{12} and x_{22}, respectively, so

$$x_{12} = \alpha_{12}P_2 \qquad x_{22} = \alpha_{22}P_2 \tag{11.42}$$

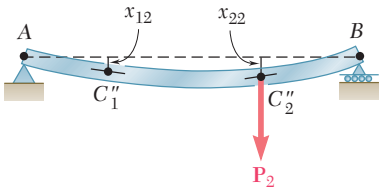


Fig. 11.33 Beam deflections at C_1 and C_2 due to single load $\mathbf{P}_2$.

where α_{12} and α_{22} are the influence coefficients representing the deflections of C_1 and C_2 when a unit load is applied at C_2. Applying the principle of superposition, the deflections x_1 and x_2 of C_1 and C_2 when both loads are applied (Fig. 11.31) are

$$x_1 = x_{11} + x_{12} = \alpha_{11}P_1 + \alpha_{12}P_2 \tag{11.43}$$

$$x_2 = x_{21} + x_{22} = \alpha_{21}P_1 + \alpha_{22}P_2 \tag{11.44}$$

To compute the work done by $\mathbf{P}_1$ and $\mathbf{P}_2$ and thus the strain energy of the beam, assume that $\mathbf{P}_1$ is first applied slowly at C_1 (Fig. 11.34*a*). Recalling the first of Eqs. (11.41), the work of $\mathbf{P}_1$ is

$$\tfrac{1}{2}P_1x_{11} = \tfrac{1}{2}P_1(\alpha_{11}P_1) = \tfrac{1}{2}\alpha_{11}P_1^2 \tag{11.45}$$

Note that $\mathbf{P}_2$ does no work while C_2 moves through x_{21}, since it has not yet been applied to the beam.

Now slowly apply $\mathbf{P}_2$ at C_2 (Fig. 11.34*b*). Recalling the second of Eqs. (11.42), the work of $\mathbf{P}_2$ is

$$\tfrac{1}{2}P_2x_{22} = \tfrac{1}{2}P_2(\alpha_{22}P_2) = \tfrac{1}{2}\alpha_{22}P_2^2 \tag{11.46}$$

But, as $\mathbf{P}_2$ is slowly applied at C_2, the point of application at $\mathbf{P}_1$ moves through x_{12} from C_1' to C_1, and load $\mathbf{P}_1$ does work. Since $\mathbf{P}_1$ is *fully applied* during this displacement (Fig. 11.35), its work is equal to P_1x_{12}, or recalling the first of Eqs. (11.42),

$$P_1x_{12} = P_1(\alpha_{12}P_2) = \alpha_{12}P_1P_2 \tag{11.47}$$

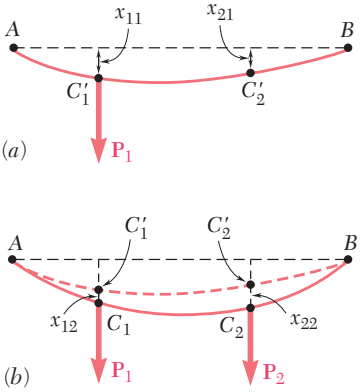


Fig. 11.34 (*a*) Deflection due to P_1 only. (*b*) Additional deflection due to subsequent application of P_2.

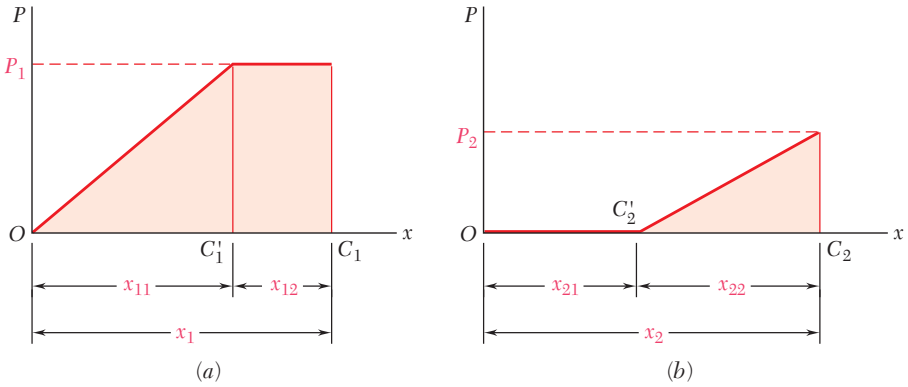


Fig. 11.35 Load-displacement diagrams for application of P_1 followed by P_2. (*a*) Load-displacement diagram for C_1. (*b*) Load-displacement diagram for C_2.

Adding the expressions in Eq. (11.45), (11.46), and (11.47), the strain energy of the beam under the loads $\mathbf{P}_1$ and $\mathbf{P}_2$ is

$$U = \tfrac{1}{2}(\alpha_{11}P_1^2 + 2\alpha_{12}P_1P_2 + \alpha_{22}P_2^2) \tag{11.48}$$

If load $\mathbf{P}_2$ had been applied first to the beam (Fig. 11.36*a*), followed by load $\mathbf{P}_1$ (Fig. 11.36*b*), the work done by each load would have been as

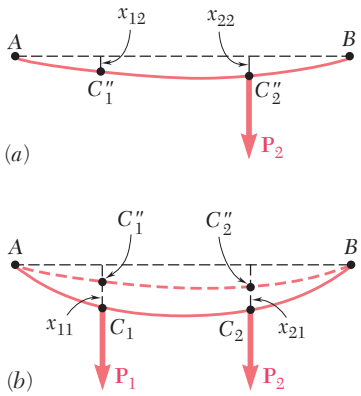


Fig. 11.36 (*a*) Deflection due to P_2 only. (*b*) Additional deflection due to subsequent application of P_1.

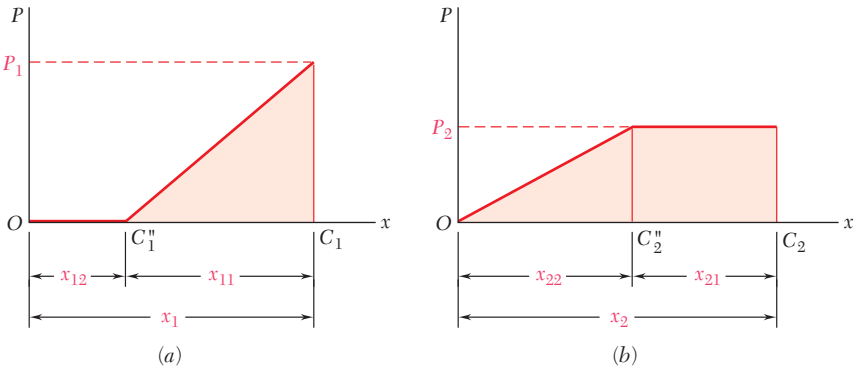


Fig. 11.37 Load-displacement diagrams for application of P_2 followed by P_1. (*a*) Load-displacement diagram for C_1. (*b*) Load-displacement diagram for C_2.

shown in Fig. 11.37. Similar calculations would lead to an alternative expression for the strain energy of the beam:

$$U = \tfrac{1}{2}(\alpha_{22}P_2^2 + 2\alpha_{21}P_2P_1 + \alpha_{11}P_1^2) \tag{11.49}$$

Equating the right-hand members of Eqs. (11.48) and (11.49), $\alpha_{12} = \alpha_{21}$, and we thus conclude that the deflection produced at C_1 by a unit load applied at C_2 is equal to the deflection produced at C_2 by a unit load applied at C_1. This is known as *Maxwell's reciprocal theorem,* after the British physicist James Clerk Maxwell (1831–1879).

While we are now able to express the strain energy U of a structure subjected to several loads as a function of these loads, the work energy method of Sec. 11.5B cannot be used determine the deflections of such a structure. Computing the strain energy U by integrating the strain-energy density u over the structure and substituting the expression obtained into Eq. (11.48) yields only one equation, which clearly can not be solved for the multiple coefficients α.

*11.7 CASTIGLIANO'S THEOREM

Recall from the previous section that the strain energy of an elastic structure subjected to two loads $\mathbf{P}_1$ and $\mathbf{P}_2$ is

$$U = \tfrac{1}{2}(\alpha_{11}P_1^2 + 2\alpha_{12}P_1P_2 + \alpha_{22}P_2^2) \tag{11.48}$$

where α_{11}, α_{12}, and α_{22} are the influence coefficients associated with the points of application C_1 and C_2 of the two loads. Differentiating Eq. (11.48) with respect to P_1 and using Eq. (11.43) gives

$$\frac{\partial U}{\partial P_1} = \alpha_{11}P_1 + \alpha_{12}P_2 = x_1 \tag{11.50}$$

Differentiating Eq. (11.48) with respect to P_2, using Eq. (11.44), and keeping in mind that $\alpha_{12} = \alpha_{21}$, we have

$$\frac{\partial U}{\partial P_2} = \alpha_{12}P_1 + \alpha_{22}P_2 = x_2 \tag{11.51}$$

More generally if an elastic structure is subjected to n loads $\mathbf{P}_1$, $\mathbf{P}_2, \ldots, \mathbf{P}_n$, the deflection x_j of the point of application of $\mathbf{P}_j$, and measured along the line of action of $\mathbf{P}_j$ is expressed as the partial derivative of the strain energy of the structure with respect to the load $\mathbf{P}_j$. Thus,

$$x_j = \frac{\partial U}{\partial P_j} \tag{11.52}$$

This is *Castigliano's theorem,* named after the Italian engineer Alberto Castigliano (1847–1884) who first stated it.†

Recall that the work of a couple $\mathbf{M}$ is $\frac{1}{2}M\theta$, where θ is the angle of rotation at the point where the couple is slowly applied. Castigliano's theorem can be used to determine the slope of a beam at the point of application of a couple $\mathbf{M}_j$. Thus,

$$\theta_j = \frac{\partial U}{\partial M_j} \tag{11.55}$$

Similarly, the angle of twist ϕ_j in a section of a shaft where a torque $\mathbf{T}_j$ is slowly applied is obtained by differentiating the strain energy of the shaft with respect to T_j:

$$\phi_j = \frac{\partial U}{\partial T_j} \tag{11.56}$$

†For an elastic structure subjected to n loads $\mathbf{P}_1$, $\mathbf{P}_2$, . . ., $\mathbf{P}_n$, the deflection of the point of application of $\mathbf{P}_j$, measured along the line of action of $\mathbf{P}_j$, is

$$x_j = \sum_k \alpha_{jk} P_k \tag{11.53}$$

and the strain energy of the structure is

$$U = \tfrac{1}{2} \sum_i \sum_k \alpha_{ik} P_i P_k \tag{11.54}$$

Differentiating U with respect to $\mathbf{P}_j$ and observing that $\mathbf{P}_j$ is found in terms corresponding to either $i = j$ or $k = j$ gives

$$\frac{\partial U}{\partial P_j} = \frac{1}{2} \sum_k \alpha_{jk} P_k + \frac{1}{2} \sum_i \alpha_{ij} P_i$$

or since $\alpha_{ij} = \alpha_{ji}$,

$$\frac{\partial U}{\partial P_j} = \frac{1}{2} \sum_k \alpha_{jk} P_k + \frac{1}{2} \sum_i \alpha_{ji} P_i = \sum_k \alpha_{jk} P_k$$

Recalling Eq. (11.53), we verify that

$$x_j = \frac{\partial U}{\partial P_j} \tag{11.52}$$

*11.8 DEFLECTIONS BY CASTIGLIANO'S THEOREM

We saw in the preceding section that the deflection x_j of a structure at the point of application of a load $\mathbf{P}_j$ can be determined by computing the partial derivative $\partial U/\partial P_j$ of the strain energy U of the structure. As we recall from Secs. 11.2A and 11.2B, the strain energy U is obtained by integrating or summing over the structure the strain energy of each element of the structure. The calculation by Castigliano's theorem of the deflection x_j is simplified if the differentiation with respect to the load P_j is carried out before the integration or summation.

For the beam from Sec. 11.2A, the strain energy was found to be

$$U = \int_0^L \frac{M^2}{2EI}\,dx \tag{11.15}$$

and the deflection x_j of the point of application of the load $\mathbf{P}_j$ is then

$$x_j = \frac{\partial U}{\partial P_j} = \int_0^L \frac{M}{EI}\frac{\partial M}{\partial P_j}\,dx \tag{11.57}$$

For a truss of n uniform members with a length L_i, cross-sectional area A_i, and internal force F_i, Eq. (11.14) can be used for the strain energy U to write

$$U = \sum_{i=1}^{n} \frac{F_i^2 L_i}{2A_i E} \tag{11.58}$$

The deflection x_j of the point of application of the load $\mathbf{P}_j$ is obtained by differentiating each term of the sum with respect to P_j. Thus,

$$x_j = \frac{\partial U}{\partial P_j} = \sum_{i=1}^{n} \frac{F_i L_i}{A_i E}\frac{\partial F_i}{\partial P_j} \tag{11.59}$$

Concept Application 11.12

The cantilever beam AB supports a uniformly distributed load w and a concentrated load $\mathbf{P}$ (Fig. 11.38). Knowing that $L = 2$ m, $w = 4$ kN/m, $P = 6$ kN, and $EI = 5$ MN·m^2, determine the deflection at A.

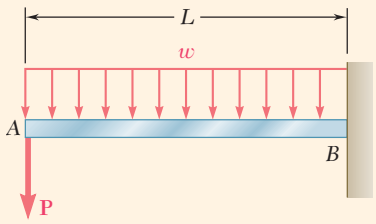


Fig. 11.38 Cantilever beam loaded as shown.

(continued)

The deflection y_A of point A where load **P** is applied is obtained from Eq. (11.57). Since **P** is vertical and directed downward, y_A represents a vertical deflection and is positive downward.

$$y_A = \frac{\partial U}{\partial P} = \int_0^L \frac{M}{EI}\frac{\partial M}{\partial P}\,dx \tag{1}$$

The bending moment M at a distance x from A is

$$M = -(Px + \tfrac{1}{2}wx^2) \tag{2}$$

and its derivative with respect to P is

$$\frac{\partial M}{\partial P} = -x$$

Substituting for M and $\partial M/\partial P$ into Eq. (1),

$$y_A = \frac{1}{EI}\int_0^L \left(Px^2 + \frac{1}{2}wx^3\right)dx$$

$$y_A = \frac{1}{EI}\left(\frac{PL^3}{3} + \frac{wL^4}{8}\right) \tag{3}$$

Substituting the given data,

$$y_A = \frac{1}{5 \times 10^6\ \text{N}\cdot\text{m}^2}\left[\frac{(6 \times 10^3\ \text{N})(2\ \text{m})^3}{3} + \frac{(4 \times 10^3\ \text{N/m})(2\ \text{m})^4}{8}\right]$$

$$y_A = 4.8 \times 10^{-3}\ \text{m} \qquad y_A = 4.8\ \text{mm} \downarrow$$

Note that the computation of the partial derivative $\partial M/\partial P$ *could not have been carried out* if the numerical value of P had been substituted for P in Eq. (2) for the bending moment.

The deflection x_j of a structure at a given point C_j can be obtained using the direct application of Castigliano's theorem only if load $\mathbf{P}_j$ is applied at C_j in the direction for which x_j is to be determined. When no load is applied at C_j or a load is applied in a direction other than the desired one, the deflection x_j still can be found using Castigliano's theorem if we use the following procedure. First, a fictitious or "dummy" load $\mathbf{Q}_j$ at C_j is applied in the direction in which the deflection x_j is to be determined. Then Castigliano's theorem is used to obtain the deflection

$$x_j = \frac{\partial U}{\partial Q_j} \tag{11.60}$$

due to $\mathbf{Q}_j$ and the actual loads. Making $Q_j = 0$ in Eq. (11.60) yields the deflection at C_j in the desired direction under the given load.

The slope θ_j of a beam at a point C_j can be found by applying a fictitious couple $\mathbf{M}_j$ at C_j, computing the partial derivative $\partial U/\partial M_j$, and making $M_j = 0$ in the expression obtained.

Concept Application 11.13

The cantilever beam AB supports a uniformly distributed load w (Fig. 11.39a). Determine the deflection and slope at A.

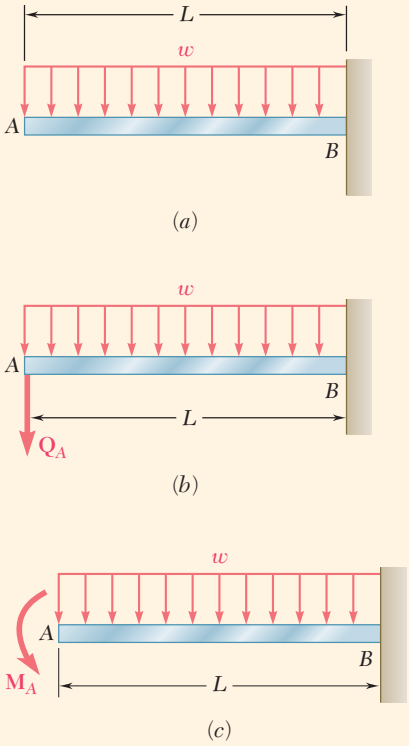


Fig. 11.39 (a) Cantilever beam supporting a uniformly distributed load. (b) Dummy load Q_A applied to determine deflection at A. (c) Dummy load M_A applied to determine the slope at A.

Deflection at *A*. Apply a dummy downward load $\mathbf{Q}_A$ at A (Fig. 11.39b) and write

$$y_A = \frac{\partial U}{\partial Q_A} = \int_0^L \frac{M}{EI}\frac{\partial M}{\partial Q_A}\,dx \tag{1}$$

The bending moment M at a distance x from A is

$$M = -Q_A x - \tfrac{1}{2}wx^2 \tag{2}$$

and its derivative with respect to Q_A is

$$\frac{\partial M}{\partial Q_A} = -x \tag{3}$$

Substituting for M and $\partial M/\partial Q_A$ from Eq. (2) and (3) into Eq. (1) and making $Q_A = 0$, the deflection at A for the given load is:

$$y_A = \frac{1}{EI}\int_0^L (-\tfrac{1}{2}wx^2)(-x)\,dx = +\frac{wL^4}{8EI}$$

Since the dummy load was directed downward, the positive sign indicates that

$$y_A = \frac{wL^4}{8EI}\downarrow$$

Slope at *A*. Apply a dummy counterclockwise couple $\mathbf{M}_A$ at A (Fig. 11.39c) and write

$$\theta_A = \frac{\partial U}{\partial M_A}$$

Recalling Eq. (11.15),

$$\theta_A = \frac{\partial}{\partial M_A}\int_0^L \frac{M^2}{2EI}\,dx = \int_0^L \frac{M}{EI}\frac{\partial M}{\partial M_A}\,dx \tag{4}$$

The bending moment M at a distance x from A is

$$M = -M_A - \tfrac{1}{2}wx^2 \tag{5}$$

and its derivative with respect to M_A is

$$\frac{\partial M}{\partial M_A} = -1 \tag{6}$$

Substituting for M and $\partial M/\partial M_A$ from Eq. (5) and (6) into Eq. (4) and making $M_A = 0$, the slope at A for the given load is:

$$\theta_A = \frac{1}{EI}\int_0^L (-\tfrac{1}{2}wx^2)(-1)\,dx = +\frac{wL^3}{6EI}$$

Since the dummy couple was counterclockwise, the positive sign indicates that the angle θ_A is also counterclockwise:

$$\theta_A = \frac{wL^3}{6EI}\measuredangle$$

Concept Application 11.14

A load **P** is supported at B by two rods of the same material and the same cross-sectional area A (Fig. 11.40*a*). Determine the horizontal and vertical deflection of point B.

We apply a dummy horizontal load **Q** at B (Fig. 11.40*b*). From Castigliano's theorem,

$$x_B = \frac{\partial U}{\partial Q} \qquad y_B = \frac{\partial U}{\partial P}$$

Using Eq. (11.14) to obtain the strain energy for the rods

$$U = \frac{F_{BC}^2 (BC)}{2AE} + \frac{F_{BD}^2 (BD)}{2AE}$$

where F_{BC} and F_{BD} represent the forces in BC and BD, respectively. Therefore,

$$x_B = \frac{\partial U}{\partial Q} = \frac{F_{BC}(BC)}{AE}\frac{\partial F_{BC}}{\partial Q} + \frac{F_{BD}(BD)}{AE}\frac{\partial F_{BD}}{\partial Q} \tag{1}$$

and

$$y_B = \frac{\partial U}{\partial P} = \frac{F_{BC}(BC)}{AE}\frac{\partial F_{BC}}{\partial P} + \frac{F_{BD}(BD)}{AE}\frac{\partial F_{BD}}{\partial P} \tag{2}$$

From the free-body diagram of pin B (Fig. 11.40*c*),

$$F_{BC} = 0.6P + 0.8Q \qquad F_{BD} = -0.8P + 0.6Q \tag{3}$$

Differentiating these equations with respect to Q and P, write

$$\frac{\partial F_{BC}}{\partial Q} = 0.8 \qquad \frac{\partial F_{BD}}{\partial Q} = 0.6$$
$$\frac{\partial F_{BC}}{\partial P} = 0.6 \qquad \frac{\partial F_{BD}}{\partial P} = -0.8 \tag{4}$$

Substituting from Eqs. (3) and (4) into both Eqs. (1) and (2), making $Q = 0$, and noting that $BC = 0.6l$ and $BD = 0.8l$, the horizontal and vertical deflections of point B under the given load **P** are

$$x_B = \frac{(0.6P)(0.6l)}{AE}(0.8) + \frac{(-0.8P)(0.8l)}{AE}(0.6)$$
$$= -0.096\frac{Pl}{AE}$$
$$y_B = \frac{(0.6P)(0.6l)}{AE}(0.6) + \frac{(-0.8P)(0.8l)}{AE}(-0.8)$$
$$= +0.728\frac{Pl}{AE}$$

Referring to the directions of the loads **Q** and **P**, we conclude that

$$x_B = 0.096\frac{Pl}{AE} \leftarrow \qquad y_B = 0.728\frac{Pl}{AE} \downarrow$$

We check that the expression found for the vertical deflection of B is the same as obtained in Concept Application 11.9.

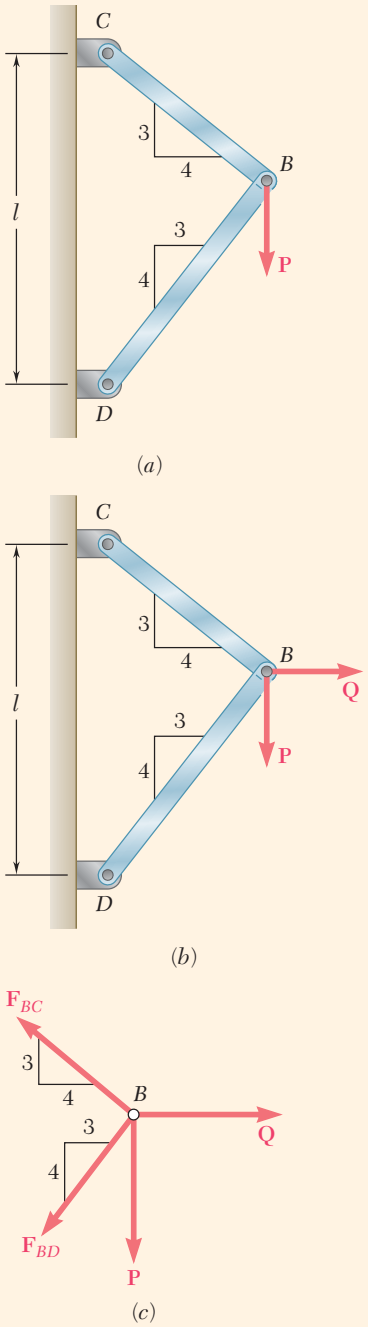


Fig. 11.40 (*a*) Frame *CBD* supporting vertical load *P*. (*b*) Frame *CBD* with horizontal dummy load *Q* applied. (*c*) Free-body diagram of joint *B* for finding member forces in terms of loads *P* and *Q*.

*11.9 STATICALLY INDETERMINATE STRUCTURES

The reactions at the supports of a statically indeterminate elastic structure can be determined using Castigliano's theorem. For example, in a structure indeterminate to the first degree, designate one of the reactions as redundant and eliminate or modify accordingly the corresponding support. The redundant reaction is treated like an unknown load that, together with the other loads, must produce deformations compatible with the original supports. First calculate the strain energy U of the structure due to the combined action of the loads and the redundant reaction. Observing that the partial derivative of U with respect to the redundant reaction represents the deflection (or slope) at the support that has been eliminated or modified, we then set this derivative equal to zero and solve for the redundant reaction.† The remaining reactions are found using the equations of statics.

†This is in the case of a rigid support allowing no deflection. For other types of support, the partial derivative of U should be set equal to the allowed deflection.

Concept Application 11.15

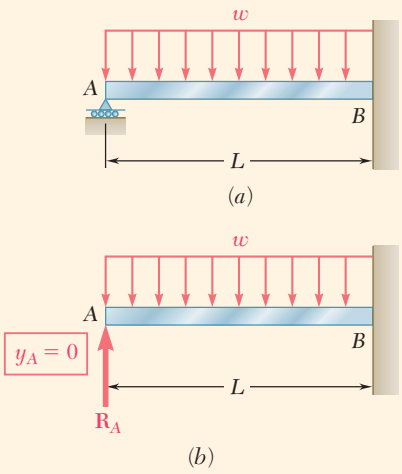


Fig. 11.41 (*a*) Beam statically indeterminate to first degree. (*b*) Redundant reaction at *A* and zero displacement boundary condition.

Determine the reactions at the supports for the prismatic beam and load shown (Fig. 11.41*a*).

The beam is statically indeterminate to the first degree. The reaction at A is redundant and the beam is released from that support. The reaction $\mathbf{R}_A$ is considered to be an unknown load (Fig. 11.41*b*) and will be determined under the condition that the deflection y_A at A must be zero. By Castigliano's theorem, $y_A = \partial U/\partial R_A$, where U is the strain energy of the beam under the distributed load and the redundant reaction. Recalling Eq. (11.57),

$$y_A = \frac{\partial U}{\partial R_A} = \int_0^L \frac{M}{EI}\frac{\partial M}{\partial R_A}\,dx \tag{1}$$

The bending moment M for the load of Fig. 11.41*b* at a distance x from A is

$$M = R_A x - \tfrac{1}{2}wx^2 \tag{2}$$

and its derivative with respect to R_A is

$$\frac{\partial M}{\partial R_A} = x \tag{3}$$

Substituting for M and $\partial M/\partial R_A$ from Eqs. (2) and (3) into Eq. (1), write

$$y_A = \frac{1}{EI}\int_0^L \left(R_A x^2 - \frac{1}{2}wx^3\right)dx = \frac{1}{EI}\left(\frac{R_A L^3}{3} - \frac{wL^4}{8}\right)$$

(continued)

Set $y_A = 0$ and solve for R_A:

$$R_A = \tfrac{3}{8}wL \qquad \mathbf{R}_A = \tfrac{3}{8}wL \uparrow$$

From the conditions of equilibrium for the beam, the reaction at B consists of the force and couple:

$$\mathbf{R}_B = \tfrac{5}{8}wL \uparrow \qquad \mathbf{M}_B = \tfrac{1}{8}wL^2 \circlearrowleft$$

Concept Application 11.16

A load **P** is supported at B by three rods of the same material and the same cross-sectional area A (Fig. 11.42*a*). Determine the force in each rod.

The structure is statically indeterminate to the first degree. The reaction at H is choosen as the redundant. Thus rod BH is released from its support at H. The reaction $\mathbf{R}_H$ is now considered to be an unknown load (Fig. 11.42*b*) and will be determined under the condition that the deflection y_H of point H must be zero. By Castigliano's theorem, $y_H = \partial U/\partial R_H$, where U is the strain energy of the three-rod system under load **P** and the redundant reaction $\mathbf{R}_H$. Recalling Eq. (11.59),

$$y_H = \frac{F_{BC}(BC)}{AE}\frac{\partial F_{BC}}{\partial R_H} + \frac{F_{BD}(BD)}{AE}\frac{\partial F_{BD}}{\partial R_H} + \frac{F_{BH}(BH)}{AE}\frac{\partial F_{BH}}{\partial R_H} \qquad (1)$$

Note that the force in rod BH is equal to R_H, or

$$F_{BH} = R_H \qquad (2)$$

Then, from the free-body diagram of pin B (Fig. 11.42*c*),

$$F_{BC} = 0.6P - 0.6R_H \qquad F_{BD} = 0.8R_H - 0.8P \qquad (3)$$

Differentiating with respect to R_H the force in each rod gives

$$\frac{\partial F_{BC}}{\partial R_H} = -0.6 \qquad \frac{\partial F_{BD}}{\partial R_H} = 0.8 \qquad \frac{\partial F_{BH}}{\partial R_H} = 1 \qquad (4)$$

Substituting from Eq. (2), (3), and (4) into Eq. (1) and noting that the lengths BC, BD, and BH are equal to $0.6l$, $0.8l$, and $0.5l$, respectively,

$$y_H = \frac{1}{AE}[(0.6P - 0.6R_H)(0.6l)(-0.6) + (0.8R_H - 0.8P)(0.8l)(0.8) + R_H(0.5l)(1)]$$

Setting $y_H = 0$ gives

$$1.228R_H - 0.728P = 0$$

and solving for R_H:

$$R_H = 0.593P$$

Carrying this value into Eqs. (2) and (3), the forces in the three rods are

$$F_{BC} = +0.244P \qquad F_{BD} = -0.326P \qquad F_{BH} = +0.593P$$

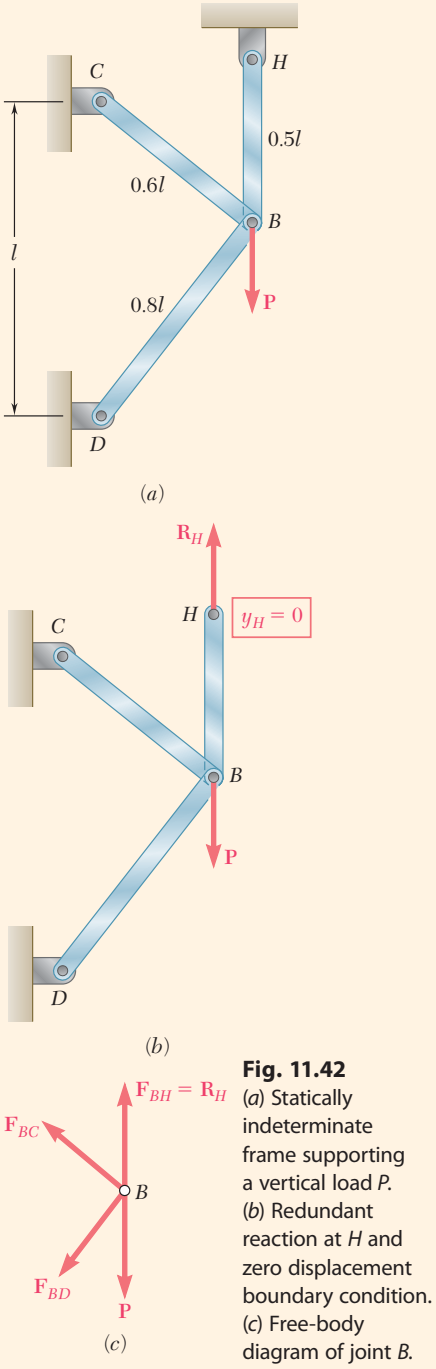
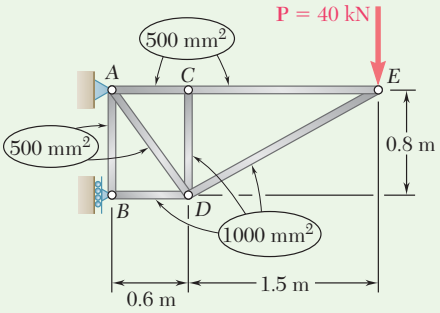


Fig. 11.42 (*a*) Statically indeterminate frame supporting a vertical load *P*. (*b*) Redundant reaction at *H* and zero displacement boundary condition. (*c*) Free-body diagram of joint *B*.

Sample Problem 11.5



For the truss and loading of Sample Prob. 11.4, determine the vertical deflection of joint *C*.

STRATEGY: Add a dummy load associated with the desired vertical deflection at joint *C*. The truss is then analyzed to determine the member forces, first by drawing a free-body diagram of the truss to find the reactions and then by using equilibrium at each joint to find the member forces. Use Eq. (11.59) to get the deflection in terms of the dummy load **Q**.

MODELING and ANALYSIS:

Castigliano's Theorem. We introduce the dummy vertical load **Q** as shown in Fig. 1. Using Castigliano's theorem where the force F_i in a given member i is caused by the combined load of **P** and **Q** and since E = constant,

$$y_C = \sum\left(\frac{F_iL_i}{A_iE}\right)\frac{\partial F_i}{\partial Q} = \frac{1}{E}\sum\left(\frac{F_iL_i}{A_i}\right)\frac{\partial F_i}{\partial Q} \tag{1}$$

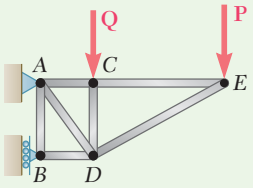


Fig. 1 Dummy load **Q** applied to joint *C* used to determine vertical deflection at *C*.

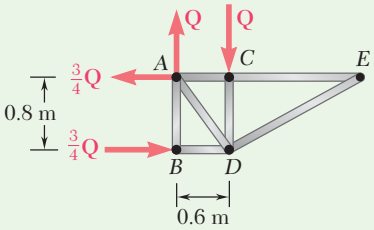


Fig. 2 Free-body diagram of truss with only dummy load *Q*.

Force in Members. Since the force in each member caused by the load **P** was previously found in Sample Prob. 11.4, we only need to determine the force in each member due to **Q**. Using the free-body diagram of the truss with load **Q**, we draw a free-body diagram (Fig. 2) to determine the reactions. Then, considering in sequence the equilibrium of joints *E, C, B* and *D* and using Fig. 3, we determine the force in each member caused by load **Q**.

Joint *E*: $F_{CE} = F_{DE} = 0$

Joint *C*: $F_{AC} = 0;\ F_{CD} = -Q$

Joint *B*: $F_{AB} = 0;\ F_{BD} = -\frac{3}{4}Q$

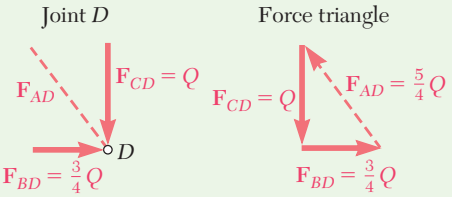


Fig. 3 Force analysis diagrams for joint *D*.

The total force in each member under the combined action of **Q** and **P** is shown in the following table. Form $\partial F_i/\partial Q$ for each member, then compute $(F_iL_i/A_i)(\partial F_i/\partial Q)$, as indicated.

(continued)

Member	F_i	$\partial F_i/\partial Q$	L_i, m	A_i, m^2	$\left(\frac{F_iL_i}{A_i}\right)\frac{\partial F_i}{\partial Q}$
AB	0	0	0.8	500×10^{-6}	0
AC	$+15P/8$	0	0.6	500×10^{-6}	0
AD	$+5P/4 + 5Q/4$	$\frac{5}{4}$	1.0	500×10^{-6}	$+3125P + 3125Q$
BD	$-21P/8 - 3Q/4$	$-\frac{3}{4}$	0.6	1000×10^{-6}	$+1181P + 338Q$
CD	$-Q$	-1	0.8	1000×10^{-6}	$+800Q$
CE	$+15P/8$	0	1.5	500×10^{-6}	0
DE	$-17P/8$	0	1.7	1000×10^{-6}	0

$$\sum\left(\frac{F_iL_i}{A_i}\right)\frac{\partial F_i}{\partial Q} = 4306P + 4263Q$$

Deflection of C. Substituting into Eq. (1), we have

$$y_C = \frac{1}{E}\sum\left(\frac{F_iL_i}{A_i}\right)\frac{\partial F_i}{\partial Q} = \frac{1}{E}(4306P + 4263Q)$$

Since load **Q** is not part of the original load, set $Q = 0$. Substituting $P = 40$ kN and $E = 73$ GPa gives

$$y_C = \frac{4306\,(40 \times 10^3\ \text{N})}{73 \times 10^9\ \text{Pa}} = 2.36 \times 10^{-3}\ \text{m} \qquad y_C = 2.36\ \text{mm}\downarrow$$

Sample Problem 11.6

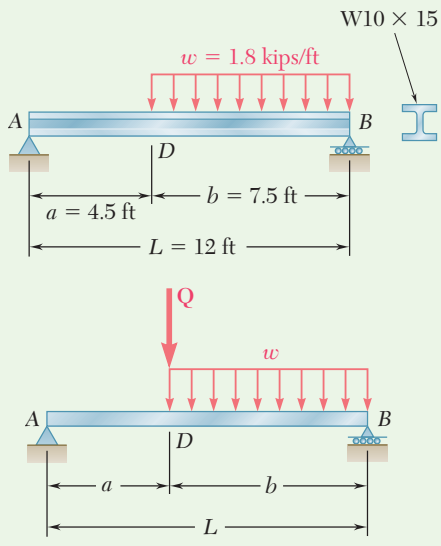


Fig. 1 Dummy load **Q** used to determine vertical deflection at point *D*.

For the beam and loading shown, determine the deflection at point *D*. Use $E = 29 \times 10^6$ psi.

STRATEGY: Add a dummy load associated with the desired vertical deflection at joint *D*. Use a free-body diagram to determine the reactions due to both the dummy load and the distributed load. The moments in each segment are then written as a function of the coordinate along the beam. Eq. (11.57) is used to determine the deflection.

MODELING and ANALYSIS:

Castigliano's Theorem. We introduce a dummy load **Q** as shown in Fig. 1. Using Castigliano's theorem and noting that *EI* is constant, write

$$y_D = \int \frac{M}{EI}\left(\frac{\partial M}{\partial Q}\right)dx = \frac{1}{EI}\int M\left(\frac{\partial M}{\partial Q}\right)dx \qquad \textbf{(1)}$$

The integration will be performed separately for segments *AD* and *DB*.

(continued)

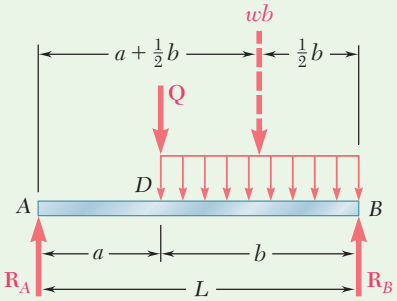


Fig. 2 Free-body diagram of beam.

From A to D

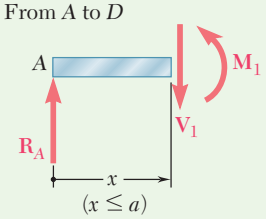


Fig. 3 Free-body diagram of left portion (in *AD*).

From B to D

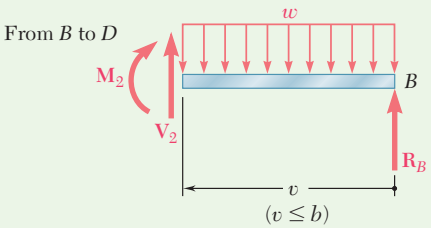


Fig. 4 Free-body diagram of right portion (in *BD*).

Reactions. Using the free-body diagram of the entire beam (Fig. 2) gives

$$\mathbf{R}_A = \frac{wb^2}{2L} + Q\frac{b}{L}\uparrow \qquad \mathbf{R}_B = \frac{wb(a + \frac{1}{2}b)}{L} + Q\frac{a}{L}\uparrow$$

Portion AD of Beam. Using the free-body diagram shown in Fig. 3,

$$M_1 = R_A x = \left(\frac{wb^2}{2L} + Q\frac{b}{L}\right)x \qquad \frac{\partial M_1}{\partial Q} = +\frac{bx}{L}$$

Substituting into Eq. (1) and integrating from A to D gives

$$\frac{1}{EI}\int M_1\frac{\partial M_1}{\partial Q}\,dx = \frac{1}{EI}\int_0^a R_A x\left(\frac{bx}{L}\right)dx = \frac{R_A a^3 b}{3EIL}$$

Then substitute for R_A and set the dummy load Q equal to zero.

$$\frac{1}{EI}\int M_1\frac{\partial M_1}{\partial Q}\,dx = \frac{wa^3b^3}{6EIL^2} \qquad \textbf{(2)}$$

Portion DB of Beam. Using the free-body diagram shown in Fig. 4, the bending moment at a distance v from end B is

$$M_2 = R_B v - \frac{wv^2}{2} = \left[\frac{wb(a + \frac{1}{2}b)}{L} + Q\frac{a}{L}\right]v - \frac{wv^2}{2} \qquad \frac{\partial M_2}{\partial Q} = +\frac{av}{L}$$

Substitute into Eq. (1) and integrate from point B (where $v = 0$) to point D (where $v = b$) for

$$\frac{1}{EI}\int M_2\frac{\partial M_2}{\partial Q}\,dv = \frac{1}{EI}\int_0^b \left(R_B v - \frac{wv^2}{2}\right)\left(\frac{av}{L}\right)dv = \frac{R_B ab^3}{3EIL} - \frac{wab^4}{8EIL}$$

Substituting for R_B and setting $Q = 0$,

$$\frac{1}{EI}\int M_2\frac{\partial M_2}{\partial Q}\,dv = \left[\frac{wb(a + \frac{1}{2}b)}{L}\right]\frac{ab^3}{3EIL} - \frac{wab^4}{8EIL} = \frac{5a^2b^4 + ab^5}{24EIL^2}w \qquad \textbf{(3)}$$

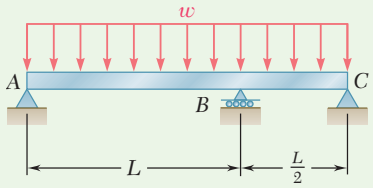
Deflection at Point D. Recalling Eqs. (1), (2), and (3),

$$y_D = \frac{wab^3}{24EIL^2}(4a^2 + 5ab + b^2) = \frac{wab^3}{24EIL^2}(4a + b)(a + b) = \frac{wab^3}{24EIL}(4a + b)$$

From Appendix C, $I = 68.9$ in^4 for a W10 × 15 beam. Substituting the numerical values for I, w, a, b, and L,

$$y_D = 0.262 \text{ in.}\downarrow$$

Sample Problem 11.7



For the uniform beam and loading shown, determine the reactions at the supports.

STRATEGY: The beam is indeterminate to the first degree, and we must choose one of the reactions as a redundant. We then use a free-body diagram to solve for the reactions due to the distributed load and the redundant reaction. Using free-body diagrams of the segments, we obtain the moments as a function of the coordinate along the beam. Using Eq. (11.57), we write Castigliano's theorem for deflection associated with the redundant reaction. We set this deflection equal to zero, and solve for the redundant reaction. Equilibrium can then be used to find the other reactions.

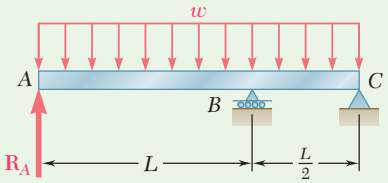


Fig. 1 Released beam, replacing support at A with redundant reaction R_A.

MODELING and ANALYSIS:

Castigliano's Theorem. Choose the reaction $\mathbf{R}_A$ as the redundant one (Fig. 1). Using Castigliano's theorem, determine the deflection at A due to the combined action of $\mathbf{R}_A$ and the distributed load. Since EI is constant,

$$y_A = \int \frac{M}{EI}\left(\frac{\partial M}{\partial R_A}\right)dx = \frac{1}{EI}\int M\frac{\partial M}{\partial R_A}\,dx \tag{1}$$

The integration will be performed separately for portions AB and BC of the beam. $\mathbf{R}_A$ is then obtained by setting y_A equal to zero.

Free Body: Entire Beam. Using Fig. 2, the reactions at B and C in terms of R_A and the distributed load are

$$R_B = \tfrac{9}{4}wL - 3R_A \qquad R_C = 2R_A - \tfrac{3}{4}wL \tag{2}$$

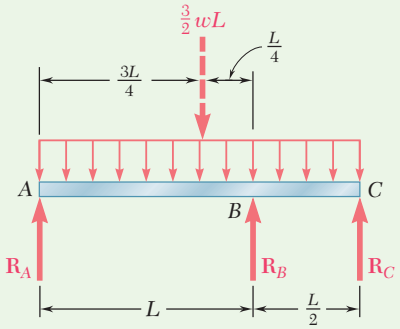


Fig. 2 Free-body diagram of beam.

From A to B

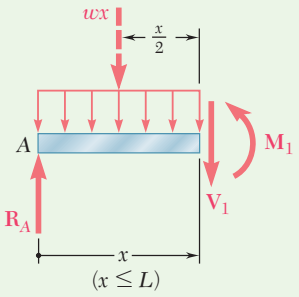


Fig. 3 Free-body diagram of left portion showing internal shear and moment.

From C to B

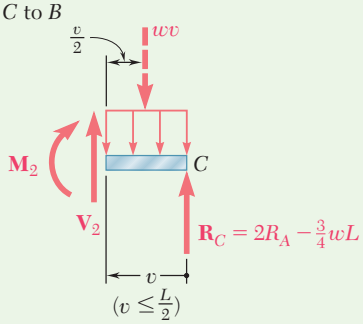


Fig. 4 Free-body diagram of right portion showing internal shear and moment.

Portion AB of Beam. Using the free-body diagram shown in Fig. 3, find

$$M_1 = R_A x - \frac{wx^2}{2} \qquad \frac{\partial M_1}{\partial R_A} = x$$

Substituting into Eq. (1) and integrating from A to B gives

$$\frac{1}{EI}\int M_1 \frac{\partial M}{\partial R_A}\,dx = \frac{1}{EI}\int_0^L \left(R_A x^2 - \frac{wx^3}{2}\right)dx = \frac{1}{EI}\left(\frac{R_A L^3}{3} - \frac{wL^4}{8}\right) \quad \textbf{(3)}$$

Portion BC of Beam. Using the free-body diagram shown in Fig. 4, find

$$M_2 = \left(2R_A - \frac{3}{4}wL\right)v - \frac{wv^2}{2} \qquad \frac{\partial M_2}{\partial R_A} = 2v$$

Substituting into Eq. (1) and integrating from C (where $v = 0$) to B (where $v = \frac{1}{2}L$) gives

$$\frac{1}{EI}\int M_2 \frac{\partial M_2}{\partial R_A}\,dv = \frac{1}{EI}\int_0^{L/2} \left(4R_A v^2 - \frac{3}{2}wLv^2 - wv^3\right)dv$$

$$= \frac{1}{EI}\left(\frac{R_A L^3}{6} - \frac{wL^4}{16} - \frac{wL^4}{64}\right) = \frac{1}{EI}\left(\frac{R_A L^3}{6} - \frac{5wL^4}{64}\right) \quad \textbf{(4)}$$

Reaction at *A*. Adding the expressions from Eqs. (3) and (4), we obtain y_A and set it equal to zero:

$$y_A = \frac{1}{EI}\left(\frac{R_A L^3}{3} - \frac{wL^4}{8}\right) + \frac{1}{EI}\left(\frac{R_A L^3}{6} - \frac{5wL^4}{64}\right) = 0$$

Thus,
$$R_A = \frac{13}{32}wL \qquad R_A = \frac{13}{32}wL \uparrow$$

Reactions at *B* and *C*. Substituting for R_A into Eqs. (2), we obtain

$$R_B = \frac{33}{32}wL \uparrow \qquad R_C = \frac{wL}{16} \uparrow$$

Problems

11.77 and 11.78 Using the information in Appendix D, compute the work of the loads as they are applied to the beam (*a*) if the load **P** is applied first, (*b*) if the couple **M** is applied first.

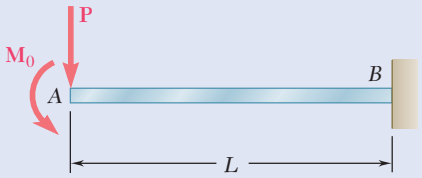


Fig. P11.77

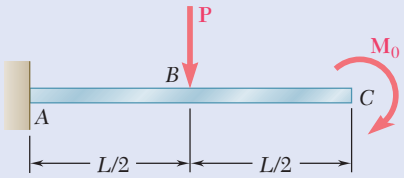


Fig. P11.78

11.79 through 11.82 For the beam and loading shown, (*a*) compute the work of the loads as they are applied successively to the beam, using the information provided in Appendix D, (*b*) compute the strain energy of the beam by the method of Sec. 11.2A and show that it is equal to the work obtained in part *a*.

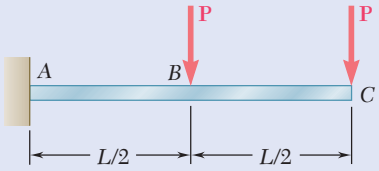


Fig. P11.79

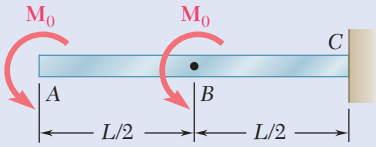


Fig. P11.80

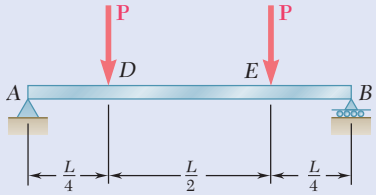


Fig. P11.81

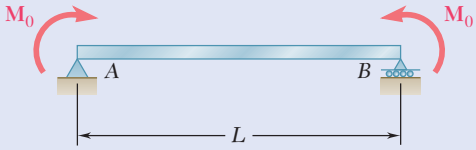


Fig. P11.82

11.83 through 11.85 For the prismatic beam shown, determine the deflection of point *D*.

11.86 through 11.88 For the prismatic beam shown, determine the slope at point *D*.

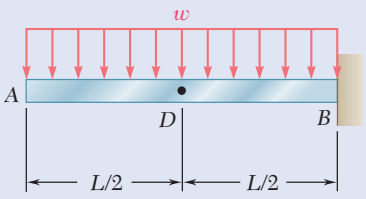


Fig. P11.83 and P11.86

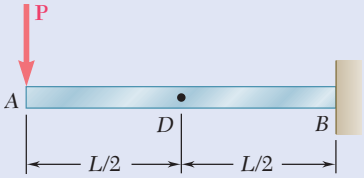


Fig. P11.84 and P11.87

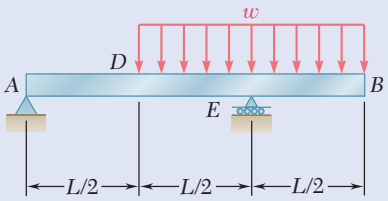


Fig. P11.85 and P11.88

11.89 For the prismatic beam shown, determine the slope at point A.

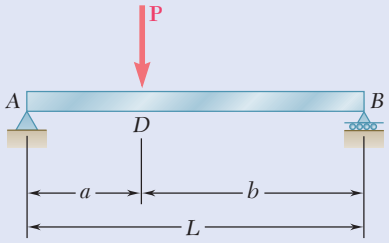


Fig. P11.89

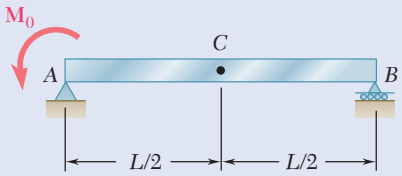


Fig. P11.90

11.90 For the prismatic beam shown, determine the slope at point B.

11.91 For the beam and loading shown, determine the deflection of point B. Use $E = 29 \times 10^6$ psi.

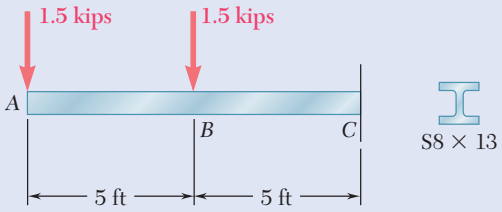


Fig. P11.91 and *P11.92*

11.92 For the beam and loading shown, determine the deflection of point A. Use $E = 29 \times 10^6$ psi.

11.93 and 11.94 For the beam and loading shown, determine the deflection at point B. Use $E = 200$ GPa.

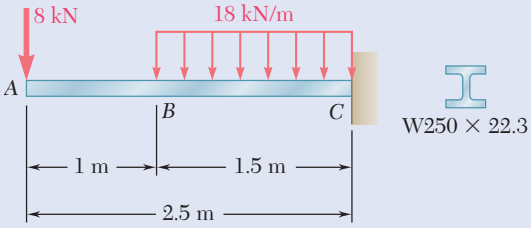


Fig. P11.93

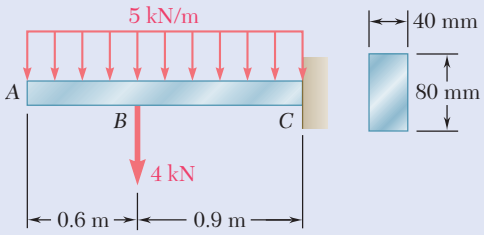


Fig. P11.94

11.95 For the beam and loading shown, determine the slope at end A. Use $E = 200$ GPa.

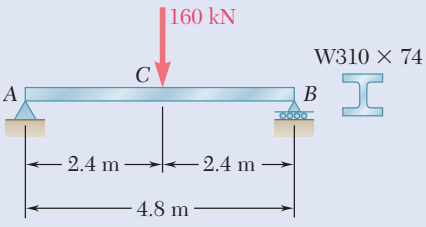


Fig. P11.95

11.96 For the beam and loading shown, determine the deflection at point D. Use $E = 200$ GPa.

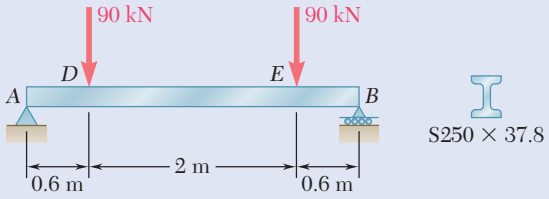


Fig. P11.96

11.97 For the beam and loading shown, determine the slope at end A. Use $E = 29 \times 10^6$ psi.

11.98 For the beam and loading shown, determine the deflection at point C. Use $E = 29 \times 10^6$ psi.

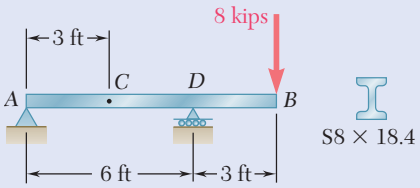


Fig. P11.97 and *P11.98*

11.99 and *11.100* For the truss and loading shown, determine the horizontal and vertical deflection of joint C.

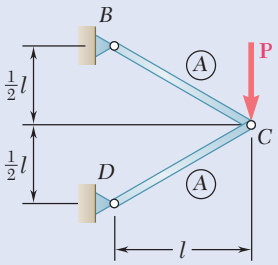


Fig. P11.99

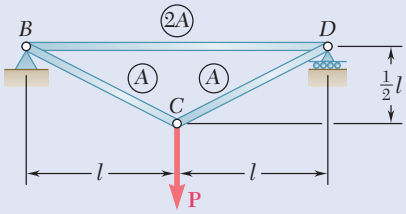


Fig. *P11.100*

11.101 and 11.102 Each member of the truss shown is made of steel and has the cross-sectional area shown. Using $E = 29 \times 10^6$ psi, determine the deflection indicated.

11.101 Vertical deflection of joint C.

11.102 Horizontal deflection of joint C.

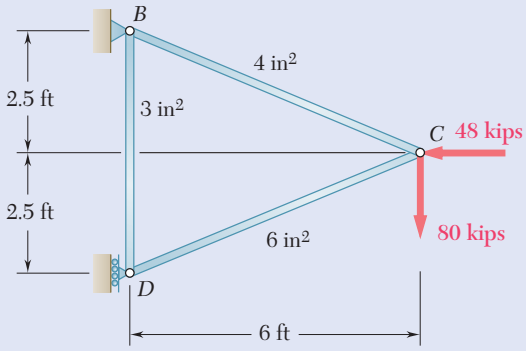


Fig. P11.101 and P11.102

11.103 and *11.104* Each member of the truss shown is made of steel and has a cross-sectional area of 500 mm^2. Using $E = 200$ GPa, determine the deflection indicated.

11.103 Vertical deflection of joint B.

11.104 Horizontal deflection of joint B.

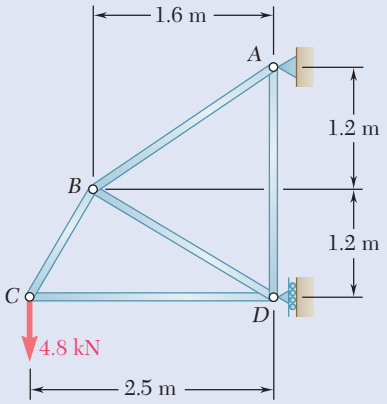


Fig. P11.103 and *P11.104*

11.105 A uniform rod of flexural rigidity EI is bent and loaded as shown. Determine (*a*) the vertical deflection of point A, (*b*) the horizontal deflection of point A.

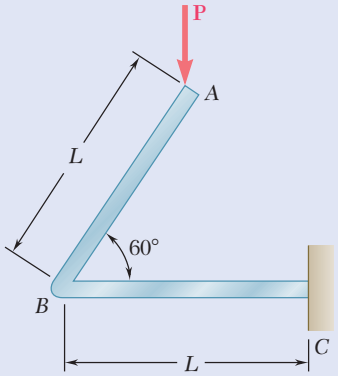


Fig. P11.105

11.106 For the uniform rod and loading shown and using Castigliano's theorem, determine the deflection of point B.

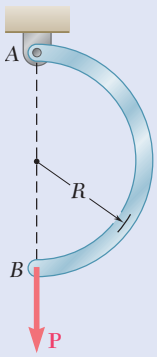


Fig. P11.106

11.107 For the beam and loading shown and using Castigliano's theorem, determine (*a*) the horizontal deflection of point *B*, (*b*) the vertical deflection of point *B*.

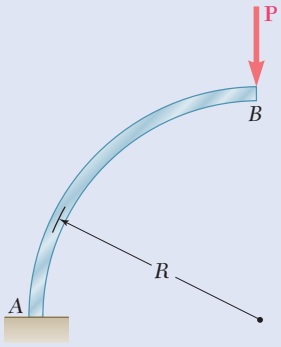


Fig. P11.107

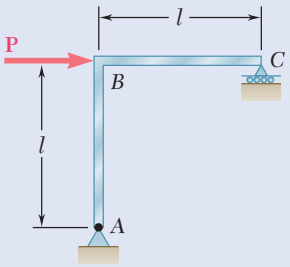


Fig. *P11.108*

11.108 Two rods *AB* and *BC* of the same flexural rigidity *EI* are welded together at *B*. For the loading shown, determine (*a*) the deflection of point *C*, (*b*) the slope of member *BC* at point *C*.

11.109 Three rods, each of the same flexural rigidity *EI*, are welded to form the frame *ABCD*. For the loading shown, determine the deflection of point *D*.

11.110 Three rods, each of the same flexural rigidity *EI*, are welded to form the frame *ABCD*. For the loading shown, determine the angle formed by the frame at point *D*.

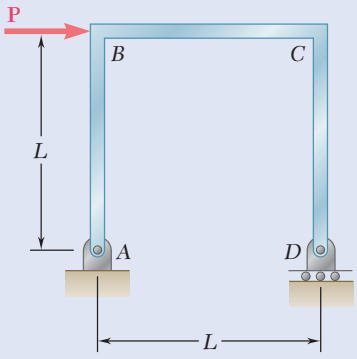


Fig. P11.109 and *P11.110*

11.111 through *11.115* Determine the reaction at the roller support and draw the bending-moment diagram for the beam and loading shown.

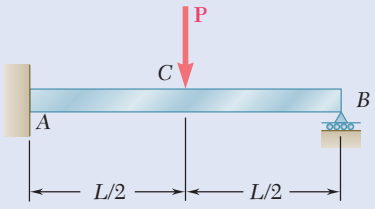


Fig. P11.111

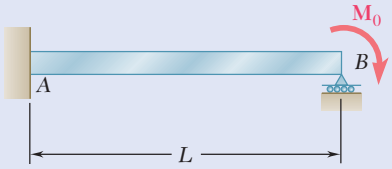


Fig. P11.112

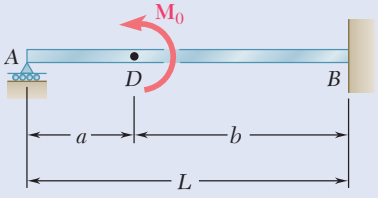


Fig. P11.113

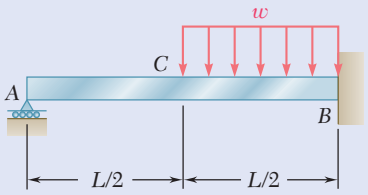


Fig. P11.114

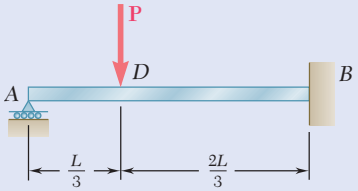


Fig. *P11.115*

11.116 For the uniform beam and loading shown, determine the reaction at each support.

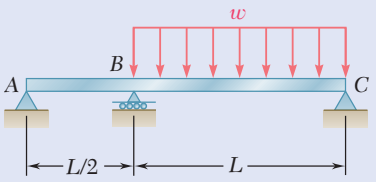


Fig. *P11.116*

11.117 through 11.120 Three members of the same material and same cross-sectional area are used to support the load **P**. Determine the force in member *BC*.

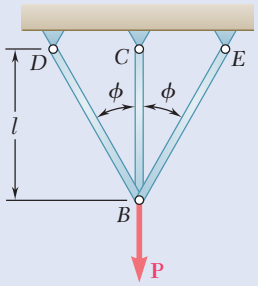


Fig. P11.117

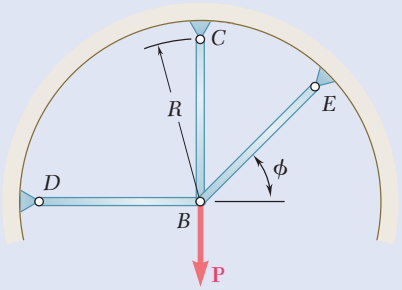


Fig. P11.118

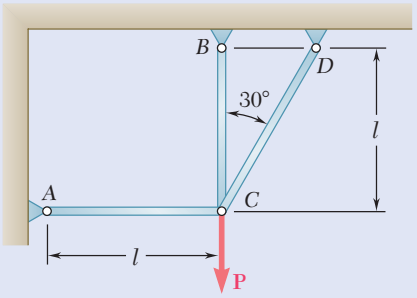


Fig. P11.119

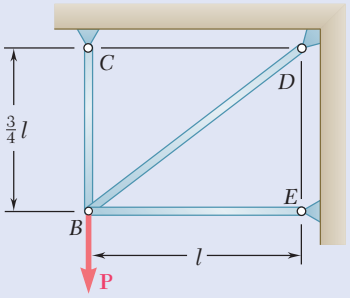


Fig. *P11.120*

11.121 and 11.122 Knowing that the eight members of the indeterminate truss shown have the same uniform cross-sectional area, determine the force in member *AB*.

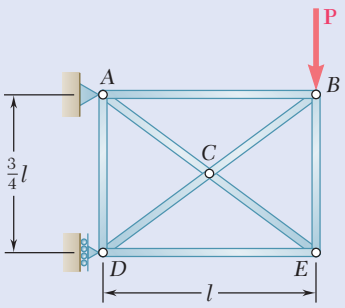


Fig. P11.121

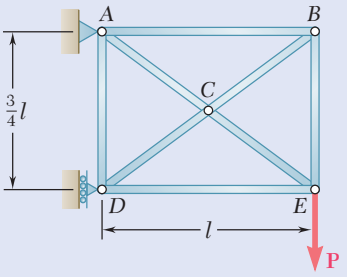


Fig. *P11.122*

Review and Summary

Strain Energy

We considered a uniform rod subjected to a slowly increasing axial load **P** (Fig. 11.43). The area under the load-deformation diagram (Fig. 11.44) represents the work done by **P**. This work is equal to the *strain energy* of the rod associated with the deformation caused by load **P**:

$$\text{Strain energy} = U = \int_0^{x_1} P\,dx \tag{11.2}$$

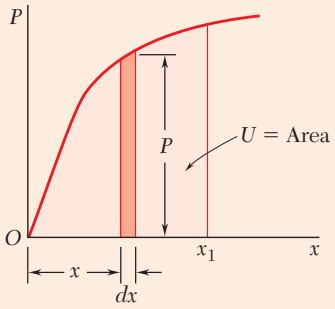


Fig. 11.44 Work due to load *P* is equal to the area under the load-deformation diagram.

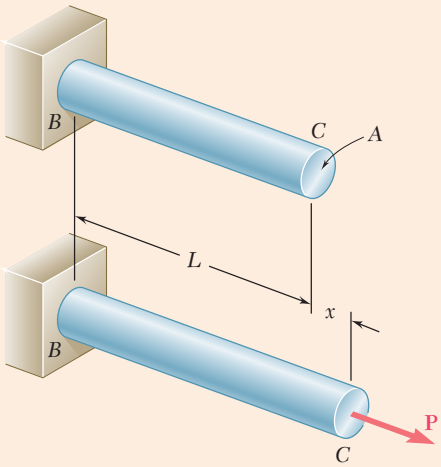


Fig. 11.43 Axially loaded rod.

Strain-Energy Density

Since the stress is uniform throughout the rod shown in Fig. 11.43, the strain energy can be divided by the volume of the rod to obtain the strain energy per unit volume. This is the *strain-energy density* of the material.

$$\text{Strain-energy density} = u = \int_0^{\epsilon_1} \sigma_x\,d\epsilon_x \tag{11.4}$$

The strain-energy density is equal to the area under the stress-strain diagram of the material (Fig. 11.45). Equation (11.4) remains valid when the stresses are not uniformly distributed, but the strain-energy density now varies from point to point. If the material is unloaded, there is a permanent strain ϵ_p, and only the strain-energy density corresponding to the triangular area is recovered. The remainder of the energy is dissipated in the form of heat during the deformation of the material.

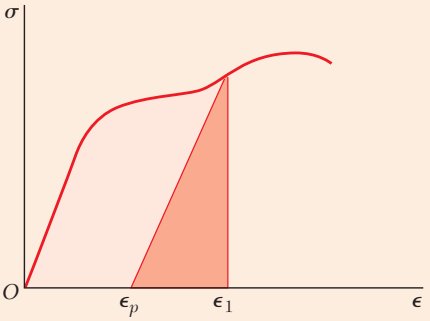


Fig. 11.45 Strain-energy density is the area under the stress-strain curve between $\epsilon_x = 0$ and $\epsilon_x = \epsilon_1$. If loaded into the plastic region, only the energy associated with elastic unloading is recovered.

Modulus of Toughness

The area under the entire stress-strain diagram (from zero to rupture) is called the *modulus of toughness* and is a measure of the total energy that can be acquired by the material.

Modulus of Resilience

If the normal stress σ remains within the proportional limit of the material, the strain-energy density u is

$$u = \frac{\sigma^2}{2E}$$

The area under the stress-strain curve from zero strain to the strain ϵ_Y at yield (Fig. 11.46) is the *modulus of resilience* of the material. It represents the energy per unit volume that the material can absorb without yielding:

$$u_Y = \frac{\sigma_Y^2}{2E} \tag{11.8}$$

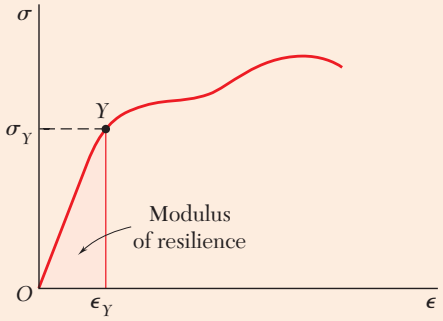


Fig. 11.46 Modulus of resilience is the area under the stress-strain curve to yield.

Strain Energy Under Axial Load

The strain energy under axial load is associated with *normal stresses.* If a rod of length L and *variable cross-sectional area* A is subjected to a centric axial load **P** at its end, the strain energy of the rod is

$$U = \int_0^L \frac{P^2}{2AE}\,dx \tag{11.13}$$

If the rod has a *uniform cross section* with an area A, the strain energy is

$$U = \frac{P^2 L}{2AE} \tag{11.14}$$

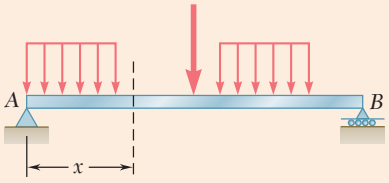


Fig. 11.47 Transversely loaded beam.

Strain Energy Due to Bending

For a beam subjected to transverse loads (Fig. 11.47), the strain energy associated with the normal stresses is

$$U = \int_0^L \frac{M^2}{2EI}\,dx \tag{11.15}$$

where M is the bending moment and EI is the flexural rigidity of the beam.

Strain Energy Due to Shearing Stresses

The strain energy also can be associated with *shearing stresses.* The strain-energy density for a material in pure shear is

$$u = \frac{\tau_{xy}^2}{2G} \tag{11.17}$$

where τ_{xy} is the shearing stress and G is the modulus of rigidity of the material.

Strain Energy Due to Torsion

For a shaft with a length of L and uniform cross section subjected to couples of magnitude T at its ends (Fig. 11.48), the strain energy is

$$U = \frac{T^2 L}{2GJ} \tag{11.20}$$

where J is the polar moment of inertia of the cross-sectional area of the shaft.

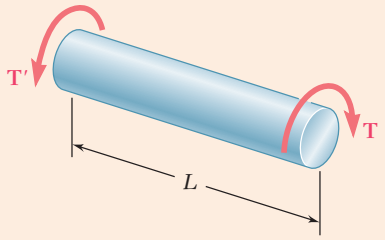


Fig. 11.48 Prismatic shaft subjected to torque.

General State of Stress

The strain energy of an elastic isotropic material under a general state of stress was considered where the strain-energy density at a given point is expressed in terms of the principal stresses σ_a, σ_b, and σ_c at that point:

$$u = \frac{1}{2E}[\sigma_a^2 + \sigma_b^2 + \sigma_c^2 - 2\nu(\sigma_a\sigma_b + \sigma_b\sigma_c + \sigma_c\sigma_a)] \tag{11.23}$$

The strain-energy density at a given point is divided into two parts: u_v, which is associated with a change in volume of the material at that point, and u_d, which is associated with a distortion of the material at the same point. Thus, $u = u_v + u_d$, where

$$u_v = \frac{1 - 2\nu}{6E}(\sigma_a + \sigma_b + \sigma_c)^2 \tag{11.28}$$

and

$$u_d = \frac{1}{12G}[(\sigma_a - \sigma_b)^2 + (\sigma_b - \sigma_c)^2 + (\sigma_c - \sigma_a)^2] \tag{11.29}$$

This equation for u_d is used to derive the maximum-distortion-energy criterion to predict whether or not a ductile material yields under a given state of plane stress.

Impact Loads

For the *impact loading* of an elastic structure being hit by a mass moving with a given velocity, it is assumed that the kinetic energy of the mass is transferred entirely to the structure. The *equivalent static load* is the load that causes the same deformations and stresses as the impact load.

A structural member designed to withstand an impact load effectively should be shaped so that the stresses are evenly distributed throughout the member. Also, the material used should have a low modulus of elasticity and a high yield strength.

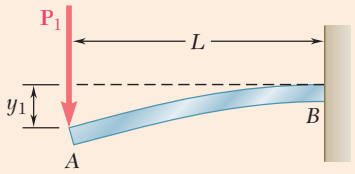


Fig. 11.49 Cantilever beam with load $\mathbf{P}_1$.

Members Subjected to a Single Load

The strain energy of structural members subjected to a *single load* was considered for the beam and loading of Fig. 11.49. The strain energy of the beam is

$$U = \frac{P_1^2 L^3}{6EI} \tag{11.37}$$

Observing that the work done by load **P** is equal to $\frac{1}{2}P_1 y_1$, the work of the load and the strain energy of the beam are equal and can be equated to determine the deflection y_1 at the point of application of the load.

The method just described is of limited value, since it is restricted to structures subjected to a single concentrated load and to the determination of the deflection at the point of application of that load. In the remaining sections of the chapter, we presented a more general method, which can be used to determine deflections at various points of structures subjected to several loads.

Castigliano's Theorem

Castigliano's theorem states that the deflection x_j of the point of application of a load $\mathbf{P}_j$ measured along the line of action of $\mathbf{P}_j$ is equal to the partial derivative of the strain energy of the structure with respect to the load $\mathbf{P}_j$. Thus,

$$x_j = \frac{\partial U}{\partial P_j} \tag{11.52}$$

Castigliano's theorem also can be used to determine the *slope* of a beam at the point of application of a couple $\mathbf{M}_j$ by writing

$$\theta_j = \frac{\partial U}{\partial M_j} \tag{11.55}$$

Similarly the *angle of twist* is determined in a section of a shaft where a torque $\mathbf{T}_j$ is applied by writing

$$\phi_j = \frac{\partial U}{\partial T_j} \tag{11.56}$$

Castigliano's theorem can be applied to determine the deflections and slopes at various points of a given structure. Dummy loads are used to determine displacements at points where no actual load is applied. The calculation of a deflection x_j is simpler if the differentiation with respect to load P_j is carried out before the integration. For a beam,

$$x_j = \frac{\partial U}{\partial P_j} = \int_0^L \frac{M}{EI}\frac{\partial M}{\partial P_j}\,dx \tag{11.57}$$

For a truss consisting of n members, the deflection x_j at the point of application of the load $\mathbf{P}_j$ is

$$x_j = \frac{\partial U}{\partial P_j} = \sum_{i=1}^{n} \frac{F_i L_i}{A_i E}\frac{\partial F_i}{\partial P_j} \tag{11.59}$$

Indeterminate Structures

Castigliano's theorem can also be used in the analysis of statically indeterminate structures, as shown in Sec. 11.9.

Review Problems

11.123 Rod AB is made of a steel for which the yield strength is $\sigma_Y = 450$ MPa and $E = 200$ GPa; rod BC is made of an aluminum alloy for which $\sigma_Y = 280$ MPa and $E = 73$ GPa. Determine the maximum strain energy that can be acquired by the composite rod ABC without causing any permanent deformations.

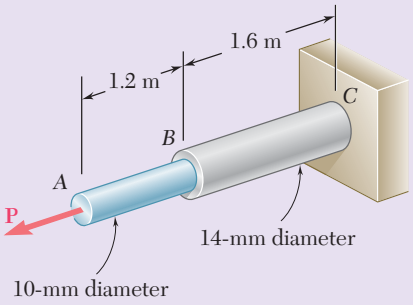


Fig. P11.123

11.124 Each member of the truss shown is made of steel and has the cross-sectional area shown. Using $E = 29 \times 10^6$ psi, determine the strain energy of the truss for the loading shown.

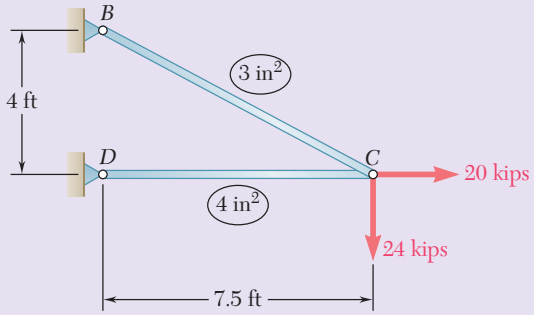


Fig. P11.124

11.125 The ship at A has just started to drill for oil on the ocean floor at a depth of 5000 ft. The steel drill pipe has an outer diameter of 8 in. and a uniform wall thickness of 0.5 in. Knowing that the top of the drill pipe rotates through two complete revolutions before the drill bit at B starts to operate and using $G = 11.2 \times 10^6$ psi, determine the maximum strain energy acquired by the drill pipe.

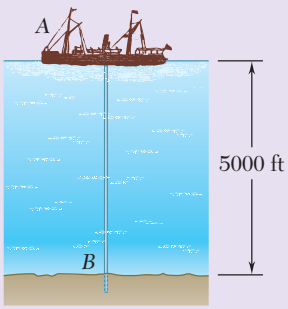


Fig. *P11.125*

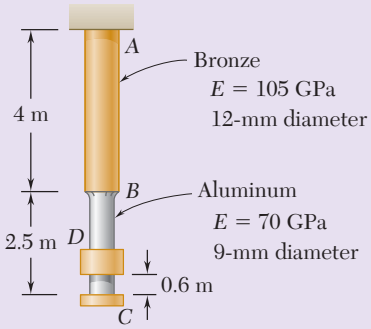


Fig. P11.126

11.126 Collar D is released from rest in the position shown and is stopped by a small plate attached at end C of the vertical rod ABC. Determine the mass of the collar for which the maximum normal stress in portion BC is 125 MPa.

11.127 Each member of the truss shown is made of steel and has a cross-sectional area of 400 mm^2. Using E = 200 GPa, determine the deflection of point D caused by the 16-kN load.

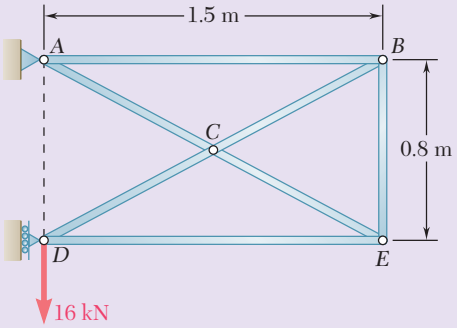


Fig. *P11.127*

11.128 A block of weight W is placed in contact with a beam at some given point D and released. Show that the resulting maximum deflection at point D is twice as large as the deflection due to a static load W applied at D.

11.129 Two solid steel shafts are connected by the gears shown. Using the method of work and energy, determine the angle through which end D rotates when $T = 820$ N · m. Use $G = 77.2$ GPa.

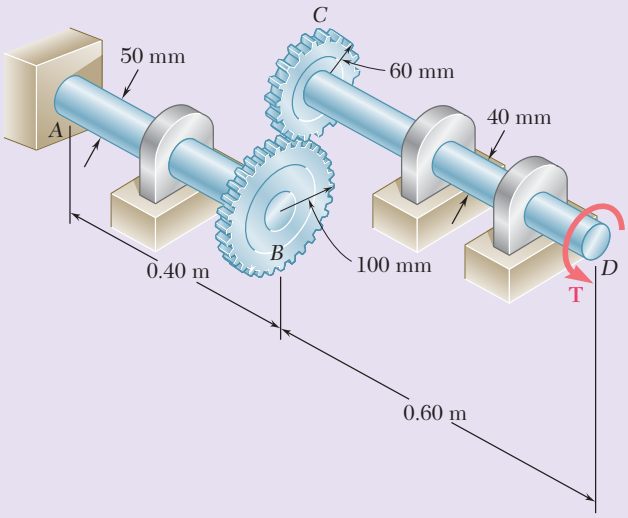


Fig. P11.129

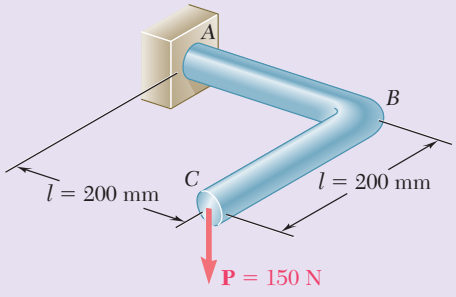


Fig. P11.130

11.130 The 12-mm-diameter steel rod ABC has been bent into the shape shown. Knowing that $E = 200$ GPa and $G = 77.2$ GPa, determine the deflection of end C caused by the 150-N force.

11.131 For the prismatic beam shown, determine the slope at point D.

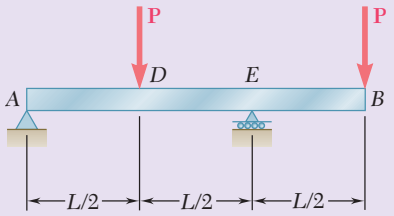


Fig. P11.131

11.132 A disk of radius a has been welded to end B of the solid steel shaft AB. A cable is then wrapped around the disk and a vertical force **P** is applied to end C of the cable. Knowing that the radius of the shaft is L and neglecting the deformations of the disk and of the cable, show that the deflection of point C caused by the application of **P** is

$$\delta_c = \frac{PL^3}{3EI}\left(1 + 1.5\frac{Ea^2}{GL^2}\right)$$

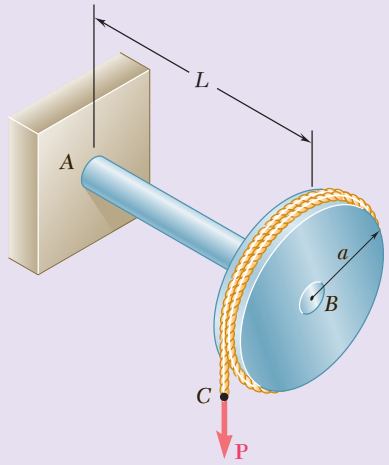


Fig. P11.132

11.133 A uniform rod of flexural rigidity EI is bent and loaded as shown. Determine (*a*) the horizontal deflection of point D, (*b*) the slope at point D.

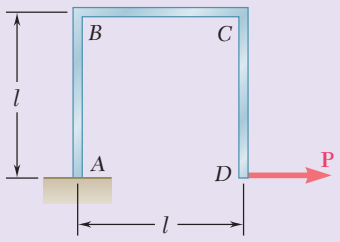


Fig. P11.133

11.134 The steel bar ABC has a square cross section of side 0.75 in. and is subjected to a 50-lb load **P**. Using $E = 29 \times 10^6$ psi for rod BD and the bar, determine the deflection of point C.

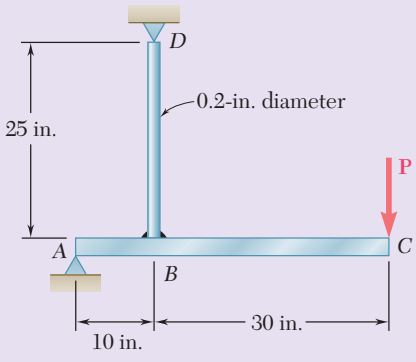


Fig. P11.134

Computer Problems

The following problems are designed to be solved with a computer.

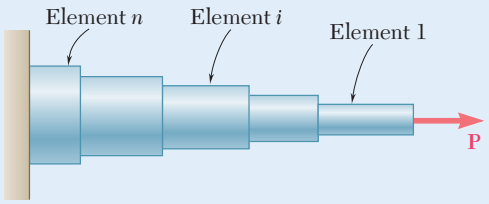


Fig. P11.C1

11.C1 A rod consisting of n elements, each of which is homogeneous and of uniform cross section, is subjected to a load **P** applied at its free end. The length of element i is denoted by L_i and its diameter by d_i. (*a*) Denoting by E the modulus of elasticity of the material used in the rod, write a computer program that can be used to determine the strain energy acquired by the rod and the deformation measured at its free end. (*b*) Use this program to determine the strain energy and deformation for the rods of Probs. 11.9 and 11.10.

11.C2 Two 0.75 × 6-in. cover plates are welded to a W8 × 18 rolled-steel beam as shown. The 1500-lb block is to be dropped from a height $h = 2$ in. onto the beam. (*a*) Write a computer program to calculate the maximum normal stress on transverse sections just to the left of D and at the center of the beam for values of a from 0 to 60 in. using 5-in. increments. (*b*) From the values considered in part *a*, select the distance a for which the maximum normal stress is as small as possible. Use $E = 29 \times 10^6$ psi.

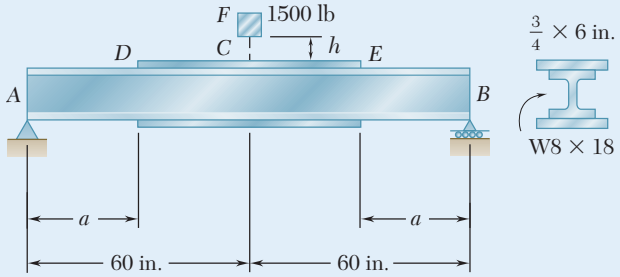


Fig. P11.C2

11.C3 The 16-kg block D is dropped from a height h onto the free end of the steel bar AB. For the steel used $\sigma_{all} = 120$ MPa and $E = 200$ GPa. (*a*) Write a computer program to calculate the maximum allowable height h for values of the length L from 100 mm to 1.2 m, using 100-mm increments. (*b*) From the values considered in part *a*, select the length corresponding to the largest allowable height.

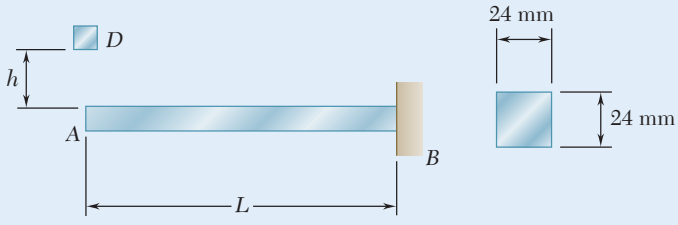


Fig. P11.C3

11.C4 The block D of mass $m = 8$ kg is dropped from a height $h = 750$ mm onto the rolled-steel beam AB. Knowing that $E = 200$ GPa, write a computer program to calculate the maximum deflection of point E and the maximum normal stress in the beam for values of a from 100 to 900 mm 900 mm, using 100-mm increments.

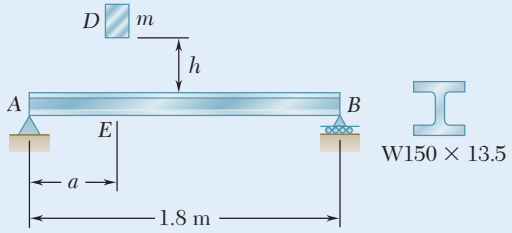


Fig. P11.C4

11.C5 The steel rods AB and BC are made of a steel for which $\sigma_Y = 300$ MPa and $E = 200$ GPa. (a) Write a computer program to calculate for values of a from 0 to 6 m, using 1-m increments, the maximum strain energy that can be acquired by the assembly without causing any permanent deformation. (b) For each value of a considered, calculate the diameter of a uniform rod of length 6 m and of the same mass as the original assembly, and the maximum strain energy that could be acquired by this uniform rod without causing permanent deformation.

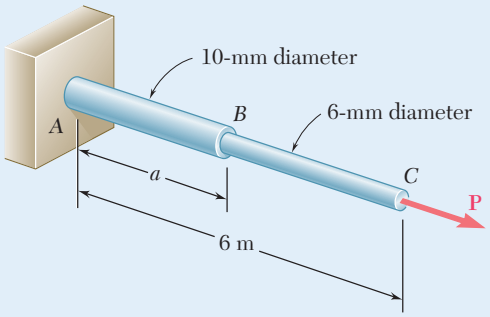


Fig. P11.C5

11.C6 A 160-lb diver jumps from a height of 20 in. onto end C of a diving board having the uniform cross section shown. Write a computer program to calculate for values of a from 10 to 50 in., using 10-in. increments, (a) the maximum deflection of point C, (b) the maximum bending moment in the board, (c) the equivalent static load. Assume that the diver's legs remain rigid and use $E = 1.8 \times 10^6$ psi.

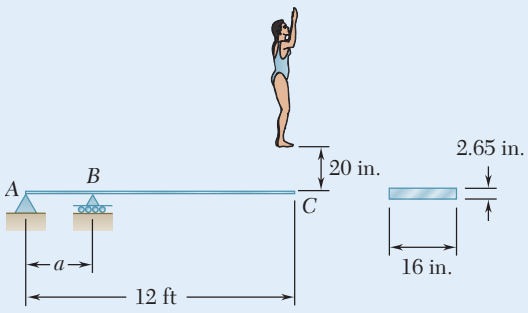


Fig. P11.C6

This page intentionally left blank

Appendices

Appendix A Moments of Areas A2

Appendix B Typical Properties of Selected Materials Used in Engineering A13

Appendix C Properties of Rolled-Steel Shapes† A17

Appendix D Beam Deflections and Slopes A29

Appendix E Fundamentals of Engineering Examination A30

†Courtesy of the American Institute of Steel Construction, Chicago, Illinois.

APPENDIX

A Moments of Areas

A.1 First Moment of an Area and Centroid of an Area

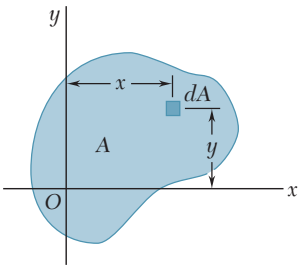


Fig. A.1 General area A with infinitesimal area dA referred to xy coordinate system.

Consider an area A located in the xy plane (Fig. A.1). Using x and y as the coordinates of an element of area dA, the *first moment of the area A with respect to the x axis* is the integral

$$Q_x = \int_A y\,dA \tag{A.1}$$

Similarly, the *first moment of the area A with respect to the y axis* is the integral

$$Q_y = \int_A x\,dA \tag{A.2}$$

Note that each of these integrals may be positive, negative, or zero, depending on the position of the coordinate axes. When SI units are used, the first moments Q_x and Q_y are given in m^3 or mm^3. When U.S. customary units are used, they are given in ft^3 or in^3.

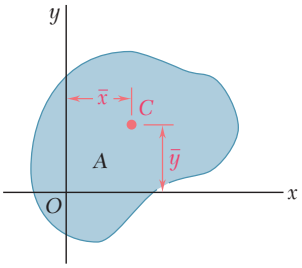


Fig. A.2 Centroid of area A.

The *centroid of the area A* is the point C of coordinates $\bar{x}$ and $\bar{y}$ (Fig. A.2), which satisfy the relationship

$$\int_A x\,dA = A\bar{x} \qquad \int_A y\,dA = A\bar{y} \tag{A.3}$$

Comparing Eqs. (A.1) and (A.2) with Eqs. (A.3), the first moments of the area A can be expressed as the products of the area and the coordinates of its centroid:

$$Q_x = A\bar{y} \qquad Q_y = A\bar{x} \tag{A.4}$$

When an area possesses an *axis of symmetry,* the first moment of the area with respect to that axis is zero. Considering area A of Fig. A.3, which is symmetric with respect to the y axis, every element of area dA of

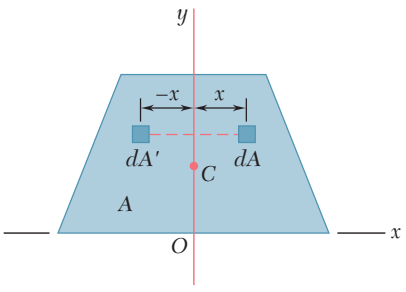


Fig. A.3 Area having axis of symmetry.

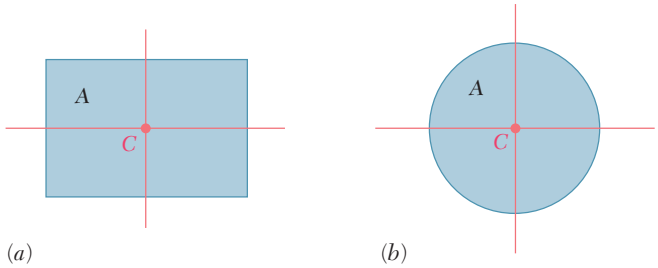


Fig. A.4 Areas having two axes of symmetry have the centroid at their intersection.

abscissa x corresponds to an element of area dA' of abscissa $-x$. Therefore, the integral in Eq. (A.2) is zero, and $Q_y = 0$. From the first of the relationships in Eq. (A.3), $\bar{x} = 0$. Thus, if an area A possesses an axis of symmetry, its centroid C is located on that axis.

Since a rectangle possesses two axes of symmetry (Fig. A.4*a*), the centroid C of a rectangular area coincides with its geometric center. Similarly, the centroid of a circular area coincides with the center of the circle (Fig. A.4*b*).

When an area possesses a *center of symmetry* O, the first moment of the area about any axis through O is zero. Considering the area A of Fig. A.5, every element of area dA with coordinates x and y corresponds to an element of area dA' with coordinates $-x$ and $-y$. It follows that the integrals in Eqs. (A.1) and (A.2) are both zero, and $Q_x = Q_y = 0$. From Eqs. (A.3), $\bar{x} = \bar{y} = 0$, so the centroid of the area coincides with its center of symmetry.

When the centroid C of an area can be located by symmetry, the first moment of that area with respect to any given axis can be obtained easily from Eqs. (A.4). For example, for the rectangular area of Fig. A.6,

$$Q_x = A\bar{y} = (bh)(\tfrac{1}{2}h) = \tfrac{1}{2}bh^2$$

and

$$Q_y = A\bar{x} = (bh)(\tfrac{1}{2}b) = \tfrac{1}{2}b^2h$$

In most cases, it is necessary to perform the integrations indicated in Eqs. (A.1) through (A.3) to determine the first moments and the centroid of a given area. While each of the integrals is actually a double integral, it is possible to select elements of area dA in the shape of thin horizontal or vertical strips and to reduce the equations to integrations in a single variable. This is illustrated in Concept Application A.1. Centroids of common geometric shapes are given in a table inside the back cover.

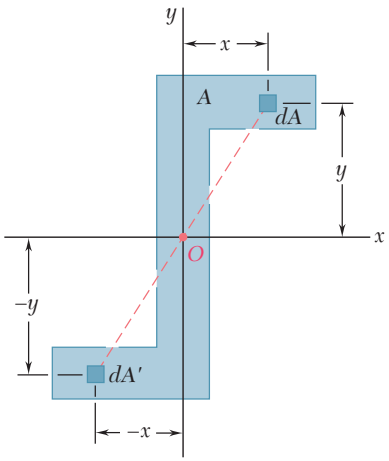


Fig. A.5 Area with center of symmetry has its centroid at the origin.

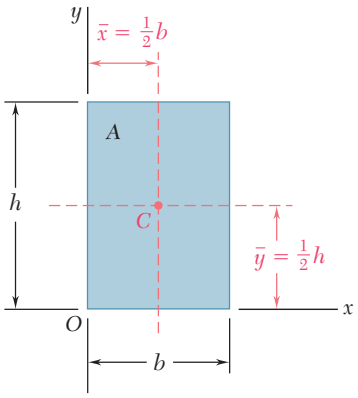


Fig. A.6 Centroid of a rectangular area.

Concept Application A.1

For the triangular area of Fig. A.7*a*, determine (*a*) the first moment Q_x of the area with respect to the x axis, (*b*) the ordinate $\bar{y}$ of the centroid of the area.

a. First Moment Q_x. We choose to select as an element of area a horizontal strip with a length of u and thickness dy. Note that all of the points within the element are at the same distance y from the x axis (Fig. A.7*b*). From similar triangles,

$$\frac{u}{b} = \frac{h - y}{h} \qquad u = b\frac{h - y}{h}$$

and

$$dA = u\,dy = b\frac{h - y}{h}\,dy$$

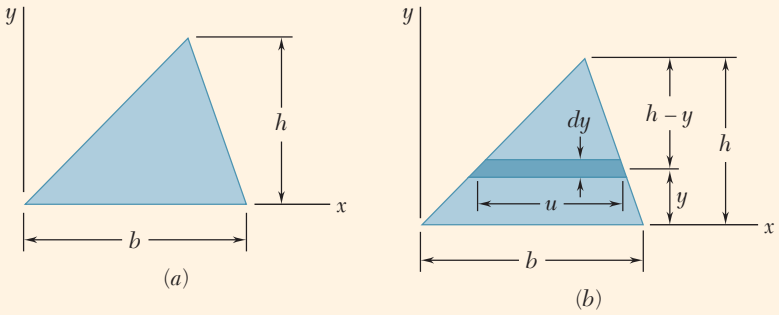


Fig. A.7 (*a*) Triangular area. (*b*) Horizontal element used in integration to find centroid.

The first moment of the area with respect to the x axis is

$$Q_x = \int_A y\,dA = \int_0^h yb\frac{h - y}{h}\,dy = \frac{b}{h}\int_0^h (hy - y^2)\,dy$$

$$= \frac{b}{h}\left[h\frac{y^2}{2} - \frac{y^3}{3}\right]_0^h \qquad Q_x = \tfrac{1}{6}bh^2$$

b. Ordinate of Centroid. Recalling the first of Eqs. (A.4) and observing that $A = \frac{1}{2}bh$,

$$Q_x = A\bar{y} \qquad \tfrac{1}{6}bh^2 = (\tfrac{1}{2}bh)\bar{y}$$

$$\bar{y} = \tfrac{1}{3}h$$

A.2 The First Moment and Centroid of a Composite Area

Consider area A of the quadrilateral area shown in Fig. A.8, which can be divided into simple geometric shapes. The first moment Q_x of the area with respect to the x axis is represented by the integral $\int y\,dA$, which extends over the entire area A. Dividing A into its component parts A_1, A_2, A_3, write

$$Q_x = \int_A y\,dA = \int_{A_1} y\,dA + \int_{A_2} y\,dA + \int_{A_3} y\,dA$$

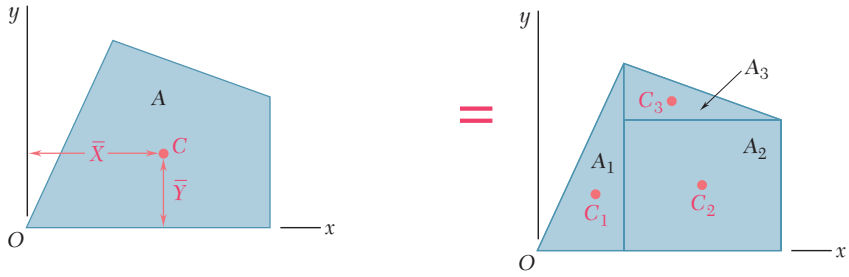


Fig. A.8 Quadrilateral area divided into simple geometric shapes.

or recalling the second of Eqs. (A.3),

$$Q_x = A_1\bar{y}_1 + A_2\bar{y}_2 + A_3\bar{y}_3$$

where $\bar{y}_1, \bar{y}_2$, and $\bar{y}_3$ represent the ordinates of the centroids of the component areas. Extending this to an arbitrary number of component areas and noting that a similar expression for Q_y may be obtained, write

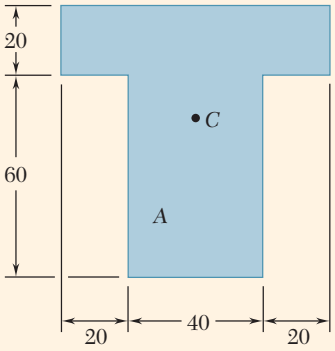
$$Q_x = \sum A_i\bar{y}_i \quad Q_y = \sum A_i\bar{x}_i \tag{A.5}$$

To obtain the coordinates $\bar{X}$ and $\bar{Y}$ of the centroid C of the composite area A, substitute $Q_x = A\bar{Y}$ and $Q_y = A\bar{X}$ into Eqs. (A.5):

$$A\bar{Y} = \sum_i A_i\bar{y}_i \quad A\bar{X} = \sum_i A_i\bar{x}_i$$

Solving for $\bar{X}$ and $\bar{Y}$ and recalling that the area A is the sum of the component areas A_i,

$$\bar{X} = \frac{\sum_i A_i\bar{x}_i}{\sum_i A_i} \quad \bar{Y} = \frac{\sum_i A_i\bar{y}_i}{\sum_i A_i} \tag{A.6}$$



Concept Application A.2

Locate the centroid C of the area A shown in Fig. A.9*a*.

Selecting the coordinate axes shown in Fig. A.9*b*, note that the centroid C must be located on the y axis, since this is an axis of symmetry. Thus, $\bar{X} = 0$.

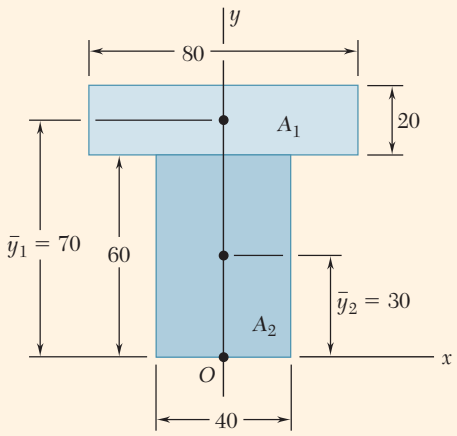
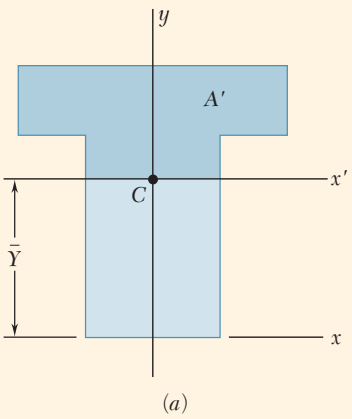


Fig. A.9 (*a*) Area *A*. (*b*) Composite areas A_1 and A_2 used to determine overall centroid.

Divide A into its component parts A_1 and A_2 and use the second of Eqs. (A.6) to determine the ordinate $\bar{Y}$ of the centroid. The actual computation is best carried out in tabular form:

	Area, mm^2	$\bar{y}_i$, mm	$A_i\bar{y}_i$, mm^3
A_1	$(20)(80) = 1600$	70	112×10^3
A_2	$(40)(60) = 2400$	30	72×10^3
	$\sum_i A_i = 4000$		$\sum_i A_i\bar{y}_i = 184 \times 10^3$

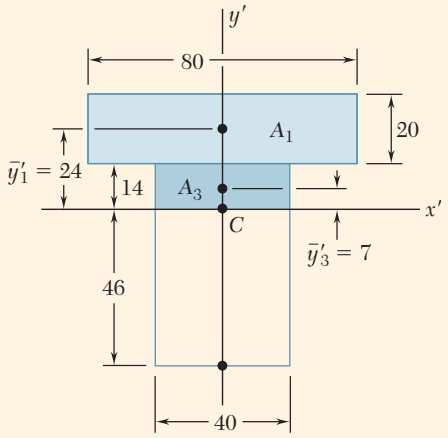
$$\bar{Y} = \frac{\sum_i A_i\bar{y}_i}{\sum_i A_i} = \frac{184 \times 10^3 \text{ mm}^3}{4 \times 10^3 \text{ mm}^2} = 46 \text{ mm}$$



(*a*)

Concept Application A.3

Referring to the area A of Concept Application A.2, consider the horizontal x' axis through its centroid C (called a *centroidal axis*). The portion of A located above that axis is A' (Fig. A.10*a*). Determine the first moment of A' with respect to the x' axis.



Dimensions in mm

(*b*)

Solution. Divide the area A' into its components A_1 and A_3 (Fig. A.10*b*). Recall from Concept Application A.2 that C is located 46 mm above the lower edge of A. The ordinates $\bar{y}'_1$ and $\bar{y}'_3$ of A_1 and A_3 and the first moment $Q'_{x'}$ of A' with respect to x' are

$$Q'_{x'} = A_1\bar{y}'_1 + A_3\bar{y}'_3$$
$$= (20 \times 80)(24) + (14 \times 40)(7) = 42.3 \times 10^3\,\text{mm}^3$$

Alternative Solution. Since the centroid C of A is located on the x' axis, the first moment $Q_{x'}$ of the *entire area* A with respect to that axis is zero:

$$Q_{x'} = A\bar{y}' = A(0) = 0$$

Using A'' as the portion of A located below the x' axis and $Q''_{x'}$ as its first moment with respect to that axis,

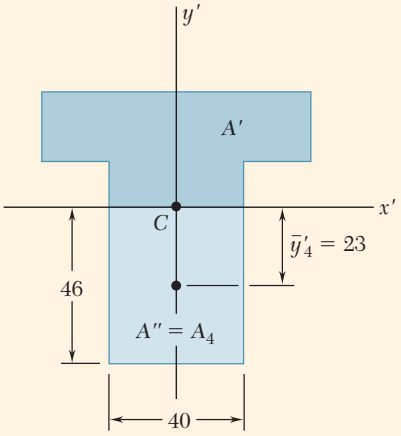
$$Q_{x'} = Q'_{x'} + Q''_{x'} = 0 \quad \text{or} \quad Q'_{x'} = -Q''_{x'}$$

This shows that the first moments of A' and A'' have the same magnitude and opposite signs. Referring to Fig. A.10*c*, write

$$Q''_{x'} = A_4\bar{y}'_4 = (40 \times 46)(-23) = -42.3 \times 10^3\,\text{mm}^3$$

and

$$Q'_{x'} = -Q''_{x'} = +42.3 \times 10^3\,\text{mm}^3$$



Dimensions in mm

(*c*)

Fig. A.10 (*a*) Area A with centroidal $x'y'$ axes, highlighting portion A'. (*b*) Areas used to determine the first moment of area A' with respect to the x' axis. (*c*) Alternative solution using the other portion A'' of the total area A.

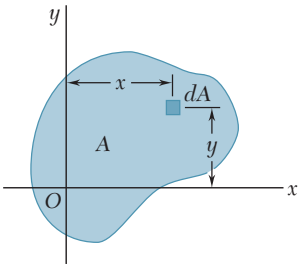


Fig. A.1 (*repeated*)

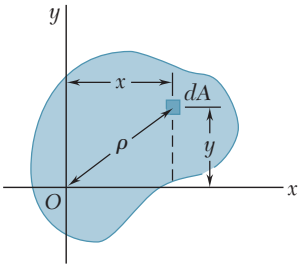


Fig. A.11 Area *dA* located by distance ρ from point *O*.

A.3 Second Moment, or Moment of Inertia of an Area, and Radius of Gyration

Consider an area A located in the xy plane (Fig. A.1) and the element of area dA of coordinates x and y. The *second moment,* or *moment of inertia,* of area A with respect to the x and y axes is

$$I_x = \int_A y^2\,dA \quad I_y = \int_A x^2\,dA \tag{A.7}$$

These integrals are called *rectangular moments of inertia,* since they are found from the rectangular coordinates of element dA. While each integral is actually a double integral, it is possible to select elements of area dA in the shape of thin horizontal or vertical strips and to reduce the equations to integrations in a single variable. This is illustrated in Concept Application A.4.

The *polar moment of inertia* of area A with respect to point O (Fig. A.11) is the integral

$$J_O = \int_A \rho^2\,dA \tag{A.8}$$

where ρ is the distance from O to the element dA. While this integral is also a double integral, for circular areas it is possible to select elements of area dA in the shape of thin circular rings and to reduce the equation of J_O to a single integration (see Concept Application A.5).

Note from Eqs. (A.7) and (A.8) that the moments of inertia of an area are positive quantities. When SI units are used, moments of inertia are given in m^4 or mm^4. When U.S. customary units are used, they are given in ft^4 or in^4.

An important relationship can be established between the polar moment of inertia J_O of a given area and the rectangular moments of inertia I_x and I_y. Noting that $\rho^2 = x^2 + y^2$,

$$J_O = \int_A \rho^2\,dA = \int_A (x^2 + y^2)\,dA = \int_A y^2\,dA + \int_A x^2\,dA$$

or

$$J_O = I_x + I_y \tag{A.9}$$

The *radius of gyration* of an area A with respect to the x axis is r_x, which satisfies the relationship

$$I_x = r_x^2 A \tag{A.10}$$

where I_x is the moment of inertia of A with respect to the x axis. Solving Eq. (A.10) for r_x,

$$r_x = \sqrt{\frac{I_x}{A}} \tag{A.11}$$

The radii of gyration with respect to the y axis and the origin O are

$$I_y = r_y^2 A \qquad r_y = \sqrt{\frac{I_y}{A}} \tag{A.12}$$

$$J_O = r_O^2 A \qquad r_O = \sqrt{\frac{J_O}{A}} \tag{A.13}$$

Substituting for J_O, I_x, and I_y in terms of the corresponding radii of gyration in Eq. (A.9),

$$r_O^2 = r_x^2 + r_y^2 \tag{A.14}$$

The results obtained in the following two Concept Applications are included in the table for moments of inertias of common geometric shapes, located inside the back cover of this book.

Concept Application A.4

For the rectangular area of Fig. A.12*a*, determine (*a*) the moment of inertia I_x of the area with respect to the centroidal x axis, (*b*) the corresponding radius of gyration r_x.

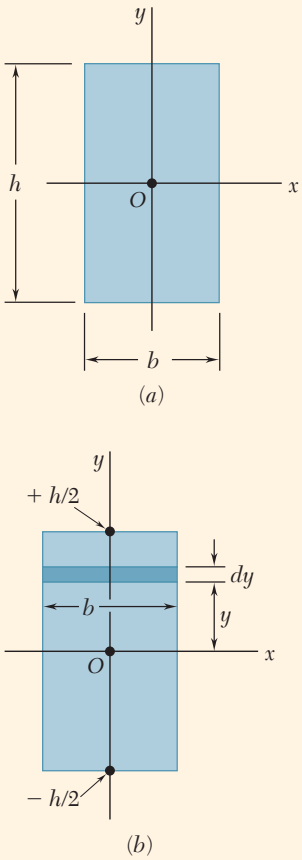


Fig. A.12 (*a*) Rectangular area. (*b*) Horizontal strip used to determine moment of inertia I_x.

a. Moment of Inertia I_x. We choose to select a horizontal strip of length b and thickness dy (Fig. A.12*b*). Since all of the points within the strip are at the same distance y from the x axis, the moment of inertia of the strip with respect to that axis is

$$dI_x = y^2\,dA = y^2(b\,dy)$$

Integrating from $y = -h/2$ to $y = +h/2$,

$$I_x = \int_A y^2\,dA = \int_{-h/2}^{+h/2} y^2(b\,dy) = \tfrac{1}{3}b[y^3]_{-h/2}^{+h/2}$$

$$= \tfrac{1}{3}b\left(\frac{h^3}{8} + \frac{h^3}{8}\right)$$

or

$$I_x = \tfrac{1}{12}bh^3$$

b. Radius of Gyration r_x. From Eq. (A.10),

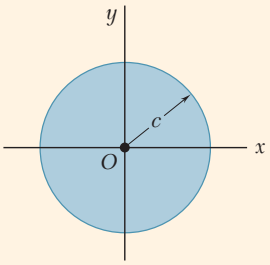
$$I_x = r_x^2 A \quad \tfrac{1}{12}bh^3 = r_x^2(bh)$$

and solving for r_x gives

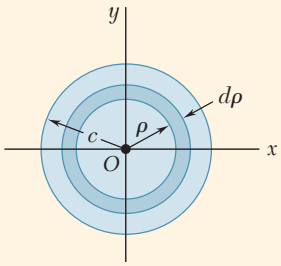
$$r_x = h/\sqrt{12}$$

Concept Application A.5

For the circular area of Fig. A.13*a*, determine (*a*) the polar moment of inertia J_O, (*b*) the rectangular moments of inertia I_x and I_y.



(*a*)



(*b*)

Fig. A.13 (*a*) Circular area. (*b*) Annular strip used to determine polar moment of inertia J_O.

a. Polar Moment of Inertia. We choose to select as an element of area a ring of radius ρ with a thickness $d\rho$ (Fig. A.13*b*). Since all of the points within the ring are at the same distance ρ from the origin O, the polar moment of inertia of the ring is

$$dJ_O = \rho^2\, dA = \rho^2(2\pi\rho\, d\rho)$$

Integrating in ρ from 0 to c,

$$J_O = \int_A \rho^2\, dA = \int_0^c \rho^2(2\pi\rho\, d\rho) = 2\pi \int_0^c \rho^3\, d\rho$$

$$J_O = \tfrac{1}{2}\pi c^4$$

b. Rectangular Moments of Inertia. Because of the symmetry of the circular area, $I_x = I_y$. Recalling Eq. (A.9), write

$$J_O = I_x + I_y = 2I_x \quad \tfrac{1}{2}\pi c^4 = 2I_x$$

and,

$$I_x = I_y = \tfrac{1}{4}\pi c^4$$

A.4 Parallel-Axis Theorem

Consider the moment of inertia I_x of an area A with respect to an arbitrary x axis (Fig. A.14). Using y as the distance from an element of area dA to that axis, recall from Sec. A.3 that

$$I_x = \int_A y^2\, dA$$

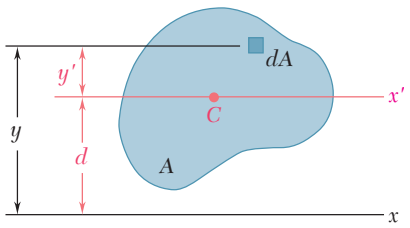


Fig. A.14 General area with centroidal x' axis, parallel to arbitrary x axis.

We now draw the *centroidal x′ axis,* which is the axis parallel to the x axis that passes through the centroid C. Using y' as the distance from element dA

to that axis, $y = y' + d$, where d is the distance between the two axes. Substituting for y in the integral representing I_x gives

$$I_x = \int_A y^2\,dA = \int_A (y' + d)^2 dA$$

$$I_x = \int_A y'^2\,dA + 2d\int_A y'\,dA + d^2\int_A dA \qquad \textbf{(A.15)}$$

The first integral in Eq. (A.15) represents the moment of inertia $\bar{I}_{x'}$ of the area with respect to the centroidal x' axis. The second integral represents the first moment $Q_{x'}$ of the area with respect to the x' axis and is equal to zero, since the centroid C of the area is located on that axis. In other words, recalling from Sec. A.1 we write

$$Q_{x'} = A\bar{y}' = A(0) = 0$$

The last integral in Eq. (A.15) is equal to the total area A. Therefore,

$$I_x = \bar{I}_{x'} + Ad^2 \qquad \textbf{(A.16)}$$

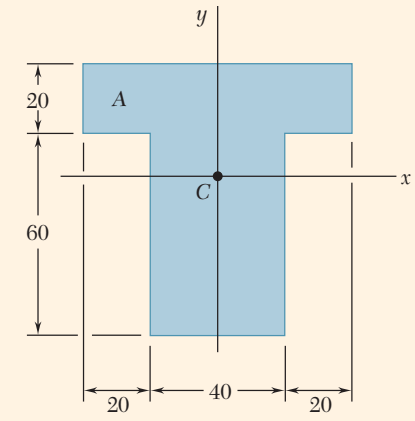
This equation shows that the moment of inertia I_x of an area with respect to an arbitrary x axis is equal to the moment of inertia $\bar{I}_{x'}$ of the area with respect to the centroidal x' axis parallel to the x axis *plus* the product Ad^2 of the area A and of the square of the distance d between the two axes. This result is known as the *parallel-axis theorem*. With this theorem, the moment of inertia of an area with respect to a given axis can be determined when its moment of inertia with respect to a centroidal axis of the same direction is known. Conversely, it makes it possible to determine the moment of inertia $\bar{I}_{x'}$ of an area A with respect to a centroidal axis x' when the moment of inertia I_x of A with respect to a parallel axis is known. This is done by *subtracting* from I_x the product Ad^2. Note that the parallel-axis theorem may be used *only if one of the two axes involved is a centroidal axis.*

A similar formula relates the polar moment of inertia J_O of an area with respect to an arbitrary point O and the polar moment of inertia $\bar{J}_C$ of the same area with respect to its centroid C. Using d as the distance between O and C,

$$J_O = \bar{J}_C + Ad^2 \qquad \textbf{(A.17)}$$

A.5 Moment of Inertia of a Composite Area

Consider a composite area A made of several component parts A_1, A_2, and so forth. Since the integral for the moment of inertia of A can be subdivided into integrals extending over A_1, A_2, etc. the moment of inertia of A with respect to a given axis is obtained by adding the moments of inertia of the areas A_1, A_2, etc. with respect to the same axis. The moment of inertia of an area made of several common shapes may be found by using the formulas shown in the inside back cover of this book. Before adding the moments of inertia of the component areas, the parallel-axis theorem should be used to transfer each moment of inertia to the desired axis. This is shown in Concept Application A.6.



Concept Application A.6

Determine the moment of inertia $\bar{I}_x$ of the area shown with respect to the centroidal x axis (Fig. A.15*a*).

Location of Centroid. The centroid C of the area has been located in Concept Application A.2 for the given area. From this, C is located 46 mm above the lower edge of area A.

Computation of Moment of Inertia. Area A is divided into two rectangular areas A_1 and A_2 (Fig. A.15*b*), and the moment of inertia of each area is found with respect to the x axis.

Rectangular Area A_1. To obtain the moment of inertia $(I_x)_1$ of A_1 with respect to the x axis, first compute the moment of inertia of A_1 *with respect to its own centroidal axis* x'. Recalling the equation in part *a* of Concept Application A.4 for the centroidal moment of inertia of a rectangular area,

$$(\bar{I}_{x'})_1 = \tfrac{1}{12}bh^3 = \tfrac{1}{12}(80\text{ mm})(20\text{ mm})^3 = 53.3 \times 10^3\text{ mm}^4$$

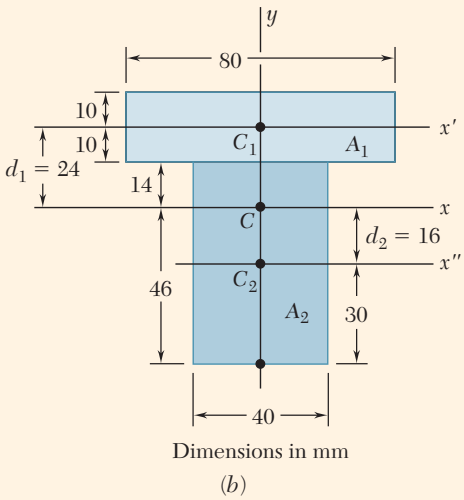


Fig. A.15 (*a*) Area *A*. (*b*) Composite areas and centroids.

Using the parallel-axis theorem, transfer the moment of inertia of A_1 from its centroidal axis x' to the parallel axis x:

$$(I_x)_1 = (\bar{I}_{x'})_1 + A_1 d_1^2 = 53.3 \times 10^3 + (80 \times 20)(24)^2$$
$$= 975 \times 10^3\text{ mm}^4$$

Rectangular Area A_2. Calculate the moment of inertia of A_2 with respect to its centroidal axis x'' and use the parallel-axis theorem to transfer it to the x axis to obtain

$$(\bar{I}_{x''})_2 = \tfrac{1}{12}bh^3 = \tfrac{1}{12}(40)(60)^3 = 720 \times 10^3\text{ mm}^4$$

$$(I_x)_2 = (\bar{I}_{x''})_2 + A_2 d_2^2 = 720 \times 10^3 + (40 \times 60)(16)^2$$

$$= 1334 \times 10^3\text{ mm}^4$$

Entire Area A. Add the values for the moments of inertia of A_1 and A_2 with respect to the x axis to obtain the moment of inertia $\bar{I}_x$ of the entire area:

$$\bar{I}_x = (I_x)_1 + (I_x)_2 = 975 \times 10^3 + 1334 \times 10^3$$

$$\bar{I}_x = 2.31 \times 10^6\text{ mm}^4$$

Appendix B Typical Properties of Selected Materials Used in Engineering[1,5]

(U.S. Customary Units)

Material	Specific Weight, lb/in^3	Ultimate Strength			Yield Strength[3]		Modulus of Elasticity, 10^6 psi	Modulus of Rigidity, 10^6 psi	Coefficient of Thermal Expansion, 10^{-6}/°F	Ductility, Percent Elongation in 2 in.
		Tension, ksi	Compression,[2] ksi	Shear, ksi	Tension, ksi	Shear, ksi				
Steel										
Structural (ASTM-A36)	0.284	58			36	21	29	11.2	6.5	21
High-strength-low-alloy										
ASTM-A709 Grade 50	0.284	65			50		29	11.2	6.5	21
ASTM-A913 Grade 65	0.284	80			65		29	11.2	6.5	17
ASTM-A992 Grade 50	0.284	65			50		29	11.2	6.5	21
Quenched & tempered										
ASTM-A709 Grade 100	0.284	110			100		29	11.2	6.5	18
Stainless, AISI 302										
Cold-rolled	0.286	125			75		28	10.8	9.6	12
Annealed	0.286	95			38	22	28	10.8	9.6	50
Reinforcing Steel										
Medium strength	0.283	70			40		29	11	6.5	
High strength	0.283	90			60		29	11	6.5	
Cast Iron										
Gray Cast Iron										
4.5% C, ASTM A-48	0.260	25	95	35			10	4.1	6.7	0.5
Malleable Cast Iron										
2% C, 1% Si, ASTM A-47	0.264	50	90	48	33		24	9.3	6.7	10
Aluminum										
Alloy 1100-H14 (99% Al)	0.098	16		10	14	8	10.1	3.7	13.1	9
Alloy 2014-T6	0.101	66		40	58	33	10.9	3.9	12.8	13
Alloy 2024-T4	0.101	68		41	47		10.6		12.9	19
Alloy 5456-H116	0.095	46		27	33	19	10.4		13.3	16
Alloy 6061-T6	0.098	38		24	35	20	10.1	3.7	13.1	17
Alloy 7075-T6	0.101	83		48	73		10.4	4	13.1	11
Copper										
Oxygen-free copper (99.9% Cu)										
Annealed	0.322	32		22	10		17	6.4	9.4	45
Hard-drawn	0.322	57		29	53		17	6.4	9.4	4
Yellow Brass (65% Cu, 35% Zn)										
Cold-rolled	0.306	74		43	60	36	15	5.6	11.6	8
Annealed	0.306	46		32	15	9	15	5.6	11.6	65
Red Brass (85% Cu, 15% Zn)										
Cold-rolled	0.316	85		46	63		17	6.4	10.4	3
Annealed	0.316	39		31	10		17	6.4	10.4	48
Tin bronze (88 Cu, 8Sn, 4Zn)	0.318	45			21		14		10	30
Manganese bronze (63 Cu, 25 Zn, 6 Al, 3 Mn, 3 Fe)	0.302	95			48		15		12	20
Aluminum bronze (81 Cu, 4 Ni, 4 Fe, 11 Al)	0.301	90	130		40		16	6.1	9	6

(Table continued on page A14)

Appendix B Typical Properties of Selected Materials Used in Engineering[1,5]

(SI Units)

Material	Density kg/m³	Ultimate Strength			Yield Strength[3]		Modulus of Elasticity, GPa	Modulus of Rigidity, GPa	Coefficient of Thermal Expansion, 10^{-6}/°C	Ductility, Percent Elongation in 50 mm
		Tension, MPa	Compression,[2] MPa	Shear, MPa	Tension, MPa	Shear, MPa				
Steel										
Structural (ASTM-A36)	7860	400			250	145	200	77.2	11.7	21
High-strength-low-alloy										
ASTM-A709 Grade 345	7860	450			345		200	77.2	11.7	21
ASTM-A913 Grade 450	7860	550			450		200	77.2	11.7	17
ASTM-A992 Grade 345	7860	450			345		200	77.2	11.7	21
Quenched & tempered										
ASTM-A709 Grade 690	7860	760			690		200	77.2	11.7	18
Stainless, AISI 302										
Cold-rolled	7920	860			520		190	75	17.3	12
Annealed	7920	655			260	150	190	75	17.3	50
Reinforcing Steel										
Medium strength	7860	480			275		200	77	11.7	
High strength	7860	620			415		200	77	11.7	
Cast Iron										
Gray Cast Iron										
4.5% C, ASTM A-48	7200	170	655	240			69	28	12.1	0.5
Malleable Cast Iron										
2% C, 1% Si, ASTM A-47	7300	345	620	330	230		165	65	12.1	10
Aluminum										
Alloy 1100-H14 (99% Al)	2710	110		70	95	55	70	26	23.6	9
Alloy 2014-T6	2800	455		275	400	230	75	27	23.0	13
Alloy-2024-T4	2800	470		280	325		73		23.2	19
Alloy-5456-H116	2630	315		185	230	130	72		23.9	16
Alloy 6061-T6	2710	260		165	240	140	70	26	23.6	17
Alloy 7075-T6	2800	570		330	500		72	28	23.6	11
Copper										
Oxygen-free copper (99.9% Cu)										
Annealed	8910	220		150	70		120	44	16.9	45
Hard-drawn	8910	390		200	265		120	44	16.9	4
Yellow-Brass (65% Cu, 35% Zn)										
Cold-rolled	8470	510		300	410	250	105	39	20.9	8
Annealed	8470	320		220	100	60	105	39	20.9	65
Red Brass (85% Cu, 15% Zn)										
Cold-rolled	8740	585		320	435		120	44	18.7	3
Annealed	8740	270		210	70		120	44	18.7	48
Tin bronze (88 Cu, 8Sn, 4Zn)	8800	310			145		95		18.0	30
Manganese bronze (63 Cu, 25 Zn, 6 Al, 3 Mn, 3 Fe)	8360	655			330		105		21.6	20
Aluminum bronze (81 Cu, 4 Ni, 4 Fe, 11 Al)	8330	620	900		275		110	42	16.2	6

(Table continued on page A15

Appendix B Typical Properties of Selected Materials Used in Engineering[1,5]

(U.S. Customary Units)

Continued from page A14

Material	Specific Weight, lb/in^3	Ultimate Strength			Yield Strength[3]		Modulus of Elasticity, 10^6 psi	Modulus of Rigidity, 10^6 psi	Coefficient of Thermal Expansion, 10^{-6}/°F	Ductility, Percent Elongation in 2 in.
		Tension, ksi	Compression,[2] ksi	Shear, ksi	Tension, ksi	Shear, ksi				
Magnesium Alloys										
Alloy AZ80 (Forging)	0.065	50		23	36		6.5	2.4	14	6
Alloy AZ31 (Extrusion)	0.064	37		19	29		6.5	2.4	14	12
Titanium										
Alloy (6% Al, 4% V)	0.161	130			120		16.5		5.3	10
Monel Alloy 400(Ni-Cu)										
Cold-worked	0.319	98			85	50	26		7.7	22
Annealed	0.319	80			32	18	26		7.7	46
Cupronickel (90% Cu, 10% Ni)										
Annealed	0.323	53			16		20	7.5	9.5	35
Cold-worked	0.323	85			79		20	7.5	9.5	3
Timber, air dry										
Douglas fir	0.017	15	7.2	1.1			1.9	.1	Varies	
Spruce, Sitka	0.015	8.6	5.6	1.1			1.5	.07	1.7 to 2.5	
Shortleaf pine	0.018		7.3	1.4			1.7			
Western white pine	0.014		5.0	1.0			1.5			
Ponderosa pine	0.015	8.4	5.3	1.1			1.3			
White oak	0.025		7.4	2.0			1.8			
Red oak	0.024		6.8	1.8			1.8			
Western hemlock	0.016	13	7.2	1.3			1.6			
Shagbark hickory	0.026		9.2	2.4			2.2			
Redwood	0.015	9.4	6.1	0.9			1.3			
Concrete										
Medium strength	0.084		4.0				3.6		5.5	
High strength	0.084		6.0				4.5		5.5	
Plastics										
Nylon, type 6/6, (molding compound)	0.0412	11	14		6.5		0.4		80	50
Polycarbonate	0.0433	9.5	12.5		9		0.35		68	110
Polyester, PBT (thermoplastic)	0.0484	8	11		8		0.35		75	150
Polyester elastomer	0.0433	6.5		5.5			0.03			500
Polystyrene	0.0374	8	13		8		0.45		70	2
Vinyl, rigid PVC	0.0520	6	10		6.5		0.45		75	40
Rubber	0.033	2							90	600
Granite (Avg. values)	0.100	3	35	5			10	4	4	
Marble (Avg. values)	0.100	2	18	4			8	3	6	
Sandstone (Avg. values)	0.083	1	12	2			6	2	5	
Glass, 98% silica	0.079		7				9.6	4.1	44	

[1]Properties of metals vary widely as a result of variations in composition, heat treatment, and mechanical working.
[2]For ductile metals the compression strength is generally assumed to be equal to the tension strength.
[3]Offset of 0.2 percent.
[4]Timber properties are for loading parallel to the grain.
[5]See also *Marks' Mechanical Engineering Handbook,* 10th ed., McGraw-Hill, New York, 1996; *Annual Book of ASTM,* American Society for Testing Materials, Philadelphia, Pa.; *Metals Handbook,* American Society for Metals, Metals Park, Ohio; and *Aluminum Design Manual,* The Aluminum Association, Washington, DC.

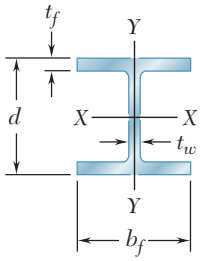
Appendix B Typical Properties of Selected Materials Used in Engineering[1,5]

(SI Units)

Continued from page A15

Material	Density kg/m³	Ultimate Strength: Tension, MPa	Ultimate Strength: Compression,[2] MPa	Ultimate Strength: Shear, MPa	Yield Strength[3]: Tension, MPa	Yield Strength[3]: Shear, MPa	Modulus of Elasticity, GPa	Modulus of Rigidity, GPa	Coefficient of Thermal Expansion, 10^{-6}/°C	Ductility, Percent Elongation in 50 mm
Magnesium Alloys										
Alloy AZ80 (Forging)	1800	345		160	250		45	16	25.2	6
Alloy AZ31 (Extrusion)	1770	255		130	200		45	16	25.2	12
Titanium										
Alloy (6% Al, 4% V)	4730	900			830		115		9.5	10
Monel Alloy 400(Ni-Cu)										
Cold-worked	8830	675			585	345	180		13.9	22
Annealed	8830	550			220	125	180		13.9	46
Cupronickel (90% Cu, 10% Ni)										
Annealed	8940	365			110		140	52	17.1	35
Cold-worked	8940	585			545		140	52	17.1	3
Timber, air dry										
Douglas fir	470	100	50	7.6			13	0.7	Varies	
Spruce, Sitka	415	60	39	7.6			10	0.5	3.0 to 4.5	
Shortleaf pine	500		50	9.7			12			
Western white pine	390		34	7.0			10			
Ponderosa pine	415	55	36	7.6			9			
White oak	690		51	13.8			12			
Red oak	660		47	12.4			12			
Western hemlock	440	90	50	10.0			11			
Shagbark hickory	720		63	16.5			15			
Redwood	415	65	42	6.2			9			
Concrete										
Medium strength	2320		28				25		9.9	
High strength	2320		40				30		9.9	
Plastics										
Nylon, type 6/6, (molding compound)	1140	75	95		45		2.8		144	50
Polycarbonate	1200	65	85		35		2.4		122	110
Polyester, PBT (thermoplastic)	1340	55	75		55		2.4		135	150
Polyester elastomer	1200	45		40			0.2			500
Polystyrene	1030	55	90		55		3.1		125	2
Vinyl, rigid PVC	1440	40	70		45		3.1		135	40
Rubber	910	15							162	600
Granite (Avg. values)	2770	20	240	35			70	4	7.2	
Marble (Avg. values)	2770	15	125	28			55	3	10.8	
Sandstone (Avg. values)	2300	7	85	14			40	2	9.0	
Glass, 98% silica	2190		50				65	4.1	80	

[1]Properties of metals very widely as a result of variations in composition, heat treatment, and mechanical working.
[2]For ductile metals the compression strength is generally assumed to be equal to the tension strength.
[3]Offset of 0.2 percent.
[4]Timber properties are for loading parallel to the grain.
[5]See also *Marks' Mechanical Engineering Handbook,* 10th ed., McGraw-Hill, New York, 1996; *Annual Book of ASTM,* American Society for Testing Materials, Philadelphia, Pa.; *Metals Handbook,* American Society of Metals, Metals Park, Ohio; and *Aluminum Design Manual,* The Aluminum Association, Washington, DC.



Appendix C Properties of Rolled-Steel Shapes

(U.S. Customary Units)

W Shapes

(Wide-Flange Shapes)

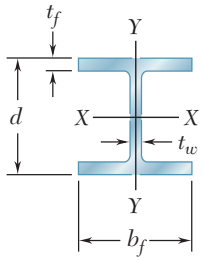
Designation†	Area A, in^2	Depth d, in.	Flange: Width b_f, in.	Flange: Thickness t_f, in.	Web Thickness t_w, in.	Axis X-X: I_x, in^4	Axis X-X: S_x, in^3	Axis X-X: r_x, in.	Axis Y-Y: I_y, in^4	Axis Y-Y: S_y, in^3	Axis Y-Y: r_y, in.
W36 × 302	88.8	37.3	16.7	1.68	0.945	21100	1130	15.4	1300	156	3.82
135	39.7	35.6	12.0	0.790	0.600	7800	439	14.0	225	37.7	2.38
W33 × 201	59.2	33.7	15.7	1.15	0.715	11600	686	14.0	749	95.2	3.56
118	34.7	32.9	11.5	0.740	0.550	5900	359	13.0	187	32.6	2.32
W30 × 173	51.0	30.4	15.0	1.07	0.655	8230	541	12.7	598	79.8	3.42
99	29.1	29.7	10.50	0.670	0.520	3990	269	11.7	128	24.5	2.10
W27 × 146	43.1	27.4	14.0	0.975	0.605	5660	414	11.5	443	63.5	3.20
84	24.8	26.70	10.0	0.640	0.460	2850	213	10.7	106	21.2	2.07
W24 × 104	30.6	24.1	12.8	0.750	0.500	3100	258	10.1	259	40.7	2.91
68	20.1	23.7	8.97	0.585	0.415	1830	154	9.55	70.4	15.7	1.87
W21 × 101	29.8	21.4	12.3	0.800	0.500	2420	227	9.02	248	40.3	2.89
62	18.3	21.0	8.24	0.615	0.400	1330	127	8.54	57.5	14.0	1.77
44	13.0	20.7	6.50	0.450	0.350	843	81.6	8.06	20.7	6.37	1.26
W18 × 106	31.1	18.7	11.2	0.940	0.590	1910	204	7.84	220	39.4	2.66
76	22.3	18.2	11.0	0.680	0.425	1330	146	7.73	152	27.6	2.61
50	14.7	18.0	7.50	0.570	0.355	800	88.9	7.38	40.1	10.7	1.65
35	10.3	17.7	6.00	0.425	0.300	510	57.6	7.04	15.3	5.12	1.22
W16 × 77	22.6	16.5	10.3	0.760	0.455	1110	134	7.00	138	26.9	2.47
57	16.8	16.4	7.12	0.715	0.430	758	92.2	6.72	43.1	12.1	1.60
40	11.8	16.0	7.00	0.505	0.305	518	64.7	6.63	28.9	8.25	1.57
31	9.13	15.9	5.53	0.440	0.275	375	47.2	6.41	12.4	4.49	1.17
26	7.68	15.7	5.50	0.345	0.250	301	38.4	6.26	9.59	3.49	1.12
W14 × 370	109	17.9	16.5	2.66	1.66	5440	607	7.07	1990	241	4.27
145	42.7	14.8	15.5	1.09	0.680	1710	232	6.33	677	87.3	3.98
82	24.0	14.3	10.1	0.855	0.510	881	123	6.05	148	29.3	2.48
68	20.0	14.0	10.0	0.720	0.415	722	103	6.01	121	24.2	2.46
53	15.6	13.9	8.06	0.660	0.370	541	77.8	5.89	57.7	14.3	1.92
43	12.6	13.7	8.00	0.530	0.305	428	62.6	5.82	45.2	11.3	1.89
38	11.2	14.1	6.77	0.515	0.310	385	54.6	5.87	26.7	7.88	1.55
30	8.85	13.8	6.73	0.385	0.270	291	42.0	5.73	19.6	5.82	1.49
26	7.69	13.9	5.03	0.420	0.255	245	35.3	5.65	8.91	3.55	1.08
22	6.49	13.7	5.00	0.335	0.230	199	29.0	5.54	7.00	2.80	1.04

†A wide-flange shape is designated by the letter W followed by the nominal depth in inches and the weight in pounds per foot.

(Table continued on page A18)

Appendix C Properties of Rolled-Steel Shapes

(SI Units)



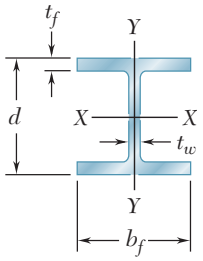
W Shapes

(Wide-Flange Shapes)

Designation†	Area A, mm²	Depth d, mm.	Flange Width b_f, mm	Flange Thickness t_f, mm	Web Thickness t_w mm	Axis X-X I_x 10^6 mm⁴	Axis X-X S_x 10^3 mm³	Axis X-X r_x mm	Axis Y-Y I_y 10^6 mm⁴	Axis Y-Y S_y 10^3 mm³	Axis Y-Y r_y mm
W920 × 449	57300	947	424	42.7	24.0	8780	18500	391	541	2560	97.0
201	25600	904	305	20.1	15.2	3250	7190	356	93.7	618	60.5
W840 × 299	38200	856	399	29.2	18.2	4830	11200	356	312	1560	90.4
176	22400	836	292	18.8	14.0	2460	5880	330	77.8	534	58.9
W760 × 257	32900	772	381	27.2	16.6	3430	8870	323	249	1310	86.9
147	18800	754	267	17.0	13.2	1660	4410	297	53.3	401	53.3
W690 × 217	27800	696	356	24.8	15.4	2360	6780	292	184	1040	81.3
125	16000	678	254	16.3	11.7	1190	3490	272	44.1	347	52.6
W610 × 155	19700	612	325	19.1	12.7	1290	4230	257	108	667	73.9
101	13000	602	228	14.9	10.5	762	2520	243	29.3	257	47.5
W530 × 150	19200	544	312	20.3	12.7	1010	3720	229	103	660	73.4
92	11800	533	209	15.6	10.2	554	2080	217	23.9	229	45.0
66	8390	526	165	11.4	8.89	351	1340	205	8.62	104	32.0
W460 × 158	20100	475	284	23.9	15.0	795	3340	199	91.6	646	67.6
113	14400	462	279	17.3	10.8	554	2390	196	63.3	452	66.3
74	9480	457	191	14.5	9.02	333	1460	187	16.7	175	41.9
52	6650	450	152	10.8	7.62	212	944	179	6.37	83.9	31.0
W410 × 114	14600	419	262	19.3	11.6	462	2200	178	57.4	441	62.7
85	10800	417	181	18.2	10.9	316	1510	171	17.9	198	40.6
60	7610	406	178	12.8	7.75	216	1060	168	12.0	135	39.9
46.1	5890	404	140	11.2	6.99	156	773	163	5.16	73.6	29.7
38.8	4950	399	140	8.76	6.35	125	629	159	3.99	57.2	28.4
W360 × 551	70300	455	419	67.6	42.2	2260	9950	180	828	3950	108
216	27500	376	394	27.7	17.3	712	3800	161	282	1430	101
122	15500	363	257	21.7	13.0	367	2020	154	61.6	480	63.0
101	12900	356	254	18.3	10.5	301	1690	153	50.4	397	62.5
79	10100	353	205	16.8	9.40	225	1270	150	24.0	234	48.8
64	8130	348	203	13.5	7.75	178	1030	148	18.8	185	48.0
57.8	7230	358	172	13.1	7.87	160	895	149	11.1	129	39.4
44	5710	351	171	9.78	6.86	121	688	146	8.16	95.4	37.8
39	4960	353	128	10.7	6.48	102	578	144	3.71	58.2	27.4
32.9	4190	348	127	8.51	5.84	82.8	475	141	2.91	45.9	26.4

†A wide-flange shape is designated by the letter W followed by the nominal depth in millimeters and the mass in kilograms permeter.

(Table continued on page A19)



Appendix C Properties of Rolled-Steel Shapes

(U.S. Customary Units)

Continued from page A18

W Shapes

(Wide-Flange Shapes)

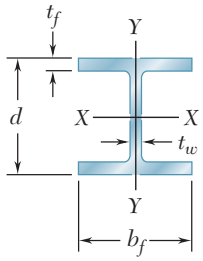
Designation†	Area A, in^2	Depth d, in.	Flange Width b_f, in.	Flange Thickness t_f, in.	Web Thickness t_w, in.	Axis X-X I_x, in^4	Axis X-X S_x, in^3	Axis X-X r_x, in.	Axis Y-Y I_y, in^4	Axis Y-Y S_y, in^3	Axis Y-Y r_y, in.
W12 × 96	28.2	12.7	12.2	0.900	0.550	833	131	5.44	270	44.4	3.09
72	21.1	12.3	12.0	0.670	0.430	597	97.4	5.31	195	32.4	3.04
50	14.6	12.2	8.08	0.640	0.370	391	64.2	5.18	56.3	13.9	1.96
40	11.7	11.9	8.01	0.515	0.295	307	51.5	5.13	44.1	11.0	1.94
35	10.3	12.5	6.56	0.520	0.300	285	45.6	5.25	24.5	7.47	1.54
30	8.79	12.3	6.52	0.440	0.260	238	38.6	5.21	20.3	6.24	1.52
26	7.65	12.2	6.49	0.380	0.230	204	33.4	5.17	17.3	5.34	1.51
22	6.48	12.3	4.03	0.425	0.260	156	25.4	4.91	4.66	2.31	0.848
16	4.71	12.0	3.99	0.265	0.220	103	17.1	4.67	2.82	1.41	0.773
W10 × 112	32.9	11.4	10.4	1.25	0.755	716	126	4.66	236	45.3	2.68
68	20.0	10.4	10.1	0.770	0.470	394	75.7	4.44	134	26.4	2.59
54	15.8	10.1	10.0	0.615	0.370	303	60.0	4.37	103	20.6	2.56
45	13.3	10.1	8.02	0.620	0.350	248	49.1	4.32	53.4	13.3	2.01
39	11.5	9.92	7.99	0.530	0.315	209	42.1	4.27	45.0	11.3	1.98
33	9.71	9.73	7.96	0.435	0.290	171	35.0	4.19	36.6	9.20	1.94
30	8.84	10.5	5.81	0.510	0.300	170	32.4	4.38	16.7	5.75	1.37
22	6.49	10.2	5.75	0.360	0.240	118	23.2	4.27	11.4	3.97	1.33
19	5.62	10.2	4.02	0.395	0.250	96.3	18.8	4.14	4.29	2.14	0.874
15	4.41	10.0	4.00	0.270	0.230	68.9	13.8	3.95	2.89	1.45	0.810
W8 × 58	17.1	8.75	8.22	0.810	0.510	228	52.0	3.65	75.1	18.3	2.10
48	14.1	8.50	8.11	0.685	0.400	184	43.2	3.61	60.9	15.0	2.08
40	11.7	8.25	8.07	0.560	0.360	146	35.5	3.53	49.1	12.2	2.04
35	10.3	8.12	8.02	0.495	0.310	127	31.2	3.51	42.6	10.6	2.03
31	9.12	8.00	8.00	0.435	0.285	110	27.5	3.47	37.1	9.27	2.02
28	8.24	8.06	6.54	0.465	0.285	98.0	24.3	3.45	21.7	6.63	1.62
24	7.08	7.93	6.50	0.400	0.245	82.7	20.9	3.42	18.3	5.63	1.61
21	6.16	8.28	5.27	0.400	0.250	75.3	18.2	3.49	9.77	3.71	1.26
18	5.26	8.14	5.25	0.330	0.230	61.9	15.2	3.43	7.97	3.04	1.23
15	4.44	8.11	4.01	0.315	0.245	48.0	11.8	3.29	3.41	1.70	0.876
13	3.84	7.99	4.00	0.255	0.230	39.6	9.91	3.21	2.73	1.37	0.843
W6 × 25	7.34	6.38	6.08	0.455	0.320	53.4	16.7	2.70	17.1	5.61	1.52
20	5.87	6.20	6.02	0.365	0.260	41.4	13.4	2.66	13.3	4.41	1.50
16	4.74	6.28	4.03	0.405	0.260	32.1	10.2	2.60	4.43	2.20	0.967
12	3.55	6.03	4.00	0.280	0.230	22.1	7.31	2.49	2.99	1.50	0.918
9	2.68	5.90	3.94	0.215	0.170	16.4	5.56	2.47	2.20	1.11	0.905
W5 × 19	5.56	5.15	5.03	0.430	0.270	26.3	10.2	2.17	9.13	3.63	1.28
16	4.71	5.01	5.00	0.360	0.240	21.4	8.55	2.13	7.51	3.00	1.26
W4 × 13	3.83	4.16	4.06	0.345	0.280	11.3	5.46	1.72	3.86	1.90	1.00

†A wide-flange shape is designated by the letter W followed by the nominal depth in inches and the weight in pounds per foot.

Appendix C Properties of Rolled-Steel Shapes

(SI Units)

Continued from page A19

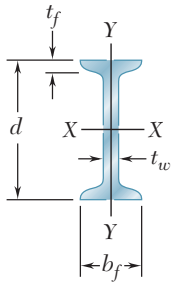


W Shapes

(Wide-Flange Shapes)

Designation†	Area A, mm²	Depth d, mm	Flange Width b_f, mm	Flange Thickness t_f, mm	Web Thickness t_w, mm	Axis X-X I_x 10^6 mm⁴	Axis X-X S_x 10^3 mm³	Axis X-X r_x mm	Axis Y-Y I_y 10^6 mm⁴	Axis Y-Y S_y 10^3 mm³	Axis Y-Y r_y mm
W310 × 143	18200	323	310	22.9	14.0	347	2150	138	112	728	78.5
107	13600	312	305	17.0	10.9	248	1600	135	81.2	531	77.2
74	9420	310	205	16.3	9.40	163	1050	132	23.4	228	49.8
60	7550	302	203	13.1	7.49	128	844	130	18.4	180	49.3
52	6650	318	167	13.2	7.62	119	747	133	10.2	122	39.1
44.5	5670	312	166	11.2	6.60	99.1	633	132	8.45	102	38.6
38.7	4940	310	165	9.65	5.84	84.9	547	131	7.20	87.5	38.4
32.7	4180	312	102	10.8	6.60	64.9	416	125	1.94	37.9	21.5
23.8	3040	305	101	6.73	5.59	42.9	280	119	1.17	23.1	19.6
W250 × 167	21200	290	264	31.8	19.2	298	2060	118	98.2	742	68.1
101	12900	264	257	19.6	11.9	164	1240	113	55.8	433	65.8
80	10200	257	254	15.6	9.4	126	983	111	42.9	338	65.0
67	8580	257	204	15.7	8.89	103	805	110	22.2	218	51.1
58	7420	252	203	13.5	8.00	87.0	690	108	18.7	185	50.3
49.1	6260	247	202	11.0	7.37	71.2	574	106	15.2	151	49.3
44.8	5700	267	148	13.0	7.62	70.8	531	111	6.95	94.2	34.8
32.7	4190	259	146	9.14	6.10	49.1	380	108	4.75	65.1	33.8
28.4	3630	259	102	10.0	6.35	40.1	308	105	1.79	35.1	22.2
22.3	2850	254	102	6.86	5.84	28.7	226	100	1.20	23.8	20.6
W200 × 86	11000	222	209	20.6	13.0	94.9	852	92.7	31.3	300	53.3
71	9100	216	206	17.4	10.2	76.6	708	91.7	25.3	246	52.8
59	7550	210	205	14.2	9.14	60.8	582	89.7	20.4	200	51.8
52	6650	206	204	12.6	7.87	52.9	511	89.2	17.7	174	51.6
46.1	5880	203	203	11.0	7.24	45.8	451	88.1	15.4	152	51.3
41.7	5320	205	166	11.8	7.24	40.8	398	87.6	9.03	109	41.1
35.9	4570	201	165	10.2	6.22	34.4	342	86.9	7.62	92.3	40.9
31.3	3970	210	134	10.2	6.35	31.3	298	88.6	4.07	60.8	32.0
26.6	3390	207	133	8.38	5.84	25.8	249	87.1	3.32	49.8	31.2
22.5	2860	206	102	8.00	6.22	20.0	193	83.6	1.42	27.9	22.3
19.3	2480	203	102	6.48	5.84	16.5	162	81.5	1.14	22.5	21.4
W150 × 37.1	4740	162	154	11.6	8.13	22.2	274	68.6	7.12	91.9	38.6
29.8	3790	157	153	9.27	6.60	17.2	220	67.6	5.54	72.3	38.1
24	3060	160	102	10.3	6.60	13.4	167	66.0	1.84	36.1	24.6
18	2290	153	102	7.11	5.84	9.20	120	63.2	1.24	24.6	23.3
13.5	1730	150	100	5.46	4.32	6.83	91.1	62.7	0.916	18.2	23.0
W130 × 28.1	3590	131	128	10.9	6.86	10.9	167	55.1	3.80	59.5	32.5
23.8	3040	127	127	9.14	6.10	8.91	140	54.1	3.13	49.2	32.0
W100 × 19.3	2470	106	103	8.76	7.11	4.70	89.5	43.7	1.61	31.1	25.4

†A wide-flange shape is designated by the letter W followed by the nominal depth in millimeters and the mass in kilograms per meter.



Appendix C Properties of Rolled-Steel Shapes

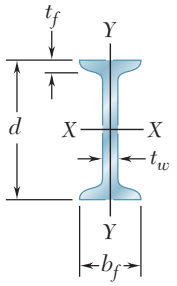
(U.S. Customary Units)

S Shapes

(American Standard Shapes)

Designation†	Area A, in^2	Depth d, in.	Flange: Width b_f, in.	Flange: Thickness t_f, in.	Web Thickness t_w, in.	Axis X-X: I_x, in^4	Axis X-X: S_x, in^3	Axis X-X: r_x, in.	Axis Y-Y: I_y, in^4	Axis Y-Y: S_y, in^3	Axis Y-Y: r_y, in.
S24 × 121	35.5	24.5	8.05	1.09	0.800	3160	258	9.43	83.0	20.6	1.53
106	31.1	24.5	7.87	1.09	0.620	2940	240	9.71	76.8	19.5	1.57
100	29.3	24.0	7.25	0.870	0.745	2380	199	9.01	47.4	13.1	1.27
90	26.5	24.0	7.13	0.870	0.625	2250	187	9.21	44.7	12.5	1.30
80	23.5	24.0	7.00	0.870	0.500	2100	175	9.47	42.0	12.0	1.34
S20 × 96	28.2	20.3	7.20	0.920	0.800	1670	165	7.71	49.9	13.9	1.33
86	25.3	20.3	7.06	0.920	0.660	1570	155	7.89	46.6	13.2	1.36
75	22.0	20.0	6.39	0.795	0.635	1280	128	7.62	29.5	9.25	1.16
66	19.4	20.0	6.26	0.795	0.505	1190	119	7.83	27.5	8.78	1.19
S18 × 70	20.5	18.0	6.25	0.691	0.711	923	103	6.70	24.0	7.69	1.08
54.7	16.0	18.0	6.00	0.691	0.461	801	89.0	7.07	20.7	6.91	1.14
S15 × 50	14.7	15.0	5.64	0.622	0.550	485	64.7	5.75	15.6	5.53	1.03
42.9	12.6	15.0	5.50	0.622	0.411	446	59.4	5.95	14.3	5.19	1.06
S12 × 50	14.6	12.0	5.48	0.659	0.687	303	50.6	4.55	15.6	5.69	1.03
40.8	11.9	12.0	5.25	0.659	0.462	270	45.1	4.76	13.5	5.13	1.06
35	10.2	12.0	5.08	0.544	0.428	228	38.1	4.72	9.84	3.88	0.980
31.8	9.31	12.0	5.00	0.544	0.350	217	36.2	4.83	9.33	3.73	1.00
S10 × 35	10.3	10.0	4.94	0.491	0.594	147	29.4	3.78	8.30	3.36	0.899
25.4	7.45	10.0	4.66	0.491	0.311	123	24.6	4.07	6.73	2.89	0.950
S8 × 23	6.76	8.00	4.17	0.425	0.441	64.7	16.2	3.09	4.27	2.05	0.795
18.4	5.40	8.00	4.00	0.425	0.271	57.5	14.4	3.26	3.69	1.84	0.827
S6 × 17.2	5.06	6.00	3.57	0.359	0.465	26.2	8.74	2.28	2.29	1.28	0.673
12.5	3.66	6.00	3.33	0.359	0.232	22.0	7.34	2.45	1.80	1.08	0.702
S5 × 10	2.93	5.00	3.00	0.326	0.214	12.3	4.90	2.05	1.19	0.795	0.638
S4 × 9.5	2.79	4.00	2.80	0.293	0.326	6.76	3.38	1.56	0.887	0.635	0.564
7.7	2.26	4.00	2.66	0.293	0.193	6.05	3.03	1.64	0.748	0.562	0.576
S3 × 7.5	2.20	3.00	2.51	0.260	0.349	2.91	1.94	1.15	0.578	0.461	0.513
5.7	1.66	3.00	2.33	0.260	0.170	2.50	1.67	1.23	0.447	0.383	0.518

†An American Standard Beam is designated by the letter S followed by the nominal depth in inches and the weight in pounds per foot.



Appendix C Properties of Rolled-Steel Shapes

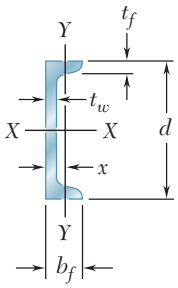
(SI Units)

S Shapes

(American Standard Shapes)

Designation†	Area A, mm^2	Depth d, mm	Flange Width b_f, mm	Flange Thickness t_f, mm	Web Thickness t_w, mm	Axis X-X I_x 10^6 mm^4	Axis X-X S_x 10^3 mm^3	Axis X-X r_x mm	Axis Y-Y I_y 10^6 mm^4	Axis Y-Y S_y 10^3 mm^3	Axis Y-Y r_y mm
S610 × 180	22900	622	204	27.7	20.3	1320	4230	240	34.5	338	38.9
158	20100	622	200	27.7	15.7	1220	3930	247	32.0	320	39.9
149	18900	610	184	22.1	18.9	991	3260	229	19.7	215	32.3
134	17100	610	181	22.1	15.9	937	3060	234	18.6	205	33.0
119	15200	610	178	22.1	12.7	874	2870	241	17.5	197	34.0
S510 × 143	18200	516	183	23.4	20.3	695	2700	196	20.8	228	33.8
128	16300	516	179	23.4	16.8	653	2540	200	19.4	216	34.5
112	14200	508	162	20.2	16.1	533	2100	194	12.3	152	29.5
98.2	12500	508	159	20.2	12.8	495	1950	199	11.4	144	30.2
S460 × 104	13200	457	159	17.6	18.1	384	1690	170	10.0	126	27.4
81.4	10300	457	152	17.6	11.7	333	1460	180	8.62	113	29.0
S380 × 74	9480	381	143	15.8	14.0	202	1060	146	6.49	90.6	26.2
64	8130	381	140	15.8	10.4	186	973	151	5.95	85.0	26.9
S310 × 74	9420	305	139	16.7	17.4	126	829	116	6.49	93.2	26.2
60.7	7680	305	133	16.7	11.7	112	739	121	5.62	84.1	26.9
52	6580	305	129	13.8	10.9	94.9	624	120	4.10	63.6	24.9
47.3	6010	305	127	13.8	8.89	90.3	593	123	3.88	61.1	25.4
S250 × 52	6650	254	125	12.5	15.1	61.2	482	96.0	3.45	55.1	22.8
37.8	4810	254	118	12.5	7.90	51.2	403	103	2.80	47.4	24.1
S200 × 34	4360	203	106	10.8	11.2	26.9	265	78.5	1.78	33.6	20.2
27.4	3480	203	102	10.8	6.88	23.9	236	82.8	1.54	30.2	21.0
S150 × 25.7	3260	152	90.7	9.12	11.8	10.9	143	57.9	0.953	21.0	17.1
18.6	2360	152	84.6	9.12	5.89	9.16	120	62.2	0.749	17.7	17.8
S130 × 15	1890	127	76.2	8.28	5.44	5.12	80.3	52.1	0.495	13.0	16.2
S100 × 14.1	1800	102	71.1	7.44	8.28	2.81	55.4	39.6	0.369	10.4	14.3
11.5	1460	102	67.6	7.44	4.90	2.52	49.7	41.7	0.311	9.21	14.6
S75 × 11.2	1420	76.2	63.8	6.60	8.86	1.21	31.8	29.2	0.241	7.55	13.0
8.5	1070	76.2	59.2	6.60	4.32	1.04	27.4	31.2	0.186	6.28	13.2

†An American Standard Beam is designated by the letter S followed by the nominal depth in millimeters and the mass in kilograms per meter.



Appendix C Properties of Rolled-Steel Shapes

(U.S. Customary Units)

C Shapes

(American Standard Channels)

Designation†	Area A, in^2	Depth d, in	Flange Width b_f, in	Flange Thickness t_f, in	Web Thickness t_w, in	Axis X-X I_x, in^4	Axis X-X S_x, in^3	Axis X-X r_x, in	Axis Y-Y I_y, in^4	Axis Y-Y S_y, in^3	Axis Y-Y r_y, in	Axis Y-Y x, in
C15 × 50	14.7	15.0	3.72	0.650	0.716	404	53.8	5.24	11.0	3.77	0.865	0.799
40	11.8	15.0	3.52	0.650	0.520	348	46.5	5.45	9.17	3.34	0.883	0.778
33.9	10.0	15.0	3.40	0.650	0.400	315	42.0	5.62	8.07	3.09	0.901	0.788
C12 × 30	8.81	12.0	3.17	0.501	0.510	162	27.0	4.29	5.12	2.05	0.762	0.674
25	7.34	12.0	3.05	0.501	0.387	144	24.0	4.43	4.45	1.87	0.779	0.674
20.7	6.08	12.0	2.94	0.501	0.282	129	21.5	4.61	3.86	1.72	0.797	0.698
C10 × 30	8.81	10.0	3.03	0.436	0.673	103	20.7	3.42	3.93	1.65	0.668	0.649
25	7.34	10.0	2.89	0.436	0.526	91.1	18.2	3.52	3.34	1.47	0.675	0.617
20	5.87	10.0	2.74	0.436	0.379	78.9	15.8	3.66	2.80	1.31	0.690	0.606
15.3	4.48	10.0	2.60	0.436	0.240	67.3	13.5	3.87	2.27	1.15	0.711	0.634
C9 × 20	5.87	9.00	2.65	0.413	0.448	60.9	13.5	3.22	2.41	1.17	0.640	0.583
15	4.41	9.00	2.49	0.413	0.285	51.0	11.3	3.40	1.91	1.01	0.659	0.586
13.4	3.94	9.00	2.43	0.413	0.233	47.8	10.6	3.49	1.75	0.954	0.666	0.601
C8 × 18.7	5.51	8.00	2.53	0.390	0.487	43.9	11.0	2.82	1.97	1.01	0.598	0.565
13.7	4.04	8.00	2.34	0.390	0.303	36.1	9.02	2.99	1.52	0.848	0.613	0.554
11.5	3.37	8.00	2.26	0.390	0.220	32.5	8.14	3.11	1.31	0.775	0.623	0.572
C7 × 12.2	3.60	7.00	2.19	0.366	0.314	24.2	6.92	2.60	1.16	0.696	0.568	0.525
9.8	2.87	7.00	2.09	0.366	0.210	21.2	6.07	2.72	0.957	0.617	0.578	0.541
C6 × 13	3.81	6.00	2.16	0.343	0.437	17.3	5.78	2.13	1.05	0.638	0.524	0.514
10.5	3.08	6.00	2.03	0.343	0.314	15.1	5.04	2.22	0.860	0.561	0.529	0.500
8.2	2.39	6.00	1.92	0.343	0.200	13.1	4.35	2.34	0.687	0.488	0.536	0.512
C5 × 9	2.64	5.00	1.89	0.320	0.325	8.89	3.56	1.83	0.624	0.444	0.486	0.478
6.7	1.97	5.00	1.75	0.320	0.190	7.48	2.99	1.95	0.470	0.372	0.489	0.484
C4 × 7.2	2.13	4.00	1.72	0.296	0.321	4.58	2.29	1.47	0.425	0.337	0.447	0.459
5.4	1.58	4.00	1.58	0.296	0.184	3.85	1.92	1.56	0.312	0.277	0.444	0.457
C3 × 6	1.76	3.00	1.60	0.273	0.356	2.07	1.38	1.08	0.300	0.263	0.413	0.455
5	1.47	3.00	1.50	0.273	0.258	1.85	1.23	1.12	0.241	0.228	0.405	0.439
4.1	1.20	3.00	1.41	0.273	0.170	1.65	1.10	1.17	0.191	0.196	0.398	0.437

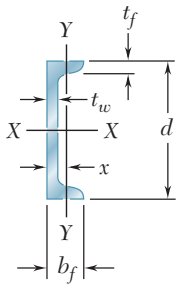
†An American Standard Channel is designated by the letter C followed by the nominal depth in inches and the weight in pounds per foot.

Appendix C Properties of Rolled-Steel Shapes

(SI Units)

C Shapes

(American Standard Channels)

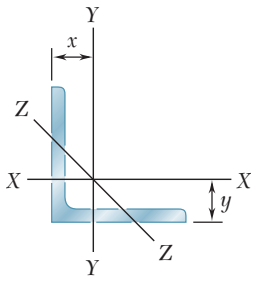


Designation†	Area A, mm²	Depth d, mm	Flange Width b_f, mm	Flange Thickness t_f, mm	Web Thickness t_w, mm	Axis X-X I_x 10^6 mm⁴	Axis X-X S_x 10^3 mm³	Axis X-X r_x mm	Axis Y-Y I_y 10^6 mm⁴	Axis Y-Y S_y 10^3 mm³	Axis Y-Y r_y mm	x mm
C380 × 74	9480	381	94.5	16.5	18.2	168	882	133	4.58	61.8	22.0	20.3
60	7610	381	89.4	16.5	13.2	145	762	138	3.82	54.7	22.4	19.8
50.4	6450	381	86.4	16.5	10.2	131	688	143	3.36	50.6	22.9	20.0
C310 × 45	5680	305	80.5	12.7	13.0	67.4	442	109	2.13	33.6	19.4	17.1
37	4740	305	77.5	12.7	9.83	59.9	393	113	1.85	30.6	19.8	17.1
30.8	3920	305	74.7	12.7	7.16	53.7	352	117	1.61	28.2	20.2	17.7
C250 × 45	5680	254	77.0	11.1	17.1	42.9	339	86.9	1.64	27.0	17.0	16.5
37	4740	254	73.4	11.1	13.4	37.9	298	89.4	1.39	24.1	17.1	15.7
30	3790	254	69.6	11.1	9.63	32.8	259	93.0	1.17	21.5	17.5	15.4
22.8	2890	254	66.0	11.1	6.10	28.0	221	98.3	0.945	18.8	18.1	16.1
C230 × 30	3790	229	67.3	10.5	11.4	25.3	221	81.8	1.00	19.2	16.3	14.8
22	2850	229	63.2	10.5	7.24	21.2	185	86.4	0.795	16.6	16.7	14.9
19.9	2540	229	61.7	10.5	5.92	19.9	174	88.6	0.728	15.6	16.9	15.3
C200 × 27.9	3550	203	64.3	9.91	12.4	18.3	180	71.6	0.820	16.6	15.2	14.4
20.5	2610	203	59.4	9.91	7.70	15.0	148	75.9	0.633	13.9	15.6	14.1
17.1	2170	203	57.4	9.91	5.59	13.5	133	79.0	0.545	12.7	15.8	14.5
C180 × 18.2	2320	178	55.6	9.30	7.98	10.1	113	66.0	0.483	11.4	14.4	13.3
14.6	1850	178	53.1	9.30	5.33	8.82	100	69.1	0.398	10.1	14.7	13.7
C150 × 19.3	2460	152	54.9	8.71	11.1	7.20	94.7	54.1	0.437	10.5	13.3	13.1
15.6	1990	152	51.6	8.71	7.98	6.29	82.6	56.4	0.358	9.19	13.4	12.7
12.2	1540	152	48.8	8.71	5.08	5.45	71.3	59.4	0.286	8.00	13.6	13.0
C130 × 13	1700	127	48.0	8.13	8.26	3.70	58.3	46.5	0.260	7.28	12.3	12.1
10.4	1270	127	44.5	8.13	4.83	3.11	49.0	49.5	0.196	6.10	12.4	12.3
C100 × 10.8	1370	102	43.7	7.52	8.15	1.91	37.5	37.3	0.177	5.52	11.4	11.7
8	1020	102	40.1	7.52	4.67	1.60	31.5	39.6	0.130	4.54	11.3	11.6
C75 × 8.9	1140	76.2	40.6	6.93	9.04	0.862	22.6	27.4	0.125	4.31	10.5	11.6
7.4	948	76.2	38.1	6.93	6.55	0.770	20.2	28.4	0.100	3.74	10.3	11.2
6.1	774	76.2	35.8	6.93	4.32	0.687	18.0	29.7	0.0795	3.21	10.1	11.1

†An American Standard Channel is designated by the letter C followed by the nominal depth in millimeters and the mass in kilograms per meter.

Appendix C Properties of Rolled-Steel Shapes

(U.S. Customary Units)



Angles

Equal Legs

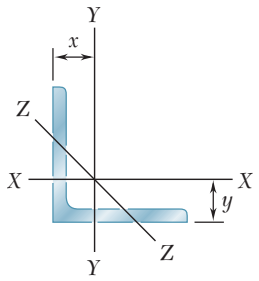
Size and Thickness, in.	Weight per Foot, lb/ft	Area, in^2	Axis *X-X* and Axis *Y-Y*				Axis *Z-Z*
			I, in^4	*S*, in^3	*r*, in.	*x* or *y*, in.	r_z, in.
L8 × 8 × 1	51.0	15.0	89.1	15.8	2.43	2.36	1.56
¾	38.9	11.4	69.9	12.2	2.46	2.26	1.57
½	26.4	7.75	48.8	8.36	2.49	2.17	1.59
L6 × 6 × 1	37.4	11.0	35.4	8.55	1.79	1.86	1.17
¾	28.7	8.46	28.1	6.64	1.82	1.77	1.17
⅝	24.2	7.13	24.1	5.64	1.84	1.72	1.17
½	19.6	5.77	19.9	4.59	1.86	1.67	1.18
⅜	14.9	4.38	15.4	3.51	1.87	1.62	1.19
L5 × 5 × ¾	23.6	6.94	15.7	4.52	1.50	1.52	0.972
⅝	20.0	5.86	13.6	3.85	1.52	1.47	0.975
½	16.2	4.75	11.3	3.15	1.53	1.42	0.980
⅜	12.3	3.61	8.76	2.41	1.55	1.37	0.986
L4 × 4 × ¾	18.5	5.44	7.62	2.79	1.18	1.27	0.774
⅝	15.7	4.61	6.62	2.38	1.20	1.22	0.774
½	12.8	3.75	5.52	1.96	1.21	1.18	0.776
⅜	9.80	2.86	4.32	1.50	1.23	1.13	0.779
¼	6.60	1.94	3.00	1.03	1.25	1.08	0.783
L3½ × 3½ × ½	11.1	3.25	3.63	1.48	1.05	1.05	0.679
⅜	8.50	2.48	2.86	1.15	1.07	1.00	0.683
¼	5.80	1.69	2.00	0.787	1.09	0.954	0.688
L3 × 3 × ½	9.40	2.75	2.20	1.06	0.895	0.929	0.580
⅜	7.20	2.11	1.75	0.825	0.910	0.884	0.581
¼	4.90	1.44	1.23	0.569	0.926	0.836	0.585
L2½ × 2½ × ½	7.70	2.25	1.22	0.716	0.735	0.803	0.481
⅜	5.90	1.73	0.972	0.558	0.749	0.758	0.481
¼	4.10	1.19	0.692	0.387	0.764	0.711	0.482
3⁄16	3.07	0.900	0.535	0.295	0.771	0.687	0.482
L2 × 2 × ⅜	4.70	1.36	0.476	0.348	0.591	0.632	0.386
¼	3.19	0.938	0.346	0.244	0.605	0.586	0.387
⅛	1.65	0.484	0.189	0.129	0.620	0.534	0.391

Appendix C Properties of Rolled-Steel Shapes

(SI Units)

Angles

Equal Legs



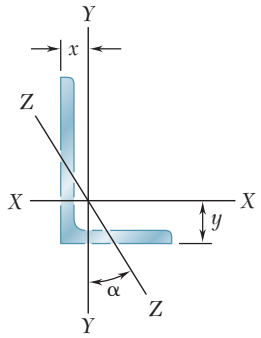
Size and Thickness, mm	Mass per Meter, kg/m	Area, mm^2	Axis *X-X* I $10^6\ mm^4$	Axis *X-X* S $10^3\ mm^3$	Axis *X-X* r mm	Axis *X-X* x or y mm	Axis *Z-Z* r_z mm
L203 × 203 × 25.4	75.9	9680	37.1	259	61.7	59.9	39.6
19	57.9	7350	29.1	200	62.5	57.4	39.9
12.7	39.3	5000	20.3	137	63.2	55.1	40.4
L152 × 152 × 25.4	55.7	7100	14.7	140	45.5	47.2	29.7
19	42.7	5460	11.7	109	46.2	45.0	29.7
15.9	36.0	4600	10.0	92.4	46.7	43.7	29.7
12.7	29.2	3720	8.28	75.2	47.2	42.4	30.0
9.5	22.2	2830	6.41	57.5	47.5	41.1	30.2
L127 × 127 × 19	35.1	4480	6.53	74.1	38.1	38.6	24.7
15.9	29.8	3780	5.66	63.1	38.6	37.3	24.8
12.7	24.1	3060	4.70	51.6	38.9	36.1	24.9
9.5	18.3	2330	3.65	39.5	39.4	34.8	25.0
L102 × 102 × 19	27.5	3510	3.17	45.7	30.0	32.3	19.7
15.9	23.4	2970	2.76	39.0	30.5	31.0	19.7
12.7	19.0	2420	2.30	32.1	30.7	30.0	19.7
9.5	14.6	1850	1.80	24.6	31.2	28.7	19.8
6.4	9.80	1250	1.25	16.9	31.8	27.4	19.9
L89 × 89 × 12.7	16.5	2100	1.51	24.3	26.7	26.7	17.2
9.5	12.6	1600	1.19	18.8	27.2	25.4	17.3
6.4	8.60	1090	0.832	12.9	27.7	24.2	17.5
L76 × 76 × 12.7	14.0	1770	0.916	17.4	22.7	23.6	14.7
9.5	10.7	1360	0.728	13.5	23.1	22.5	14.8
6.4	7.30	929	0.512	9.32	23.5	21.2	14.9
L64 × 64 × 12.7	11.4	1450	0.508	11.7	18.7	20.4	12.2
9.5	8.70	1120	0.405	9.14	19.0	19.3	12.2
6.4	6.10	768	0.288	6.34	19.4	18.1	12.2
4.8	4.60	581	0.223	4.83	19.6	17.4	12.2
L51 × 51 × 9.5	7.00	877	0.198	5.70	15.0	16.1	9.80
6.4	4.70	605	0.144	4.00	15.4	14.9	9.83
3.2	2.40	312	0.0787	2.11	15.7	13.6	9.93

Appendix C Properties of Rolled-Steel Shapes

(U.S. Customary Units)

Angles

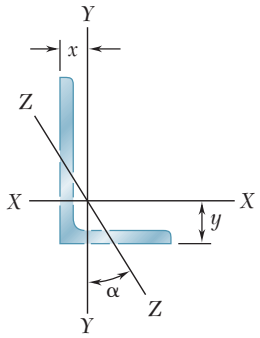
Unequal Legs



Size and Thickness, in.	Weight per Foot, lb/ft	Area, in^2	Axis *X-X*				Axis *Y-Y*				Axis *Z-Z*	
			I_x, in^4	S_x, in^3	r_x, in.	y, in.	I_y, in^4	S_y, in^3	r_y, in.	x, in.	r_z, in.	tan α
L8 × 6 × 1	44.2	13.0	80.9	15.1	2.49	2.65	38.8	8.92	1.72	1.65	1.28	0.542
¾	33.8	9.94	63.5	11.7	2.52	2.55	30.8	6.92	1.75	1.56	1.29	0.550
½	23.0	6.75	44.4	8.01	2.55	2.46	21.7	4.79	1.79	1.46	1.30	0.557
L6 × 4 × ¾	23.6	6.94	24.5	6.23	1.88	2.07	8.63	2.95	1.12	1.07	0.856	0.428
½	16.2	4.75	17.3	4.31	1.91	1.98	6.22	2.06	1.14	0.981	0.864	0.440
⅜	12.3	3.61	13.4	3.30	1.93	1.93	4.86	1.58	1.16	0.933	0.870	0.446
L5 × 3 × ½	12.8	3.75	9.43	2.89	1.58	1.74	2.55	1.13	0.824	0.746	0.642	0.357
⅜	9.80	2.86	7.35	2.22	1.60	1.69	2.01	0.874	0.838	0.698	0.646	0.364
¼	6.60	1.94	5.09	1.51	1.62	1.64	1.41	0.600	0.853	0.648	0.652	0.371
L4 × 3 × ½	11.1	3.25	5.02	1.87	1.24	1.32	2.40	1.10	0.858	0.822	0.633	0.542
⅜	8.50	2.48	3.94	1.44	1.26	1.27	1.89	0.851	0.873	0.775	0.636	0.551
¼	5.80	1.69	2.75	0.988	1.27	1.22	1.33	0.585	0.887	0.725	0.639	0.558
L3½ × 2½ × ½	9.40	2.75	3.24	1.41	1.08	1.20	1.36	0.756	0.701	0.701	0.532	0.485
⅜	7.20	2.11	2.56	1.09	1.10	1.15	1.09	0.589	0.716	0.655	0.535	0.495
¼	4.90	1.44	1.81	0.753	1.12	1.10	0.775	0.410	0.731	0.607	0.541	0.504
L3 × 2 × ½	7.70	2.25	1.92	1.00	0.922	1.08	0.667	0.470	0.543	0.580	0.425	0.413
⅜	5.90	1.73	1.54	0.779	0.937	1.03	0.539	0.368	0.555	0.535	0.426	0.426
¼	4.10	1.19	1.09	0.541	0.953	0.980	0.390	0.258	0.569	0.487	0.431	0.437
L2½ × 2 × ⅜	5.30	1.55	0.914	0.546	0.766	0.826	0.513	0.361	0.574	0.578	0.419	0.612
¼	3.62	1.06	0.656	0.381	0.782	0.779	0.372	0.253	0.589	0.532	0.423	0.624

Appendix C Properties of Rolled-Steel Shapes

(SI Units)

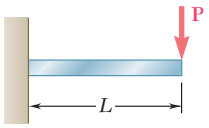
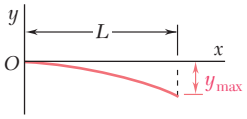
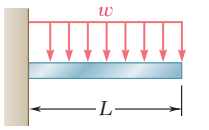
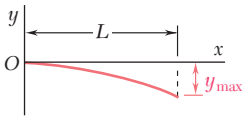
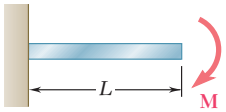
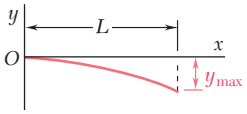
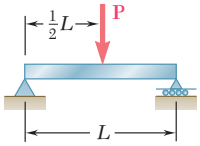
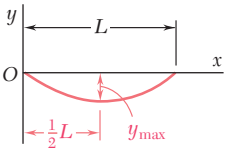
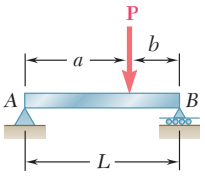
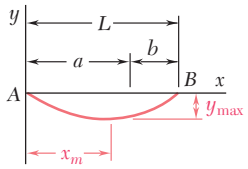
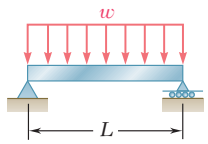
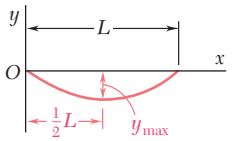
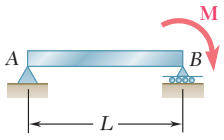
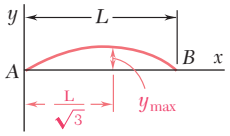


Angles

Unequal Legs

			Axis *X-X*				Axis *Y-Y*				Axis *Z-Z*	
Size and Thickness, mm	Mass per Meter kg/m	Area mm^2	I_x 10^6 mm^4	S_x 10^3 mm^3	r_x mm	y mm	I_y 10^6 mm^4	S_y 10^3 mm^3	r_y mm	x mm	r_z mm	tan α
L203 × 152 × 25.4	65.5	8390	33.7	247	63.2	67.3	16.1	146	43.7	41.9	32.5	0.542
19	50.1	6410	26.4	192	64.0	64.8	12.8	113	44.5	39.6	32.8	0.550
12.7	34.1	4350	18.5	131	64.8	62.5	9.03	78.5	45.5	37.1	33.0	0.557
L152 × 102 × 19	35.0	4480	10.2	102	47.8	52.6	3.59	48.3	28.4	27.2	21.7	0.428
12.7	24.0	3060	7.20	70.6	48.5	50.3	2.59	33.8	29.0	24.9	21.9	0.440
9.5	18.2	2330	5.58	54.1	49.0	49.0	2.02	25.9	29.5	23.7	22.1	0.446
L127 × 76 × 12.7	19.0	2420	3.93	47.4	40.1	44.2	1.06	18.5	20.9	18.9	16.3	0.357
9.5	14.5	1850	3.06	36.4	40.6	42.9	0.837	14.3	21.3	17.7	16.4	0.364
6.4	9.80	1250	2.12	24.7	41.1	41.7	0.587	9.83	21.7	16.5	16.6	0.371
L102 × 76 × 12.7	16.4	2100	2.09	30.6	31.5	33.5	0.999	18.0	21.8	20.9	16.1	0.542
9.5	12.6	1600	1.64	23.6	32.0	32.3	0.787	13.9	22.2	19.7	16.2	0.551
6.4	8.60	1090	1.14	16.2	32.3	31.0	0.554	9.59	22.5	18.4	16.2	0.558
L89 × 64 × 12.7	13.9	1770	1.35	23.1	27.4	30.5	0.566	12.4	17.8	17.8	13.5	0.485
9.5	10.7	1360	1.07	17.9	27.9	29.2	0.454	9.65	18.2	16.6	13.6	0.495
6.4	7.30	929	0.753	12.3	28.4	27.9	0.323	6.72	18.6	15.4	13.7	0.504
L76 × 51 × 12.7	11.5	1450	0.799	16.4	23.4	27.4	0.278	7.70	13.8	14.7	10.8	0.413
9.5	8.80	1120	0.641	12.8	23.8	26.2	0.224	6.03	14.1	13.6	10.8	0.426
6.4	6.10	768	0.454	8.87	24.2	24.9	0.162	4.23	14.5	12.4	10.9	0.437
L64 × 51 × 9.5	7.90	1000	0.380	8.95	19.5	21.0	0.214	5.92	14.6	14.7	10.6	0.612
6.4	5.40	684	0.273	6.24	19.9	19.8	0.155	4.15	15.0	13.5	10.7	0.624

Appendix D Beam Deflections and Slopes

Beam and Loading	Elastic Curve	Maximum Deflection	Slope at End	Equation of Elastic Curve
1 		$-\frac{PL^3}{3EI}$	$-\frac{PL^2}{2EI}$	$y = \frac{P}{6EI}(x^3 - 3Lx^2)$
2 		$-\frac{wL^4}{8EI}$	$-\frac{wL^3}{6EI}$	$y = -\frac{w}{24EI}(x^4 - 4Lx^3 + 6L^2x^2)$
3 		$-\frac{ML^2}{2EI}$	$-\frac{ML}{EI}$	$y = -\frac{M}{2EI}x^2$
4 		$-\frac{PL^3}{48EI}$	$\pm\frac{PL^2}{16EI}$	For $x \le \frac{1}{2}L$: $y = \frac{P}{48EI}(4x^3 - 3L^2x)$
5 		For $a > b$: $-\frac{Pb(L^2 - b^2)^{3/2}}{9\sqrt{3}EIL}$ at $x_m = \sqrt{\frac{L^2 - b^2}{3}}$	$\theta_A = -\frac{Pb(L^2 - b^2)}{6EIL}$ $\theta_B = +\frac{Pa(L^2 - a^2)}{6EIL}$	For $x < a$: $y = \frac{Pb}{6EIL}[x^3 - (L^2 - b^2)x]$ For $x = a$: $y = -\frac{Pa^2b^2}{3EIL}$
6 		$-\frac{5wL^4}{384EI}$	$\pm\frac{wL^3}{24EI}$	$y = -\frac{w}{24EI}(x^4 - 2Lx^3 + L^3x)$
7 		$\frac{ML^2}{9\sqrt{3}EI}$	$\theta_A = +\frac{ML}{6EI}$ $\theta_B = -\frac{ML}{3EI}$	$y = -\frac{M}{6EIL}(x^3 - L^2x)$

APPENDIX

E Fundamentals of Engineering Examination

Engineers are required to be licensed when their work directly affects the public health, safety, and welfare. The intent is to ensure that engineers have met minimum qualifications, involving competence, ability, experience, and character. The licensing process involves an initial exam, called the *Fundamentals of Engineering Examination,* professional experience, and a second exam, called the *Principles and Practice of Engineering*. Those who successfully complete these requirements are licensed as a *Professional Engineer*. The exams are developed under the auspices of the *National Council of Examiners for Engineering and Surveying.*

The first exam, the *Fundamentals of Engineering Examination*, can be taken just before or after graduation from a four-year accredited engineering program. The exam stresses subject material in a typical undergraduate engineering program, including *Mechanics of Materials*. The topics included in the exam cover much of the material in this book. The following is a list of the main topic areas with references to appropriate sections in this book. Also included are problems that can be solved to review this material.

Stresses (1.2–1.4)
Problems: 1.4, 1.10, 1.30, 1.37

Strains (2.1–2.4; 2.7–2.8)
Problems: 2.4, 2.19, 2.41, 2.47, 2.61, 2.68

Torsion (3.1–3.3; 3.9–3.10)
Problems: 3.6, 3.27, 3.35, 3.53, 3.129, 3.137

Bending (4.1–4.4; 4.7)
Problems: 4.9, 4.22, 4.33, 4.49, 4.103, 4.107

Shear and Bending–Moment Diagrams (5.1–5.2)
Problems: 5.5, 5.11, 5.39, 5.43

Normal Stresses in Beams (5.3)
Problems: 5.18, 5.21, 5.56, 5.60

Shear (6.1; 6.3–6.4)
Problems: 6.1, 6.11, 6.32, 6.38

Transformation of Stresses and Strains (7.1–7.2; 7.5–7.6)
Problems: 7.5, 7.15, 7.32, 7.43, 7.81, 7.87, 7.100, 7.104

Deflection of Beams (9.1; 9.4)
Problems: 9.5, 9.13, 9.71, 9.77

Columns (10.1)
Problems: 10.11, 10.19, 10.22

Strain Energy (11.1–11.2)
Problems: 11.9, 11.15, 11.21

Answers to Problems

Answers to problems with a number set in straight type are given on this and the following pages. Answers to problems with a number set in italic and red are not listed.

CHAPTER 1

1.1 (*a*) 84.9 MPa. (*b*) −96.8 MPa.
1.2 $d_1 = 22.6$ mm, $d_2 = 40.2$ mm.
1.3 (*a*) 17.93 ksi. (*b*) 22.6 ksi.
1.4 6.75 kips.
1.7 (*a*) 101.6 MPa. (*b*) −21.7 MPa.
1.8 1084 ksi.
1.9 285 mm^2.
1.10 (*a*) 11.09 ksi. (*b*) −12.00 ksi.
1.13 −4.97 MPa.
1.14 (*a*) 12.73 MPa. (*b*) −4.77 MPa.
1.15 43.4 mm.
1.16 2.25 kips.
1.17 889 psi.
1.18 67.9 kN.
1.20 29.4 mm.
1.21 (*a*) 3.33 MPa. (*b*) 525 mm.
1.23 (*a*) 1.030 in. (*b*) 38.8 ksi.
1.24 8.31 kN.
1.25 (*a*) 11.45 mm. (*b*) 134.9 MPa. (*c*) 90.0 MPa.
1.28 (*a*) 9.94 ksi. (*b*) 6.25 ksi.
1.29 (*a*) $\sigma = 489$ kPa; $\tau = 489$ kPa.
1.30 (*a*) 13.95 kN. (*b*) 620 kPa.
1.31 $\sigma = 70.0$ psi; $\tau = 40.4$ psi.
1.32 (*a*) 1.500 kips. (*b*) 43.3 psi.
1.35 $\sigma = -21.6$ MPa; $\tau = 7.87$ MPa.
1.36 833 kN.
1.37 3.09 kips.
1.40 (*a*) 181.3 mm^2. (*b*) 213 mm^2.
1.41 (*a*) 3.97. (*b*) 265 mm^2.
1.42 0.268 in^2.
1.45 2.87.
1.46 0.798 in.
1.47 10.25 kN.
1.48 (*a*) 2.92. (*b*) $b = 40.3$ mm, $c = 97.2$ mm.
1.50 3.24.
1.52 283 lb.
1.53 2.42.
1.54 2.05.
1.55 3.72 kN.
1.56 3.97 kN.
1.57 (*a*) 362 kg. (*b*) 1.718.
1.58 (*a*) 629 lb. (*b*) 1.689.
1.59 195.3 MPa.
1.60 (*a*) 14.64 ksi. (*b*) −9.96 ksi.
1.62 25.2 mm.
1.64 (*a*) −640 psi. (*b*) −320 psi.
1.65 (*a*) 444 psi. (*b*) 7.50 in. (*c*) 2400 psi.
1.67 3.45.
1.68 $\sigma_{all}\, d/4\, \tau_{all}$.
1.70 $21.3° < \theta < 32.3°$.
1.C2 (*c*) 16 mm ≤ *d* ≤ 22 mm. (*d*) 18 mm ≤ *d* ≤ 22 mm.
1.C3 (*c*) 0.70 in. ≤ *d* ≤ 1.10 in. (*d*) 0.85 in. ≤ *d* ≤ 1.25 in.
1.C4 (*b*) For $\beta = 38.66°$, $\tan\beta = 0.8$; *BD* is perpendicular to *BC*.
(*c*) *F.S.* = 3.58 for $\alpha = 26.6°$; **P** is perpendicular to line *AC*.
1.C5 (*b*) *Member of Fig. P 1.29, for* $\alpha = 60°$*:*
(1) 70.0 psi; (2) 40.4 psi; (3) 2.14; (4) 5.30; (5) 2.14.
Member of Fig. P 1.31, for $\alpha = 45°$*:*
(1) 489 kPa; (2) 489 kPa; (3) 2.58; (4) 3.07; (5) 2.58.
1.C6 (*d*) $P_{all} = 5.79$ kN; stress in links is critical.

CHAPTER 2

2.1 (*a*) 0.546 mm. (*b*) 36.3 MPa.
2.2 (*a*) 0.0303 in. (*b*) 15.28 ksi.
2.3 (*a*) 9.82 kN. (*b*) 500 MPa.
2.4 (*a*) 81.8 MPa. (*b*) 1.712.
2.6 (*a*) 5.32 mm. (*b*) 1.750 m.
2.7 (*a*) 0.381 in. (*b*) 17.58 ksi.
2.9 9.21 mm.
2.11 48.4 kips.
2.13 0.429 in.
2.14 1.988 kN.
2.15 0.868 in.
2.17 (*a*) 25.5×10^{-3} in. (*b*) 15.56×10^{-3} in.
2.19 (*a*) 32.8 kN. (*b*) 0.0728 mm ↓.
2.20 (*a*) 0.0189 mm ↑. (*b*) 0.0919 mm ↓.
2.21 (*a*) $\delta_{AB} = -2.11$ mm; $\delta_{AC} = 2.03$ mm.
2.23 (*a*) 0.1767 in. (*b*) 0.1304 in.
2.24 50.4 kN.
2.25 14.74 kN.
2.26 (*a*) −0.0302 mm. (*b*) 0.01783 mm.
2.27 4.71×10^{-3} in. ↓.
2.29 (*a*) $\rho g l^2/2E$. (*b*) $W/2$.
2.30 $Ph/\pi Eab$ ↓.
2.33 (*a*) 140.6 MPa. (*b*) 93.8 MPa.
2.34 (*a*) 15.00 mm. (*b*) 288 kN.
2.35 $\sigma_s = -8.34$ ksi; $\sigma_c = -1.208$ ksi.
2.36 695 kips.
2.39 (*a*) $R_A = 2.28$ kips ↑; $R_C = 9.72$ kips ↑. (*b*) $\sigma_{AB} = +1.857$ ksi; $\sigma_{BC} = -3.09$ ksi.
2.41 (*a*) 62.8 kN ← at *A*; 37.2 kN ← at *E*. (*b*) 46.3 μm →.
2.42 (*a*) 45.5 kN ← at *A*; 54.5 kN ← at *E*. (*b*) 48.8 μm →.
2.43 0.536 mm ↓.
2.44 (*a*) $P_{BE} = 205$ lb; $P_{CF} = 228$ lb. (*b*) 0.0691 in. ↓.
2.45 $P_A = 0.525\,P$; $P_B = 0.200\,P$; $P_C = 0.275\,P$.
2.47 −8.15 MPa.
2.48 −56.2 MPa.
2.50 $\sigma_s = -1.448$ ksi; σ_C 54.2 psi.
2.51 142.6 kN.
2.52 (*a*) $\sigma_{AB} = -5.25$ ksi; $\sigma_{BC} = -11.82$ ksi. (*b*) 6.57×10^{-3} in. →.

2.54 (*a*) −98.3 MPa. (*b*) −38.3 MPa.
2.55 (*a*) 21.4°C. (*b*) 3.67 MPa.
2.56 5.70 kN.
2.58 (*a*) 201.6°F. (*b*) 18.0107 in.
2.59 (*a*) 52.3 kips. (*b*) 9.91×10^{-3}in.
2.61 29×10^3 psi; 10.03×10^3 psi; 0.444.
2.63 0.399.
2.64 (*a*) 0.0358 mm. (*b*) −0.00258 mm. (*c*) −0.000344 mm. (*d*) −0.00825 mm^2.
2.66 94.9 kips.
2.67 (*a*) −0.0724 mm. (*b*) −0.01531 mm.
2.68 (*a*) 0.00312 in. (*b*) 0.00426 in. (*c*) 0.00505 in.
2.69 (*a*) 352×10^{-6} in. (*b*) 82.8×10^{-6} in. (*c*) 307×10^{-6} in.
2.70 (*a*) −63.0 MPa. (*b*) −13.50 mm^2. (*c*) −540 mm^3.
2.77 $a = 42.9$ mm; $b = 160.7$ mm.
2.78 75.0 kN; 40.0 mm.
2.79 (*a*) 10.42 in. (*b*) 0.813 in.
2.80 $\tau = 62.5$ psi; $G = 156.3$ psi.
2.81 16.67 MPa.
2.82 19.00×10^3 kN/m
2.83 (*a*) 588×10^{-6} in. (*b*) 33.2×10^{-3} in^3. (*c*) 0.0294%.
2.84 (*a*) −0.0746 mm; −143.9 mm^3. (*b*) −0.0306 mm; −521 mm^3.
2.85 (*a*) 193.2×10^{-6}; 1.214×10^{-3} in^3. (*b*) 396×10^{-6}; 2.49×10^{-3} in^3.
2.88 3.00.
2.91 (*a*) 0.0303 mm. (*b*) $\sigma_x = 40.6$ MPa, $\sigma_y = \sigma_z = 5.48$ MPa.
2.92 (*a*) $\sigma_x = 44.6$ MPa; $\sigma_y = 0$; $\sigma_z = 3.45$ MPa. (*b*) −0.0129 mm.
2.93 (*a*) 58.3 kN. (*b*) 64.3 kN.
2.94 (*a*) 87.0 MPa. (*b*) 75.2 MPa. (*c*) 73.9 MPa.
2.97 (*a*) 11.4 mm. (*b*) 28.8 kN.
2.98 36.7 mm.
2.99 (*a*) 12.02 kips. (*b*) 108.0%.
2.100 23.9 kips.
2.101 (*a*) 15.90 kips; 0.1745 in. (*b*) 15.90 kips; 0.274 in.
2.102 (*a*) 44.2 kips; 0.0356 in. (*b*) 44.2 kips; 0.1606 in.
2.105 176.7 kN; 3.84 mm.
2.106 176.7 kN; 3.16 mm.
2.107 (*a*) 0.292 mm. (*b*) $\sigma_{AC} = 250$ MPa; $\sigma_{BC} = -307$ MPa. (*c*) 0.0272 mm.
2.108 (*a*) 990kN. (*b*) $\sigma_{AC} = 250$ MPa; $\sigma_{BC} = -316$ MPa. (*c*) 0.0313 mm.
2.111 (*a*) 112.1 kips. (*b*) 50 ksi in low-strength steel; 82.9 ksi in high-strength steel. (*c*) 0.00906 in.
2.112 (*a*) 0.0309 in. (*b*) 64.0 ksi. (*c*) 0.00387 in.
2.113 (*a*) $\sigma_{AD} = 250$ MPa. (*b*) $\sigma_{BE} = 124.3$ MPa. (*c*) 0.622 mm ↓.
2.114 (*a*) $\sigma_{AD} = 233$ MPa; $\sigma_{BE} = 250$ MPa. (*b*) 1.322 mm ↓.
2.115 (*a*) $\sigma_{AD} = -4.70$ MPa; $\sigma_{BE} = 19.34$ MPa. (*b*) 0.0967 mm ↓.
2.116 (*a*) −36.0 ksi. (*b*) 15.84 ksi.
2.117 (*a*) $\sigma_{AC} = -150.0$ MPa; $\sigma_{CB} = -250$ MPa. (*b*) −0.1069 mm →.
2.118 (*a*) $\sigma_{AC} = 56.5$ MPa; $\sigma_{CB} = 9.41$ MPa. (*b*) 0.0424 mm →.
2.121 (*a*) 915°F. (*b*) 1759°F.
2.122 (*a*) 0.1042 mm. (*b*) $\sigma_{AC} = \sigma_{CB} = -65.2$ MPa.
2.123 (*a*) 0.00788 mm. (*b*) $\sigma_{AC} = \sigma_{CB} = -6.06$ MPa.
2.125 1.219 in.
2.127 4.67°C.
2.128 (*a*) 9.53 kips. (*b*) 1.254×10^{-3} in.
2.130 (steel) − 15.80 ksi; (concrete) − 1.962 ksi.
2.131 (*a*) 9.73 kN. (*b*) 2.02 mm ←.
2.133 0.01870 in.
2.135 (*a*) $A\,\sigma_Y/\mu g$. (*b*) $E\,A/L$.

2.C1 *Prob. 2.126:* (*a*) 11.90×10^{-3} in. ↓. (*b*) 5.66×10^{-3} in. ↑.
2.C3 *Prob. 2.60:* (*a*) −116.2 MPa. (*b*) 0.363 mm.
2.C5 $r = 0.25$ in.: 3.89 kips; $r = 0.75$ in.: 2.78 kips.
2.C6 (*a*) −0.40083. (*b*) −0.10100. (*c*) −0.00405.

CHAPTER 3

3.1 641 N·m.
3.2 87.3 MPa.
3.3 (*a*) 5.17 kN·m. (*b*) 87.2 MPa.
3.4 (*a*) 7.55 ksi. (*b*) 7.64 ksi.
3.6 (*a*) 70.7 MPa. (*b*) 35.4 MPa. (*c*) 6.25%.
3.7 (*a*) 19.21 kip·in. (*b*) 2.01 in.
3.9 (*a*) 8.35 ksi. (*b*) 5.94 ksi.
3.10 (*a*) 1.292 in. (*b*) 1.597 in.
3.11 (*a*) shaft *CD*. (*b*) 85.8 MPa.
3.13 (*a*) 77.6 MPa. (*b*) 62.8 MPa. (*c*) 20.9 MPa.
3.15 9.16 kip·in.
3.16 (*a*) 1.503 in. (*b*) 1.853 in.
3.18 (*a*) $d_{AB} = 52.9$ mm. (*b*) $d_{BC} = 33.3$ mm.
3.20 3.18 kN·m.
3.21 (*a*) 59.6 mm. (*b*) 43.9 mm.
3.22 (*a*) 72.5 MPa. (*b*) 68.7 MPa.
3.23 1.189 kip·in.
3.25 4.30 kip·in.
3.27 73.6 N·m.
3.28 (*a*) $d_{AB} = 38.6$ mm. (*b*) $d_{CD} = 52.3$ mm. (*c*) 75.5 mm.
3.29 1.0; 1.025; 1.120; 1.200; 1.0.
3.31 11.87 mm.
3.32 9.38 ksi.
3.33 (*a*) 1.390°. (*b*) 1.482°.
3.35 (*a*) 1.384°. (*b*) 3.22°.
3.37 (*a*) 14.43°. (*b*) 46.9°.
3.38 6.02°.
3.40 1.140°.
3.41 3.77°.
3.42 3.78°.
3.44 53.8°.
3.45 36.1 mm.
3.46 0.837 in.
3.47 1.089 in.
3.48 62.9 mm.
3.49 42.0 mm.
3.50 22.5 mm.
3.53 (*a*) 4.72 ksi. (*b*) 7.08 ksi. (*c*) 4.35°.
3.54 7.37°.
3.56 (*a*) $T_A = 1090$ N·m; $T_C = 310$ N·m. (*b*) 47.4 MPa. (*c*) 28.8 MPa.
3.57 $\tau_{AB} = 68.9$ MPa; $\tau_{CD} = 14.70$ MPa.
3.59 12.24 MPa.
3.61 0.241 in.
3.63 $T/2\pi t r_1^2$ at r_1.
3.64 (*a*) 9.51 ksi. (*b*) 4.76 ksi.
3.65 (*a*) 46.9 MPa. (*b*) 23.5 MPa.
3.66 (*a*) 0.893 in. (*b*) 0.709 in.
3.67 (*a*) 20.1 mm. (*b*) 15.94 mm.
3.68 25.6 kW.
3.69 2.64 mm.
3.71 (*a*) 51.7 kW. (*b*) 6.17°.
3.73 (*a*) 47.5 MPa. (*b*) 30.4 mm.
3.76 (*a*) 4.08 ksi. (*b*) 6.79 ksi.

3.77 (*a*) 0.799 in. (*b*) 0.947 in.
3.78 (*a*) 16.02 Hz. (*b*) 27.2 Hz.
3.79 1917 rpm.
3.80 50.0 kW.
3.81 36.1 mm.
3.84 10.8 mm.
3.86 (*a*) 5.36 ksi. (*b*) 5.02 ksi.
3.87 63.5 kW.
3.88 42.6 Hz.
3.89 (*a*) 2.61 ksi. (*b*) 2.01 ksi.
3.90 (*a*) 203 N·m. (*b*) 165.8 N·m.
3.92 (*a*) 9.64 kN·m. (*b*) 9.91 kN·m.
3.93 2230 lb·in.
3.94 (*a*) 18.86 ksi; 1.500 in. (*b*) 21.0 ksi; 0.916 in.
3.95 (*a*) 113.3 MPa; 15.00 mm.
(*b*) 145.0 MPa; 6.90 mm.
3.98 (*a*) 6.72°. (*b*) 18.71°.
3.99 (*a*) 2.47°. (*b*) 4.34°.
3.100 (*a*) 977 N·m. (*b*) 8.61 mm.
3.101 (*a*) 52.1 kip·in. (*b*) 80.8 kip·in.
3.102 $\tau_{max} = 145.0$ MPa; $\phi = 19.70°$.
3.104 (*a*) 8.17 mm. (*b*) 42.1°.
3.106 (*a*) 8.02°. (*b*) 14.89 kN·m.
3.107 (*a*) 11.71 kN·m; 3.44°. (*b*) 14.12 kN·m; 4.81°.
3.110 (*a*) 5.24 kip·in. (*b*) 6.88°.
3.111 (*a*) 1.322 kip·in. (*b*) 12.60 ksi.
3.112 2.32 kN·m.
3.113 2.26 kN·m.
3.114 5.63 ksi.
3.115 14.62°.
3.118 68.0 MPa at inner surface.
3.119 20.2°.
3.120 (*a*) $c_0 = 0.1500c$. (*b*) $T_0 = 0.221\tau_y c^3$.
3.121 0.0505 in.
3.122 68.2 in.
3.123 (*a*) 189.2 N·m; 9.05°. (*b*) 228 N·m; 7.91°.
3.124 (*a*) 74.0 MPa; 9.56°. (*b*) 61.5 MPa; 6.95°.
3.127 5.07 MPa.
3.128 59.2 MPa.
3.129 0.944.
3.131 0.198.
3.132 0.883.
3.133 (*a*) 1.193 in. (*b*) 1.170 in. (*c*) 0.878 in.
3.135 (*a*) 157.0 kN·m. (*b*) 8.70°.
3.136 (*a*) 7.52 ksi. (*b*) 4.61°.
3.137 (*a*) 1007 N·m. (*b*) 9.27°.
3.138 (*a*) 4.55 ksi. (*b*) 2.98 ksi. (*c*) 2.56°.
3.139 (*a*) 5.82 ksi. (*b*) 2.91 ksi.
3.142 (*a*) 16.85 N·m.
3.143 8.45 N·m.
3.144 $\tau_a = 4.73$ MPa, $\tau_b = 9.46$ MPa.
3.146 0.894 in.
3.147 (*a*) 12.76 MPa. (*b*) 5.40 kN·m.
3.149 (*a*) $3c/t$. (*b*) $3c^2/t^2$.
3.150 (*b*) 0.25% , 1.000%, 4.00%.
3.151 637 kip·in.
3.153 12.22°.
3.155 1.285 in.
3.156 (*a*) 73.7 MPa. (*b*) 34.4 MPa. (*c*) 5.06°.
3.157 4.12 kN·m.
3.158 (*a*) 18.80 kW. (*b*) 24.3 MPa.
3.160 7.34 kip·ft.
3.162 (*a*) 0.347 in. (*b*) 37.2°.
3.C2 *Prob. 3.44:* 2.21°.
3.C5 (*a*) −3.282%. (*b*) −0.853%.
(*c*) −0.138%. (*d*) −0.00554%.
3.C6 (*a*) −1.883%. (*b*) −0.484%.
(*c*) −0.078%. (*d*) −0.00313%.

CHAPTER 4

4.1 (*a*) −61.6 MPa. (*b*) 91.7 MPa.
4.2 (*a*) −2.38 ksi. (*b*) −0.650 ksi.
4.3 80.2 kN·m.
4.4 24.8 kN·m.
4.5 (*a*) 1.405 kip·in. (*b*) 3.19 kip·in.
4.6 (*a*) −39.3 MPa. (*b*) 26.2 MPa.
4.9 −14.71 ksi; 8.82 ksi.
4.10 −10.38 ksi; 15.40 ksi.
4.11 −102.4 MPa; 73.2 MPa.
4.12 61.3 kN.
4.15 20.4 kip·in.
4.16 106.1 N·m.
4.18 4.63 kip·in.
4.19 3.79 kN·m.
4.21 (*a*) 96.5 MPa. (*b*) 20.5 N·m.
4.22 (*a*) 0.602 mm. (*b*) 0.203 N·m.
4.23 (*a*) 145.0 ksi. (*b*) 384 lb·in.
4.24 (*a*) $\sigma = 75.0$ MPa, $\rho = 26.7$ m.
(*b*) $\sigma = 125.0$ MPa, $\rho = 9.60$ m.
4.25 (*a*) 9.17 kN·m (*b*) 10.24 kN·m.
4.26 (*a*) 45.1 kip·in. (*b*) 49.7 kip·in.
4.29 (*a*) (8/9) h_0. (*b*) 0.949.
4.30 (*a*) 1007 in. (*b*) 3470 in. (*c*) 0.01320°.
4.31 (*a*) 139.1 m. (*b*) 480m.
4.32 (*a*) $[(\sigma_x)_{max}/2\ \rho c](y^2 - c^2)$. (*b*) $-(\sigma_x)_{max}\ c/2\rho$.
4.33 1.240 kN·m.
4.34 887 N·m.
4.37 689 kip·in.
4.38 335 kip·in.
4.39 (*a*) −56.0 MPa. (*b*) 66.4 MPa.
4.40 (*a*) −56.0 MPa. (*b*) 68.4 MPa.
4.41 (*a*) −1.979 ksi. (*b*) 16.48 ksi.
4.43 8.70 m.
4.44 8.59 m.
4.45 625 ft.
4.47 3.87 kip·ft.
4.48 2.88 kip·ft.
4.49 (*a*) 212 MPa. (*b*) −15.59 MPa.
4.50 (*a*) 210 MPa. (*b*) −14.08 MPa.
4.54 (*a*) 1674 mm^2. (*b*) 90.8 kN·m.
4.55 (*a*) $\sigma_A = 6.86$ ksi; $\sigma_B = 6.17$ ksi; $\sigma_S = 4.11$ ksi. (*b*) 151.9 ft.
4.57 (*a*) −22.5 ksi. (*b*) 17.78 ksi.
4.59 (*a*) 6.15 MPa. (*b*) −8.69 MPa.
4.61 (*a*) 219 MPa. (*b*) 176.0 MPa.
4.63 (*a*) 6.79 kip·in. (*b*) 5.59 kip·in.
4.64 (*a*) 4.71 ksi. (*b*) 5.72 ksi.
4.65 (*a*) 147.0 MPa. (*b*) 119.0 MPa.
4.67 (*a*) 38.4 N·m. (*b*) 52.8 N·m.
4.68 (*a*) 57.6 N·m. (*b*) 83.2 N·m.
4.69 2460 lb·in.
4.71 (*a*) 5.87 mm. (*b*) 2.09 m.
4.72 (*a*) 21.9 mm. (*b*) 7.81 m.
4.75 (*a*) 1759 kip·in. (*b*) 2650 kip·in.

4.77 (*a*) 29.2 kN·m. (*b*) 1.500.
4.78 (*a*) 27.5 kN·m. (*b*) 1.443.
4.79 (*a*) 2840 kip·in. (*b*) 1.611.
4.80 (*a*) 4820 kip·in. (*b*) 1.443.
4.81 1.866 kN·m.
4.82 19.01 kN·m.
4.84 22.8 kip·in.
4.86 212 kip·in.
4.87 120 MPa.
4.88 106.4 MPa.
4.91 (*a*) 106.7 MPa. (*b*) $y_0 = -31.2$ mm, 0, 31.2 mm. (*c*) 24.1 m.
4.92 (*a*) 13.36 ksi. (*b*) $y_0 = -1.517$ in., 0, 1.517 in. (*c*) 168.8 ft.
4.94 (*a*) $0.707\rho_Y$. (*b*) $6.09\rho_Y$.
4.96 (*a*) 4.69 m. (*b*) 7.29 kN·m.
4.99 (*a*) −102.8 MPa. (*b*) 80.6 MPa.
4.100 (*a*) −212 psi. (*b*) −637 psi. (*c*) −1061 psi.
4.101 (*a*) $-2P/\pi r^2$. (*b*) $-5P/\pi r^2$.
4.103 (*a*) −37.8 MPa. (*b*) −38.6 MPa.
4.105 (*a*) 288 lb. (*b*) 209 lb.
4.106 1.994 kN.
4.107 14.40 kN.
4.108 16.04 mm.
4.109 43.0 kips.
4.110 0.500*d*.
4.113 7.86 kips ↓; 9.15 kips ↑.
4.114 5.32 kips ↓; 10.79 kips ↑.
4.115 (*a*) 47.6 MPa. (*b*) −49.4 MPa. (*c*) 9.80 mm below top of section.
4.116 (*a*) $-P/2at$. (*b*) $-2P/at$. (*c*) $-P/2at$.
4.117 (*a*) 1125 kN. (*b*) 817 kN.
4.121 (*a*) 30.0 mm. (*b*) 94.5 kN.
4.122 (*a*) 5.00 mm. (*b*) 243 kN.
4.124 $P = 44.2$ kips; $Q = 57.3$ kips.
4.125 (*a*) 152.3 kips. (*b*) $x = 0.59$ in. (*c*) 300 μ.
4.127 (*a*) −3.37 MPa. (*b*) −18.60 MPa. (*c*) 3.37 MPa.
4.128 (*a*) 9.86 ksi. (*b*) −2.64 ksi. (*c*) −9.86 ksi.
4.129 (*a*) −29.3 MPa. (*b*) −144.8 MPa. (*c*) −125.9 MPa.
4.130 (*a*) 0.321 ksi. (*b*) −0.107 ksi. (*c*) 0.427 ksi.
4.133 (*a*) 57.8 MPa. (*b*) −56.8 MPa. (*c*) 25.9 MPa.
4.134 (*a*) 57.4°. (*b*) 75.7 MPa.
4.135 (*a*) 18.29°. (*b*) 13.74 ksi.
4.137 (*a*) 10.03°. (*b*) 54.2 MPa.
4.138 (*a*) 27.5°. (*b*) 5.07 ksi.
4.139 (*a*) 32.9°. (*b*) 61.4 MPa.
4.141 113.0 MPa.
4.143 10.46 ksi.
4.144 (*a*) $\sigma_A = 31.5$ MPa; $\sigma_B = -10.39$ MPa. (*b*) 94.0 mm above point *A*.
4.145 (*a*) 17.11 mm.
4.146 0.1638 in.
4.147 53.9 kips.
4.150 29.1 kip·in.
4.151 29.1 kip·in.
4.152 733 N·m.
4.153 1.323 kN·m.
4.155 900 N·m.
4.161 (*a*) −77.3 MPa. (*b*) −55.7 MPa.
4.162 $\sigma_A = -65.1$ MPa; $\sigma_B = 39.7$ MPa.
4.163 (*a*) 12.19 ksi. (*b*) 11.15 ksi.
4.164 $\sigma_A = 10.77$ ksi; $\sigma_B = -3.22$ ksi.
4.167 655 lb.
4.169 73.2 mm.
4.170 (*a*) −82.4 MPa. (*b*) 36.6 MPa.
4.171 (*a*) 3.06 ksi. (*b*) −2.81 ksi. (*c*) 0.529 ksi.
4.173 13.80 kN·m.
4.174 8.49 kN·m.
4.175 (*a*) 16.05 ksi. (*b*) −9.84 ksi.
4.177 (*a*) 41.8 MPa. (*b*) −20.4 MPa.
4.178 27.2 mm.
4.179 107.8 N·m.
4.180 (*a*) −32.5 MPa. (*b*) 34.2 MPa.
4.181 (*a*) −3.65 ksi. (*b*) 3.72 ksi.
4.183 (*a*) −5.96 ksi. (*b*) 3.61 ksi.
4.184 (*a*) −6.71 ksi. (*b*) 3.24 ksi.
4.185 (*a*) 63.9 MPa. (*b*) −52.6 MPa.
4.191 −0.536 ksi.
4.192 67.8 MPa; −81.8 MPa
4.194 (*a*) $\sigma_{\max} = 6\,M/a^3$, $1/\rho = 12M/Ea^4$.
(*b*) $\sigma_{\max} = 8.49\,M/a^3$, $1/\rho = 12M/Ea^4$.
4.195 48.6 kN·m.
4.196 (*a*) 46.9 MPa. (*b*) 18.94 MPa. (*c*) 55.4 m.
4.198 (*a*) −20.9 ksi. (*b*) −22.8 ksi.
4.199 60.9 mm.
4.201 (*a*) 56.7 kN·m. (*b*) 20.0 mm.
4.202 $P = 75.6$ kips ↓; $Q = 87.1$ kips ↓.
4.203 (*a*) $\sigma_A = -\frac{1}{2}\,\sigma$; $\sigma_B = \sigma_1$; $\sigma_C = -\sigma_1$; $\sigma_D = \frac{1}{2}\,\sigma_1$. (*b*) $4/3\,\rho_1$.
4.C1 *a = 4 mm:* $\sigma_a = 50.6$ MPa, $\sigma_s = 107.9$ MPa.
a = 14 mm: $\sigma_a = 89.7$ MPa, $\sigma_s = 71.8$ MPa.
(*a*) 1 11.6 MPa. (*b*) 6.61 mm.
4.C2 $y_Y = 65$ mm, $M = 52.6$ kN.m, $\rho = 43.3$; $y_Y = 45$ mm, $M = 55.6$ kN·m, $\rho = 30.0$ m.
4.C3 $\beta = 30°$: $\sigma_A = -7.83$ ksi, $\sigma_B = -5.27$ ksi, $\sigma_C = 7.19$ ksi, $\sigma_D = 5.91$ ksi;
$\beta = 120°$: $\sigma_A = 1.557$ ksi, $\sigma_B = 6.01$ ksi, $\sigma_C = -2.67$ ksi, $\sigma_D = -4.89$ ksi.
4.C4 $r_1/h = 0.529$ for 50% increase in $\sigma_{\max}$.
4.C5 *Prob. 4.10:* −102.4 MPa; 73.2 MPa.
4.C6 $y_Y = 0.8$ *in.:* 76.9 kip·in., 552 in.;
$y_Y = 0.2$ *in.:* 95.5 kip·in., 138.1 in.
4.C7 *a = 0.2 in.:* − 7.27 ksi, *a = 0.8 in.:* − 6.61 ksi.
For $a = 0.625$ in., $\sigma = -6.51$ ksi.

CHAPTER 5

5.1 (*b*) $V = w(L/2 - x)$; $M = wx(L - x)/2$.
5.2 (*b*) *A* to *B*: $V = \dfrac{Pb}{L}$; $M = Pbx/L$.
B to *C*: $V = Pa/L$; $M = Pa\,(L - x)/L$.
5.3 (*b*) $V = w_0L/2 - w_0\,x^2/2L$; $M = -w_0L^2/3 + w_0Lx/2 - w_0x^3/6L$
5.4 (*b*) $V = w(L - x)$; $M = w/2\,(L - x)^2$.
5.5 (*b*) $(0 < x < a)$: $V = -P$; $M = Px$. $(a < x < 2a)$: $V = 2P$; $M = -2Px + Pa$.
5.6 (*b*) *A* to *B*: $V = w(a - x)$; $M = w(ax - x^2/2)$.
B to *C*: $V = 0$; $M = wa^2/2$.
C to *D*: $V = w(L - x - a)$; $M = w[a(L - x) - (L - x)^2/2]$.
5.7 (*a*) 3.00 kN. (*b*) 0.800 kN·m.
5.8 (*a*) 150.0 lb. (*b*) 1500 lb·in.
5.9 (*a*) 62.5 kN. (*b*) 47.6 kN·m.
5.11 (*a*) 3.45 kN. (*b*) 1125 N·m.
5.12 (*a*) 2000 lb. (*b*) 19200 lb·in.
5.13 (*a*) 900 N. (*b*) 112.5 N·m.
5.15 10.89 MPa.
5.16 950 psi.

5.18 139.2 MPa.
5.20 9.90 ksi.
5.21 14.17 ksi.
5.23 $|V|_{max} = 342$ N; $|M|_{max} = 51.6$ N·m; $\sigma = 17.19$ MPa.
5.25 10.34 ksi.
5.26 $|V|_{max} = 6.00$ kN; $|M|_{max} = 4.00$ kN·m; $\sigma_{max} = 14.29$ MPa.
5.27 (*a*) 10.67 kN. (*b*) 9.52 MPa.
5.29 (*a*) 866 mm. (*b*) 99.2 MPa.
5.30 (*a*) 819 mm. (*b*) 89.5 MPa.
5.31 (*a*) 3.09 ft. (*b*) 12.95 ksi.
5.32 1.021 in.
5.33 (*a*) 33.3 mm. (*b*) 6.66 mm.
5.34 See 5.1.
5.35 See 5.2.
5.36 See 5.3.
5.37 See 5.4.
5.38 See 5.5.
5.39 See 5.6.
5.40 See 5.7.
5.41 See 5.8.
5.42 See 5.9.
5.43 See 5.10.
5.46 See 5.15.
5.47 See 5.16.
5.48 See 5.18.
5.49 See 5.20.
5.52 (*a*) $V = (w_0L/\pi)\cos(\pi x/L)$; $M = (w_0L^2/\pi^2)\sin(\pi x/L)$. (*b*) w_0L^2/π^2.
5.53 (*a*) $V = w_0(L^2 - 3x^2)/6L$; $M = w_0(Lx - x^3/L)/6$. (*b*) $0.0642\ w_0L^2$.
5.54 $|V|_{max} = 15.75$ kips; $|M|_{max} = 27.8$ kip·ft; $\sigma = 13.58$ ksi.
5.55 $|V|_{max} = 16.80$ kN; $|M|_{max} = 8.82$ kN·m; $\sigma = 73.5$ MPa.
5.56 $|V|_{max} = 20.7$ kN; $|M|_{max} = 9.75$ kN·m; $\sigma = 60.2$ MPa.
5.58 $|V|_{max} = 1400$ lb; $|M|_{max} = 19.20$ kip·in; $\sigma = 6.34$ ksi.
5.59 $|V|_{max} = 76.0$ kN; $|M|_{max} = 67.3$ kN·m; $\sigma = 68.5$ MPa.
5.60 $|V|_{max} = 48.0$ kN; $|M|_{max} = 12.00$ kN·m; $\sigma = 62.2$ MPa.
5.61 $|V|_{max} = 30.0$ lb; $|M|_{max} = 24.0$ lb·ft; $\sigma = 6.95$ ksi.
5.63 (*a*) $|V|_{max} = 24.5$ kips; $|M|_{max} = 36.3$ kip·ft; (*b*) 15.82 ksi.
5.64 $|V|_{max} = 1150$ N; $|M|_{max} = 221$ N·m; $P = 500$ N; $Q = 250$ N.
5.65 $h > 173.2$ mm.
5.68 $b > 6.20$ in.
5.69 $h > 203$ mm.
5.70 $b > 48.0$ mm.
5.71 W21 × 62.
5.72 W27 × 84.
5.73 W530 × 92.
5.74 W250 × 28.4.
5.76 S15 × 42.9.
5.77 S510 × 98.2.
5.79 9 mm.
5.80 C180 × 14.6.
5.81 C9 × 15.
5.82 3/8 in.
5.83 W610 × 101.
5.84 W24 × 68.
5.85 176.8 kN/m.
5.86 108.8 kN/m.
5.89 (*a*) 1.485 kN/m. (*b*) 1.935 m.
5.91 (*a*) S15 × 42.9. (*b*) W27 × 84.
5.92 (*a*) 6.49 ft. (*b*) W16 × 31.
5.94 383 mm.
5.95 336 mm.
5.96 W27 × 84.
5.97 +23.2%.
5.98 (*a*) $V = -w_0x + w_0\langle x - a\rangle^1$; $M = w_0x^2/2 + (w_0/2)\langle x - a\rangle^2$. (*b*) $-3\ w_0a^2/2$.
5.100 (*a*) $V = -w_0x + w_0x^2/2a - (w_0/2a)\langle x - a\rangle^2$; $M = -w_0x^2/2 + w_0x^3/6a - (w_0/6a)\langle x - a\rangle^3$. (*b*) $-5\ w_0a^2/6$.
5.102 (*a*) $V = -w_0\langle x - a\rangle^1 - 3w_0a/4 + (15\ w_0a/4)\langle x - 2a\rangle^0$; $M = -(w_0/2)\langle x - a\rangle^2 - 3w_0ax/4 + (15\ w_0a/4)\langle x - 2a\rangle^1$. (*b*) $-w_0a^2/2$.
5.103 (*a*) $V = 1.25\ P - P\langle x - a\rangle^0 - P\langle x - 2a\rangle^0$; $M = 1.25\ Px - P\langle x - a\rangle^1 - P\langle x - 2a\rangle^1$. (*b*) $0.750\ Pa$.
5.104 (*a*) $V = -P/2 - P\langle x - a\rangle^0$; $M = Px/2 - P\langle x - a\rangle^1 + Pa + Pa\langle x - a\rangle^0$. (*b*) $3\ Pa/2$.
5.105 (*a*) $V = -P\langle x - a\rangle^0$; $M = -P\langle x - a\rangle^1 - Pa\langle x - a\rangle^0$. (*b*) $-Pa$.
5.106 (*a*) $V = 40 - 48\langle x - 1.5\rangle^0 - 60\langle x - 3.0\rangle^0 + 60\langle x - 3.6\rangle^0$ kN; $M = 40x - 48\langle x - 1.5\rangle^1 - 60\langle x - 3.0\rangle^1 + 60\langle x - 3.6\rangle^1$ kN·m. (*b*) 60.0 kN·m.
5.107 (*a*) $V = -3 + 9.75\langle x - 3\rangle^0 - 6\langle x - 7\rangle^0 - 6\langle x - 11\rangle^0$ kips; $M = -3x + 9.75\langle x - 3\rangle^1 - 6\langle x - 7\rangle^1 - 6\langle x - 11\rangle^1$ kip·ft. (*b*) 21.0 kip·ft.
5.108 (*a*) $V = 62.5 - 25\langle x - 0.6\rangle^1 + 25\langle x - 2.4\rangle^1 - 40\langle x - 0.6\rangle^0 - 40\langle x - 2.4\rangle^0$ kN; $M = 62.5x - 12.5\langle x - 0.6\rangle^2 + 12.5\langle x - 2.4\rangle^2 - 40\langle x - 0.6\rangle^1 - 40\langle x - 2.4\rangle^1$ kN·m (*b*) 47.6 kN·m.
5.109 (*a*) $V = 13 - 3x + 3\langle x - 3\rangle^1 - 8\langle x - 7\rangle^0 - 3\langle x - 11\rangle^1$ kips; $M = 13x - 1.5x^2 + 1.5\langle x - 3\rangle^2 - 8\langle x - 7\rangle^1 - 1.5\langle x - 11\rangle^2$ kip·ft. (*b*) 41.5 kip·ft.
5.110 (*a*) $V = 30 - 24\langle x - 0.75\rangle^0 - 24\langle x - 1.5\rangle^0 - 24\langle x - 2.25\rangle^0 + 66\langle x - 3\rangle^0$ kN; $M = 30x - 24\langle x - 0.75\rangle^1 - 24\langle x - 1.5\rangle^1 - 24\langle x - 2.25\rangle^1 + 66\langle x - 3\rangle^1$ kN·m. (*b*) 87.7 MPa.
5.114 (*a*) 122.7 kip·ft at $x = 6.50$ ft. (*b*) W16 × 40.
5.115 (*a*) 121.5 kip·ft at $x = 6.00$ ft. (*b*) W16 × 40.
5.118 $|V|_{max} = 35.6$ kN; $|M|_{max} = 25.0$ kN·m.
5.119 $|V|_{max} = 89.0$ kN; $|M|_{max} = 178.0$ kN·m.
5.120 $|V|_{max} = 15.30$ kips; $|M|_{max} = 38.0$ kip·ft.
5.122 (*a*) $|V|_{max} = 13.80$ kN; $|M|_{max} = 16.16$ kN·m. (*b*) 83.8 MPa.
5.123 (*a*) $|V|_{max} = 40.0$ kN; $|M|_{max} = 30.0$ kN·m. (*b*) 40.0 MPa.
5.124 (*a*) $|V|_{max} = 3.84$ kips; $|M|_{max} = 3.80$ kip·ft. (*b*) 0.951 ksi.
5.126 (*a*) $h = h_0\,[(x/L)\,(1 - x/L)]^{1/2}$. (*b*) 4.44 kip·in.
5.127 (*a*) $h = h_0\,(x/L)^{1/2}$. (*b*) 20.0 kips.
5.128 (*a*) $h = h_0\,(x/L)^{3/2}$. (*b*) 167.7 mm.
5.130 (*a*) $h = h_0\sqrt{2x/L}$. (*b*) 60.0 kN.
5.132 $l_2 = 6.00$ ft; $l_2 = 4.00$ ft.
5.134 1.800 m.
5.135 1.900 m.
5.136 $d = d_0\,(2x/L)^{1/3}$ for $0 \le x \le L/2$; $d = d_0\,[2\,(L - x)/L]^{1/3}$ for $L/2 \le x \le L$.
5.139 (*a*) $b = b_0\,(1 - x/L)^2$. (*b*) 160.0 lb/in.
5.140 (*a*) 155.2 MPa. (*b*) 143.3 MPa.
5.141 (*a*) 25.0 ksi. (*b*) 18.03 ksi.
5.143 193.8 kN.
5.144 (*a*) 152.6 MPa. (*b*) 133.6 MPa.
5.145 (*a*) 4.49 m. (*b*) 211. mm.

5.147 (*a*) 11.16 ft. (*b*) 14.31 in.
5.149 (*a*) 240 mm. (*b*) 150.0 MPa.
5.150 (*a*) 15.00 in. (*b*) 320 lb/in.
5.151 (*a*) 30.0 in. (*b*) 12.80 kips.
5.152 (*a*) 85.0 N. (*b*) 21.3 N·m.
5.154 (*a*) 1.260 ft. (*b*) 7.24 ksi.
5.156 $|V|_{\max} = 200$ kN; $|M|_{\max} = 300$ kN·m; 136.4 MPa.
5.158 $h > 14.27$ in.
5.159 W27 × 84.
5.161 (*a*) 225.6 kN·m at $x = 3.63$ m.
(*b*) 60.6 MPa.
5.163 (*a*) $b_0\,(1 - x/L)$. (*b*) 20.8 mm.
5.C4 *For $x = 13.5$ ft:* $M_1 = 131.25$ kip·ft;
$M_2 = 156.25$ kip·ft; $M_C = 150.0$ kip·ft.
5.C6 *Prob. 5.112:* $V_A = 29.5$ kN, $M_{\max} = 28.3$ kN·m,
at 1.938 m from *A*.

CHAPTER 6

6.1 60.0 mm.
6.2 2.00 kN.
6.3 326 lb.
6.4 (*a*) 155.8 N. (*b*) 329 kPa.
6.5 193.5 kN.
6.7 10.56 ksi.
6.9 (*a*) 8.97 MPa. (*b*) 8.15 MPa.
6.11 (*a*) 13.15 ksi. (*b*) 11.16 ksi.
6.12 (*a*) 3.17 ksi. (*b*) 2.40 ksi.
6.13 114.0 kN.
6.15 1733 lb.
6.17 (*a*) 84.2 kips. (*b*) 60.2 kips.
6.18 87.3 mm.
6.19 (*b*) $h = 320$ mm; $b = 97.7$ mm.
6.21 (*a*) 1.745 ksi. (*b*) 2.82 ksi.
6.22 (*a*) 31.0 MPa. (*b*) 23.2 MPa.
6.23 3.21 ksi.
6.24 32.7 MPa.
6.26 (*a*) Line at mid-height. (*b*) 2.00.
6.28 (*a*) Line at mid-height. (*b*) 1.500.
6.29 1.672 in.
6.30 10.79 kN.
6.31 (*a*) 59.9 psi. (*b*) 79.8 psi.
6.32 (*a*) 379 kPa. (*b*) 0.
6.35 (*a*) 95.2 MPa. (*b*) 112.8 MPa.
6.36 (*a*) 101.6 MPa. (*b*) 79.9 MPa.
6.37 $\tau_a = 33.7$ MPa; $\tau_b = 75.0$ MPa; $\tau_c = 43.5$ MPa.
6.38 (*a*) 40.5 psi. (*b*) 55.2 psi.
6.40 $\tau_a = 0$; $\tau_b = 1.262$ ksi; $\tau_c = 3.30$ ksi;
$\tau_d = 6.84$ ksi; $\tau_e = 7.86$ ksi.
6.42 (*a*) 18.23 MPa. (*b*) 14.59 MPa. (*c*) 46.2 MPa.
6.43 7.19 ksi.
6.44 9.05 mm.
6.45 0.371 in.
6.46 83.3 MPa.
6.48 $\tau_a = 10.76$ MPa; $\tau_b = 0$; $\tau_c = 11.21$ MPa;
$\tau_d = 22.0$ MPa; $\tau_e = 9.35$ MPa.
6.49 (*a*) 50.9 MPa. (*b*) 62.4 MPa.
6.51 1.4222 in.
6.52 10.53 ksi.
6.56 (*a*) 6.73 MPa. (*b*) 1.515 MPa.
6.57 (*a*) 23.3 MPa. (*b*) 109.7 MPa.
6.58 (*a*) 1.323 ksi. (*b*) 1.329 ksi.
6.59 (*a*) 0.888 ksi. (*b*) 1.453 ksi.
6.61 0.345*a*.
6.62 0.714*a*.
6.63 1.250*a*.
6.64 $3(b^2 - a^2)/[6(a + b) + h]$.
6.65 (*a*) 19.06 mm. (*b*) $\tau_A = 0$; $(\tau_B)_{AB} = 50.5$ MPa;
$(\tau_B)_{BD} = 25.3$ MPa; $\tau_c = 59.0$ MPa.
6.68 (*a*) 10.22 mm. (*b*) 0 at *B* and *E*; 41.1 MPa at *A*;
68.5 MPa just above *D*; 13.71 MPa just to the right of *D*;
77.7 MPa just below *D*; 81.8 MPa at center of *DF*.
6.69 0.727 in.
6.70 20.2 mm.
6.71 1.265 in.
6.72 6.14 mm.
6.75 2.37 in.
6.76 21.7 mm.
6.77 40.0 mm.
6.78 3.75 in.
6.81 (maximum) P/at.
6.82 (maximum) 1.333 P/at.
6.83 (*a*) 144.6 N·m. (*b*) 65.9 MPa.
6.84 (*a*) 144.6 N·m. (*b*) 106.6 MPa.
6.87 (maximum) 0.428 ksi at B'.
6.88 (maximum) 1.287 ksi at C'.
6.89 738 N.
6.90 (*a*) 17.63 MPa. (*b*) 13.01 MPa.
6.91 143.3 kips.
6.93 189.6 lb.
6.94 (*a*) 41.4 MPa. (*b*) 41.4 MPa.
6.96 53.9 kips.
6.97 (*a*) 146.1 kN/m. (*b*) 19.99 MPa.
6.99 40.0 mm.
6.100 0.433 in.
6.C1 (*a*) $h = 173.2$ mm. (*b*) $h = 379$ mm.
6.C2 (*a*) $L = 37.5$ in.; $b = 1.250$ in.
(*b*) $L = 70.3$ in.; $b = 1.172$ in.
(*c*) $L = 59.8$ in.; $b = 1.396$ in.
6.C4 (*a*) $\tau_{\max} = 2.03$ ksi; $\tau_B = 1.800$ ksi. (*b*) 194 psi.
6.C5 *Prob. 6.66:* (*a*) 2.67 in. (*b*) $\tau_B = 0.917$ ksi;
$\tau_D = 3.36$ ksi; $\tau_{\max} = 4.28$ ksi.

CHAPTER 7

7.1 $\sigma = 9.46$ ksi; $\tau = 1.013$ ksi.
7.2 $\sigma = 32.9$ MPa; $\tau = 71.0$ MPa.
7.3 $\sigma = 10.93$ ksi; $\tau = 0.536$ ksi.
7.4 $\sigma = -0.521$ MPa; $\tau = 56.4$ MPa.
7.5 (*a*) −37.0°, 53.0°. (*b*) −13.60 MPa. (*c*) −86.4 MPa.
7.7 (*a*) − 26.6°; 63.4°. (*b*) 190.0 MPa, −10.00 MPa.
7.9 (*a*) 8.0°, 98.0°. (*b*) 36.4 MPa. (*c*) −50.0 MPa.
7.10 (*a*) −26.6°, 63.4°. (*b*) 5.00 ksi. (*c*) 6.00 ksi.
7.11 (*a*) 18.4°, 108.4°. (*b*) 100.0 MPa. (*c*) 90.0 MPa.
7.12 (*a*) −31.0°, 59.0° (*b*) 17.00 ksi. (*c*) 3.00 ksi.
7.13 (*a*) $\sigma_{x'} = -2.40$ ksi; $\tau_{x'y'} = 0.1498$ ksi; $\sigma_{y'} = 10.40$ ksi.
(*b*) $\sigma_{x'} = 1.951$ ksi; $\tau_{x'y'} = 6.07$ ksi; $\sigma_{y'} = 6.05$ ksi.
7.15 (*a*) $\sigma_{x'} = 9.02$ ksi; $\tau_{x'y'} = 3.80$ ksi; $\sigma_{y'} = -13.02$ ksi.
(*b*) $\sigma_{x'} = 5.34$ ksi; $\tau_{x'y'} = -9.06$ ksi; $\sigma_{y'} = -9.34$ ksi.
7.17 (*a*) 217 psi. (*b*) −125.0 psi.
7.18 (*a*) −0.300 MPa. (*b*) −2.92 MPa.
7.19 16.58 kN.
7.21 (*a*) 18.4°. (*b*) 16.67 ksi.
7.23 (*a*) 18.9°, 108.9°, 18.67 MPa, −158.5 MPa. (*b*) 88.6 MPa.

7.24 (*a*) 25.1 ksi, −0.661 ksi, 12.88 ksi.
7.25 5.12 ksi, −1.640 ksi, 3.38 ksi.
7.26 12.18 MPa, −48.7 MPa; 30.5 MPa.
7.27 205 MPa.
7.29 (*a*) −2.89 MPa. (*b*) 12.77 MPa, 1.226 MPa.
7.53 (*a*) −8.66 MPa. (*b*) 17.00 MPa, −3.00 MPa.
7.55 33.8°, 123.8°; 168.6 MPa, 6.42 MPa.
7.56 0°, 90°; σ_0, $-\sigma_0$.
7.57 −30°, 60°; $-\sqrt{3}\tau_0$, $\sqrt{3}\tau_0$.
7.58 $-120.0 \text{ MPa} \le \tau_{xy} \le 120.0 \text{ MPa}$.
7.59 $-141.4 \text{ MPa} \le \tau_{xy} \le 141.1 \text{ MPa}$.
7.61 $16.5° \le \theta \le 110.1°$.
7.62 $-5.1° \le \theta \le 132.0°$.
7.63 (*a*) 33.7°, 123.7°. (*b*) 18.00 ksi. (*c*) 6.50 ksi.
7.65 (*b*) $|\tau_{xy}| = \sqrt{\sigma_x \sigma_y - \sigma_{\max}\sigma_{\min}}$.
7.66 (*a*) 13.00 ksi. (*b*) 15.00 ksi.
7.68 (*a*) 94.3 MPa. (*b*) 105.3 MPa.
7.69 (*a*) 100.0 MPa. (*b*) 110.0 MPa.
7.70 (*a*) 91.0 MPa. (*b*) 91.0 MPa. (*c*) 108.0 MPa.
7.71 (*a*) 113.0 MPa. (*b*) 91.0 MPa. (*c*) 143.0 MPa.
7.73 (*a*) 18.5 ksi. (*b*) 13.00 ksi. (*c*) 11.00 ksi.
7.74 (*a*) ±6.00 ksi. (*b*) ±11.24 ksi.
7.75 ±60.0 MPa.
7.77 2.00 ksi; 9.33 ksi.
7.79 −40.0 MPa; 130.0 MPa.
7.80 (*a*) 45.7 MPa. (*b*) 92.9 MPa.
7.81 (*a*) 1.228. (*b*) 1.098. (*c*) Yielding occurs.
7.82 (*a*) 1.083. (*b*) Yielding occurs. (*c*) Yielding occurs.
7.83 (*a*) 1.287. (*b*) 1.018. (*c*) Yielding occurs.
7.84 (*a*) 1.119. (*b*) Yielding occurs. (*c*) Yielding occurs.
7.87 8.19 kip·in.
7.88 9.46 kip·in.
7.89 Rupture will occur.
7.90 Rupture will occur.
7.91 No Rupture.
7.92 Rupture will occur.
7.94 ±8.49 MPa.
7.95 50.0 MPa.
7.96 196.9 N·m.
7.98 (*a*) 1.290 MPa. (*b*) 0.852 mm.
7.100 5.49.
7.102 10.25 ksi; 5.12 ksi.
7.103 2.94 MPa.
7.104 12.76 m.
7.105 $\sigma_{\max} = 113.7$ MPa; $\tau_{\max} = 56.8$ MPa.
7.106 $\sigma_{\max} = 136.0$ MPa; $\tau_{\max} = 68.0$ MPa.
7.108 $\sigma_{\max} = 78.5$ MPa; $\tau_{\max} = 39.3$ MPa.
7.109 251 psi.
7.111 0.307 in.
7.112 3.29 MPa.
7.113 3.80 MPa.
7.114 (*a*) 44.2 MPa. (*b*) 15.39 MPa.
7.115 56.8°.
7.117 (*a*) 3750 psi. (*b*) 1079 psi.
7.118 387 psi.
7.120 (*a*) 3.15 ksi. (*b*) 1.9993 ksi.
7.121 (*a*) 1.486 ksi. (*b*) 3.16 ksi.
7.122 $\sigma_{\max} = 68.6$ MPa; $\tau_{\max} = 34.3$ MPa.
7.124 $\sigma_{\max} = 77.4$ MPa; $\tau_{\max} = 38.7$ MPa.
7.126 (*a*) 5.64 ksi. (*b*) 282 psi.
7.127 (*a*) 2.28 ksi. (*b*) 228 psi.
7.128 $\epsilon_{x'} = -653\ \mu$; $\epsilon_{y'} = 303\ \mu$; $\gamma_{x'y'} = -829\ \mu$.
7.129 $\epsilon_{x'} = 115.0\ \mu$; $\epsilon_{y'} = 285\ \mu$; $\gamma_{x'y'} = -5.72\ \mu$.
7.131 $\epsilon_{x'} = 36.7\ \mu$; $\epsilon_{y'} = 283\ \mu$; $\gamma_{x'y'} = 227\ \mu$.
7.132 $\epsilon_{x'} = -653\ \mu$; $\epsilon_{y'} = 303\ \mu$; $\gamma_{x'y'} = -829\ \mu$.
7.133 $\epsilon_{x'} = 115.0\ \mu$; $\epsilon_{y'} = 285\ \mu$; $\gamma_{x'y'} = -5.72\ \mu$.
7.135 $\epsilon_{x'} = 36.7\ \mu$; $\epsilon_{y'} = 283\ \mu$; $\gamma_{x'y'} = 227\ \mu$.
7.136 (*a*) −33.7°, 56.3°; −420 μ, 100 μ, 160 μ. (*b*) 520 μ. (*c*) 580 μ.
7.137 (*a*) −30.1°, 59.9°; −702 μ, −298 μ, 500 μ. (*b*) 403 μ. (*c*) 1202 μ.
7.139 (*a*) −26.6°, 64.4°; −150.0 μ, 750 μ, −300 μ. (*b*) 900 μ. (*c*) 1050 μ.
7.140 (*a*) 7.8°, 97.8°; 56.6 μ, 243 μ, 0. (*b*) 186.8 μ.(*c*) 243 μ.
7.141 (*a*) 121.0°, 31.0°; 513 μ, 87.5 μ, 0. (*b*) 425 μ.(*c*) 513 μ.
7.143 (*a*) 127.9°, 37.9°; −383 μ, −57.5 μ, 0. (*b*) 325 μ.(*c*) 383 μ.
7.146 (*a*) -300×10^{-6} in./in. (*b*) 435×10^{-6} in./in., -315×10^{-6} in./in.; 750×10^{-6} in./in.
7.149 (*a*) 30.0°, 120.0°; 560×10^{-6} in./in, -140.0×10^{-6} in./in. (*b*) 700×10^{-6} in./in.
7.150 $P = 69.6$ kips; $Q = 30.3$ kips.
7.151 $P = 34.8$ kips; $Q = 38.4$ kips.
7.154 1.421 MPa.
7.155 1.761 MPa.
7.156 −22.5°, 67.5°; 426 μ, −952 μ, −224 μ.
7.157 −32.1°, 57.9°; −70.9 MPa, −29.8 MPa.
7.158 −4.76 ksi; −0.467 ksi.
7.159 (*a*) 47.9 MPa. (*b*) 102.7 MPa.
7.161 $\theta/2$, $(\theta + \pi)/2$; $\sigma_0 + \sigma_0 \cos\theta$, $\sigma_0 - \sigma_0 \cos\theta$.
7.163 (*a*) 40.0 MPa. (*b*) 72.0 MPa.
7.164 (*a*) 1.286. (*b*) 1.018. (*c*) Yielding occurs.
7.165 $\sigma_{\max} = 45.1$ MPa; $\tau_{\max}$ (in-plane) = 9.40 MPa.
7.167 3.43 ksi (compression).
7.169 415×10^{-6} in./in.
7.C1 *Prob. 7.14:* (*a*) −56.2 MPa, 86.2 MPa, −38.2 MPa. (*b*) −45.2 MPa, 75.2 MPa, 53.8 MPa.
Prob. 7.16: (*a*) 24.0 MPa, −104.0 MPa, −1.50 MPa. (*b*) −19.51 MPa, −60.5 MPa, −60.7 MPa.
7.C4 *Prob. 7.93:* Rupture occurs at $\tau_0 = 3.67$ ksi.
7.C6 *Prob. 7.138:* (*a*) −21.6°, 68.4°; 279μ, −599μ, 160.0μ. (*b*) 877μ. (*c*) 877μ.
7.C7 *Prob. 7.142:* (*a*) 11.3°, 101.3°; 310μ, 50.0μ, 0. (*b*) 260μ. (*b*) 310μ.
7.C8 *Prob. 7.144:* $\epsilon_x = 253\mu$; $\epsilon_y = 307$; $\gamma_{xy} = -893$. $\epsilon_a = 727\mu$; $\epsilon_b = -167.2$; $\gamma_{\max} = -894$.
Prob. 7.145: $\epsilon_x = 725\mu$; $\epsilon_y = -75.0$; $\gamma_{xy} = 173.2$. $\epsilon_a = 734\mu$; $\epsilon_b = -84.3$; $\gamma_{\max} = 819$.

CHAPTER 8

8.1 (*a*) 10.69 ksi. (*b*) 19.18 ksi. (*c*) Not acceptable.
8.2 (*a*) 10.69 ksi. (*b*) 13.08 ksi. (*c*) Acceptable.
8.3 (*a*) 94.6 MPa. (*b*) 93.9 MPa. (*c*) Acceptable.
8.4 (*a*) 91.9 MPa. (*b*) 95.1 MPa. (*c*) Acceptable.
8.5 (*a*) W 310 × 38.7. (*b*) 147.8 MPa; 18.18 MPa; 140.2 MPa.
8.6 (*a*) W 690 × 125. (*b*) 118.2 MPa; 34.7 MPa; 122.3 MPa.
8.9 (*a*) 137.5 MPa. (*b*) 129.5 MPa.
8.11 (*a*) 17.90 ksi. (*b*) 17.08 ksi.
8.12 (*a*) 19.39 ksi. (*b*) 20.7 ksi.
8.13 (*a*) 131.3 MPa. (*b*) 135.5 MPa.
8.15 41.2 mm.
8.19 873 lb.
8.20 1.578 in.
8.22 (*a*) *H :* 6880 psi; *K* : 6760 psi. (*b*) *H :* 7420 psi; *K :* 7010 psi.

8.23 57.7 mm.
8.24 54.3 mm.
8.27 37.0 mm.
8.28 43.9 mm.
8.29 1.822 in.
8.30 1.792 in.
8.31 (*a*) 11.06 ksi; 0. (*b*) −0.537 ksi; 1.610 ksi. (*c*) −12.13 ksi; 0.
8.32 (*a*) −12.34 ksi; 0. (*b*) −1.073 ksi; 0.805 ksi. (*c*) 10.20 ksi; 0.
8.35 (*a*) −37.9 MPa; 14.06 MPa. (*b*) −131.6 MPa; 0.
8.36 (*a*) −32.5 MPa; 14.06 MPa. (*b*) −126.2 MPa; 0.
8.37 (*a*) 0; 3.34 ksi. (*b*) −8.80 ksi; 2.93 ksi.
8.38 (*a*) 20.4 MPa; 14.34 MPa. (*b*) −21.5 MPa; 19.98 MPa.
8.39 (*a*) 4.79 ksi; 3.07 ksi. (*b*) −2.57 ksi; 3.07 ksi.
8.40 −14.98 MPa; 17.29 MPa.
8.42 55.0 MPa, −55.0 MPa; −45.0°, 45.0°; 55.0 MPa.
8.43 (*a*) 4.30 MPa, −93.4 MPa; 12.1°, 102.1°. (*b*) 48.9 MPa.
8.46 (*a*) 3.47 ksi; 1.042 ksi. (*b*) 7.81 ksi; 0.781 ksi. (*c*) 12.15 ksi; 0.
8.47 (*a*) 18.39 MPa; 0.391 MPa. (*b*) 21.3 MPa; 0.293 MPa. (*c*) 24.1 MPa; 0.
8.48 (*a*) −7.98 MPa; 0.391 MPa. (*b*) −5.11 MPa; 0.293 MPa. (*c*) −2.25 MPa; 0.
8.49 1506 psi, −4150 psi; 31.1°, 121.1°; 2830 psi.
8.51 25.2 MPa, −0.870 MPa; 13.06 MPa.
8.52 34.6 MPa, −10.18 MPa; 22.4 MPa.
8.53 (*a*) 86.5 MPa; 0. (*b*) 57.0 MPa; 9.47 MPa.
8.55 12.94 MPa, −1.328 MPa; 7.13 MPa.
8.57 4.05 ksi, −0.010 ksi; 2.03 ksi.
8.58 1.468 ksi, −3.90 ksi; 2.68 ksi.
8.60 (*a*) 51.0 kN. (*b*) 39.4 kN.
8.61 12.2 MPa, −12.2 MPa; 12.2 MPa.
8.62 (*a*) 12.90 ksi, −0.32 ksi; −8.9°, 81.1°.; 6.61 ksi. (*b*) 6.43 ksi, −6.43 ksi; ± 45.0°; 6.43 ksi.
8.64 0.48 ksi, −44.7 ksi; 22.6 ksi.
8.65 (*a*) W14 × 22. (*b*) 23.6 ksi, 4.89 ksi; 22.4 ksi.
8.66 *BC*: 21.7 mm; *CD*: 33.4 mm.
8.68 46.5 mm.
8.69 (*a*) −11.07 ksi; 0. (*b*) 2.05 ksi; 2.15 ksi. (*c*) 15.17 ksi; 0.
8.71 $P\,(2R + 4r/3)/\pi r^3$.
8.74 30.1 MPa, −0.62 MPa; −8.2°, 81.8°; 15.37 MPa.
8.75 (*a*) −16.41 ksi; 0. (*b*) −15.63 ksi; 0.0469 ksi. (*c*) −7.10 ksi; 1.256 ksi.
8.76 (*a*) 7.50 MPa. (*b*) 11.25 MPa. (*c*) 56.3°; 13.52 MPa.
8.C3 *Prob. 8.18*: 37.3 mm.
8.C5 *Prob. 8.45*: $\sigma = 6.00$ ksi; $\tau = 0.781$ ksi.

CHAPTER 9

9.1 (*a*) $y = -(Px^2/6EI)\,(3L - x)$. (*b*) $PL^3/3EI\downarrow$. (*c*) $PL^2/2EI\measuredangle$.
9.2 (*a*) $y = (M_0/2EI)\,(L - x)^2$. (*b*) $M_0L^2/2EI\uparrow$. (*c*) $M_0\,L/EI\measuredangle$.
9.3 (*a*) $y = -(w/24EI)\,(x^4 - 4\,L^3x + 3L^4)$. (*b*) $wL^4/8EI\downarrow$. (*c*) $wL^3/6EI\measuredangle$.
9.4 (*a*) $y = -(w_0/120EIL)\,(x^5 - 5L^4x)$. (*b*) $w_0L^4/30\,EI\downarrow$. (*c*) $w_0L^3/24\,EI\measuredangle$.
9.5 (*a*) $y = (w/72\,EI)\,(3x^4 - 16ax^3)$. (*b*) $10\,wa^4/9\,EI\downarrow$. (*c*) $4\,wa^3/3EI\measuredangle$.
9.7 (*a*) $y = (w_0/EIL)\,(L^2x^3/48 - x^5/120 - L^4x/80)$. (*b*) $w_0\,L^4/256\,EI\downarrow$. (*c*) $w_0\,L^3/120\,EI\measuredangle$.
9.9 (*a*) 3.92×10^{-3} rad $\measuredangle$. (*b*) 0.1806 in. ↓.
9.10 (*a*) 2.79×10^{-3} rad $\measuredangle$. (*b*) 1.859 mm ↓.
9.11 (*a*) $0.00652w_0L^4/EI\downarrow$; $0.481L$. (*b*) 0.229 in. ↓.
9.12 (*a*) $0.211L$; $0.01604M_0L^2/EI$. (*b*) 6.08 m.
9.13 0.398 in. ↓.
9.16 (*a*) $(P/EI)\,(ax^2/2 - aLx/2 + a^3/6)$. (*b*) 1.976 mm ↓.
9.17 (*a*) $y = -(w_0/EIL^2)\,(L^2x^4/24 - LX^5/30 + X^6/120 - L^4x^2/24)$. (*b*) $w_0\,L^4/40\,EI\downarrow$.
9.18 (*a*) $y = w_0\,(x^6 - 15\,L^2x^4 + 25L^3x^3 - 11\,L^5x)/360\,EIL^2$. (*b*) $11w_0L^3/360\,EI\measuredangle$. (*c*) $0.00916\,w_0L^4/EI\downarrow$.
9.19 $3wL/8\uparrow$.
9.20 $3M_0/2L\uparrow$.
9.23 4.00 kips ↑.
9.24 9.75 kN ↑.
9.25 $R_B = 5P/16\uparrow$; $M_A = -3PL/16$, $M_C = 5PL/32$, $M_B = 0$.
9.26 $R_B = 9M_0/8L\uparrow$; $M_A = M_0/8$, $M_{C-} = -7M_0/16$, $M_{C+} = 9M_0/16$.
9.27 $R_A = 9w_0L/640\uparrow$; $M_M = 0.00814\,w_0L^2$, $M_B = -0.0276\,w_0L^2$.
9.28 $R_A = 7wL/128\uparrow$; $M_C = 0.0273\,wL^2$, $M_B = -0.0703\,wL^2$, $M = 0.0288\,wL^2$ at $x = 0.555L$.
9.30 $R_B = 17wL/64\uparrow$; $y_C = wL^4/1024\,EI\downarrow$.
9.32 $R_B = 5M_0/6L\downarrow$; $y_D = 7M_0L^2/486\,EI\uparrow$.
9.33 $wL/2\uparrow$, $wL^2/12\,\curvearrowleft$; $M = w\,[6x\,(L - x) - L^2]/12$.
9.34 $R_A = w_0L/4\uparrow$, $M_A = 0.0521\,w_0L^2\curvearrowleft$; $M_C = 0.0313\,w_0L_2$.
9.35 (*a*) $y = w\{Lx^3/48 - \langle x - L/2\rangle^4/24 - 7L^3x/384\}/EI$. (*b*) $7wL^3/384\,EI\measuredangle$. (*c*) $5wL^4/768\,EI\downarrow$.
9.36 (*a*) $y = (M_0/6EIL)\,\{x^3 - 3L\langle x - a\rangle^2 + (3b^2 - L^2)\,x\}$ (*b*) $M_0\,(3b^2 - L^2)/6EIL\measuredangle$. (*c*) $M_0\,ab\,(b - a)/3\,EIL\uparrow$.
9.37 (*a*) $9Pa^3/4EI\downarrow$. (*b*) $19Pa^3/6EI\downarrow$. (*c*) $9Pa^3/4EI\downarrow$.
9.38 (*a*) $5Pa^3/2EI\downarrow$. (*b*) $49Pa^3/6EI$. (*c*) $15Pa^3/EI$.
9.41 (*a*) $y = w\,\{ax^3/6 - \langle x - a\rangle^4/24 + \langle x - 3a\rangle^4/24 - 11\,a^3x/6\}/EI$. (*b*) $19\,wa^4/8EI\downarrow$.
9.43 (*a*) $y = w_0\,\{-5L^3x^2/48 + L^2\,x^3/24 - \langle x - L/2\rangle^5/60\}/EIL$. (*b*) $w_0L^4/48\,EI\downarrow$. (*c*) $121\,w_0L^4/1920\,EI\downarrow$.
9.44 (*a*) $y = (w/24\,EI)\,\{-x^4 + \langle x - L/2\rangle^4 - \langle x - L\rangle^4 + Lx^3 + 3L\,\langle x - L\rangle^3 - L^3x/16\}$. (*b*) $wL^4/768\,EI\uparrow$. (*c*) $5wL^4/256\,EI$.
9.45 (*a*) 9.51×10^{-3} rad $\measuredangle$. (*b*) 5.80 mm ↓.
9.46 (*a*) 8.66×10^{-3} rad $\measuredangle$. (*b*) 0.1503 in. ↓.
9.48 (*a*) 5.40×10^{-3} rad $\measuredangle$. (*b*) 3. 06 mm ↓.
9.49 (*a*) $5P/16\uparrow$. (*b*) $7\,PL^3/168EI\downarrow$.
9.50 (*a*) $9M_0/8L\uparrow$. (*b*) $M_0L^2/128EI\downarrow$.
9.51 (*a*) $2P/3\uparrow$. (*b*) $5PL^3/486EI\downarrow$.
9.53 (*a*) 11.54 kN ↑. (*b*) 4.18 mm ↓.
9.54 (*a*) 41.3 kN ↑. (*b*) 0.705 mm ↓.
9.56 (*a*) 7.38 kips ↑. (*b*) 0.0526 in. ↓.
9.57 (*a*) $1.280wa\uparrow$; $1.333wa^2\,\curvearrowleft$. (*b*) $0.907\,wa^4/EI\downarrow$.
9.58 (*a*) $20P/27\uparrow$; $4PL/27\,\curvearrowleft$. (*b*) $5PL^3/1296\,EI\downarrow$.
9.59 5.80 mm ↓ at $x = 0.991$ m.
9.60 0.1520 in. ↓ at $x = 26.4$ in.
9.61 0.281 in. ↓ at $x = 8.40$ ft.
9.62 3.07 mm ↓ at $x = 0.942$ m.
9.65 $wL^3/48EI\measuredangle$; $wL^4/384EI\uparrow$.
9.66 $PL^2/24\,EI\measuredangle$; $PL^3/48\,EI$.
9.67 $3PL^2/4\,EI\measuredangle$; $13\,PL^3/24\,EI\downarrow$.
9.68 $Pa\,(2L - a)/2\,EI\measuredangle$; $Pa\,(3L^2 - 3aL + a^2)/6\,EI\uparrow$.
9.71 (*a*) $wL^4/128\,EI$. (*b*) $wL^3/72\,EI$.
9.72 (*a*) $PL^3/486\,EI$. (*b*) $PL^2/81\,EI\measuredangle$.
9.73 6.32×10^{-3} rad $\measuredangle$; 5.55 mm ↓.
9.75 7.91×10^{-3} rad $\measuredangle$; 0.340 in. ↓.
9.76 6.98×10^{-3} rad $\measuredangle$; 0.1571 in. ↓.
9.77 (*a*) 0.601×10^{-3} rad $\measuredangle$. (*b*) 3.67 mm ↓.
9.79 (*a*) $4P/3\uparrow$; $PL/3\,\curvearrowleft$. (*b*) $2P/3\uparrow$.
9.80 (*a*) $41\,wL/128\uparrow$. (*b*) $23\,wL/128\uparrow$; $7wL^2/128\,\curvearrowright$.

9.82 $R_A = 2M_0/L \uparrow$; $R_B = 3M_0/L \downarrow$; $R_C = M_C/L \uparrow$.
9.84 $wL/2 \uparrow$, $wL^2/2 \circlearrowright$.
9.85 (*a*) 5.94 mm ↓. (*b*) 6.75 mm ↓.
9.86 $y_B = 0.210$ in. ↓; $y_c = 0.1709$ in. ↓.
9.87 (*a*) 5.06×10^{-3} rad ↻. (*b*) 0.0477 in. ↓.
9.88 121.5 N/m.
9.90 5.63 kN.
9.91 (*a*) 0.00937 mm ↓. (*b*) 229 N ↑.
9.93 0.278 in. ↓.
9.94 9.31 mm ↓.
9.95 (*a*) M_0L/EI ↻. (*b*) $M_0L^2/2EI \uparrow$.
9.96 (*a*) $PL^2/2EI \circlearrowright$. (*b*) $PL^3/3\ EI \downarrow$.
9.97 (*a*) $wL^3/6EI \circlearrowright$. (*b*) $wL^4/8EI \downarrow$.
9.98 (*a*) $w_0L^3/24EI \circlearrowright$. (*b*) $w_0L^4/30\ EI \downarrow$.
9.101 (*a*) 4.24×10^{-3} rad ↻. (*b*) 0.0698 in. ↓.
9.102 (*a*) 5.20×10^{-3} rad $\circlearrowright$. (*b*) 10.85 mm ↓.
9.103 (*a*) 5.84×10^{-3} rad ↻. (*b*) 0.300 in. ↓.
9.104 (*a*) 7.15×10^{-3} rad $\circlearrowright$. (*b*) 17.67 mm ↓.
9.105 (*a*) $wL^3/16EI \circlearrowright$. (*b*) $47wL^4/1152\ EI \downarrow$.
9.107 (*a*) 3.43×10^{-3} rad $\circlearrowright$. (*b*) 6.66 mm ↓.
9.109 (*a*) $PL^2/16EI$ ↻. (*b*) $PL^3/48EI \downarrow$.
9.110 (*a*) $Pa(L - a)/2EI$ ↻. (*b*) $Pa\ (3L^2 - 4a^2)/24EI \downarrow$.
9.111 (*a*) $PL^2/32\ EI$ ↻. (*b*) $PL^3/128EI \downarrow$.
9.112 (*a*) $wa^2\ (3L - 2a)/12EI$ ↻. (*b*) $wa^2\ (3L^2 - 2a^2/48EI) \downarrow$.
9.113 (*a*) $M_0\ (L - 2a)/2EI$ ↻. (*b*) $M_0\ (L^2 - 4a^2)/8EI \downarrow$.
9.115 (*a*) $5Pa^2/8EI$ ↻. (*b*) $3Pa^3/4EI \downarrow$.
9.118 (*a*) 4.71×10^{-3} rad ↻. (*b*) 5.84 mm ↓.
9.119 (*a*) 4.50×10^{-3} rad ↻. (*b*) 8.26 mm ↓.
9.120 (*a*) 5.21×10^{-3} rad ↻. (*b*) 21.2 mm ↓.
9.122 3.84 kN/m.
9.123 $0.211L$.
9.124 $0.223L$.
9.125 (*a*) $4PL^3/243EI \uparrow$. (*b*) $14\ PL^2/81\ EI \circlearrowright$.
9.126 (*a*) $5PL^3/768EI \downarrow$. (*b*) $3PL^2/128\ EI$ ↻.
9.128 (*a*) $5w_0L^4/768\ EI \downarrow$. (*b*) $7w_0\ L^3/360\ EI$ ↻.
9.129 (*a*) 8.74×10^{-3} rad ↻. (*b*) 15.10 mm ↓.
9.130 (*a*) 7.48×10^{-3} rad ↻. (*b*) 5.35 mm ↓.
9.132 (*a*) 5.31×10^{-3} rad ↻. (*b*) 0.204 in. ↓.
9.133 (*a*) $M_0\ (L + 3a)/3EI \circlearrowright$. (*b*) $M_0a\ (2L + 3a)/6\ EI \downarrow$.
9.135 (*a*) 5.33×10^{-3} rad $\circlearrowright$. (*b*) 0.01421 in. ↓.
9.136 (*a*) 3.61×10^{-3} rad ↻. (*b*) 0.960 mm ↑.
9.137 (*a*) 2.34×10^{-3} rad ↻. (*b*) 0.1763 in. ↓.
9.139 (*a*) $9wL^3/256\ EI$ ↻. (*b*) $7wL^3/256\ EI \circlearrowright$.
(*c*) $5wL^4/512EI \downarrow$.
9.140 (*a*) $17PL^3/972\ EI \downarrow$. (*b*) $19PL^3/972\ EI \downarrow$.
9.142 $0.00652\ w_0L^4/EI$ at $x = 0.519L$.
9.144 0.212 in. at $x = 5.15$ ft.
9.145 0.1049 in.
9.146 1.841 mm.
9.147 $5P/16 \uparrow$.
9.148 $9M_0/8L$.
9.150 $7wL/128 \uparrow$.
9.152 $R_A = 3P/32 \downarrow$; $R_B = 13P/32 \uparrow$; $R_C = 11P/16 \uparrow$.
9.153 (*a*) 6.87 mm ↑. (*b*) 46.3 kN ↑.
9.154 10.18 kips ↑; $M_A = -87.9$ kip·ft; $M_D = 46.3$ kip·ft; $M_B = 0$.
9.155 $48\ EI/7L^3$.
9.156 $144\ EI/L^3$.
9.157 (*a*) $y = (w_0/EIL)\ (L^3x^2/6 - Lx^4/12 + x^5/120)$.
(*b*) $11w_0L^4/120\ EI \downarrow$. (*c*) $w_0L^3/8EI$ ↻.
9.158 (*a*) $0.0642\ M_0L^2/EI$ a+ $x = 0.423\ L$. (*b*) 45.3 kN·m.
9.160 $R_A = R_B = P/2 \uparrow$, $M_A = PL/8 \curvearrowleft$; $M_B = PL/8 \curvearrowright$; $M_C = PL/8$.
9.161 (*a*) 2.49×10^{-3} rad ↻. (*b*) 1.078 mm ↓.
9.163 0.210 in. ↓.
9.165 (*a*) 2.55×10^{-3} rad ↻. (*b*) 6.25 mm ↓.
9.166 (*a*) 5.86×10^{-3} rad $\circlearrowright$. (*b*) 0.0690 in. ↑.
9.168 (*a*) 65.2 kN ↑; $M_A = 0°$; $M_D = 58.7$ kN·m;
$M_B = -82.8$ kN·m.
9.C1 *Prob. 9.74:* 5.56×10^{-3} rad ↻; 2.50 mm ↓.
9.C2 *a = 6 ft:* (*a*) 3.14×10^{-3} rad ↻, 0.292 in. ↓;
(*b*) 0.397 in. ↓ at 11.27 ft to the right of A.
9.C3 *x = 1.6 m:* (*a*) 7.90×10^{-3} rad ↻, 8.16 mm ↓;
(*b*) 6.05×10^{-3} rad ↻, 5.79 mm ↓;
(*c*) 1.021×10^{-3} rad ↻, 0.314 mm ↓.
9.C5 (*a*) *a = 3 ft:* 1.586×10^{-3} rad ↻; 0.1369 in. ↓;
(*b*) *a = 1.0 m:* 0.293×10^{-3} rad ↻, 0.479 mm ↓.
9.C7 *x = 2.5 m:* 5.31 mm ↓; *x = 5.0 m:* 11.2.28 mm ↓.

CHAPTER 10

10.1 kL.
10.2 k/L.
10.3 $kL/4$.
10.4 $2\ kL/9$.
10.6 120.0 kips.
10.7 $ka^2/2l$.
10.9 305 kN.
10.10 8.37 lb.
10.11 1.421.
10.13 14.10 mm; round strut; 61.4 kN; square strut: 64.3 kN.
10.15 70.2 kips.
10.16 467 kN.
10.17 335 kips.
10.19 2.27.
10.21 (*a*) 0.500. (*b*) 2.46.
10.22 (*a*) $L_{BC} = 4.20$ ft; $L_{CD} = 1.050$ ft. (*b*) 4.21 kips.
10.24 657 mm.
10.25 (*a*) 0.500. (*b*) $b = 14.15$ mm; $d = 28.3$ mm.
10.27 (*a*) 2.55. (*b*) $d_2 = 28.3$ mm; $d_3 = 14.14$ mm;
$d_4 = 16.72$ mm; $d_5 = 20.0$ mm.
10.28 (1) 319 kg; (2) 79.8 kg; (3) 319 kg; (4) 653 kg.
10.29 (*a*) 4.32 mm. (*b*) 44.4 MPa.
10.30 (*a*) 1.658 mm. (*b*) 78.9 MPa.
10.32 (*a*) 0.0399 in. (*b*) 19.89 ksi.
10.34 (*a*) 0.247 in. (*b*) 12.95 ksi.
10.35 (*a*) 13.29 kips. (*b*) 15.50 ksi.
10.36 (*a*) 235 kN. (*b*) 149.6 MPa.
10.37 (*a*) 151.6 kN. (*b*) 109.5 MPa.
10.39 (*a*) 370 kN. (*b*) 104.6 MPa.
10.40 (*a*) 224 kN. (*b*) 63.3 MPa.
10.41 58.9°F.
10.43 (*a*) 189.0 kN. (*b*) 229 kN.
10.44 (*a*) 147.0 kN. (*b*) 174.0 kN.
10.45 (*a*) 49.6 kips. (*b*) 0.412.
10.47 1.302 m.
10.49 (*a*) 26.8 ft. (*b*) 8.40 ft.
10.50 (*a*) 4.54 m. (*b*) 2.41 m.
10.51 W 200 × 26.6.
10.53 2.125 in.
10.54 2.625 in.
10.56 3.09.
10.57 (*a*) 220 kN. (*b*) 841 kN.
10.58 (*a*) 86.6 kips. (*b*) 88.1 kips.
10.59 414 kN.
10.60 35.9 kN.

10.62 (*a*) 26.6 kN. (*b*) 33.0 kN.
10.64 76.8 kips.
10.65 76.3 kips.
10.66 1596 kN.
10.68 173.5 kips.
10.69 (*a*) 66.3 kN. (*b*) 243 kN.
10.71 123.1 mm.
10.72 6.53 in.
10.74 1.615 in.
10.75 22.3 mm.
10.77 W200 × 46.1.
10.78 W14 × 82.
10.79 W10 × 54.
10.80 (*a*) 30.1 mm. (*b*) 33.5 mm.
10.83 L89 × 64 × 12.7.
10.84 56.1 kips.
10.86 (*a*) $P_D = 433$ kN; $P_L = 321$ kN.
(*b*) $P_D = 896$ kN; $P_L = 664$ kN.
10.87 W310 × 74.
10.88 5/16 in.
10.89 76.7 kN.
10.91 (*a*) 18.26 kips. (*b*) 14.20 kips.
10.92 (*a*) 21.1 kips. (*b*) 18.01 kips.
10.93 (*a*) 329 kN. (*b*) 280 kN.
10.95 (*a*) 0.698 in. (*b*) 2.11 in.
10.97 16.44 ft.
10.99 5.48 m.
10.100 4.81 m.
10.101 1.021 m.
10.102 1.175 m.
10.103 83.4 mm.
10.104 87.2 mm.
10.105 12.00 mm.
10.106 15.00 mm.
10.107 140.0 mm.
10.109 1.882 in.
10.110 1.735 in.
10.111 $t = ¼$ in.
10.113 W14 × 145.
10.114 W14 × 68.
10.116 W250 × 58.
10.117 (*a*) 647 lb. (*b*) 0.651 in. (*c*) 58.8%.
10.118 $k > 4.91$ kN/m.
10.120 (*a*) 47.2°. (*b*) 1.582 kips.
10.121 2.44.
10.123 $\Delta T = \pi^2 b^2 / 12 L^2 \alpha$.
10.125 107.7 kN.
10.126 W250 × 67.
10.128 (*a*) 0.0987 in. (*b*) 0.787 in.
10.C1 *r = 8 mm:* 9.07 kN. *r = 16 mm:* 70.4 kN.
10.C2 *b = 1.0 in.:* 3.85 kips. *b = 1.375 in.:* 6.07 kips.
10.C3 *h = 5.0 m:* 9819 kg. *h = 7.0 m:* 13,255 kg.
10.C4 *P = 35 kips:* (*a*) 0.086 in.; (*b*) 4.69 ksi.
P = 55 kips: (*a*) 0.146 in.; (*b*) 7.65 ksi.
10.C6 *Prob. 10.113:* $P_{all} = 282.6$ kips.
Prob. 10.114: $P_{all} = 139.9$ kips.

CHAPTER 11

11.1 (*a*) 43.1 in · lb/in^3. (*b*) 72.8 in · lb/in^3.
(*c*) 172.4 in · lb/in^3.
11.2 (*a*) 21.6 kJ/m^3. (*b*) 336 kJ/m^3, (*c*) 163.0 kJ/m^3.
11.3 (*a*) 177.9 kJ/m^3. (*b*) 712 kJ/m^3. (*c*) 160.3 kJ/m^3.
11.5 (*a*) 58.0 in · lb/in^3. (*b*) 20.0 in · kip/in^3.
11.6 (*a*) 1296 kJ/m^3. (*b*) 90.0 MJ/m^3.
11.7 (*a*) 1.750 MJ/m^3. (*b*) 71.2 MJ/m^3.
11.9 (*a*) 176.2 in · lb.
(*b*) $u_{AB} = 11.72$ in · lb/in^3; $u_{BC} = 5.65$ in · lb/in^3.
11.10 (*a*) 12.18 J. (*b*) $u_{AB} = 15.83$kJ/m^3; $u_{BC} = 38.6$ kJ/m^3.
11.11 (*a*) 168.8 in · lb.
(*b*) $u_{CD} = 0.882$ in · lb/in^3; $u_{EF} = 5.65$ in · lb/in^3.
11.12 0.846 J.
11.15 (*a*) 3.28. (*b*) 4.25.
11.17 102.7 in · lb.
11.18 $1.398\, P^2 l/EA$.
11.20 $2.37\, P^2 l/EA$.
11.21 $0.233\, P^2 l/EA$.
11.23 6.68 kip · in.
11.24 $W^2 L^5/40\, EI$.
11.25 $(P^2 a^2/6\, EI)\,(a + L)$.
11.27 $(M_0^2/6\, EIL^2)\,(a^3 + b^3)$.
11.28 89.5 in · lb.
11.30 1048 J.
11.31 670 J.
11.33 12.70 J.
11.37 (*a*) No yield. (*b*) Yield occurs.
11.39 (*a*) 2.33. (*b*) 2.02.
11.40 $(2M_0^2\, L\, /\, Ebd^3)\,(1 + 3Ed^2/10GL^2)$.
11.41 $(Q^2/4\pi GL)\ln(R_2\, /\, R_1)$.
11.42 24.7 mm.
11.43 25.5 ft/sec.
11.44 9.12 lb.
11.45 841 mm.
11.48 11.09 ft/s.
11.50 (*a*) 7.54 kN. (*b*) 41.3 MPa. (*c*) 3.18 mm.
11.51 (*a*) 9.60 kN. (*b*) 32.4 MPa. (*c*) 2.50 mm.
11.52 (*a*) 15.63 mm. (*b*) 83.8 N·m. (*c*) 208 MPa.
11.53 (*a*) 7.11 mm. (*b*) 140.1 MPa.
11.54 (*a*) 0.903 in. (*b*) 511 lb·in. (*c*) 21.3 ksi.
11.56 (*b*) 7.12.
11.57 (*b*) 0.152.
11.58 $Pa^2 b^2/3EI\,\downarrow$.
11.59 $Pa^2\,(a + L)/3EI\,.$
11.61 $M_0\,(L + 3a)/3EI\,\searrow$.
11.62 $3PL^3/16\, EI\,\downarrow$.
11.63 $3Pa^3/4\, EI\,\downarrow$.
11.65 $M_0 L/16\, EI\,\searrow$.
11.66 59.8 mm ↓.
11.67 32.4 in.
11.68 3.12°.
11.72 $2.38Pl/EA\,\rightarrow$.
11.73 0.650 in. ↓.
11.75 0.366 in. ↓.
11.76 1.111 mm ↓.
11.77 (*a*) and (*b*) $P^2 L^3/6\, EI + PM_0 L^2/2EI + M_0^2 L/2\, EI$.
11.78 (*a*) and (*b*) $P^2 L^3/48\, EI + M_0 PL^2/8EI + M_0^2 L/2\, EI$.
11.80 (*a*) and (*b*) $5\, M_0^2 L/4\, EI$.
11.82 (*a*) and (*b*) $M_0^2 L/2\, EI$.
11.83 $0.0443 wL^4/EI\,\downarrow$.
11.85 $wL^4/768\, EI\,\uparrow$.
11.86 $7wL^3/48\, EI\,\measuredangle$.
11.88 $wL^3/384\, EI\,\measuredangle$.
11.89 $(Pab/6EIL^2)\,(3La + 2a^2 + 2b^2)\,\searrow$.
11.90 $M_0 L/6\, EI\,\searrow$.

11.91 0.329 in. ↓.
11.93 5.12 mm ↓.
11.94 7.25 mm ↓.
11.95 7.07×10^{-3} rad ↘.
11.96 3.80 mm ↓.
11.97 2.07×10^{-3} rad ◿.
11.99 $x_C = 0$, $y_C = 2.80\ P_L/EA$ ↓.
11.101 0.1613 in. ↓.
11.102 0.01034 in. ← .
11.103 0.1459 mm ↓.
11.105 (*a*) $PL^3/6EI$ ↓. (*b*) 0.1443 PL^3/EI.
11.106 $\pi PR^3/2\ EI$ ↓.
11.107 (*a*) $PR^3/2\ EI$ →. (*b*) $\pi PR^3/4\ EI$ ↓.
11.109 $5PL^3/6EI$.
11.111 $5P/16$ ↑.
11.112 $3M_0/2L$ ↑.
11.113 $3M_0\, b(L + a)\ /2L^3$ ↑.
11.114 $7wL/128$ ↑.
11.117 $P/(1 + 2\cos^3\phi)$.
11.118 $7P/8$.
11.119 $0.652P$.
11.121 $2P/3$.
11.123 136.6 J.
11.124 1.767 in · kip.
11.126 4.76 kg.
11.129 2.55°.
11.130 11.57 mm ↓.
11.134 0.807 in . ↓.
11.C2 (*a*) *a = 15 in.:* $\sigma_D = 17.19$ ksi, $\sigma_C = 21.0$ ksi;
a =45 in.: $\sigma_D = 36.2$ ksi, $\sigma_C = 14.74$ ksi.
(*b*) $a = 18.34$ in., $\sigma = 20.67$ ksi.
11.C3 (*a*) *L = 200 mm: h* = 2.27 mm;
L = 800 mm: h = 1.076 mm.
(*b*) *L = 440 mm: h* = 3.23 mm.
11.C4 *a = 300 mm:* 1.795 mm, 179.46 MPa;
a = 600 mm: 2.87 mm, 179.59 MPa.
11.C5 *a = 2 m:* (*a*) 30.0 J; (*b*) 7.57 mm, 60.8 J.
a = 4 m: (*a*) 21.9 J; (*b*) 8.87 mm, 83.4 J.
11.C6 *a = 20 in:* (*a*) 13.26 in.; (*b*) 99.5 kip · in.; (*c*) 803 lb.
a = 50 in: (*a*) 9.46 in.; (*b*) 93.7 kip · in.; (*c*) 996 lb.

Photo Credits

Image Research by Danny Meldung/Photo Affairs, Inc.

CHAPTER 1

Opener: © Pete Ryan/Getty Images RF; 1.1: © David R. Frazier/Science Source; 1.2: © Walter Bibikow/agefotostock; 1.3: © John DeWolf.

CHAPTER 2

Opener: © Sylvain Grandadam/agefotostock; 2.1: © John DeWolf; 2.2: Courtesy of Tinius Olsen Testing Machine Co., Inc.; 2.3-2.5: © John DeWolf; 2.6: © John Fisher.

CHAPTER 3

Opener: © incamerastock/Alamy; 3.1: © 2008 Ford Motor Company; 3.2: © John DeWolf; 3.3: Courtesy of Tinius Olsen Testing Machine Co., Inc.; 3.4: © koi88/Alamy RF.

CHAPTER 4

Opener: © Mel Curtis/Getty Images RF; 4.1: Courtesy of Flexifoil; 4.2: © Tony Freeman/PhotoEdit; 4.3: © Hisham Ibrahim/Getty Images RF; 4.4: © Bohemian Nomad Picturemakers/Corbis; 4.5: © Tony Freeman/PhotoEdit; 4.6: © John DeWolf.

CHAPTER 5

Opener: © Digital Vision/Getty Images RF; 5.1: © Huntstock/agefotostock RF; 5.2: © David Nunuk/Science Source.

CHAPTER 6

Opener: © Aurora Photos/Alamy; 6.1: © John DeWolf; 6.2: © Jake Wyman/Getty Images; 6.3: © Rodho/shutterstock.com.

CHAPTER 7

Opener: NASA; 7.1: © Walter G. Allgöwer Image Broker/Newscom; 7.2: © FELLOW/agefotostock; 7.3: © Clair Dunn/Alamy; 7.4: © Spencer C. Grant/PhotoEdit.

CHAPTER 8

Opener: © S. Meltzer/PhotoLink/Getty Images RF.

CHAPTER 9

Opener: © Jetta Productions/Getty Images RF; 9.1: © Royalty-Free/Corbis; 9.2–9.3: © John DeWolf; 9.4: © FOTOG/Getty Images RF; 9.5: © Royalty-Free/Corbis.

CHAPTER 10

Opener: © Jose Manuel/Getty Images RF; 10.1: Courtesy of Fritz Engineering Laboratory, Lehigh University; 10.2a: © Steve Photo/Alamy RF; 10.2b: © Peter Marlow/Magnum Photos.

CHAPTER 11

Opener: © Corbis Super RF/Alamy; 11.1: © Israel Antunes/Alamy; 11.2: © Tony Freeman/PhotoEdit; 11.3: © TRL Ltd./Science Source.

Index

A

Allowable (working) load, 32–33
Allowable stress, 32–33
Allowable stress design, 723–728, 739, 751
Aluminum column design, 726
American Association of Safety and Highway Officials, 34
American Concrete Institute, 34
American Forest and Paper Association, 34, 726
American Institute of Steel Construction (AISC), 34, 723–724, 728
American standard beam (S-beam), 424
Angle of twist
  elastic range and, 151, 167–170
  circular shafts, 167–170, 224
  non-circular shafts, 210
  torque (τ) and, 151, 167–170
  tubes (thin-walled hollow shafts), 214
Anisotropic materials, 64, 134
Anticlastic curvature, 249, 335
Area (A)
  centroid of, A2–A7
  composite, A4–A7, A11–A12
  moments of, A2–A12
  radius of gyration, A8–A10
Average shearing stress, 11, 45, 422, 468
Average value of stress, 7, 44
Axial loading
  eccentric, 238–239, 291–295, 307–312, 337–338
  member stresses from, 7–10
  multiaxial, 95–97, 137
  oblique plane stresses from, 27–28
  plane of symmetry with, 291–295, 337
  pure bending and, 238–239, 291–295, 307–312, 337–338
  strain energy under, 764, 824
  stress and strain under, 55–145
  stress components under, 31
Axial stresses, 7–10
Axisymmetry of circular shafts, 151–152

B

Bauschinger effect, 66
Beam analysis and design, 344–415
  bending and, 344–415
  elastic section modulus (S) for, 347–348, 371–372, 396, 408, 410
  load and resistant factor design (LRFD), 373
  nonprismatic beams, 348, 396–401, 410
  prismatic beams, 371–376, 408
  relationships between load, shear, and bending moment, 260–368, 408
  shear and bending moment diagrams for, 348–354, 407–408
  shear and stress distributions, 347–348, 407
  sign convention for, 349
  singularity functions for shear and bending moment, 348, 383–391, 409
  step functions, 385, 409
  transverse loadings, 346–348, 407
Beam of constant strength, 396, 410
Beams. *See also* Beam analysis and design; Cantilever beams
  boundary conditions, 604, 679
  cantilever, 604–605
  deflection of, 598–689
  longitudinal shear on arbitrary elements, 437–439, 468
  normal stress in, 558–561, 591
  overhang, 604
  plastic deformations, 441–442, 469
  principal stresses in, 559–561, 591
  shearing stress in, 558–561, 591
  shearing stress distribution in, 347–348, 407, 422–431, 468
  simply supported, 604, 606
  singularity functions for, 348, 383–391, 409, 623–630, 681–682
  slopes and deflections of, A29
  span, 346
  statically determinate, 346–347, 407
  statically indeterminate, 347, 600, 611–617, 679–681
  thin-walled members, 439–466, 469
  unsymmetric loading of, 454–462, 469
Bearing stresses, connections with, 12, 45
Bearing surface, 12, 45
Bending
  beam analysis and design for, 344–415
  couple moment (M), 240–241
  modulus of rupture (R), 274
  prismatic members, 237–343
  pure, 237–343
  strain energy due to, 766, 824
Bending moment diagrams
  beam analysis using, 348–354, 407–408
  by parts for moment-area theorems, 654–659, 684
  sign convention for, 349
Bending moments
  couples, 240–241
  pure bending in symmetric members, 240–241, 334
  relationships with load and shear 260–368, 408
  singularity functions for, 348, 383–391, 409
Boundary conditions of beams, 604, 679
Breaking strength, 60–61
Bridges, design specifications for, 34
Brittle materials
  compression test for, 62
  concrete, 62, 134
  cracks, 511
  maximum-normal-stress criterion, 506
  Mohr's criterion for, 510–511, 549
  rupture of, 60–62
  stress and strain transformations, 509–511, 549
  stress-strain diagram determination of, 60–62, 133
  tensile test for, 60–61
  under plane stress, 509–511, 549
Buckling, 692–694
Bulk modulus (k), dilatation and, 97–99, 137

C

Cantilever beams
  deflection of, 604–605, 651–653, 684
  moment-area theorem for, 651–653, 684
  shearing stresses in, 426–427
Castigliano's theorem, 804–809, 826
Center of symmetry, 460
Centric load design, 722–732, 751
Centric loading, 9, 45
Centroid of the area, A2–A7
Circular shafts
  angle of twist, 151, 167–170, 224
  axisymmetry of, 151–152
  deformations in, 151–153
  modulus of rupture (R), 196, 225–226
  plastic deformation in, 195–204, 225–227
  residual stresses in, 199–204, 226–227
  shearing strain in, 153, 223
  stress concentrations in, 187–190, 225
  stresses in, 150–151, 153–161, 223–224
  torsion in, 148–204, 223–227
Coefficient of thermal expansion, 82, 136
Columns, 690–756
  allowable stress design, 723–728, 739, 751
  aluminum, 726
  buckling, 692–694
  centric load design, 722–732, 751
  critical load, 692–694, 750
  eccentric load design, 739–745, 751
  eccentric loading, 709–714, 751
  effective length, 698–700, 750
  Euler's formula for, 694–702, 750
  fixed ends, 698–700
  interaction method, 740–741, 751
  load and resistance factor design (LRFD), 728
  pin-ended, 694–697
  secant formula for, 711–712, 751
  slenderness ratio, 696, 750
  stability of structures and, 692–702
  structural steel, 723–724
  wood, 726
Combined loads, principal stresses under, 575–583, 592
Composite area (A)
  centroid of, A4–A7
  moment of inertia and, A11–A12

Composite materials, 259–262, 335
moduli of elasticity and, 259–260, 335
pure bending of members of, 259–262, 335
transformed section of, 260–335
Compression test, 62
Computation error detection, 16
Concentrated loads, 8, 346
Concrete
design specifications for, 34
stress-strain diagram for, 62, 134
Connections, bearing stress in, 12
Constant strength, 348
Coulomb's criterion, 509
Couple (bending) moments, 240–241
Cracks, 511
Critical load, 692–694, 750
Critical stress, 696
Curvature
analysis of curved members, 319–327, 338
anticlastic, 249, 335
pure bending and, 241–244, 319–327, 334–335, 338
radius of (ρ), 247, 334, 335
stresses and, 320–323, 338
transverse cross section, 248–252
transverse loading, 238–239, 334
Cylindrical pressure vessels, stresses in, 520–522, 549

D

Deflection of beams, 598–689, 790–795, 806–809
bending moment and, 600–601
boundary conditions and, 604, 679
Castigliano's theorem for, 806–809
deformation under transverse loading, 602–610, 679–680
elastic curve, equation of for, 603–606, 679
energy methods for, 790–795, 806–809
flexural rigidity (EI), 603–604, 679
method of superposition for, 601, 635–643
moment-area theorems for, 601–602, 649–659, 664–674, 682–684
singularity functions for, 623–630, 681–682
slope and, 607–608, 623–630, 681–682, A29
statically determinate, 635–636
statically indeterminate, 600, 611–617, 636–637, 679–681
work-energy method for, 790–795
Deformation (δ). *See also* Elastic deformation; Plastic deformation
axial loading and, 56–58, 68–69, 102–104, 119–122, 135, 139
bending in symmetric members, 241–244
circular shafts, 151–153, 195–204, 223, 225
deflection of beams under transverse loading, 602–610, 679–680
elastic behavior and, 68–69, 135
elastic range stresses and, 244–248, 334
multiaxial loadings, 95–96
per unit length, 57–58, 133
plastic behavior and, 65–67, 135
pure bending, 241–252
rectangular parallelepiped, 96
relationships of E, G, and ν, 102–104, 139
relative displacement for, 69
shafts, 148–149, 151–153, 209–218, 223, 225–227
strain energy and, 760–762, 823
transmission shafts, 148–149
torsion and, 148–149, 151–153, 209–218, 223, 225–227
Design considerations
allowable stress and, 32–33
allowable stress design, 723–728, 739, 751
centric load design, 722–732, 751
columns, 722–745, 751
eccentric load design, 739–745, 751
factor of safety, 32–34
impact loads, 786–787, 725–726
interaction method, 740–741, 751
load and resistance factor design (LRFD), 34, 728
power (P), 185–186, 225
specifications for, 34
stress (σ) and, 31–37
transmission shafts, 185–187, 225
ultimate strength, 31–32
working (allowable) load, 32–33
Dilatation (e), 98–99, 137
Dimensionless quantities, 58
Distributed loads, 346
Double shear, 12, 45
Ductile materials
breaking strength, 60–61
maximum-distortion-energy criterion, 508
maximum-shearing-stress criterion, 507–508
necking, 60
percent elongation, 61
percent reduction in area, 62
strain-hardening, 61
stress and strain transformations, 507–508, 548
stress-strain diagram determination of, 59–62, 133–134
ultimate strength, 60–61
yield, 59, 134
yield criteria, 507–508, 548
yield strength, 60–61, 134

E

Eccentric axial loading
analysis of, 307–312, 338
columns, 709–714, 751
forces of, 238–239
neutral axis, 292
plane of symmetry with, 291–295, 337
pure bending and, 238–239, 291–295, 307–312, 337–338
secant formula for, 711–712, 751
Eccentric load design, 739–745, 751
Eccentric loading, 8–9, 44. *See also* Eccentric axial loading
Effective length, 698–700, 750
Elastic behavior, 65–67, 134
plastic behavior compared to, 65–67
stress-strain diagrams for, 65–66, 134
Elastic curve
equation of, 603–606, 679
flexural rigidity (EI), 603–604, 679
load distribution and determination of, 609–610
Elastic deformation, 68–69, 135
Elastic flexural formulas, 245, 334
Elastic limit, 65, 134
Elastic range
angle of twist in, 167–170
internal torque and, 156
shearing stresses in, 153–160, 223–224
stresses and deformation, 244–248, 334
torsion and, 153–160, 167–170, 223–224
Elastic section modulus (S)
beam analysis and design for bending, 347–348, 371–372, 396, 408, 410
elastic range and cross section of members, 246, 335
nonprismatic beam design, 396, 410
prismatic beam design, 371–372, 408
Elastic strain energy, 763–769, 824
Elastic torsion formulas, 155–156, 223
Elasticity (E), modulus of, 63–65, 102–104, 134, 139
composite material members, 259–260, 335
Hooke's law and, 63–65, 134
pure bending and, 259–260, 335
relationships with G and ν, 102–104, 139
stress and strain directional relationships, 65, 134
Elastoplastic material
plastic deformation of, 119–122, 139
pure bending in members, 274–278, 336
torsion in circular shafts, 196–199, 226
Elementary work, 761
Endurance limit, 67–68, 135
Energy methods, 758–822
Castigliano's theorem, 804–809, 826
deflection by, 790–795, 806–809
elastic strain energy, 763–769, 824
impact loads, 784–787, 725–726
multiple loads and, 802–804
single-loaded members, 788–790, 826
statically indeterminate structures, 810–816
strain energy, 760–775, 823–725
strain-energy density, 762–763, 823
work and, 788–795, 802–804, 826
work-energy method, 790–795
Engineering materials, properties of, A13–A16
Engineering stress and engineering strain, 63
Equilibrium equations for problem solutions, 16, 46
Euler's formula, 694–702, 750
fixed-end columns, 698–700
pin-ended columns, 694–697

F

Factor of safety, 32–34, 46
Failure
brittle materials under plane stress, 509–511, 549
cracks, 511
design consideration of, 33
ductile materials, 507–508, 548
fracture criteria, 509–511, 549
stress and strain transformations, 507–513, 548–549
theories of, 507–513, 548–549
yield criteria, 507–508, 548

Fatigue, 67–68, 135
endurance limit, 67–68, 135
limit of, 67
repeated loadings and, 67–68
Fiber-reinforced composite materials, 64–65, 104–108, 134, 139
Hooke's law for, 64–65, 134
lamina, 64
laminate, 64–65, 105
matrix, 64
multiaxial loading, 105
stress-strain relationships for, 104–108, 139
Fillets, stress concentrations in, 117–118, 122
Fixed-end columns, 698–700
Flexural rigidity (*EI*), 603–604, 679
Force
internal, 10–12
shearing stresses and, 10–12
transverse, 44–45
Fracture criteria for brittle materials, 509–511
Free-body diagrams, 4–6, 16, 45
problem solutions from, 16, 45
two-force member stress analysis, 4–6
Fundamentals of Engineering Examination, A30

G

Gauge length, 58–59
General loading conditions, 28–31

H

Hertz (Hz), 185
Hollow shafts (tubes)
circular, 154–155, 158–160, 223–224
thin-walled non-circular, 211–216, 227
Homogeneous materials, 94
Hooke's law
axial loadings, 63–65, 134
fiber-reinforced composite materials and, 64–65
modulus of elasticity (*E*), 63–65, 134
modulus of rigidity (*G*), 100–101, 138
multiaxial loadings, 95–97, 137
proportional limit for stress, 64, 134
shearing stress and strain, 100–101, 138–139
Horsepower (hp), 185, 225

I

Impact loads, 725–726, 784–787
design for, 725–726, 786–787
energy from, 725, 784–785
In-plane shearing stress, 484, 547
Inertia, moments of, A8–A12
Interaction method, 740–741, 751
Internal forces, 10–12
Internal torque, 156
Isotropic materials, 64, 94, 134

L

Lamina, 64
Laminate, 64–65, 105
Lateral strain, 94–95, 137
Line of action, 8
Load and resistance factor design (LRFD), 34, 46, 373, 728
Load-deformation curve, 57
Loadings. *See also* Torsion
axial, 7–10, 27–28, 31, 55–145
beam deflection and, 651–653, 664–667, 684–685
bending and, 238–239, 346–348
centric, 9, 44
columns, 692–694, 709–714, 728, 750–751
combined, 575–583, 592
concentrated, 8, 346
critical, 692–694, 750
design considerations of, 32–34
distributed, 346
eccentric, 8–9, 44, 709–714, 751
factor of safety, 32–34, 46
general conditions, 28–31, 46
impact, 784–787, 725–726
line of action for, 8
moment-area theorems and, 651–653, 664–667, 684–685
multiaxial, 95–97, 137
plane stress and, 556–597
relationships with shear and bending moment, 260–368, 408
repeated, 67–68
reverse, 66–67
singularity functions for equivalent open-ended, 385–386, 410
singularity in, 383
stress and strain under, 55–145
stress components under, 29–31
stresses from, 7–10, 27–28, 44
symmetric, 651–653, 684
transverse, 238–239, 346–348
ultimate, 728
uniformly distributed, 346
unsymmetric, 454–462, 469, 664–674, 684–685
working (allowable), 32–33
Longitudinal shear on arbitrary beam elements, 437–439, 468

M

Macaulay brackets, 384–385, 387
Macroscopic cracks, 511
Matrix, 64
Maximum absolute strain, 244, 334
Maximum absolute stress, 244, 334
Maximum deflection, 666–667, 685
Maximum-distortion-energy criterion, 508
Maximum elastic moment, 275–276, 336
Maximum-normal-stress criterion, 506
Maximum-shearing-stress criterion, 507–508
Members
axial stress in, 7–10
bearing stress in, 12
shearing stress in, 10–12
two-force diagrams for, 4–6
stability of, 9
Membrane analogy, 210–211
Microscopic cracks, 511
Modulus
bulk (*k*), 97–99, 137
elastic section (*S*), 246, 335, 347–348, 371–372, 396, 408, 410
elasticity (*E*), 63–65, 102–104, 134, 259–260, 335
relationships of *E*, *G*, and ν, 102–104, 139
resilience (σ_Y), 763, 824
rigidity (*G*), 100–101, 102–104, 138–139
rupture (*R*), 196, 225–226, 274
toughness (ε_R), 762–763, 823
Young's (*E*), 63
Mohr's circle
plane strain, 532–534, 550
plane stress, 492–502, 547
Mohr's criterion for brittle materials, 510–511, 549
Moment-area theorems
bending-moment diagrams by parts, 654–659, 684
cantilever beams, 651–653, 684
deflection and, 601–602, 649–659, 664–674, 682–685
first, 601, 649–650, 682
general principles of, 649–651, 664
maximum deflection and, 666–667, 685
second, 601, 650–651, 683
statically indeterminate beams, 668–674, 685
symmetric loadings and, 651–653, 684
unsymmetric loadings, 664–674, 684–685
Moment of inertia, A8–A12
Moments of areas, A2–A12
centroid of the area, A2–A7
composite area, A4–A7, A11–A12
first, A2–A10
moment of inertia of, A11–A12
moment of inertia, A8–A12
parallel-axis theorem, A10–A11
radius of gyration, A8–A10
second, A11–A12
Multiaxial loadings, 95–97, 105, 137
fiber-reinforced composite materials, 105
Hooke's law for, 95–97, 137
principle of superposition for, 96
rectangular parallelepiped deformation from, 96
Multiple loads, work and energy under, 802–804

N

Neutral axis, 243, 334
Neutral surface, 242–243, 334
Non-circular shafts, 209–216, 227
angle of twist, 210
membrane analogy for, 210–211
thin-walled (tubes), 211–216, 227
torsion in, 209–216, 227
uniform rectangular cross sections, 210, 227
Non-rectangular cross sections, plastic deformation in, 277
Nonprismatic beams
analysis and design for bending, 348, 396–401, 410
elastic section modulus (*S*) for, 396, 410
Normal strain, axial loading and, 57–58, 133

Normal stress
beams, 558–561, 591
determination of, 7, 44
maximum criterion for brittle materials, 506
strain energy and, 763–767, 824
Numerical accuracy, 16

O

Oblique parallelepiped deformation, 99–100
Oblique planes, stresses on from axial loading, 27–28, 46
Orthotropic materials, 105
Overhanging beam, 604

P

Parabolic beam, 424–425
Parallel-axis theorem, A10–A11
Parallelepipeds
oblique, 99–100
rectangular, 96
Percent elongation, 61
Percent reduction in area, 62
Permanent set, 65, 134. *See also* Plastic deformation
Pin-ended columns, 694–697
Plane strain, 529–537, 549–550
Mohr's circle for, 532–534, 550
three-dimensional analysis of, 534–537
transformation equations, 529–531, 549
transformation of, 529–534, 546–550
Plane stress, 478–479, 480–506, 546
Mohr's circle for, 492–502, 547
principal stresses, 482–487, 546
state of, 478–479
three-dimensional analysis, 504–506
transformation equations for, 480–482, 546
transformation of, 480–487, 546
Plastic behavior, 65–67, 134
elastic behavior compared to, 65–67
permanent set, 65, 134
stress-strain diagrams for, 65–66, 134
reverse loadings and, 66–67
Plastic deformation
Bauschinger effect, 66
beams, 441–440, 469
circular shafts, 195–204, 225–227
creep, 65
elastic behavior and, 65–67, 134
elastic limit, 65–66, 134
elastoplastic material, 119–122, 139
elastoplastic members, 274–278, 336
members with single plane of symmetry, 278–279
modulus of rupture (R), 196, 225–226, 274
non-rectangular cross sections, 277
permanent deformation and, 200–201, 226–227
permanent set, 65–67, 134
pure bending and, 273–285, 336
rectangular cross sections, 274–277
residual stresses, 122–126, 139, 199–204, 226–227, 279, 336
reverse loadings and, 66–67
single-plane symmetric members, 278–279
slip, 65
stress and strain under axial loads, 65–67, 119–122, 134, 139
stress concentrations and, 122
thin-walled members, 440–441, 469
torsion and, 195–204, 225–227
Plastic hinge, 441
Plastic moment, 275–276, 336
Polar moment of inertia, A8
Poisson's ratio (ν), 94–95, 102–104, 137
lateral strain and, 94–95, 137
relationships with E and G, 102–104, 139
Power (P) transmitted by shafts, 185–186, 225
Pressure vessels, 520–524, 549
cylindrical, 520–522, 549
spherical, 522, 549
stresses in, 520–524, 549
thin-walled, 520–524, 549
Principal planes of stress, 482–487, 546
Principal strains, 523
Principal stresses, 483, 546, 556–597
beams, 559–561, 591
combined loads and, 575–583, 592
loading and, 556–597
plane stress transformation and, 483, 546
transmission shaft design for, 562–569, 592
Prismatic beams, design for bending, 371–376, 408
Prismatic members, pure bending of, 237–343
Problems
computation error detection, 16
equilibrium equations for, 16, 46
free-body diagrams for, 16, 45
numerical accuracy of, 16
Saint-Venant's principle for, 115–117, 139
SMART methodology for, 15–16
solution, method of, 15–19, 45–46
statically equivalent, 115–117
statically indeterminate, 78–81, 135–136
superposition method for, 79–81
temperature changes and, 82–88, 136–137
Properties of materials, A13–A28
Proportional limit for stress, 64, 134
Pure bending, 237–343
composite members, 259–262, 335
curved members, 319–327, 338
deformations from, 241–252
eccentric axial loading, 238–239, 291–295, 307–312, 337–338
elastic range stresses and deformation, 244–248, 334
elastoplastic members, 274–278, 336
members with single plane of symmetry, 278–279
plastic deformations, 273–285, 336
prismatic members, 237–343
residual stresses from, 279–280
stress concentrations from, 263–267, 336
symmetric members in, 240–244, 334
transverse cross sections, 248–252
transverse loading, 238–239, 334
unsymmetric bending analysis, 302–307, 337

R

Radius of curvature (ρ), 247, 334
Radius of gyration, A8–A10
Rectangular cross sections, plastic deformation in, 274–277
Rectangular parallelepiped deformation, 96
Redundant reactions, 810
Relative displacement, 69,
Repeated loadings, fatigue from, 67–68
Residual stresses
circular shafts, 199–204, 226–227
permanent deformation and, 200–201, 226–227
plastic deformation and, 122–126, 136, 199–204, 226–227, 279
pure bending and, 279, 336
temperature change and, 124
torsion and, 199–204, 226–227
Resilience (u_Y), modulus of, 763, 824
Resistance factor (ϕ), 728
Reverse loadings, plastic behavior and, 66–67
Rigidity (G), modulus of, 100–101, 102–104, 138–139
Hooke's law and, 100–101, 138
relationships with E and ν, 102–104, 139
shearing strain and, 100–101, 138
Rolled steel shapes, properties of, A17–A28
Rotation, speed of, 185
Rupture (R), modulus of, 196, 225–226, 274
Rupture of brittle materials, 60–62

S

Saint Venant's criterion, 509
Saint Venant's principle, 115–117, 139
Secant formula, 711–712, 751
Section modulus (S), *see* Elastic section modulus
Shafts, 147–234
circular, 148–204, 223–227
deformation of, 148–149, 151–153, 209–218, 223, 225–227
hollow (tubes), 154–155, 158–160, 223–224
non-circular, 209–216, 227
plastic deformation of, 195–204, 225–227
residual stresses in, 199–204, 226–227
statically indeterminate, 170–176, 225
stresses in, 150–151, 153–161, 209–218, 223–224
thin-walled hollow (tubes), 211–216, 227
torsion in, 147–234
transmission, 148–149, 185–187, 225
Shear
double, 12, 45
relationships with loads and bending moments, 260–368, 408
single, 11, 45
ultimate strength in, 32
Shear center, 419, 455, 469
Shear diagrams, 348–354, 407–408
beam analysis for bending, 348–354, 407–408
sign convention for, 349
Shear flow, 419, 421, 440–441, 468
Shear moments, singularity functions for, 348, 383–391, 409
Shearing strain
axial loading and, 99–102, 138

circular shafts, 153, 223
Hooke's law for, 100–101, 138
modulus of rigidity (G), 100–101, 138
oblique parallelepiped deformation, 99–100
Shearing stresses
average, 11, 45, 422, 468
beam design for, 417–475
beams, distribution of in, 347–348, 407, 422–431, 468
bending and, 347–348, 407
circular shafts, 153–160, 223
components of, 30–31
elastic range with, 153–160
forces exerted on transverse prismatic beams, 418–419, 467
horizontal, 419–426, 467
in-plane, 484, 547
internal force and, 10–12
longitudinal, 437–439, 468
maximum criterion for ductile materials, 507–508
plastic deformation and, 441–446
points of application, 44
strain energy due to, 767–769, 824
thin-walled member design for, 439–466, 469
unsymmetric loading and, 454–462, 469
vertical, 418, 467
Simple structures, analysis and design of, 12–15
Simply supported beam, 604, 606
Single-loaded members, work of, 788–790, 826
Single shear, 11, 45
Singularity functions
application to computer programming, 388
beams, 348, 383–391, 409, 623–630, 681–682
bending analysis and design using, 348, 383–391, 409
equivalent open-ended loadings for, 385–386, 410
Macaulay brackets, 384–385, 387
shear and bending moments using, 348, 383–391, 409
slope and deflection using, 623–630, 681–682
Singularity in beam loading, 383
Slenderness ratio, 696, 698, 750
Slope and deflection
beams, 607–608, 623–630, 681–682, A29
relationship of, 607–608
singularity functions for, 623–630, 681–682
SMART methodology, 15–16
Span, 346
Speed of rotation, 185
Spherical pressure vessels, stresses in, 522, 549
Stability
critical load, 692–694, 750
members, 9
structures, 692–702
Stable system, 692–693
Statically determinate members
beams, 346–347, 407, 635–636, 682
deflection and, 635–636, 682
method of superposition and, 635–636, 682
Statically equivalent problems, 115–117
Saint-Venant's principle, 115–117
uniform distribution of, 116–117
Statically indeterminate members
beams, 347, 600–601, 611–617, 636–637, 668–674, 679–682
deflection and, 611–617, 636–637, 668–674, 697, 680–682
first degree, 381, 612
forces, 56
method of superposition and, 636–637, 682
moment-area theorems for, 668–674, 685
problems, 78–81, 135–136
second degree, 381, 612
shafts, 170–176, 225
stress distribution, 8, 56
Statically indeterminate structures, 810–816
Statics
free-body diagrams, 4–6
review of methods, 4–6
Steel, design specifications for, 34
Step functions, 385, 409
Strain (ε). *See also* Stress and strain transformations; Stress and strain under axial loading
bending, 244, 334
circular shafts, 153, 223
engineering, 63
lateral, 94–95, 137
maximum absolute, 244, 334
measurement of, 538–541
normal, 57–58, 133
plane, 529–537, 549–550
Poisson's ratio (ν), 94–95, 102–104, 137
shearing, 99–102, 138, 153, 223
thermal, 82, 136
true, 63
Strain energy, 760–775, 823–725
axial loading and, 764, 824
bending and, 766, 824
deformation and, 760–762, 823
elastic, 763–769, 824
general state of stress and, 770–775, 825
modulus of resilience and, 763, 824
modulus of toughness and, 762–763, 823
normal stresses and, 763–767, 824
shearing stresses and, 767–769, 824
torsion and, 767–768, 825
transverse loading and, 769
Strain-energy density, 762–763, 823
Strain-hardening, 61
Strain gages, 480, 538, 547
Strain rosette, 480, 538, 547
Stress. *See also* Stress and strain transformations; Stress and strain under axial loading
allowable, 32–33
applications to analysis and design of simple structures, 12–15
average value of, 7, 44
axial, 7–10, 31
beams, distribution of in, 347–348, 407
bearing, 12, 45
bending, 244–248, 334, 347–348, 407
circular shafts, 150–151, 153–160, 223–224
components of, 28–31
concept of, 2–53
critical, 696
curved members, 320–323, 338
defined, 7
direction of the component, 29
design considerations, 31–37
elastic range deformation and, 244–248, 334
engineering, 63
exerted on a surface, 29
factor of safety, 32–34, 46
general loading conditions, 28–31, 46
internal forces and, 10–12
load and resistance factor design (LRFD), 34, 46
loadings and, 7–10, 27–31
maximum absolute, 244, 334
method of problem solution, 15–19, 45–46
normal, 7, 44
oblique planes under axial loading, 27–28, 46
plane, 478–479, 480–506, 546
proportional limit, 64, 134
residual, 122–126, 139
shearing, 10–12, 30–31, 44–45, 153–160
statically indeterminate distribution of, 8
true, 63
ultimate strength, 31–32
uniaxial, 242
uniform, 44
Stress and strain transformations, 476–555
brittle materials, 509–511, 549
ductile materials, 507–508, 548
failure, theories of, 507–513, 548–549
general state of stress, 503–504, 548
in-plane shearing stress, 484, 547
measurement of strain, 538–541
Mohr's circle for, 492–502, 547
plane strain, 529–537, 549–550
plane stress, 478–479, 480–506, 546
states of stress, 478–479
thin-walled pressure vessels, 520–524, 549
three-dimensional stress analysis, 504–506
yield criteria, 479
Stress and strain under axial loading, 55–145
bulk modulus (k), 97–99, 137
deformations from, 56–57, 68–69, 102–104, 119–122, 135, 139
dilatation, 97–99, 137
elastic limit, 65, 134
elastic versus plastic behavior, 65–67
endurance limit, 67–68, 135
fatigue from, 67–68, 135
fiber-reinforced composite materials, 64–65, 104–108
Hooke's law, 63–65, 95–97, 100–101, 134
lateral strain, 94–95, 137
modulus of elasticity (E), 63–65, 102–104, 134
modulus of rigidity (G), 100–101, 102–104, 138–139
multiaxial loadings, 95–97, 137
normal strain, 57–58, 133
plastic deformation, 65–67, 119–126, 134, 139
Poisson's ratio (ν), 94–95, 102–104, 137
repeated loadings, 67–68
residual stresses, 122–126, 139
Saint-Venant's principle, 115–117, 139
shearing strain, 99–102, 138
statically equivalent problems, 115–117
statically indeterminate problems, 78–81, 135–136
stress concentrations, 117–118, 122, 139
stress-strain diagram, 58–62, 65–67, 133–134
temperature change effects on, 82–88, 136–137
true stress and true strain, 63
uniform distribution of, 116–117

Stress concentrations
circular shafts, 187–190, 225
circular stress distribution, 117–118
discontinuity factor (K), 117–118, 139
fillets, 117–118, 122
flat stress distribution, 117–118
plastic deformations and, 122
pure bending, 263–267, 336
torsion and, 187–190, 225
Stress-strain diagrams, 57–62, 65–67, 133–134
axial loading and, 57–62, 65–67, 133–134
breaking strength, 60–61
brittle material determination, 60–61, 133
compression test for, 62
ductile material determination, 59–62, 133–134
gage length of specimen, 58–59
load-deformation curve, 57
rupture and, 60–61
tensile test for, 58–62
ultimate strength, 60–61
yield strength, 60–61, 134
Structural steel column design, 723–724
Superposition
method of for deflection, 601, 635–643, 682
multiaxial problems, 96–97
principle of, 96
statically determinate beams, 635–636, 682
statically indeterminate beams, 636–637, 682
statically indeterminate problems, 79–81
Symmetric loadings, moment-area theorems for, 651–653, 684
Symmetric members, 240–244, 334
bending (couple) moments in, 240–241, 334
deformation from pure bending, 241–244, 334
plastic deformation in, 278–279

T

Temperature change
coefficient of thermal expansion, 82, 136
plastic deformation and, 124
problems involving, 82–88, 136–137
residual stresses and, 124
stress and strain under axial loads and, 82–88, 124, 136–137
thermal strain, 82, 136
Tensile test, 58–62
Thermal expansion, coefficient of, 82, 136
Thermal strain, 82, 136
Thin-walled members
beam design for shearing stresses, 439–466, 469
non-circular (tubes), 211–216, 227
plastic deformations in, 440–441, 469
shear flow, 440–441
shearing stresses in, 439–466, 469
unsymmetric loading of, 454–462, 469
Three-dimensional analysis
strain, 534–537
stress, 504–506
Timber, design specifications for, 34
Torque (T), 148, 151, 156, 167–170
Torsion, 147–234
angle of twist, 151, 167–170, 210, 214, 224
circular shafts, 148–204, 223–227
elastic range, 153–160, 167–170, 223–224
elastoplastic materials, 196–199, 226
hollow shafts (tubes), 154–155, 158–160, 223–224
modulus of rupture (R), 196, 225–226
non-circular shafts, 209–216, 227
plastic deformation and, 195–204, 225–227
residual stresses from, 199–204, 226–227
shearing stresses from, 153–160, 167–170, 209–218, 224–227
strain energy due to, 767–768, 825
stress concentrations and, 187–190, 225
stresses in, 150–151, 153–161, 223–224
thin-walled hollow shafts (tubes), 211–216, 227
transmission shafts, 148–149, 185–187, 225
Torsion formulas
elastic range, 155–156, 223
variable circular cross sections, 188, 225
Toughness (ε_R), modulus of, 762–763, 823
Transformed section, 240
Transmission shafts
deformation of, 148–149
design of, 185–187, 225, 562–569, 592
power transmitted by, 185–186, 225
principle stresses and, 562–569, 592
speed of rotation of, 185
Transverse cross sections, 248–252
Transverse forces, 44–45
Transverse loading
beam analysis and design for, 346–348, 407
concentrated, 346
deflection of beams under, 602–610, 679–680
distributed, 346
pure bending and, 238–239, 334
shear and stress distributions, 347–348, 407
strain energy under, 769
support reactions, 347–348
uniformly distributed, 346
True stress and true strain, 63
Tubes, 211–216. *See also* Shafts
Two-force member analysis, 4–6

U

Ultimate load, 728
Ultimate strength, 31–32, 60–61
Uniaxial stress, 242
Uniform distribution of stress and strain, 116–117
Uniform stress, 44
Uniformly distributed loads, 346
Unstable system, 692–693
Unsymmetric bending analysis, 302–307, 337
Unsymmetric loading
beam deflection and, 664–674, 684–685
maximum deflection and, 666–667, 685
moment-area theorems for, 664–674, 684–685
thin-walled members, 454–462, 469

V

Volume change, 97–99, 137
axial loadings and, 97–99, 137
bulk modulus (k) for, 97–99, 137
dilatation, 98–99, 137
von Mises criterion, 508

W

Watts (W), 185, 225
Wide-flange beam (W-beam), 424
Wood column design, 726
Work, 788–795, 802–804, 826
deflection by, 790–795, 806–809
energy and, 788–795, 802–804, 826
multiple loads and, 802–804
single-loaded members, 788–790, 826
Work-energy method, 790–795

Y

Yield, 59, 134
Yield criteria for ductile materials, 507–508, 548
Yield points, 61
Yield strength, 60–61, 134
Yielding, design consideration of, 33
Young's modulus (E), 63. *See also* Elasticity

SI Prefixes

Multiplication Factor	Prefix†	Symbol
$1\,000\,000\,000\,000 = 10^{12}$	tera	T
$1\,000\,000\,000 = 10^{9}$	giga	G
$1\,000\,000 = 10^{6}$	mega	M
$1\,000 = 10^{3}$	kilo	k
$100 = 10^{2}$	hecto‡	h
$10 = 10^{1}$	deka‡	da
$0.1 = 10^{-1}$	deci‡	d
$0.01 = 10^{-2}$	centi‡	c
$0.001 = 10^{-3}$	milli	m
$0.000\,001 = 10^{-6}$	micro	μ
$0.000\,000\,001 = 10^{-9}$	nano	n
$0.000\,000\,000\,001 = 10^{-12}$	pico	p
$0.000\,000\,000\,000\,001 = 10^{-15}$	femto	f
$0.000\,000\,000\,000\,000\,001 = 10^{-18}$	atto	a

† The first syllable of every prefix is accented so that the prefix will retain its identity. Thus, the preferred pronunciation of kilometer places the accent on the first syllable, not the second.

‡ The use of these prefixes should be avoided, except for the measurement of areas and volumes and for the nontechnical use of centimeter, as for body and clothing measurements.

Principal SI Units Used in Mechanics

Quantity	Unit	Symbol	Formula
Acceleration	Meter per second squared	···	m/s^2
Angle	Radian	rad	†
Angular acceleration	Radian per second squared	···	rad/s^2
Angular velocity	Radian per second	···	rad/s
Area	Square meter	···	m^2
Density	Kilogram per cubic meter	···	kg/m^3
Energy	Joule	J	$N \cdot m$
Force	Newton	N	$kg \cdot m/s^2$
Frequency	Hertz	Hz	s^{-1}
Impulse	Newton-second	···	$kg \cdot m/s$
Length	Meter	m	‡
Mass	Kilogram	kg	‡
Moment of a force	Newton-meter	···	$N \cdot m$
Power	Watt	W	J/s
Pressure	Pascal	Pa	N/m^2
Stress	Pascal	Pa	N/m^2
Time	Second	s	‡
Velocity	Meter per second	···	m/s
Volume, solids	Cubic meter	···	m^3
Liquids	Liter	L	$10^{-3}\ m^3$
Work	Joule	J	$N \cdot m$

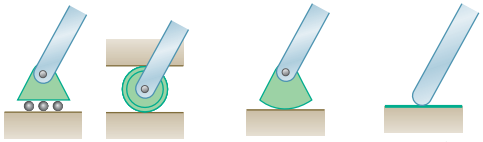
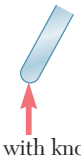
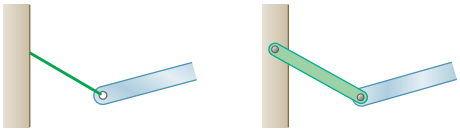
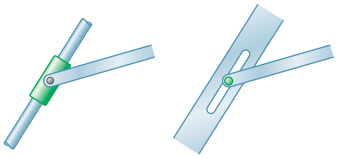
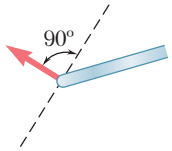
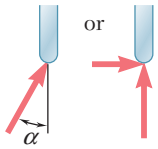
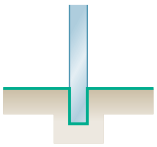
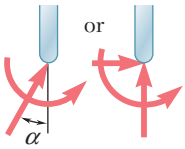
† Supplementary unit (1 revolution = 2π rad = 360°).

‡ Base unit.

U.S. Customary Units and Their SI Equivalents

Quantity	U.S. Customary Units	SI Equivalent
Acceleration	ft/s^2	0.3048 m/s^2
	$in./s^2$	0.0254 m/s^2
Area	ft^2	0.0929 m^2
	in^2	645.2 mm^2
Energy	ft · lb	1.356 J
Force	kip	4.448 kN
	lb	4.448 N
	oz	0.2780 N
Impulse	lb · s	4.448 N · s
Length	ft	0.3048 m
	in.	25.40 mm
	mi	1.609 km
Mass	oz mass	28.35 g
	lb mass	0.4536 kg
	slug	14.59 kg
	ton	907.2 kg
Moment of a force	lb · ft	1.356 N · m
	lb · in.	0.1130 N · m
Moment of inertia		
Of an area	in^4	0.4162 × 10^6 mm^4
Of a mass	lb · ft · s^2	1.356 kg · m^2
Power	ft · lb/s	1.356 W
	hp	745.7 W
Pressure or stress	lb/ft^2	47.88 Pa
	lb/in^2 (psi)	6.895 kPa
Velocity	ft/s	0.3048 m/s
	in./s	0.0254 m/s
	mi/h (mph)	0.4470 m/s
	mi/h (mph)	1.609 km/h
Volume, solids	ft^3	0.02832 m^3
	in^3	16.39 cm^3
Liquids	gal	3.785 L
	qt	0.9464 L
Work	ft · lb	1.356 J

Reactions at Supports and Connections for a Two-Dimensional Structure

Support or Connection	Reaction	Number of Unknowns
 Rollers; Rocker; Frictionless surface	 Force with known line of action	1
 Short cable; Short link	 Force with known line of action	1
 Collar on frictionless rod; Frictionless pin in slot	 Force with known line of action	1
 Frictionless pin or hinge; Rough surface	 Force of unknown direction	2
 Fixed support	 Force and couple	3

The first step in the solution of any problem concerning the equilibrium of a rigid body is to construct an appropriate free-body diagram of the body. As part of that process, it is necessary to show on the diagram the reactions through which the ground and other bodies oppose a possible motion of the body. The figures on this and the facing page summarize the possible reactions exerted on two- and three-dimensional bodies.

Reactions at Supports and Connections for a Three-Dimensional Structure

